

ASRDI OXYGEN

TECHNOLOGY SURVEY

Volume VII: Characteristics of

Metals That Influence System Safety

PELOUCH

**CASE FILE
COPY**



NATIONAL AERONAUTICS AND SPACE ADMINISTRATION

ASRDI OXYGEN

TECHNOLOGY SURVEY

Volume VII: Characteristics of

Metals That Influence System Safety

By James J. Pelouch, Jr.

Aerospace Safety Research and Data Institute
NASA Lewis Research Center



Scientific and Technical Information Office

NATIONAL AERONAUTICS AND SPACE ADMINISTRATION
Washington, D.C.

1974

For sale by the National Technical Information Service
Springfield, Virginia 22151
Price — \$3.75

PREFACE

This document is one of a series of publications being developed by the NASA Aerospace Safety Research and Data Institute for use as oxygen system design and operation guidelines. This Special Publication reviews the major issues in the safety and reliability of metals usage in oxygen systems and is presented as a descriptive summary covering these issues.

A microfiche supplement of references is attached inside the back cover to make pertinent pages of listed references readily available to the reader. Some references are included in their entirety, while only selected pages or sections of others are reproduced. Commonly available handbooks and copyrighted textbooks are not included in the microfiche supplement. The location of each reference in the microfiche supplement is noted in the list of references at the end of the report.

This review recognizes the cost in time and dollars that results from any system failure regardless of the cause. Although oxygen initiated failures are emphasized, all types of failures are considered since the results of oxygen system failures are generally more serious because of the chemical and physical properties of the oxidizer.

A second objective of this volume is to bring together available information that will help define the limiting conditions of use that oxygen "compatible" materials may be expected to withstand when used in oxygen systems.

The following representatives at the NASA centers and at the National Bureau of Standards participated in the critical review of the text: Melvin G. Olsen of the Kennedy Space Center; Robert L. Johnston and Glenn M. Ecord of the Johnson Space Center; James H. Hess of the Marshall Space Flight Center; John M. Kazaroff and George Tulusiak of the Lewis Research Center; and Alan F. Clark and Jerome G. Hust of the Cryogenics Division, National Bureau of Standards.

Frank E. Belles, Director
Aerospace Safety Research and Data Institute
National Aeronautics and Space Administration

CONTENTS

	Page
SUMMARY	1
INTRODUCTION	2
BRITTLE FRACTURE OF METALS - BASIC INFLUENCES	3
Capacity to Absorb Energy	4
Fracture Mechanics Considerations	4
Effect of Crystal Structure	5
Effect of Elevated Temperature	5
STEEL	6
Application in Oxygen Systems - Alloys Suitable for Use	7
Phase Transition and Brittle Failure of Steels	8
Effect of steel plate thickness	11
Effect of specimen orientation	11
Effect of metallurgical factors	12
Characteristics of Various Stainless Alloys	15
Types of and Specifications for Stainless Steel Alloys for Oxygen Service	17
ALUMINUM AND ALUMINUM ALLOYS	17
Applications and Limitations in Oxygen Systems	17
Aluminum Alloys Suitable for Oxygen Use	20
Processing and Fabrication Factors	20
Strengthening and temper designation	20
Casting	22
Forging	23
Welding	23
Surface treatments	24
Design and Use Factors	24
Thermal conductivity	24
Metallurgical factors	27
NICKEL AND NICKEL ALLOYS	29
Applications in Oxygen Systems - Code Restrictions	29
Nickel Alloys Suitable for Oxygen Use	30
Fabrication	32
Plating	32
Lubrication	32
Thermal Conductivity	33

	Page
COPPER AND COPPER ALLOYS	33
Applications in Oxygen Systems	33
Copper Alloys Suitable for Oxygen Use	34
Restrictions on Heat Treatable Copper Alloys	35
MISCELLANEOUS METALS	35
Magnesium	36
Titanium	36
Beryllium	36
Gold and Platinum	37
IGNITION AND COMBUSTION OF METALS - RELATIVE COMPARISON	37
Symbols	38
Influence of Metal Properties and Ignition Temperature	38
Relative energy rate to ignite	38
Energy of combustion	39
Summary comparison of various metals from the standpoints mentioned previously	40
APPENDIX - TABLES OF SPECIFICATIONS, USES, AND SPECIAL CONSIDERATIONS FOR METALS AND ALLOYS IN OXYGEN SYSTEMS	43
REFERENCES	64
BIBLIOGRAPHY	67

SUMMARY

This report contains the results of a literature survey and analysis of the material and process factors affecting the safety of metals in oxygen systems. In addition, the practices of those who specify, build, or use oxygen systems relative to the previous is summarized. Alloys based on iron, copper, nickel, and aluminum were investigated representing the bulk of metals found in oxygen systems. Safety-related characteristics of other miscellaneous metals are summarized.

It was found that factors affecting the safety of metals in oxygen systems exist in all phases of the evolutionary process, from smelting and mill techniques through end-product fabrication.

The interplay of safety-related material and process factors became most complicated when iron alloys (steels) were considered, because of the existence of multiple metallurgical phases. Aluminum, although widely used in oxygen systems, can liberate relatively large amounts of heat in an oxygen fire. Nickel is highly fire resistant and easily fabricated, but it is too expensive and limited in availability for extensive use. Copper is also highly fire resistant, but lower strength and fabrication difficulties curtail its use in large structures.

Steels, due to large available property ranges, are found in the construction of all kinds of oxygen system components including gears, shafts, plumbing, tankage, and fasteners; aluminum is used principally in tankage and forged parts such as valve bodies; nickel is used in more critical (high pressure, high temperature) applications as lines and cast and forged components; and copper is found in small oxygen components as castings, forgings, and wrought shapes in the form of low pressure tubing, springs, valve components, and gaskets.

Of the miscellaneous metals, magnesium, titanium, and beryllium are distinctly hazardous because of the ease and severity of reaction or because of the toxicity of the reaction products. The metals gold and platinum are exceedingly safe due to their high stability against oxidation.

The safety of a given metal in an oxygen system was determined to be influenced by the particular service requirement. The metal characteristics should favorably influence fulfillment of these requirements. Thus, no singular metal or alloy could be classified as safest for all types of oxygen service.

INTRODUCTION

This survey examines the properties and characteristics of technically important metals and alloys as influencing factors in oxygen system safety, complemented with a summary of prevailing practices with these metals and alloys in oxygen systems. The reader is thus (1) exposed to the types of engineering considerations he would have to make when selecting a metal for oxygen service, and (2) provided with the "metal selection practice" of the technical community with which to substantiate his selection.

The vulnerability of an oxygen system to fire or hazardous mechanical malfunctions is in part influenced by the physical characteristics of the metals used herein. For example, oxygen, in common with all cryogenic liquids, can cause certain metals to be brittle, facilitating failure. Pressure burst in a high pressure gaseous oxygen system can likewise be affected by some characteristic in the containment metal (such as low toughness) resulting in a bomb-like explosion. Fires often result when metal failures occur because (1) the rate of energy release is very high when highly stressed metals fail, (2) fragmentation and impact sometimes occur, and (3) other, perhaps less compatible, portions of the structure or surroundings are suddenly exposed to oxygen. Oxygen can produce other effects on structural metals, but these effects are of little consequence to the engineer. For example, the fatigue resistance of certain metals, typically nickel alloys, is lowered by the presence of oxygen. This effect is, however, produced by the presence of only 0.01 millimeter mercury oxygen partial pressure in the environmental gas; concentrations in excess of this have no further effect (ref. 1). As a further example, oxygen by itself is not corrosive to structural metals, and because of the necessity for internal system cleanliness to minimize fire hazards, sufficient containment is not typically present inside the system to induce corrosion. Emphasis is therefore placed on the threats mentioned in the previous paragraph; namely, metal fires and metal rupture (principally brittle fracture).

Four basic alloy systems commonly used in oxygen systems are discussed: steels, aluminum and aluminum alloys, nickel and nickel alloys, and copper and copper alloys. A summary of more exotic metals is also provided.

For each alloy system, the basic influencing properties are discussed. The effect of alloy composition and processing variables on these properties is shown.

For each alloy system, the prevailing metal selection practice of those who specify, build, or use oxygen systems is summarized. This information includes codes, use restrictions and limitations and reasons therefore (if known).

It should be noted that not all pertinent issues on oxygen safety are discussed for each metal. This would make the report repetitious. The issue is raised at the first opportunity and only repeated if it is vital to the alloy being discussed. Table I is presented as a guide to determine the relevancy of various considerations to various metals in oxygen system service.

TABLE I. - RELEVANCE OF ISSUES TO METALS

[1, usually irrelevant or of little concern; 2, should receive attention depending on application; 3, should receive attention at all times; 4, very important, always a potential contributor to hazard; 5, critically important, principal contributor to hazard.]

Issue	Alloy				
	Steel	Aluminum	Nickel	Copper	Miscellaneous
Brittle transition	5	2	1	1	2
Strengthening	5	2	3	4	2
Casting	2	2	1	2	2
Welding	3	4	2	N/A ^a	N/A
Forging	3	3	3	3	2
Surface smoothness	3	4	2	2	2
Thermophysical properties	2	4	3	3	3
Code and use history restrictions	4	2	3	3	3
Plating and passivating	3	1	2	1	2
Lubrication	3	1	1	1	2
Tolerance to contamination	5	5	4	4	4

^aN/A, not applicable.

BRITTLE FRACTURE OF METALS - BASIC INFLUENCES

Any system is subject to inadvertent overloads. The behavior of the system to an overload may be tolerance or failure. The behavior of structural components under overload situations can be divided into three categories: (1) where yield of the structure relieves the overload and rupture does not occur, (2) where yield of the structure does not relieve the overload and rupture occurs, and (3) where yield of the structure constitutes failure in itself regardless of rupture. Examples of (1) may be bolts in bolted joints, struts, and closed containers completely full of pressurized but incompressible fluids. Examples of (2) are all pressure vessels containing compressible fluids such as lines, fittings, and tanks, and rotating components subject to centripetal loads such as pump impellers, etc. Examples of (3) are bearing surfaces, gears, cams, etc. Category (1) is a forgiving situation. Category (3) involves prevention of yield failure by providing high yield strength, often at the sacrifice of toughness. In oxygen systems, category (2) is the condition for potential explosion compounded by fire, the most common and severe hazard. The behavior of metals in this category (2) situation and the resultant safety is the subject of this section.

Capacity to Absorb Energy

Toughness is the ability of a metal or alloy to absorb mechanical energy prior to rupture. The most important singular factor in the selection of materials for items such as pressure vessels is to assure that toughness (and, to be discussed, ductility) is inherent in the material at all use temperatures. A tough material will resist failure by deforming plastically (yielding) when subject to substantial amounts of energy as illustrated in figure 1. Conversely, a low toughness material, although usually much stronger, will

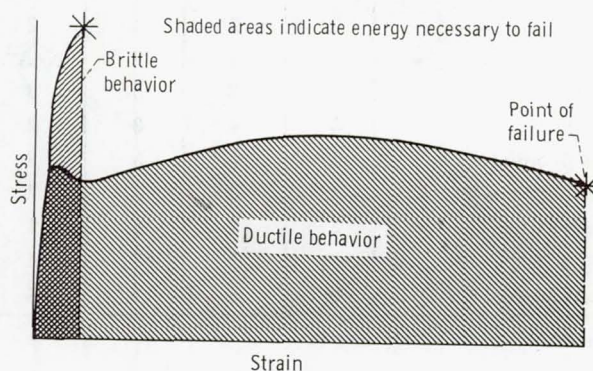


Figure 1. - Ductile and brittle behavior.

fail with little or no plastic deformation when subject to smaller amounts of energy (ref. 2, pp. 188 and 189). Energy can be supplied from abrupt pressurization, inadvertent impact, thermal shock, etc. While a pressure vessel should not intentionally yield in service, it should yield before rupture rather than rupture in a low toughness mode in the event of an overload. The reason is simple: the energy contained in the fluid is partially absorbed in the plastic deformation of the vessel which reduces the energy of the explosion.

Fracture Mechanics Considerations

All structures contain flaws either introduced during fabrication (such as welding porosity, gas bubble formation during mill operations, etc.) or during operation (cracks generated from cyclic stressing, cracks generated from stress corrosion, surface nicks from impact, etc.). Structures occasionally fail at stress levels far below the yield strength, where the failure initiates at some flaw site. What has happened is that localized yielding in the region of the flaw was prevented and the stress across the flaw had to be absorbed by the flaw tip causing the material at the flaw tip to fail. If the load is

not released by this action, the flaw will further progress and, because progressively smaller amounts of sound material are left, the process will continue in an unstable manner until the component separates. If, on the other hand, the material at the flaw tip could flow plastically to relieve the local stress, the flaw would not extend and failure would not occur. The previous separates ductile from brittle behavior in metals. Ductility is therefore the ability of the material to deform plastically while toughness is the ability to absorb energy during plastic deformation. Ductile to brittle transition in a particular metal is facilitated by high strain rates (impact), decreasing temperature, and a state of complex stress acting to constrain the material. A liquid oxygen pressure vessel embodies all of the conditions necessary for brittle explosion: low temperatures, the existence of a compressible fluid, a state of complex constraining stresses in the vessel wall, and the potential for sudden overload (impact or internal reaction).

Effect of Crystal Structure

The ductile or brittle behavior of metals is dependent on the structure of the crystals contained therein. Metals with cubic lattice structure and one atom in the center of each face (FCC) show no loss in ductility down to at least liquid oxygen temperature. Examples are aluminum, copper, and nickel. Metals with cubic lattice structure and one atom in the center of each cube (BCC) and metals with a hexagonal crystal structure show a marked ductile to brittle transition. Examples are iron, carbon steel, and titanium. Fortunately, iron can be alloyed in a way that the ductility improves. One can never rely on the previous criterion as the only one for predicting the ductile or brittle behavior of a given metal because other metallurgical factors are also at play in a real alloy system. For example, dissolved gases, metallic precipitates, grain size, and component size also have relevance in ductile or brittle behavior as evidenced in the following sections.

Effect of Elevated Temperature

Certain alloys sustain a loss in ductility as the temperature is raised to a substantial fraction (one-quarter to three-quarters) of the melting temperature. This is evidenced by a loss of elongation of metal samples in tensile testing. In an oxygen system, should a heat-producing reaction occur that would elevate the temperature of a pressure containment structure, a brittle failure of this otherwise ductile structure could occur. This is especially serious if the alloy sustains a loss of ductility before it sustains a loss of strength with increasing temperature: this prevents failure in a ductile mode by loss

of strength due to heating. Paradoxically, those alloys that exhibit a high degree of ductile behavior at cryogenic temperatures generally suffer a loss of ductility at high temperatures. Examples of alloys that lose substantial ductility before losing substantial strength at high temperatures are Inconel X-750, Monel K-500, and nickel silvers. Examples of alloys that lose ductility and strength more or less simultaneously are austenitic (300 series) stainless steels, brasses, and bronzes. Examples of alloys that do not lose ductility (or, in some cases, gain ductility in a continuous manner) are low alloy steels, martensitic (400 series) stainless steels, Inconel 718, Hastelloy X and, apart from the aforementioned paradox, copper and aluminum alloys.

STEEL

Steels comprise the most widely used group of alloys in oxygen systems because of their diversity of properties, low cost, and ease of fabrication. Reference 3, in a review of applicable literature, has concluded that ignition of steels in oxygen generally occurs near the melting temperature of 1300°C . Combustion is continuous and moderate, intermediate between nickel alloys (which gradually quench) and aluminum alloys (which burn vigorously). At 800 psi the ignition temperature for low alloy steels is lowered 200° to 400°C below the melting temperature and the burning rate is increased. The ignition temperature of steels is probably further lowered at still higher pressures

TABLE II. - BASIC FACTORS AFFECTING THE SELECTION OF
STEEL FOR OXYGEN SERVICE

Carbon steel	For - The cost is low and ease of fabrication in large commercial ground structures. Good strength exists considering cost. Against - Surface scales (rust) form with moisture creating a potential contamination trap. These scales can also be carried in the fluid stream to initiate reactions elsewhere in the system. Ductility is lost at subzero temperatures prohibiting pressure containment of LOX.
Alloy steel (high-strength, low-alloy steel)	For - Such alloys possess exceptional hardness and strength for wear resistant surfaces and containment of high pressure gaseous oxygen. Against - Same as Carbon steel.
Stainless steel	For - Retention of ductility at LOX temperatures (austenitic grades only) permits containment of LOX. Only a very thin oxide film forms which facilitates cleaning and minimizes contaminant accumulation. Against - The cost is higher than for others. The strength is lower than alloy steels.

by virtue of the observed trend at lower pressure ranges. Reference 4 (pp. 32 to 34) indicates that the ignition of steels can be promoted easier than the ignition of copper or nickel at 7500 psi. Combustion characteristics for various steels will differ if the alloying elements chromium or nickel are present in large (>10 percent) amounts. Chromium (such as in 400 series stainless steels) will invigorate the combustion, and nickel (such as in 300 series stainless steels) will passify the combustion. Selection criteria are shown in table II.

Application in Oxygen Systems - Alloys Suitable for Use

Table III (from refs. 5 and 6) lists the uses for steel in oxygen systems and the

TABLE III. - SELECTION OF STEELS FOR USE IN OXYGEN SERVICE^a

Applications (with reference to text)	Major factors influencing selection	Steels commonly used in oxygen service					
		Service temperature extremes, °F					
		500	80	-20	-75	-170	-300
Category I - Pressure vessels: lines, fittings, valve bodies, tanks, etc.	Notch impact toughness						
	Fracture toughness						
	Notch strength						
	Thermal shock resistance						
	Creep resistance						
	Weldability						
	Formability						
	Avoidance of phase-transformation-induced brittle behavior						
	Ability to provide smooth surface finishes - resistance to surface corrosion						
	Fire compatibility with oxygen						
Category II - Load bearing surfaces: bushings, rolling-element bearings, gears, pivot-joints, shafts, etc.	Resistance to stress corrosion						
	Hardness						
	High modulus						
	Fatigue strength						
	Dimensional stability						
	Machinability						
	Acceptance of phase-transformation-induced brittle behavior to improve performance						
	Ability to provide smooth surface finishes - resistance to surface corrosion						
	Fire compatibility with oxygen						
	Resistance to stress corrosion						
Category III - Locating hardware: fasteners, struts, ties, brackets	Compatibility in oxygen when lubricated						
	Resistance to galling, seizure						
	Strengthenability by thermomechanical treatments						
	Creep resistance						
	Formability						
	Compatible thermal expansion characteristics						
	Ability to provide smooth surface finishes - resistance to surface corrosion						
	Fire compatibility with oxygen						
	Resistance to stress corrosion						
	Compatibility in oxygen when lubricated						
	Resistance to galling, seizure						

^aFrom information in ref. 5 (pp. 63 to 536) and ref. 6 (secs. 11XX to 16XX).

types of steels to fulfill these uses. There are over 500 alloys classified as carbon steels, alloy steels, high strength steels, and stainless steels as listed in reference 7 (pp. 1 to 14). Each of these alloys has certain properties which permit specific uses in oxygen such as those listed in table III. Engineering considerations such as welding, machining, forging, and casting for most of these alloys are given in reference 5 (pp. 63 to 536) and are not summarized here because of the extensive volume of such information.

Phase Transition and Brittle Failure of Steels

The three basic factors that contribute to brittle behavior in a given steel are high strain rates (impact), low temperatures, and the presence of notches (fig. 2 from ref. 8,

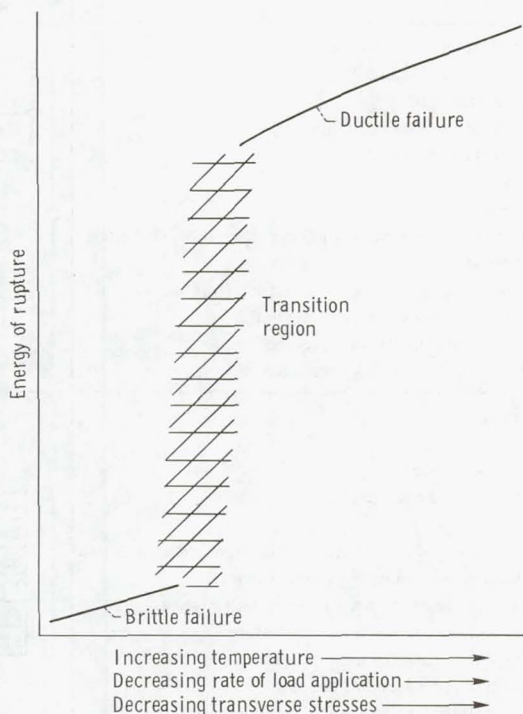


Figure 2. - Effect of temperature, rate of loading, and transverse stresses on type of failure (ref. 8, p. 17).

p. 17). According to present knowledge, there is always a considerable increase in yield strength with a corresponding loss in ductility at high strain rates; the yield point for mild steel doubles for an increase in strain rate from 10^{-3} to 10^2 inch per inch per second. At some point in decreasing temperature, called the nil ductility transition

TABLE IV. - MINIMUM ACCEPTABLE IMPACT VALUES FOR STEELS^a

Material	Specified minimum tensile strength	Operating temperature range, °F		Charpy V-notch impact energy, ft-lb		Lateral expansion, in. (mil)
				Fully deoxidized steel	Other than fully deoxidized	
Carbon, low alloy steels	65 000 psi and less	-20 to 100	Average for 3 specimens	13	10	-----
			Minimum for 1 specimen	10	7	
Carbon, low alloy steels	Over 65 000 to 75 000 psi inclusive	-20 to 100	Average for 3 specimens	15	13	-----
			Minimum for 1 specimen	12	10	
Carbon, low alloy steels	Over 75 000 to but not including 100 000 psi	-20 to 100	Average for 3 specimens	15	13	-----
			Minimum for 1 specimen	12	10	
Carbon, low alloy steels	100 000 psi and over	-20 to 100	Minimum for 3 specimens	---	---	0.015 (15)
Types 304, 304L, 347 stainless	-----	below -325		---	---	↓
FeM (chromium) stainless	-----	below -20		---	---	
FeA (chromium-nickel) stainless with carbon greater than 0.10 percent	-----	below -20				
FeA stainless with alloy content in excess of AISI limits	-----	below -20		---	---	
High alloy steels in castings	-----	below -20		---	---	
Types 309, 310, 316, 309Cb, 310Cb, or 316Cb stainless	-----	All temperatures		---	---	

^aFrom information in ref. 11.

temperature (NDT), the metallurgical structure of the steel changes with a resulting change from ductile to brittle behavior. Metallurgical influences on the NDT will be discussed later. The presence of the notch constrains the material in a triaxial state of tensile stress at the root of the notch which reduces plastic behavior: tensile strains in the longitudinal direction cannot be made up for by necking-in deformations in the transverse directions (ref. 9, pp. 81 to 85).

The most widely recognized test to measure the brittle nature of metals is the notched bar impact test (ASTM E23-66, ref. 10, pp. 275 to 289). Therein, the energy necessary to fracture a notched specimen and the bulge or lateral expansion at the fracture site are measured. The impact energy level that the particular metal must survive is a function of the end use. The ASME Pressure Vessel Code (ref. 11) recognizes the following (table IV) minimum acceptable impact energy conditions for steels for pressure vessel construction at the temperature and condition for which service is intended. Paragraph UG-84 of Division 1 and Article M-2 of Division 2 of Section VIII of the ASME Boiler and Pressure Vessel Code must be consulted when defining the impact test requirements for steels for pressure vessel applications.

The specimen configurations for the Charpy tests are shown in figure 3. A more complete description of specimen types is given in reference 10 (pp. 282 and 287).

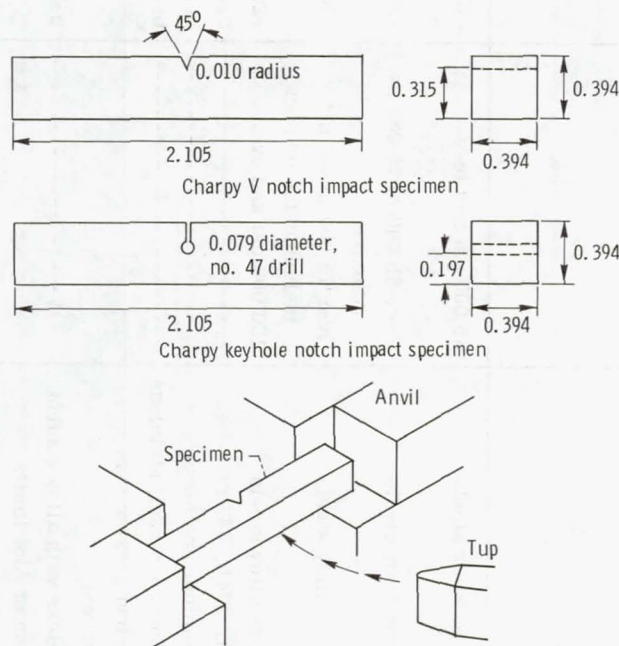


Figure 3. - Charpy test specimens and test method (ref. 8, p. 159). All dimensions are in inches.

Three things must be recognized when reviewing data on impact strength:

(1) The results are functions of the specimen configuration such that Charpy key-hole, Charpy V-notch, Izod specimen, etc. tests will not correlate.

(2) The impact test provides quantitative comparisons on a selected specimen, but data cannot be converted into energy values that would serve for engineering design calculations.

(3) Impact strength is a criteria that must be applied regardless of the type of oxygen service, whether it be a stainless steel for the containment of LOX or a carbon steel for gaseous oxygen service at room temperature (ref. 10, p. 287).

An excellent discussion on the transition between ductile-to-brittle behavior as evidenced by impact testing is given in reference 8 (pp. 18 to 27).

Effect of steel plate thickness. - In general, the NDT temperature increases as the rolled plate thickness increases (fig. 4). This is principally due to a lack of grain refinement as one progresses into the center of a thick rolled section. The transition temperature should be determined from specimens of full plate thickness if the standard range of Charpy specimen widths can accommodate this restriction (see ref. 10, pp. 275 to 289).

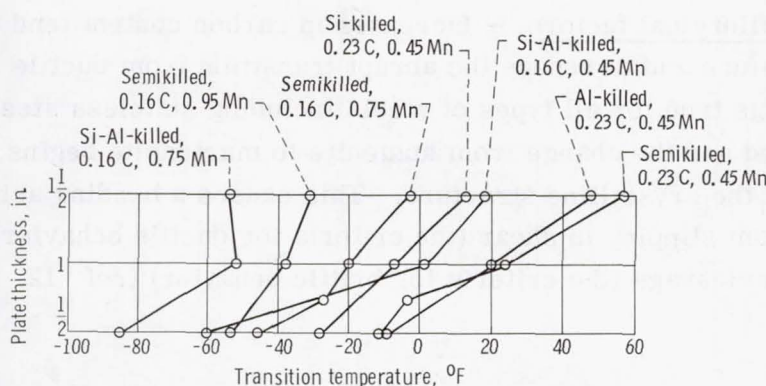


Figure 4. - Average curves showing effect of plate thickness on keyhole Charpy ductility transition temperatures of various carbon steels (ref. 8, p. 30).

Effect of specimen orientation. - In general, specimens oriented parallel to the rolling direction and notches parallel to the plate surface give higher impact energy values than specimens oriented transverse to the rolling direction and notches normal to the plate surface (fig. 5). The usual procedure is to use the LH specimen orientation shown in the figure.

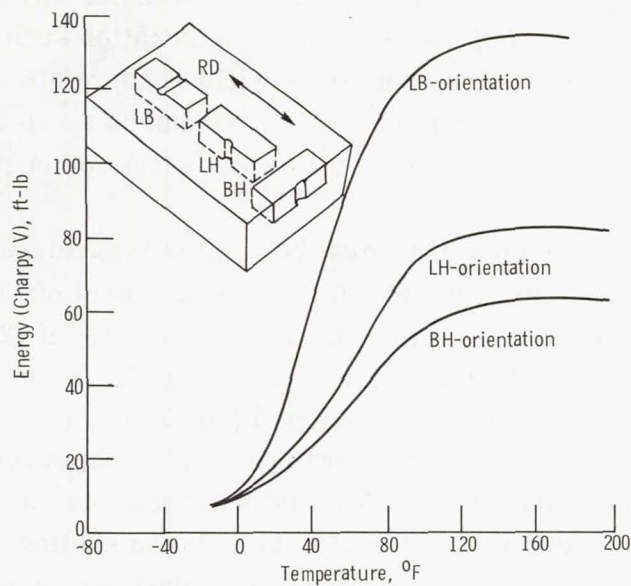


Figure 5. - Effect of Charpy V transition curves of notch and specimen orientation relative to rolling direction (ref. 8, p. 66).

Effect of metallurgical factors. - Increases in carbon content tend to increase the transition temperature and to reduce the abrupt transition from ductile to brittle behavior (fig. 6). This is true for all types of steels including stainless steels. As the temperature is lowered and the change from austenite to martensite begins, the carbon is precipitated out of the crystalline structure. This causes a bonding action which prevents the metal from slipping in shear (the criteria for ductile behavior) causing the failure to occur in cleavage (the criteria for brittle behavior) (ref. 12, pp. 144 and 145).

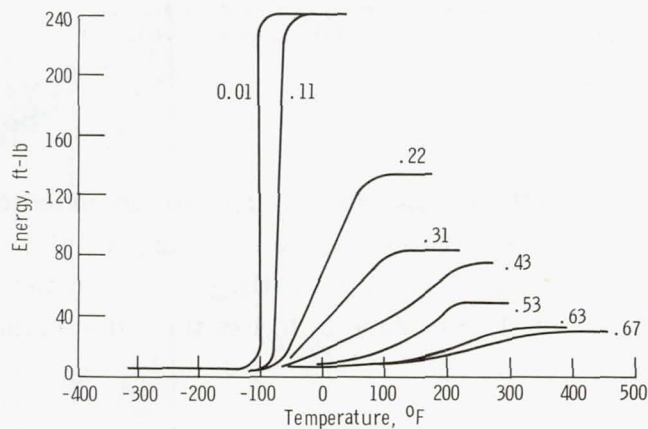


Figure 6. - Effect of carbon on shape of Charpy V transition curve (ref. 8, p. 36).

Increases in nickel content tend to decrease the transition temperature and to reduce the abrupt transition between ductile and brittle behavior (fig. 7). At high (>42 percent) nickel content, the austenite phase is completely stabilized such that no brittle transformation is possible (ref. 12, p. 58).

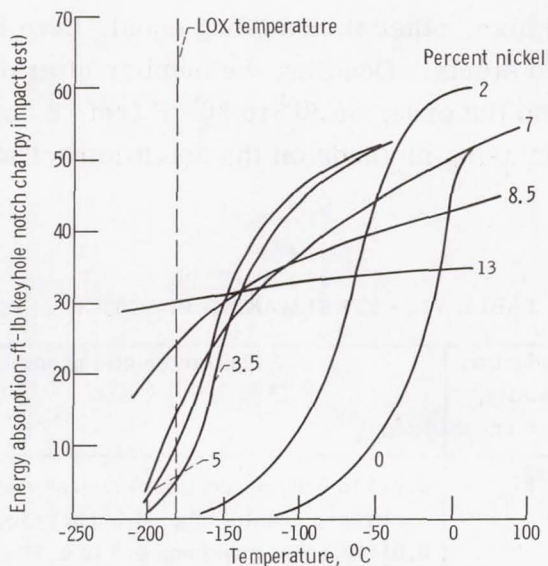


Figure 7. - Effect of nickel on impact properties of steel (ref. 13, p. 48). Source, International Nickel Company.

Table V lists the constituents that are commonly found or added during the manufacture of carbon or low alloy steel that have a significant effect on impact strength.

TABLE V. - EFFECT OF ALLOY CONSTITUENT ON IMPACT STRENGTH OF LOW ALLOY STEELS^a

Alloy	
Manganese	Lowers NDT temperature 0.75° to 1° F for every 0.01 percent increase in manganese up to 1.5 percent
Silicon	Present in killed steels in amounts of 0.15 to 0.30 percent; silicon seems to lower NDT temperature
Phosphorus	Drastically raises NDT temperature, about 7° to 13° F for each 0.01 percent of phosphorus
Nitrogen	Moderately raises NDT temperature; most evident in strained and aged material
Aluminum	Lowers NDT temperature in silicon-killed steels, especially in thick plates where problem is more critical

^aFrom information in ref. 8, pp. 36 to 39.

Specifically, the manganese-to-carbon ratio is of most important note in the selection of pressure vessel steels. The Mn/C ratios greater than 2.5 provide a steel for use down to about -20°F ; Mn/C greater than 4.5 are used down to -70°F ; and fine grained manganese, low carbon steels treated with aluminum, niobium, or vanadium for extra grain refinement can be used down to -130°F .

Steels with finer grain size, other things being equal, have lower transition temperatures than coarser grained steels. Doubling the number of grains lowers the Charpy keyhole NDT temperature on the order of 20° to 30°F (ref. 8, pp. 36 and 37).

The relevance of steelmaking methods on the notch impact strength is presented in tables VI and VII.

TABLE VI. - STEELMAKING PRACTICE^a

Method	Production quantity, percent	Characteristic product
Open hearth	87	0.025 to 0.03 percent sulfur, less than 0.006 percent nitrogen results in good impact toughness
Acid Bessimer	3	0.015 Percent nitrogen; 0.7 to 0.12 percent phosphorus results in compromised impact toughness; tube and pipe frequently fabricated from acid Bessimer stock
Electric furnace	10	Similar to open hearth except slightly higher nitrogen; therefore, slightly lower impact toughness

^aFrom information in ref. 8, pp. 33 to 35.

TABLE VII. - DEOXIDATION PRACTICE^a

Method	Characteristic product
Rimmed steel	Strong evolution of carbon monoxide takes place during freezing of ingot resulting in variable carbon content; low Mn/C ratio, relatively high oxygen, nitrogen content results in poor impact toughness
Killed steel	Silicon and/or aluminum added to completely stop carbon/oxygen reaction resulting in superior impact toughness; expensive
Semi-killed steel	Lie between rimmed and killed steels in practice and resultant impact toughness

^aFrom information in ref. 8, pp. 33 to 35.

Characteristics of Various Stainless Alloys

Reference 6 divides stainless steels into two basic types - austenitic (FeA) and martensitic (FeM). In addition, two other groups of steels, age hardening (FeAH) and nickel steels, are closely allied to stainless steels and will be discussed here. The FeA steels are the most widely used stainless steels in oxygen systems (ref. 13, pp. 39 to 42). These steels are annealed by quenching from the austenitic temperature range. Strength is improved from the annealed condition only by cold working. The FeA stainless steels with less than 18 percent nickel will partially revert to martensite when exposed to LOX temperatures, especially when the material is strained (forced to change shape) at LOX temperatures. Carbon and nitrogen tend to stabilize (prevent) this transition, but the resulting metallurgical structure will be more brittle due to the formation of compounds at the grain boundaries containing residual carbon and nitrogen. The preference (from a toughness standpoint) is to allow or sometimes encourage the formation of some martensite but not to allow sufficient carbon and nitrogen to be present to precipitate as a result of this transformation. The low carbon (designated by the suffix L) versions of the FeA steels are therefore favored for cryogenic LOX applications. Due to the many variables involved in the amount and properties of the martensite formed the subject can only be discussed qualitatively, such as is done in table VIII.

TABLE VIII. - MARTENSITE TRANSFORMATION IN AUSTENITIC STAINLESS STEEL^a

Factor	Amount	Type of stainless steel	Amount of martensite formed at LOX temperature	Nature of martensite formed	Prevailing threat or advantage
Nickel content	Low	201	Much	Could be brittle	Low toughness, dimensional change
	Medium	304	Some	Most likely ductile	Dimensional change
	High	310	None	-----	No toughness change, no dimensional change
Carbon, nitrogen content	Low	304L	Much	Tough	Acceptable toughness, dimensional change
	High	304	Some	Very brittle	Possible ^b brittle behavior
Low (LOX) temperature straining	Mild	----	Some	Tough	Acceptable toughness
	Severe	----	Much	Tough	Possible ^b brittle behavior
Room temperature straining before LOX use	Mild	----	None	-----	None
	Severe	----	Some	Tough	Minimizes brittle behavior of low nickel or high carbon alloys

^aFrom information in ref. 12, pp. 57 to 65.

^bWhen combined with other bad factors.

Some of the FeA stainless steels (most notably type 304) exhibit yield strengths that are only one-third to one-quarter of the tensile strength. To prevent permanent structural deformations, the designer must base the working stress below the yield strength. The strength to weight ratio of these FeA stainless steels is therefore compromised over the other types to be discussed. The FeM stainless steels can be quenched from the temperature at which austenite exists (1700° to 1900° F) and tempered between 400° and 1400° F to develop high (180 000 to 200 000 psi) tensile strength. These steels contain little or no nickel and 11.5 to 18 percent chromium and can be welded or cast. The most commonly used types are 410 (12Cr, low carbon) and 430 (16Cr, low carbon). While these steels are acceptable for use in gaseous oxygen systems at room temperature, the inherent martensitic structure is brittle at LOX temperatures prohibiting them from use in pressure vessel applications with LOX but making them ideal for applications (including LOX) requiring hardness and wear resistance. Carbon is added to FeM stainless steels to further enhance the characteristic of high hardness. The prime example, type 440C, is commonly used in bearings in LOX systems.

Age hardening (FeAH) stainless steels derive their strength from complex (often proprietary) combinations of strain and age hardening. Tensile strengths up to 240 000 psi can be obtained. Because of the nickel content of these steels, fire compatibility with gaseous oxygen is as good as FeA stainless steels, permitting their use therewith. However, as with FeM stainless steels, FeAH steels generally become notch sensitive at liquid oxygen temperatures, similarly curtailing their use.

Nickel steels are commonly used in LOX systems (where large amounts of material are required) to avoid the high cost of FeA stainless steels. A minimum of 9 percent nickel (ASTM-A353) is required to keep the notch toughness acceptably high at LOX temperatures. Even so, the notch toughness of 9 percent nickel steel is reduced to 50 percent of the toughness of FeA type 304 at LOX temperatures, suggesting a smaller critical flaw size for 9 percent nickel steel. ASME allowable stresses for this material (22 500 psi, $1/4$ of the yield) should therefore be respected. For applications where the ASME pressure vessel code does not apply and stresses closer to yield are necessary, 9 percent nickel steels should not be used in favor of materials with a greater notch toughness ratio at liquid oxygen temperatures. Nine percent nickel steel is not corrosion resistant. Oxide scales will form in the presence of moist or saline air. Scales of this sort can be carried as reactants by fluid flow through the system. It is therefore necessary to establish relatively tight controls on moisture and other atmospheric contaminants from the inside of 9 percent nickel oxygen vessels, even during periods of nonuse.

Types of and Specifications for Stainless Steel Alloys for Oxygen Service

Tables A-I and A-II in the appendix (ref. 6, secs. 13XX to 16XX) list the applicable specifications and special considerations governing the use of stainless steels.

ALUMINUM AND ALUMINUM ALLOYS

Aluminum and its alloys require a relatively large amount of energy to react with oxygen and are therefore considered acceptable, with basic precautions, for structural use in oxygen systems. Aluminum alloys derive their resistance to reaction in oxygen by the natural formation of a thin protective oxide surface film that protects the substrate from further oxidation. High (7500 psi) pressure of oxygen does not effect this film, but temperatures in excess of 1200⁰ F cause a loss of film coherence. A situation such as this is not inconceivable, since a rapid surface reaction could produce a molton zone at this temperature while the rest of the structure remained structurally intact at ambient temperature. Above 1200⁰ F it becomes possible to burn the metal (ref. 3, p. 12). For rapid combustion to proceed, the temperature must exceed the melting point of aluminum oxide (3700⁰ F). Sudden disruption of the film at lower temperatures such as by mechanical or chemical means permits ignition, and under these conditions the ignition point also becomes influenced by oxygen pressure. The quantitative levels of energy rate causing ignition of aluminum at various temperatures and pressures are not known, so the process of designing aluminum into an oxygen system in a fire-safe manner consists of rigidly adhering to criteria developed from use experience.

Applications and Limitations in Oxygen Systems

Aluminum and aluminum alloys are found in all phases of oxygen manufacture and use. Table IX summarizes the advantages and disadvantages of each major application.

In ground liquid oxygen systems, aluminum is used extensively for tankage, lines, pump and valve components, and heat exchangers (ref. 14, pp. 305 to 310). Aluminum is the lowest cost material suitable for use with liquid oxygen and directly competes with 9 percent nickel steel in this application.

In aerospace liquid oxygen systems, aluminum frequently becomes the primary structural material by virtue of its light weight. Figure 8 shows the application of aluminum alloys to the Saturn V, S-1C stage. The critical failure mode of such a structure is buckling; therefore, the added wall thickness permitted within the weight allowance by the low density of aluminum is beneficial (ref. 14, p. 441). However, very special

TABLE IX. - FACTORS AFFECTING USE OF ALUMINUM IN OXYGEN SYSTEMS

Application	Favorable factor	Unfavorable factor
General O ₂ use	High amount of energy required to ignite aluminum (ref. 14, p. 922)	Combustion characterized as violent (ref. 4, p. 8)
Liquid oxygen (LOX)	No brittle phase transformation at cryogenic temperatures; low cost	Coefficient of thermal expansion higher than other acceptable materials (ref. 13, p. 75)
Ground LOX systems	Light weight improves payload efficiency of ground transport (ref. 14, p. 309)	High heat extraction of aluminum increases boiloff losses (ref. 13, pp. 26 and 27)
Aerospace LOX systems	Good strength to weight ratio, ease of fabrication, especially in large construction (ref. 14, pp. 441 to 451)	Surface scales may form (due to atmospheric exposure) perhaps hindering maintenance of cleanliness; certain high-strength alloys difficult to purchase in small quantities
Oxygen heat exchangers	High thermal conductivity provides compact design (ref. 14, pp. 305 and 306)	Must be fabricated by flux-brazing; selection of alloys limited (ref. 14, pp. 305 and 306)
Gaskets	Good conductivity, nil creep or relaxation at LOX temperature	Requires higher compression to seal than non-metallic gaskets, thermal expansion characteristics usually different from surrounding structure creating possibility of leakage

- 1 Forward skirt structure, alloy 7075-T6
- 2 Gox distributor, alloys 2219-T87, T81 and T6
- 3 Oxidizer tank, alloys 2219-T87, T81 and T6
- 4 Antislosh baffles, alloys 2024-T3 and 7178-T6
- 5 Antivortex device
- 6 Cruciform baffle
- 7 Intertank structure, alloy 7075-T6
- 8 Fuel tank, alloys 2219-T87, T81 and T6
- 9 Suction line tunnels, alloy 2219-T81
- 10 Oxidizer suction lines
- 11 Fuel suction lines
- 12 Center engine support, alloys 7075-T6 and 7079-T6
- 13 Thrust column, alloy 7075-T6
- 14 Holddown post, alloy 7079-T6
- 15 Upper thrust ring, alloy 7075-T6
- 16 Lower thrust ring, alloy 7075-T6
- 17 Engine fairing, alloy 7075-T6
- 18 Fin, alloys 2024-T3 and 7075-T6
- 19 F-1 engine
- 20 Retrorockets
- 21 Gox line
- 22 Helium line
- 23 Helium bottles, alloy 2014-T6
- 24 Helium distributor
- 25 Oxidizer vent line
- 26 Instrumentation panels
- 27 Cable tunnel
- 28 Umbilical panel

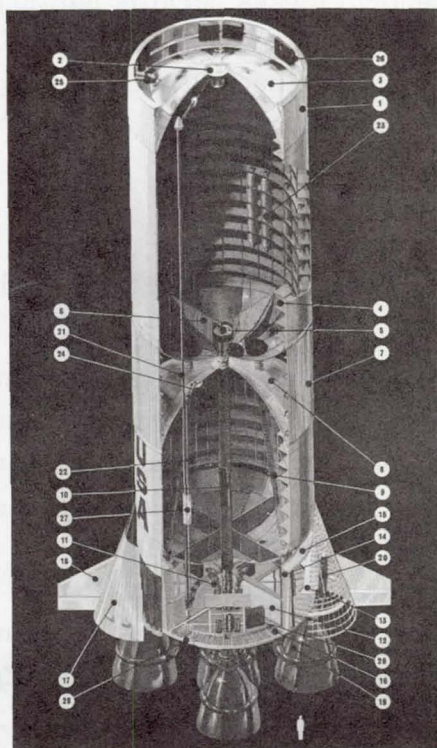


Figure 8. - Use of aluminum on S-1C stage (ref. 14, pp. 442 and 443).

treatment of aluminum is necessary in aerospace applications, especially with the 7XXX series alloys. Most of these aluminum parts are given detailed stress analysis and most are subsequently painted on exterior surfaces after assembly to counter the high susceptibility to stress corrosion when high stresses are present.

In room temperature oxygen systems, the role of aluminum is generally relegated to small component construction, because carbon or alloy steels have the advantage of either lower cost or lighter weight by virtue of their high strength. These steels cannot be used at cryogenic temperatures because of brittle phase transformation.

In elevated temperature oxygen systems, aluminum is not used because its strength deteriorates rapidly above 400° F (ref. 5, pp. 878 and 879).

In high pressure oxygen systems, the relatively low strength of aluminum necessitates a greater wall thickness, favoring the use of high strength nickel or iron base al-

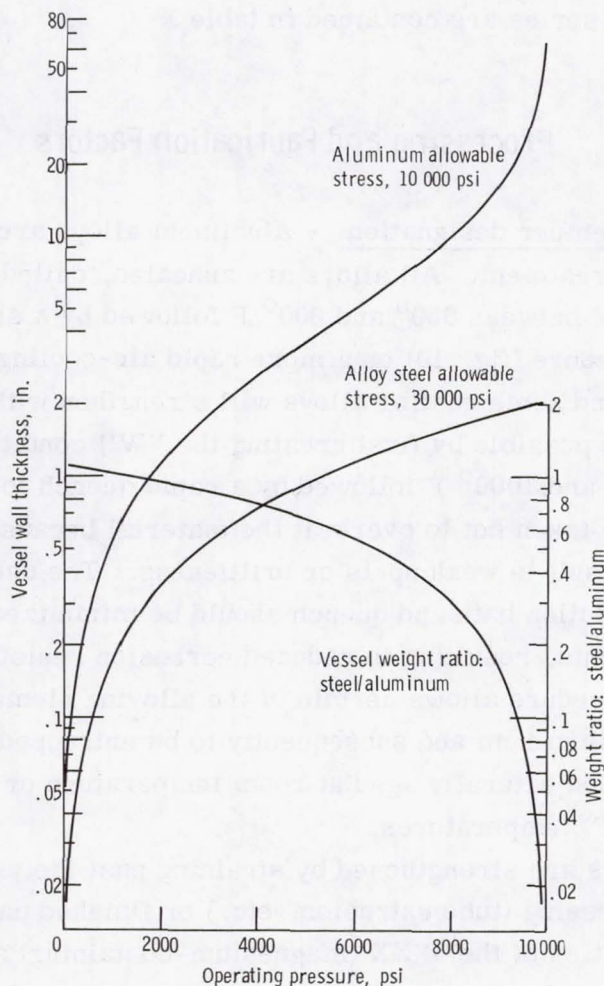


Figure 9. - Aluminum against steel for high pressure gaseous oxygen containment in a 10-inch inside diameter cylindrical vessel.

loys. This is exemplified in figure 9, based on ASME Pressure Vessel Code Requirements (ref. 11).

In situations where no practical recourse exists to avoid injury or loss of life in the event of fire, aluminum is not used because of the observed violence of combustion in concentrated oxygen (ref. 4, p. 8). Alloys of nickel or copper are somewhat more difficult to ignite, and they burn much less violently than aluminum (ref. 4, pp. 32 to 34 and ref. 15, pp. 917 to 923).

Aluminum Alloys Suitable for Oxygen Use

Subject to the factors herein, all alloys of aluminum defined by processing factors given in reference 16 and by specifications as shown in table A-III (ref. 17, pp. 162 to 164) of the appendix can be used in oxygen systems. Descriptions and attributes of various aluminum alloy series are contained in table X.

Processing and Fabrication Factors

Strengthening and temper designation. - Aluminum alloys are strengthened by strain hardening and/or heat treatment. All alloys are annealed, called the "O" condition, by heating to a temperature between 650° and 800° F followed by a slow (50° F/hr) furnace-controlled cooling procedure (fig. 10) or a more rapid air-cooling procedure. Alloys 2XXX, 6XXX, 7XXX, and some casting alloys will strengthen with age and temperature. Aging response is made possible by first creating the "W" condition which consists of heating to between 900° and 1000° F followed by a rapid quench to hold constituents in solution. Care must be taken not to overheat the material because local melting or oxide formation will either result in weak spots or brittleness. The delay between extraction of the alloy from the solution bath and quench should be minimized because of possible segregation of constituents, resulting in reduced corrosion resistance (ref. 6, secs. 32XX-33XX). This procedure allows certain of the alloying elements to enter into a solid solution with the aluminum and subsequently to be entrapped in solution during the quench. The alloy is then naturally aged at room temperature or artificially aged at elevated (250° to 400° F) temperatures.

All aluminum alloys are strengthened by straining past the yield point. This can be done during stock processing (tube extrusion, etc.) or finished part processing (die forging, etc.). The properties of the 5XXX (magnesium-containing) alloys should be stabilized by a low temperature heating cycle after strain hardening if properties changes are to be avoided over a long time at room temperature. Alloys 2XXX and 7XXX that are

TABLE X. - DESCRIPTION OF ALUMINUM ALLOYS^a

Alloy series	Composition	Strengthening methods	Factors affecting use
1XXX	99.0 to 99.6 per cent pure aluminum	Cold work only	All 1XXX are readily weldable by all methods. All are very ductile and suitable for deep forming operations. All are more tough at cryogenic temperatures than at room temperature, even after severe cold working. Annealed or partially worked stock is too soft to machine to a high surface finish. High thermal conductivity produced by low alloy content improves fire safety. Low strength curtails high performance applications.
2XXX	93 to 95 percent aluminum, balance principally copper	Cold work plus aging at room or elevated temperature	Weldability and formability decrease with increasing strength. Weldable by gas-tungsten-arc (GTA) or gas-metal-arc (GMA) methods only. Alloy 2219 has excellent weldability, medium strength, good cryogenic toughness, and excellent stress corrosion resistance, allowing its use in LOX and GOX pressure vessel applications. Alloys 2014 and 2024 progressively sacrifice the above for strength improvements. Alloy 2219 can develop weld strength equal to parent metal strength if postweld heat treatment is employed.
3XXX	98 to 99 percent aluminum, balance manganese	Cold work only	Strength slightly higher than 1XXX but considerably lower than other aluminum alloys. All have excellent cryogenic toughness. Alloy 3003 is readily brazed and has high thermal conductivity and for this reason is used extensively in heat exchangers.
5XXX	94 to 96 percent aluminum, balance principally magnesium	Cold work only	Readily welded by GTA and GMA methods. Welding reanneals the material in the heat affected zone but the as-welded strength is typically higher than other alloys. The 5XXX alloys are the most widely documented and characterized of the aluminum family. All are more tough at LOX temperature than at room temperature. Because of the above, 5XXX alloys, notably 5083 and 5456, are widely used for LOX tankage where postweld heat treatment is avoided because of difficulty or expense.
6XXX	98 to 99 percent aluminum, balance magnesium and silicon	Cold work plus aging at room or elevated temperature	Easily forged, excellent cold formability, weldable by GTA or GMA methods. Welds must be heat treated to approach the strength of 5XXX weldments. Good cryogenic toughness. Used mainly as extrusions, forgings, and small weldments such as pipe, pipe fittings, and valve bodies in LOX service. Alloy 6061 is the most documented and widely used of this group. Alloy 6063 is lower in cost and strength.
7XXX	88 to 93 percent aluminum, balance principally zinc	Cold work plus aging at room or elevated temperature	Highest strength of all aluminum alloys. The copper-free X7005, 7039, and X7106 are weldable by GTA and GMA methods; all others are not weldable. Toughness is generally reduced at cryogenic temperatures. Used in aerospace LOX systems as forged and machined components where high strength is essential and high levels of process control and inspection are possible. Unfavorable for use as LOX pressure vessels because of low toughness.
Casting alloys	-----	Age hardenable	Casting alloys with low alloy content or with silicon or magnesium silicide are well suited for LOX applications with no loss in toughness. Alloys C355 (5Si, 1.3Cu, 0.5Mg) or A356 (7Si, 0.3Mg) are ideal representations of the above. The conventional forms of these alloys, 355 and 356, contain more impurity and are relegated to conventional casting practice with no guarantee on minimum mechanical properties.

^aFrom information in ref. 6, secs. 32XX and 33XX.

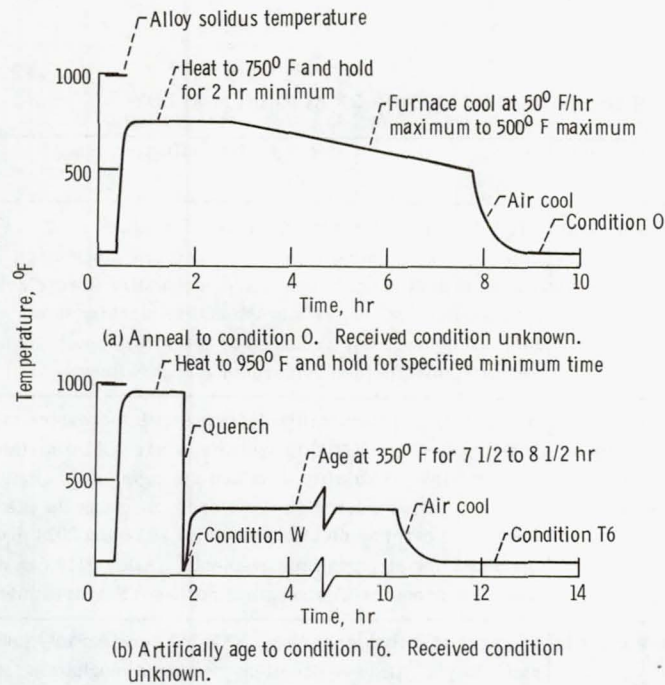


Figure 10. - Typical heat treatments for aluminum alloys.

strain hardened and aged to high strength levels should receive special processes to reduce residual stresses. These processes include (1) application of plastic strain prior to aging (called stretching), (2) initiation of strain hardening as quickly as possible after solution treatment, (3) quench using hot (180°F) water bath or spray, and (4) liquid nitrogen cool after quench followed by a steam spray. These and other special processes serve to reduce high residual stresses by localized yielding while the metal is in a ductile condition (ref. 16, pp. 371 to 381). Removal of high residual stresses reduces the threat of failure by stress corrosion or thermal shock. Tempers of aluminum are designated in accordance with table A-IV (see appendix).

Casting. - Aluminum is cast by all known practices. The selection of casting practice for oxygen system components should be in accordance with the following criteria:

(1) Alloys C355 or A356 should be used unless a particular requirement is not satisfied by this selection. These alloys have been highly characterized and widely used in the aerospace industry. These alloys are recommended because they possess excellent pressure tightness and can be used in a casting process (permanent mold) that produces smooth surface finishes.

(2) Sand and shell mold castings should be avoided in favor of die, investment, or permanent mold castings specifically because of the superior surface finish produced by the latter.

(3) Castings used for oxygen containment purposes should each be proof pressure tested with leakage rate included as a condition of acceptance.

(4) Castings should not be applied where high resistance to fatigue through cyclic loading is required.

Forging. - No restriction is placed on the forging practice; however, the designer would do well to design the forging and create controls on the forging process such that flow lines are in the direction of the major applied service load. Alloys 2024 and 7075 should be avoided except where high strength is essential. This is because of the low toughness level of these alloys and their strong properties dependency on temperature. Where 2024 and/or 7075 must be used, fracture mechanics analyses should be employed to determine critical flaw sizes, and 100 percent nondestructive inspection should be used that will detect these flaw sizes. Alloys 2219, 5052, and 5456 are preferred in that order for forging. Alloy 2014 is used extensively for forgings but its resistance to corrosion is compromised because of the residual stresses induced by forging (ref. 6, sec. 3201).

Welding. - Alloys 7075 and 7178 cannot be welded. Alloy 2024 is very difficult to weld. Most other alloys of aluminum are weldable. All internal weld areas in oxygen systems should be dressed smooth and continuous to the parent metal. Weld joints exposed to the inside of the oxygen system should be designed to facilitate dressing and weld surface inspection. Only those weld joint designs should be used that provide for full-thickness weld penetration; crevices between welds and parent surfaces in contact with oxygen due to lack of penetration can trap contamination.

Table XI shows several alloys that can be welded by all conventional processes. It

TABLE XI. - WELDING OF
ALUMINUM ALLOYS^a

Alloys	Weld filler
A356	4043
1060	1260
1100	1110
2219	2319
5052	5154
5456	5556
6061	4043

^aFrom ref. 6, secs. 32XX
and 33XX.

is suggested, however, that only GTA (gas tungsten arc), GMA (gas metal arc), or EB (electron beam) processes be used for routine oxygen system welds because (1) the possibility of introducing contaminants by the shielding media is minimized, (2) flux residues are eliminated, and (3) the soundness and surface smoothness of GTA, GMA, and EB welds are generally superior. The GMA and EB welds eliminate the possibility of tungsten inclusions. Weld soundness is better with EB and GTA processes. The EB welds may produce a sharp radius crown that requires machining off to produce smooth surface continuity. Hydrocarbons and water soluble lubricants must be controlled on the weld surfaces and the weld filler material as these contaminants are capable of destroying the favorable mechanical properties of the joint. When a weld overpass is delayed for a period of time, the cleanliness of the general weld area must be maintained. In an oily shop atmosphere this problem may require special controls. Those alloys exhibiting the highest weldability are 5456, 5052, 5083, 1100, 6061, and 2219, followed by C355, A356, 2014, and 2014 (ref. 6, secs. 31XX to 33XX).

Surface treatments. - The use of anodic films and passivation techniques offer no advantage on aluminum surfaces in contact with oxygen and are therefore not recommended. These surface treatments may, in fact, produce an undesirable effect such as rough surfaces or the introduction of less desirable metal oxides in the surface film. A bright, shiny, smooth aluminum surface, protected within its own film, is the superior surface. Surface treatments on exterior surfaces, however, are required where corrosive atmospheres are encountered and/or where the alloy of aluminum is relatively sensitive to the effects of corrosion. Zinc chromate primers are impact sensitive with oxygen and are therefore prohibited on surfaces in contact with oxygen. Because of the possibility of spray contamination, exterior surface protection consisting of zinc chromate is also prohibited in favor of anodic coatings (ref. 18, p. 71).

Design and Use Factors

Thermal conductivity. - Thermal conductivity of metals and alloys is viewed with only casual interest in most structural design applications. However, thermal conductivity in a structure in an oxygen system becomes a direct measure of the resistance of the structure to fire. The structure ignites because sudden energy from some source is momentarily supplied to the surface raising it to the ignition temperature. High thermal conductivity will lower the surface temperature and will therefore increase the resistance to ignition.

The thermal conductivity of aluminum alloys in particular can vary significantly depending on certain processing and compositional variables as shown herein. It is therefore important to use these variables to produce high thermal conductivity as well as meeting other design considerations.

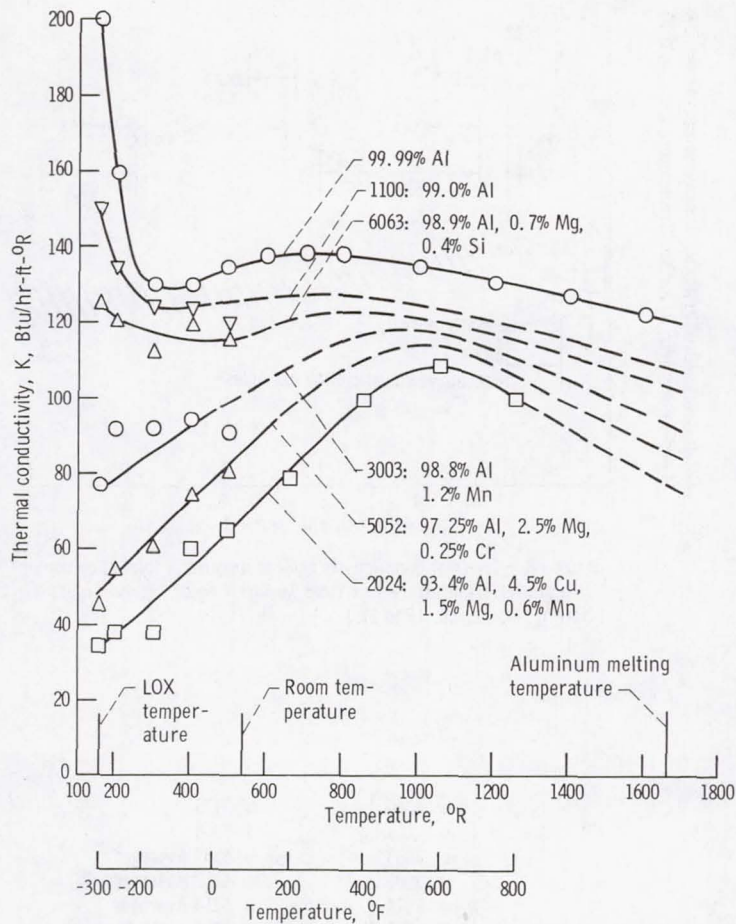


Figure 11. - Comparison of thermal conductivity of several aluminum alloys.
(From information in refs. 19, 20, and 21 (pp. 5 to 32).)

Aluminum alloy thermal conductivity decreases with increasing alloy content especially at cryogenic temperatures. This is illustrated in figure 11. The most dramatic change takes place when small amounts of alloy are introduced into pure aluminum. The change becomes very small when the alloy content increases above 7 or 8 percent (see fig. 12). Because of this, the designer should favor the 1XXX or low alloy content 6XXX aluminum alloys where possible.

Aluminum alloy thermal conductivity decreases as the alloy strength level is raised (see fig. 13). The logical reason for this is that the two strengthening mechanisms, cold work and precipitation hardening, either increase the number of grain boundaries (grain refinement) or add to the thickness of the grain boundary, both acting as barriers to the flow of heat. Because of this, the designer should specify that the alloy be strengthened no higher than the requirements of the application.

It is important to note that thermal conductivity does not alone determine the rate of

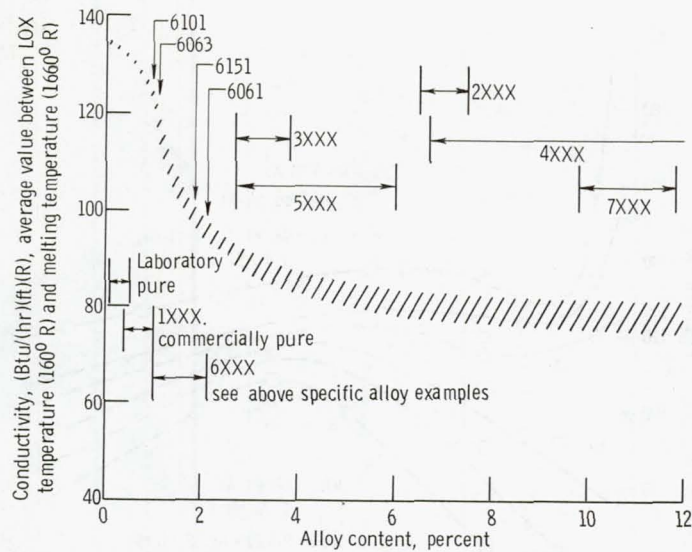


Figure 12. - Thermal conductivity against amount of total alloy constituent for aluminum alloys (cold worked + aged). (From information in ref. 22, pp. 12 to 27.)

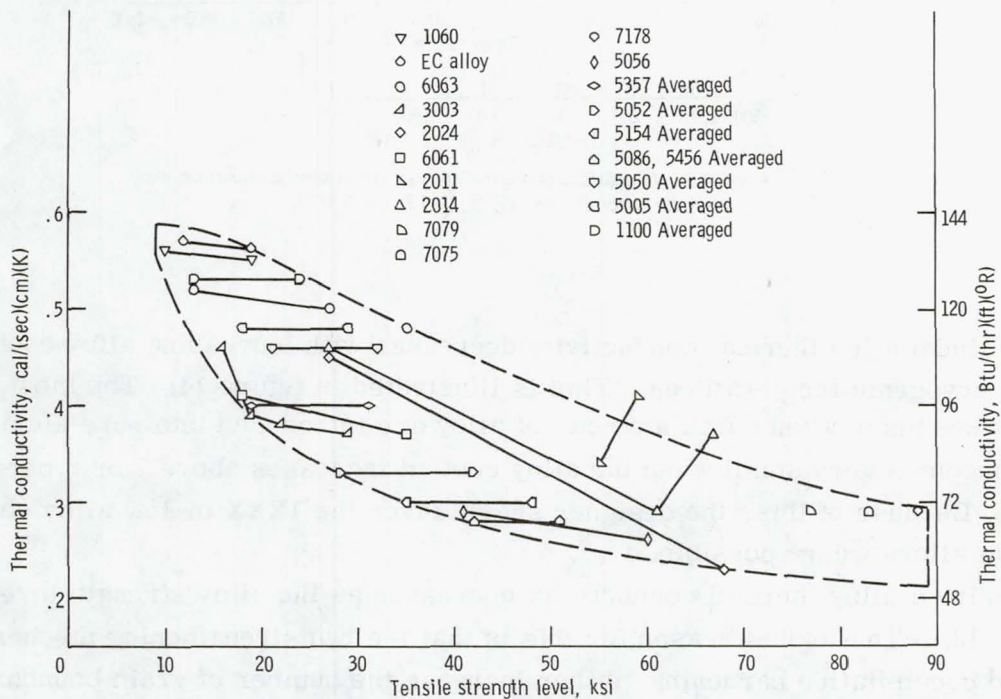


Figure 13. - Effect of strength on room temperature thermal conductivity. Alloys of aluminum strengthened by cold work and/or aging. (From information in ref. 5, pp. 935 to 958; ref. 6, sections 13XX to 16XX; and ref. 23, vol. 1, pp. 42, 43, 75, 96, 97, 176, 204, 227, 238, and 246.)

heat transfer into the metal from a surface reaction. It also depends on the metal specific heat and density. These properties, however, are not highly dependent on the alloy content or the strength level. A discussion of the combined effect of conductivity, specific heat, and density is presented in the concluding section of this report.

Metallurgical factors. - Pure aluminum has been shown not to ignite in oxygen until temperatures of 800° to 1000° C, far in excess of its melting point, are reached. Both the melting temperature and the ignition temperature will change as alloying elements are added. Noneutectic alloys that are heated through the melting range will undergo a "slush" phase wherein both liquid and solid exist simultaneously. The chemical composition of the liquid and solid may vary markedly from the composition of the base alloy (ref. 9, pp. 101 to 107). Consider the following phase diagram (fig. 14). A metal of

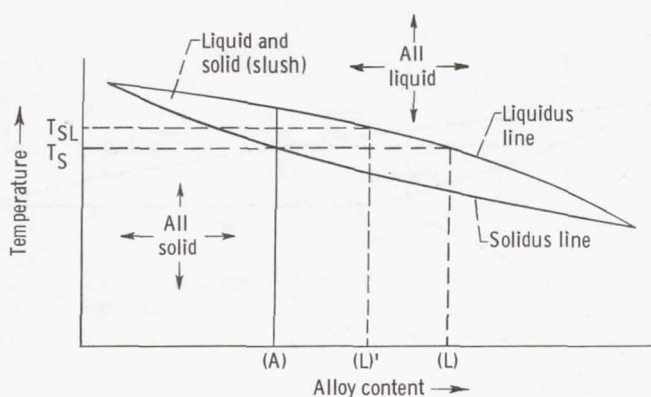


Figure 14. - Illustration of phase relations and compositions at various temperatures.

alloy content (A) is heated to the solidus temperature T_S and a minute amount of liquid is formed. The alloy content of this liquid is not (A) but is (L). Further heating of the metal to T_{SL} produces more liquid but it is now of composition (L)' (ref. 9, pp. 101 to 107). It is important to recognize that should melting of an aluminum alloy take place in an oxygen system, the first liquid to appear will be of substantially different chemical composition and therefore the ignition temperature of this first liquid may be distinctly different from the base aluminum alloy. Ignition of the first liquid will be a sufficient impetus to promote combustion of the remainder of the alloy. The presence of magnesium, for instance, in aluminum in amounts in excess of 20 or 30 percent tends to grossly lower the ignition temperature (fig. 15). The first liquid formed from alloy 5456 (5 percent Mg) will contain approximately 20 percent magnesium (fig. 16). It must be presumed that the resistance of an aluminum - 20 percent magnesium alloy to fire will be somewhat less than pure aluminum. Conversely, the first liquid obtained from aluminum-copper alloys will be enriched in copper (fig. 17) and since copper is very

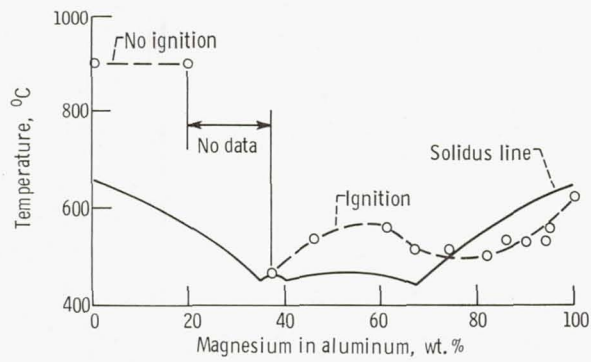


Figure 15. - Solidus line and ignition temperatures for aluminum-magnesium alloys. (From information in ref. 3, pp. A1 and A2.)

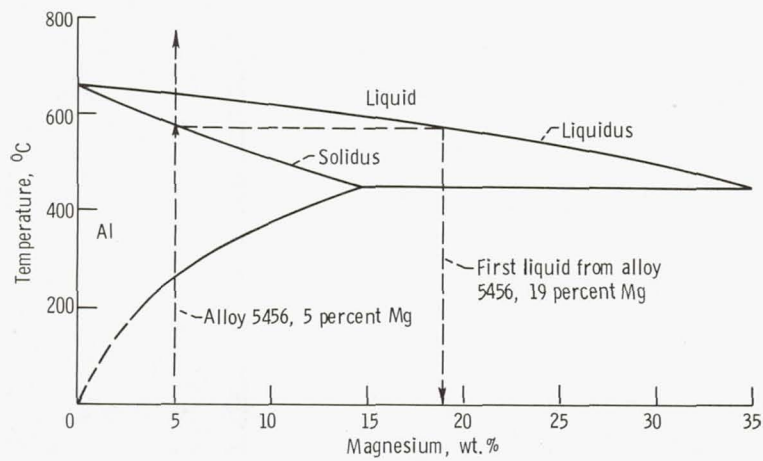


Figure 16. - Phase diagram of aluminum-magnesium system.

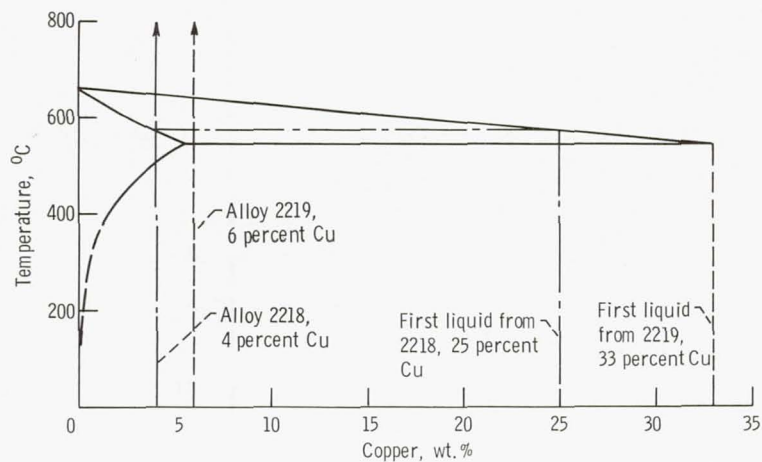


Figure 17. - Phase diagram aluminum-copper system.

reluctant to ignite in oxygen it is presumed that a copper enriched liquid alloy will be more resistant to fire than pure aluminum. More aluminum alloy phase diagrams are found in reference 24 (pp. 368 to 396).

NICKEL AND NICKEL ALLOYS

Nickel and nickel alloys form a group of metals that are, together with copper, the most resistant to ignition and combustion in oxygen except for the precious metals platinum, gold, and silver. Nickel alloys can be developed to high strengths with no significant impairment in low-temperature toughness whereas copper cannot. Nickel is characterized by its low heat of combustion and high thermal conductivity in its pure form such that combustion is self-terminating even at high (8000 psi) pure oxygen pressure (ref. 4, pp. 32 to 34). Alloying elements raise the heat of combustion (except copper) and substantially lower the thermal conductivity such that steady but slow combustion is possible. The oxide film that forms on nickel is thin but extremely protective against further oxidation, and the surface remains bright and shiny, even in relatively corrosive environments. High temperature, however, will cause the film to break down resulting in further oxidation. This effects the life of high-temperature components. Inspection for and maintenance of high levels of surface cleanliness is facilitated by this bright surface. The addition of alloying elements (typically Cu, Cr, or Mo) with nickel generally tends to depress the ignition temperature to 100⁰ to 200⁰ C below the melting temperature. However, these alloying elements also greatly improve the strength, hardness, and creep resistance of the metal, with tensile strengths of the order of 90 to 100 ksi. Small quantities of titanium and/or aluminum are added to each of the previous types of alloys to render them precipitation hardening to tensile strengths of 150 to 200 ksi.

Applications in Oxygen Systems - Code Restrictions

Most of the nickel alloys were originally developed for applications requiring strength and oxidation resistance at high temperatures such as jet engine internal components; their use in oxygen systems is a spin-off of the original intent of these developments. Nickel and its alloys are now used extensively in aerospace oxygen systems where extreme (-300⁰ to 2000⁰ F) temperature changes are regularly encountered such as rocket combustion chambers, injectors, and manifolding. Because of high strength and fire resistance, the age hardenable nickel alloys are used for lines and tanks in supercritical oxygen systems.

The high cost of nickel-base alloys generally precludes their use on ground equipment except in small amounts. Invar, the exception, is used in short tubular lengths as fire breaks in long oxygen transfer lines. Invar has the unique characteristic of almost zero thermal expansion (ref. 5, pp. 816 to 819) and is therefore used in situations where temperature-induced dimensional change cannot be tolerated.

Nickel or nickel alloys generally do not undergo a brittle phase transformation in the liquid oxygen temperature environment (ref. 12, p. 56); therefore, they are well suited for pressure-containment applications in such cases. As temperatures are lowered to cryogenic values, the smooth strength and notch strength actually improve while the impact strength remains constant or goes down just slightly. Certain alloys, namely Hastelloy X and those containing cobalt, lose impact strength at cryogenic temperatures and are therefore not well suited for LOX pressure containment applications.

Oxygen systems that are required to meet the ASME Boiler and Pressure Vessel Code (ref. 11, pp. 144 to 149) are constrained in the selection of nickel alloys to those listed in table XII. None of these alloys are precipitation hardenable and must be oper-

TABLE XII. - NICKEL ALLOYS RECOGNIZED BY
ASME BOILER AND PRESSURE VESSEL CODE

Alloy	Composition	Specified minimum tensile strength, ksi
Nickel	99 percent minimum Ni	50 to 55
Monel 400	70Ni, 30Cu	70 to 75
Inconel 600	78Ni, 15Cr, 7Fe	80 to 85
Incoloy	32Ni, 21Cr, 47Fe	65 to 75
Ni-O-Nel	42Ni, 22Cr, 36Fe	85

ated at stresses less than one quarter of ultimate. In applications outside the province of the ASME Pressure Vessel Code, precipitation hardenable alloys may readily be used provided proof testing combined with nondestructive inspection techniques are implemented. As with any high strength material, precipitation hardenable nickel alloys are less tolerant to flaws than lower strength versions. Critical flaw size calculations using fracture mechanics techniques should be made to confirm the suitability of the nondestructive test techniques to be used.

Nickel Alloys Suitable for Oxygen Use

All currently developed and commercially available nickel alloys are suitable for use in oxygen systems except where purchase specifications do not exist. References 5 (pp. 1118 to 1130) and 6 (secs. 41XX and 42XX) list those alloys and applicable specifications. A list of alloys with characteristics representative of the entire spectrum is given in table XIII.

TABLE XIII. - DESCRIPTION OF NICKEL ALLOYS^a

Alloy	Composition, percent	Strengthening methods	Factors affecting use
Nickel	99.4 Ni	Cold work	Outstanding resistance to fire; characterized as self-extinguishing in pure oxygen to 8000 psi total pressure (ref. 4, pp. 32 and 33). High thermal conductivity. Remains ductile at LOX temperature due to retention of face-centered-cubic (FCC) crystalline structure. Relatively low strength (<40 ksi) compared to other nickel alloys.
Monel 400	70Ni, 30Cu	Cold work	Outstanding resistance to fire. Fabricated by all conventional methods. Develops 140 ksi tensile strength in fully cold worked condition. Ductile at LOX temperatures.
Monel K500	67Ni, 30Cu, 3Al	Cold work plus age hardening	Same as Monel 400 except aging due to aluminum content produces strengths approaching 200 ksi. High strength causes a small but acceptable loss in ductility at LOX temperature and produces a small properties dependency on direction of cold reduction.
Inconel 600	78Ni, 15Cr, 7Fe	Cold work	Fire resistance slightly reduced, conductivity lower, otherwise similar in properties to Monel 400. Available in a wide range of wrought shapes.
Inconel 718	54Ni, 19Cr, 17Fe, 5Cb, 3Mo, 1Ti, 1Al	Cold work plus age hardening	Used as manifolds, lines, bellows, injector plates in LOX chemical rocket systems. High (>200 ksi) strength in the aged condition is typical while retention of toughness at LOX temperatures is acceptably high. Aging response is sluggish permitting welding and high temperature forming without leaving high residual stresses.
Inconel X750	73Ni, 15Cr, 7Fe, 3Ti, 1Cb, 1Al	Cold work plus age hardening	Similar to Inconel 718. Also used in supercritical oxygen service (tubing, valve bodies) in space life-support systems. Welded only in annealed condition except where service temperatures below 1000° F exist.
Hastelloy C	58Ni, 16Cr, 16Mo, 5Fe, 4W	Cold work plus age hardening	Lower strength and higher density than other age-hardenable nickel-base alloys. Used where sliding contact exists because of its good wear resistance.
Hastelloy X	48Ni, 22Cr, 18Fe, 9Mo, 2Co, 1W	Cold work	Excellent resistance to oxidation at high temperatures. Becomes decidedly brittle at LOX temperatures (impact strength, 20 ft-lb) curtailing its use in pressure vessel applications. High hardness and wear resistance allows use where sliding exists.
Invar	31 to 53Ni, Balance Fe	Cold work plus quench and temper	Used as fire breaks in oxygen lines. Very low coefficient of thermal expansion which can actually be altered to zero or negative values by controls on chemistry and processes. Used where dimensional change due to temperature change must be minimized.

^aFrom information in ref. 6, secs. 41XX and 42XX.

Fabrication

A distinct attribute of nickel alloys (especially the nonage hardenable alloys Inconel 600 and Monel 400) is that they are readily fabricated using all conventional industrial techniques for casting, forging, welding, brazing soft soldering, and machining. These techniques are applied with reduced threats that are attendant to certain other metal alloys such as stress corrosion, hot cracking, and carbide precipitation (high temperature sensitization). Heat treatment of age or precipitation-hardenable nickel alloys follows the same general procedure as with aluminum alloys. Over-heating during solution treatment will weaken or detract from the corrosion resistance of the finished product. Special considerations for particular alloys are listed in table A-V (see appendix).

Plating. - Nickel is easily plated on other metal substrates, a practice that can be used to improve the fire resistance of less-compatible metal surfaces. Electrolysis plating techniques provide the least porosity and access of oxygen to the base metal and are therefore recommended. Nickel plating cannot be used to permit an otherwise unacceptable substrate metal in an oxygen system. A complete discussion on nickel plating is contained in references 5 (p. 1114) and 25 (pp. 56 to 61).

Lubrication. - Nickel alloys, especially Hastelloy, are very resistant to sliding wear, galling, and seizure. This property makes them ideally suited for items such as valve stems, screw leads, shafts, bolts, and nuts. Lubricant should be avoided except

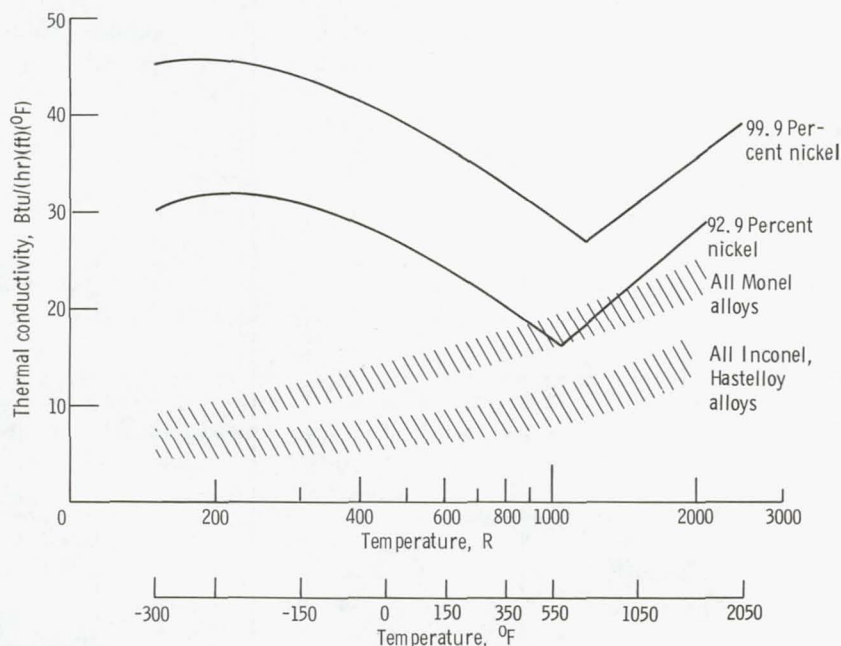


Figure 18. - Thermal conductivity of nickel and nickel alloys. (From information in ref. 5, sections 41XX and 42XX; ref. 23, vol. II, pp. 13, 14, 25, 41, 55, 81, and 144.)

where it has been shown by use to be necessary. Fully fluorinated lubricants subjected to batch testing per a specification such as MSFC-SPEC-106B should be used. Holes may be threaded directly into nickel alloys without the need for inserts.

Thermal Conductivity

The thermal conductivity of nickel is lowered by the addition of alloying elements but, unlike aluminum, the amount of cold work or heat treatment has only a small effect. Addition of copper (Monel) does not lower the thermal conductivity as much as addition of chromium or iron (Inconel, Hastelloy) (see fig. 18). Pure nickel should be favored over nickel alloys except where strength or hardness considerations dictate otherwise.

COPPER AND COPPER ALLOYS

Copper and copper alloys provide a highly compatible group of metals for use in both liquid and gaseous oxygen systems. Pure copper must be forced by a massive donor to ignite even in 7500 psi oxygen (ref. 4, pp. 32 to 34). Even then combustion is moderate and, more often than not, self-quenching. The effect of alloying elements on the ignition of copper is not known but it is presumed that ignition temperatures are lowered by virtue of the more reactive species present. Furthermore, the high thermal conductivity of pure copper is significantly lowered by the addition of alloying elements, causing the surface temperature of the alloy to rise more rapidly than that of the pure metal under conditions of identical heating.

Applications in Oxygen Systems

Copper and its alloys exist as a face-centered-cubic crystalline structure from absolute zero to several hundred degrees above room temperature providing for outstanding toughness and notch insensitivity at both liquid and gaseous oxygen temperatures. Copper and copper alloys are used in the fabrication of castings, forgings, gaskets, screw machine parts, and as low pressure tubing in virtually all phases of oxygen manufacture and use. Copper alloy castings have replaced aluminum alloy castings in certain instances, such as LOX centrifugal pump impellers to combat fires initiated by rubbing friction and wear. Further applications are limited for two reasons:

(1) Copper can be readily cold formed only in its unalloyed or annealed state where its strength is limited to 10 000 to 20 000 psi limiting its use in such applications as pressure vessels and high pressure tubing.

(2) Copper is often difficult to weld so the resort is to silver brazing techniques and sleeve joints (potential contaminant traps) or inert-gas furnace brazing techniques which limit the size of the assembly.

Moreover, copper alloys are no different from any other cold workable metal in that exposure to the solution temperature such as with brazing, welding, etc., will destroy most of the strength derived from the cold work, resulting in low joint efficiencies (ref. 5, pp. 962 and 963).

Oxygen by itself will not corrode copper, but outdoor exposure will eventually produce a characteristic green patina which could if swept away by the working fluid and become the stimulus for a reaction elsewhere within the oxygen system. It is therefore necessary to seal and protect copper-containing oxygen systems from such exposure much as with 9 percent nickel steel systems.

If mild tool rake angles are used, and the material is cold worked to greater than half-hard, copper alloys are easily machined and can be readily finished to low surface roughness values. Production of a good machine finish on annealed or low strength copper alloys is difficult.

Copper Alloys Suitable for Oxygen Use

Tables A-VI and A-VII (in the appendix) list the properties and applications of copper and copper alloys for use in oxygen systems.

Zinc contents in excess of 30 percent in copper alloys (brass) should be avoided because of the appearance of the relatively brittle beta phase. Brasses are supplied in all cold wrought forms and are commonly used in the manufacture of machined hardware suitable for LOX or GOX service such as tube fittings and parts for valves. The addition of 0.5 to 3 percent lead improves the machinability. Aluminum, tin, silicon, iron, and manganese additions to brass greatly improve the strength as a function of the amount of cold work and enhance the resistance to corrosion. This is important because excessive amounts of cold work in copper alloys will leave high enough residual stresses to cause stress corrosion cracking.

Copper-tin (bronze) alloys are generally cast, some time forged. Aluminum, manganese, silicon, and nickel are additives that increase the tensile strength. Manganese and aluminum bronzes produce high quality castings with tensile strengths of 115 000 psi with 20-percent elongation. Lead in these bronzes should not exceed 0.1 percent because of detrimental effect on toughness and strength. Bronzes are used extensively in oxygen systems where sliding contact is required such as with gears, bushings, and screw leads. Aluminum bronzes have a high fatigue limit, considerably in excess of manganese bronze or any other copper casting alloy.

Phosphor bronzes are copper-tin bearing and gear alloys with between 0.01 and 1 percent residual phosphorus which, depending on the amount, imparts high hardness to the surface. As with beryllium copper, however, these alloys are relatively brittle.

Nickel silvers are casting alloys of copper containing 17 to 20 percent zinc and 10 to 25 percent nickel plus lead and tin. Tensile strengths vary with nickel content up to 65 000 psi for the 25 percent nickel alloy. Nickel silvers are marked by exceptional corrosion resistance and notch toughness between cryogenic and room temperatures and (except for strength) approach Monel and Inconel castings in these attributes. Copper-nickel alloys (containing 10 or 30 percent nickel, balance copper) are similar in characteristics to nickel-silvers except for somewhat reduced strength and better resistance to stress corrosion cracking. Copper-nickel alloys require full stress relieving or solution annealing prior to exposure to solders or brazes, otherwise brittle alloy phases will appear due to migration of the filler metal into the base metal.

Restrictions on Heat Treatable Copper Alloys

Certain copper alloys containing small amounts of beryllium, nickel and silicon, chromium, zirconium, and nickel and phosphorus are designated as heat treatable. These coppers are cold worked and then age hardened to tensile strengths considerably higher than brasses or bronzes. The most common and highly characterized of these alloys is beryllium copper (97.85Cu, 1.90Be, 0.25Co) which can be worked and aged to tensile strengths up to 200 000 psi. Springs, bellows, diaphragms, and bushings are commonly fabricated from this material. Care must be taken in use, because the impact strength of this material is uniformly low from -400° to 300° F, approximately six times lower than nickel-based alloys (such as Inconel 718) with equivalent strengths (ref. 23, vol. II, p. 226). In critical applications where brittle failure could constitute a hazard, a material such as aged Inconel X-750 or Monel K500 should be used in lieu of aged beryllium copper.

MISCELLANEOUS METALS

Several metals, most notably magnesium, titanium, and beryllium are found in aerospace structures because of their good strength to density ratio. The ignition and combustion of titanium and magnesium in oxygen have been widely studied.

Magnesium

Magnesium can be expected to ignite between 500⁰ and 630⁰ C at low oxygen pressures, or at 300⁰ C below its melting point of 930⁰ C (ref. 3, pp. 15 and 16). Apparently the protective oxide film on magnesium loses coherency at this relatively low temperature. Magnesium is also impact sensitive in LOX. Magnesium is therefore less safe than aluminum in oxygen systems and is not recommended for use.

Titanium

Titanium (and, to the same extent, zirconium) will resist ignition to near its melting temperature of 1940⁰ C if the oxide film is not disturbed; however, sudden removal of the oxide film will cause ignition and violent combustion in room temperature and 350 psi pressure (ref. 3, pp. 6 to 12). The high heat of oxidation compounded by the very low thermal conductivity of these metals causes the near-instantaneous generation of high temperatures on the fresh surface. Combustion of titanium is not steady but marked by random violent explosions, perhaps due to failures caused by large thermal gradients due to the low thermal conductivity. These metals, or alloys containing major amounts thereof, are not safe in compressed oxygen or LOX systems where there is any possibility that the protective oxide film could be removed. Therefore, titanium and zirconium are not recommended for use.

Beryllium

The ignition temperature of beryllium in oxygen is within approximately 400⁰ C of the melting point of beryllium oxide (3000⁰ C), and is higher than the ignition temperature of aluminum (ref. 26, p. iv). However, the heat of formation of the oxide is extremely high (16 000 cal/g of beryllium compared to 7500 cal/g for aluminum) suggesting that a beryllium fire would be more energetic, therefore more hazardous, than any other fire involving a common metal of construction. In addition, beryllium metal, its oxides, and salts are highly toxic in transient concentrations higher than 25 micrograms per cubic meter of atmosphere (ref. 27, p. 76). Concentrations of this order are certainly possible in the event of a beryllium fire. For the previous reasons, beryllium should not be used in oxygen systems or near oxygen systems where it could be consumed in the event of a fire.

Gold and Platinum

The metal gold, and possible platinum, are the only metals where more energy is required to form the oxide film than is liberated by oxidation. In other words, these metals are not reactive with oxygen at room temperatures and this dissociation tendency further increases as temperature increases (ref. 3, p. i). This property allows gold and platinum to be used safely in oxygen systems where energy stimuli are high, perhaps high enough to ignite metals other than these. Electrical contacts, commutators and heater elements are some examples of these applications. The use of these metals as platings is perhaps more common than their use in bulk form. It is debatable whether plating can be relied upon for fire protection of a less compatible metal. Gold plating of electrical contacts will principally provide an oxide-free surface to facilitate electrical continuity. Loss of this plating will not only expose less compatible substrate metal, but will create oxide films, thereby increasing electrical resistance and contact temperature. If a fire would result with a loss of gold plating, solid gold substrate should be favored over gold plating.

IGNITION AND COMBUSTION OF METALS - RELATIVE COMPARISON

As with any material, the conditions necessary to enable a metal to ignite and burn involve a heat balance. If the rate of heating exceeds the rate of dissipation, the temperature will rise until either the protective oxide film fails or the metal beneath the film vaporizes and moves through the film to the oxygen resulting in combustion. The heat of formation of the oxide film contributes to the heat input and, together with the specific heat and thermal conductivity of the metal, influences the rise in temperature of the metal.

The shape, or more specifically the surface to volume ratio, of the metal influences the temperature rise due to heating. Sharp points such as burrs, metal particles, or powders do not contain much thermal capacity to prevent the generation of high temperatures. In fact, it is possible to divide a metal sample into small enough particles to cause combustion in oxygen by sudden exposure only: the heat liberated by surface oxide film formation is sufficient in itself. This is why it is important to provide smooth, continuous metal surfaces in oxygen systems and to assure that metal particles are not generated by operating wear or left in the system from fabrication processes.

It is of interest to understand how metals are relatively influenced by their properties to resist fire in oxygen. This is necessary to lend credence to the information in this report and to provide a means for appraisal of metals in oxygen where no prior experience exists. Unfortunately, an exact treatment of this subject is impossible because of the immense number of influencing factors. Attempts have been made (refs. 28

and 29) to calculate the ignition conditions for metals based on these influencing factors, but these are currently too theoretical to be of engineering value. A simplified approach is provided herein that (1) summarizes various metal ignition temperatures (as measured by test), (2) shows the metal properties that influence attainment of this temperature, and (3) lists the thermophysical properties of metals that are measures of the energy of combustion. Again, please remember that metal-oxygen fire hazards consist of (1) the ease with which the metal is ignited and (2) the violence of the fire, once ignited.

Symbols

		FPS units ¹	CGS units ¹	SI units ²
c	specific heat	Btu/(lb)(°F)	cal/(g)(°C)	J/(kg)(K)
E	heat of oxide formation	Btu/lb metal	cal/g metal	J/kg metal
F _O	heat flux	Btu/(ft ²)(hr)	cal/(cm ²)(sec)	J/(m ²)(sec)
k	thermal conductivity	Btu/(hr)(ft)(°F)	cal/(sec)(cm)(°C)	J/(sec)(m)(K)
Q	heat of oxide formation		cal/g mol	J/kg mol
S	allowable working stress	psi or ksi	-----	kg/m ²
T	surface temperature	°F	°C	K
T _{ign}	ignition temperature	°F	°C	K
t	time			
ρ	density	lb/ft ³	g/cm ³	kg/m ³

Influence of Metal Properties and Ignition Temperature

Relative energy rate to ignite. - Carslaw and Jaeger (ref. 30, p. 56) give the relation which describes the surface temperature of a semi-infinite solid subject to a given heat flux:

$$T = 2F_o \sqrt{\frac{t}{\pi k \rho c}} \quad (1)$$

¹These units are typically given in the references and are therefore repeated in this report.

²These units are used in the original analysis of this report.

When rearranging terms it can be seen that

$$F_o \sqrt{t} \propto T \sqrt{k\rho c} \quad (2)$$

If the flux F_o exists for a fixed time t (analogous to situations involving different metals subject to identical amounts of heating) and the ignition temperature T_{ign} is substituted for T , the relative resistance of the metal to ignition will be proportional to

$$T_{\text{ign}} \sqrt{k\rho c} \quad (3)$$

Thus, metals with high values for T_{ign} , k , ρ , and c are more resistant to ignition than metals with low values of same. It must be noted that the previous does not consider the following:

(1) The physical boundaries of the metal object other than the flat surface receiving the heat flux are not considered. This is acceptable if the duration of heating is short or the object is massive. If not, three-dimensional, nonsteady heat conduction models must be resorted to such as given in reference 31 (pp. 331 to 436).

(2) The effect of surface (oxidation) reactions prior to ignition are not considered. If this precision is desired, techniques such as provided by reference 28 must be implemented.

Energy of combustion. - The heat of oxide formation such as is listed in reference 3 (p. 17) for various metals is also a relative measure of the heat liberated during combustion of the metal. The heats of formation Q are given in reference 3 in units of calories per gram mole of oxide. To convert these to E , the calories per gram of metal consumed (by fire) divide Q by the metal atomic weight times the number of metal atoms in the oxide molecule. For example, for aluminum, the oxide is Al_2O_3 , Q is 1.68×10^9 joules per kilogram-mole, and the atomic weight is 26.98. Therefore, the heat liberated in an aluminum fire E is

$$E = \frac{1.68 \times 10^9}{2 \times 26.98} = 3.11 \times 10^7 \text{ J/kg metal} \quad (4)$$

The previous is useful when comparing the potential fire severity of various metals comprising an equal weight structure. If various metals comprising an equal volume structure are to be compared, the value of E is multiplied by the metal density. For aluminum,

$$\begin{aligned}
 E\rho &= 3.11 \times 10^7 \text{ J/kg metal} \times 2700 \text{ kg/m}^3 \\
 &= 8.39 \times 10^{10} \text{ J/m}^3 \text{ metal}
 \end{aligned}
 \tag{5}$$

If various metals comprising an equal strength structure are to be compared (perhaps the most realistic comparison), the value $E\rho$ is divided by S , the allowable working stress of the metal. For aluminum (assuming $S = 7 \times 10^5 \text{ kg/m}^2$)

$$\frac{E\rho}{S} = \frac{8.39 \times 10^{10}}{7 \times 10^5} = 1.20 \times 10^5 \frac{\text{J}}{(\text{kg})(\text{m})}
 \tag{6}$$

Thus, low strength metals can liberate more heat in a fire because more metal is necessary to provide the strength.

Summary comparison of various metals from the standpoints mentioned previously. - Table XIV lists the thermal and physical properties for several metals. Aluminum, steel, copper, and nickel are commonly used in oxygen systems and are discussed in this report. The metals magnesium, titanium, and silver are also included in this table for illustrative purposes. In the table, densities and specific heats are center values, and thermal conductivities are ranges based on the ranges of common alloy compositions and operating temperatures. Magnesium is known to ignite quite easily and burn quite energetically in oxygen. Titanium is a recognized ignition hazard in oxygen (see Miscellaneous Metals section). Conversely, silver is recognized as being superior in its resistance to fire in oxygen (ref. 4, p. 33), but it is too expensive for routine component fabrication. Figures 19 to 22 show the results of the previous calculations for the seven metals listed in table XIV. The following is apparent from examination of these figures:

(1) Figure 19: Aluminum is more difficult to ignite than steel. Copper and nickel are very difficult to ignite. Titanium is very easy to ignite. Silver is extremely difficult to ignite.

(2) Figures 20 to 22: Aluminum, magnesium, and titanium burn very energetically. Steel, copper, and nickel burn less energetically than aluminum. Silver burns the least energetically.

TABLE XIV. - SUMMARY OF THERMAL AND PHYSICAL PROPERTIES FOR SEVERAL METALS

Metal	Heat of oxide for- mation, Q , J/kg mol	Metal atomic weight	Number of metal atoms in oxide molecule	Density, kg/m^3	Specific heat, c , J/(kg)(K)	Thermal con- ductivity range, k , J/(sec)(m)(K)	Minimum ob- served ignition temperature, T_{ign} , K	Allowable work- ing stress range, S , kg/m^2
Aluminum	168.0×10^7	26.98	2	2.70×10^3	938	104 to 243	920	0.14 to 1.0×10^6
Steel	26.6	55.85	1	7.87	503	12 to 42	1200	.70 to 1.8
Copper	17.5	63.54	2	8.96	385	104 to 390	1350	.21 to 1.5
Nickel	24.0	58.69	1	8.90	469	17 to 67	1720	.56 to 2.0
Magnesium	60.2	24.32	1	1.74	1026	71 to 109	880	.21 to 0.7
Titanium	94.5	47.90	1	4.50	578	4 to 17	1100	.56 to 1.1
Silver	3.01	107.90	2	10.49	234	209 to 419	could not ignite	.42 to 0.7

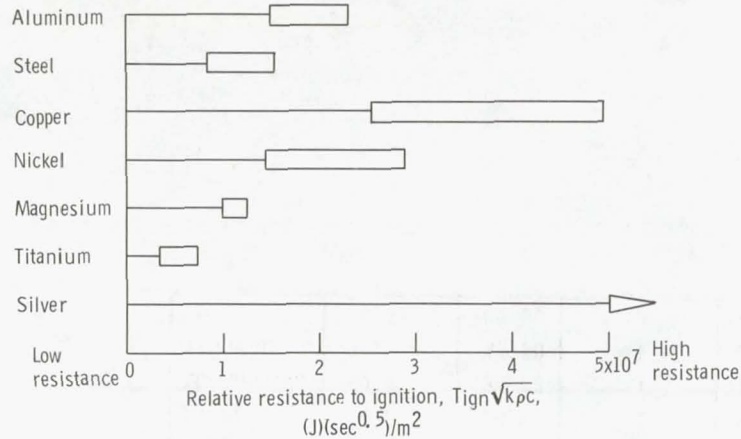


Figure 19. - Relative resistance to ignition.

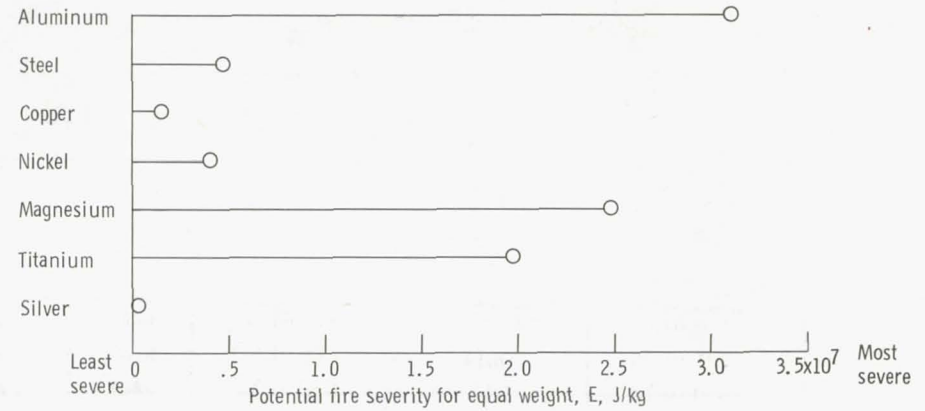


Figure 20. - Potential fire severity for equal weight (comparison of components of equal weight but made of different materials).

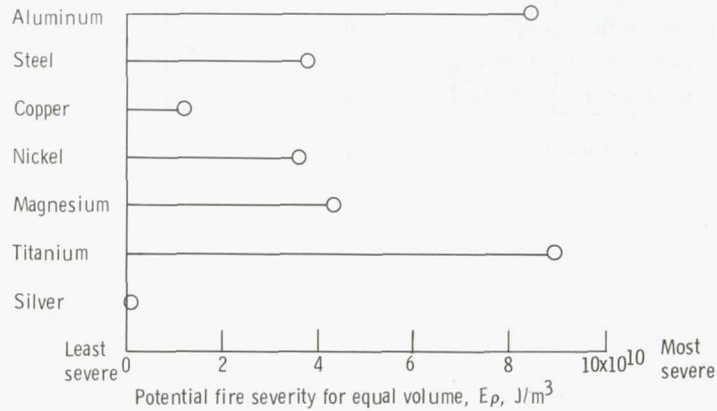


Figure 21. - Potential fire severity for equal volume (comparison of components of equal volume but made of different metals).

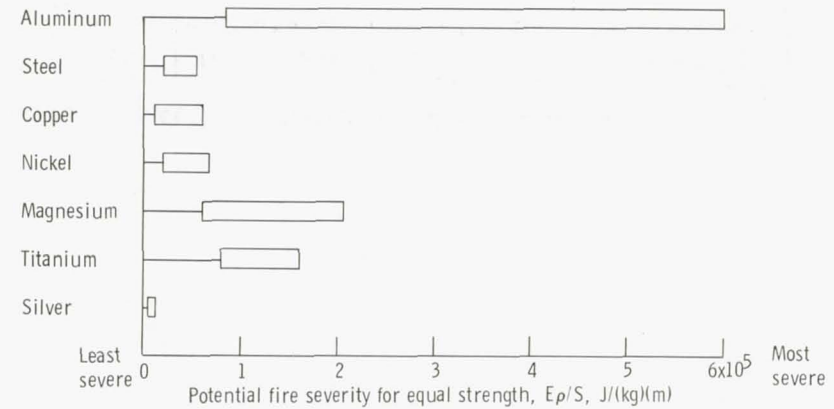


Figure 22. - Potential fire severity for equal strength (comparison of components of equal strength but made of different materials).

APPENDIX - TABLES OF SPECIFICATIONS, USES, AND SPECIAL CONSIDERATIONS FOR METALS AND ALLOYS IN OXYGEN SYSTEMS

TABLE A-I. - CORRELATION OF SPECIFICATIONS FOR STAINLESS STEELS^a

Wrought alloys			Cast alloys		
AISI	SAE	ASTM	SAE	ACI	ASTM
Martensitic					
403	51403	Plate, sheet, strip: A176 Bars, billets: A276	-----	-----	-----
410	51410	Plate, sheet, strip: A176, A240 Bars, billets: A276 Pipe, tube: A268	60410	CA-15	A296
414	51414	Bars, billets: A276	-----	-----	-----
416,	51416,	Bars, billets: A276	-----	-----	-----
416Se	51416Se				
420	51420	Bars, billets: A276	60420	CA-40	-----
431	51431	Bars, billets: A276	-----	-----	-----
440A, 440B, 440C	-----	Bars, billets: A276	-----	-----	A296
Ferritic					
405	51405	Plate, sheet, strip: A240 Bars, billets: A276 Pipe, tube: A268	-----	-----	A351
430, 430F, 430SeF	51430, 51430F, 51430SeF	Plate, sheet, strip: A176, A240 Bars, billets: A276 Pipe, tube: A268	-----	-----	-----
442	51442	Plate, sheet, strip: A176 Bars, billets: A276 Pipe, tube: A268	60442	CB-30	A296
446	51446	Plate, sheet, strip: A176 Bars, billets: A276 Pipe, tube: A268	70446	HC	A297
Austenitic					
301	30301	Plate, sheet, strip: A167, A264 (clad)	-----	-----	-----
302	30302	Plate, sheet, strip: A167, A240, A264 (clad) Bars, billets: A276, A314	-----	CF-20	A296
302B	30302B	Plate, sheet, strip: A167 Bars, billets: A276, A314	-----	HF	A297
303, 303Se	30303, 30303Se	Bars, billets: A276, A314 Nuts, bolts: A194, A320	-----	CF-16F	A296
304, 304L	30304, 30304L	Plate, sheet, strip: A167, A177, A240, A264 Bars, billets: A276, A314 Pipe, tube: A213, A249, A269, A270, A271, A312, A358, A376 Nuts, bolts: A193, A194, A320 Forgings, fittings: A182, A336	60304, 60304L	CF-8, CF-3	A296, A351
305	30305	Plate, sheet, strip: A240 Bars, billets: A314 Pipe, tube: A249	-----	-----	-----

^aFrom information in ref. 7, p. 6.

TABLE A-I. - Concluded. CORRELATION OF SPECIFICATIONS FOR STAINLESS STEELS^a

Wrought alloys			Cast alloys		
AISI	SAE	ASTM	SAE	ACI	ASTM
Austenitic					
308	30308	Plate, sheet, strip: A167, A264 Bars, billets: A276, A314 Welding electrodes: A298	-----	-----	-----
309, 309S	30309, 30309S	Plate, sheet, strip: A167, A240, A264 Bars, billets: A276, A314 Pipe, tube: A249, A312, A358 Welding electrodes: A298	60309, 70309	CH-20, HH	A296, A297, A351
310, 310S	30310, 30310S	Plate, sheet, strip: A167, A240, A264 Bars, billets: A276, A314 Pipe, tube: A213, A249, A312, A358 Forgings, fittings: A182, A336 Welding electrodes: A298	60310, 70310	CK-20, HK	A296, A297, A351
314	30314	Bars, billets: A314	-----	-----	-----
316, 316L	30316, 30316L	Plate, sheet, strip: A167, A240, A264 Bars, billets: A276, A314 Pipe, tube: A213, A249, A269, A312, A358, A376 Nuts, bolts: A193 Forgings, fittings: A182, 336 Welding electrodes: A298	60316, 60316L	CF-3M, CF-8M, CF-12M	A296 A351
317	30317	Plate, sheet, strip: A240 Bars, billets: A314 Pipe, tube: A249, A269, A312 Welding electrodes: A298	60317	CG-8M	A296
321	30321	Plate, sheet, strip: A167, A240, A264 Bars, billets: A276, A314 Pipe, tube: A213, A249, A269, A271, A312, A358, A376 Nuts, bolts: A193, A194, A320 Forgings, fittings: A182, A336	-----	-----	-----
347	30347	Plate, sheet, strip: A167, A240, A264 Bars, billets: A276, A314 Pipe, tube: A213, A249, A269, A271, A298, A358, A376 Nuts, bolts: A193, A194, A320 Forgings, fittings: A182, A336 Welding electrodes: A298	60347	CF-8C	A296, A351
348	30348	Plate, sheet, strip: A240 Bars, billets: A276, A314 Pipe, tube: A213, A249, A269, A358, A376 Nuts, bolts: A320	-----	-----	-----

^aFrom information in ref. 7, p. 6.

TABLE A-II. - SPECIAL CONSIDERATIONS FOR STAINLESS STEEL ALLOYS^a

(a) FeA steels

Steel	Special considerations
Types 301, 302: Fe 18 Cr 8 Ni	<p>The effect of cold work on the properties of these steels, particularly of type 301, depends to a considerable extent on the content of nickel, carbon, and possibly other elements, as well as on not well recognized processing conditions, such as speed and temperature of rolling. Materials can be obtained for special requirements to closer composition on limits than those listed in specifications in order to secure higher uniformity in properties or performance on fabrication.</p> <p>Cold rolled sheet in these alloys exhibits a very pronounced directionality. While the tensile strength and tensile yield strengths are nearly the same in both directions, the compressive yield strength and compressive stress strain curves are much higher in the transverse than in the longitudinal direction. This condition is only partly improved by stress relief.</p> <p>Small amount of cold work during straightening and handling can raise considerably the low yield strength of annealed material. Heating for long times at 800° F and short times at 1600° F or slow cooling through this range must be avoided. Carburizing conditions at high temperature reduce corrosion resistance. Adhering zinc and lead particles which lead to embrittlement at elevated temperatures must be removed prior to heating.</p>
Types 304, 304L: Fe Low C 19 Cr 10 Ni	Intergranular corrosion after welding or heating may occur in type 304, but usually not in type 304L.
19-9 DL 8, 19-9 DX: Fe 20 Cr 10 Ni 1.5 Mo 1.5 W	<p>Alloy is susceptible to stress cracking after forming unless stress relieved or annealed. Heat at temperatures in the vicinity of 1100° to 1200° F sensitizes the alloy (i. e., develops susceptibility to intergranular attack).</p> <p>Alloy may crack after cold work or welding unless annealed or stress relieved.</p>
Types 310, 310S: Fe 24 Cr 20 Ni	<p>Intergranular carbide precipitation can occur after prolonged heating in the range between 800° and 1600° F, on slow cooling through this range. The tendency to carbide precipitation will be reduced by lowering the carbon content (as in 310S) and this grade is preferred for welding or when the service condition could promote carbide precipitation. Sigma formation can occur during prolonged heating in the temperature range between 1200° and 1800° F. The tendency to form sigma will be increased by cold work. The amount of sigma formed in this alloy is much less than in silicon containing grades such as 312.</p> <p>The alloy is free from LOX temperature strain induced phase changes which can produce embrittlement in the lower nickel grades (e. g., 301 and 302). The crack propagation resistance at cryogenic temperatures is excellent in longitudinal direction even for heavily cold worked material. However, such material is characterized by a pronounced mechanical anisotropy and the crack propagation resistance is considerably lower in the transverse than in the longitudinal direction.</p>
Type 314: Fe 25 Cr 20 Ni 2 Si	<p>Prolonged exposure at 1200° to 1600° F may cause embrittlement through carbide precipitation and sigma phase formation. Ductility may be restored by annealing at 1900° to 1950° F for 10 to 60 minutes. This treatment is recommended after a 1000-hour exposure at 1400° to 1600° F.</p>
Types 316, 317: Fe 18 Cr 13 Ni + Mo	<p>Prolonged heating at temperatures from 800° to 1600° F may result in embrittlement and stress corrosion sensitivity. Because of its reduced stress corrosion sensitivity, type 316L is recommended when heavy cross sections cannot be annealed after welding or where low temperature stress relieving is desired.</p>
Type 321: Fe 18 Cr 10 Ni + Ti	<p>Heating above 1900° F followed by heating about 1200° F may sensitize this steel.</p> <p>Use type 347 welding wire for shielded-metal-arc welding type 321 to prevent loss of stabilization.</p> <p>Cold work greatly reduces the deep ductility at 1100° and 1200° F, particularly if grain size is less than 5. Annealing is recommended to restore the ductility.</p>

^aFrom information in ref. 6, secs. 13XX to 16XX.

TABLE A-II. - Continued. SPECIAL CONSIDERATIONS FOR STAINLESS STEEL ALLOYS^a

(b) FeM steels

Steel	Special considerations
Types 403, 410, 416: Fe Low C 12 Cr	Avoid tempering at 550 ⁰ to 1050 ⁰ F because of reduced resistance to stress corrosion and increased notch sensitivity. Corrosion resistance of type 410 castings may not be satisfactory for many applications. Casting quality should be evaluated by penetrant inspection rather than by magnetic inspection, because of inconsistency of the latter method. Type 416 castings are primarily used for small parts at temperatures up to 1000 ⁰ F. Corrosion resistance is lower than that of type 410 castings but machinability is better. The proper chemical balance is necessary in types 403 and 410 to ensure against the formation of free or delta ferrite which can affect the mechanical properties, especially hardness and toughness. The hardness decreases with an increase in the free ferrite content while the toughness as measured by impact strength increases for longitudinal tests but decreases for transverse tests. These effects on impact strength are due to the mechanical fibering associated with the presence of free ferrite and their magnitude will depend on both the amount of ferrite present and the degree of work in the structure.
Type 420: Fe Med C 13 Cr	See also type 410. Stress corrosion may occur if the steel is exposed at 700 ⁰ to 800 ⁰ F. It should not be used for heavily stressed parts that will operate at subzero temperatures.
Type 422: Fe 12 Cr 1 Mo 1 W 0.8 Ni 0.25 V	See type 420.
Type 431: Fe 0.2 C 16 Cr 2 Ni	The composition of this steel is such that difficulties are sometimes encountered in obtaining the expected mechanical properties. The high chromium content tends to keep the structure ferritic during austenitizing. This tendency is overcome by the addition of nickel which tends to promote austenite formation. However, the composition limits are rather broad, and significant variations in response to heat treatment and mechanical properties can be expected within the normal ranges of chemistry. If the chromium is high and the nickel low, the quenched steel may contain ferrite and not develop full strength. If the chromium is low and the nickel high, retained austenite may be a problem and subcooling after quenching will be required. In such cases it is recommended to refrigerate rather than water quench to avoid potential cracking. Carbon contents on the high side tend to increase tensile strength but lower the corrosion resistance. Castings are available in more than one range of carbon contents. Stress relief or tempering in the range between 700 ⁰ to 1100 ⁰ F is not recommended since embrittlement in this range may be encountered. Hydrogen embrittlement may be a problem with this steel at high hardness and strength levels.
Type 440A, B, and C: Fe High C 17 Cr 0.5 Mo	Cracking may occur on heating, cooling, pickling or after welding. Steels are particularly subject to decarburization because of high carbon content.
USS-12 MoV: Fe 12 Cr 1 Mo 0.65 Ni 0.3 V	See types 410 and 420. This material is susceptible to stress-corrosion cracking when stressed and simultaneously exposed to some corrosive environment.

^aFrom information in ref. 6, secs. 13XX to 16XX.

TABLE A-II. - Continued. SPECIAL CONSIDERATIONS FOR STAINLESS STEEL ALLOYS^a

(c) FeAH steels

Shell	Special considerations
17-4 PH: Fe 17 Cr 4 Ni 4 Cu	No special precautions are necessary for this alloy except the need for cleanliness as for any stainless steel. The alloy also has a wide allowance in compositional range.
17-7 PH: Fe 17 Cr 7 Ni 1 Al	<p>The crack propagation resistance as measured by the sharp notch strength exhibits a pronounced minimum at aging temperature between 900° and 1050° F. This is the region of aging temperature producing the highest strength and having the greatest commercial interest. Very high toughness at considerable sacrifice in strength can be obtained by over-aging at temperatures of 1100° F and above. The impact strength of all heat treated conditions of this alloy decrease at subzero temperatures. At a given low test temperature the impact strength increases with aging temperature but at cryogenic temperatures only the overaged relatively low strength conditions exhibit a useful degree of toughness. Poor crack propagation resistance at subzero temperatures is indicated by K_{IC} values ranging from about 40 to 50 ksi-in.^{1/2} at -50° F.</p> <p>The room temperature tensile strength of the heat treated conditions increases with exposure to temperatures between about 600° to 900° F. Tensile tests at elevated temperatures show the same effects of exposure. It might be expected that this increase in strength would be accompanied by a decrease in crack propagation resistance. Such an embrittling effect is noted for PH14-8Mo.</p> <p>The crack propagation resistance is lower in the transverse than in the longitudinal direction. Cold work following heat treatment to condition A and subsequent to aging can produce large reductions in tensile properties as compared with those that would be obtained in the absence of the cold work. Dimensional changes during heat treatment require special consideration. There is a volume contraction on hardening.</p>
PH15-7Mo: Fe 15 Cr 7 Ni 2.5 Mo	<p>Alloy is available in numerous forms, but the primary usage is in the sheet and strip form. In common with the general class of precipitation hardening stainless steels, this alloy is unstable during exposure to temperatures exceeding about 500° F. This instability is reflected in an increase in the yield strength and a decrease in fracture toughness. The transverse direction has lower toughness than the longitudinal direction.</p> <p>Dimensional changes during heat treating to conditions TH 1050 or RH 950 need consideration and special provisions must be made for machining and tooling. Thorough cleaning prior to thermal treatments is recommended in order to avoid carburization and to minimize difficulties when descaling.</p>
AM 350: Fe 17 Cr 4 Ni 3 Mo	<p>Heating to temperature above those specified for condition H should be avoided because of excessive delta ferrite formation and loss of response to hardening.</p> <p>Annealing of heavy bar and forging to condition H may result in loss of response to heat treating.</p> <p>Forging of heavy sections should be finished at about 1750° F to ensure adequate response to heat treating.</p> <p>CRT (cold-rolled, tempered condition alloy) has optimum stress corrosion resistance. SCT (subcooled, tempered condition alloy) requires either a minimum of 10 percent delta ferrite or a 1000° F temper for optimum stress corrosion resistance.</p>
AM 355: Fe 15.5 Cr 4.5 Ni 3 Mo	Heating to temperatures above those specified for condition H (anneal) should be avoided because of grain coarsening and loss of response to hardening. AM 355, when hardened by the carbide solution subzero treatment, has stress corrosion resistance superior to that of AM 350 in the SCT (850) condition and comparable to that of AM 350 in the SCT (1000) condition.
PH14-8Mo: Fe 14 Cr 8 Ni 2.5 Mo Al	<p>When PH14-8Mo is fabricated in condition A (anneal), and subsequently heat treated, an allowance should be made for the dimensional change (an overall expansion of approximately 0.004 in./in.) that occurs during heat treatment. Thorough cleaning prior to thermal treatments is recommended in order to avoid carburization and to minimize difficulties when descaling.</p> <p>This alloy exhibits a metallurgical instability which is manifest as an increase in the tensile yield strength and decrease in the static crack propagation resistance when cracked or sharply notched specimens are exposed for long periods of time at moderately elevated temperatures and then tested at the exposure temperature or at a lower temperature. These instability effects are not reduced by vacuum melting and appear to be larger the higher the strength level of the material. There is insufficient data to establish the time-</p>

^aFrom information in ref. 6, secs. 13XX to 16XX.

TABLE A-II. Continued. SPECIAL CONSIDERATIONS FOR STAINLESS STEEL ALLOYS^a

(c) Continued. FeAH steels

Steel	Special considerations
<p>AF 71:</p> <p>Fe</p> <p>18 Mn</p> <p>12 Cr</p> <p>3 Mo</p> <p>+ V</p> <p>+ B</p>	<p>temperature relation for the effect of the instability on the mechanical properties; however, it would appear that exposure at temperatures below about 400° F produces negligible embrittlement. In general, the longitudinal direction of sheet has a higher toughness than the transverse direction. However, this directionality is reduced by vacuum melting. The alloy has poor fracture toughness below about -200° F and should not be used at cryogenic temperatures.</p> <p>The high quenching temperature of 2050° F has been considered by some consumers to be objectionable in the processing of material in thin gages because of the excessive thickness loss incurred in scaling and pickling. To avoid such losses expensive heat treating equipment (vacuum furnaces or controlled-atmosphere furnaces) are required.</p>
<p>PH13-8Mo:</p> <p>Fe</p> <p>13 Cr</p> <p>8 Ni</p> <p>2 Mo</p>	<p>The fracture toughness of this alloy is good in heavy sections at room temperature and above but decreases rapidly at temperatures below about 0° F. Heavy sections appear to exhibit negligible directionality of tensile properties. Insufficient data are available to define the directionality of fracture toughness; however, limited information indicates that it is probably small. In common with other alloys of this class the impact strength and presumably the fracture toughness decrease as a result of long time exposure to moderately elevated temperature. It should be noted that nearly all information available for this chapter relates to the double vacuum melted product. Lower toughness and greater directionality can be expected of air-melted material.</p>
<p>AFC 77:</p> <p>Fe</p> <p>0.15 C</p> <p>14.5 Cr</p> <p>13.5 Co</p> <p>5 Mo</p> <p>0.5 V</p> <p>0.05 N₂</p>	<p>This alloy is subject to a severe embrittlement when tempered above about 700° F. The tempering temperature range over which this embrittlement occurs is much more extensive than in other FeM stainless steels and extends to nearly 1400° F. No substantial recovery in the embrittlement is noted for 1200° F tempering even though this temperature is well beyond the secondary hardening peak. Cold rolling preceding tempering in the brittle range can substantially increase the strength but also increases the embrittlement. The alloy is not stable during elevated temperature exposure and long time exposures to moderately elevated temperatures can substantially increase the embrittlement. As might be expected, the low temperature crack and notch strength are very poor for conditions tempered in the brittle range.</p> <p>If tempering is confined to temperatures below about 700° F, the yield strength is below about 170 ksi and the room temperature fracture toughness is high. No valid values of K_{Ic} are available for these tempered conditions. It would be expected that the low tempered conditions would not be stable during elevated temperature exposure, and that a time temperature dependent embrittlement would develop.</p>
<p>AM 362:</p> <p>Fe</p> <p>15 Cr</p> <p>7 Ni</p> <p>Ti</p>	<p>This alloy like the conventional 12Cr steels is subject to an embrittlement when held for long times at temperatures between 700° and 1000° F. This is also reflected in low impact strength for tempering temperatures below about 1000° F. The toughness of the alloy is strongly influenced by the titanium content and decreases with increasing titanium.</p>
<p>15-5 PH:</p> <p>Fe</p> <p>15 Cr</p> <p>5 Ni</p> <p>4 Cu</p>	<p>Precipitation-hardening stainless steel alloys are used in many applications requiring large and medium size sections. In many cases, loading transverse to the fiber is involved. It has been demonstrated that certain structural characteristics, particularly delta ferrite and some precipitates, cause substantial reductions in transverse ductility, and presumably fracture toughness, for many of these alloys. For compositions in which delta ferrite is present, vacuum remelting does not improve this situation.</p> <p>15-5 PH is a delta ferrite-free compositional modification of 17-4 PH alloy containing less chromium and slightly higher nickel. Its short-transverse ductility at edge and intermediate locations is superior to 17-4 PH in heavy sections. However, in products made from air-cast ingots of 15-5 PH, the short transverse ductility at the center location may be lower than at edge or intermediate locations. This nonuniformity of ductility is evidently the result of gross segregation which may be reduced by vacuum remelting. Martensitic and precipitation-hardening stainless steels are subject to an embrittling reaction when heated between about 500° to 900° F. This is evidenced by an increase in yield strength and a reduction in the resistance to crack propagation. Its magnitude depends on a number of factors including the exposure time, composition, and previous treatment.</p>

^aFrom information in ref. 6, secs. 13XX to 16XX.

TABLE A-II. - Concluded. SPECIAL CONSIDERATIONS FOR STAINLESS STEEL ALLOYS^a

(c) Concluded. FeAH steels

Steel	Special considerations
	<p>Insufficient data are available to quantitatively define the effects of these variables for any of the commercial steels subject to this embrittlement. However, on the basis of the information available for the PH steels, it would be expected that long time exposures at temperatures in the lower portion of the embrittling range would produce the maximum embrittling effects.</p> <p>It has been reported that the embrittling is associated with the formation of a copper-rich alpha prime ferrite phase and that the following factors are important in establishing its magnitude:</p> <ol style="list-style-type: none"> 1. Increased amounts of chromium, silicon and columbium increase the rate of embrittlement at 800° F. When silicon and columbium are low, chromium becomes the sole controlling factor, except that the nickel content as related to the chromium influences the result (Cr-Ni balance influences the martensite reaction). The highest nickel content which can be used at a given level of chromium without inhibiting martensite transformation is best from the standpoint of embrittlement. 2. The embrittlement is completely reversible by reapplying the initial precipitation hardening temperature, if that temperature is 1025° F or higher. 3. Lowering the solution-treating temperature, at least down to 1650° F, slightly lessens the tendency toward embrittlement at 800° F. <p>Consumers have sometimes complained that the composition limits of precipitation-hardenable semi-austenitic steels are too wide to permit uniform response to heat treatment. The impact strength of 17-4 PH type precipitation-hardening stainless steel both before and after exposure at 800° F are affected by variations in chemistry within the recommended composition range. It would be expected that 15-5 PH would be similarly affected. For many applications, 15-5 PH should not be used in condition A. This is true even though the desired hardness may fall within the range of condition A. While the alloy is relatively soft in condition A, the structure is untempered martensite that has low ductility and poor resistance to stress corrosion cracking.</p>
N-155:	Unless stress relieved, hot cold-worked forgings may warp during machining.
Fe	
20 Co	
20 Cr	
20 Ni	
3 Mo	
2.5 W	
1 Cb	
S-590:	Avoid large grain forgings.
Fe	
20 Co	
20 Cr	
20 Ni	
4 Cb	
4 Mo	
4 W	
16-25-6:	Avoid heating alloy to high temperatures in stagnant oxidizing atmosphere, because of molybdenum reactions.
Fe	
25 Ni	
16 Cr	
6 Mo	
Incoloy:	At 1800° F the scaling resistance of Incoloy is comparable to that of the high nickel alloys such as Inconel and Nimonic 75.
Fe	
34 Ni	
20 Cr	
Incoloy alloy 802:	This alloy is not recommended for use at temperatures above 1700° F. Dispersion reactions in the temperature range between about 1200° and 1600° F reduce the tensile elongations and impact strength.
Fe	
0.35 C	
33 Ni	
21 Cr	
0.75 Ti	
0.60 Al	

^aFrom information in ref. 6, secs. 13XX to 16XX.

TABLE A-III - SPECIFICATIONS AND FORMS FOR WROUGHT
ALUMINUM ALLOYS*

Com- mer- cial Desig- nation	Sheet and Plate	Drawn Tube	Pipe ^a and Round Seamless Extruded Tube	Welded Tube	Extruded Bar, Rod, Shapes, and Tube ^a	Bar, Rod, Wire, and Shapes Rolled or Drawn ^c Spray Wire	Brazing or Welding Rod and Electrode	Rivets and Rivet Wire	Forgings and Forging Stock
1100	QQ-A-250/1 AMS 4001 AMS 4003 ASTM B209 USA H38.2	WW-T-700/1 AMS 4062 ASTM B307 ASTM B210 USA H38.3	ASTM B241 USA H38.7	ASTM B313 USA H38.11	ASTM B221 USA H38.5	QQ-A-225/1 MIL-W-6712 AMS 4102 AMS 4180 ASTM B211 USA H38.4	QQ-R-566 MIL-E-15597 MIL-E-16053 ASTM B285 ASTM B184	MIL-R-5674 QQ-A-430 AMS 7220 ASTM B316 USA H38.12	ASTM B247 USA H38.8
1230									
2011						QQ-A-225/3 ASTM B211 USA H38.4			
2014	AMS 4028 AMS 4029 AMS 4014 ASTM B209 USA H38.2	ASTM B210 USA H38.3	ASTM B241 USA H38.7		QQ-A-200/2 AMS 4153 ASTM B221 USA H38.5	QQ-A-225/4 AMS 4121 ASTM B211 USA H38.4			QQ-A-367 AMS 4134 AMS 4135 ASTM B247 MIL-A-22771 USA H38.8
Alclad 2014	QQ-A-250/3 ASTM B209 USA H38.2								
2017						QQ-A-225/5 AMS 4110 AMS 4118 ASTM B211 USA H38.4		MIL-R-5674 QQ-A-430 ASTM B316 USA H38.1	
2024	AMS 4033 AMS 4035 AMS 4037 AMS 4097 AMS 4098 AMS 4099 AMS 4103 AMS 4104 AMS 4105 AMS 4106 QQ-A-250/4 ASTM B209 USA H38.2	WW-T-700/3 AMS 4087 AMS 4088 AMS 4086 ^b ASTM B210 USA H38.3	ASTM B241 USA H38.7		QQ-A-200/3 AMS 4152 AMS 4164 AMS 4165 ASTM B221 USA H38.5	QQ-A-225/6 AMS 4112 AMS 4119 AMS 4120 ASTM B211 USA H38.4		MIL-R-5674 QQ-A-430 ASTM B316 AMS 7223 USA H38.12	
Alclad 2024	QQ-A-250/5 AMS 4034 AMS 4040 AMS 4041 AMS 4042 AMS 4060 AMS 4061 AMS 4072 AMS 4073 AMS 4074 AMS 4075 ASTM B209 USA H38.2								
2117								USA H38.12 MIL-R-27384 MIL-R-5674 MIL-R-8814 AMS 7222 ASTM B316 QQ-A-430	
2219	MIL-A-8920 ASTM B209 USA H38.2 AMS 4031		ASTM B241 USA H38.7		ASTM B221 USA H38.5	ASTM B211 USA H38.4			ASTM B247 QQ-A-367 AMS 4143 AMS 4144 USA H38.8
Alclad 2219	ASTM B209 USA H38.2								
3003	QQ-A-250/2 AMS 4006 AMS 4008 ASTM B209 USA H38.2	WW-T-700/2 AMS 4065 AMS 4067 ASTM B210 ASTM B234 ASTM B307 USA H38.9 USA H38.6 USA H38.3	ASTM B241 ^a ASTM B345 ^a MIL-P-25995 USA H38.7 USA H38.13	ASTM B313 USA H38.11	QQ-A-200/1 ASTM B221 USA H38.5	QQ-A-225/2 ASTM B211 USA H38.4	MIL-E-15597	MIL-R-1150 QQ-A-430	ASTM B247 USA H38.8

*From information in ref. 17, pp. 162 to 164.

TABLE A-III - Concluded. SPECIFICATIONS AND FORMS FOR WROUGHT ALUMINUM ALLOYS*

Commercial Designation	Sheet and Plate	Drawn Tube	Pipe ^a and Round Seamless Extruded Tube	Welded Tube	Extruded Bar, Rod, Shapes, and Tube ^a	Bar, Rod, Wire, and Shapes Rolled or Drawn ^c Spray Wire	Brazing or Welding Rod and Electrode	Rivets and Rivet Wire	Forgings and Forging Stock
5457	ASTM B209 USA H38.2								
5557	ASTM B209 USA H38.2								
5657	ASTM B209 USA H38.2								
6061	QQ-A-250/11 AMS 4025 AMS 4026 AMS 4027 ASTM B209 USA H38.2	WW-T-700/6 AMS 4079 AMS 4080 AMS 4081 ^b MIL-T-7081 ^b AMS 4082 AMS 4083 ^b ASTM B210 ASTM B234 USA H38.3 USA H38.6	ASTM B241 ^a ASTM B345 ^a MIL-P-25995 USA H38.7 USA H38.13 ASTM B429	ASTM B313 USA H38.11	QQ-A-200/8 AMS 4150 AMS 4160 AMS 4161 ASTM B221 USA H38.5	QQ-A-225/8 ASTM B211 AMS 4115 AMS 4116 AMS 4117 USA H38.4		QQ-A-430 ASTM B316 USA H38.12 MIL-R-1150	QQ-A-367 AMS 4127 AMS 4146 ASTM B247 USA H38.8 MIL-A-22771
Alclad 6061	AMS 4020 AMS 4021 AMS 4022 AMS 4023 ASTM B209 USA H38.2								
6063		ASTM B210 USA H38.3	ASTM B241 ^a ASTM B345 ^a MIL-P-25995 USA H38.7 USA H38.13		QQ-A-200/9 AMS 4156 ASTM B221 USA H38.5				
6151									QQ-A-367 AMS 4125 ASTM B247 USA H38.8
6262		ASTM B210 USA H38.3			ASTM B221 USA H38.5	QQ-A-225/10 ASTM B211 USA H38.4			
6463					ASTM B221 USA H38.5				
6951									
7039	ASTM B209 USA H38.2								
7072									
7075	QQ-A-250/12 AMS 4038 AMS 4044 AMS 4045 AMS 4078 ASTM B209 USA H38.2	ASTM B210 USA H38.3	ASTM B241 USA H38.7		USA H38.5 QQ-A-200/11 AMS 4154 AMS 4167 AMS 4168 AMS 4169 ASTM B221	QQ-A-225/9 AMS 4122 AMS 4123 AMS 4124 ASTM B211 USA H38.4		ASTM B316 QQ-A-430 USA H38.12	QQ-A-367 AMS 4139 AMS 4141 ASTM B247 MIL-A-22771 USA H38.8
Alclad 7075	QQ-A-250/13 AMS 4039 AMS 4048 AMS 4049 AMS 4047 ^d ASTM B209 USA H38.2								
7079	QQ-A-250/17 AMS 4024 ASTM B209 USA H38.2		ASTM B241 USA H38.7		QQ-A-200/12 AMS 4171 ASTM B221 USA H38.5				QQ-A-367 MIL-A-22771 AMS 4138 AMS 4136 ASTM B247 USA H38.8
7178	QQ-A-250/14 ASTM B209 USA H38.2		ASTM B241 USA H38.7		AMS 4158 QQ-A-200/13 ASTM B221 USA H38.5			MIL-R-24243	
No. 11 Brazing Sheet									
No. 12									
No. 21									
No. 22									
No. 23									
No. 24									

^a Pipe made by any process.

^b Tube Hydraulic.

^c Includes Structural Shapes.

^d Plate and Sheet Roll tapered.

*From information in ref. 17, pp. 162 to 164.

TABLE A-III - Continued. SPECIFICATIONS AND FORMS FOR WROUGHT ALUMINUM ALLOYS*

Com- mercial Design- ation	Sheet and Plate	Drawn Tube	Pipe ^a and Round Seamless Extruded Tube	Welded Tube	Extruded Bar, Rod, Shapes, and Tube ^a	Bar, Rod, Wire, and Shapes Rolled or Drawn ^c Spray Wire	Brazing or Welding Rod and Electrode	Rivets and Rivet Wire	Forgings and Forging Stock
Alclad 3003	ASTM B209 USA H38.2	ASTM B210 ASTM B234 ASTM B307 USA H38.3 USA H38.6 USA H38.9	ASTM B241 ASTM B345 ^a USA H38.7 USA H38.13		ASTM B221 USA H38.5				
3004	ASTM B209 USA H38.2	ASTM B210 ASTM B307 USA H38.3 USA H38.9		ASTM B313 USA H38.11	ASTM B221 USA H38.5				
Alclad 3004	ASTM B209 USA H38.2			ASTM B313 USA H38.11					
4032									QQ-A-367 AMS 4145 ASTM B247 USA H38.8
4043						MIL-W-6712 (Spray Gun Wire)	QQ-B-655 QQ-R-566 MIL-E-15597 MIL-E-16053 AMS 4190 ASTM B184 ASTM B260 ASTM B285		
4343							QQ-B-655 MIL-B-20148		
5005	ASTM B209 USA H38.2	ASTM B307 USA H38.9				ASTM B396 (Electrical Wire)		QQ-A-430	
5050	ASTM B209 USA H38.2	ASTM B210 ASTM B307 USA H38.3 USA H38.9	ASTM B345 ^a	ASTM B313 USA H38.11					
5052	QQ-A-250/8 AMS 4015 AMS 4016 AMS 4017 ASTM B209 USA H38.2	WW-T-700/4 AMS 4069 AMS 4070 AMS 4071 ASTM B210 ASTM B307 ASTM B234 USA H38.3 USA H38.13	ASTM B345 ^a USA H38.13	ASTM B313 USA H38.11	ASTM B221 USA H38.5	QQ-A-225/7 AMS 4114 ASTM B211 USA H38.4		QQ-A-430 ASTM B316 USA H38.12 MIL-R-24243	
5083	QQ-A-250/6 ASTM B209 AMS 4056 AMS 4057 AMS 4058 AMS 4059 USA H38.2	ASTM B210 USA H38.3	ASTM B241 ^a ASTM B345 ^a USA H38.7 USA H38.13		QQ-A-200/4 ASTM B221 USA H38.5				ASTM B247 QQ-A-367 USA H38.8
5086	QQ-A-250/7 ASTM B209 USA H38.2	WW-T-700/5 ASTM B210 USA H38.3	ASTM B241 ^a ASTM B345 ^a USA H38.7 USA H38.13	ASTM B313 USA H38.11	QQ-A-200/5 ASTM B221 USA H38.5				
5154	AMS 4018 AMS 4019 ASTM B209 USA H38.2	ASTM B210 USA H38.3	ASTM B345 ^a ASTM B241 ^a MIL-P-25995 USA H38.13 USA H38.7	ASTM B313 USA H38.11	ASTM B221 USA H38.5	ASTM B211 USA H38.4	MIL-E-16053 ASTM B285 QQ-R-566		
5252	ASTM B209 USA H38.2								
5454	QQ-A-250/10 ASTM B209 USA H38.2	ASTM B234 USA H38.6	ASTM B241 ^a MIL-P-25995 USA H38.7		QQ-A-200/6 ASTM B221 USA H38.5				
5456	QQ-A-250/9 ASTM B209 USA H38.2		MIL-P-25995 ASTM B241 ^a ASTM B345 ^a USA H38.7 USA H38.13		QQ-A-200/7 ASTM B221 USA H38.5				ASTM B247 USA H38.8

*From information in ref. 17, pp. 162 to 164.

As shown in table A-IV, the standard temper designation system for aluminum and aluminum alloys, both wrought and cast, consists of a letter indicating the basic temper which, except for the annealed and as-fabricated tempers, is more specifically defined by adding one or more digits. The four main basic tempers are as follows: O, annealed; F, as-fabricated; H, strain hardened; and T, heat treated. The symbol W is used to designate the unstable condition following solution heat treatment, and if time subsequent to heat treatment is indicated, it may be considered a basic temper. It is a principle of this system that a change in a temper designation is made only when some variation in the same basic operation significantly alters the characteristics of the product.

TABLE A-IV. - TEMPER DESIGNATION SYSTEM FOR ALUMINUM ALLOYS^a

Designation	Description
F As-fabricated	Designation applies to products supplied in the condition resulting from normal manufacturing operations, without special practices to control the amount of strain or thermal treatment. For wrought products, there is no guarantee of mechanical properties. For castings, the term means as-cast. An example of 43-F.
H Strain hardened	Designation applies to those wrought products that are not subjected to thermal treatments to increase their mechanical properties but that have their strength increased by strain hardening, with or without supplementary thermal treatment to produce partial softening. The H is always followed by two or more digits. First digit indicates the specific combination of basic operations and the following digit or digits the final degree of strain hardening. (The digital system is explained subsequently.)
H1 Strain hardened only	As indicated previously, the second digit designates the amount of cold work performed. The digit 8 has been selected to represent the hardest commercially practical temper, written as H18. Material with tensile strength half-way between soft and full hard, half hard, is designated H14; quarter hard, H12; and so on. A third digit is often used to identify a special set of properties. For example, H141 may represent the same minimum properties as H14, but with maximum values that are closer than standard. The third digit may also denote values slightly different from those of H14, but not sufficiently different to place it in the H13 or H15 classification. Extra hard tempers are designated by using the second digit 9, with or without a third digit. The H112 temper for wrought alloys is generally considered a "controlled" F-temper with guaranteed mechanical properties.
H2 Strain hardened and partial annealed	It is often desirable to obtain a certain strength range in the strain hardened alloys by working to a harder temper and then reducing the strength to the desired level by partial annealing. This process is identified by the number 2 in the first digit place, and the residual amount of cold work is then designated by the same method employed for the H1 series. Thus, H28 is full hard, H24 half hard, and so on. For alloys that age soften at room temperature, the H2 tempers have approximately the same tensile strength as the corresponding H3 tempers. For other alloys, the H2 tempers have approximately the same tensile strength as the corresponding H1 tempers and slightly higher elongations.
H3 Strain hardened and then stabilized	The properties of magnesium-containing alloys in the strain hardened condition are stabilized by a low-temperature hearing, thus slightly lowering their strength and increasing their ductility. If the treatment is not employed, then the change of properties occurs over a long time at room temperature. Use of this treatment is indicated by the digit 3 following the H, and the degree of strain hardening is indicated in the usual way by one or two following digits.
O Annealed, recrystallized	Designation applies to the softest temper of wrought alloy products.

^aInformation from ref. 5, pp. 888 and 889.

TABLE A-IV. - Concluded. TEMPER DESIGNATION SYSTEM FOR ALUMINUM ALLOYS^a

Designation	Description
T Treated to produce stable tempers other than F, O, or H	Designation applies to products thermally treated to produce stable tempers with or without supplementary strain hardening. The T followed by the numerals 2 to 9 inclusive, designates one specific combination of basic operations, thus 6061-T6. Should variation of the same basic operation be applied to the same alloy, resulting in different characteristics, other digits are added to the basic designation (6061-T61 or 6061-T62). It should be understood that a period of natural aging at room temperature may occur between or after the operations listed. Control of this period is exercised when it is metallurgically important, but it is not indicated by the designation. Basic subdivisions of the T-temper, ranging from annealing to complex aging treatments, are now given.
T2 Annealed (cast products only)	Designation applies to castings only. Annealing is used for such purposes as improving ductility and increasing dimensional stability.
T3 Solution heat treated and cold worked, naturally aged to substantially stable condition	Designation applies to those wrought products that are cold worked for the primary purpose of improving the strength (for instance, 2024-T36) and also applies to those products in which the effect of cold work, such as flattening or straightening, is recognized in applicable specifications (flat sheet of 2024 heat treated by the supplier is designated 2024-T3). No control is exercised to cold work at any particular stage during the natural aging cycle.
T4 Solution heat treated and naturally aged to a substantially stable condition	Designation applies when the product is not cold worked after heat treatment (2024 sheet heat treated by the user becomes 2024-T4), and also when applicable specifications do not recognize the effect of cold work resulting from flattening and straightening operations (6061 flat sheet heat treated by the supplier is designated 6061-T4). The alloy 7075 does not have a commercial T4 designation. (An example for a casting alloy is 195-T4.)
T5 Artificially aged only	Designation applied to products that are artificially aged without prior solution heat treatment. The artificial aging of these products improves mechanical properties (6063-T5 extrusions) and dimensional stability (D132-T4 castings).
T6 Solution heat treated and then artificially aged	Designation applies to products that are not cold worked after solution heat treatment or in which the effect, if any, of flattening or straightening is not recognized in applicable specifications. Whether flattened or not, 6061 heat treated and aged is designated 6061-T6, and 7075 treated in the same manner is 7075-T6. Casting alloy example, 356-T6.
T7 Solution heat treated and then stabilized	Designation applies to products in which the temperature and time conditions for stabilizing are such that the alloy is carried beyond the point of maximum hardness, providing control of growth or residual stress, or both (2018-T71, 4032-T72, 355-T71).
T8 Solution heat treated, cold worked, then artificially aged	Designation applies when the cold working is done for the purpose of improving strength (2011-T8, Alclad 2024-T86), and also when the cold working effect of flattening or straightening is recognized in applicable specifications (Alclad 2024-T81 flat sheet).
T9 Solution heat treated, artificially aged, then cold worked	Wire of 6061 heat treated, artificially aged, and then cold worked 6061-T91.
W Unstable condition following solution heat treatment	Designation, because of natural aging, is specific only when the period of aging is indicated - for example, 2024-W (1/2 hr), 7075-W (2 months).

^aInformation from ref. 5, pp. 888 and 889.

TABLE A-V. - SPECIAL CONSIDERATIONS FOR NICKEL ALLOYS^a

Nickel alloy	Special considerations
Inconel alloy 600: Ni 15 Cr 7 Fe	Contact with sulfur-containing atmospheres at elevated temperatures should be avoided.
Inconel alloy 702: Ni 15 Cr 3 Al 0.5 Ti	Contact with sulfur-containing atmospheres at elevated temperatures should be avoided.
Inconel alloy 722: Ni 15 Cr 7 Fe 2.5 Ti 0.7 Al	Solution treating of this alloy at high temperatures (2100° F) should be avoided because subsequent small deformations reduce the high temperature properties. Slow heating of welded parts may result in cracking.
Inconel alloy 718: Ni 19 Cr 17 Fe 5 Cb 3 Mo 0.8 Ti 0.6 Al	Outstanding weld characteristics are due largely to slow response to aging, which keeps restraints to a minimum and avoids buildup of welding stresses. Material is outstanding over a wide range of temperatures in fatigue and fatigue crack propagation; hence, it is useful in applications involving large temperature changes, especially if sub-zero temperature are involved (e.g., rocket motor parts and supersonic aircraft parts). Because of iron content (which contributes to the outstanding weld characteristics) strength at high temperatures is lower than other nickel base superalloys; hence, its usefulness is restricted to a lower maximum temperature than other nickel base superalloys. Elevated temperature notch sensitivity of the alloy under creep conditions, while not completely understood, is related to the thermal and mechanical history. High finish forging temperature contributes to notch embrittlement. To avoid embrittlement one producer, the Special Metals Corporation speaking of Udimet 718, recommends that the forging be started at 2050° F (max.) and finished at approximately 1750° F. The last 30 percent of reduction should be below 1900° F, preferably below 1850° F. They recommend a maximum solution temperature of 1750° F. They also believe that notch embrittlement can best be evaluated at 1200° F, 100 ksi rather than the more commonly used condition 1300° F, 75 ksi for evaluating notch embrittlement due to thermomechanical history.
Inconel alloy X-750: Ni 15 Cr 7 Fe 25 Ti 1 Cb 0.7 Al	Avoid heating in sulfur containing atmospheres. Dimensional changes on aging require attention.

^aFrom information in ref. 6, secs. 41XX and 42XX.

TABLE A-V. - Continued. SPECIAL CONSIDERATIONS FOR NICKEL ALLOYS^a

Nickel alloy	Special considerations
Monel alloy K-500:	Welding of this alloy requires special considerations to avoid degradation of soundness and mechanical properties in the weld area. Alloy may be welded by the oxyacetylene, inert gas tungsten arc, or metallic arc processes, using proper filler rods. Oxyacetylene flame should be kept strongly reducing, and the heated end of the filler rod should be kept in the protective atmosphere of the flame to avoid oxidizing the rod. Number 44 K-Monel gas welding wire should be used with a paste flux. For metallic arc welding, number 34 K-Monel rod should be used in a shielded arc. Welding should be performed on annealed material and the welded assembly stress relieved before aging. The welded assembly should be taken through the age hardening range as quickly as possible.
Ni	
29 Cu	
3 Al	
0.5 Ti	
Incoloy alloy 901:	Heating in sulfur-containing atmospheres should be avoided. Forgings in this alloy exhibit a pronounced directionality.
Ni	
35 Fe	
13 Cr	
6 Mo	
2.5 Ti	
713 LC	The developments of steep thermal gradients in large components such as turbine wheels during cooling from casting or heat treatment at high temperature (2150° F) can introduce extremely high residual stresses which must either be eliminated or allowed for in selection of service stresses. The simplest method of reducing these stresses during heat treatment is by reducing cooling rates combined with methods of minimizing section size temperature difference by padding with insulating material.
Ni	
12 Cr	
6 Al	
4.5 Mo	
2 Cb	
0.7 Ti	
Hastelloy C:	This alloy is very sensitive to overheating on solution treating. Both its strength and its corrosion resistance may be impaired when heated to 2285° F or higher.
Ni	
16 Cr	
16 Mo	
5 Fe	
4 W	
TD Nickel	The radiation levels experienced during handling and during fabrication of the alloy are well below the AEC established tolerances.
Ni	
2 ThO ₂	Although the special merit of the alloy is reflected by its retention of strength at high temperatures for long service periods, it must be protected from oxidation by suitable coating or cladding. Because the alloy achieves a major component of strength from the cold work induced during processing, its strength is very sensitive to test direction. Caution should be exercised in use to insure that the principal loads are supported by material oriented in the major working direction. Directionality of strength is reflected in shear strengths measured in direction of principal deformation. Care should be exercised to avoid introduction of shear loads in weak directions. Joining by welding or other processes involving high temperature, especially in the presence of foreign elements or alloys, can seriously degrade long-time properties even if short-time tensile strengths are retained.

^aFrom information in ref. 6, secs. 41XX and 42XX.

TABLE A-V. - Continued. SPECIAL CONSIDERATIONS FOR NICKEL ALLOYS^a

Nickel alloy	Special considerations
713C: Ni 13 Cr 6 Al 4 Mo 2 Cb 0.7 Ti	<p>Control of cleanliness and properties is inadequate for air castings.</p> <p>Although alloy is not intended for welding, improved weldability can be obtained by maintaining low aluminum content. Improved high temperature properties, thermal shock, and impact resistance can be achieved by directional solidification. Material prepared from pre-alloy powders has improved tensile strength properties up to about 1400° F, and superplasticity properties above approximately 1900° F, thus rendering the forming properties very easy at this temperature or above. Heat treatment after forming can remove superplasticity characteristics at high temperature while retaining a strength advantage over the cast form up to 1400° F, and only minor loss in strength above this temperature.</p>
René 41: Ni 19 Cr 11 Co 10 Mo 3 Ti 1.5 Al	<p>A major problem in the use of this alloy has been the occurrence of cracking during the heat treatment of welded parts. Recent developments have, however, provided major directions toward the solution of this problem. Two basic approaches have been developed. One is the overaging treatment prior to welding followed by standard heat treatment after welding; the other is solution treating prior to welding with controlled cooling after solution treatment. Weld patch tests have also been developed to identify heats that have high susceptibility to weld cracking.</p> <p>Recent studies on sheet have indicated that under certain conditions the alloy may become highly notch sensitive in creep rupture tests. The reason for this behavior is not completely understood.</p>
TD NiCr: Ni 18 Cr 2 ThO ₂	<p>Considerable scatter characterizes the reported strength values for TD NiCr sheet and foil at both room and elevated temperature. The producer's specified properties for thermomechanically processed sheet are at the lower end of the scatter band at room temperature and near the midpoint at elevated temperatures. It is likely that the specified minimum properties will change with the further development of the alloy.</p> <p>Processing conditions producing high strength at elevated temperatures result in low values of tensile elongation for sheet and low reduction in area values for bar. At 2200° F, creep rupture specimens of thermomechanically processed materials exhibit essentially zero elongation. Mild notch tests on sheet with an unspecified processing history exhibited notch weakening at 2200° F. The significance of these low values of ductility on the fracture toughness should be determined by suitable tests using specimens containing fatigue cracks. Material which has been cold worked or thermomechanically processed to obtain high strength at elevated temperatures exhibits considerable directionality with the transverse direction being of lower strength in tensile and creep rupture tests.</p> <p>TD NiCr is slightly radioactive due to the ThO₂ content. It is an alpha emitter and requires precautions be taken if dust is generated by dry grinding.</p>
Inconel alloy 700: Ni 30 Co 15 Cr 3 Al 3 Mo 2 Ti	<p>Contact with sulfur containing atmospheres at elevated temperatures should be avoided. Overheating and lack of lubrication during forging will cause cracks and checks.</p>

^aFrom information in ref. 6, secs. 41XX and 42XX.

TABLE A-V. - Continued. SPECIAL CONSIDERATIONS FOR NICKEL ALLOYS^a

Nickel alloy	Special considerations
Waspaloy:	Solution treating in an oxidizing atmosphere may result in intergranular oxidation.
Ni	There is limited information available which indicates that the alloy may become embrittled upon long time exposure to stress in an oxidizing atmosphere.
20 Cr	
14 Co	Sharp notch embrittlement in creep has been observed at temperatures of 1000° and 1200° F for both solution treated and aged and cold rolled and aged sheet. These are insufficient data to establish the time-temperature dependence of this embrittlement.
4 Mo	
3 Ti	However, the effects appear to be larger at 1200° F than 1000° F for the solution treated and aged sheet. The cold rolled and aged material exhibits considerable notch embrittlement at both test temperatures at rupture times between 10 and 1000 hours, with the transverse direction being considerably more notch sensitive than the longitudinal direction. Sharp notch brittleness is also observed for cold rolled and aged sheet following an exposure to 650° or 1000° F at 40 ksi for 1000 hours. The effect is considerably larger at 1000° F than at 650° F. Similar exposure conditions produce no embrittlement for solution treated and aged sheet.
1 Al	
Mar-M-200:	Freckles have been observed in directionally solidified polycrystalline and monocrystalline materials. It has been determined that such freckles are linear assemblies of small random equiaxed grains which are enriched in all but the inversely segregated solute species. Excessive interdendritic porosity and feeding shrinkage are observed in the vicinity of a freckle line. Freckling tendency varies with solidification and alloy composition. Freckles degrade physical properties, and must be avoided.
Ni	
12.5 W	The PWA 1422 alloy containing 2 percent hafnium provides increased transverse ductility and creep rupture strength in thin sections. A minimum in elongation characterizes the test temperature range between 1400° and 1600° F.
10 Co	
9 Cr	
5 Al	
2 Ti	
1 Cb	
+ B	
+ Zr	
IN-100:	Because of the low chromium content, as well as the presence of vanadium, oxidation resistance is not adequate at the high temperatures where the strength of the alloy assumes special advantage. The problem is usually overcome by the use of aluminum or aluminum-base coatings. Many of these are proprietary, and the compositions as well as heat treatments are not revealed. Information provided by the coating produces shows beneficial effects of coatings as protection against oxidation and sulfidation and improvement of thermal shock resistance. These benefits are apparently obtained without impairing the tensile and creep properties at high temperature. The high hardener content of the alloy make it particularly prone to the precipitation of embrittling phases, such as sigma, upon prolonged exposure to high temperature, especially if stress is simultaneously applied. Special compositions, low in titanium content, have been found advantageous for avoiding such embrittlement. The International Nickel Company, original developer of IN-100, has developed a modification designated as IN-731X, and the General Electric Company has developed René 100 for this purpose. Both use the Pha Comp techniques, wherein electron vacancy of the remaining matrix after the major hardening precipitates have formed is used as a basis for the determination of whether sigma will form. Every heat requires a separate computation to determine sigma-proneness because of the large variations permitted in the chemistry of individual heats; however, in general, the revised composition limits with lower titanium contents are usually sigma-free within the specified limits of the other elements. The tendency toward sigma-proneness was first reported to be a
Ni	
15 Co	
9.5 Cr	
5.5 Al	
5 Ti	
3 Mo	
0.95 V	
0.015 B	

^aFrom information in ref. 6, secs. 41XX and 42XX.

TABLE A-V. - Concluded. SPECIAL CONSIDERATIONS FOR NICKEL ALLOYS^a

Nickel alloy	Special considerations
<p>Udimet 700:</p> <p>Ni</p> <p>18 Co</p> <p>15 Cr</p> <p>5 Mo</p> <p>4.5 Al</p> <p>3.5 Ti</p> <p>0.03 B</p>	<p>result of exposure to high temperatures for long times, especially at stress. It was also shown that sigma formed at 1650° F could be solutioned at 1900° to 2000° F, in 2 to 4 hours and that a 2000° F, 2-hour heat treatment delayed sigma formation. This heat treatment was observed to delay sigma formation whether applied to an as-cast bar or whether applied to a bar previously exposed to 1650° F containing sigma. This observation points to the possibility of beneficial effects of heat treatment, in contrast to the normally used as-cast structure. It also points to the possibility of removing creep damage by reheat treatment for this alloy.</p> <p>Special note should be made of recent developments to avoid sigma phase formation using the Pha Comp procedure and of modifications in composition and heat treatment resulting in optimization of properties.</p>

^aFrom information in ref. 6, secs. 41XX and 42XX.

TABLE A-VI. - PROPERTIES AND APPLICATIONS OF COPPER AND COPPER ALLOYS^a

Alloy name	Number	Nominal composition, percent	Fabricating characteristics	Typical applications
Oxygen-free copper	102	99.95 Cu	Excellent hot and cold workability; good forgeability. Fabricated by coining, coppersmithing, drawing and upsetting, hot forging and pressing, spinning swaging, stamping.	Gaskets
Electrolytic tough pitch copper	110	99.90 Cu 0.04 O	Fabricating characteristics same as alloy 102.	Gaskets
Silver-bearing tough pitch copper	113, 114, 116	99.90 Cu 0.04 O Ag(e)	Fabricating characteristics same as alloy 102.	Gaskets, chemical process equipment
Phosphorus deoxidized copper, high residual phosphorus	122	99.90 Cu 0.02 P	Fabricating characteristics same as alloy 102.	Lines; plumbing pipe and tubing, condenser tubing, evaporator, and heat exchanger tubing
Beryllium copper	172	99.5 Cu 1.9 Be 0.20 Co	Excellent hot workability. Commonly fabricated by blanking, drawing, forming, and bending, turning, drilling, tapping.	Bellows, bourdon tubing, diaphragms, fuse clips, fasteners, lock washers, springs, switch parts, roll pins, valves, welding equipment
Gilding 95 percent	210	95.0 Cu 5.0 Zn	Excellent cold workability, good hot workability for blanking, coining, drawing, piercing and punching, shearing, spinning, squeezing and swaging, stamping.	Screws, rivets
Commercial bronze, 50 percent	220	90.0 Cu 10.0 Zn	Fabricating characteristics same as alloy 210 plus heading and upsetting, roll threading and knurling, hot forging and pressing.	Screws, rivets
Red brass, 85 percent	230	85.0 Cu	Fabricating characteristics same as alloy 210.	Condenser and heat exchanger tubing, plumbing pipe
Low brass, 80 percent	240	80.0 Cu 20.0 Zn	Excellent cold workability. Fabrication characteristics same as alloy 210.	Bellows, pump lines, flexible hose
Cartridge brass, 70 percent	260	70.0 Cu 30.0 Zn	Excellent cold workability. Fabricating characteristics same as alloy 240, except for coining, roll threading and knurling.	Radiator cores and tanks, fasteners, hinges, plumbing accessories, pins, rivets
Yellow brass	268, 270	65.0 Cu	Excellent cold workability. Fabricating characteristics same as alloy 240.	Same as alloy 260
Muntz metal	280	60.0 Cu 40.0 Zn	Excellent hot formability and forgeability for blanking, forming and bending, hot forging and pressing, hot heading and upsetting, shearing.	Architectural, large nuts and bolts, brazing rod, condenser plates, condenser, evaporator and heat exchanger tubing, hot forgings
Leaded commercial bronze	314	89.0 Cu 1.75 Pb 9.25 Zn	Excellent machinability.	Screws, machine parts
Low-leaded brass tube	330	66.0 Cu 0.5 Pb 33.5 Zn	Combines good machinability and excellent cold workability. Fabricated by forming and bending, machining, piercing and punching.	Pump and power cylinders and liners
High-leaded brass tube	332	66.0 Cu 1.6 Pb 32.4 Zn	Excellent machinability. Fabricated by piercing, punching, and machining.	General purpose screw machine parts
Low-leaded brass	335	65.0 Cu 0.5 Pb 34.5 Zn	Similar to alloy 332. Commonly fabricated by blanking, drawing, machining, piercing and punching, and stamping.	Butts, hinges
Medium-leaded brass	340	65.0 Cu 1.0 Pb 34.0 Zn	Similar to alloy 332. Fabricated by blanking, heading and upsetting, machining, piercing and punching, roll threading and knurling, stamping.	Butts, gears, nuts, rivets, screws

^aFrom ref. 7, pp. 26 and 27.

TABLE A-VI. - Continued. PROPERTIES AND APPLICATIONS OF COPPER AND COPPER ALLOYS^a

Alloy name	Number	Nominal composition, percent	Fabricating characteristics	Typical applications
High-leaded brass	342, 353	65.0 Cu 2.0 Pb 33.0 Zn	Fabricating characteristics same as alloy 340.	Clock plates and nuts, gears, wheels and channel plate
Extra-high-leaded brass	356	63.0 Cu 2.5 Pb 34.5 Zn	Excellent machinability. Fabricated by blanking, machining, piercing and punching, stamping.	Same as alloys 342 and 353
Free-cutting brass	360	61.5 Cu 3.0 Pb 35.5 Zn	Excellent machinability. Fabricated by machining, roll threading and knurling.	Gears, pinions, automatic high speed screw machine parts
Leaded muntz metal	365 to 368	60.0 Cu 0.6 Pb 39.4 Zn	Combines good machinability with excellent hot formability.	Condenser tube plates
Free-cutting muntz metal	370	60.0 Cu 1.0 Pb 39.0 Zn	Fabricating characteristics similar to alloys 365 to 368.	Automatic screw machine parts
Forging brass	377	59.0 Cu 2.0 Pb 39.0 Zn	Excellent hot workability. Fabricated by heading and upsetting, hot forging and pressing, hot heading and upsetting, machining.	Forgings and pressings of all kinds
Inhibited admiralty	443, 444, 445	71.0 Cu 28.0 Zn 1.0 Sn	Excellent cold workability for forming and bending.	Condenser, evaporator and heat exchanger tubing, condenser tubing plates, distiller tubing, ferrules.
Naval brass	464 to 467	60.0 Cu 39.25 Zn 0.75 Sn	Excellent hot workability and hot forgeability. Fabricated by blanking, drawing, bending, heading and upsetting, hot forging, pressing.	Aircraft turnbuckle barrels, balls, bolts, nuts, rivets, valve stems, condenser plates, welding rod
Leaded naval	485	60.0 Cu 1.75 Pb 37.5 Zn 0.75 Sn	Combines excellent hot forgeability and machinability. Fabricated by hot forging and pressing, machining.	Marine hardware, screw machine parts, valve stems
Phosphor bronze, 1.25-percent E	505	98.75 Cu 1.25 Sn Trace P	Excellent cold workability, good hot formability. Fabricated by blanking, bending, heading and upsetting, shearing and swaging.	Flexible hose
Phosphor bronze, 5-percent A	510	95.0 Cu 5.0 Sn Trace P	Excellent cold workability. Fabricated by blanking, drawing, bending, heading and upsetting, roll threading and knurling, shearing, stamping.	Bellows, bourdon tubing, clutch disks, cotter pins, diaphragms, fasteners, lock washers, wire brushes, chemical hardware, welding rod
Phosphor bronze, 8-percent C	521	92.0 Cu 8.0 Sn Trace P	Good cold workability for blanking, drawing, forming and bending, shearing, stamping.	Generally for more severe service conditions than alloy 510
Phosphor bronze, 10-percent D	524	90.0 Cu 10.0 Sn Trace P	Good cold workability for blanking, forming and bending shearing.	Heavy bars and plates for severe compression, bridge and expansion plates and fittings articles requiring good spring qualities, resiliency, fatigue resistance, good wear and corrosion resistance

^aFrom ref. 7, pp. 26 and 27.

TABLE A-VI. - Concluded. PROPERTIES AND APPLICATIONS OF COPPER AND COPPER ALLOYS^a

Alloy name	Number	Nominal composition, percent	Fabricating characteristics	Typical applications
Free-cutting phosphor bronze	544	88.0 Cu 4.0 Pb 4.0 Zn 4.0 Sn	Excellent machinability, good workability. Fabricated by blanking, drawing, bending, machining, shearing, stamping.	Bearings, bushings, gears, pinions shafts, thrust washers, valve parts
Aluminum bronze, D	614	91.0 Cu 7.0 Al 2.0 Fe	Fabricated by blanking, drawing, forming and bending, heading and roll threading.	Nuts, bolts, stringers and threaded members, corrosion resistant vessels and tanks, structural components, machine parts and members, condenser tubing and pipe, protective sheathing and fastening
Low-silicon bronze, B	651	98.5 Cu 1.5 Si	Excellent hot and cold workability. Fabricated by forming and bending, heading and upsetting, hot forging and pressing, roll threading and knurling, squeezing and swaging.	Hydraulic pressure lines, anchor screws, bolts, cable clamps, cap screws, machine screws, nuts, rivets, U-bolts, electrical conduits, heat exchanger tubing, welding rod
High-silicon bronze, A	655	97.0 Cu 3.0 Si	Excellent hot and cold workability. Fabricated by blanking, drawing, forming and bending, heading and upsetting, hot forging and pressing, roll threading and knurling, shearing, squeezing and swaging.	Similar to alloy 651
Manganese bronze, A	675	58.5 Cu 1.4 Fe 39.0 Zn 1.0 Sn 0.1 Mn	Excellent hot workability. Fabricated by hot forging and pressing, hot heading and upsetting.	Clutch disks, pump rods, shafting, balls, valve stems and bodies
Aluminum brass	687	77.5 Cu 20.5 Zn 2.0 Al	Excellent cold workability for forming and bending.	Same as alloys 443, 444, and 445.
Copper nickel, 10 percent	706	88.7 Cu 1.3 Fe 10.0 Ni	Good hot and cold workability. Fabricated by forming and bending, welding.	Condensers, condenser plates, evaporator and heat exchanger tubing, ferrules
Copper, nickel, 30 percent	715	70.0 Cu 30.0 Ni	Similar to alloy 706.	
Nickel silver, 65-10	745	65.0 Cu 25.0 Zn 10.0 Ni	Excellent cold workability. Fabricated by blanking, drawing, etching, forming and bending, heading and upsetting, roll threading and knurling, shearing, spinning, squeezing and swaging.	Rivets, screws, slide fasteners
Nickel silver, 65-18	752	65.0 Cu 17.0 Zn 18.0 Ni	Fabricating, characteristics similar to alloy 745.	Rivets, screws
Nickel silver, 65-15	754	65.0 Cu 20.0 Zn 15.0 Ni	Fabricating characteristics similar to alloy 745.	
Nickel silver, 65-12	757	65.0 Cu 23.0 Zn 12.0 Ni	Fabricating characteristics similar to alloy 745.	
Nickel silver, 55-18	770	55.0 Cu 27.0 Zn 18.0 Ni	Good cold workability. Fabricated by blanking forming and bending and shearing.	Springs and resistance wire

^aFrom ref. 7, pp. 26 and 27.

**TABLE A-VII - PROPERTIES AND USES FOR HEAT TREATABLE
COPPER ALLOYS¹**

	Beryllium Copper (Strip) CDA 172	Copper-Nickel- Silicon (Strip) CDA 647	Chromium Copper (Strip) CDA 182	Zirconium Copper (Strip) CDA 150	Copper-Nickel- Phosphorus CDA 190
Nominal composition, %	97.85 Cu, 1.90 Be, 0.25 Co	97.50 Cu, 1.90 Ni, 0.60 Si	99.10 Cu, 0.90 Cr	99.85 Cu, 0.15 Zn	97.55 Cu, 1.20 Ni, 0.25 P
Properties					
Tensile strength, psi					
Soft (SA)*	69,000	41,000	30,000	32,000	38,000
SA + HT	177,000	85,000	56,000	34,000	65,000
1 2 hard	92,000	48,000	43,000	48,000	61,000
1 2 hard + HT	195,000	91,000	62,000	53,000	82,000
Hard	110,000	58,000	52,000	55,000	66,000
Hard + HT	200,000	98,000	67,000	59,000	90,000
Yield strength, psi					
Soft (SA)	32,000	14,000	8,000	14,000	10,000
SA + HT	155,000	65,000	45,000	18,000	40,000
1 2 hard	82,000	46,000	40,000	46,000	54,000
1 2 hard + HT	175,000	81,000	57,000	45,000	71,000
Hard	104,000	57,000	51,000	53,000	59,000
Hard + HT	180,000	85,000	63,000	53,000	78,000
Elongation in 2 in., %					
Soft (SA)	47	39	42	51	40
SA + HT	7	16	15	51	33
1 2 hard	10	17	7	11	8
1 2 hard + HT	3	13	9	18	6
Hard	4	3	2	7	6
Hard + HT	2	9	6	14	4
Electrical conductivity, % IACS					
Soft (SA)	18	23	36	70	32
SA + HT	24	40	81	84	60
1 2 hard	16	23	35	72	32
1 2 hard + HT	24	40	78	88	60
Hard	16	23	35	73	32
Hard + HT	24	40	78	88	60
Thermal conductivity, Btu/sq ft/hr/°F					
Soft (SA)	46	58	90	167	80
SA + HT	61	100	189	195	145
1 2 hard	43	58	88	171	80
1 2 hard + HT	61	100	183	202	145
Hard	43	58	88	173	80
Hard + HT	61	100	183	202	145
Fabricating Characteristics					
Hot working temperature (SA or HT)	1050 to 1475 F	1300 to 1375 F	1650 to 1695 F	1650 to 1760 F	1300 to 1550 F
Solution annealing temperature	1400 to 1475	1375 to 1475	1830	1650 to 1750	1300 to 1450
Aging temperature (1 to 2 hr)	600	800 to 900	850 to 930	750 to 950	800 to 900
Machinability rating, (SA, CW, HT)†	20%	30%	20%	20%	30%
Cold workability	Good	Excellent	Good	Excellent	Excellent
Hot workability	Excellent	Excellent	Good	Excellent	Excellent
Joining Characteristics					
Soft soldering	Excellent	Excellent	Excellent	Excellent	Excellent
Silver brazing	Good	Excellent	Excellent	Excellent	Excellent
Oxyacetylene welding	Poor	Good	—	Fair to good	Good
Carbon arc welding	Excellent	Fair to poor	—	Fair	Good
Gas shielded arc welding	Good	Good	—	Good	Good
Resistance welding	Excellent	Good	—	Not recommended	Fair
Typical Applications					
	Diaphragms, bellows, relays, circuit breakers, switches; fuse and component holders; cantilever flat springs; Belleville, curved spring and wavy spring washers; brush springs used at ambient temperature up to 300 F	Fasteners, electrical parts, marine hardware, resistance welded assemblies, resistance welding tip holders, rotors and rings, springs, switch gear, wire connectors, wire forms and wire products	Similar to coppers, such as circuit breakers, parts where high strength and high thermal and electrical conductivity are needed. Used where higher softening point than that provided by copper is needed	Commutator segments, conductors, electrical parts, gaskets, resistance welding tips, rotor bars and plates, switch parts, washers, wave guides, wire forms and wire products	Springs, clips, electronic parts, high strength electrical connectors, bolts, nails, screws, rivets, fasteners

Note: Data Sheet lists only those alloys containing 97% Cu (min).

*SA, solution annealed; CW, cold worked; HT, aged. †Based on 100% for free-cutting brass (CDA 360).

¹From ref. 7, p. 25.

REFERENCES

In parentheses after most references are given the Microfiche card numbers denoting the location of the references in the Microfiche supplement and the pages of the references reproduced in the Microfiche supplement.

1. Smith, H. H.; and Shahinian, P.: Effect of Oxygen and of Water Vapor on the Fatigue Life of Nickel at 300 C. Effects of Environment and Complex Load History on Fatigue Life. Spec. Tech. Publ. No. 462, ASTM, 1970, pp. 217-233.
2. Davis, Harmer E.; Troxell, George E.; and Wiskocil, Clement T.: The Testing and Inspection of Engineering Materials. Second ed., McGraw-Hill Book Co., Inc., 1955.
3. White, E. L.; and Ward, J. J.: Ignition of Metals in Oxygen. DMIC Rep. 224, Battelle Memorial Inst., Feb. 1, 1966. (Card 1: pp. i, ii, 6-16, A1-A3.)
4. Nihart, G. J.; and Smith, C. P.: Compatibility of Materials With 7500 PSI Oxygen. Union Carbide Corp. (AMRL-TDR-64-67, AD-608260), Oct. 1964. (Card 1: pp. v, 8, 32-34.)
5. Lyman, Taylor, ed.: Metals Handbook. Vol. I. Properties and Selection of Metals. Eighth ed., Am. Soc. Metals, 1961.
6. Wolf, J.; and Brown, W. F., Jr., eds.: Aerospace Structural Metals Handbook. Vols. 1, 2, and 3. Stulen, Inc. (AFML-TR-68-115), 1972.
7. Anon.: Metal Progress Materials and Process Engineering Data Book. Am. Soc. Metals, 1968. (Most recent available edition at time of writing, 1970 edition.) (Card 1: pp. 1-14, 25-27.)
8. Shank, M. E., ed.: Control of Steel Construction to Avoid Brittle Failure. Welding Research Council, 1967.
9. Sisco, Frank T.: Engineering Metallurgy. Pitman Publ. Co., 1957.
10. Anon.: 1971 Annual Book of ASTM Standards. Part 31. ASTM, 1971.
11. Anon.: ASME Boiler and Pressure Vessel Code. Section VIII. Rules for Construction of Pressure Vessels. Divisions 1 and 2. ASME, 1971.
12. Wigley, D. A.: Mechanical Properties of Materials at Low Temperatures. Plenum Press, 1971.
13. Anon.: Low Temperature and Cryogenic Steels. Materials Manual. United States Steel. (Cards 1 and 2: pp. 5-81.)

14. Van Horn, Kent R., ed.: Aluminum. Vol. II. Design and Application. Am. Soc. Metals, 1967.
15. Dean, L. E.; and Thompson, W. R.: Ignition Characteristics of Metals and Alloys. ARS J., vol. 31, no. 7, July 1961. (Card 2: pp. 917-923.)
16. Van Horn, Kent R., ed.: Aluminum. Vol. III. Fabrication and Finishing. Am. Soc. Metals, 1967.
17. Anon.: SAE Handbook. Soc. Automotive Eng., 1969.
18. Key, C. F.; and Riehl, W. A.: Compatibility of Materials with Liquid Oxygen. NASA TM X-985, 1964.
19. Touloukian, Y. S.: Thermophysical Properties of High Temperature Solid Materials. Vol. 2. Parts I and II. MacMillan Co., 1966.
20. Hust, J. G.; Powell, Robert L.; and Weitzel, D. H.: Thermal Conductivity, Electrical Resistivity and Thermopower of Aerospace Alloys From 4 to 300 K. Rep. 9732, National Bureau of Standards (NASA CR-108088), June 9, 1969.
21. Eldridge, E. A.; and Deem, H. W.: Report on Physical Properties of Metals and Alloys from Cryogenic to Elevated Temperatures. Spec. Tech. Publ. No. 296, ASTM, 1961. (Cards 2 and 3: pp. iii, 5-32.)
22. Coston, R. M.: Handbook of Thermal Design Data for Multilayer Insulation Systems. Vol. II. Rep. LMSC-A847882, Vol. II, Lockheed Missiles and Space Co. (NASA CR-87485), June 25, 1967. (Card 3: pp. 2-1 - 2-7, 2-9 - 2-13, 2-15, 2-17, 2-19 - 2-21, 2-23, 2-25, 2-27 - 2-29, 2-31, 2-33 - 2-35, 2-37, 2-39 - 2-41, 2-43, 2-45 - 2-49, 2-51.)
23. Schwartzberg, Fred H.; Osgood, Samuel, H.; Bryant, Carol; and Knight, Marvin: Cryogenic Materials Data Handbook. Rep. AFML-TDR-64-280, Air Force Materials Lab. July 1970.
Vol. I (AD-713619) -- Sections A, B, and C. (Card 3: pp. 42, 43, 75, 96, 97, 176, 204, 227, 238, 246.)
Vol. II (AD-713620) -- Sections D, E, F, G, H, and I. (Card 3: pp. 13, 14, 25, 41, 55, 81, 144, 226.)
24. Van Horn, Kent R., ed.: Aluminum. Vol. I. Properties, Physical Metallurgy and Phase Diagrams. Am. Soc. Metals, 1967.
25. Rosenberg, Samuel J.: Nickel and Its Alloys. Monograph 106, National Bureau of Standards, May 1968. (Card 3: pp. 56-61.)
26. Keuhl, D. K.; and Zwillenberg, M. L.: Investigation of the Ignition and Combustion of Metal Wires. Rep. F910336-24, United Aircraft Research Lab. (NASA CR-89788), May 1967.

27. Browning, Ethel: Toxicity of Industrial Metals. Second ed., Butterworths & Co., 1969.
28. Reynolds, W. C.: Investigation of Ignition Temperatures of Solid Metals. NASA TN D-182, 1959. (Card 4: All.)
29. Glassman, I.; Mellor, A. M.; Sullivan, H. F.; and Laurendeau, N. M.: A Review of Metal Ignition and Flame Models. Reactions between Gases and Solids. Conf. Proc. No. 52, AGARD, Feb. 1970. (Cards 4 and 5: pp. 19-1 - 19-30, 19-App-1 - 19-App-9.)
30. Carslaw, H. S.; and Jaeger, J. C.: Conduction of Heat in Solids. Clarendon Press, 1950.
31. Arpaci, Vedat S.: Conduction Heat Transfer. Addison-Wesley Publ. Co., 1966.

BIBLIOGRAPHY

- Anon.: ALCOA Structural Handbook. Aluminum Company of America, 1960.
- Anon.: Behavior of Materials at Cryogenic Temperatures. Spec. Tech. Publ. No. 387, ASTM, 1966.
- Anon.: Evaluation of Metallic Materials in Design for Low Temperature Service. Spec. Tech. Publ. No. 302, ASTM, 1962.
- Anon.: Low Temperature Mechanical Properties of Various Alloys. NASA SP-5921(01), 1970.
- Anon.: Military Standardization Handbook - Metallic Materials and Elements for Aerospace Vehicle Structures, Two Volumes, MIL-HDBK-5B, Sept. 1, 1971.
- Anon.: The Mechanical Properties of Copper-Beryllium Alloy Strip. Spec. Tech. Publ. No. 367, ASTM, 1964.
- Bell, Joseph H., Jr.: Cryogenic Engineering. Prentice-Hall, Inc., 1963.
- Boyd, G. M., ed.: Brittle Fracture in Steel Structures. Butterworth & Co., 1970.
- Christian, J. L.: Evaluation of Materials and Test Methods at Cryogenic Temperatures. Rep. ERR-AN-400, General Dynamics/Astronautics, Dec. 10, 1963.
- Frank, Robert G.; and Zimmerman, William F.: Materials for Rockets and Missiles. MacMillan Co., 1959.
- Groenveld, T. P.; et al.: High-Strength Steel 9Ni-4Co - Processes and Properties Handbook. Battelle Memorial Inst., Apr. 1968.
- Martin, H. L.; et al.: Effects of Low Temperatures on the Mechanical Properties of Structural Metals - Revised and Enlarged Edition. NASA SP-5012(01), 1968.
- Parker, Earl R., ed.: Materials for Missiles and Spacecraft. McGraw-Hill Book Co., Inc., 1963.
- Sessler, J., and Weiss V.: Materials Data Handbook(s):
Aluminum Alloy 2014. NASA Tech. Support Pkg. 67-10089, Apr. 1966.
Aluminum Alloy 2219. NASA Tech. Support Pkg. 67-10089, Mar. 1966.
Aluminum Alloy 5456. NASA Tech. Support Pkg. 67-10089, May 1966.
Aluminum Alloy 6061. NASA Tech. Support Pkg. 69-10065, June 1969.
Inconel Alloy 718. NASA Tech. Support Pkg. 67-10282, Sept. 1966.
Type 301 Stainless Steel, NASA Tech. Support Pkg. 67-10089, June 1966.
- Touloukian, Y. S., ed.: Recommended Values of the Thermophysical Properties of Eight Alloys, Major Constituents and Their Oxides. Purdue University, Feb. 1966.

- Varley, P. C.: The Technology of Aluminum and its Alloys. CRC Press, 1970.
- Williams, L. R.; Schmidt, E. H.; and Young, J. D.: Design and Development Engineering Handbook of Thermal Expansion Properties of Aerospace Materials at Cryogenic and Elevated Temperatures. Rep. R-6981, North American Aviation (NASA CR-102331), Mar. 30, 1969.
- Wood, R. A.: A New Aluminum Sand Casting Alloy of High Toughness (M-45). SP-5091, 1970.

NASA SP-3077
MF SUPPLEMENT

REFERENCES

In parentheses after most references are given the Microfiche card numbers denoting the location of the references in the Microfiche supplement and the pages of the references reproduced in the Microfiche supplement.

1. Smith, H. H.; and Shahinian, P.: Effect of Oxygen and of Water Vapor on the Fatigue Life of Nickel at 300 C. Effects of Environment and Complex Load History on Fatigue Life. Spec. Tech. Publ. No. 462, ASTM, 1970, pp. 217-233.
2. Davis, Harmer E.; Troxell, George E.; and Wiskocil, Clement T.: The Testing and Inspection of Engineering Materials. Second ed., McGraw-Hill Book Co., Inc., 1955.
3. White, E. L.; and Ward, J. J.: Ignition of Metals in Oxygen. DMIC Rep. 224, Battelle Memorial Inst., Feb. 1, 1966. (Card 1: pp. i, ii, 6-16, A1-12.)
4. Nihart, G. J.; and Smith, C. P.: Compatibility of Materials With 7500 PSI Oxygen. Union Carbide Corp. (AMRL-TDR-64-67, AD-608260), Oct. 1964. (Card 1: pp. v, 8, 32-34.)
5. Lyman, Taylor, ed.: Metals Handbook. Vol. I. Properties and Selection of Metals. Eighth ed., Am. Soc. Metals, 1961.
6. Wolf, J.; and Brown, W. F., Jr., eds.: Aerospace Structural Metals Handbook. Vols. 1, 2, and 3. Stulen, Inc. (AFML-TR-68-115), 1972.
7. Anon.: Metal Progress Materials and Process Engineering Data Book. Am. Soc. Metals, 1968. (Most recent available edition at time of writing, 1970 edition.) (Card 1: pp. 1-14, 25-27.)
8. Shank, M. E., ed.: Control of Steel Construction to Avoid Brittle Failure. Welding Research Council, 1967.
9. Sisco, Frank T.: Engineering Metallurgy. Pitman Publ. Co., 1957.
10. Anon.: 1971 Annual Book of ASTM Standards. Part 31. ASTM, 1971.
11. Anon.: ASME Boiler and Pressure Vessel Code. Section VIII. Rules for Construction of Pressure Vessels. Divisions 1 and 2. ASME, 1971.
12. Wigley, D. A.: Mechanical Properties of Materials at Low Temperatures. Plenum Press, 1971.
13. Anon.: Low Temperature and Cryogenic Steels. Materials Manual. United States Steel. (Cards 1 and 2: pp. 5-81.)

14. Van Horn, Kent R., ed.: Aluminum. Vol. II. Design and Application. Am. Soc. Metals, 1967.
15. Dean, L. E.; and Thompson, W. R.: Ignition Characteristics of Metals and Alloys. ARS J., vol. 31, no. 7, July 1961. (Card 2: pp. 917-923.)
16. Van Horn, Kent R., ed.: Aluminum. Vol. III. Fabrication and Finishing. Am. Soc. Metals, 1967.
17. Anon.: SAE Handbook. Soc. Automotive Eng., 1969.
18. Key, C. F.; and Riehl, W. A.: Compatibility of Materials with Liquid Oxygen. NASA TM X-985, 1964.
19. Touloukian, Y. S.: Thermophysical Properties of High Temperature Solid Materials. Vol. 2. Parts I and II. MacMillan Co., 1966.
20. Hust, J. G.; Powell, Robert L.; and Weitzel, D. H.: Thermal Conductivity, Electrical Resistivity and Thermopower of Aerospace Alloys From 4 to 300 K. Rep. 9732, National Bureau of Standards (NASA CR-108088), June 9, 1969.
21. Eldridge, E. A.; and Deem, H. W.: Report on Physical Properties of Metals and Alloys from Cryogenic to Elevated Temperatures. Spec. Tech. Publ. No. 296, ASTM, 1961. (Cards 2 and 3: pp. iii, 5-32.)
22. Coston, R. M.: Handbook of Thermal Design Data for Multilayer Insulation Systems. Vol. II. Rep. LMSC-A847882, Vol. II, Lockheed Missiles and Space Co. (NASA CR-87485), June 25, 1967. (Card 3: pp. 2-1 - 2-7, 2-9 - 2-13, 2-15, 2-17, 2-19 - 2-21, 2-23, 2-25, 2-27 - 2-29, 2-31, 2-33 - 2-35, 2-37, 2-39 - 2-41, 2-43, 2-45 - 2-49, 2-51.)
23. Schwartzberg, Fred H.; Osgood, Samuel, H.; Bryant, Carol; and Knight, Marvin: Cryogenic Materials Data Handbook. Rep. AFML-TDR-64-280, Air Force Materials Lab. July 1970.
Vol. I (AD-713619) -- Sections A, B, and C. (Card 3: pp. 42, 43, 75, 96, 97, 176, 204, 227, 238, 246.)
Vol. II (AD-713620) -- Sections D, E, F, G, H, and I. (Card 3: pp. 13, 14, 25, 41, 55, 81, 144, 226.)
24. Van Horn, Kent R., ed.: Aluminum. Vol. I. Properties, Physical Metallurgy and Phase Diagrams. Am. Soc. Metals, 1967.
25. Rosenberg, Samuel J.: Nickel and Its Alloys. Monograph 106, National Bureau of Standards, May 1968. (Card 3: pp. 56-61.)
26. Keuhl, D. K.; and Zwillenberg, M. L.: Investigation of the Ignition and Combustion of Metal Wires. Rep. F910336-24, United Aircraft Research Lab. (NASA CR-89788), May 1967.

27. Browning, Ethel: Toxicity of Industrial Metals. Second ed., Butterworths & Co., 1969.
28. Reynolds, W. C.: Investigation of Ignition Temperatures of Solid Metals. NASA TN D-182, 1959. (Card 4: All.)
29. Glassman, I.; Mellor, A. M.; Sullivan, H. F.; and Laurendeau, N. M.: A Review of Metal Ignition and Flame Models. Reactions between Gases and Solids. Conf. Proc. No. 52, AGARD, Feb. 1970. (Cards 4 and 5: pp. 19-1 - 19-30, 19-App-1 - 19-App-9.)
30. Carslaw, H. S.; and Jaeger, J. C.: Conduction of Heat in Solids. Clarendon Press, 1950.
31. Arpaci, Vedat S.: Conduction Heat Transfer. Addison-Wesley Publ. Co., 1966.

REFERENCE

1

SMITH, H. H.; AND SHAHINIAN, P.: EFFECT OF OXYGEN AND OF WATER VAPOR ON THE FATIGUE LIFE OF NICKEL AT 300C. EFFECTS OF ENVIRONMENT AND COMPLEX LOAD HISTORY ON FATIGUE LIFE. SPEC. TECH. PUBL. NO. 462, ASTM, 1970.

THIS REFERENCE IS COPYRIGHTED MATERIAL AND THEREFORE THE CONTENTS HAVE NOT BEEN REPRODUCED FROM THE TEXT.

END OF REFERENCE

1

REFERENCE

2

DAVIS, HARMER E.; TROXELL, GEORGE E.; AND WISKOCIL, CLEMENT T.: THE TESTING AND INSPECTION OF ENGINEERING MATERIALS. SECOND ED., MCGRAW-HILL BOOK CO., INC., 1955.

**THIS REFERENCE IS COPYRIGHTED MATERIAL AND THEREFORE
THE CONTENTS HAVE NOT BEEN REPRODUCED FROM THE TEXT.**

END OF REFERENCE

2

REFERENCE

3

**WHITE, E. L.; AND WARD, J. J.: IGNITION OF METALS IN
OXYGEN. DMIC REP. 224, BATTELLE MEMORIAL INST.,
FEB. 1, 1966.**

LEWIS RESEARCH CENTER
Aerospace Safety Research
and Data Institute

RECEIVED
TO
PEOVCH
H.S. 6-2

X66-21588
DMIC Report 224
February 1, 1966

3.1-0-1 X

1.1.2

IGNITION OF METALS IN OXYGEN

DEFENSE METALS INFORMATION CENTER

Battelle Memorial Institute
Columbus, Ohio 43201

LIBRARY COPY

JUL 22 1970

LEWIS LIBRARY, NASA
CLEVELAND, OHIO

DMIC Report 224
February 1, 1966

IGNITION OF METALS IN OXYGEN

by

E. L. White and J. J. Ward

to

**OFFICE OF THE DIRECTOR OF DEFENSE
RESEARCH AND ENGINEERING**

DEFENSE METALS INFORMATION CENTER
Battelle Memorial Institute
Columbus, Ohio 43201

IGNITION OF METALS IN OXYGEN

E. L. White and J. J. Ward*

SUMMARY AND CONCLUSIONS

The ignition of metals in oxygen and oxygen atmospheres was reviewed from the viewpoints of (a) methods that have been used to study behavior, (b) experimental values that have been obtained, and (c) the status of theories that permit the calculation of ignition temperatures.

While no clearcut definition of ignition temperature has been developed, it appears probable that a definite or an absolute ignition temperature does exist for a particular metal-oxygen system. In general terms, if the energy input as converted to heat is greater than the heat dissipation, a temperature will be reached at which ignition of the metal will occur. Practically, this temperature appears dependent on many factors some of which are relatively static (e. g. , atmosphere, composition, purity, metal surface area and condition, etc.) and others that may be dynamic (e. g. , pressure, impact, impact velocity, vibration, etc.). No standard test procedures or methods have been developed to evaluate the ignition temperatures of metals. The net result is that varying values have been reported for the same or similar metal-oxygen systems.

Despite these differences, the following generalizations can be offered on the basis of the experimental evaluations performed to date:

- (1) All metals, with the possible exception of gold and platinum, can be expected to ignite in oxygen at some elevated temperature.
- (2) Alloys of several systems have been shown to ignite in oxygen systems at relatively low temperatures and some at LOX temperatures if some external source of energy input is present. Generally, the presence of a fresh metal surface is also necessary to cause ignition at these low temperatures. These ignition-sensitive alloy systems include the alloys of titanium, zirconium, thorium, uranium, lead, tin, and magnesium.
- (3) A number of secondary energy input sources have been shown to cause ignition of these sensitive alloys in oxygen systems. These sources also probably produce a fresh metal surface and are identified as follows:

In Gaseous Oxygen

Electric spark	Stress rupture
Puncture	Explosive shock.

In Liquid Oxygen

Mechanical impact	Puncture
Explosive shock.	

- (4) A number of other methods of secondary energy input and methods of exposing fresh metal do not produce ignition. These are as follows:

In Gaseous Oxygen

High-velocity flow
Low-cycle fatigue cracking
Impact on the outside of a container without puncture
High-velocity flow through a small orifice
Rapid pressurization

In Liquid Oxygen

Impact on the outside of a container without puncture
Rapid pressurization
Machining
Friction and galling
Tensile rupture
Mechanical vibration
Sonic vibration
Ultrasonic vibration
High-velocity flow through an orifice.

- (5) An increase in pressure of a gaseous oxygen system tends to promote ignition at lower temperatures or with lower secondary energy inputs. The dilution of oxygen with an inert material, gaseous or liquid, tends to reduce sensitivity of metals in oxygen systems. However, propagation is not affected much until the dilution is very great, on the order of 90 percent inert gas or liquid.

*Research Chemical Engineer and Fellow in the Corrosion Research and Materials Thermodynamics Divisions, respectively, Battelle Memorial Institute, Columbus, Ohio.

(6) A number of alloy systems have been shown to be relatively insensitive to ignition in an oxygen environment either at high temperatures or at low temperatures with high secondary energy inputs. These alloy systems include: austenitic stainless steels, nickel alloys, cobalt alloys, copper alloys, and silver alloys. Alloys of these systems show the best service record and also show the least sensitivity in laboratory tests.

(7) Another group of alloys appears to be somewhat intermediate between the sensitive and insensitive groups cited in Items 2 and 6. This group includes aluminum alloys, the 400 series stainless steels, and carbon and low-alloy high-strength steels. These materials would be expected to find limited use in relatively nonsensitive applications.

A review of the theoretical analysis of the spontaneous ignition of metals in oxygen has shown the following:

(1) A theoretical model for the spontaneous ignition of massive metal in gaseous oxygen at high temperatures (above 1500 F) has been developed, based on low-temperature oxidation-reaction data and thermophysical property data.

(2) Several theoretical models for the calculation of ignition temperature of metal particles in gaseous oxidation have been developed that agree qualitatively. These models explain why particle radius is an important variable in powder combustion. Much of this work has been directed to the application of metal powder as a fuel.

(3) Practically no quantitative method is available for the calculation of ignition temperatures of massive metal in cryogenic oxidizers, such as liquid oxygen. Several good qualitative descriptions of the possible mechanism for massive metal-liquid oxygen reactions have been made. For this reason, the possible role of shock loading and energy input sufficient to give local ignition temperatures has been considered and reviewed in this report.

In the development and discussion of theoretical calculational models, a number of thermochemical and thermophysical constants are required. Therefore, a literature search was made, and a compilation of data for these constants was given. The data included standard free energy of oxide formation as an extent of metal-oxygen reaction. Also, heat-capacity values, vapor-pressure data, and thermophysical properties of melting and boiling points were included. Thermal-conductivity values of metals and oxides were included when they could be found. Heats of metal-oxide formation were tabulated. These values, with heat-capacity data, were used in calculating temperature rise on reaction.

For those who may be interested in pursuing the theoretical-calculation ignition temperatures, this report also summarizes the following thermochemical and thermophysical data for most metals and their oxides:

- (a) Standard free energy of formation
- (b) Heat capacity
- (c) Vapor pressure
- (d) Melting and boiling points
- (e) Thermal conductivity.

done by impacting an hydraulic cylinder or by pressurization. The orifices have been formed by several means; by drilling, or by using a small pinhole or small crack already in the metal. High-velocity flow through small holes and cracks has not resulted in ignition with either LOX or gaseous oxygen, even with the more sensitive metals.

Fatigue Tests

A few fatigue tests have been conducted in gaseous oxygen. These were in 60-psi oxygen at room temperature. (17) Though actual ignition did not occur in these tests, tarnished spots indicated that it is possible to ignite at least the active metals by fatigue failures. It is probable that ignition would not occur until the piece actually cracked completely through or at least under conditions under which the crack begins to propagate very rapidly.

EXPERIMENTAL VALUES OF IGNITION TEMPERATURE

The following sections of this report describe the results of tests that have been performed with a variety of conditions and methods to determine the ignition temperatures of metals in oxygen systems. Both reactions with liquid and gaseous oxygen are considered.

Most of the data generated have been for titanium and its alloys with somewhat lesser attention being given to aluminum, magnesium, and stainless steels. Correspondingly less information is available for other metals and their alloys. Also, more attention has been given to the ignition of metals in gaseous oxygen and oxygen mixtures than in liquid oxygen. To assist the reader in comparing the ignition temperatures that have been measured for all of these metals and alloys in gaseous oxygen and oxygen mixtures, Appendix A summarizes the available data.

Titanium Alloys

Ignition in Gaseous Oxygen at High Temperatures

It has been shown that titanium and its alloys will ignite in gaseous oxygen when they are heated to temperatures several hundred degrees below the metal melting point of titanium, 3034 F (1668 C). Relatively massive specimens (1/16-in. wires to 0.5-in. tubes) have been shown to ignite in the range of 2372 to 2912 F (1300 to 1600 C), when resistance heated in static oxygen atmospheres.

Effect of Oxygen Pressure. An increase in oxygen pressure above atmospheric pressure has been shown to lower the ignition point several hundred degrees C. At oxygen pressures of 300 to 500 psi, the ignition temperature is lowered to 1598 to 2012 F (870 to 1100 C). (3,4)

Effect of Dilution of Oxygen. Titanium also will ignite in air in the same temperature range as in oxygen. (2) Some titanium alloys (Ti-8Mn and Ti-5Al-2.5Sn) ignite at somewhat higher temperatures in air than in oxygen. (2) This ignition takes place at temperatures at or just above their melting points.

It has been shown that titanium will ignite in more dilute mixtures than air, such as 50CO₂-50CO₂ mixture, if the range is the same as in oxygen at 300 psi. Titanium will also ignite in CO₂ atmospheres and in nitrogen at temperatures below the melting point under pressure. (3,4)

Effect of Velocity. The ignition temperatures of titanium and its alloys have been shown to be nearly the same in high-velocity air streams as in static or slow-moving air. (2)

Ignition in Gaseous Oxygen at Ambient and Moderate Temperatures

Massive titanium will not ignite in air or oxygen at ambient or moderate temperatures, unless there is a secondary input of energy usually accompanied by the exposure of a fresh metal surface. Titanium powders will ignite at as low as 680 F (360 C) in clouds or 950 F (510 C) in layers. (21)

Ignition by Electric Spark. An electric spark with an energy input of 25 millijoules will ignite a cloud of titanium powder at room temperature and atmospheric pressure. (21) Massive titanium can also be ignited by an electric spark in gaseous oxygen at room temperature and atmospheric pressure with a spark energy of 1 to 10 joules. (16) Lower energies were required for 0.005-in. sheet than for 0.007- and 0.010-in. sheet. The test was performed by bringing a steel needle close to a titanium plate and allowing a spark to jump from one to the other. A modification in which the needle was the titanium sample gave similar results. Neither steel nor aluminum ignited in the same type of test. The oxygen flow rate, the extent of confinement, and the point of spark impingement appeared to affect the results.

The variations observed would indicate that the heat balance of the system is one of the controlling factors in ignition by spark, as has been found with ignition in high-temperature oxygen. Also, since the point of impingement seemed to be involved, there may be spots on a titanium surface that are more active than others or have a thinner or cracked scale.

Ignition by Stress Rupture. Massive metal will ignite in gaseous oxygen at room temperature at pressures above atmospheric pressure, if there is also a secondary input of energy from tensile rupture of the metal, accompanied by exposure of a fresh metal surface. (16) The pressure required was shown to be 350 psi. (20)

These effects of pressure on ignition temperature are shown in Figure 2. Ignition at somewhat lower pressures (about 60 psi) was indicated in other tests, (22) as shown in Figure 3. The Ti-6Al-4V alloy required a slightly higher pressure than the pure metal. The dilution of oxygen with helium increased the pressure required to cause ignition. At 65 percent oxygen about 1000 psi pressure is required. Below 35 percent oxygen (see Figure 4) titanium would not be expected to ignite, even at very high pressures. Under dynamic flow conditions such as caused by puncturing a pressure vessel, the pressures required for ignition are approximately 250 psi less than under static conditions. (20)

An increase in temperature above room temperature lowers the pressure required to ignite titanium under stress-rupture conditions. The pressure decreases from 350 to 50 psi at 1200 F (Figure 2).

The observation has been that once a piece of titanium is ignited, it continues to burn until all of the metal or all of the oxygen is gone. Propagation data have been developed that indicate that even in dilute mixtures of oxygen, burning can propagate at moderate pressures of 200 psi even though ignition cannot occur. Therefore, dilution of the oxygen after ignition would not be expected to cause quenching until the oxygen became very dilute or the temperature was lowered rapidly.

Effect of Low-Cycle Fatigue. The energy concentration by low-cyclic fatigue is probably smaller than with stress rupture. However, as a crack propagates, fresh metal surfaces are exposed. Fatigue tests in gaseous oxygen at 60 psi and room temperature did not result in burning at the bare metal areas. (17) However, slightly tarnished spots were observed, which indicated that high temperatures had been reached.

Effect of Mechanical Impact on the Outside of a Gaseous-Oxygen Container. No reactions occurred when the outside of a gaseous-oxygen (50 psi) container was struck with 140 ft-lb force. In four trials, the blow crushed the container but did not puncture it. (16) This indicates the energy input in the form of heat was not concentrated enough to cause ignition.

Ignition of Titanium in Gaseous Oxygen Below Room Temperature

Effect of Stress Rupture. At the low temperatures associated with LOX (-250 F), titanium ruptured under stress requires a higher pressure for ignition to occur than when ruptured at room temperature (see Figure 3). (19)

Effect of Flow Through a Small Orifice. A specimen of welded titanium containing a minute orifice was pressurized twice to 100 psig, which caused a stream of oxygen to flow through the orifice. No reaction occurred. In another experiment, a specimen containing a small crack was

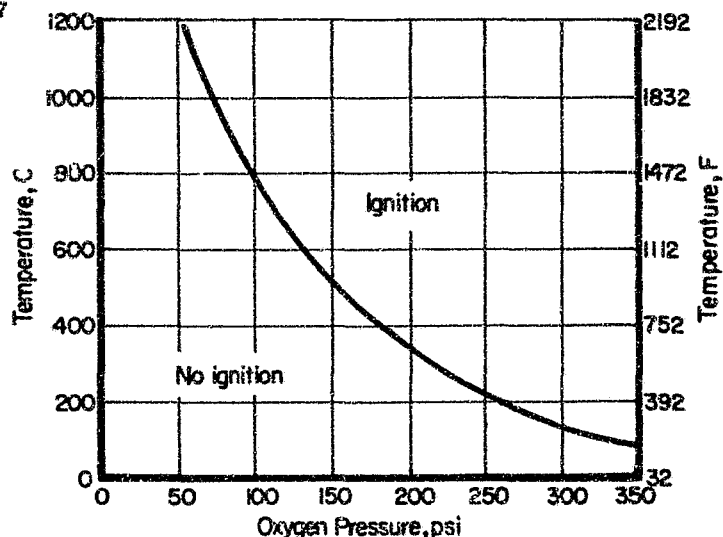


FIGURE 2. EFFECT OF TEMPERATURE ON SPONTANEOUS IGNITION OF RUPTURED TITANIUM IN OXYGEN(22)

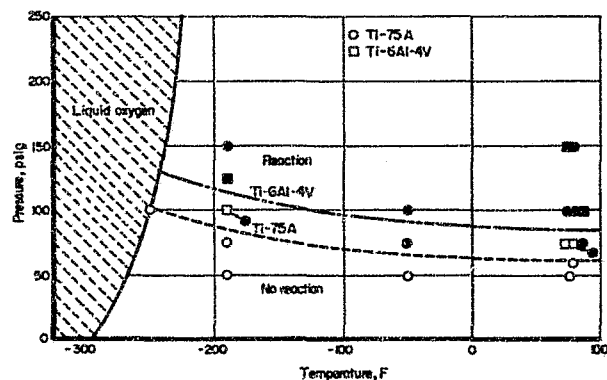


FIGURE 3. REACTIVITY OF TITANIUM RUPTURED IN GASEOUS OXYGEN(18)

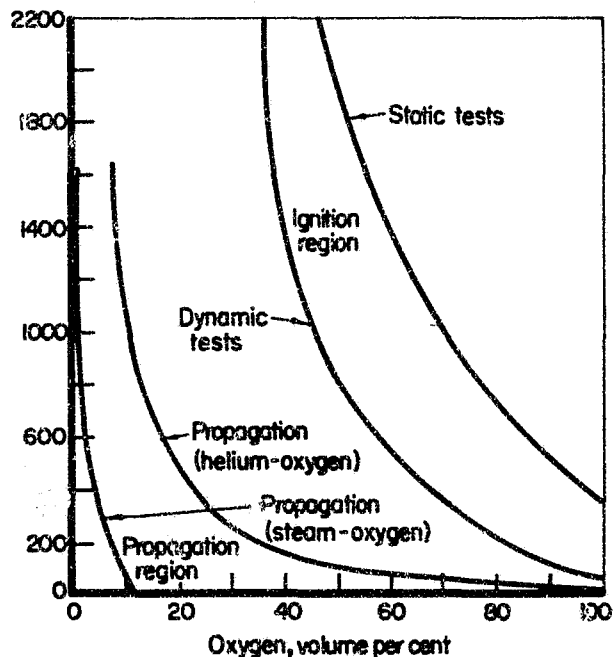


FIGURE 4. IGNITION AND PROPAGATION LIMITS OF TITANIUM IN HELIUM-OXYGEN AND STEAM-OXYGEN MIXTURES(22)

pressurized with 100-psig oxygen until it propagated to 1-1/2 inches in length. No reaction occurred. (16)

Reaction of Titanium Alloys With Liquid Oxygen

Titanium and its alloys are not expected to react violently with LOX under static conditions at the boiling point of the liquid. The normal oxidation rate is quite low at this temperature. However, it has been found that, under these conditions, titanium and its alloys can be caused to ignite with only a small amount of energy input. The factors that appear critical here are those that lead to concentrations of energy in the form of heat to raise the temperature at local sites, and the exposure of fresh metal surfaces.

Ignition by Impact. Investigators are agreed that mechanical impact is one source of energy that causes the ignition of titanium and its alloys in LOX. In the study of impact ignition of titanium and other materials, it has been found that organic materials, such as oils and greases, that are often found on metals, are very sensitive to impact. If the titanium surface were contaminated with organic compounds, ignition of the metal would occur more readily. Therefore, the degree of cleanliness of the surface may affect test results or cause unexplained field failures. Other types of dirt, such as metal filings and grit on the metal surface, produce more reactivity in impact tests.

The effect of impacting titanium in LOX has been investigated by a number of people using drop-weight-type testers. (11-12, 14-18, 23-24) In these experiments, various weights were dropped from different heights with various striker designs and areas of impact. These variations in equipment resulted in the same ft-lb input with different heights of fall and different velocities and area effects.

In addition to titanium, the following alloys have been evaluated:

Ti-5Al-2.5Sn
Ti-6Al-4V
Ti-40A
Ti-13V-11Cr-3Al
Ti-25Zr (experimental alloy).

After examining data from various sources, it was concluded⁽²⁵⁾ that the unalloyed titanium is slightly less sensitive to impact in LOX than the titanium alloys studied. Most of the data show impact sensitivities in the 10 to 70 ft-lb range, and many ignitions in the 10 to 30 ft-lb range. As has been mentioned before, no ignitions in 20 tests or one ignition in 60 tests are the accepted limits of impact sensitivity for safe practice. By these criteria, titanium alloys have been ranked

as unacceptable as a LOX container material and are ranked as being similar to such organic materials as Buna N, polyethylene, and Styrofoam. (16)

A number of surface treatments and coatings have been evaluated as to their effect on the impact sensitivity of titanium alloys in LOX. Some treatments found either to increase or to have little effect on impact sensitivity are noted as follows:

- (1) Mechanical polishing was shown to improve the resistance by one investigator, (18) whereas in another case, it seemed to increase sensitivity. (16)
- (2) Pickling was shown to increase both the frequency and the violence of the ignition reactions. (16)
- (3) Passivation with H_2O_2 increased the sensitivity to LOX. (16) Passivation in boiling nitric acid also increased the sensitivity. (19) Treatment in boiling potassium hydroxide may have produced some slight reduction in sensitivity. (16)
- (4) A number of phosphate-coating treatments have been tried on titanium. These include manganese phosphate, iron phosphate, and others. None of these conversion-coating treatments produced a substantial improvement in the impact-sensitivity situation. (16) The fluoride-phosphate treatment, which forms a heavy coating, produced only a small decrease in sensitivity. (26)
- (5) Anodizing of a titanium surface by several methods to prepare both thin or thick coatings did not improve the resistance of the base metal to impact sensitivity. (16)
- (6) The ceramic coatings that have been tried have produced no improvement in LOX sensitivity over that of the base metal. (16)
- (7) Teflon coatings reduced the LOX sensitivity, but not enough to be useful. (16)
- (8) Flame-sprayed aluminum coatings (16) and vapor-deposited aluminum coatings (26) provide some protection, but not enough to be useful.
- (9) Oxide films produced by annealing in vacuum and air cooling decreased the sensitivity somewhat, but not enough to be of any real value. (16)

- (10) Although the data regarding the method of application or thickness were not discussed in detail, gold and silver coatings were ineffective in reducing impact sensitivity.

Other types of coatings appear to provide enough reduction in impact sensitivity so that they might find limited use. Even these protective measures would be limited by the fact that damage to the coatings probably would destroy their effectiveness. These coatings are described as follows:

- (1) A nitrided layer can be formed on titanium alloys by heating at 1500 F in a nitrogen atmosphere for 3 hours. This surface treatment produced good results in that no burning occurred in the tests and only two flashes were produced. (16) This treatment might be undesirable because the metal becomes slightly embrittled by the treatment.
- (2) Electroplated coatings (about 0.5 mil thick) of copper and nickel effectively reduce the impact sensitivity of titanium in LOX. (16) These coatings may be of some practical value, although they are difficult to apply to large items.
- (3) Electroless copper and nickel coatings would be much easier to apply to the inside of such items as tanks. Thin coatings, about 0.2 mil thick, effectively reduce impact sensitivity to an acceptable level for limited use. The weight added is somewhat less than with the electroplated coatings, but the adherence may be somewhat less. (16) The latter may be a function of the method of application.
- (4) It has been found that aluminum cladding, probably a thick coating, prevents the spontaneous ignition of titanium when exposed to pressurized LOX. (28)

Ignition by Explosive Shock. Titanium and titanium alloys can be caused to ignite in LOX by explosive shock waves. (16) Three different test methods were used in this study. In the first test procedure, the spacing between the charge and the acceptor (test specimen) was fixed and the size of the charge was varied. No direct measure was made of the shock, but the variations in amount of charge required to ignite several materials can be compared. It was found that in the equipment for 0.010- and 0.035-in.-thick Ti-5Al-2.5Sn alloy sheet, only the cap (M36Al) was required to cause ignition. Only 0.84 inch of No. 40 primacord had to be added to the cap to ignite

0.063-in.-thick specimens. In contrast, Mg-HK31XA-H24, Al 5052-H34, or stainless Type 301 required much larger charges (see Table 1). Titanium was more sensitive than two gasket materials, Allpax 500 and Johns Manville 76, and was even more sensitive than No. 400 or No. 200 primacord in the same system, with water substituted for the LOX.

The other test methods were designed so that the spacing could be varied and the donor charge and the specimens kept constant. (16) Titanium was again found to be far more sensitive than either an aluminum alloy or a stainless steel (Table 1).

Copper or nickel electroless plating on unalloyed titanium results in some improvement over the uncoated Ti-5Al-2.5Sn alloy. However, the slight improvement gained with these coatings would not be sufficient protection. Nickel- and copper-coated titanium are rated more sensitive than a magnesium alloy, an aluminum alloy, or stainless steel.

Ignition of Titanium in Liquid Oxygen by Puncture. A number of experiments have been conducted to determine the effect of puncturing a container of LOX. In the standard gun-fire test, a 50-calibre, armor-piercing incendiary bullet was fired through a plywood sheet to produce tumbling upon entry into a titanium pressure bottle. Upon impact, a huge flash was observed together with a violent reaction. (14) The pressure bottle was fragmented. Fusion and burning had occurred on some of the fractured faces. However, the reaction did not propagate and the LOX was not consumed. Similar tests showed that the reactions were more violent when the LOX was not dry (i. e., when it contained ice particles).

In other tests, (16) nonincendiary bullets and 1/8-in. pointed rods were fired into Ti-5Al-2.5Sn tanks filled with LOX. With the rods, one of two burned fast and then detonated; another rod sealed the hole, but later the tank exploded by an unexplained mechanism. With the bullet, the LOX tank first burned and then exploded. The burning started immediately after the puncture, then subsided slightly before the explosion.

In tests on Ti-5Al-2.5Sn (16,29) and Ti-6Al-4V, (29) LOX containers were punctured by pins driven by falling weights. The containers did not burn every time, but the frequency was very high, i. e., in 12 of 15 times in one test and in 20 of 21 times in another. No reactions occurred with aluminum or stainless steel under these conditions. It has also been reported that punctures of LOX tanks caused by small steel and nylon pellets resulted in violent explosions. (16)

From the above experiments, it is clear that the puncture of a titanium-alloy LOX tank will

TABLE 1. SUMMARY OF SHOCK-SENSITIVITY RESULTS

Material	Thick- ness, inch	Test Method I - Stimulus From Donor (Cap and Primacord)		Test Method II - Stimulus From Donor (Cap and Primacord)		Gap(a) for Ignition, inches	Test Method III - Stimulus From Donor (Cap and Primacord)		Gap(a) for Ignition, inches
		Inches of Prima- cord(b)	Size of Primacord, gr/ft(b)	Inches of Prima- cord(b)	Size of Primacord, gr/ft(b)		Inches of Prima- cord(b)	Size of Primacord, gr/ft(b)	
<u>Reactions With LOX</u>									
Ti-5Al-2.5Sn	0.063	0.84	40	2	400	2.88	Cap only	--	1.55
Ditto	0.063	--	--	--	--	--	2	400	2.92
"	0.035	Cap only	--	--	--	--	12	400	2.44
"	0.035	--	--	--	--	--	12	400	3.00
"	0.010	Cap only	--	Cap only	--	0.36	12	400	3.90
Al-5052-T34	0.063	12	238	2	400	0.61	12	400	0.95
Ditto	0.035	12	224	--	--	--	12	400	2.10
Type 301 stainless steel	0.035	>>12	400	--	--	--	--	--	--
Titanium, copper plated	0.010	12	100	--	--	--	12	400	2.50
Titanium, nickel plated	0.010	12	84	--	--	--	12	400	2.50
Mg-HK31XA-H34	--	12	189	--	--	--	--	--	--
<u>Reactions in Gaseous Oxygen</u>									
Ti-5Al-2.5Sn	0.063	1.5	40	--	--	--	12	400	2.13
Ditto	0.032	--	--	--	--	--	12	400	2.75
"	0.010	Cap only	--	--	--	--	--	--	--
Al-5052-H34	0.063	12	283	2	400	0.46	12	400	1.37
Ditto	0.035	12	224	--	--	--	--	--	--

(a) Larger gap indicates the material is more sensitive.

(b) Smaller size or shorter primacord means more sensitive.

almost certainly result in burning that may be accompanied by a violent detonation. Three sensitizing mechanisms appear to be at work:

- (1) Impact by the puncturing tool
- (2) Exposure of fresh titanium surface
- (3) High-velocity flow past the bare metal surface.

A secondary mechanism may be that rapid pressurization, due to liquid evaporation, takes place because of the heat produced from the initial reaction. This accompanying pressure increase results in the violent detonation.

The effect of the size of the puncturing tool is illustrated by micrometeoroid puncture tests.⁽²⁹⁾ These tests, using very small "bullets" (0.1 to 0.2 gram) fired at high velocities of 9,100 to 15,000 ft/sec, resulted in ignition of the titanium at the side of entry about half the time, and on the opposite side in 15 of 16 times.

The data indicate that puncture caused by either small particles at high velocity or larger tools at much lower velocities results in ignition of titanium alloy in contact with LOX.

Effect of Mechanical Impact on the Outside of a Liquid-Oxygen Container. Experiments were conducted at as high as 140 ft-lb impact to determine if mechanical impact on the outside of a LOX container would have the same effect as impact in contact with the LOX. These tests did not result in ignition; the input of energy is probably

less than that from the detonation-type tests but is at least 7 times as great as the "in LOX" type of impact that produces ignition.⁽¹⁶⁾

Similar tests⁽¹⁸⁾ showed no reaction when titanium tubes containing LOX were crushed with 70 ft-lb of impact.

Effect of Rapid Pressurization. Titanium-alloy LOX tanks have been shown to withstand 250 pressurization cycles 0 to 1500 psi without ignition. The pressurization cycle consisted of almost instantaneous rise to 1500 psi in 0.6 second and back to 0 psi in a total of 2 seconds.⁽¹⁶⁾ LOX was also compressed in an hydraulic cylinder by application of 70 ft-lb of force from a dropped weight. A titanium specimen at the bottom of the pressurized cavity did not ignite.

Effect of Dilution by Liquid Nitrogen. Experiments have shown that titanium is impact sensitive in LOX even when it is diluted with large amounts of liquid nitrogen (LN₂).⁽¹⁶⁾ Only when the LN₂ dilution reaches 70 percent (almost liquid air) does the titanium become nonreactive at the 70 ft-lb level (see Table 2).

TABLE 2. EFFECT OF LIQUID-NITROGEN DILUTION ON LIQUID-OXYGEN IMPACT SENSITIVITY OF Ti-5Al-2.5Sn TITANIUM⁽¹⁶⁾ (0.063 in. thick)

LN ₂ , percent	Reactions per No. of Tests at Indicated Impact, ft-lb							
	72	65	58	51	43	36	22	7
0	11/20	--	--	--	--	3/20	1/20	0/20
50	1/20	3/20	3/20	0/20	0/20	--	--	--
60	2/20	--	--	2/20	1/20	0/20	--	--
70	0/20	0/20	--	--	--	--	--	--
100	0/20	--	--	--	--	--	--	--

Machining or Galling. Titanium panels were machined under LOX with no reaction. (16) The chips thus produced were shiny and bright. However, when heat was generated with galling under a rotating stainless-steel cylinder, an observable reaction occurred. Propagation did not occur at contact pressures of 2600 psi and speeds of 220 ft/min.

In experiments on the effect of galling under LOX, tests were conducted by rotating the end of a stainless-steel rod on a titanium specimen in an aluminum cup filled with LOX. The rod was mounted in a drill press and operated at peripheral speeds of up to 40 in./sec (200 ft/min) and different pressures up to 1600 psi. The reaction, as indicated by the intensity of the light flash, increased when speed and/or pressure increased. The temperature generated was estimated to be about 1000 F, as observed from the color of the stainless-steel rod.

An explanation for propagation not occurring even though ignition can be made to take place by heat generated by friction is that propagation probably is dependent upon the heat balance of the system. In the above experiments, it is clear that a high enough temperature does exist at some points in the overall cold system. The titanium-oxygen interface, however, only momentarily reaches ignition conditions, after which the heat balance shifts and quenching occurs.

Ignition by Tensile Rupture. The reactivity of a freshly formed titanium surface was investigated by rupturing titanium tensile specimens exposed to LOX. No propagating reactions were obtained in over 30 experiments at strain rates from 100 to 10,000 in./in./min. One small discolored spot was found only on one specimen. However, a bright flash of light was observed when the specimen ruptured. (26,27) Aluminum foil also flashes when ruptured. It is believed the flash is the result of the rapid oxidation of the fresh surface.

Effect of Vibration. High vibration levels, as associated with space vehicles, were studied. Vibration tests (16) of LOX-filled tanks, made with up to 200 cycles per second at 20 G's with a 0.03-inch double amplitude, caused no reactions.

In other experiments, a "sloshing" vibration was investigated using a LOX-filled tank in a Rotap machine for 10 minutes in each of 5 tests. In a similar test, the top vent port was left open and tapped lightly by the machine as dense vapors passed over the impact area. No reaction occurred.

Effect of Ultrasonic Energy. Titanium coupons were placed in LOX and subjected to ultrasonic energy from a 400-watt, 25-kc magnetostrictive transducer. (16) Three runs using disks 0.010, 0.025, and 0.063 inch thick, for 15 minutes' duration produced no reaction.

Effect of Sonic Energy. Two 0.010-in.-wall titanium tanks filled with LOX and pressurized to 50 psig were located 8 feet from a rocket motor. (16) A 4000-pound thrust LOX-kerosene rocket engine was fired to produce a 150-db acoustic pressure level. Four tests for a total of 210 seconds produced no reactions.

Simulated Loose Equipment in a Liquid-Oxygen Tank. The effect of components breaking loose and vibrating in a LOX tank during flight was simulated. (16) A 2-in. cube of Type 321 stainless steel was rough cut with a power hack saw and placed in a Ti-5Al-2.5Sn tank. The tank was filled with LOX and pressurized with 35 to 40 psig oxygen. The tank was then vibrated in a Rotap machine. After about 15 minutes, the LOX evaporated, and the cube rattled around in gaseous oxygen. Examination of the tank showed a surface peppered with minute dents but no reaction was indicated. Similar results are reported in gaseous oxygen on compressive impact studies. (18) Steel balls were impacted up to 20 mils deep into a titanium sample with no reaction.

Effect of Flow Through an Orifice. LOX was forced through a small orifice using an hydraulic cylinder. There was no apparent reaction. (18)

Summary of Oxygen-Titanium Reaction Information

The following conclusions can be drawn about ignition reactions of oxygen-titanium alloy systems.

Gaseous Oxygen

- (1) Ignition of titanium in gaseous oxygen occurs at temperatures about 482 F (250 C) below its melting point at atmospheric pressure
- (2) An increase in pressure lowers the ignition temperature
- (3) Dilution of oxygen up to the amount in air causes little change in ignition temperatures
- (4) Titanium will ignite in both carbon dioxide and nitrogen at temperatures somewhat higher than in oxygen at the same pressures
- (5) The ignition temperature in high-velocity air streams is about the same as under static conditions
- (6) Massive titanium will not ignite at ambient and moderate temperatures in air or oxygen unless some secondary source of energy other than heat is available

- (7) As with other metals, clouds and layers of powder can be ignited at substantially lower temperatures than can massive metal
- (8) Titanium can be ignited in both powder and massive form by electric spark at room temperature
- (9) The massive metal can be ignited by stress rupture at room temperature at oxygen pressures above about 60 psi but not at atmospheric pressure. If the temperature is increased, ignition occurs at lower pressures
- (10) Titanium is not ignited by low-cycle fatigue cracking at pressure up to 60 psi. Ignition is likely at higher pressure
- (11) The metal is not ignited by impact up to 70 ft-lb in gaseous oxygen at low temperatures and atmospheric pressure
- (12) Impact on the outside of a gaseous oxygen container is not likely to cause ignition if puncture does not occur
- (13) Ignition can be expected when titanium containers of gaseous oxygen are punctured either by large low-velocity projectiles or small high-velocity projectiles
- (14) High-velocity flow through small orifices is not expected to ignite titanium.

Liquid Oxygen

- (1) Titanium will not ignite in LOX without an external energy source and exposure of a fresh metal surface
- (2) Ignition may occur when titanium is impacted in LOX, even at impact levels as low as about 10 ft-lb
- (3) Unalloyed titanium may be slightly less sensitive to impact than some of its alloys
- (4) The following surface treatments, to some extent, reduce the impact sensitivity of titanium alloys: nitriding, electroplated nickel or copper, electroless nickel or copper, and cladding with a thick layer of aluminum

- (5) Titanium alloys are much more sensitive to ignition by explosive shock than magnesium, aluminum, and stainless steel. Plating the titanium alloys with nickel or copper gives some small improvement
- (6) Puncture of titanium-LOX tanks is almost sure to result in ignition
- (7) Impact of the outside of a tank that does not puncture is not likely to cause ignition
- (8) Ignition is not likely to occur in LOX-titanium systems by rapid pressurization, by machining, friction and galling, tensile rupture, mechanical vibration, sonic vibration, ultrasonic vibration, or high-velocity flow through an orifice.

Aluminum Alloys

Ignition in Gaseous Oxygen at High Temperatures

Aluminum in the massive form has been shown to ignite only at temperatures above its melting point 1220 F (660 C) at atmospheric pressure. (4) If the molten metal is confined, the ignition temperature may be as high as 1832 F (1000 C). At higher pressures of oxygen, up to 800 psi, the ignition temperature is still higher than the melting point. (3,4)

Aluminum has been broken by stress rupture to expose a fresh surface in 2000-psi gaseous oxygen at 572 F (300 C). No reaction occurred. (22)

Experiments involving impact and puncture of a diaphragm of a container of gaseous oxygen at 35 to 40 psi resulted in no reactions in 47 tests with pure aluminum, Aluminum 2014-T6, and Aluminum 6061-T6. (16) These tests were conducted at both room temperature and LOX temperature. Diaphragms pressurized with gaseous oxygen at 60 psi were punctured by simulated micrometeoroid particles traveling at 9,100 to 15,000 ft/sec. No reactions occurred, but there was some oxidation around the holes. (30) No reaction occurred as a result of puncturing Al-2024 diaphragms in LOX by metal shot traveling at 25,000 to 29,000 ft/sec through vacuum.

Aluminum can be ignited by explosive shock when in contact with gaseous oxygen. (16) Table 1 shows the effects under three different conditions. (16) In these tests, based on the amount of explosive needed and on the spacing between the charge and specimen, Aluminum

5052 is shown to be much less sensitive than titanium, but more sensitive than stainless steel.

Small particles of aluminum or aluminum-magnesium alloys can be ignited in clouds in air by low-energy sparks (50 to 80 millijoules). (21) Massive aluminum can be sparked with very much higher energies (10 joules) in pure oxygen and no evidence of reaction is found. (16)

Small particles of aluminum in clouds or layers have been ignited in air at 1202 and 1382 F (650 and 750 C), respectively. (21) In more dilute mixtures than air, ignition temperatures of 3632 F (2000 C) are indicated. (31)

Ignition in Liquid Oxygen

When aluminum foil is ruptured in LOX, bright flashes of light are emitted, but there is no other evidence of ignition. (18,27) It is believed that these flashes are merely the result of rapid oxidation of the fresh metal surface and cannot really be called ignition. (25)

Aluminum and its alloys are not usually ignited by impact energies up to 70 ft-lb of force. (16,18) There was some indication that if grit is impacted on aluminum, ignition may occur.

In puncture tests, the effect of both rupture and impact was studied. When a 30-calibre bronze-jacketed bullet was fired through an aluminum-LOX tank, the slug passed through both sides, leaving clean holes; no reaction occurred. Milder tests on aluminum tanks punctured by steel pins produced no reaction. (16)

Diaphragms pressurized with LOX were punctured by very small, high-velocity particles (9,100 to 15,000 ft/sec) to simulate micro-meteoroids. (30) There were no reactions when the particles penetrated Aluminum 2024 alloy diaphragms. However, there was a small amount of oxidation around the holes. When 1/16-in. shots traveling at 25,000 to 29,000 ft/sec in vacuum passed through diaphragms in LOX, no reaction occurred, but the metal was mechanically ruptured. (16)

It has been shown that aluminum alloys can be ignited by explosive shock in LOX. In these experiments, the amount of explosive required to ignite Aluminum 5052 was much greater than that necessary for titanium, and somewhat more than for magnesium (Table 1). However, this aluminum alloy was shown to be more sensitive than stainless steel. (16) The same trend was indicated in tests in which the spacing between the explosive and the specimen was varied. (16)

The experimental data above indicate that aluminum and its alloys are not easily ignited in

either gaseous oxygen or in LOX. However, the data show that stainless steel is even less sensitive, indicating that stainless steel would be the choice between the two materials, based on ignition reactions.

Stainless Steels

Ignition in Gaseous Oxygen

It has been found that the austenitic stainless steels in massive form ignite at or above their melting points at oxygen pressures up to 300 psi. (2,4) At 800 psi, Types 302, 304, and 347 ignite at their melting points, while Types 310 and 210 ignite at slightly lower temperatures. (4) The precipitation-hardening steels, 17-7PH and AM-350, ignite at their melting points at 50 psi and slightly lower at 300 and 800 psi. (4) Types 410 and 430 steels behave more like carbon steels than like the 300-series steels and ignite at temperatures between 2372 and 2480 F (1300 and 1360 C) at pressures up to 300 psi, (2,4) and as low as about 2192 F (1200 C) at 800 psi. (4)

At lower temperatures, the 300-series stainless steels do not ignite when ruptured in 2000-psi gaseous oxygen at 572 F (300 C). (22) Type 301 stainless steel diaphragms at 60 psi were impacted and ruptured by small particles traveling 9,100 to 15,000 ft/sec; no reaction occurred. (30) Type 301 diaphragms on gaseous oxygen containers, at 35 to 40 psi at room temperature and LOX temperature, have been punctured with 1/16-in. steel shot; no reaction occurred. (16) In the above experiments, the effects of impact, rupture, and high flow rates were involved, and no reactions occurred.

In other experiments, higher velocity flows were used. Oxygen gas at pressures of 12,000 psi was released through small orifices, 0.005 to 0.013 inch in diameter. No reaction occurred, but some erosion of the orifices took place. (32)

In air as in oxygen, the ignition temperature of Type 302 is above the melting point. (2) A higher temperature is required to ignite Type 430 steel in air than in oxygen. The temperature is at or above the melting point of the alloy. (2) High-velocity air flow, Mach 1.25, also had little effect on the air ignition temperature. In 50O₂-50CO₂, the 300-series steels ignite at or above their melting point.

It is reported that 18-8 stainless steel in fine powder form does not ignite at temperatures up to 1832 F (1000 C) either in clouds or layers. (21)

The effect of sudden increases in pressure has been studied. Stainless steel receivers were suddenly pressurized by releasing oxygen gas at 10,000 to 16,000 psi into low-pressure receivers.

The pressure in the receiver rose quickly from 15 to 8,000 psi, raising the bulk temperature 21 to 42 F. These pressure surges did not produce ignition. (32)

Ignition in Liquid Oxygen

The effect of impact and rupture of LOX tanks has been investigated. Type 301 stainless steel diaphragms on LOX containers have been punctured by micrometeoroid particles traveling at 9,100 to 15,000 ft/sec. No reaction was observed under these conditions. When 1/16-in. steel spheres traveling at 25,000 to 29,000 ft/sec were shot through diaphragms 0.010 inch thick, no reaction occurred, but the diaphragms ruptured mechanically. (16)

Type 304 LOX pressure bottles penetrated by incendiary 50-calibre bullets do not ignite and burn, but they do exhibit tearing. Occasionally, the bottles shatter if the material has defects at the grain boundaries. (33)

The effect of friction and galling on the ignition of stainless steels has been investigated. When a stainless-steel cylinder was rotated on a titanium plate at 2600 psi contact pressure at 220 ft/min in LOX, the titanium reacted, but the stainless steel showed no reaction. (18) A stainless-steel rod was rotated on a titanium plate at 200 ft/min at 1600 psi contact pressure in LOX. The temperature of the stainless steel reached about 1000 F, but there was no ignition of the stainless steel. (27)

It is possible to ignite stainless steel in LOX by explosive shock. (16) In this respect, Type 304 stainless steel requires much larger explosive charges to cause the LOX metal reaction than does aluminum.

All of the experiments that have been reported indicate that the 300-series stainless steels are among the materials most resistant to ignition in both LOX and gaseous oxygen. The various methods of additional external heat input that have been investigated have substantiated this insensitivity. The instances in which stainless steels have been ignited in oxygen can usually be traced to the ignition of another material that in turn ignited the stainless steel.

Copper Alloys

Ignition in Gaseous and Liquid Oxygen

Copper does not ignite in gaseous oxygen at atmospheric pressure and below its melting point. (2,4) An increase in pressure up to 500 psi does not change this situation. (3,4) Berylco 25 also does not ignite at its melting point at least at 50 psi. (2) However, Berylco 10 does ignite at about 1760 F (960 C) in oxygen. (2)

Copper, Berylco 10, and Berylco 25 behave about the same in air as in oxygen. (2) Data for copper in high-velocity air indicate that its ignition temperature is still above the melting point of the metal. Also, copper did not ignite at its melting point in a 50O₂-50CO₂ mixture. (3)

Small particles of copper in a cloud in air will ignite at 1292 F (700 C). (21) Berylco 25 powder does not ignite at 1832 F (1000 C) in either a cloud or a layer. (21) Brass powder (70-30) will ignite as low as 374 F (190 C) in a layer and 698 F (370 C) in a cloud. (21) Manganese bronze would not ignite in a cloud at 1832 F (1000 C) but did in a layer at 1670 F (910 C). Cu-50Al ignited in a cloud at 1706 F (930 C) and in a layer at 1526 F (830 C).

The effect of high-velocity-oxygen gas flow was studied with 0.005- to 0.013-in. orifices in copper and brass. The oxygen was released through the orifices from a container at 12,000 psi. No reaction occurred, but a fair amount of erosion did appear on the orifices. (32)

Impact studies in LOX have shown that copper alloys have a low sensitivity to ignition by this means. At the 72 ft-lb force level, Ampco 24, Cu-34Zn-1Pb, bronze, and 70-30 cupronickel showed no reactions in 20 tries. (34)

Nickel Alloys

Ignition in Gaseous and Liquid Oxygen

It has been shown that nickel does not ignite at its melting point at oxygen pressures up to 800 psi. (4) Inconel, Monel, Hastelloy C, Hastelloy B, and Hastelloy X behave in a similar manner up to 300 to 500 psi. (2,4) Inconel X may ignite at slightly below its melting point at 300 psi. Monel, Hastelloy B, and Hastelloy X may ignite slightly below their melting points at 800 psi. (4)

In air, nickel and Inconel in massive form do not ignite at their melting points at pressures up to 300 to 500 psi. (2,3) The ignition temperature of Inconel is not affected by high-velocity air flow. (3) Nickel powder in clouds or layers does not ignite at 1832 F (1000 C). (21) The ignition point of nickel powder in clouds and layers is lowered by alloying with 50 to 60 percent aluminum, being as low as 1022 to 1202 F (550 to 650 C) in layers and 1724 F (940 C) in clouds. (21)

The effect of various mechanical inputs of energy and the exposing of fresh metal has not been extensively investigated for nickel alloys. Drop-weight sensitivity tests on the K6 alloy (Karl Harrison Co.) and Kovar A show no reaction at 72 ft-lb impact in LOX. (34)

The effect of high-velocity flow through orifices in Monel was investigated by releasing

12,000-psi oxygen gas through 0.005- and 0.013-in. orifices.⁽³²⁾ Only a small amount of erosion was observed and no reactions occurred.

The data available, although not so complete as for the stainless steels, indicate that nickel alloys can be classed as being very resistant to ignition in oxygen.

Iron Alloys

Ignition in Gaseous and Liquid Oxygen

Pure iron in massive form has been shown to ignite in gaseous oxygen at atmospheric pressure at 1706 F (930 C).⁽¹⁾ The ignition temperature of mild steel in oxygen has been shown to be about the melting point at 50 psi and decreases to 1904 F (1040 C) at 800 psi.⁽⁴⁾ The alloy steels 4130 and Graphana tool steel ignited at similar temperature levels.⁽³⁾

Steels behave much the same in air as in pure oxygen, igniting in the range of 2192 to 2372 F (1200 to 1300 C).⁽²⁾ High-velocity air streams also have little effect on the ignition temperature.⁽³⁾ Likewise, dilution of oxygen with 50 percent CO₂ does not change this ignition temperature.⁽⁴⁾

Finely divided powders ignite in air at much lower temperatures than the massive metal. Pure iron powder in clouds or layers ignites at about 590 to 608 F (310 to 320 C) in air.⁽²¹⁾ Very fine powder will ignite at room temperature in air. Alloying iron with large additions of aluminum, silicon, chromium, manganese, vanadium, and even titanium (descending order) raises the ignition temperature of clouds of particles.⁽³⁵⁾ The Fe-50Al alloy did not ignite at 1832 F (1000 C). The others ignited in the range between 680 and 1652 F (360 and 900 C).⁽²¹⁾

The data on the effect of the various other factors such as impact, rupture, puncture, and explosive shock are very limited. Steel wool has been shown to be sensitive to impact in LOX with three out of four reactions at 72 ft-lb impact.⁽³⁴⁾ However, no reaction occurred when iron was ruptured in 2000-psi gaseous oxygen at 572 F (300 C).⁽²²⁾

Although the data are somewhat limited, iron and low-alloy steels probably should be rated as having a moderately high sensitivity in oxygen systems. Therefore, these alloys probably should not be used in critical conditions.

Cobalt Alloys

Ignition in Gaseous Oxygen

Limited data on cobalt alloys suggest that they may be nearly as resistant to ignition as the nickel systems in oxygen. Multimet and Haynes 25 do not ignite until above their melting points

at atmospheric pressure, but may ignite at or slightly below their melting points at higher pressures.⁽⁴⁾

Ignition data for cobalt powder in layers and clouds in air suggest that cobalt is more susceptible to ignition than cobalt alloys or nickel. The data show ignition of cobalt at 1454 F (790 C) in clouds and 1238 F (670 C) in layers as compared with no ignition of nickel at 1832 F (1000 C) under similar conditions.⁽²¹⁾

Magnesium Alloys

Ignition in Gaseous and Liquid Oxygen

The ignition temperature of magnesium in oxygen at atmospheric pressure has been shown to be slightly below its melting point at 1153 F (623 C).⁽⁵⁾ At 500 psi, the ignition temperature was shown to be near the melting point of 1202 F (650 C).⁽³⁾ The ignition point of a number of alloys has been investigated.⁽⁵⁾ Parts of the following alloy systems were studied: alloys of magnesium with the following metals; (binary alloys) aluminum, nickel, antimony, silver, bismuth, cadmium, cobalt, copper, calcium, indium, lithium, manganese, silicon, tin, lead, zinc; (ternary alloys) aluminum-zinc, aluminum-cadmium, cadmium-silver, and cadmium-zinc.⁽⁵⁾ Except for alloys over 80 percent aluminum, these alloy additions usually resulted in lowering the melting point and the ignition temperature. The ignition temperature ranged from 932 to 1112 F (500 to 600 C). Merely being in contact with some other metals also changed the ignition temperature of magnesium. Contact with nickel, brass, and aluminum lowered the ignition temperature, while contact with steel and silver did not affect it.

Massive magnesium has been shown to ignite in air at the same temperature as in oxygen.⁽¹⁾ Also, in other oxygen-inert gas mixtures the ignition temperatures were found to be 1141 to 1200 F (616 to 649 C) for 10O₂-90N₂⁽⁵⁾ and 1202 F (650 C) for 20O₂-80A mixtures.⁽³⁶⁾

Magnesium powder in air as a cloud ignites at 1148 F (620 C) and in a layer at 914 F (490 C).⁽²¹⁾ Other investigations show that the density of particles in a cloud affects the apparent ignition temperatures. Less dense clouds require high temperatures for ignition, ranging as high as 1292 to 1472 F (700 or 800 C), much above the melting point.⁽⁷⁾ It has been shown that the smaller particles, in the size range of 12 to 70 microns, may require a higher temperature to cause ignition. The ignition temperatures of powder clouds in oxygen is about the same range as in air.

Impact studies in LOX show that magnesium and its alloys must be considered sensitive to this type of ignition. Tests have been conducted on

pure magnesium, Mg-Li alloys, HK-31 alloy, and AZ-31 alloy. All these alloys were shown to be sensitive to impact at the 72 ft-lb level. Reduction in the impact force to about 35 ft-lb would not be expected to produce any reaction in 20 tries. (34)

In contrast to the above results, magnesium did not react when ruptured in 2000-psi oxygen at 572 F (300 C). Diaphragm-puncture tests with MgHK31 at room temperature and 2 to 40 psig oxygen resulted in one flash of light in 20 tests. At higher pressures of 60 and 100 psig, reactions were more frequent, i. e., 9 times in 20 tries at each pressure. (16) These results can be compared with ignition and burning with titanium and no reactions with aluminum.

From the above data, it can be concluded that though magnesium alloys are not so sensitive to ignition as titanium alloys, they are probably sensitive enough to be rated as unusable in oxygen systems.

Tin and Lead Alloys

Ignition in Gaseous and Liquid Oxygen

The ignition temperature of massive tin in oxygen at atmospheric pressure is reported as 1589 F (865 C), which is above the melting point of tin. (1) Likewise, powdered tin has been shown to ignite at 1220 F (660 C) in clouds and 968 F (520 C) in layers in air. (21) No data are available for massive lead in oxygen, but powdered lead has been shown to ignite in clouds at 1310 F (710 C) and layers at 518 F (270 C) in air. (21) The above data indicate that both lead and tin ignite only above their melting points in oxygen or air. But, since the melting points of tin and lead are low, they could still be sensitive to ignition by mechanical sources of energy.

Tin as tin plate has been shown to ignite at as low as 35 ft-lb impact and react about 2 out of 20 times at 72 ft-lb in LOX. Lead alone has not been tested in impact but many commercial solders have been studied. These soft solders containing lead or tin were all sensitive to impact in LOX at 70 ft-lb and most of them at 35 ft-lb. (34)

Generally speaking, the above results suggest that lead, tin, and soft solders should be avoided in LOX systems. They may be satisfactory in gaseous systems since, due to their low strength, they are not usually used under high pressures.

Silver and Silver Solders

Ignition in Gaseous and Liquid Oxygen

No ignition data are available for silver in oxygen or air. However, thermodynamic data indicate that the oxide is unstable at moderate

temperatures. These data, coupled with the location of silver in the periodic table, suggest that silver will not ignite easily.

Drop-weight impact data on silver solders show that some of these solders, usually the higher melting types are not impact sensitive at the 72 ft-lb level in LOX. Silver plating on stainless steel was not impact sensitive. (34)

Other Metals and Alloys

Ignition in Gaseous Oxygen

Ignition temperatures for both massive and powdered forms of a variety of other metals are given in Appendix A. These include antimony, barium, beryllium, bismuth, boron, cadmium, calcium, chromium, lithium, manganese, molybdenum, sodium, strontium, tantalum, tellurium, thorium, tungsten, uranium, vanadium, and zinc. Either from actual data on massive metal or inferred from powder data, the following metals are expected to ignite below their melting points: barium, beryllium, calcium, strontium, thorium, vanadium, tantalum, chromium, molybdenum, tungsten, uranium, manganese, silicon, and boron. The following probably would ignite above their melting points: lithium, sodium, potassium, cesium, platinum, gold, mercury, antimony, bismuth, silicon, and tellurium. Though the metals in the second group, which also includes nickel, copper, aluminum, and cobalt, possess the desirable property of igniting above their melting points, some of the melting points are so low that their use is limited. Conversely, some metals in the first group may be relatively insensitive because they have a high melting point and ignite only slightly below these temperatures. These exceptions include beryllium, chromium, and possibly columbium, tantalum, molybdenum, and tungsten.

THEORETICAL ANALYSIS AND CALCULATION OF IGNITION TEMPERATURES

Basic Data Required

The theoretical evaluation of the compatibility of metals with liquid or gaseous oxygen involves a number of thermochemical and thermo-physical constants. Data for these constants are available in the literature but are widely scattered. For this reason, the data were collected in this section in tabular form. A discussion of the data and their application follows.

Thermochemical Data for Metal Oxides of Interest

In Table 3, the standard heat of formation, ΔH_f , of the metal oxides is shown at several temperatures. The negative value indicates that the metal reacts exothermically, that is, heat is evolved in the oxide formation. The negative sign

TABLE A-1. SUMMARY OF EXPERIMENTAL IGNITION TEMPERATURES OF MASSIVE METALS AND ALLOYS IN OXYGEN SYSTEMS

Ignition Temperature, C

Metal or Alloy	In Oxygen, psi					In Air, psi				High Flow Rates	In Mixtures More Dilute Than Air, psi			
	15-50	50-200	200-400	400-700	Above 700	15-50	50-200	400-700			15-50	50-200	200-400	400-700
Aluminum 660	>1000(1) >MP(4) 900-1000	--	--	>600(3)	--	--	--	--	--	--	2050(31)	1730(31)	1730(31)	--
Antimony 630	650(1)	--	--	--	--	1600(M)	--	--	--	--	--	--	>MP(4)	--
Barium 720	175(1) 570(6)	560(6)	--	--	--	--	--	--	--	--	--	--	--	--
Beryllium	--	--	--	--	--	--	--	--	--	--	2100-2360(53)	2100-2360(53)	--	--
Beryllco 10	955-960(2)	955-960(2)	--	--	--	955-960(2)	955-960(2)	--	--	--	--	--	--	--
Beryllco 25	>MP(2)	>MP(2)	--	--	--	>MP(2)	>MP(2)	--	--	--	--	--	--	--
Bismuth 271	775(1) 760(6)	735(6)	--	--	--	1600(M)	--	--	--	--	--	--	--	--
Boron 2160	--	--	--	--	--	700(M)	--	--	--	--	1530-2000(51)	--	--	--
Cadmium 321	760(1)	--	--	--	--	--	--	--	--	--	--	--	--	--
Calcium 850	790(6) → 550(1) 320(52)	780(6)	--	--	--	704-743(2)	--	--	--	--	--	--	--	--
Cesium 28	--	--	--	--	--	--	--	--	--	--	--	--	--	--
Cobalt	--	--	--	--	--	--	--	--	--	--	--	--	--	--
Multimet	(a)MP(4)	--	(a)MP(4)	--	1315(4)	--	--	--	--	--	--	--	--	--
Co-60Al	--	--	--	--	--	--	--	--	--	--	--	--	--	--
Haynes 25	(a)MP(4)	--	(a)MP(4)	--	(a)MP(4)	--	--	--	--	--	--	--	>MP(4)	--
Copper A-50 (7)	>MP(2,4)	>MP(2)	(a)MP(4)	>MP(3)	--	>MP(2)	>MP(2)	--	>MP(3)	--	--	--	>MP(4)	--
Beryllco 25	>MP(2)	>MP(2)	--	--	--	>MP(2)	>MP(2)	--	--	--	--	--	--	--
Cu-29Zn	--	--	--	--	--	--	--	--	--	--	--	--	--	--
Mn-Bronze	--	--	--	--	--	--	--	--	--	--	--	--	--	--
Cu-50Al	--	--	--	--	--	--	--	--	--	--	--	--	--	--
Beryllco 10	955-960(2)	955-960(2)	--	--	--	955-960(2)	955-960(2)	--	--	--	--	--	--	--
Iron (1535) A-50 (7)	930(1) 1720(6)	1300(6)	--	--	--	--	--	--	--	--	--	--	--	--
Carbon steel	--	(a)MP(4)	>MP(4)	--	1040(4)	--	--	--	--	--	--	--	1370(4)	--
Mild steel	--	--	--	1150-1320(3)	--	1230-1280(2)	1230-1280(2)	--	1320(3)	--	--	--	--	--
4130	--	--	--	--	--	--	--	--	1320(3)	--	--	--	--	--
Tool steel	--	1230-1320(3)	1230-1320(3)	--	--	--	--	--	--	--	--	--	--	--
Stainless steel (18-8)	--	--	--	>MP(1)	--	--	--	--	--	--	--	--	--	--
Type 302	>MP(2)	>MP(2)	--	--	--	>MP(2)	>MP(2)	--	--	--	--	--	--	--
Type 304	--	(a)MP(4)	(a)MP(4)	--	(a)MP(4)	--	--	--	--	--	--	--	>MP(4)	--
Type 310	--	(a)MP(4)	(a)MP(4)	--	980(4)	--	--	--	--	--	--	--	>MP(4)	--
Type 321	--	(a)MP(4)	(a)MP(4)	--	1315(4)	--	--	--	--	--	--	--	>MP(4)	--
Type 347	--	(a)MP(4)	(a)MP(4)	--	(a)MP(4)	--	--	--	--	--	--	--	(a)MP(4)	--
Type 410	--	1315(4)	1315(4)	--	1200(4)	--	--	--	--	--	--	--	1040(4)	--
Type 430	1350-1365(2)	1350-1365(2)	--	--	--	>MP(2)	>MP(2)	--	>MP(2)	--	--	--	--	--
17-7PH	--	(a)MP(4)	1370(4)	--	1315(4)	--	--	--	--	--	--	--	1370(4)	--
AM-350	--	(a)MP(4)	>MP(4)	--	1315(4)	--	--	--	--	--	--	--	>MP(4)	--
Lithium (179)	190(1)	--	--	--	--	--	--	--	--	--	--	--	--	--

CHROMIUM (1900)

2000 M

LEAD (1320)

870 (1)

1000 (1)

A-1

TABLE A-1. (CONTINUED)

Metal or Alloy	In Oxygen, psi					In Air, psi				High Flow Rates	In Mixtures More Dilute Than Air, psi			
	15-50	50-200	200-400	400-700	Above 700	15-50	50-200	400-700	15-50		50-200	200-400	400-700	
	15-50 (4)	50-200 (4)	200-400 (4)	400-700 (4)	Above 700 (4)	15-50 (4)	50-200 (4)	400-700 (4)	15-50 (4)		50-200 (4)	200-400 (4)	400-700 (4)	
Magnesium 650	623-630(5)	633-639(5)	--	(a)MP(3)	--	623(1)	--	--	--	616-649(5)	--	--	<MP(31)	
Mg-6 to 63 Al	462-558(5)	--	--	--	--	--	--	--	--	--	--	--	--	
Mg-80 to 94 Al	900 or above(5)	--	--	--	--	--	--	--	--	--	--	--	--	
Mg-5 to 20 Ni	508-517(5)	--	--	--	--	--	--	--	--	--	--	--	--	
Mg-1, 2 to 29 Sb	582-593(5)	--	--	--	--	--	--	--	--	--	--	--	--	
Mg-5 to 14 Ag	540-550(5)	--	--	--	--	--	--	--	--	--	--	--	--	
Mg-10 to 20 Bi	500-548(5)	--	--	--	--	--	--	--	--	--	--	--	--	
Mg-7 to 91 Cd	552-612(5)	--	--	--	--	--	--	--	--	--	--	--	--	
Mg-1 to 5 Co	616-617(5)	--	--	--	--	--	--	--	--	--	--	--	--	
Mg-10 to 31 Cu	532-537(5)	--	--	--	--	--	--	--	--	--	--	--	--	
Mg-1 to 5 Ca	624-633(5)	--	--	--	--	--	--	--	--	--	--	--	--	
Mg-10 to 30 In	586-613(5)	--	--	--	--	--	--	--	--	--	--	--	--	
Mg-0, 3 to 11 Li	518-553(5)	--	--	--	--	--	--	--	--	--	--	--	--	
Mg-1 to 3 Mn	621-631(5)	--	--	--	--	--	--	--	--	--	--	--	--	
Mg-1, 8 to 3, 1 Si	610-625(5)	--	--	--	--	--	--	--	--	--	--	--	--	
Mg-10 to 26 Sn	560-571(5)	--	--	--	--	--	--	--	--	--	--	--	--	
Mg-16 to 58 Pb	504-575(5)	--	--	--	--	--	--	--	--	--	--	--	--	
Mg-3 to 89 Zn	509-588(5)	--	--	--	--	--	--	--	--	--	--	--	--	
Mg-1 to 11 Al, 1 to 14 Zn	534-610(5)	--	--	--	--	--	--	--	--	--	--	--	--	
Mg-10 to 15 Al, 5 to 11 Cd	534-544(5)	--	--	--	--	--	--	--	--	--	--	--	--	
Mg-22 to 27 Cd, 0, 3 to 2, 3 Ag	560-592(5)	--	--	--	--	--	--	--	--	--	--	--	--	
Mg-20 Cd-3Zn	553(5)	--	--	--	--	--	--	--	--	--	--	--	--	
Mg in contact with Ni	588(5)	--	--	--	--	--	--	--	--	--	--	--	--	
Mg in contact with Ag	623(5)	--	--	--	--	--	--	--	--	--	--	--	--	
Mg in contact with 70-30 brass	538(5)	--	--	--	--	--	--	--	--	--	--	--	--	
Mg in contact with steel	623(5)	--	--	--	--	--	--	--	--	--	--	--	--	
Mg in contact with Al	533(5)	--	--	--	--	--	--	--	--	--	--	--	--	
Molybdenum 2020	750(1)	765(6)	--	--	--	--	--	--	--	--	--	--	--	
Nickel	>MP(2,4)	>MP(2)	>MP(4)	--	>MP(4)	>MP(2)	>MP(2)	--	--	--	--	>MP(4)	--	
Inconel	>MP(2)	>MP(2)	--	>MP(2)	--	>MP(2)	>MP(2)	--	>MP(2)	--	--	--	--	
Inconel X	>MP(2,4)	>MP(2)	1200(4)	--	1150(4)	>MP(2)	>MP(2)	>MP(2)	--	--	--	>MP(4)	--	
Monel	>MP(4)	--	>MP(4)	>MP(3)	1200(4)	--	--	--	--	--	--	>MP(4)	--	
Ni-50Al	--	--	--	--	--	--	--	--	--	--	--	--	--	
Ni-58Al	--	--	--	--	--	--	--	--	--	--	--	--	--	
Hastelloy C	(a)MP(4)	--	(a)MP(4)	--	>MP(4)	--	--	--	--	--	--	>MP(4)	--	
Hastelloy R	1370(4)	--	(a)MP(4)	--	1370(4)	--	--	--	--	--	--	(a)MP(4)	--	
Hastelloy X	>MP(4)	--	(a)MP(4)	--	1370(4)	--	--	--	--	--	--	>MP(4)	--	
Potassium 63	69(1)	--	--	--	--	--	--	--	--	--	--	--	--	
Sodium 98	118(1)	--	--	--	--	--	--	--	--	--	--	--	--	
Strontium 771	720(1)	1150(6)	--	--	--	--	--	--	--	--	--	--	--	
Tantalum 2996	1240-1290(2)	1240-1290(2)	--	--	--	--	--	--	--	--	--	--	--	
Thorium 9800	500(1)	--	--	--	--	400(4)	--	--	--	--	--	--	--	
Tin 232	970(5)	965(6)	--	--	--	2700(4)	--	--	--	--	--	--	--	
Sn-2Pb	--	--	--	--	--	--	--	--	--	--	--	--	--	

TABLE A-1. (CONTINUED)

Metal or Alloy	In Oxygen, psi					In Air, psi				High Flow Rates	In Mixtures More Dilute Than Air, psi			
	15-50	50-200	200-400	400-700	Above 700	15-50	50-200	400-700			15-50	50-200	200-400	400-700
Titanium 1730	610(24) 1315(4)	1580-1630(2)	870(4)	1100(3)	--	1580-1630(2)	--	--	1580-1630(2)	--	--	--	815(4)	1100(3)
RS-110A	--	1570-1600(2)	--	--	--	>MP(2)	--	--	>MP(2)	--	--	--	--	--
RS-110BX	--	1570-1600(2)	--	--	--	>MP(2)	--	--	1530-1660(2)	--	--	--	--	--
Ti, Cu coated	--	--	--	--	--	--	--	--	--	--	--	--	--	--
Ti-8Al-2.5Sn-3.5Fe-1Cu	--	--	--	--	--	--	--	--	--	--	--	--	--	--
Ti-2.8H ₂	--	--	--	--	--	--	--	--	--	--	--	--	--	--
Ti-3.8H ₂	--	--	--	--	--	--	--	--	--	--	--	--	--	--
Ti-70Fe-7.0C	--	--	--	--	--	--	--	--	--	--	--	--	--	--
Ti-74Fe-0.06C	--	--	--	--	--	--	--	--	--	--	--	--	--	--
Ti (broken by stress rupture)	>1200(22)	300-1200(22)	RT-300(22)	--	--	--	--	--	--	--	--	--	--	--
Tungsten	--	--	--	--	--	1240-1290(2)	1240-1290(2)	--	--	--	--	--	--	--
Zinc (415)	900(11) 870(10)	1135(10)	--	--	--	505(14)	--	--	--	--	--	--	--	--
Zn-2Pb	--	--	--	--	--	--	--	--	--	--	--	--	--	--

ZIRCONIUM (1845)

END OF REFERENCE

REFERENCE

4

**NIHART, G. J.; AND SMITH, C. P.: COMPATIBILITY OF
MATERIALS WITH 7500 PSI OXYGEN. UNION CARBIDE CORP.
(AMRL-TDR-64-67, AD-608260), OCT. 1964.**

79811-59N

AD-708-51-75

COPY 1

N65 11897
AD 608260

COMPATIBILITY OF MATERIALS WITH 7500 PSI OXYGEN

G. J. NIHAET
C. P. SMITH

UNION CARBIDE CORPORATION, LINDE DIVISION

OCTOBER 1964

LIBRARY COPY

DEC 16 1964

LEWIS LIBRARY, NASA
CLEVELAND, OHIO

BIOMEDICAL LABORATORY
AEROSPACE MEDICAL RESEARCH LABORATORIES
AEROSPACE MEDICAL DIVISION
AIR FORCE SYSTEMS COMMAND
WRIGHT-PATTERSON AIR FORCE BASE, OHIO

COMPATIBILITY OF MATERIALS WITH 7500 PSI OXYGEN

**G. J. NIHART
C. P. SMITH**

TABLE OF CONTENTS

	<u>Page</u>
INTRODUCTION	1
PROGRAM DEVELOPMENT	1
Selection of Test Methods	1
Oxygen Bomb Test	2
Impact Sensitivity Test	2
Velocity Impact Test	2
Hot Wire Test.	2
Promoted Ignition Test	3
Adiabatic Compression Test	3
Selection of Materials for Test	3
Thread Lubricants and Thread Sealants	3
Fluorocarbon Plastics and Elastomers	5
Metals and Alloys.	6
Design of Equipment	8
High Pressure Oxygen Warm Converter	11
High Pressure Oxygen Bomb.	11
Valves, Fittings, and Tubing	11
Simulated System	11
EXPERIMENTAL PROGRAM	14
High Pressure Laboratory	14
Construction of Laboratory	14
Physical Arrangement of Test Equipment	14
Cleaning and Assembly of Equipment	14
High Pressure Oxygen Bomb Tests	14
Purpose.	14
Procedure	17
Preliminary Tests of Prototype Bomb and Final Bomb	17
7500 psi Tests	20
Adiabatic Compression Tests	26
Purpose and Discussion	26
Preliminary Tests	26
7500 psi Tests	28
Promoted Ignition Tests	28
Purpose	28
Procedure	28
Preliminary Tests	30
7500 psi Tests	32
Simulated System Tests	45
Purpose	45
Philosophy	45
Materials of Construction and Arrangement of Equipment	45
Procedure	49
7500 psi Tests	50
Evaluation of Hardware Used in the Experimental Program	52
Gemini Regulator	52
High Pressure Valves	52
Tubing Connection and Fittings	53
Miscellaneous	55

1. In general, metal alloys with a high percentage of nickel such as the Monels and Inconels have the highest resistance to combustion.
2. The resistance to combustion appeared to be related to the percentage of iron in an alloy.
3. The size of the metal sample will affect its resistance to combustion (e.g. the more subdivided a metal specimen, the easier it will ignite).

The results of Dean and Thompson (3) referred to earlier were evaluated in regard to the relative resistance to ignition and combustion of each metal tested and the metals are listed in Table 1 in the order of their decreasing resistance, with the most resistant metal at the top of the list.

The relative resistance of metals as determined by the "Velocity Impact Test" and the "Promoted Ignition Test" at Linde are also listed in Table 1 for comparison. It should be pointed out that there might be some shifting in the position of the metals in the "Promoted Ignition Test" column because in those cases where two or more metals showed similar resistance to ignition, the violence of the combustion determined the position. Also if a large enough number of tests were to be performed on each metal, statistically the position of a metal might be changed.

Of particular interest is the position occupied by aluminum. Dean and Thompson's work would place it at the top of the list while it is at the bottom of the list in the Linde Tests. This is no doubt due to the fact that Dean and Thompson only heated the tube to its melting point. Grosse and Conway (6) have shown the ignition temperature of aluminum to be $> 1000^{\circ}\text{C}$ which is considerably above its melting point of 660°C . Aluminum is at the bottom of the ladder on the Linde tests because of its violent reaction once it becomes ignited.

It will be noted that nickel and copper alloys are at the top of the list in all three columns.

For the present investigation, metals and alloys were selected which would be representative of materials already tested in oxygen pressures up to 2000 psi. Results at 7500 psi could thus be compared to those obtained at the lower pressures. Additionally some other metals were chosen because of their possible usefulness in high pressure systems.

The metals and alloys selected for test, the melting point of each, and the reported ignition temperature in oxygen are presented in Table 2.

Design of Equipment

The materials of construction and the design of the equipment to be used in the test program was an area that received considerable attention. Because of the inherent hazards with gaseous oxygen and the magnification of these hazards with 7500 psi oxygen, it was necessary to select those materials which would be considered relatively safe by present available knowledge. Consequently nickel alloys were used in all critical pieces of apparatus. This resulted in considerable delay in initial construction of equipment.

that results were significantly different from those obtained in the 2000 psi tests in that the weight of neoprene required to bring about combustion of the metal was less. This was attributed to the geometric configuration of the bomb, the physical position of the metal specimen in the test tube during preliminary tests, and the difference in oxygen pressures. All of these factors would favor the blanketing of the metal specimen by the ignition products of CO_2 and H_2O formed during combustion of the neoprene. At the lower pressure of 2000 psi the combustion products would occupy a much greater volume than at 7500 psi.

Although the tests at 2000 psi were informative it was necessary to develop new parameters at 7500 psi. Original intentions had been to perform identical tests at 2000 psi and at 7500 psi for comparison purposes, but tests at 2000 psi now had to be eliminated and only the 7500 psi tests were made.

7500 psi Tests

1. Discussion of Test

After completion of a number of tests at 7500 psi, a geometrical configuration of 5 millimeters by 30 millimeters was selected as the standard size for the 5-mil metal foil samples. By determining the weight of neoprene necessary to combust, partially combust, melt, or partially melt a specimen, the relative resistance to ignition and combustion was obtained for the metals and alloys.

The metals and alloys have been arranged in Table 4 in order of their decreasing resistance to ignition as determined by these tests in 7500 psi oxygen. Complete data on the tests is presented in Table 10 of Appendix IV.

It had been hopefully expected that we might be able to extract some temperature data from the pressure profiles in the bomb during the ignitions and a pressure transducer was connected into the bomb system. The pressure was recorded on a Sanborn 150 recorder which permitted suppression of several thousand pounds of pressure and, by means of an attenuator, the recorder could be spanned over a narrow pressure range if it were so desired. After a large number of tests and a study of the pressure profiles, the conclusion was reached that prediction of ignition temperatures could not be determined from the profiles. A typical pressure profile is shown in Figure 22.

2. Discussion of Results

a. From Table 4 it can be seen that nickel is by far the most resistant to ignition (gold and silver excepted) but if enough energy is present nickel will burn.

b. A standard specimen of Monel alloy 400 was never completely combusted so the amount of neoprene shown in Table 4 to completely combust the standard size specimen was estimated. The required weight of neoprene might actually be higher than the estimate which would improve the relative position of Monel 400.

TABLE 4

METALS AND ALLOYS ARRANGED IN ORDER OF DECREASING
RESISTANCE TO IGNITION AND COMBUSTION IN 7500 PSI OXYGEN

Metal or Alloy	Weight of Neoprene to Completely Combust Standard Specimen 5 mm x 30 mm x 0.005"
Gold	Only melts
Silver	Only melts
Nickel	48 to 56 mg*
Monel alloy 400	18 to 19 mg*
Yellow Brass (partial combustion only)	11.8 to 15.2 mg
Inconel alloy 600	13.2 mg
Aluminum	11.0 to 16.4 mg
Copper	10.5 mg*
Inconel alloy X-750	9.0 mg
Stainless steels	7.1 to 8.5 mg

*Estimated from results of a number of tests which were either standard with only part of the specimen consumed or were not standard and either complete or partial combustion occurred.

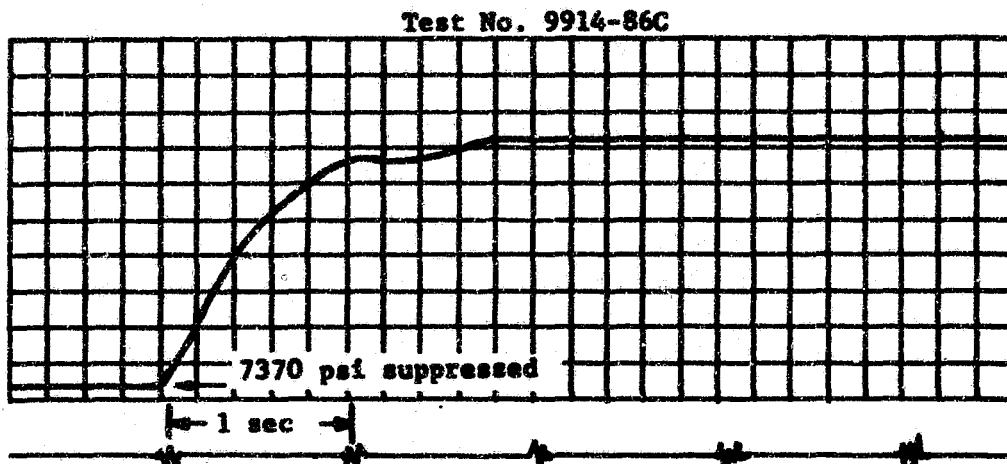


FIGURE 22. PRESSURE PROFILE OF PROMOTED IGNITION TEST

c. It has been possible to demonstrate with some of the metals (e.g. copper, brass, Monel 400, and nickel) that ignition can be started and part of the specimen combusted without consuming all of the specimen. By varying the weight of neoprene only slightly, it has been possible to combust a small part of the specimen, a large part of the specimen, or all of the specimen. This is characteristic of these metals and demonstrates their quenching effect once ignition has started. This is no doubt due to the low heats of combustion of these materials. Evidence of this is shown in Figures 26, 27, 29, and 30. Figures 23, 24, 25, 28, 31 and 32 show other ignition results.

d. Lead was not listed in Table 4 because 12.6 mg of neoprene melted the specimen into a ball with very little oxidation and no further tests were run. Therefore it was difficult to position it in the table.

e. Aluminum was tested with two different anodized surface thicknesses and also with what was thought to be normal surface condition if just exposed to the atmosphere. The amount of neoprene necessary to ignite the aluminum was not as clear cut as with other metals. However a range was established between 11.0 and 16.4 mg. Once ignited, the aluminum burned violently.

f. Gold and silver required more neoprene to melt the specimens than was required to ignite most of the other metals.

g. Brass had high resistance to ignition but it was always heavily oxidized.

h. Stainless steels were least resistant to ignition.

i. Samples of stainless steel enclosed in 5-mil Kel-F and 5-mil Teflon FEP were tested. This was intended to simulate a coating of these materials on the metal. Complete ignition occurred in all cases.

j. Two samples of aluminum coated on one side with Kel-F were tested. The Kel-F disappeared in one case without ignition and ignited in the other case. The aluminum was not affected in either case.

3. Evaluation of Test Results

a. With the exception of aluminum, results of these tests generally agree with those previously made at Linde in 2000 psi oxygen and with those of Dean and Thompson (3). (See Table 1.)

b. Nickel has the highest resistance to ignition and combustion. Therefore it would be the first choice for construction of a high pressure oxygen receiver from the standpoint of compatibility with oxygen.

c. Monel alloy 400, Inconel alloy 600, and brass, would be rated as the next best materials.

END OF REFERENCE

REFERENCE

5

**LYMAN, TAYLOR, ED.: METALS HANDBOOK. VOL. I.
PROPERTIES AND SELECTION OF METALS. EIGHTH ED.,
AMERICAN SOCIETY FOR METALS, 1961.**

**THIS REFERENCE IS A COPYRIGHTED HANDBOOK AND
THEREFORE THE CONTENTS HAVE NOT BEEN REPRODUCED
FROM THE TEXT.**

END OF REFERENCE
5

REFERENCE

6

**WOLF, J.; AND BROWN, W. F., JR., EDS.: AEROSPACE
STRUCTURAL METALS HANDBOOK. VOLS. 1, 2, AND 3.
STULEN, INC. (AFML-TR-68-115), 1972.**

**THIS REFERENCE IS A COPYRIGHTED HANDBOOK AND
THEREFORE THE CONTENTS HAVE NOT BEEN REPRODUCED
FROM THE TEXT.**

END OF REFERENCE

6

REFERENCE

7

ANON.: METAL PROGRESS MATERIALS AND PROCESS
ENGINEERING DATA BOOK. AM. SOC. METALS, 1968
(MOST RECENT AVAILABLE EDITION AT TIME OF WRITING,
1970 EDITION.).

THIS MATERIAL HAS BEEN APPROVED TO BE MADE AVAILABLE FOR THE
TECHNICAL AND SCIENTIFIC COMMUNITY PER AMERICAN SOCIETY FOR
METAL'S APPROVAL (ELIZABETH M. ALDRICH, JUNE 14, 1973).

METAL PROGRESS

MATERIALS and PROCESS
ENGINEERING

DATABOOK



1

Selection of Materials in Design

2

Processing and Fabrication

THIS MATERIAL HAS BEEN APPROVED TO BE MADE AVAILABLE FOR THE
TECHNICAL AND SCIENTIFIC COMMUNITY PER AMERICAN SOCIETY FOR
METAL'S APPROVAL (ELIZABETH M. ALDRICH, JUNE 14, 1973).

About This Book

#20.00
This Databook will serve its purpose if you find information in it which helps you make a technical decision in minimum time or solve a problem in your production operations. It is based on what has been one of our most popular features in Metal Progress—our monthly Data Sheets, in which we present practical information on the selection of materials for design and on their processing and fabrication.

We can always count on an impressive number of requests for extra copies each time we publish a Metal Progress Data Sheet. And we can always count on compliments from readers which add up to, "this is a compact way of conveying a wealth of useful technical information on specific subjects." Also, one question has been asked with great regularity: "Are Metal Progress Data Sheets available in separate form? This would add to their utility to us." Thus, this volume is published in response to the need expressed by many engineers to have information of this type readily available in book form.

The Databook contains recent information on the 100 subjects covered. Part I deals with practical information on the selection of materials in design applications. Part II comprises five divisions with individual sections devoted to heat treatment, forming, welding, machining, and finishing. You will find a table of contents on the divider preceding Part I on materials in design and on the dividers preceding each of the five sections comprising Part II on processing and fabrication. Plastic paper is used for the pages in the Databook to provide resistance to tearing and soiling, which might be encountered in frequent use. The sheet is also resistant to water and oil.

C 50576-B
The engineering and economic requirements of materials performance are constantly changing and becoming more demanding. The materials and process engineer must continually examine his basis for selecting materials, for evaluating their properties, and for determining their processing and fabricating characteristics in light of the most recent information. Thus keep in mind that in a sense this Databook is a do-it-yourself reference book. In fact, we regard this as a strength. You can keep it current by adding new Data Sheets to it as they appear in Metal Progress.

Allen G. Gray
Editor, Metal Progress
Engineering Publications ASM

LIBRARY COPY

RETURN TO
LEWIS LIBRARY

Copyright © 1968 by the
American Society for Metals

1

USEFUL DATA FOR SELECTING MATERIALS

AISI-SAE Standard Carbon Steels, Including Free-Machining Grades	1
Stainless Steels—Properties and Applications	2
Stainless Steels—Correlation of Specifications	6
SAE Standard Alloy Steel Compositions	7
AISI-SAE Standard H-Steel Compositions	8
High-Strength Steels—Compositions, Properties, Producers	9
Nickel-Base Superalloys—Selection Criteria	15
Iron-Nickel-Base Superalloys—Selection Criteria	16
Cobalt-Base Superalloys—Selection Criteria	16
Refractory Metal Alloys—Compositions and Properties	17
Gray Iron Castings—Specifications and Properties	18
Ductile (Nodular) Iron Castings—Specifications and Properties	20
Carbon and Low-Alloy Steel Castings—Properties and Applications	21
Malleable Iron Castings—Designation and Properties	22
Corrosion-Resistant Stainless and High-Alloy Steel Castings— Properties and Applications	23
Heat-Resistant Stainless and High-Alloy Steel Castings— Properties and Applications	24
Heat-Treatable Copper Alloys—Properties and Uses	25
Copper and Copper Alloys— Properties, Fabricating Characteristics, and Uses	26
Powder Metallurgy Parts—Properties and Applications	28
Aluminum Alloys—Properties and Uses for Wrought Grades	30
Titanium Alloys—Specifications, Properties, and Uses	31
Noble Metals—Properties	32
Plastics—Properties and Applications	33
Comparison of Properties of Common Plastics	33
Materials for Boilers and Nuclear Reactor Vessels	34
Spring Materials—Selection Criteria	35
Fastener Materials—Selection Criteria	36
Metals for Cryogenic Service— Mechanical Properties at Cryogenic Temperature	
Strength-to-Density Ratio	

LIBRARY COPY

RETURN TO

LEWIS LIBRARY

CLEVELAND, OHIO

AISI-SAE Standard Carbon Steels

Free-Machining Grades

Nonresulfurized Grades

AISI No.*	Composition †, %				SAE No.	AISI No.*	Composition †, %				SAE No.
	C	Mn	P	S			C	Mn	P Max	S Max	
Resulfurized						1008	0.10 max	0.30 to 0.50	0.040	0.050	—
1109	0.08 to 0.13	0.60 to 0.90	0.040 max	0.08 to 0.13	1109	1010	0.08 to 0.13	0.30 to 0.60	0.040	0.050	1010
1110	0.08 to 0.13	0.30 to 0.60	0.040 max	0.08 to 0.13	—	1012	0.10 to 0.15	0.30 to 0.60	0.040	0.050	1012
B1111	0.13 max	0.60 to 0.90	0.07 to 0.12	0.10 to 0.15	—	—	0.10 to 0.16	1.10 to 1.40	0.040	0.050	1513§
B1112	0.13 max	0.70 to 1.00	0.07 to 0.12	0.16 to 0.23	1112	1015	0.13 to 0.18	0.30 to 0.60	0.040	0.050	1015
B1113	0.13 max	0.70 to 1.00	0.07 to 0.12	0.24 to 0.33	1113	1016	0.13 to 0.18	0.60 to 0.90	0.040	0.050	1016
1116	0.14 to 0.20	1.10 to 1.40	0.040 max	0.16 to 0.23	—	1017	0.15 to 0.20	0.30 to 0.60	0.040	0.050	1017
1117	0.14 to 0.20	1.00 to 1.30	0.040 max	0.08 to 0.13	1117	1018	0.15 to 0.20	0.60 to 0.90	0.040	0.050	1018
1118	0.14 to 0.20	1.30 to 1.60	0.040 max	0.08 to 0.13	1118	—	0.15 to 0.21	1.10 to 1.40	0.040	0.050	1518
1119	0.14 to 0.20	1.00 to 1.30	0.040 max	0.24 to 0.33	1119	1019	0.15 to 0.20	0.70 to 1.00	0.040	0.050	1019
1132	0.27 to 0.34	1.35 to 1.65	0.040 max	0.08 to 0.13	1132	1020	0.18 to 0.23	0.30 to 0.60	0.040	0.050	1020
1137	0.32 to 0.39	1.35 to 1.65	0.040 max	0.08 to 0.13	1137	1021	0.18 to 0.23	0.60 to 0.90	0.040	0.050	1021
1139	0.35 to 0.43	1.35 to 1.65	0.040 max	0.13 to 0.20	—	1022	0.18 to 0.23	0.70 to 1.00	0.040	0.050	1022
1140	0.37 to 0.44	0.70 to 1.00	0.040 max	0.08 to 0.13	1140	—	0.18 to 0.24	1.10 to 1.40	0.040	0.050	1522
1141	0.37 to 0.45	1.35 to 1.65	0.040 max	0.08 to 0.13	1141	1023	0.20 to 0.25	0.30 to 0.60	0.040	0.050	1023
1144	0.40 to 0.48	1.35 to 1.65	0.040 max	0.24 to 0.33	1144	—	0.19 to 0.25	1.35 to 1.65	0.040	0.050	1524
1145	0.42 to 0.49	0.70 to 1.00	0.040 max	0.04 to 0.07	1145	1025	0.22 to 0.28	0.30 to 0.60	0.040	0.050	1025
1146	0.42 to 0.49	0.70 to 1.00	0.040 max	0.08 to 0.13	1146	—	0.23 to 0.29	0.80 to 1.10	0.040	0.050	1525
1151	0.48 to 0.55	0.70 to 1.00	0.040 max	0.08 to 0.13	1151	1026	0.22 to 0.28	0.60 to 0.90	0.040	0.050	1026
Resulfurized and Rephosphorized						—	0.22 to 0.29	1.10 to 1.40	0.040	0.050	1526
1211	0.13 max	0.60 to 0.90	0.07 to 0.12	0.10 to 0.15	—	—	0.22 to 0.29	1.20 to 1.50	0.040	0.050	1527
1212	0.13 max	0.70 to 1.00	0.07 to 0.12	0.16 to 0.23	1112	1029	0.25 to 0.31	0.60 to 0.90	0.040	0.050	—
1213	0.13 max	0.70 to 1.00	0.07 to 0.12	0.24 to 0.33	1113	1030	0.28 to 0.34	0.60 to 0.90	0.040	0.050	1030
1215	0.09 max	0.75 to 1.05	0.04 to 0.09	0.26 to 0.35	—	1035	0.32 to 0.38	0.60 to 0.90	0.040	0.050	1035
12L14 ‡	0.15 max	0.85 to 1.15	0.04 to 0.09	0.26 to 0.35	—	—	0.30 to 0.37	1.20 to 1.50	0.040	0.050	1536

* Prefix B indicates acid bessemer steel; others are made by the electric furnace, open hearth, or basic oxygen furnace processes.

† When silicon is required, the following ranges and limits are commonly used: for nonresulfurized steels: up to 1015, 0.10% max; 1015 to 1025, 0.10% max, or 0.10 to 0.20%, or 0.15 to 0.30%; over 1025, 0.10 to 0.20%, or 0.15 to 0.30%; 1513 to 1524, 0.10% max, or 0.10 to 0.20%, or 0.15 to 0.30%; 1525 and over, 0.10 to 0.20%, or 0.15 to 0.30%. For resulfurized steels: to 1110, 0.10% max; 1116 and over, 0.10% max, or 0.10 to 0.20%, or 0.15 to 0.30%. It is not common practice to produce resulfurized and rephosphorized steels to specified limits for silicon because of its adverse effect on machinability.

Copper can be added to a standard steel.

‡ 0.15 to 0.35% Pb. When lead is required as an added element to a standard steel, a range of 0.15 to 0.35%, inclusive, is generally used. Such a steel is identified by inserting the letter "L" between the second and third numeral of the AISI number.

§ SAE 15XX designations (with the exception of 1513, 1518, 1522, 1525, and 1526) were formerly SAE 10XX. The AISI has approved these high-manganese carbon steel compositions and it will publish them shortly. The grades are applicable only to semifinished products for forging, to hot rolled and cold finished bars, to wire rods, and to seamless

1037	0.32 to 0.38	0.70 to 1.00	0.040	0.050	1037
1038	0.35 to 0.42	0.60 to 0.90	0.040	0.050	1038
1039	0.37 to 0.44	0.70 to 1.00	0.040	0.050	1039
1040	0.37 to 0.44	0.60 to 0.90	0.040	0.050	1040
—	0.36 to 0.44	1.35 to 1.65	0.040	0.050	1541
1042	0.40 to 0.47	0.60 to 0.90	0.040	0.050	1042
1043	0.40 to 0.47	0.70 to 1.00	0.040	0.050	1043
1044	0.43 to 0.50	0.30 to 0.60	0.040	0.050	1044
1045	0.43 to 0.50	0.60 to 0.90	0.040	0.050	1045
1046	0.43 to 0.50	0.70 to 1.00	0.040	0.050	1046
—	0.45 to 0.51	1.35 to 1.65	0.040	0.050	1547
—	0.44 to 0.52	1.10 to 1.40	0.040	0.050	1548
1049	0.46 to 0.53	0.60 to 0.90	0.040	0.050	1049
1050	0.48 to 0.55	0.60 to 0.90	0.040	0.050	1050
—	0.45 to 0.56	0.85 to 1.15	0.040	0.050	1551
—	0.47 to 0.55	1.20 to 1.50	0.040	0.050	1552
1053	0.48 to 0.55	0.70 to 1.00	0.040	0.050	—
1055	0.50 to 0.60	0.60 to 0.90	0.040	0.050	1055
1060	0.55 to 0.65	0.60 to 0.90	0.040	0.050	1060
—	0.55 to 0.65	0.75 to 1.05	0.040	0.050	1561
—	0.60 to 0.71	0.85 to 1.15	0.040	0.050	1566
1070	0.65 to 0.75	0.60 to 0.90	0.040	0.050	1070
—	0.65 to 0.75	1.00 to 1.30	0.040	0.050	1572
1078	0.72 to 0.85	0.30 to 0.60	0.040	0.050	1078
1080	0.75 to 0.88	0.60 to 0.90	0.040	0.050	1080
1084	0.80 to 0.93	0.60 to 0.90	0.040	0.050	1084
1090	0.85 to 0.98	0.60 to 0.90	0.040	0.050	1090
1095	0.90 to 1.03	0.30 to 0.50	0.040	0.050	1095

* Prefix B indicates acid bessemer steel; others are made by the electric furnace, open hearth, or basic oxygen furnace processes.

† When silicon is required, the following ranges and limits are commonly used: for nonresulfurized steels: up to 1015, 0.10% max; 1015 to 1025, 0.10% max, or 0.10 to 0.20%, or 0.15 to 0.30%; over 1025, 0.10 to 0.20%, or 0.15 to 0.30%; 1513 to 1524, 0.10% max, or 0.10 to 0.20%, or 0.15 to 0.30%; 1525 and over, 0.10 to 0.20%, or 0.15 to 0.30%. For resulfurized steels: to 1110, 0.10% max; 1116 and over, 0.10% max, or 0.10 to 0.20%, or 0.15 to 0.30%. It is not common practice to produce resulfurized and rephosphorized steels to specified limits for silicon because of its adverse effect on machinability.

Copper can be added to a standard steel.

‡ 0.15 to 0.35% Pb. When lead is required as an added element to a standard steel, a range of 0.15 to 0.35%, inclusive, is generally used. Such a steel is identified by inserting the letter "L" between the second and third numeral of the AISI number.

§ SAE 15XX designations (with the exception of 1513, 1518, 1522, 1525, and 1526) were formerly SAE 10XX. The AISI has approved these high-manganese carbon steel compositions and it will publish them shortly. The grades are applicable only to semifinished products for forging, to hot rolled and cold finished bars, to wire rods, and to seamless tubing.

Sources: American Iron & Steel Institute, New York; SAE Standard J403c.

Typical Properties of

AISI Type	Typical Composition, % (a)	Form (b)	Mechanical Properties of Annealed Material at Room Temperature				Nominal Properties of Annealed Material at Low Temperature						
			Tensile Strength, 1000 Psi	Yield Strength (0.2% Offset), 1000 Psi	Elongation in 2 in., %	Hardness	Temperature, F	Tensile Strength, 1000 Psi	Yield Strength, 1000 Psi	Elongation in 2 in., %	Reduction in Area, %	120° Impact Strength, Ft-Lb	
Austenitic (c)													
201	16-18 Cr, 3.5-5.5 Ni, 0.15 C, 5.5-7.5 Mn, 1.0 Si, 0.060 P, 0.030 S, 0.25 N	Sheets Strips	115 115	55 55	55 55	Rb 90 Rb 90	+ 70 -300	— —	— —	— —	— —	110 - 120 38-70	
202	17-19 Cr, 4-6 Ni, 0.15 C, 7.5-10.0 Mn, 1.0 Si, 0.060 P, 0.030 S, 0.25 N	Sheets Strips	105 105	55 55	55 55	Rb 90 Rb 90	+ 70 -100 -300 -423	100 145 200 220	55 95 156 170	55 38 15 5	—	110 - 120 — 42-120 —	
301	16-18 Cr, 6-8 Ni, 0.15 C, 2.0 Mn, 1.0 Si, 0.045 P, 0.030 S	Plates Sheets Strips	105 110 110	40 40 40	55 60 60	Rbm 165 Rb 85 Rb 85	+ 70 + 32 - 40 - 80 -320	105 155 180 195 275	40 43 48 50 75	60 53 42 40 30	70 64 63 62 57	100 110 110 110 110	
302	17-19 Cr, 8-10 Ni, 0.15 C, 2.0 Mn, 1.0 Si, 0.045 P, 0.030 S	Bars Plates Sheets Strips	85 90 90 90	35 35 40 40	60 60 50 50	Bhn 150 Rb 80 Rb 85 Rb 85	+ 70 + 32 - 40 - 80 -320 -423	94 122 145 161 219 250	37 40 48 50 68 125	68 65 60 57 46 41	78 76 73 70 70 55	110 110 110 110 110 —	
302B	17-19 Cr, 8-10 Ni, 0.15 C, 2.0 Mn, 2.0-3.0 Si, 0.045 P, 0.030 S	Bars Plates Sheets Strips	90 90 95 95	40 40 40 40	50 50 55 55	Rb 85 Rb 85 Rb 85 Rb 85	+ 70	Not applicable. Silicon added to type 302 for oxidation resistance					90
303	17-19 Cr, 8-10 Ni, 0.15 C, 2.0 Mn, 1.0 Si, 0.20 P, 0.15 S min, 0.60 Mo (optional)	Bars	90	35	50	Bhn 160	+ 70 + 32 - 40 - 80 -320 -452	100 114 145 162 235 267	40 40 40 40 37 —	67 61 45 40 35 30	67 65 62 60 52 37	85 90 100 106 125 —	
303Se	17-19 Cr, 8-10 Ni, 0.15 C, 2.0 Mn, 1.0 Si, 0.20 P, 0.05 S, 0.15 Se min												
304	18-20 Cr, 8-12 Ni, 0.08 C, 2.0 Mn, 1.0 Si, 0.045 P, 0.030 S	Bars Plates Sheets Strips	85 82 84 84	35 35 42 42	60 60 55 55	Bhn 149 Bhn 149 Rb 80 Rb 80	+ 70 + 32 - 40 - 80 -320 -423	95 130 155 170 221 243	35 34 34 34 39 50	65 55 47 39 40 40	71 68 64 63 55 50	110 110 110 110 110 110	
304L	18-20 Cr, 8-12 Ni, 0.03 C, 2.0 Mn, 1.0 Si, 0.045 P, 0.030 S	Plates Sheets Strips	79 81 81	33 39 39	60 55 55	Bhn 143 Rb 79 Rb 79	+ 70 + 32 - 40 - 80 -320 -423	— — — — — —	— — — — — —	— — — — — —	— — — — — —	— — — — — —	
305	17-19 Cr, 10-13 Ni, 0.12 C, 2.0 Mn, 1.0 Si, 0.045 P, 0.030 S	Plates Sheets Strips	85 85 85	35 38 38	55 50 50	Rb 80 Rb 80 Rb 80	+ 70	—	—	—	—	110	
308	19-21 Cr, 10-12 Ni, 0.08 C, 2.0 Mn, 1.0 Si, 0.045 P, 0.030 S	Bars Plates Sheets Strips	85 85 85 85	30 30 35 35	55 55 50 50	Rb 80 Bhn 150 Rb 80 Rb 80	+ 70	—	—	—	—	110	
309	22-24 Cr, 12-15 Ni, 0.20 C, 2.0 Mn, 1.0 Si, 0.045 P, 0.030 S	Bars Plates Sheets Strips	95 95 95 95	40 40 45 45	45 45 45 45	Rb 83 Bhn 170 Rb 85 Rb 85	+ 70	—	—	—	—	110	
309S	22-24 Cr, 12-15 Ni, 0.08 C, 2.0 Mn, 1.0 Si, 0.045 P, 0.030 S												
310	24-26 Cr, 19-22 Ni, 0.25 C, 2.0 Mn, 1.5 Si, 0.045 P, 0.030 S	Bars Plates Sheets Strips	95 95 95 95	45 45 45 45	50 50 45 45	Rb 89 Bhn 170 Rb 95 Rb 95	+ 70 + 32 - 40 - 80 -320 -423	86 85 95 100 152 176	37 32 39 40 74 108	55 64 57 55 54 56	70 75 75 75 64 61	130 130 130 130 85 —	
310S	24-26 Cr, 19-22 Ni, 0.08 C, 2.0 Mn, 1.5 Si, 0.045 P, 0.30 S												
314	23-25 Cr, 19-22 Ni, 0.25 C, 2.0 Mn, 1.5-3.0 Si, 0.045 P, 0.030 S	Bars Plates Sheets Strips	100 100 100 100	30 30 30 30	45 45 40 40	Bhn 180 Bhn 180 Rb 85 Rb 85	Not applicable. High silicon added to type 310 for carburization resistance						
316	16-18 Cr, 10-14 Ni, 0.05 C, 2.0 Mn, 1.0 Si, 0.045 P, 0.030 S, 2.0-3.0 Mo	Bars Plates Sheets Strips	80 82 84 84	30 36 42 42	40 45 50 50	Rb 70 Bhn 149 Rb 75 Rb 75	+ 70 + 32 - 40 - 80 -320 -423	85 90 104 118 165 210	37 39 41 37 75 84	65 60 50 57 99 92	76 75 75 73 76 60	130 130 130 130 — —	
316L	16-18 Cr, 10-14 Ni, 0.03 C, 2.0 Mn, 1.0 Si, 0.025 P, 0.030 S, 2.0-3.0 Mo	Plates Sheets Strips	81 81 81	34 42 42	55 50 50	Bhn 146 Rb 70 Rb 70	+ 70 + 32 - 40 - 80 -320 -423	— — — — — —	— — — — — —	— — — — — —	— — — — — —	— — — — — —	
317	18-20 Cr, 11-15 Ni, 0.05 C, 2.0 Mn, 1.0 Si, 0.045 P, 0.030 S, 3.0-4.0 Mo	Bars Plates Sheets Strips	85 85 85 85	40 40 40 40	50 50 45 45	Bhn 160 Bhn 160 Rb 85 Rb 85	Same as type 316						

Wrought Stainless Steel

Mechanical Properties at Elevated Temperatures							Thermal Treatment				AISI Type	Characteristics and Applications
Creep Strength					Soaking Temperature		Initial Forging Temperature, F	Annealing Temperature, F (d)	Stress-Relief Annealing Temperature, F	Melting Range, F		
Load for 1% Elongation in 10,000 Hr, 1000 Psi					Max Continuous Service in Air, F	Max Inter-mittent Service in Air, F						
1000 F	1100 F	1200 F	1300 F	1500 F								
—	—	—	—	—	1550	1450	2100-2250	1850-2050	—	—	201	High work hardening rate; low-nickel equivalent of type 301.
—	—	—	—	—	1550	1450	2100-2250	1850-2050	—	—	202	General purpose low-nickel equivalent of type 302.
19	12.5	8	4.5	1.8	1650	1500	2100-2300	1850-2050	400-750	2250-2500	301	High work hardening rate; good for structural applications where high strength plus high ductility is required in railroad cars, trailer bodies, aircraft structures.
20	12.5	7.5	4.3	1.5	1650	1500	2100-2300	1850-2050	400-750	2550-2580	302	General purpose austenitic stainless steel for trim, food handling equipment, aircraft cooling, antennas, springs, architectural, cookware.
—	—	7	4.5	1	1750	1600	2050-2250	1850-2050	—	2500-2550	302B	More resistant to scale than type 302. Used for furnace parts, oil flues, heating elements.
16.5	11.5	6.5	3.5	0.7	1650	1400	2100-2350	1850-2050	400-750	2550-2590	303	Free-machining modification of type 302 for heavier cuts. Used for screw machine products, shafts, valves.
											303Se	Free machining modification of type 302, for lighter cuts and where hot working or cold heading may be involved.
20	12	7.5	4	1.5	1650	1550	2100-2300	1850-2050	400-750	2550-2600	304	Low-carbon modification of type 302 for restriction of carbide precipitation during welding. Used for chemical and food processing equipment, recording wire.
											304L	Extra-low-carbon modification of type 304 for further restriction of carbide precipitation during welding.
19	12.5	8	4.5	2	1650	—	2100-2300	1850-2050	—	2550-2600	305	Low work hardening rate; used for spin forming and severe drawing operations. Used for nuclear energy applications.
—	—	—	—	—	1700	1550	2100-2300	1850-2050	—	2550-2580	306	Higher alloy steel having higher corrosion and heat resistance. Primarily used for welding filler metals to compensate for alloy loss in welding.
16.5	12.5	10	6	3	1900	1850	2000-2250	1900-2000	—	2500-2600	307	Used for its high temperature strength and scale resistance in aircraft heaters, heat treating equipment, annealing furnaces, furnace parts.
											307B	Low-carbon modification of type 307, for welded construction.
33	23	15	10	3	2050	1900	2000-2250	1900-2100	400-750	2550-2600	310	Higher elevated temperature strength and scale resistance than type 307. Used for heat exchangers, furnace parts, combustion chambers, welding filler metal.
											310B	Low-carbon modification of type 310, for welded construction.
20	10	7.5	5	2.5	—	—	1900-2000	2100	—	—	314	More resistant to scale than type 310.
25	17.4	11.6	7.5	2.4	1600	1400	2100-2300	1850-2000	400-750	2520-2590	316	Higher corrosion resistance than types 302 and 304, high creep strength. Used for chemical and pulp handling equipment, photographic and food equipment.
											316L	Extra-low-carbon modification of type 316, for welded construction where intergranular carbide precipitation must be avoided.
23	16.0	11.2	6.9	2.0	1750	1600	2100-2300	1850-2000	—	2500-2600	317	Higher corrosion and creep resistance than type 316.

Typical Properties of Wrought Stainless Steel (Continued)

AISI Type	Typical Composition, % (a)	Form (b)	Mechanical Properties of Annealed Material at Room Temperature				Nominal Properties of Annealed Material at Low Temperature					
			Tensile Strength, 1000 Psi	Yield Strength (0.2% Offset), 1000 Psi	Elongation in 2 in., %	Hardness	Temperature, F	Tensile Strength, 1000 Psi	Yield Strength, 1000 Psi	Elongation in 2 in., %	Reduction in Area, %	Charpy Impact Strength, Ft-Lb
Austenitic (c)												
321	17-19 Cr, 9-12 Ni, 0.08 C, 2.0 Mn, 1.0 Si, 0.045 P, 0.030 S (Ti, 5xC min)	Bars	85	35	55	Bhn 150	+ 70	89	37	62	76	110
		Plates	85	35	55	Bhn 160	+ 32	99	38	58	73	110
		Sheets	90	35	45	Rb 80	- 40	117	44	58	70	115
		Strips	90	35	45	Rb 80	- 80	130	45	57	68	117
							Rb 80	- 320	208	64	44	57
							- 423	238	92	35	—	—
347	17-19 Cr, 9-13 Ni, 0.08 C, 2.0 Mn, 1.0 Si, 0.045 P, 0.030 S (Cb+Ta, 10xC min)	Bars	90	35	55	Bhn 160	+ 70	93	38	55	68	110
		Plates	90	35	55	Bhn 160	+ 32	105	42	62	72	110
		Sheets	95	40	45	Rb 85	- 40	117	44	53	71	117
		Strips	95	40	45	Rb 85	- 80	130	45	57	70	110
						Rb 85	- 320	209	47	43	65	95
							- 423	228	55	39	53	60
Ferritic (c)												
405	11.5-14.5 Cr, 0.08 C, 1.0 Mn, 1.0 Si, 0.040 P, 0.030 S, 0.1-0.3 Al	Bars	70	40	30	Bhn 150	+ 70	Approximately same as type 410 in annealed condition				20-35
		Plates	65	40	30	Bhn 150						
		Sheets	65	40	25	Rb 75						
430	14-18 Cr, 0.12 C, 1.0 Mn, 1.0 Si, 0.040 P, 0.030 S	Bars	75	45	30	Bhn 155	+ 70	65	38	37	73	35
		Plates	75	40	30	Bhn 160	+ 32	69	40	37	72	20
		Sheets	75	50	25	Rb 85	- 40	76	41	36	72	10
		Strips	75	50	25	Rb 85	- 80	81	44	36	70	6
							- 320	90	87	2	4	2
430F	14-18 Cr, 0.12 C, 1.25 Mn, 1.0 Si, 0.080 P, 0.15 S min, 0.80 Mn (optional)											
430FSe	14-18 Cr, 0.12 C, 1.25 Mn, 1.0 Si, 0.080 P, 0.080 S, 0.15 Se min	Bars	80	55	25	Bhn 170	+ 70 - 100 - 300	—	—	—	—	5-50 4 1
442	18-23 Cr, 0.20 C, 1.0 Mn, 1.0 Si, 0.040 P, 0.030 S	Bars	80	45	20	Rb 90	+ 70	—	—	—	—	5-15
446	23-27 Cr, 0.20 C, 1.5 Mn, 1.0 Si, 0.040 P, 0.030 S, 0.25 N	Bars	80	50	25	Rb 86	+ 70	—	—	—	—	2-10
		Plates	85	55	25	Rb 84						
		Sheets	80	50	20	Rb 83						
		Strips	80	50	20	Rb 83						
Martensitic (c)												
403	11.5-13.0 Cr, 0.15 C, 1.0 Mn, 0.5 Si, 0.040 P, 0.030 S	Bars	75	40	35	Rb 82		Some as type 410				
		Sheets	70	45	25	Rb 80						
		Strips	70	45	25	Rb 80						
410	11.5-13.5 Cr, 0.15 C, 1.0 Mn, 1.0 Si, 0.040 P, 0.030 S	Bars	75	40	35	Rb 82	+ 70	110	87	21	68	85
		Plates	70	35	30	Bhn 150	+ 32	115	89	24	69	40
		Sheets	70	45	25	Rb 90	- 40	122	90	23	64	25
		Strips	70	45	25	Rb 90	- 80	128	94	22	60	25
							- 320	138	148	10	11	5
414	11.5-13.5 Cr, 1.25-2.50 Ni, 0.15 C, 1.0 Mn, 1.0 Si, 0.040 P, 0.030 S	Bars	115	50	20	Bhn 235	+ 70	—	—	—	—	40-50
		Plates	115	90	20	Bhn 235						
		Sheets	120	105	15	Rb 92						
		Strips	120	105	15	Rb 92						
416	12-14 Cr, 0.15 C, 1.25 Mn, 1.0 Si, 0.030 P, 0.15 S min, 0.80 Mn (optional)											
416Se	12-14 Cr, 0.15 C, 1.25 Mn, 1.0 Si, 0.030 P, 0.080 S, 0.15 Se min	Bars	75	40	30	Rb 82	+ 70 - 100 - 300	—	—	—	—	20-64 50 3
420	12-14 Cr, 0.15 C min, 1.0 Mn, 1.0 Si, 0.040 P, 0.030 S	Bars	95	50	25	Rb 92	+ 70 + 32 - 40 - 80	—	—	—	—	10 10 8 7
431	15-17 Cr, 1.25-2.50 Ni, 0.20 C, 1.0 Mn, 1.0 Si, 0.040 P, 0.030 S	Bars	125	55	20	Bhn 260	+ 70 + 32 - 40 - 80	—	—	—	—	50 50 30 17
440A	16-18 Cr, 0.80-0.75 C, 1.0 Mn, 1.0 Si, 0.040 P, 0.030 S, 0.75 Nb	Bars	105	60	20	Rb 95	—	—	—	—	—	—
440B	16-18 Cr, 0.75-0.95 C, 1.0 Mn, 1.0 Si, 0.040 P, 0.030 S, 0.75 Nb	Bars	107	62	18	Rb 96	—	—	—	—	—	—
440C	16-18 Cr, 0.95-1.20 C, 1.0 Mn, 1.0 Si, 0.040 P, 0.030 S, 0.75 Nb	Bars	110	65	14	Rb 97	—	—	—	—	—	—

(a) Single values are maximums, except as noted; (b) Forms listed are only those for which mechanical properties are given. Most types are available in many forms; (c) Austenitic, hardenable by cold working; not hardenable by heat treatment. Ferritic, not hardenable by heat treatment or cold working. Martensitic, hardenable by heat treatment; (d) Followed by rapid cooling. H is hardening temperature, T is tempering temperature.

Mechanical Properties at Elevated Temperature							Thermal Treatment				AISI Type	Characteristics and Applications
Creep Strength					Scaling Temperature		Initial Forging Temperature, F	Annealing Temperature, F (d)	Stress-Relief Annealing Temperature, F	Melting Range, F		
Load for 1% Elongation in 10,000 Hr, 1000 Psi					Max Continuous Service in Air, F	Max Intermittent Service in Air, F						
1000 F	1100 F	1200 F	1300 F	1500 F								
18	17	9	5	1.5	1650	1550	2100-2300	1750-2050	400-750(e)	2550-2600	321	Stabilized for weldments subject to severe corrosive conditions and for service from 800 to 1800 F. Used for aircraft exhaust manifolds, boiler shells, process equipment, expansion joints.
											347	Similar to type 321.
32	23	16	10	2	1650	1550	2100-2300	1850-2050	400-750(e)	2550-2600	348	Similar to type 321. Used for nuclear energy applications due to low reactivity.
8.4	—	—	—	—	1400	1450	1950-2050	Low anneal 1350-1500	—	2700-2750	405	Nonhardenable grade for assemblies where air-hardening types (410 or 403) are objectionable.
8.5	4.7	2.6	1.4	—	1550	1650	1900-2050	Low anneal 1400-1500	—	2600-2750	430	General purpose nonhardenable chromium type. Used for decorative trim, nitric acid tanks, annealing baskets.
8.5	4.6	1.9	1.3	—	1500	1600	1950-2100	Low anneal 1250-1400	—	2600-2750	430F	Free-machining modification of type 430, for heavier cuts and screw machine parts.
											430FSo	Free-machining modification of type 430, for lighter cuts and where hot working or cold heading may be involved.
8.5	5	1.6	1	0.6	1600	1900	1600-2100	1300	—	2600-2750	442	High chromium steel. Used principally for parts which must resist high temperatures in service, without scaling—furnace parts, nozzles, combustion chambers.
6.4	2.9	1.4	0.6	0.4	1950	2050	1950-2050	1450-1600	—	2600-2750	446	High resistance to corrosion and scaling at high temperature especially for intermittent service. Often used in sulfur-bearing atmosphere.
									Hardening and Tempering Temperature, F			
11	4.5	2	1.4	—	1300	1450	2000-2200(f)	1500-1650(g) 1200-1400(h)	H1700-1850(d) T 400-1400(i)	2700-2750	403	"Turbine quality" grade for steam turbine blades and other highly stressed parts.
11.5	4.3	2	1.5	—	1300	1450	2000-2200(f)	1500-1650(g) 1200-1400(h)	H1700-1850(d) T 400-1400(i)	2700-2750	410	General purpose heat treatable type, for machine parts, pump shafts.
—	—	—	—	—	1300	1450	2100-2200	— 1300-1300(h)	H1600-1900(d) T 400-1300(i)	—	414	Higher hardenability than type 410, for springs, tempered valves, machine parts.
											415	Free-machining modification of type 410, for heavier cuts.
11	4.6	2	1.2	—	1250	1400	2100-2300(f)	1500-1650(g) 1200-1400(h)	H1700-1850(d) T 400-1400(i)	2700-2750	416a	Free-machining modification of type 410, for lighter cuts and where hot working or cold heading may be involved.
9.2	4.2	2	1	—	1200	1400	2000-2200(j)	1500-1600(g) 1300-1400(h)	H1600-1900(d) T 300-700	2600-2750	420	Higher carbon modification of type 410 often used for cutlery, surgical instruments, valves and other wear-resisting parts.
6.8	3.5	—	—	—	1600	1600	2100-2250(j)	— 1150-1225(h)	H1600-1900(d) T 400-1200(i)	—	431	Special-purpose hardenable steel used where particularly high mechanical properties are required—stencil fittings, boiler bars, paper machinery rolls.
—	—	—	—	—	1400	1500	1900-2250(j)	1500-1650(g) 1300-1450(h)	H1600-1900(d) T 300-650	2600-2750	440A	Hardenable to higher hardness than type 420 with good corrosion resistance. Used for cutlery, bearings, surgical tools.
—	—	—	—	—	1400	1500	1900-2100(j)	1500-1650(g) 1350-1450(h)	H1600-1900(d) T 300-650	2500-2750	440B	Cutlery grade; for fixed type of stainless cutlery, valve parts, and other wear-resisting and high hardness parts.
—	—	—	—	—	1400	1500	1900-2100(j)	1500-1650(g) 1350-1450(h)	H1600-1900(d) T 300-650	2500-2750	440C	Yields highest hardness of hardenable stainless steels for tools, bearings, rolls.

Notes: (a) Stabilizing temperature, 1900 to 1800 F; (f) Rotated cast; (g) Full anneal, followed by slow cooling; (h) Low anneal; (i) Tempering within the range of 600 to 1300 F is not recommended because of resulting low and erratic impact properties and reduced corrosion resistance. Time at temperature and temperatures may vary depending on part size; (j) Rotated cast and anneal.

Data supplied by the American Iron and Steel Institute Committee of Stainless Steel Producers.

Correlation of Specifications for Stainless Steels

By J. Gordon Parr and Albert Hanson*

Many of the common composition ranges of wrought stainless steels are classified as standard AISI (American Iron and Steel Institute) types. The AISI number designates a specified composition range based on the ladle analysis of the steel. The Society of Automotive Engineers (SAE) uses a five-digit system in which the last three digits correspond to the AISI number. The numbers in either system offer no rational clues as to composition except

that the austenitic series in the AISI system begins with the number 3; the manganese-substituted austenitic steels begin with a 2 (there are only two such standard steels); both ferritic and martensitic classes in the AISI system begin with the number 4, and the lower numbers in the martensitic class have a lower carbon content.

Specifications of the Alloy Casting Institute (ACI) refer exclusively to cast alloys, although

some of the ACI alloys approximate compositions of wrought alloys. The American Society for Testing and Materials (ASTM) calls for requirements in addition to composition including mechanical properties, heat treatments and testing procedures.

*Adapted from the book by the authors, "An Introduction to Stainless Steel", published by the American Society for Metals, Metals Park, Ohio.

Wrought Alloys			Cast Alloys		
AISI	SAE	ASTM	SAE	ACI	ASTM
Martensitic					
403	51403	Plate, sheet, strip: A176 Bars, billets: A276	—	—	—
410	51410	Plate, sheet, strip: A176, A240 Bars, billets: A276 Pipe, tube: A268	60410	CA-15	A296
414	51414	Bars, billets: A276	—	—	—
416, 416Se	51416, 51416Se	Bars, billets: A276	—	—	—
420	51420	Bars, billets: A276	60420	CA-40	—
431	51431	Bars, billets: A276	—	—	—
440A, 440B, 440C	—	Bars, billets: A276	—	—	A296
Ferritic					
405	51405	Plate, sheet, strip: A240 Bars, billets: A276 Pipe, tube: A268	—	—	A351
430, 430F, 430SeF	51430, 51430F, 51430SeF	Plate, sheet, strip: A176, A240 Bars, billets: A276 Pipe, tube: A268	—	—	—
442	51442	Plate, sheet, strip: A175 Bars, billets: A276 Pipe, tube: A268	60442	CB-30	A296
446	51446	Plate, sheet, strip: A176 Bars, billets: A276 Pipe, tube: A268	70446	HC	A297
Austenitic					
301	30301	Plate, sheet, strip: A167, A264 (clad)	—	—	—
302	30302	Plate, sheet, strip: A167, A240, A264 (clad) Bars, billets: A276, A314	—	CF-20	A296
302B	30302B	Plate, sheet, strip: A167 Bars, billets: A276, A314	—	HF	A297
303, 303Se	30303, 30303Se	Bars, billets: A276, A314 Nuts, bolts: A194, A320	—	CF-16F	A296
304, 304L	30304, 30304L	Plate, sheet, strip: A167, A177, A240, A264 Bars, billets: A276, A314 Pipe, tube: A213, A249, A269, A270, A271, A312, A358, A376 Nuts, bolts: A193, A194, A320 Forgings, fittings: A182, A336	60304, 60304L	CF-8, CF-3	A296, A351
305	30305	Plate, sheet, strip: A240 Bars, billets: A314 Pipe, tube: A249	—	—	—
308	30308	Plate, sheet, strip: A167, A264 Bars, billets: A276, A314	—	—	—

Wrought Alloys			Cast Alloys		
AISI	SAE	ASTM	SAE	ACI	ASTM
Manganese-Substituted Austenitic					
309, 309S	30309, 30309S	Welding electrodes: A298 Plate, sheet, strip: A167, A240, A264 Bars, billets: A276, A314 Pipe, tube: A249, A312, A358 Welding electrodes: A298	60309, 70309	CH-20, HH	A296, A297, A351
310, 310S	30310, 30310S	Plate, sheet, strip: A167, A240, A264 Bars, billets: A276, A314 Pipe, tube: A213, A249, A312, A358 Forgings, fittings: A182, A336 Welding electrodes: A298	60310, 70310	CK-20, HK	A296, A297, A351
314	30314	Bars, billets: A314	—	—	—
316, 316L	30316, 30316L	Plate, sheet, strip: A167, A240, A264 Bars, billets: A276, A314 Pipe, tube: A213, A249, A269, A312, A358, A376 Nuts, bolts: A193 Forgings, fittings: A182, A336 Welding electrodes: A298	60316, 60316L	CF-3M, CF-8M, CF-12M	A296, A351
317	30317	Plate, sheet, strip: A240 Bars, billets: A314 Pipe, tube: A249, A269, A312 Welding electrodes: A298	60317	CG-8M	A296
321	30321	Plate, sheet, strip: A167, A240, A264 Bars, billets: A276, A314 Pipe, tube: A213, A249, A269, A271, A312, A358, A376 Nuts, bolts: A193, A194, A320 Forgings, fittings: A182, A336	—	—	—
347	30347	Plate, sheet, strip: A167, A240, A264 Bars, billets: A276, A314 Pipe, tube: A213, A249, A269, A271, A298, A358, A376 Nuts, bolts: A193, A194, A320 Forgings, fittings: A182, A336 Welding electrodes: A298	60347	CF-8C	A296, A351
348	30348	Plate, sheet, strip: A240 Bars, billets: A276, A314 Pipe, tube: A213, A249, A269, A358, A376 Nuts, bolts: A320	—	—	—
Precipitation Hardening					
201	30201	—	—	—	—
202	30202	—	—	—	—
630	—	Bars, forgings: A461	—	—	—
631	—	Bars, forgings: A461	—	—	—
632	—	Bars, forgings: A461	—	—	—
633	—	Bars, forgings: A461	—	—	—
634	—	Bars, forgings: A461	—	—	—

SAE Standard Alloy Steel Compositions (Bars, Blooms, Billets and Slabs)

SAE J404c, Revised July 1964

SAE No.	Composition, %								Corresponding AISI No.
	C	Mn	P	S	Si	Ni	Cr	Other	
1330	0.78-0.33	1.80-1.90	0.035	0.040	0.20-0.35	—	—	—	1330
1335	0.33-0.38	1.80-1.90	0.035	0.040	0.20-0.35	—	—	—	1335
1340	0.38-0.43	1.80-1.90	0.035	0.040	0.20-0.35	—	—	—	1340
1345	0.43-0.48	1.80-1.90	0.035	0.040	0.20-0.35	—	—	—	1345
4012	0.09-0.14	0.75-1.00	0.035	0.040	0.20-0.35	—	—	0.15-0.25	4012
4023	0.20-0.25	0.70-0.90	0.035	0.040	0.20-0.35	—	—	0.20-0.30	4023
4024	0.20-0.25	0.70-0.90	0.035	0.035-0.050	0.20-0.35	—	—	0.20-0.30	4024
4027	0.25-0.30	0.70-0.90	0.035	0.040	0.20-0.35	—	—	0.20-0.30	4027
4028	0.25-0.30	0.70-0.90	0.035	0.035-0.050	0.20-0.35	—	—	0.20-0.30	4028
4032	0.30-0.35	0.70-0.90	0.035	0.040	0.20-0.35	—	—	0.20-0.30	4032
4037	0.35-0.40	0.70-0.90	0.035	0.040	0.20-0.35	—	—	0.20-0.30	4037
4042	0.40-0.45	0.70-0.90	0.035	0.040	0.20-0.35	—	—	0.20-0.30	4042
4047	0.45-0.50	0.70-0.90	0.035	0.040	0.20-0.35	—	—	0.20-0.30	4047
4118	0.12-0.23	0.70-0.90	0.035	0.040	0.20-0.35	—	0.40-0.60	0.30-0.15	4118
4130	0.28-0.33	0.40-0.80	0.035	0.040	0.20-0.35	—	0.80-1.10	0.15-0.25	4130
4135	0.33-0.38	0.70-0.90	0.035	0.040	0.20-0.35	—	0.80-1.10	0.15-0.25	—
4137	0.35-0.40	0.70-0.90	0.035	0.040	0.20-0.35	—	0.80-1.10	0.15-0.25	4137
4140	0.38-0.43	0.75-1.00	0.035	0.040	0.20-0.35	—	0.80-1.10	0.15-0.25	4140
4142	0.40-0.45	0.75-1.00	0.035	0.040	0.20-0.35	—	0.80-1.10	0.15-0.25	4142
4145	0.43-0.48	0.75-1.00	0.035	0.040	0.20-0.35	—	0.80-1.10	0.15-0.25	4145
4147	0.45-0.50	0.75-1.00	0.035	0.040	0.20-0.35	—	0.80-1.10	0.15-0.25	4147
4150	0.48-0.53	0.75-1.00	0.035	0.040	0.20-0.35	—	0.80-1.10	0.15-0.25	4150
4161	0.55-0.65	0.75-1.00	0.035	0.040	0.20-0.35	—	0.70-0.90	0.25-0.35	—
4320	0.17-0.22	0.45-0.65	0.035	0.040	0.20-0.35	1.65-2.00	0.40-0.60	0.20-0.30	4320
4340	0.30-0.43	0.80-0.90	0.035	0.040	0.20-0.35	1.65-2.00	0.70-0.90	0.20-0.30	4340
E4340	0.30-0.43	0.65-0.85	0.025	0.025	0.20-0.35	1.65-2.00	0.70-0.90	0.20-0.30	E4340
4419	0.18-0.23	0.45-0.65	0.035	0.040	0.20-0.35	—	—	0.45-0.60	4419
4422	0.20-0.25	0.70-0.90	0.035	0.040	0.20-0.35	—	—	0.35-0.45	—
4427	0.24-0.29	0.70-0.90	0.035	0.040	0.20-0.35	—	—	0.35-0.45	—
4615	0.13-0.18	0.45-0.65	0.035	0.040	0.20-0.35	1.65-2.00	—	0.20-0.30	4615
4617	0.15-0.20	0.45-0.65	0.035	0.040	0.20-0.35	1.65-2.00	—	0.20-0.30	—
4620	0.17-0.22	0.45-0.65	0.035	0.040	0.20-0.35	1.65-2.00	—	0.20-0.30	4620
4621	0.18-0.23	0.70-0.90	0.035	0.040	0.20-0.35	1.65-2.00	—	0.20-0.30	4621
4626	0.24-0.29	0.45-0.65	0.035	0.04 max	0.20-0.35	0.70-1.00	—	0.15-0.25	—
4718	0.16-0.21	0.70-0.90	—	—	—	0.90-1.20	0.25-0.55	0.30-0.40	4718
4720	0.17-0.22	0.50-0.70	0.035	0.040	0.20-0.35	0.90-1.20	0.35-0.55	0.15-0.25	4720
4815	0.13-0.18	0.40-0.60	0.035	0.040	0.20-0.35	3.25-3.75	—	0.20-0.30	4815
4817	0.15-0.20	0.40-0.60	0.035	0.040	0.20-0.35	3.25-3.75	—	0.20-0.30	4817
4820	0.18-0.23	0.50-0.70	0.035	0.040	0.20-0.35	3.25-3.75	—	0.20-0.30	4820
5015	0.12-0.17	0.30-0.50	0.035	0.040	0.20-0.35	—	0.30-0.50	—	5015
5040	0.30-0.43	0.75-1.00	0.035	0.040	0.20-0.35	—	0.40-0.60	—	—
5044	0.43-0.48	0.75-1.00	0.035	0.040	0.20-0.35	—	0.40-0.60	—	5044
5046	0.43-0.48	0.75-1.00	0.035	0.040	0.20-0.35	—	0.20-0.35	—	—
5044H	0.44-0.49	0.75-1.00	0.035	0.040	0.20-0.35	—	0.20-0.35	—	5044H
5045H	0.46-0.53	0.75-1.00	0.035	0.040	0.20-0.35	—	0.40-0.60	—	5045H
5046H	0.50-0.64	0.75-1.00	0.035	0.040	0.20-0.35	—	0.40-0.60	—	5046H
5115	0.13-0.18	0.70-0.90	0.035	0.040	0.20-0.35	—	0.70-0.90	—	—
5120	0.17-0.22	0.70-0.90	0.035	0.040	0.20-0.35	—	0.70-0.90	—	5120
5130	0.28-0.33	0.70-0.90	0.035	0.040	0.20-0.35	—	0.80-1.10	—	5130
5132	0.30-0.35	0.80-0.90	0.035	0.040	0.20-0.35	—	0.75-1.00	—	5132
5135	0.33-0.38	0.80-0.90	0.035	0.040	0.20-0.35	—	0.80-1.05	—	5135
5140	0.38-0.43	0.70-0.90	0.035	0.040	0.20-0.35	—	0.70-0.90	—	5140
5145	0.43-0.48	0.70-0.90	0.035	0.040	0.20-0.35	—	0.70-0.90	—	5145
5147	0.45-0.51	0.70-0.90	0.035	0.040	0.20-0.35	—	0.65-1.15	—	5147
5150	0.48-0.53	0.70-0.90	0.035	0.040	0.20-0.35	—	0.70-0.90	—	5150
5155	0.51-0.59	0.70-0.90	0.035	0.040	0.20-0.35	—	0.70-0.90	—	5155
5160	0.54-0.64	0.75-1.00	0.035	0.040	0.20-0.35	—	0.70-0.90	—	5160
5160H	0.56-0.64	0.75-1.00	0.035	0.040	0.20-0.35	—	0.70-0.90	—	5160H
52100	0.50-1.00	0.25-0.45	0.025	0.025	0.20-0.35	—	0.40-0.60	—	—
52100	0.50-1.00	0.25-0.45	0.025	0.025	0.20-0.35	—	0.90-1.15	—	52100
52100	0.50-1.00	0.25-0.45	0.025	0.025	0.20-0.35	—	1.30-1.60	V	52100
6130	0.16-0.21	0.50-0.70	0.035	0.040	0.20-0.35	—	0.50-0.70	0.10-0.15	6130
6130	0.40-0.53	0.70-0.90	0.035	0.040	0.20-0.35	—	0.60-1.10	0.15	6130
6135	0.13-0.18	0.70-0.90	0.035	0.040	0.20-0.35	0.20-0.40	0.30-0.50	0.00-0.15	6135
6135H	0.43-0.48	0.75-1.00	0.035	0.040	0.20-0.35	0.20-0.40	0.35-0.55	0.00-0.15	6135H
6415	0.13-0.18	0.70-0.90	0.035	0.040	0.20-0.35	0.40-0.70	0.40-0.60	0.15-0.25	—
6417	0.15-0.20	0.70-0.90	0.035	0.040	0.20-0.35	0.40-0.70	0.40-0.60	0.15-0.25	6417
6420	0.18-0.23	0.70-0.90	0.035	0.040	0.20-0.35	0.40-0.70	0.40-0.60	0.15-0.25	6420
6422	0.20-0.25	0.70-0.90	0.035	0.040	0.20-0.35	0.40-0.70	0.40-0.60	0.15-0.25	6422
6425	0.23-0.28	0.70-0.90	0.035	0.040	0.20-0.35	0.40-0.70	0.40-0.60	0.15-0.25	6425
6427	0.25-0.30	0.70-0.90	0.035	0.040	0.20-0.35	0.40-0.70	0.40-0.60	0.15-0.25	6427
6430	0.28-0.33	0.70-0.90	0.035	0.040	0.20-0.35	0.40-0.70	0.40-0.60	0.15-0.25	6430
6432	0.30-0.35	0.75-1.00	0.035	0.040	0.20-0.35	0.40-0.70	0.40-0.60	0.15-0.25	6432
6435	0.33-0.38	0.75-1.00	0.035	0.040	0.20-0.35	0.40-0.70	0.40-0.60	0.15-0.25	6435
6437	0.35-0.40	0.75-1.00	0.035	0.040	0.20-0.35	0.40-0.70	0.40-0.60	0.15-0.25	6437
6440	0.38-0.43	0.75-1.00	0.035	0.040	0.20-0.35	0.40-0.70	0.40-0.60	0.15-0.25	6440
6442	0.40-0.45	0.75-1.00	0.035	0.040	0.20-0.35	0.40-0.70	0.40-0.60	0.15-0.25	6442
6445	0.43-0.48	0.75-1.00	0.035	0.040	0.20-0.35	0.40-0.70	0.40-0.60	0.15-0.25	6445
6447	0.45-0.51	0.75-1.00	0.035	0.040	0.20-0.35	0.40-0.70	0.40-0.60	0.15-0.25	6447
6450	0.48-0.53	0.75-1.00	0.035	0.040	0.20-0.35	0.40-0.70	0.40-0.60	0.15-0.25	6450
6452	0.50-0.59	0.75-1.00	0.035	0.040	0.20-0.35	0.40-0.70	0.40-0.60	0.15-0.25	6452
6455	0.53-0.64	0.75-1.00	0.035	0.040	0.20-0.35	0.40-0.70	0.40-0.60	0.15-0.25	6455
6457	0.56-0.64	0.75-1.00	0.035	0.040	0.20-0.35	0.40-0.70	0.40-0.60	0.15-0.25	6457
6460	0.59-0.64	0.75-1.00	0.035	0.040	0.20-0.35	0.40-0.70	0.40-0.60	0.15-0.25	6460
6462	0.62-0.65	0.75-1.00	0.035	0.040	0.20-0.35	0.40-0.70	0.40-0.60	0.15-0.25	6462
6465	0.65-0.68	0.75-1.00	0.035	0.040	0.20-0.35	0.40-0.70	0.40-0.60	0.15-0.25	6465
6467	0.68-0.73	0.75-1.00	0.035	0.040	0.20-0.35	0.40-0.70	0.40-0.60	0.15-0.25	6467
6470	0.71-0.76	0.75-1.00	0.035	0.040	0.20-0.35	0.40-0.70	0.40-0.60	0.15-0.25	6470
6472	0.74-0.79	0.75-1.00	0.035	0.040	0.20-0.35	0.40-0.70	0.40-0.60	0.15-0.25	6472
6475	0.77-0.82	0.75-1.00	0.035	0.040	0.20-0.35	0.40-0.70	0.40-0.60	0.15-0.25	6475
6477	0.80-0.85	0.75-1.00	0.035	0.040	0.20-0.35	0.40-0.70	0.40-0.60	0.15-0.25	6477
6480	0.83-0.88	0.75-1.00	0.035	0.040	0.20-0.35	0.40-0.70	0.40-0.60	0.15-0.25	6480
6482	0.86-0.91	0.75-1.00	0.035	0.040	0.20-0.35	0.40-0.70	0.40-0.60	0.15-0.25	6482
6485	0.89-0.94	0.75-1.00	0.035	0.040	0.20-0.35	0.40-0.70	0.40-0.60	0.15-0.25	6485
6487	0.92-0.97	0.75-1.00	0.035	0.040	0.20-0.35	0.40-0.70	0.40-0.60	0.15-0.25	6487
6490	0.95-1.00	0.75-1.00	0.035	0.040	0.20-0.35	0.40-0.70	0.40-0.60	0.15-0.25	6490
6492	0.98-1.03	0.75-1.00	0.035	0.040	0.20-0.35	0.40-0.70	0.40-0.60	0.15-0.25	6492
6495	1.01-1.06	0.75-1.00	0.035	0.040	0.20-0.35	0.40-0.70	0.40-0.60	0.15-0.25	6495
6497	1.04-1.09	0.75-1.00	0.035	0.040	0.20-0.35	0.40-0.70	0.40-0.60	0.15-0.25	6497
6500	1.07-1.12	0.75-1.00	0.035	0.040	0.20-0.35	0.40-0.70	0.40-0.60	0.15-0.25	6500
6502	1.10-1.15	0.75-1.00	0.035	0.040	0.20-0.35	0.40-0.70	0.40-0.60	0.15-0.25	6502
6505	1.13-1.18	0.75-1.00	0.035	0.040	0				

AISI-SAE Standard H-Steel Compositions

AISI-SAE No. (a)	C	Mn	Ni	Cr	Other
1330 H	0.27-0.33	1.45-2.05	—	—	—
1335 H	0.32-0.38	1.45-2.05	—	—	—
1340 H	0.37-0.44	1.45-2.05	—	—	—
1345 H	0.42-0.49	1.45-2.05	—	—	—
					Mo
4027 H	0.24-0.30	0.60-1.00	—	—	0.20-0.30
4028 H(b)	0.24-0.30	0.60-1.00	—	—	0.20-0.30
4032 H (c)	0.29-0.35	0.60-1.00	—	—	0.20-0.30
4037 H	0.34-0.41	0.60-1.00	—	—	0.20-0.30
4042 H (c)	0.39-0.46	0.60-1.00	—	—	0.20-0.30
4047 H	0.44-0.51	0.60-1.00	—	—	0.20-0.30
4118 H	0.17-0.23	0.60-1.00	—	0.30-0.70	0.08-0.15
4130 H	0.27-0.33	0.30-0.70	—	0.75-1.20	0.15-0.25
4135 H (c)	0.32-0.38	0.60-1.00	—	0.75-1.20	0.15-0.25
4137 H	0.34-0.41	0.60-1.00	—	0.75-1.20	0.15-0.25
4140 H	0.37-0.44	0.65-1.10	—	0.75-1.20	0.15-0.25
4142 H	0.39-0.46	0.65-1.10	—	0.75-1.20	0.15-0.25
4145 H	0.42-0.49	0.65-1.10	—	0.75-1.20	0.15-0.25
4147 H	0.44-0.51	0.65-1.10	—	0.75-1.20	0.15-0.25
4150 H	0.47-0.54	0.65-1.10	—	0.75-1.20	0.15-0.25
4161 H	0.55-0.65	0.65-1.10	—	0.65-0.95	0.25-0.35
4320 H	0.17-0.23	0.40-0.70	1.55-2.00	0.35-0.65	0.20-0.30
4340 H	0.37-0.44	0.55-0.90	1.55-2.00	0.55-0.95	0.20-0.30
E4340 H (d)	0.37-0.44	0.60-0.95	1.55-2.00	0.65-0.95	0.20-0.30
4419 H	0.17-0.23	0.35-0.75	—	—	0.45-0.60
4620 H	0.17-0.23	0.35-0.75	1.55-2.00	—	0.20-0.30
4621 H	0.17-0.23	0.60-1.00	1.55-2.00	—	0.20-0.30
4626 H (c)	0.23-0.29	0.40-0.70	0.65-1.05	—	0.15-0.25
4718 H	0.15-0.21	0.60-0.95	0.85-1.25	0.30-0.60	0.30-0.40
4720 H	0.17-0.23	0.45-0.75	0.85-1.25	0.30-0.60	0.15-0.25
4815 H	0.12-0.18	0.30-0.70	3.20-3.80	—	0.20-0.30
4817 H	0.14-0.20	0.30-0.70	3.20-3.80	—	0.20-0.30
4820 H	0.17-0.23	0.40-0.80	3.20-3.80	—	0.20-0.30
50B40 H (c) (e)	0.37-0.44	0.65-1.10	—	0.30-0.70	—
50B44 H (e)	0.42-0.49	0.65-1.10	—	0.30-0.70	—
5046 H (c)	0.43-0.50	0.65-1.10	—	0.13-0.43	—
50B46 H (e)	0.43-0.50	0.65-1.10	—	0.13-0.43	—
50B50 H (e)	0.47-0.54	0.65-1.10	—	0.30-0.70	—
50B60 H (e)	0.55-0.65	0.65-1.10	—	0.30-0.70	—
5120 H	0.17-0.23	0.60-1.00	—	0.60-1.00	—
5130 H	0.27-0.33	0.60-1.00	—	0.75-1.20	—
5132 H	0.29-0.35	0.50-0.90	—	0.65-1.10	—
5135 H	0.32-0.38	0.50-0.90	—	0.70-1.15	—
5140 H	0.37-0.44	0.60-1.00	—	0.60-1.00	—
5145 H	0.42-0.49	0.60-1.00	—	0.60-1.00	—
5147 H	0.45-0.52	0.60-1.05	—	0.80-1.25	—
5150 H	0.47-0.54	0.60-1.00	—	0.60-1.00	—
5155 H	0.50-0.60	0.60-1.00	—	0.60-1.00	—
5160 H	0.55-0.65	0.65-1.10	—	0.60-1.00	—
51B60 H (e)	0.55-0.65	0.65-1.10	—	0.60-1.00	—
					V
6118 H	0.15-0.21	0.40-0.80	—	0.40-0.80	0.10-0.15
6150 H	0.47-0.54	0.60-1.00	—	0.75-1.20	0.15 min.
					Mo
81B45 H (e)	0.42-0.49	0.70-1.05	0.15-0.45	0.30-0.60	0.08-0.15
8617 H	0.14-0.20	0.60-0.95	0.35-0.75	0.35-0.65	0.15-0.25
8620 H	0.17-0.23	0.80-0.95	0.35-0.75	0.35-0.65	0.15-0.25
8622 H	0.19-0.25	0.60-0.95	0.35-0.75	0.35-0.65	0.15-0.25
8625 H	0.22-0.28	0.80-0.95	0.35-0.75	0.35-0.65	0.15-0.25
8627 H	0.24-0.30	0.80-0.95	0.35-0.75	0.35-0.65	0.15-0.25
8630 H	0.27-0.33	0.60-0.95	0.35-0.75	0.35-0.65	0.15-0.25
8637 H	0.34-0.41	0.70-1.05	0.35-0.75	0.35-0.65	0.15-0.25
8640 H	0.37-0.44	0.70-1.05	0.35-0.75	0.35-0.65	0.15-0.25
8642 H	0.39-0.46	0.70-1.05	0.35-0.75	0.35-0.65	0.15-0.25
8645 H	0.42-0.49	0.70-1.05	0.35-0.75	0.35-0.65	0.15-0.25
88B45 H (c) (e)	0.42-0.49	0.70-1.05	0.35-0.75	0.35-0.65	0.15-0.25
8850 H (c)	0.47-0.54	0.70-1.05	0.35-0.75	0.35-0.65	0.15-0.25
8855 H	0.50-0.60	0.70-1.05	0.35-0.75	0.35-0.65	0.15-0.25
8880 H (c)	0.55-0.65	0.70-1.05	0.35-0.75	0.35-0.65	0.15-0.25
8720 H	0.17-0.23	0.80-0.95	0.35-0.75	0.35-0.65	0.20-0.30
8740 H	0.37-0.44	0.70-1.05	0.35-0.75	0.35-0.65	0.20-0.30
8822 H	0.19-0.25	0.70-1.05	0.35-0.75	0.35-0.65	0.30-0.40
9280 H (f)	0.55-0.65	0.65-1.10	—	—	—
9310 H (c) (d)	0.07-0.13	0.40-0.70	2.95-3.55	1.00-1.45	0.08-0.15
94B15 H (c) (e)	0.12-0.18	0.70-1.05	0.25-0.65	0.25-0.55	0.08-0.15
94B17 H (e)	0.14-0.20	0.70-1.05	0.25-0.65	0.25-0.55	0.08-0.15
94B36 H (e)	0.27-0.33	0.70-1.05	0.25-0.65	0.25-0.55	0.08-0.15

(a) H-steels contain 0.20 to 0.35% Si, except for 9260 H. Maximum phosphorus and sulfur contents for each steelmaking process are as follows: basic electric, 0.025 P, 0.025 S; basic open hearth or basic oxygen, 0.035 P, 0.040 S; acid electric, 0.050 P, 0.050 S; acid open hearth, 0.050 P, 0.050 S. Minimum silicon limit for acid open hearth or acid electric furnace alloy steel is 0.15%. Small quantities of certain elements are present in alloy steels which are considered as incidental and may be present to the following maximum amounts: 0.35 Cu, 0.25 Ni, 0.20 Cr, and 0.06 Mo. Standard H-steels can be produced with 0.15 to 0.35% Pb. Such steels are identified by inserting the letter "L" between the second and third numerals of the AISI number. A ladle analysis for lead is not determinable, since lead is added to the ladle stream while each ingot is poured. (b) Resulfurized; 0.035 to 0.050% S. (c) SAE designations only. 4626 H is AISI only. (d) Electric furnace steel. (e) 0.0005% B min. (f) 1.70 to 2.20% Si.

Source: AISI Steel Products Manual, February 1964, and 1968 SAE Handbook

Composition, Properties and Producers of High Strength Steels

I. Columbium or Vanadium Group

SAE J410b, 945X, 950X, 955X, 960X, 965X and 970X

With added copper there may be limited application to ASTM A242, A347 and A375. Usually these are semikilled steels but may be killed, particularly at higher strength levels.

Name	Producer Code	Composition, %								Mechanical Properties		
		C	Mn	P	S	Si	Cu (Min)	Cb (Min)	or V (Min)	Yield, 1000 Psi	Tensile, 1000 Psi	Elongation in 2 in., %
AWX-45	AW	(0.12)	(0.45)	(0.02)	(0.03)	(0.04)	—	(0.02)	—	45	63	24
50	AW	(0.14)	(0.50)	(0.02)	(0.03)	(0.04)	—	(0.02)	—	50	67	22
55	AW	(0.16)	(0.55)	(0.02)	(0.03)	(0.04)	—	(0.02)	—	55	70	20
AW-Ten	AW	(0.18)	(0.75)	(0.02)	(0.03)	(0.04)	(0.25)	(0.02)	—	50	70	18
High Strength												
#7	ARM	(0.13)	(0.70)	—	—	—	Opt	(0.02)	—	45	65	22
#6	ARM	(0.17)	(0.70)	—	—	—	Opt	(0.02)	—	50	70	22
C-45	ARM	0.22	1.15	0.04	0.05	0.10	—	0.005	—	45	65	19
C-50	ARM	0.22	1.15	0.04	0.05	0.10	—	0.005	—	50	70	18
C-55	ARM	0.26	1.35	0.04	0.05	0.30	—	0.005	—	55	75	16
C-60	ARM	0.26	1.60	0.04	0.05	0.30	—	0.005	—	60	80	14
V42(a)	B	0.22	1.25	0.04	0.05	—	Opt	—	0.02	42	63	20 (c)
V45	B	0.22	1.25	0.04	0.05	—	Opt	—	0.02	45	65	18 (c)
V50	B	0.22	1.25	0.04	0.05	—	Opt	—	0.02	50	70	18 (c)
V55(b)	B	0.25	1.35	0.04	0.05	—	Opt	—	0.02	55	70	17 (c)
V60	B	0.25	1.35	0.04	0.05	—	Opt	—	0.02	60	75	16 (c)
V65	B	0.22	1.25	0.04	0.05	—	Opt	—	0.02	65	80	15 (c)
Hi-Yield 42	GC	0.21	0.90	0.04	0.05	—	—	0.01	—	42	63	24
45	GC	0.22	1.25	0.04	0.05	—	—	0.01	—	45	60	22
50	GC	0.22	1.25	0.04	0.05	—	—	0.01	—	50	65	20
55	GC	0.25	1.35	0.04	0.05	—	—	0.01	—	55	70	18
(Sheet)												
INX-45	IN	0.20	1.00	0.04	0.05	0.30	Opt	0.01	0.01	45	60	25
50	IN	0.20	1.00	0.04	0.05	0.30	Opt	0.01	0.01	50	65	22
55	IN	0.21	1.25	0.04	0.05	0.30	Opt	0.01	0.01	55	70	20
60	IN	0.22	1.25	0.04	0.05	0.30	Opt	0.01	0.01	60	75	20
65	IN	0.24	1.35	0.04	0.05	0.30	Opt	0.01	0.01	65	80	18
70	IN	0.26	1.35	0.04	0.05	0.30	Opt	0.01	0.01	70	85	16
(Plate)												
INX-42	IN	0.20	0.90	0.04	0.05	0.30	Opt	0.01	0.01	42	63	20 (c)
45	IN	0.20	1.25	0.04	0.05	0.30	Opt	0.01	0.01	45	65	19 (c)
50	IN	0.22	1.25	0.04	0.05	0.30	Opt	0.01	0.01	50	70	18 (c)
55	IN	0.22	1.35	0.04	0.05	0.30	Opt	0.01	0.01	55	75	17 (c)
60	IN	0.24	1.35	0.04	0.05	0.30	Opt	0.01	0.01	60	80	16 (c)
65	IN	0.25	1.35	0.04	0.05	0.30	Opt	0.01	0.01	65	85	15 (c)
70	IN	0.26	1.35	0.04	0.05	0.30	Opt	0.01	0.01	70	90	14 (c)
Amscol 45	IA	0.16	0.70	0.04	0.05	—	—	0.015	—	45	60	30
50	IA	0.18	0.70	0.04	0.05	0.04	—	0.015	—	50	63	30
IH "50"	IH	0.22	1.50	0.04	0.05	0.70	0.20	—	—	50	75	20
"65"	IH	0.22	1.65	0.04	0.05	0.70	0.20	0.01	0.01	65	90	18
INX-45	IH	0.20	1.00	0.04	0.05	0.10	—	0.01	0.01	45	60	22
50	IH	0.22	1.10	0.04	0.05	0.10	Opt	0.01	0.01	50	65	20
55	IH	0.24	1.40	0.04	0.05	0.30	Opt	0.01	0.01	55	70	18
60	IH	0.26	1.55	0.04	0.05	0.30	Opt	0.01	0.01	60	75	18
65	IH	0.26	1.60	0.04	0.05	0.30	Opt	0.01	0.01	65	80	17
70	IH	0.26	1.65	0.04	0.05	0.30	Opt	0.01	0.01	70	85	16
JLX-42	JL	0.20	1.00	0.04	0.05	0.30	Opt	0.01	0.01	42	57	25
45	JL	0.20	1.10	0.04	0.05	0.30	Opt	0.01	0.01	45	60	24
50	JL	0.22	1.20	0.04	0.05	0.30	Opt	0.01	0.01	50	65	22
55	JL	0.24	1.20	0.04	0.05	0.20	Opt	0.01	0.01	55	70	20
60	JL	0.25	1.35	0.04	0.05	0.30	Opt	0.01	0.01	60	75	18
65	JL	0.26	1.50	0.04	0.05	0.30	Opt	0.01	0.01	65	80	16
70	JL	0.26	1.65	0.04	0.05	0.30	Opt	0.01	0.01	70	85	14

I. Columbium or Vanadium Group—Continued

Name	Producer Code	Composition, %								Mechanical Properties		
		C	Mn	P	S	Si	Cu (Min)	Cb (Min)	or V (Min)	Yield, 1000 Psi	Tensile, 1000 Psi	Elongation in 2 in., %
Kaisaloy												
42-CV	K	0.20	0.90	0.04	0.05	0.30	—	0.01	0.01	42	65	24
45-CB	K	0.20	1.00	0.04	0.05	0.10	—	0.01	—	45	60	22
50-CB	K	0.22	1.10	0.04	0.05	0.10	—	0.01	—	50	65	22
55-CB	K	0.24	1.40	0.04	0.05	0.10	—	0.01	—	55	70	20
60-CB	K	0.26	1.60	0.04	0.05	0.10	—	0.01	—	60	75	18
MLX-45	McL	0.15	1.00	0.04	0.05	0.10	—	0.005	0.02	45	60	25
50	McL	0.20	1.00	0.04	0.05	0.10	—	0.005	0.02	50	65	22
55	McL	0.24	1.20	0.04	0.05	0.30	—	0.005	0.02	55	70	22
60	McL	0.26	1.50	0.04	0.05	0.30	—	0.005	0.02	60	75	20
GLX-45W	N	0.20	1.25	0.04	0.05	—	Opt	0.01	—	45	60	22
50W	N	0.22	1.25	0.04	0.05	—	Opt	0.01	—	50	65	22
55W	N	0.22	1.35	0.04	0.05	—	Opt	0.01	—	55	70	22
60W	N	0.22	1.35	0.04	0.05	—	Opt	0.01	—	60	75	22
65W	N	0.24	1.35	0.04	0.05	—	Opt	0.01	—	65	80	18
70W	N	0.26	1.35	0.04	0.05	—	Opt	0.01	—	70	85	16
SK42 (A529)	P	0.27	1.20	0.04	0.05	—	Opt	—	—	42	60	19 (c)
SKA45	P	0.22	1.25	0.04	0.05	0.10	Opt	—	0.02	45	65	19 (c)
SKA50	P	0.26	1.30	0.04	0.05	0.10	Opt	—	0.02	50	70	18 (c)
Pitt-Ten												
X45W	PGH	0.20	1.00	0.04	0.05	0.10	—	0.01	—	45	60	24
X50W	PGH	0.20	1.00	0.04	0.05	0.10	—	0.01	—	50	65	22
X55W	PGH	0.20	1.00	0.04	0.05	0.10	—	0.01	—	55	70	20
X60W	PGH	0.20	1.00	0.04	0.05	0.10	—	0.01	—	60	75	18
X42W	R	0.22	1.10	0.04	0.05	0.10	—	0.01	0.01	42	57	24
X45W	R	0.20	1.00	0.04	0.05	0.10	—	0.01	0.01	45	60	25
X50W	R	0.20	1.00	0.04	0.05	0.10	—	0.01	0.01	50	65	22
X55W	R	0.25	1.50	0.04	0.05	0.10	—	0.01	0.01	55	70	20
X60W	R	0.25	1.50	0.04	0.05	0.10	—	0.01	0.01	60	75	18
X65W	R	0.26	1.50	0.04	0.05	0.30	—	0.01	0.01	65	80	16
X70W	R	0.26	1.65	0.04	0.05	0.30	—	0.01	0.01	70	85	14
(Sheet)												
Ex-Ten 45	US	0.20	1.00	0.04	0.05	0.30	Opt	0.01	—	45	60	25
50	US	0.20	1.00	0.04	0.05	0.30	Opt	0.01	—	50	65	22
55	US	0.20	1.25	0.04	0.05	0.30	Opt	0.01	—	55	70	20
60	US	0.22	1.25	0.04	0.05	0.30	Opt	0.01	—	60	75	18
65	US	0.22	1.35	0.04	0.05	0.30	Opt	0.01	—	65	80	16
70	US	0.26	1.35	0.04	0.05	0.30	Opt	0.01	and 0.01	70	85	14
(Plate)												
Ex-Ten 42	US	0.21	0.90	0.04	0.05	0.30	Opt	0.01	0.01	42	63	20 (c)
45	US	0.22	1.25	0.04	0.05	0.30	Opt	0.01	0.01	45	65	19 (c)
50	US	0.22	1.35	0.04	0.05	0.30	Opt	0.01	0.01	50	70	18 (c)
55	US	0.24	1.35	0.04	0.05	0.30	Opt	0.01	0.01	55	75	17 (c)
60	US	0.25	1.35	0.04	0.05	0.30	Opt	0.01	0.01	60	80	16 (c)
65	US	0.26	1.35	0.04	0.05	0.30	Opt	0.01	0.02	65	85	15 (c)
70	US	0.26	1.35	0.04	0.05	0.30	Opt	0.01	and 0.02	70	90	14 (c)
YSW-42	Y	0.20	1.10	0.04	0.05	—	Opt	0.01	0.01	42	62	25
45	Y	0.20	1.25	0.04	0.05	—	Opt	0.01	0.01	45	60	25
50	Y	0.22	1.25	0.04	0.05	—	Opt	0.01	0.01	50	65	22
55	Y	0.25	1.35	0.04	0.05	—	Opt	0.01	0.01	55	70	20
60(d)	Y	0.26	1.35	0.04	0.05	—	Opt	0.01	0.01	60	75	18
65	Y	0.26	1.35	—	—	—	Opt	0.01	0.01	65	80	18
70(d)	Y	0.26	1.50	—	—	—	Opt	0.01	0.01	70	85	16
CB/V45	ALG	0.20	1.25	0.04	0.05	—	—	0.01	0.01	45	60	25
CB/V50	ALG	0.20	1.25	0.04	0.05	—	—	0.01	0.01	50	65	22
CB/V55	ALG	0.20	1.25	0.04	0.05	—	—	0.01	0.01	55	70	20
CB/V60	ALG	0.22	1.25	0.04	0.05	—	—	0.01	0.01	60	75	18
Defascoloy												
45W	DF	0.25	1.25	0.04	0.05	0.10	—	0.01	—	45	65	22
50W	DF	0.25	1.25	0.04	0.05	0.10	—	0.01	—	50	70	22
55W	DF	0.25	1.25	0.04	0.05	0.10	—	0.01	—	55	70	20
60W	DF	0.25	1.25	0.04	0.05	0.10	—	0.01	—	60	75	18
Stalco CB45	SC	0.20	1.20	0.04	0.05	—	—	0.005	—	45	60	25
50	SC	0.20	1.20	0.04	0.05	—	—	0.005	—	50	65	22
55	SC	0.20	1.20	0.04	0.05	—	—	0.005	—	55	70	20
60	SC	0.20	1.20	0.04	0.05	—	—	0.005	—	60	75	18

Note: Steels in Group I do not normally contain more than residual copper; therefore, the atmospheric corrosion resistance is usually equal to that of plain carbon steel. If 0.20% minimum Cu is added, then corrosion resistance is up to twice that of plain carbon steel.

(a) V42, 45, 50, 55, 60, 65 licensed to Alan Wood Steel Co.; (b) V55, 60, 65 contain up to 0.015 N; (c) elongation in 8 in.; (d) 0.012% P, min.

II. Low Manganese-Vanadium Group

Copper is usually omitted for better formability

Name	Pro-ducer Code	Composition, %							Mechanical Properties			Corrosion Resistance
		C	Mn	P	S	Si	Cu	Other (a)	Yield, 1000 Psi	Tensile, 1000 Psi	Elonga-tion in 2 In., %	
High Strength #3	ARM	0.10	0.30-0.50	0.04	0.05	0.10	0.20	0.02 V	(40)	(60)	(35)	2
High Strength	JL	0.12	0.75	0.04	0.05	0.10	—	0.01 V	Properties to meet specific form-			1
Bumper Steel	McL	0.12	0.75	(0.02)	(0.02)	0.25	0.22	0.015 Cb	(45)	(62)	(28)	1 to 2
ML-F	N	(0.10)	(0.46)	(0.01)	(0.02)	(0.18)	(0.09)	(0.02 Zr)	(45)	(62)	(29)	1
NAX-Fine Grain	PGH	0.15	0.75	0.04	0.05	0.10	—	0.035 V	Properties to meet specific form-			1
Pitt-Ten #2												
Par-Ten	US	0.12	0.75	0.04	0.05	0.10	—	0.07 V max	(45)	(62)	(29)	1
YB-Ten	Y	0.12	0.75	0.04	0.05	0.10	—	0.01 V	(45)	(62)	(28)	1

(a) Minimum unless otherwise specified.

III. Manganese and Manganese-Copper Groups

Name	Pro-ducer Code	Composition, %						Condition	Mechanical Properties			Corrosion Resistance	
		C	Mn	P	S	Si	Cu (Min)		Yield, 1000 Psi	Tensile, 1000 Psi	Elonga- gation in 2 In., %		
A. Manganese Group—Copper not usually indicated													
Shef-Lo-Temp	ARM	0.20	0.70-1.35	0.04	0.05	0.15-0.30	—	HT	50	70	21 (a)	1	
Shef-Super-Lo-Temp	ARM	0.20	1.20-1.45	0.04	0.05	0.20-0.50	—	HT	60	80	21	1	
IH "50"	IH	0.22	1.50	0.04	0.05	0.70	0.20	—	50	75	20	2	
LT-75N	L	0.20	0.70-1.35	0.035	0.04	0.15-0.30	—	HT	50	70	24	2	
LT-75QT	L	0.20	0.70-1.35	0.035	0.04	0.15-0.30	—	HT	60	80	24	2	
Lukens 45	L	0.20	1.20	0.04	0.05	—	—	—	45	65	24	1	
50	L	0.20	1.35	0.04	0.05	—	—	—	50	70	24	1	
55	L	0.22	1.35	0.04	0.05	—	—	—	55	75	23	1	
60	L	0.22	1.60	0.04	0.05	0.15-0.30	—	—	60	80	23	1	
NAX-Fine Grain(b)	N	(0.15)	(0.79)	(0.010)	(0.017)	(0.51)	—	—	50	70	22	1 to 2	
Char-Pac	US	0.20	0.70-1.35	0.04	0.05	0.15-0.50	—	N or Q&T	50	70	19 (a)	1	
								Q&T	60	80	23	1	
Con-Pac	US	0.20	1.00-1.50	0.04	0.05	0.30-0.60	0.25	—	80	100	18	2	
Tower 50	ALG	0.33	1.20	0.04	0.05	—	—	—	50	75	17	1	
55	ALG	0.33	1.65	0.04	0.05	—	—	—	55	80	17	1	
60 (c)	ALG	0.33	1.65	0.04	0.05	—	—	—	60	80	16	1	
Strenlite 50	SC	0.33	1.65	0.04	0.05	—	—	—	50	70	17 (a)	1	
B. Manganese-Copper Group—ASTM A440, SAE 950C; limited application for ASTM A242 and A375													
High Strength #4S	ARM	0.25	1.10-1.60	0.045	0.05	0.35	0.20	K	50	70	22	2	
#4R	ARM	0.25	1.10-1.60	0.045	0.05	0.10	0.20	SK	50	70	22	2	
Shef-Ten (d)	ARM	0.28	1.10-1.60	0.045	0.05	0.30	0.20	—	50	70	18 (a)	2	
Med. Mn (A440)	B	0.28	1.10-1.60	0.04	0.05	0.30	0.20-0.35	—	50	70	20	2	
Hi-Man	IN	0.25	1.10-1.60	0.04	0.05	0.30	0.20	SK	50	75	22	2	
Hi-Killed	IN	0.25	1.10-1.60	0.04	0.05	0.30	0.20	K	50	75	22	2	
Hi-440	IN	0.28	1.10-1.60	0.04	0.05	0.30	0.20	—	50	70	18 (a)	2	
Jellan-3S	JL	0.25	1.60	0.04	0.05	0.30	0.20	K	50	70	22	2	
3R	JL	0.25	1.60	0.04	0.05	—	0.20	SK	50	70	22	2	
Kaisley 50 MM	K	0.27	1.10-1.60	0.045	0.05	0.30	0.20	—	50	70	—	2	
Lukens 440	L	0.28	1.10-1.60	0.04	0.05	0.30	0.20	—	50	70	18 (a)	2	
ML-M	McL	0.25	1.10-1.60	0.045	0.05	0.30	0.20	—	50	70	22	2	
NAX-Hi Mang.	N	(0.22)	(1.25)	(0.011)	(0.018)	0.30	(0.22)	—	50	70	22	2	
Orelloy 440	O	(0.19)	(1.28)	(0.020)	(0.030)	(0.23)	(0.35)	—	50	70	18 (a)	2	
Republic M-1	R	0.25	1.10-1.60	0.045	0.05	0.30	0.20	K	50	75	20	2	
M-2	R	0.25	1.10-1.60	0.045	0.05	0.30	0.20	SK	50	75	20	2	
Man-Ten	US	0.25	1.10-1.60	0.045	0.05	0.30	0.20	SK	50	75	20	2	
Man-Ten A440	US	0.28	1.10-1.60	0.04	0.05	0.30	0.20	—	50	70	—	2	
Yo Man B	Y	0.25	1.60	0.04	0.05	0.30	0.20	—	50	75	25	2	
Defaceloy M	DF	0.25	1.50	0.04	0.05	0.30	0.20	—	50	70	22	2	
Strenlite (440)	SC	0.27	1.10-1.60	0.04	0.05	0.30	0.20	—	50	70	22	2	

Note: HT, heat treated; N, normalized; Q&T, quenched and tempered; K, killed; SK, semikilled.

(a) Elongation in 8 in.; (b) 0.07 Zr; (c) 0.05 V; (d) 0.04 Ni.

IV. Manganese-Vanadium-Copper Group
SAE 950B, ASTM A441, A242, A374, A375

Name	Producer Code	Composition, %							Mechanical Properties			Corrosion Resistance
		C	Mn	P	S	Si	Cu (Min)	V (Min)	Yield, 1000 Psi	Tensile, 1000 Psi	Elongation in 2 in., %	
AW-441	AW	0.22	1.25	0.04	0.05	0.30	0.20	0.02	50	70	22	2
High Strength #5	ARM	0.22	1.25	0.04	0.05	0.30	0.20	0.02	45	60	25	2
Hi-Strength B	ARM	0.22	1.25	0.04	0.05	0.30	0.20	0.02	50	70	18 (a)	2
Mn-V A441	B	0.22	1.25	0.04	0.05	0.30	0.20	0.02	50	70	—	2
Tri-Steel	IN	0.22	1.25	0.04	0.05	0.30	0.20	0.02	50	70	22	2
Jaken 1	JL	0.22	1.25	0.04	0.05	0.30	0.20	0.02	50	70	22	2
Kaisaloy 50 MV	K	0.22	1.25	0.04	0.05	0.30	0.20	0.02	50	70	24	2
Mn-V	L	0.22	1.25	0.04	0.05	0.30	0.20	0.02	50	70	—	2
GLS-441	N	0.22	1.25	0.04	0.04	0.30	0.20	0.02	50	70	22	2
NAX-Fine Grain (b)	N (c)	0.18	0.50-1.00	0.04	0.05	0.50-0.90	0.25	—	50	70	22	2
ML-F (A441)	MCL	0.22	1.25	0.04	0.05	0.30	0.20	0.02	50	70	22	2
Orelloy 441	O	0.22	1.25	0.04	0.05	0.30	0.20	0.02	50	70	22	2
Clay-Loy (A441)	P	0.22	1.25	0.05	0.05	0.35	0.20	0.02	50	70	—	2
Republic A-441	R	0.22	1.25	0.04	0.05	0.30	0.20	0.02	50	70	22	2
Tri-Ten	US	0.22	1.25	0.04	0.05	0.30	0.20	0.02	50	70	18 (a)	2
YSW A441	Y	0.22	1.25	0.04	0.05	0.30	0.20	0.02	50	70	22	2
Dofasco MV	DF	0.22	1.25	0.04	0.05	0.30	0.20	0.02	50	70	22	2
Stelco-Vanadium	SC	0.22	1.25	0.04	0.05	0.30	0.20	0.02	50	70	22	2

(a) Elongation in 8 in.; (b) 0.15 Zr; (c) NAX-Fine Grain is licensed to Republic, Sharon and Pittsburgh Steel. It competes with but does not comply with A441 steels.

V. Multiple Alloy and Copper Group

SAE 950A; limited application to ASTM A242, A374, A375

Name	Producer Code	Composition, %										Mechanical Properties			Corrosion Resistance
		C	Mn	P	S	Si	Cu	Mo	Cr	Ni	Other (Min)	Yield, 1000 Psi	Tensile, 1000 Psi	Elongation in 2 in., %	
Hi-Strength A	ARM	0.12	(0.40)	0.04	0.05	0.45	0.30-0.50	0.10	(0.60)	(0.70)	0.03 Ti	50	70	18 (a)	4 to 5
Ni-Cu-Ti	JL	0.15	1.00	0.04	0.05	0.50	0.30 min	—	—	0.70	0.05 Ti	50	70	22	4
Kaisaloy 45FG	K	0.12	0.60	0.04	0.04	0.50	0.30	0.10	0.25	0.60	0.02 V, 0.005 Ti	45	60	25	6 max
50CR	K	0.20	1.25	0.05	0.05	0.75	0.35	0.15	0.25	0.60	0.02 V, 0.005 Ti	50	75	22	6 max
60WR	K	0.35	1.50	0.04	0.05	0.35	0.35	0.10	0.25	0.40	0.05 V, 0.005 Ti	60	80	—	3
70MB	K	0.15	0.60	0.04	0.04	0.35	—	0.60	—	—	0.001 B	70	85	—	2
NAX-High Tensile	N (b)	0.15	(0.70)	0.04	0.04	0.90	0.25	—	(0.60)	—	0.03 Zr	50	70	22	4
Republic 50	R	0.15	(0.75)	0.04	0.05	—	0.30-1.00	0.10	0.30	(0.70)	—	50	70	22	4 to 6
Cor-Ten	US	0.19	(1.07)	0.04	0.05	0.30	0.25-0.40	—	(0.52)	—	0.02 V	50	70	19 (a)	4
Yoloy HS(c)	Y	0.15	1.00	0.04	0.05	0.35	0.50-1.00	0.25	—	(1.00)	—	50	70	22	4 to 5
HSX	Y	0.15	1.00	0.04	0.05	0.35	0.50-1.00	0.25	—	(1.00)	—	45	62	25	4 to 5
S	Y	0.20	1.00	0.04	0.05	0.30	0.75-1.25	—	—	(1.90)	—	50	70	22	4 to 6
Algo Tuf 50	ALG	0.20	(1.15)	0.03	0.05	0.35	—	—	—	0.50	0.02 V	50	80	18	2
Dofasco #1	DF	0.18	1.00	0.04	0.05	0.30	0.60	—	—	0.90	—	50	70	22	4 to 5
#2	DF	0.15	1.00	0.04	0.05	0.30	0.60	—	—	0.90	—	45	65	22	4 to 5
Stelcoloy S	SC	0.15	1.35	0.03	0.04	0.30	0.20-0.50	—	(0.37)	(0.35)	0.01 V	50	70	22	4 to 5

(a) Elongation in 8 in.; (b) NAX-High Tensile is licensed to Republic, Sharon and Pittsburgh Steel; (c) Yoloy alloys can be precipitation hardened (stress relief annealed) to increase tensile properties.

Maximum values for composition are listed except where ranges, minimum or typical values are indicated. Typical values are enclosed in parentheses. Mechanical properties are those of sheet or hot rolled plate up to 1/2 in. thick and are minimums unless typical is indicated by parentheses.

Atmospheric corrosion resistance for these high strength steels is compared to that of carbon steel. Example: 2 indicates twice the corrosion resistance of carbon steel.

Producer Code: AW—Alan Wood Steel Co.; ALG—Algoma Steel Corp.; ARM—Armco Steel Corp.; B—Bethlehem Steel Corp.; C—Crucible Steel Co.; DF—Dominion Foundries & Steel Ltd.; GC—Granite City Steel Co.; IN—Inland Steel Co.; IA—Interlake (Acme) Steel Co.; IH—International Harvester (Wisconsin Steel Div.); IHW—Isaacson Iron Works; JL—Jones & Laughlin Steel Corp.; K—Kaiser Steel Corp.; L—Lukens Steel Co.; MCL—McLouth Steel Corp.; N—National Steel Corp.; O—Oregon Steel Mills; P—Phoenix Steel Corp.; PGH—Pittsburgh Steel Co.; R—Republic Steel Corp.; SH—Sharon Steel Corp.; SC—Steel Co. of Canada Ltd.; US—United States Steel Corp.; Y—Youngstown Sheet & Tube Co.

VI. Multiple Alloy and Copper and Phosphorus Group
SAE 950D; limited application to ASTM A242, A374, A375

Name	Pro-ducer Code	Composition, %								Mechanical Properties			Corrosion Resistance
		C	Mn	P	S	Si	Cu	Cr	Ni	Yield, 1000 Psi	Tensile, 1000 Psi	Elongation in 2 in., %	
AW Dynalloy 50	AW	0.15	(1.00)	0.10	0.05	0.30	0.30-0.60	0.15 Mo	0.40-0.70	50	70	22	4 to 5
High Strength #1(a) #2	ARM	0.15	(0.62)	0.07	0.04	0.15	0.50-0.75	—	0.60-0.90	50	70	22	4 to 5
	ARM	0.15	(0.62)	0.07	0.04	0.15	0.50-0.75	—	0.60-0.90	(45)	(64)	—	4 to 5
Mayari-R(b)	B	0.12	(0.75)	0.12	0.05	(0.55)	0.50	0.40-1.00	1.00	50	70	22	4 to 6
Maxeloy 4	C	0.15	1.20	0.07	0.04	0.50	0.20 min	—	0.50	50	70	22	4 to 5
Hi Stee(a)	IN	0.12	(0.75)	0.12	0.05	0.15	0.55-1.30	0.18 Mo	0.30-0.75	50	70	22	4 to 6
Jalten 2	JL	0.15	1.40	0.14	0.05	0.10	0.30 min	—	—	50	70	22	4 to 5
ML-50(c) 60 70	McL	(0.13)	(0.48)	(0.01)	(0.02)	(0.17)	(0.22)	(0.40)	(0.51)	50	70	22	3
	McL	(0.13)	(0.90)	(0.01)	(0.02)	(0.20)	(0.29)	(0.51)	(0.68)	60	75	22	3
	McL	(0.16)	(0.95)	(0.01)	(0.02)	(0.17)	(0.30)	(0.55)	(0.73)	70	85	20	3
Orelloy 242	O	(0.10)	(0.50)	(0.09)	(0.03)	(0.48)	(0.43)	(0.86)	(0.43)	50	70	22	4 to 5
Pitt-Ten #1(a)	PGH	0.12	(0.75)	0.07	0.05	0.20	0.60-1.05	—	0.45-0.95	50	70	22	4 to 5
Cor-Ten(d)	US	0.12	(0.35)	0.15	0.05	(0.50)	0.25-0.55	0.31-1.25	0.65	50	70	19(e)	5 to 8
Dofascloy P	DF	0.16	0.60	0.12	0.04	(0.25)	0.60	0.60	0.90	50	70	22	4 to 6
Stelcoloy G	SC	0.12	0.75	0.12	0.04	(0.32)	0.30-0.60	0.30-0.60	0.30-0.60	50	70	22	4 to 6

(a) Precipitation hardening is possible; (b) 0.10 Zr; (c) ML-50, 60 and 70 contain 0.01% Mo. ML-50 and 60 contain 0.014% Cb, ML-70 0.029% Cb; (d) Cor-Ten is licensed to Algoma, Crucible, Granite City, Greer, Inland, Interlake (Acme), Jones & Laughlin, Lukens, Republic, Sharon and Wheeling Steel; (e) elongation in 8 in.

VII. Precipitation Hardening Alloys

Name	Producer Code	Composition, %								Mechanical Properties			Corrosion Resistance
		C	Mn	P	S	Si	Cu	Mo	Ni	Yield, 1000 Psi	Tensile, 1000 Psi	Elongation in 2 in., %	
Republic 65 70	R	0.15	1.00	0.04	0.04	0.15	0.90-1.40	0.20-0.30	1.00-1.50	65	85	20	4 to 6
	R	0.20	1.00	0.04	0.04	0.15	1.00-1.50	0.20-0.30	1.20-1.75	70	90	18	4 to 6
Cu-Ni-Mo	US	0.21	0.80-1.10	0.04	0.05	0.15-0.30	0.50-0.80	0.20-0.30	1.20-1.50	65	140	18	4 to 6
Yoloy S	Y	0.20	1.00	0.04	0.05	0.30	0.75-1.25	—	1.60-2.20	65	(90)	20	4 to 6

VIII. Constructional Alloys (Extra High Strength Steels)

Name	Pro- ducer Code	Composition, %									Mechanical Properties (b)		
		C	Mn	P	S	Si	Ni	Cr	Mo	Other (a)	Yield, 1000 Psi	Tensile, 1000 Psi	Elonga- tion in 2 in., %
SSS-100	ARM	0.12-0.20	0.40-0.70	0.04	0.05	0.20-0.35	—	1.40-2.00	0.60	0.40 Cu max, 0.04 Ti, 0.0015 B	100	115	18
SSS-100A	ARM	0.13-0.20	0.40-0.70	0.04	0.05	0.20-0.35	—	0.85-1.20	0.25	0.40 Cu max, 0.04 Ti, 0.0015 B	100	115	18
HY80	ARM	0.18	0.10-0.40	0.025	0.025	0.15-0.35	2.00-3.25	1.00-1.80	0.60	—	80	—	20
HY100	ARM	0.20	0.10-0.40	0.025	0.025	0.15-0.35	2.25-3.50	1.00-1.80	0.60	—	100	—	18
Ni-Mn	IIW	0.26	0.15-0.45	0.02	0.02	0.15-0.35	2.75-3.25	—	0.60	—	75	95	20
I-90	IIW	0.16-0.20	0.60-0.90	0.03	0.03	0.20-0.30	1.10-1.40	0.50-0.75	0.60	0.06 V	90	100	20
Jalloy S- 90	JL	0.10-0.20	1.10-1.50	0.04	0.04	0.15-0.30	—	—	0.30	0.0005 B	90	(100)	(18)
S-100	JL	0.10-0.20	1.10-1.50	0.04	0.04	0.15-0.30	—	—	0.30	—	100	(110)	(18)
S-110	JL	0.10-0.20	1.10-1.50	0.04	0.04	0.15-0.30	—	—	0.30	—	110	(120)	(17)
Jalloy I(c)	JL	0.10-0.20	1.10-1.50	0.04	0.04	0.15-0.30	—	—	0.20	—	—	—	—
N-A-XTRA- 80	N	0.10-0.20	0.60-1.10	0.04	0.04	0.40-0.80	—	0.40-0.80	0.28	0.05 Zr	80	95	18
90	N	0.10-0.20	0.60-1.10	0.04	0.04	0.40-0.80	—	0.40-0.80	0.28	0.05 Zr	90	105	18
100	N	0.10-0.20	0.60-1.10	0.04	0.04	0.40-0.80	—	0.40-0.80	0.28	0.05 Zr	100	115	18
110	N	0.10-0.20	0.60-1.10	0.04	0.04	0.40-0.80	—	0.40-0.80	0.28	0.05 Zr	110	125	18
PX80 Plus	P	0.15-0.21	0.80-1.10	0.035	0.04	0.40-0.90	—	0.50-0.90	0.28	0.05 Zr, 0.0025 B max	80	95	18
PX90 Plus	P	0.15-0.21	0.80-1.10	0.035	0.04	0.40-0.90	—	0.50-0.90	0.28	0.05 Zr, 0.0025 B max	90	105	18
PX100 Plus	P	0.15-0.21	0.80-1.10	0.035	0.04	0.40-0.90	—	0.50-0.90	0.28	0.05 Zr, 0.0025 B max	100	115	18
PX110 Plus	P	0.15-0.21	0.80-1.10	0.035	0.04	0.40-0.90	—	0.50-0.90	0.28	0.05 Zr, 0.0025 B max	110	125	18
PX360 Bhr(d)	P	0.15-0.21	0.80-1.10	0.035	0.04	0.40-0.90	—	0.50-0.90	0.28	0.05 Zr, 0.0025 B max	(165)	(180)	(16)

VIII. Constructional Alloys (Extra High Strength Steels)—Continued

Name	Pro- ducer Code	Composition, %									Mechanical Properties (b)		
		C	Mn	P	S	Si	Ni	Cr	Mo	Other (a)	Yield, 1000 Psi	Tensile, 1000 Psi	Elonga- tion in 2 in., %
T-1-Reg. Qual.	US/L	0.10-0.20	0.60-1.00	0.035	0.04	0.15-0.35	0.70-1.00	0.40-0.65	0.60	0.15-0.50 Cu, 0.002 B, 0.03 V	90	105	16
T-1-A-Reg. Qual.(a)	US/L	0.12-0.21	0.70-1.00	0.035	0.04	0.20-0.35	—	0.40-0.65	0.25	0.0005 B, 0.01 Ti, 0.03 V	100	115	18
T-1-B(a)	US/L	0.12-0.21	0.95-1.30	0.035	0.04	0.20-0.35	0.30-0.70	0.40-0.65	0.30	0.0005 B, 0.03 V	100	115	18
Algoma 90	ALG	0.12	1.60	0.04	0.04	0.15-0.45	—	3.00-3.75	0.40	0.02 V	90	115	18

Note: Bars, structural shapes and tubing can also be supplied in these alloys.

(a) Minimum unless otherwise specified; (b) all alloys quenched and tempered except J alloy 1 and Algoma 90 which are hot rolled; (c) Brinell hardness, 200 to 250; (d) Brinell hardness, 360; (e) copper optional.

IX. Abrasion Resistant Alloys

Name	Pro- ducer Code	Composition, %									Con- dition	Mechanical Properties		
		C	Mn	P	S	Si	Cu	Cr	Mo	Other (a)		Hard- ness, Bhn	Yield, 1000 Psi	Tensile 1000 Psi
SSS-321	ARM	0.13-0.25	0.40-0.70	0.04	0.05	0.35	0.20-0.40	0.85-2.0	0.15-0.60	0.0015 B	Q&T	321	—	—
SSS-360	ARM	0.13-0.25	0.40-0.70	0.04	0.05	0.35	0.20-0.40	0.85-2.0	0.15-0.60	0.10 Ti	Q&T	360	—	—
SSS-400	ARM	0.13-0.25	0.40-0.70	0.04	0.05	0.35	0.20-0.40	0.85-2.0	0.15-0.60	—	Q&T	400	—	—
Sheffield AR	ARM	0.43	1.55-2.00	0.05	0.05	0.35	—	—	—	—	HR	225	—	—
AR-No. 235	B	0.35-0.50	1.40-2.00	0.05	0.05	0.30	—	—	—	—	HR	(235)	70	110
Abrasion Resisting, Med. Hard	IN	0.35-0.50	1.20-2.00	0.04	0.05	0.30	—	—	—	—	HR	235	—	—
Abrasion Resisting, Full Hard	IN	0.70-0.85	0.60-1.00	0.04	0.05	0.30	—	—	—	—	HR	270	—	—
J alloy AR-280	JL	0.25-0.31	1.35-1.65	0.04	0.04	0.30	0.20 min	—	0.10-0.20	0.0005 B	Q&T	260	110	117
320	JL	0.25-0.31	1.35-1.65	0.04	0.04	0.30	0.20 min	—	0.10-0.20	0.0005 B	Q&T	300	135	142
360	JL	0.25-0.31	1.35-1.65	0.04	0.04	0.30	0.20 min	—	0.10-0.20	0.0005 B	Q&T	340	160	166
400	JL	0.25-0.31	1.35-1.65	0.04	0.04	0.30	0.20 min	—	0.10-0.20	0.0005 B	Q&T	400	184	190
J alloy S-340	JL	0.10-0.20	1.10-1.50	0.04	0.04	0.30	—	—	0.20-0.30	0.0005 B	Q&T	320	149	157
J alloy 3 (AR)	JL	0.10-0.20	1.10-1.50	0.04	0.04	0.30	—	—	0.20-0.30	0.0005 B	HR	(225)	90	104
Kaisaloy AR	K	0.35-0.50	1.50-2.00	0.05	0.05	0.35	—	—	—	—	—	—	—	—
T-1-A-360	L	0.12-0.21	0.70-1.00	0.04	0.05	0.35	Opt	0.40-0.65	0.15-0.25	0.0005 B, 0.03 V	Q&T	360	(145)	(180)
XAR-15	N	0.10-0.20	0.60-1.00	0.04	0.04	0.90	—	0.45-0.85	0.15-0.25	0.03 Zr	Q&T	360	165	180
XAR-30	N	0.25-0.30	0.60-1.00	0.04	0.04	0.90	—	0.45-0.85	0.15-0.25	0.03 Zr	Q&T	360	165	180
USS-AR	US	0.35-0.50	1.50-2.00	0.05	0.05	0.35	—	—	—	—	HR	(235)	—	—
T-1	US/L	0.10-0.20	0.60-1.00	0.035	0.04	0.35	0.15-0.50	0.40-0.65	0.40-0.60	0.70-1.00 Ni, 0.002 B, 0.03 V	Q&T	321	(100)	(115)
T-1-A	US/L	0.12-0.21	0.60-1.00	0.035	0.04	0.35	Opt	0.40-0.65	0.15-0.25	0.0005 B, 0.01 Ti, 0.03 V	Q&T	321	(100)	(115)
T-1-A-321	US/L	0.12-0.21	0.70-1.00	0.035	0.04	0.35	Opt	0.40-0.65	0.15-0.25	0.0005 B, 0.03 V	Q&T	321	(137)	(171)
T-1-B-321	US/L	0.12-0.21	0.95-1.30	0.035	0.04	0.35	Opt	0.40-0.65	0.20-0.30	0.30-0.70 Ni, 0.0005 B, 0.03 V	Q&T	321	(137)	(171)
T-1-321	US/L	0.10-0.20	0.60-1.00	0.035	0.04	0.35	0.15-0.50	0.40-0.65	0.40-0.65	0.70-1.00 Ni, 0.002 B, 0.03 V	Q&T	321	(141)	(175)
T-1-360	US/L	0.10-0.20	0.60-1.00	0.035	0.04	0.35	0.15-0.50	0.40-0.65	0.40-0.65	0.70-1.00 Ni, 0.002 B, 0.03 V	Q&T	360	(145)	(180)

Note: Q&T, quenched and tempered; HR, hot rolled.

(a) Minimum unless otherwise specified.

Maximum values for composition are listed except where ranges, minimum or typical values are indicated. Typical values are enclosed in parentheses. Mechanical properties are those of sheet or hot rolled plate up to 1/2 in. thick and are minimums unless typical is indicated by parentheses.

Atmospheric corrosion resistance for these high strength steels is compared to that of carbon steel. Example: 2 indicates twice the corrosion resistance of carbon steel.

Producer Code: AW—Alan Wood Steel Co.; ALG—Algoma Steel Corp.; ARM—Armco Steel Corp.; B—Bethlehem Steel Corp.; C—Crucible Steel Co.; DF—Dominion Foundries & Steel Ltd.; GC—Granite City Steel Co.; IN—Inland Steel Co.; IA—Interlake (Acme) Steel Co.; IH—International Harvester (Wisconsin Steel Div.); IIW—Isaacson Iron Works; JL—Jones & Laughlin Steel Corp.; K—Kaiser Steel Corp.; L—Lukens Steel Co.; McL—McLouth Steel Corp.; N—National Steel Corp.; O—Oregon Steel Mills; P—Phoenix Steel Corp.; PGH—Pittsburgh Steel Co.; R—Republic Steel Corp.; SH—Sharon Steel Corp.; SC—Steel Co. of Canada Ltd.; US—United States Steel Corp.; Y—Youngstown Sheet & Tube Co.

Properties and Uses for Heat Treatable Copper Alloys

Compiled by C. Lawrence Bulow
Bridgeport Brass Co.

	Beryllium Copper (Strip) CDA 172	Copper-Nickel- Silicon (Strip) CDA 647	Chromium Copper (Strip) CDA 182	Zirconium Copper (Strip) CDA 150	Copper-Nickel- Phosphorus CDA 150
Nominal composition, %	97.85 Cu, 1.90 Be, 0.25 Co	97.50 Cu, 1.90 Ni, 0.60 Si	99.10 Cu, 0.90 Cr	99.85 Cu, 0.15 Zn	97.55 Cu, 1.20 Ni, 0.25 P
Properties					
Tensile strength, psi					
Soft (SA)*	69,000	41,000	30,000	32,000	38,000
SA + HT	177,000	85,000	56,000	34,000	65,000
1/2 hard	92,000	48,000	43,000	48,000	61,000
1/2 hard + HT	195,000	91,000	62,000	53,000	82,000
Hard	110,000	58,000	52,000	55,000	66,000
Hard + HT	200,000	98,000	67,000	59,000	90,000
Yield strength, psi					
Soft (SA)	32,000	14,000	8,000	14,000	10,000
SA + HT	155,000	65,000	45,000	18,000	40,000
1/2 hard	82,000	46,000	40,000	46,000	54,000
1/2 hard + HT	175,000	81,000	57,000	45,000	71,000
Hard	104,000	57,000	51,000	53,000	59,000
Hard + HT	180,000	85,000	63,000	53,000	78,000
Elongation in 2 in., %					
Soft (SA)	47	39	42	51	40
SA + HT	7	16	15	51	33
1/2 hard	10	17	7	11	8
1/2 hard + HT	3	13	9	18	6
Hard	4	3	2	7	6
Hard + HT	2	9	6	14	4
Electrical conductivity, % IACS					
Soft (SA)	18	23	36	70	32
SA + HT	24	40	81	84	60
1/2 hard	16	23	35	72	32
1/2 hard + HT	24	40	78	88	60
Hard	16	23	35	73	32
Hard + HT	24	40	78	88	60
Thermal conductivity, Btu/sq ft/ft/hr/°F					
Soft (SA)	46	58	90	167	80
SA + HT	61	100	189	195	145
1/2 hard	43	58	88	171	90
1/2 hard + HT	61	100	183	202	145
Hard	43	58	88	173	80
Hard + HT	61	100	183	202	145
Fabricating Characteristics					
Hot working temperature (SA or HT)	1050 to 1475 F	1300 to 1375 F	1650 to 1695 F	1650 to 1760 F	1300 to 1550 F
Solution annealing temperature	1400 to 1475	1375 to 1475	1830	1650 to 1750	1300 to 1450
Aging temperature (1 to 2 hr)	600	800 to 900	850 to 930	750 to 950	800 to 900
Machinability rating, (SA, CW, HT)†	20%	30%	20%	20%	30%
Cold workability	Good	Excellent	Good	Excellent	Excellent
Hot workability	Excellent	Excellent	Good	Excellent	Excellent
Joining Characteristics					
Soft soldering	Excellent	Excellent	Excellent	Excellent	Excellent
Silver brazing	Good	Excellent	Excellent	Excellent	Excellent
Oxyacetylene welding	Poor	Good	—	Fair to good	Good
Carbon arc welding	Excellent	Fair to poor	—	Fair	Good
Gas shielded arc welding	Good	Good	—	Good	Good
Resistance welding	Excellent	Good	—	Not recommended	Fair
Typical Applications					
	Diaphragms, bellows, relays, circuit breakers, switches; fuse and component holders; cantilever flat springs; Belleville, curved spring and wavy spring washers; brush springs used at ambient temperature up to 300 F	Fasteners, electrical parts, marine hardware, resistance welded assemblies, resistance welding tip holders, rotors and rings, springs, switch gear, wire connectors, wire forms and wire products	Similar to coppers, such as circuit breakers, parts where high strength and high thermal and electrical conductivity are needed. Used where higher softening point than that provided by copper is needed	Commutator segments, conductors, electrical parts, gaskets, resistance welding tips, rotor bars and plates, switch parts, washers, wave guides, wire forms and wire products	Springs, clips, electronic parts, high strength electrical connectors, bolts, nails, screws, rivets, fasteners

Note: Data Sheet lists only those alloys containing 97% Cu (min).

*SA, solution annealed; CW, cold worked; HT, aged. †Based on 100% for free-cutting brass (CDA 360).

Properties and Applications

Name and Number	Nominal Composition, %	Commercial Form (a)	Mechanical Properties (b)			Corrosion Resistance (c)	Machinability Rating (d)	Fabricating Characteristics and Typical Applications
			Tensile Strength, 1000 Psi	Yield Strength, 1000 Psi	Elongation in 2 in., %			
102 Oxygen-free copper	99.95 Cu	F, R, W, T, P, S	66-32	53-10	4-55	G-E	20	Excellent hot and cold workability; good forgeability. Fabricated by rolling, cupping, drawing and upsetting, hot forging and pressing, spinning, swaging, stamping. Uses: bushings, waveguides.
110 Electrolytic tough pitch copper	99.90 Cu, 0.04 O	F, R, W, T, P, S	66-32	53-10	4-55	G-E	20	Fabricating characteristics same as No. 102. Uses: downspouts, gutters, roofing, gaskets, auto radiators, bushings, coils, printing rolls, rivets, radio parts.
113, 114, 116 Silver-bearing - tough pitch copper	99.90 Cu, 0.04 O, Ag (v)	F, R, W, T, S	66-32	53-10	4-55	G-E	20	Fabricating characteristics same as No. 102. Uses: gaskets, radiators, bushings, windings, switches, chemical process equipment, clad metals, printed circuit foil.
122 Phosphorus deoxidized copper, high residual phosphorus	99.90 Cu, 0.02 P	F, R, T, P	55-32	50-10	8-45	G-E	20	Fabricating characteristics same as No. 102. Uses: gas and heater lines; oil burner tubing; plumbing pipe and tubing; condenser tubing, evaporator and heat exchanger tubing; dairy and distiller tubing; steam and water lines; air, gasoline and hydraulic lines.
150 Zirconium copper	99.80 Cu, 0.15 Zr	F, R, W	60-45	52-38	12-18	G-E	20	Excellent hot and cold workability. Uses: resistance welding tips and wheels, stud bases for power transistors and rectifiers, commutators, electrical switches.
162 Cadmium copper	99.75 Cu, 1.0 Cd	W	80-37	—	2-45 in 10 in.	G-E	30	Uses: trolley wire.
172 Beryllium copper	99.5 Cu, 1.9 Be, 0.20 Co	F, R, W, T, P, S	165-60	130-25	3-35	G-E	20	Excellent hot workability. Commonly fabricated by blanking, drawing, forming and bending, turning, drilling, tapping. Uses: bellows, boudon tubing, diaphragms, fuse clips, fasteners, lock washers, springs, switch parts, roll pins, valves, welding equipment.
182 Chromium copper	98.5 Cu, 0.9 Cr	F, W, R, S	62-35	55-15	12-40	G-E	20	Good hot and cold workability. Uses: resistance-welding electrode tips and wheels, circuit breaker parts, cable connectors, parts for electronic devices.
210 Gilding, 95%	95.0 Cu, 5.0 Zn	F, W	64-34	58-10	4-45	G-E	20	Excellent cold workability, good hot workability for blanking, coining, drawing, piercing and punching, shearing, spinning, squeezing and swaging, stamping. Uses: coins, medals, bullet jackets, fuse caps, primers, plaques, jewelry, base for gold plate.
220 Commercial bronze, 50%	90.0 Cu, 10.0 Zn	F, R, W, T	72-37	62-10	3-50	G-E	20	Fabricating characteristics same as alloy No. 210, plus heading and upsetting, roll threading and knurling, hot forging and pressing. Uses: etching bronze, mill-work, screen cloth, weatherstripping, lipstick cases, compacts, marine hardware, screws, rivets.
226 Jewelry bronze, 87.5%	87.5 Cu, 12.5 Zn	F, W	97-39	62-11	3-46	F-E	30	Fabricating characteristics same as alloy No. 210, plus heading and upsetting, roll threading and knurling. Uses: Angles, channels, chain, fasteners, costume jewelry, lipstick cases, compacts, base for gold plate.
230 Red brass, 85%	85.0 Cu, 15.0 Zn	F, W, T, P	105-39	63-10	3-55	G-E	30	Fabricating characteristics same as alloy No. 226. Uses: Weatherstripping, conduit, sockets, fasteners, fire extinguishers, condenser and heat exchanger tubing, plumbing pipe, radiator cores.
240 Low brass, 80%	80.0 Cu, 20.0 Zn	F, W	125-42	65-12	3-55	F-E	30	Excellent cold workability. Fabricating characteristics same as alloy No. 226. Uses: battery caps, bellows, musical instruments, clock dials, pump lines, flexible hose.
260 Cartridge brass, 70%	70.0 Cu, 30.0 Zn	F, R, W, T	130-44	65-11	3-66	F-E	30	Excellent cold workability. Fabricating characteristics same as alloy No. 240, except for coining, roll threading and knurling. Uses: Radiator cores and tanks, flashlight shells, lamp fixtures, fasteners, locks, hinges, ammunition components, plumbing accessories, pins, rivets.
268, 270 Yellow brass	65.0 Cu, 35.0 Zn	F, R, W	128-46	62-14	3-65	F-E	30	Excellent cold workability. Fabricating characteristics same as alloy No. 240. Uses: Same as alloy No. 260 except not used for ammunition.
280 Muntz metal	60.0 Cu, 40.0 Zn	F, R, T	74-54	55-21	10-52	F-E	40	Excellent hot formability and forgeability for blanking, forming and bending, hot forging and pressing, hot heading and upsetting, shearing. Uses: architectural, large nuts and bolts, brazing rod, condenser plates, condenser, evaporator and heat exchanger tubing, hot forgings.
314 Leaded commercial bronze	89.0 Cu, 1.75 Pb, 9.25 Zn	F, R	60-37	55-12	10-45	G-E	80	Excellent machinability. Uses: screws, machine parts, pickling crates.
330 Low-leaded brass tube	66.0 Cu, 0.5 Pb, 33.5 Zn	T	75-47	60-15	7-60	F-E	60	Combines good machinability and excellent cold workability. Fabricated by forming and bending, machining, piercing and punching. Uses: Pump and power cylinders and liners, ammunition primers, plumbing accessories.
332 High-leaded brass tube	66.0 Cu, 1.6 Pb, 32.4 Zn	T	75-52	60-20	7-50	F-E	80	Excellent machinability. Fabricated by piercing, punching and machining. Uses: general purpose screw machine parts.
335 Low-leaded brass	65.0 Cu, 0.5 Pb, 34.5 Zn	F	74-46	60-14	8-65	F-E	60	Similar to alloy No. 332. Commonly fabricated by blanking, drawing, machining, piercing and punching, stamping. Uses: butts, hinges, watch backs.
340 Medium-leaded brass	65.0 Cu, 1.0 Pb, 34.0 Zn	F, R, W, S	88-47	60-15	7-60	F-E	70	Similar to alloy No. 335. Fabricated by blanking, heading and upsetting, machining, piercing and punching, roll threading and knurling, stamping. Uses: butts, gears, nuts, rivets, screws, disks, engravings, instrument plates.
342, 353 High-leaded brass	65.0 Cu, 2.0 Pb, 33.0 Zn	F, R	85-49	62-17	5-52	F-E	90	Fabricating characteristics same as alloy No. 340. Uses: Clock plates and nuts, clock and watch backs, gears, wheels and channel plate.
356 Extra-high leaded brass	63.0 Cu, 2.5 Pb, 34.5 Zn	F	74-49	60-17	7-50	F-E	100	Excellent machinability. Fabricated by blanking, machining, piercing and punching, stamping. Uses: same as alloy No. 342 and 353.
360 Free-cutting brass	61.5 Cu, 3.0 Pb, 35.5 Zn	F, R, S	68-49	45-18	18-53	F-E	100	Excellent machinability. Fabricated by machining, roll threading and knurling. Uses: gears, pistons, automatic high speed screw machine parts.
365 to 368 Leaded muntz metal	60.0 Cu, 0.6 Pb, 39.4 Zn	F	54 (As hot rolled)	20	45	F-E	60	Combines good machinability with excellent hot formability. Uses: condenser tube plates.
370 Free-cutting muntz metal	60.0 Cu, 1.0 Pb, 39.0 Zn	T	80-54	60-20	6-40	F-E	70	Fabricating characteristics similar to alloy No. 365 to 368. Uses: automatic screw machine parts.

of Copper and Copper Alloys

Name and Number	Nominal Composition, %	Commercial Forms (a)	Mechanical Properties (b)			Corrosion Resistance (c)	Machinability Rating (d)	Fabricating Characteristics and Typical Applications
			Tensile Strength, 1000 Psi	Yield Strength, 1000 Psi	Elongation in 2 in., %			
377 Forging brass	59.0 Cu, 2.0 Pb, 39.0 Zn	R, S	52 (As extruded)	20	45	F-E	80	Excellent hot workability. Fabricated by heading and upsetting, hot forging and pressing, hot heading and upsetting, machining. Uses: Forgings and pressings of all kinds.
385 Architectural bronze	57.0 Cu, 3.0 Pb, 40.0 Zn	R, S	60 (As extruded)	20	30	F-E	90	Excellent machinability and hot workability. Fabricated by hot forging and pressing, forming, bending and machining. Uses: architectural extrusions, stairs fronts, thresholds, trim, bolts, hinges, lock bodies and forgings.
443, 444, 445 Inhibited admiralty	71.0 Cu, 29.0 Zn, 1.0 Sn	F, W, T	55-48	22-18	60-65	E	30	Excellent cold workability for forming and bending. Uses: Condenser, evaporator and heat exchanger tubing, condenser tubing plates, distiller tubing, ferrules.
464 to 467 Naval brass	60.0 Cu, 39.25 Zn, 0.75 Sn	F, R, T, S	88-55	66-25	17-50	F-E	30	Excellent hot workability and hot forgeability. Fabricated by blanking, drawing, bending, heading and upsetting, hot forging, pressing. Uses: aircraft turnbuckle barrels, bolts, bolts, marine hardware, nuts, propeller shafts, rivets, valve stems, condenser plates, welding rod.
485 Leaded naval brass	60.0 Cu, 1.75 Pb, 37.5 Zn, 0.75 Sn	F, R, S	77-55	53-25	15-40	F-E	70	Combines excellent hot forgeability and machinability. Fabricated by hot forging and pressing, machining. Uses: marine hardware, screw machine parts, valve stems.
505 Phosphor bronze 1.25% E	98.75 Cu, 1.25 Sn, trace P	F, W	79-40	50-14	4-48	G-E	20	Excellent cold workability; good hot formability. Fabricated by blanking, bending, heading and upsetting, shearing and swaging. Uses: electrical contacts, flexible hose, pole-line hardware.
510 Phosphor bronze, 5% A	95.0 Cu, 5.0 Sn, trace P	F, R, W, T	140-47	80-19	2-64	G-E	20	Excellent cold workability. Fabricated by blanking, drawing, bending, heading and upsetting, roll threading and knurling, shearing, stamping. Uses: bellows, bourdon tubing, clutch disks, cotter pins, diaphragms, fasteners, lock washers, wire brushes, chemical hardware, textile machinery, welding rod.
521 Phosphor bronze, 8% C	92.0 Cu, 8.0 Sn, trace P	F, R, W	140-55	80-24	2-70	E	20	Good cold workability for blanking, drawing, forming and bending, shearing, stamping. Uses: generally for more severe service conditions than alloy No. 510.
524 Phosphor bronze, 10% D	90.0 Cu, 10.0 Sn, trace P	F, R, W	147-66 (Annealed)	28	3-70	E	20	Good cold workability for blanking, forming and bending, shearing. Uses: heavy bars and plates for severe compression, bridge and expansion plates and fittings, articles requiring good spring qualities, resiliency, fatigue resistance, good wear and corrosion resistance.
544 Free-cutting phosphor bronze	88.0 Cu, 4.0 Pb, 4.0 Zn, 4.0 Sn	F, R	75-44	63-19	15-50	G-E	80	Excellent machinability; good cold workability. Fabricated by blanking, drawing, bending, machining, shearing, stamping. Uses: bearings, bushings, gears, pinions, shafts, thrust washers, valve parts.
614 Aluminum bronze, D	91.0 Cu, 7.0 Al, 2.0 Fe	F, R, W, T, P, S	89-76	60-33	32-45	E	20	Fabricated by blanking, drawing, forming and bending, heading and roll threading. Uses: nuts, bolts, springs and threaded members, corrosion resistant vessels and tanks, structural components, machine parts and members, condenser tubing and pipe, protective sheathing and fastening, mixing troughs and blending chambers.
651 Low-silicon bronze, B	98.5 Cu, 1.5 Si	R, W, T	95-40	69-15	11-55	G-E	30	Excellent hot and cold workability. Fabricated by forming and bending, heading and upsetting, hot forging and pressing, roll threading and knurling, squeezing and swaging. Uses: hydraulic pressure lines, anchor screws, bolts, cable clamps, cap screws, machine screws, marine hardware, nuts, pole-line hardware, rivets, U-bolts, electrical conduits, heat exchanger tubing, welding rod.
655 High-silicon bronze, A	97.0 Cu, 3.0 Si	F, R, W, T	145-56	70-21	3-63	G-E	30	Excellent hot and cold workability. Fabricated by blanking, drawing, forming and bending, heading and upsetting, hot forging and pressing, roll threading and knurling, shearing, squeezing and swaging. Uses: similar to alloy No. 651 including propeller shafts.
675 Manganese bronze, A	58.5 Cu, 1.4 Fe, 39.0 Zn, 1.0 Sn, 0.1 Mn	R, S	84-65	60-30	19-33	F-E	30	Excellent hot workability. Fabricated by hot forging and pressing, hot heading and upsetting. Uses: clutch disks, pump rods, shafting, balls, valve stems and bodies.
687 Aluminum brass	77.5 Cu, 20.5 Zn, 2.0 Al	T	60 (Annealed)	27	55	E	30	Excellent cold workability for forming and bending. Uses: same as alloy No. 443 444 and 445.
706 Copper nickel, 10%	88.7 Cu, 1.3 Fe, 10.0 Ni	F, T	60-44	57-16	10-42	E	20	Good hot and cold workability. Fabricated by forming and bending, welding. Uses: condensers, condenser plates, distiller tubing, evaporator and heat exchanger tubing, ferrules, salt water piping.
715 Copper nickel, 30%	70.0 Cu, 30.0 Ni	F, R, T	75-54	70-20	15-45	E	20	Similar to alloy No. 706.
745 Nickel silver, 65-10	65.0 Cu, 25.0 Zn, 10.0 Ni	F, W	130-49	76-18	1-50	E	20	Excellent cold workability. Fabricated by blanking, drawing, etching, forming and bending, heading and upsetting, roll threading and knurling, shearing, spinning, squeezing and swaging. Uses: rivets, screws, slide fasteners, optical parts, etching stock, hollow ware, nameplates, platers' bars.
752 Nickel silver, 65-18	65.0 Cu, 17.0 Zn, 18.0 Ni	F, R, W	103-56	90-25	3-45	E	20	Fabricating characteristics similar to alloy No. 745. Uses: rivets, screws, table flatware, brass wire, zippers, bows, camera parts, core bars, temples, base for silver plate, costume jewelry, etching stock, hollow ware, nameplates, radio dials.
754 Nickel silver, 65-15	65.0 Cu, 20.0 Zn, 15.0 Ni	F	92-53	79-18	2-43	E	20	Fabricating characteristics similar to alloy No. 745. Uses: camera parts, optical equipment, etching stock, jewelry.
757 Nickel silver, 65-12	65.0 Cu, 23.0 Zn, 12.0 Ni	F, W	93-52	79-18	2-48	E	20	Fabricating characteristics similar to alloy No. 745. Uses: slide fasteners, camera parts, optical parts, etching stock, nameplates.
770 Nickel silver, 55-18	55.0 Cu, 27.0 Zn, 18.0 Ni	F, R, W	145-60	90-27	2-40	E	30	Good cold workability. Fabricated by blanking, forming and bending and shearing. Uses: optical goods, springs and resistance wire.

(a) F, hot products; R, rod; W, wire; T, tube; P, pipe; S, shapes.

(b) Hardest to softest commercial forms. The strength of the standard copper alloys depend on the temper (annealed grain size or degree of cold work) and the section thickness of the mill product. Ranges cover standard tempers (eight hard, quarter hard, half hard) for each alloy.

(c) E, excellent; G, good; F, fair.

(d) Based on 100% for alloy No. 360.

(e) Alloy No. 113 contains 8 oz per ton silver; No. 114, 10 oz per ton; No. 116, 25 oz per ton. Compiled by Copper Development Assn., New York.

END OF REFERENCE

REFERENCE

8

**SHANK, M. E., ED.: CONTROL OF STEEL CONSTRUCTION TO
AVOID BRITTLE FAILURE. WELDING RESEARCH COUNCIL, 1967.**

**THIS REFERENCE IS COPYRIGHTED MATERIAL AND THEREFORE
THE CONTENTS HAVE NOT BEEN REPRODUCED FROM THE TEXT.**

END OF REFERENCE

REFERENCE

9

SISCO, FRANK T.: ENGINEERING METALLURGY. PITMAN PUBL. CO., 1957.

**THIS REFERENCE IS COPYRIGHTED MATERIAL AND THEREFORE
THE CONTENTS HAVE NOT BEEN REPRODUCED FROM THE TEXT.**

END OF REFERENCE

REFERENCE

10

**ANON.: 1971 ANNUAL BOOK OF ASTM STANDARDS. PART 31.
ASTM, 1971.**

**THIS REFERENCE IS A COPYRIGHTED STANDARD AND THEREFORE
THE CONTENTS HAVE NOT BEEN REPRODUCED FROM THE TEXT.**

END OF REFERENCE

10

REFERENCE

II

ANON.: ASME BOILER AND PRESSURE VESSEL CODE. SECTION VIII. RULES FOR CONSTRUCTION OF PRESSURE VESSELS. DIVISIONS I AND 2. ASME, 1971.

THIS REFERENCE IS A COPYRIGHTED STANDARD AND THEREFORE THE CONTENTS HAVE NOT BEEN REPRODUCED FROM THE TEXT.

END OF REFERENCE

II

REFERENCE

12

**WIGLEY, D. A.: MECHANICAL PROPERTIES OF MATERIALS AT
LOW TEMPERATURES. PLENUM PRESS, 1971.**

**THIS REFERENCE IS A COPYRIGHTED MATERIAL AND THEREFORE
THE CONTENTS HAVE NOT BEEN REPRODUCED FROM THE TEXT.**

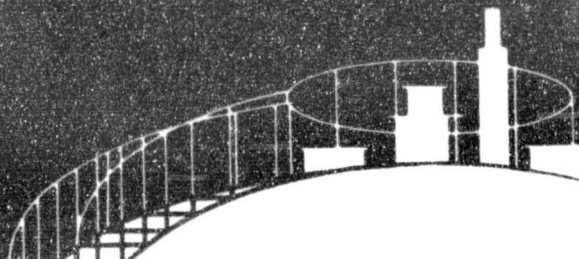
END OF REFERENCE
12

REFERENCE
13

**ANON.: LOW TEMPERATURE AND CRYOGENIC STEELS. MATERIALS
MANUAL. UNITED STATES STEEL.**



Low Temperature and Cryogenic Steels



THIS MATERIAL HAS BEEN APPROVED TO BE MADE AVAILABLE
FOR THE TECHNICAL AND SCIENTIFIC COMMUNITY PER LETTER
R. S. HOLMES TO JOANNE FOLK DATED OCT. 9, 1972.



United States Steel

I. Introduction

The fundamental characteristics of low-temperature and cryogenic technology have already found their way into segments of almost every major industry. Cryogenic applications in space, in the new oxygen process for the manufacture of steel, in the chemical-process industries, and in the metal fabrication and medical fields have been well known and publicized for many years.

These, together with additional applications of cryogenic processes to the petroleum, natural gas, glass, cement, food, and electronics industries, give the cryogenic field a firm foundation for future growth. The low-temperature and cryogenic products of commercial importance include refrigerated propane and anhydrous ammonia, carbon dioxide, nitrous oxide, ethane, ethylene, methane, oxygen, nitrogen, argon, chlorine, hydrogen, and helium. The chemical formulas and boiling points of these and the other products normally associated with low-temperature and cryogenic applications are shown in Table I (Page 6), along with the designations of classes of steels used in equipment for service at the boiling-point temperatures of the products. "Low-temperature" and "cryogenic" technologies may be defined for present purposes as involving temperatures to -150°F and -459°F , respectively.

In terms of volume of products, the steel and chemical-processing industries represent the largest single commercial consumers for all of these products. Various agencies of the government, of course, have been and will continue to be consumers of considerable importance. Presently, the steel industry and chemical-processing industries consume

over half of the total atmospheric-gas production in the country and will continue to take that portion for the foreseeable future.

In the steel industry, as elsewhere, these commodities are used in two general types of equipment. The first, primarily plant equipment, represents relatively complex machinery performing specific functions in production operations. This type of equipment includes heat exchangers, cold-box equipment, distillation columns, compressors, controls and instrumentation. The other type of equipment is devoted primarily to material-handling aspects of storage, transportation, distribution, and ultimate consumption of cryogenic fluids (as either liquids or gases). Carbon, alloy, and stainless steels for low-temperature and cryogenic service are used in both areas.

United States Steel produces a family of steels covering the entire range of low-temperature and cryogenic applications. Individual steels may be best suited only to certain areas of use. Their mechanical and physical properties vary with alloy content and the steelmaking process. To fabricate these steels successfully, a knowledge of their properties and characteristics is essential. The detailed applications of materials given in this publication are offered as a guide to successful workmanship.

When ordering cryogenic and low-temperature steels, the purchaser should always inform the supplier of the end-use of the material and the fabrication techniques to be employed in order to obtain the most suitable material. For applications under unusual conditions, or where special suggestions may be

Table 1. Boiling Points of Gases and a List of Steels for Service at Boiling Points

Commodity	Chemical Formula	Approximate Boiling Point at 1 Atm				Steels Normally Considered for Service at Boiling Point
		°C	°K	°F	°R	
Butane	C ₄ H ₁₀	-0.6	272.5	30.9	490.6	A 201† A 212† A 516† CHAR-PAC USS "T-1" (A 517) 2½% Nickel Steel (A 203)
Sulfur Dioxide	SO ₂	-10.0	263.1	14.0	473.7	
Isobutane	(CH ₃) ₂ C ₂ H ₆	-10.2	262.9	13.6	473.3	
Methyl Chloride	CH ₃ Cl	-23.7	249.4	-10.7	449.0	
Fluorocarbon Refrigerant ₁₂	CCl ₂ F ₂	-30.0	243.1	-22.0	437.7	
Ammonia	NH ₃	-33.3	239.8	-27.9	431.8	
Fluorocarbon Refrigerant ₂₂	CHClF ₂	-40.6	232.5	-41.0	418.7	
Ketene	C ₂ H ₂ O	-41.0	232.1	-41.8	417.9	
Propane	C ₃ H ₈	-42.3	230.8	-44.1	415.6	
Propylene	C ₃ H ₆	-47.0	226.1	-52.6	407.1	
Hydrogen Sulfide	H ₂ S	-59.6	213.5	-75.3	394.4	
Carbon Dioxide*	CC ₂	-78.5	194.6	-109.3	350.4	Stainless Steels (AISI 300 Series) 3½% Nickel Steels (A 203)
Acetylene	C ₂ H ₂	-84.0	189.1	-119.2	340.5	
Ethane	C ₂ H ₆	-83.3	184.8	-126.9	332.8	
Nitrous Oxide	N ₂ O	-89.5	183.6	-129.1	330.6	
Ethylene	C ₂ H ₄	-103.8	169.3	-154.8	304.9	
Xenon	Xe	-109.1	164.0	-164.4	295.3	
Ozone	O ₃	-111.9	161.3	-169.4	290.3	9% Nickel Steel (A 353) Stainless Steels (AISI 300 Series)
Krypton	Kr	-151.8	121.3	-241.2	218.5	
Methane	CH ₄	-161.4	111.7	-258.5	201.2	
Oxygen	O ₂	-183.0	90.1	-297.4	162.3	
Argon	A	-185.7	87.4	-302.3	157.4	
Fluorine	F ₂	-187.0	86.0	-304.6	155.1	
Carbon Monoxide	CO	-192.0	81.1	-313.6	146.1	
Nitrogen	N ₂	-195.8	77.3	-320.4	139.3	Stainless Steels (AISI 300 Series)
Neon	Ne	-245.9	27.2	-410.6	49.1	
Tritium	T ₂	-248.0	25.1	-414.4	45.3	
Deuterium	D ₂	-249.5	23.6	-417.1	42.6	
Hydrogen	H ₂	-252.7	20.4	-422.9	36.8	
Helium	He ⁴	-268.9	4.2	-452.1	7.6	
Helium	He ³	-269.9	3.2	-453.8	5.9	

*Sublimes.

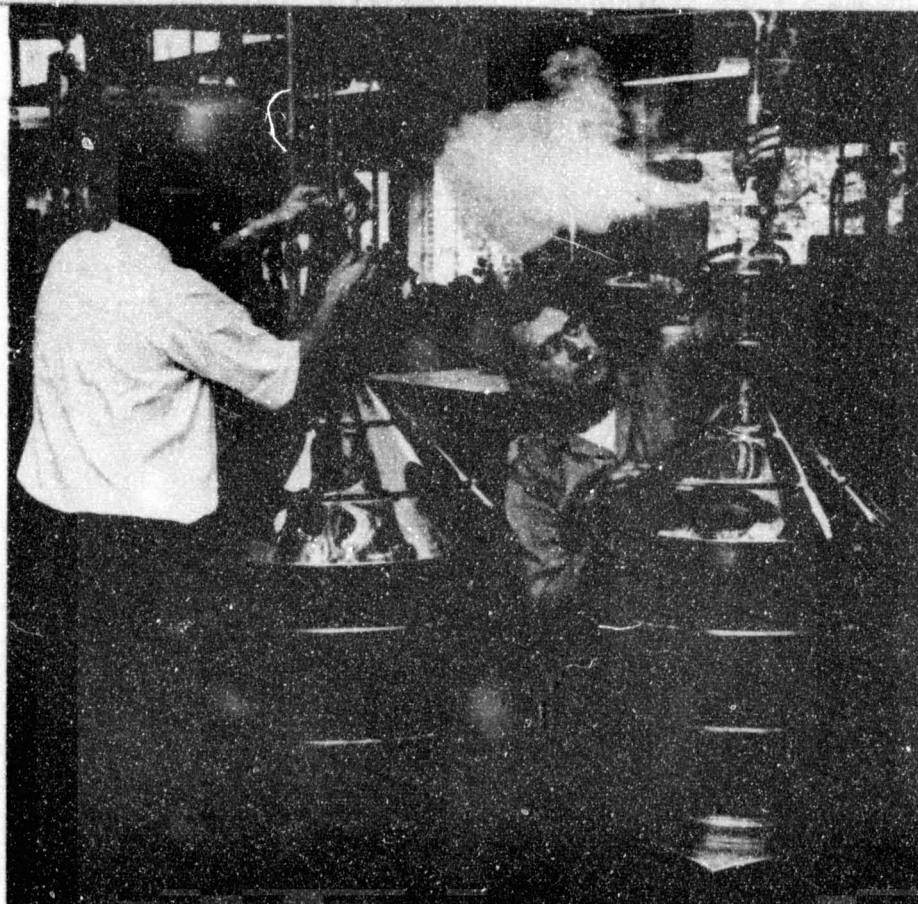
†To ASTM A 300 specification.

needed, the nearest Sales Office of United States Steel will supply additional assistance on request.

The total commercial effort of United States Steel is aimed at providing better customer service in the sale and use of steel and steel products. This sales effort is reinforced by such USS departments as Marketing, Metallurgical, Engineering, and Research & Technology—the last consisting of a staff of 1,700 in the steel industry's largest and best equipped Research Center.

Low-temperature and cryogenic steels are a group of ferrous metals which possess desirable metallurgical characteristics for tanks, pressure vessels, and piping (used principally for the processing, transporting, and storing of liquefied gases), as well as certain other items of process equipment, and for structural uses requiring ductile steels at temperatures for which the more conventional materials are unsuitable.

The "low-temperature" steels are those especially suited for extremely cold



One of the most significant advances in cryogenic technology was the ADL-Collins Helium Cryostat. More than 250 of these helium liquefiers are used in low-temperature installations

throughout the Free World. Here, a product development team at Arthur D. Little, Inc., experiments with liquefaction of helium gas, using a 200-liter stainless steel Dewar vessel.

climates and for the handling of relatively "warm" (to -150°F) liquefied gases such as propane, anhydrous ammonia, carbon dioxide, and ethane. Cryogenic steels, such as 9% nickel steel, and the austenitic stainless steels, are capable of retaining toughness in applications involving the storing and handling of liquefied methane, oxygen, nitrogen, argon, hydrogen, and helium to -459°F .

The following pages are intended to provide designers with summary information pertaining to the composition and properties of those carbon, alloy, and stainless steels which possess desirable metallurgical characteristics for

low-temperature and cryogenic service. Table 2 gives the nominal composition of the steels included in the USS "Family of Steels" for low-temperature and cryogenic service. Table 3 identifies the pertinent ASTM Specifications, ASME Specifications and Code Cases, and AISI designations relating to carbon, alloy and stainless steels for these applications. The mechanical and physical properties having major significance for applications in low-temperature and cryogenic service are shown in Tables 4 and 5, respectively, and Table 6 shows the availability of these steels by product classification.

Table 2. Composition Ranges of USS Family of Steels for Low-Temperature and Cryogenic Service^{1,2}

Carbon Steels

USS Designation	ASTM Spec. & Grade	Chemical Composition (percent)			
		Carbon	Manganese	Silicon	Other Elements
USS CHAR-PAC	A 537 (*)	0.20	0.70-1.35	0.15-0.50	P, 0.04; S, 0.05; small amounts of Cu, Cr, Ni and Mo
	A 291 (*)				
	Grade A	0.20	0.85-1.20	0.15-0.30	P, 0.04; S, 0.05
	Grade B	0.24	0.85-1.20	0.15-0.30	P, 0.04; S, 0.05
	A 212(*)				
	Grade A	0.20	0.85-1.20	0.15-0.30	P, 0.04; S, 0.05
	Grade B	0.31	0.85-1.20	0.15-0.30	P, 0.04; S, 0.05
	A 533				
	Grade 1	0.30	0.40-1.06	not spec.	P, 0.05; S, 0.06
	Grade 6	0.30	0.29-1.06	0.10 min.	P, 0.048; S, 0.058
	A 534				
	Grade 1	0.30	0.40-1.06	not spec.	P, 0.05; S, 0.06
	Grade 6	0.30	0.29-1.06	0.10 min.	P, 0.048; S, 0.058
	A 442				
	Grade 55	0.22	0.30-1.10	0.15-0.30	P, 0.04; S, 0.05
	Grade 60	0.24	0.30-1.10	0.15-0.30	P, 0.04; S, 0.05
	A 516 (*)				
	Grade 55	0.18	0.60-0.90	0.15-0.30	P, 0.04; S, 0.05
	Grade 60	0.21	0.60-0.90	0.15-0.30	P, 0.04; S, 0.05
	Grade 65	0.24	0.85-1.20	0.15-0.30	P, 0.04; S, 0.05
	Grade 70	0.27	0.85-1.20	0.15-0.30	P, 0.04; S, 0.05

Alloy Steels³

USS Designation	ASTM Spec. No. & Grade	Chemical Composition (percent)					
		Carbon	Manganese	Silicon	Chromium	Nickel	Other Elements
USS "T-1"	ASTM A 517 Grade F	0.10-0.20	0.60-1.00	0.15-0.35	0.40-0.65	0.70-1.00	Mo, 0.40-0.60; V, 0.03-0.08; Cu, 0.15-0.50; B, 0.002-0.006; P, 0.035; S, 0.040
USS 2 1/4% Ni	ASTM A 203 Grade A	0.17-0.23	0.70-0.80	0.15-0.30	2.10-2.50	P, 0.035; S, 0.040
	Grade B	0.21-0.25	0.70-0.80	0.15-0.30	2.10-2.50	P, 0.035; S, 0.040
USS 3 1/2% Ni	ASTM A 203 Grade D	0.17-0.20	0.70-0.80	0.15-0.30	3.25-3.75	P, 0.035; S, 0.040
	Grade E	0.20-0.23	0.70-0.80	0.15-0.30	3.25-3.75	P, 0.035; S, 0.040
USS 0% Ni	ASTM A 353 Grade A	0.13	0.80	0.15-0.30	8.50-9.50	P, 0.035; S, 0.040
	Grade B	0.13	0.90	0.15-0.30	8.50-9.50	P, 0.035; S, 0.040

Stainless Steels³

USS Designation and AISI Type No.	Chemical Composition (percent)					
	Carbon	Manganese	Silicon	Chromium	Nickel	Other Elements
USS 17-7 (AISI 301)	0.15	2.00	1.00	16.00-18.00	6.00-8.00	P, 0.045; S, 0.030
USS 18-8 (AISI 302)	0.075	2.00	1.00	17.00-19.00	8.00-10.00	P, 0.045; S, 0.030
USS 18-8S (AISI 304)	0.08	2.00	1.00	18.00-20.00	8.00-12.00	P, 0.045; S, 0.030
USS 18-8L (AISI 304L)	0.03	2.00	1.00	18.00-20.00	8.00-12.00	P, 0.045; S, 0.030
USS 18-8FS (AISI 308)	0.12	2.00	1.00	17.00-19.00	10.00-13.00	P, 0.045; S, 0.030
USS 25-12 (AISI 309)	0.20	2.00	1.00	22.00-24.00	12.00-15.00	P, 0.045; S, 0.030
USS 25-12S (AISI 309S)	0.08	2.00	1.00	22.00-24.00	12.00-15.00	P, 0.045; S, 0.030

(Continued on next page)

Table 2 (continued). Composition Ranges of USS Family of Steels for Low-Temperature and Cryogenic Service
Stainless Steels¹

USS Designation and AISI Type No.	Chemical Composition (percent)					
	Carbon	Manganese	Silicon	Chromium	Nickel	Other Elements
USS 25-20 (AISI 310)	0.25	2.00	1.50	24.00-26.00	19.00-22.00	P, 0.045; S, 0.030
USS 25-20S (AISI 310S)	0.08	2.00	1.50	24.00-26.00	19.00-22.00	P, 0.045; S, 0.030
USS 18-8 Mo (AISI 316)	0.08	2.00	1.00	16.00-18.00	10.00-14.00	Mo, 2.00-3.00; P, 0.045; S, 0.030
USS 18-8 MoL (AISI 316L)	0.03	2.00	1.00	16.00-18.00	10.00-14.00	Mo, 2.00-3.00; P, 0.045; S, 0.030
USS 18-8 Ti (AISI 321)	0.08	2.00	1.00	17.00-19.00	9.00-12.00	Ti, 5xC, min.; P, 0.045; S, 0.030
USS 18-8 Cb Ti (AISI 347)	0.08	2.00	1.00	17.00-19.00	9.00-13.00	Cb+Ti, 10xC, min.; P, 0.045; S, 0.030
USS 18-8 Cb (AISI 348)	0.08	2.00	1.00	17.00-19.00	9.00-13.00	Cb+Ti, 10xC, min.; Ti, 0.10; Cb, 0.20; P, 0.045; S, 0.030

(1) Exact composition selected for a given application is dependent upon type of product (e.g., plates, tubular products) and/or section size (e.g., thickness). For more information consult pertinent specifications identified in table 3 or your USS salesman.

(2) Values are maximum unless otherwise specified or a range is given.

(3) See table 3 for ASTM specification and ASME code case numbers corresponding to USS designations.

(4) To ASTM A 300 specifications. (5) With modifications.

Table 3. ASME Specification and Code Case Numbers, ASTM Specification Numbers, and AISI Type Numbers Related to Flat-Rolled and Tubular Products of USS Steels for Low-Temperature and Cryogenic Service

USS Designation	AISI Type No.	Plates		Tubular Products		
		ASME		ASTM Spec. Number	ASME	
		Code Case No.	Spec. No.		Code Case No.	Spec. No.
Carbon Steels USS CHAR-PAC			SA-201* SA-212* SA-442	A 537** A 201† A 212† A 442		
Alloy Steels USS "T-1"		1346	SA-516*	A 516†	SA-333 SA-334	A 333 A 334
USS 2 1/4% Ni		1204	SA-203 (Grades A & B)	A 517 (Grade F) A 203 (Grades A & B)	SA-333 (Grade 7) SA-334 (Grade 7)	A 333 A 334
USS 3 1/4% Ni			SA-203 (Grades D & E)	A 203 (Grades D & E)	SA-333 (Grade 3) SA-334 (Grade 3)	A 333 A 334
USS 9% Ni		1308	SA-353 (Grades A & B)	A 353 (Grades A & B)	1308 SA-333 (Grade 8) SA-334 (Grade 8)	A 333 A 334
Stainless Steels						
USS 17-7	301			A 177		
USS 18-8	302		3A-240	A 240 Type 302		
USS 18-8S	304		3A-240	A 240 Type 304		
USS 18-8L	304L		3A-240	A 240 Type 304L	SA-213	A 269 Grade TP-304 A 213 Grade TP-304L
USS 18-8FS	305		3A-240	A 240 Type 305		
USS 25-12	309					A 312 Grade TP-309
USS 25-12S	309S		3A-240	A 240 Type 309S		
USS 25-20	310				SA-213	A 213 Grade TP-310
USS 25-20S	310S		3A-240	A 240 Type 310S		
USS 18-8 Mo	316		3A-240	A 240 Type 316		A 269 Grade TP-316
USS 18-8 MoL	316L		3A-240	A 240 Type 316L		A 269 Grade TP-316L
USS 18-8 Ti	321		3A-240	A 240 Type 321		A 269 Grade TP-321
USS 18-8 Cb Ti	347		3A-240	A 240 Type 347		A 269 Grade TP-347
USS 18-8 Cb	348		3A-240	A 240 Type 348		A 269 Grade TP-348

*To ASME SA-300 specifications.

†To ASTM A 300 specifications.

**With modifications.

Table 4. Room Temperature Mechanical Properties of USS Family of Steels for Low-Temperature and Cryogenic Service (a)(b)

Designation	Tensile Strength (1,000 Lb. per Sq. In.)	Yield Point (1,000 Lb. per Sq. In.)	Yield Strength (1,000 Lb. per Sq. In.)(c)	Elongation (Percent)		Modulus of Elasticity (Million Lb. per Sq. In.)
				in 2 in.	in 8 in.	
Carbon Steels						
USS CHAR-PAC (ASTM A 537)(^b)						
Normalized(^c)	70-90	50			19	28-30
Quenched & Tempered(^c)	80-100	..	60(^d)	23	..	28-30
ASTM A 201(^d)						
Grade A	55-65	30	..	28(^e)	24(^e)	28-30
Grade B	60-72	32	..	25(^e)	22(^e)	28-30
ASTM A 212(^d)						
Grade A	65-77	35	..	23(^e)	20(^e)	28-30
Grade B	70-85	38	..	21(^e)	18(^e)	28-30
ASTM A 333						
Grade 1	55	30	..	35(^e)
Grade 6	60	35	..	30(^e)
ASTM A 334						
Grade 1	55	30	..	35(^e)
Grade 6	60	35	..	30(^e)
ASTM A 442						
Grade 55	55-65	30	..	28(^e)	24(^e)	28-30
Grade 60	60-72	32	..	25(^e)	22(^e)	28-30
ASTM A 516 (^d)						
Grade 55	55-65	30	..	28(^e)	24(^e)	..
Grade 60	60-72	32	..	26(^e)	22(^e)	..
Grade 65	65-77	35	..	24(^e)	20(^e)	..
Grade 70	70-85	38	..	22(^e)	18(^e)	..
Alloy Steels						
USS "T-1"						
ASTM A 517 Grade F	115-135	..	100(^d)	18	..	30
USS 2¼% Ni						
ASTM A 203 Grade A	65	37	..	25(^e)	21(^e)	29
ASTM A 203 Grade B	70	40	..	23(^e)	19(^e)	29
ASTM A 333 Grade 7	65	35	..	30(^e)
ASTM A 334 Grade 7	65	35	..	30(^e)
USS 3¼% Ni						
ASTM A 203 Grade D	65	37	..	24(^e)	21(^e)	29
ASTM A 203 Grade E	70	40	..	22(^e)	19(^e)	..
ASTM A 333 Grade 3	65	35	..	30(^e)
ASTM A 334 Grade 3	65	35	..	30(^e)
USS 9% Ni						
ASME Code Case 1308	100-120	..	75	22
ASTM A 353 Grade A	90	..	60	22	..	29
ASTM A 353 Grade B	95	..	65	20
ASTM A 333 Grade 8	100	75	..	22(^e)
ASTM A 334 Grade 8	100	75	..	22(^e)

(a) Minimum values except where ranges are indicated. Exact values related to chemical composition and section size. Values shown for modulus of elasticity are typical values and are not covered by specifications.

(b) Impact properties are given in Chapter III, Section B, under "Toughness."

(c) For plates to 1 1/4 in., incl., in thickness. Plates are available up to 2 in. thick.

(d) Elongation measured in 2 in. or 8 in. depending on plate thickness. See specification.

(e) Basic minimum elongation for tubular products with walls 1/4 in. and over in thickness, strip tests, and for all small sizes tested in full section. See specification for details relating to elongation values for products of lesser wall thickness.

Table 4 (continued). Room Temperature Mechanical Properties of USS Family of Steels for Low-Temperature and Cryogenic Service (a)(b)

Designation	Tensile Strength (1000 Lb. per Sq. In.)	Yield Point (1000 Lb. per Sq. In.)	Yield Strength (100 Lb. per Sq. In.)(c)	Elongation (Percent)		Modulus of Elasticity (Million Lb. per Sq. In.)
				In 2 In.	In 8 In.	
Stainless Steels						
USS 17-7 (ASTM A 177)						
1/4 Hard	125	..	75	25(h)	..	28(i)
1/2 Hard	150	..	110	10(h)
3/4 Hard	175	..	135	5(h)
Full Hard	185	..	140	4(h)
USS 18-8 (ASTM A 240, Type 302)	75	..	30	40	..	28
USS 18-8S (ASTM A 240, Type 304)	75	..	30	40	..	28
USS 18-8L (ASTM A 240, Type 304L)	70	..	25	40	..	28
USS 18-8FS (ASTM A 240, Type 305)	70	..	25	40	..	28
USS 25-12 (ASTM A 312, Grade TP 309)	75	..	30	35	..	29
USS 25-12S (ASTM A 240, Type 309S)	75	..	30	40	..	29
USS 25-20 (ASTM A 213, Grade TP 310)	75	..	30	35	..	29
USS 25-20S (ASTM A 240, Type 310S)	75	..	30	40	..	29
USS 18-8 Mo (ASTM A 240, Type 316)	75	..	30	40	..	28
USS 18-8 MoL (ASTM A 240, Type 316L)	70	..	25	40	..	28
USS 18-8 Ti (ASTM A 240, Type 321)	75	..	30	40	..	28
USS 18-8 CbTa (ASTM A 240, Type 347)	75	..	30	40	..	28
USS 18-8 Cb (ASTM A 240, Type 348)	75	..	30	40	..	28

(f) Determined by total extension-under-load method.

(g) Determined by the 0.2% offset method, unless otherwise noted.

(h) For thicknesses 0.016 to .030 in., see specification for minimum elongation values for other thickness ranges.

(i) Annealed.

(j) To ASTM A 300 specification.

(k) With modifications.

Table 5A. Physical Properties of USS Carbon and Alloy Steels for Low-Temperature and Cryogenic Service (Properties Determined at Room Temperature Unless Otherwise Indicated)

Property	Carbon Steels			Alloy Steels			
	ASTM A 537*	ASTM A 442	ASTM A 516	USS "T-1" ASTM A 517	USS 2 1/4% Ni ASTM A 263	USS 3 1/2% Ni ASTM A 263	USS 9% Ni ASTM A 263
Density Lb. per Cu. In. Gm. per Cu. Cm.		0.283 7.83	0.283 7.83				
Specific Electrical Resistance Microhm-in. Microhm-Cm.		3.82 9.71	3.82 9.71				
Specific Heat, Btu/lb./°F -320 To +80°F -150 To +80°F At 58°F		0.11	0.11		0.080	0.0798	0.0878
+80 To +700°F +80 To +1000°F					0.144	0.147	0.119
Thermal Conductivity Btu/hr./sq. ft./°F/in. -320°F -150°F -50°F +68°F +200°F		349	349		248 267 280	214 253 270	91.3 169 189 208
Mean Coefficient of Thermal Expansion, in./in./°F At -300°F -300 To 0°F -300 To +200°F -50 To +150°F 0 To +200°F At 68°F +70 To +1300°F	6.5 x 10 ⁻⁶	6.53 x 10 ⁻⁶	6.53 x 10 ⁻⁶	6.5 x 10 ⁻⁶	6.2 x 10 ⁻⁶ 7.74 x 10 ⁻⁶	6.15 x 10 ⁻⁶	4.0 x 10 ⁻⁶ 5.3 x 10 ⁻⁶ 5.6 x 10 ⁻⁶ 5.8 x 10 ⁻⁶

*With modifications.

Table 5B. Physical Properties of USS Stainless Steels for Low-Temperature and Cryogenic Service (Properties Determined at Room Temperature Unless Otherwise Indicated)

USS Designation	USS 17-7	USS 18-8	USS 18-8S and 18-11	USS 18-8FS	USS 25-12 and 25-12S	USS 25-20	USS 25-20S	USS 18-8Mo and 18-9Mo	USS 18-8Ti	USS 18-8Cb and 18-8Cb
AISI Type No.	301	302	304, 304L	305	309, 309S	310	310S	316, 316L	321	347, 348
Property										
Density Lb. per Cu. In. Gm. per Cu. Cm.	0.29 7.9	0.29 7.9	0.29 7.9	0.29 7.9	0.29 7.9	0.29 7.9	0.29 7.9	0.29 7.9	0.29 7.9	0.29 7.9
Specific Electrical Resistance Microhm-in. Microhm-Cm.	28.4 72	28.4 72	28.4 72	28.4 72	30.8 78	30.8 78	30.8 78	29.2 74	28.4 72	28.6 73
Magnetic Permeability Annealed 10% Cold Worked Heavily Cold Worked			1.003 1.10 7.0		1.003 1.003			1.003		1.02
Specific Heat, Btu/lb./°F -320°F -150°F 32 To 212°F			0.037 0.088 0.12		0.12 0.12	0.12 0.12	0.12 0.12	0.12 0.12	0.12 0.12	0.12 0.12
Thermal Conductivity Btu/hr./sq. ft./°F/in. -320°F -155°F +70°F +212°F +600°F			56.4 80.0 117.6 120.0		109	73.8	73.8	113	112	112
Mean Coefficient of Thermal Expansion, in./in./°F -300 To +70° -200 To +70° -100 To +70° 32 To 212°F 32 To 600°F			7.4 x 10 ⁻⁶ 7.7 x 10 ⁻⁶ 8.2 x 10 ⁻⁶		8.3 x 10 ⁻⁶ 9.3 x 10 ⁻⁶	8.8 x 10 ⁻⁶ 9.0 x 10 ⁻⁶	8.8 x 10 ⁻⁶ 9.0 x 10 ⁻⁶	8.9 x 10 ⁻⁶ 9.0 x 10 ⁻⁶	9.3 x 10 ⁻⁶ 9.5 x 10 ⁻⁶	9.3 x 10 ⁻⁶ 9.5 x 10 ⁻⁶

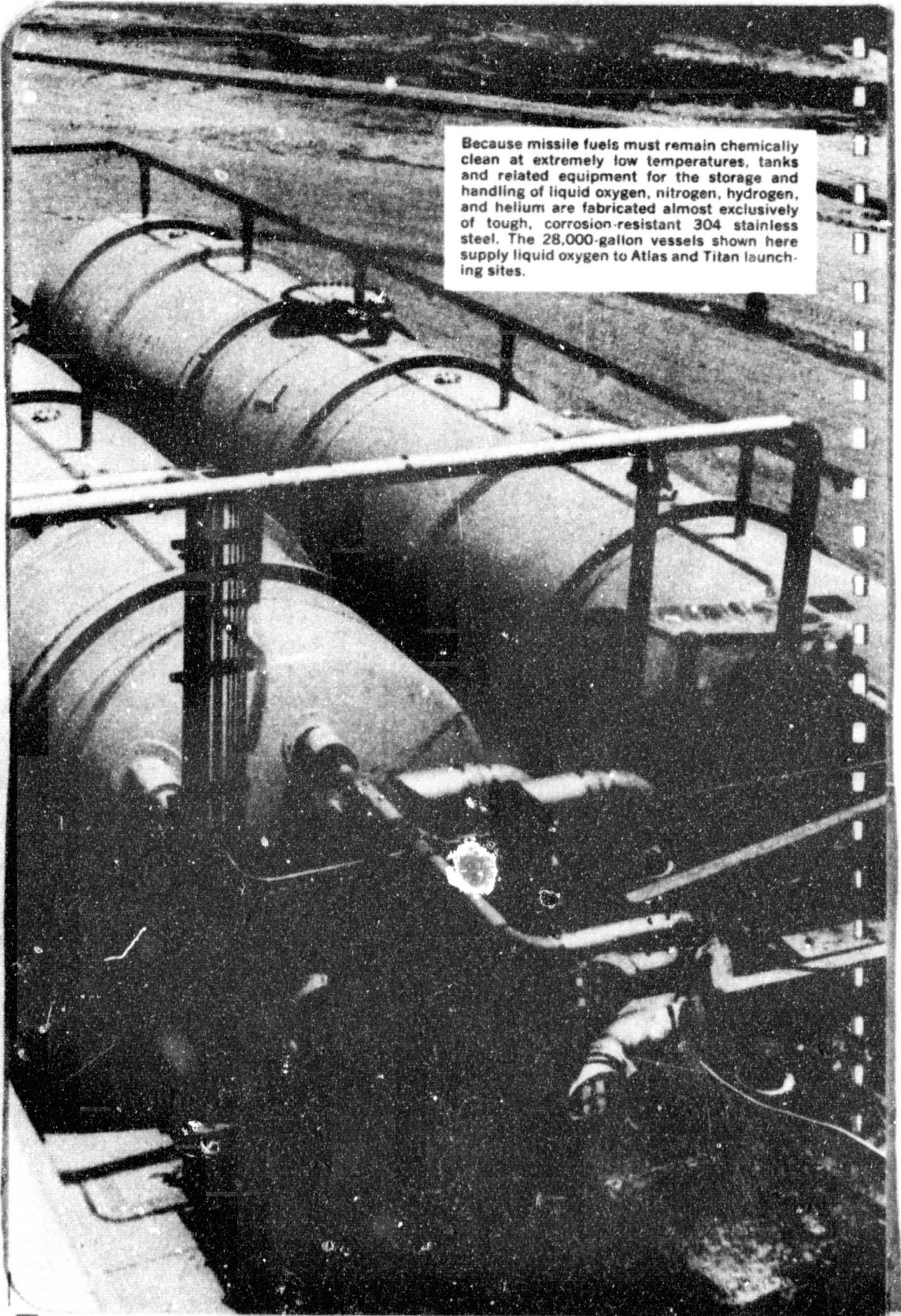
Table 6. Availability of USS Low-Temperature and Cryogenic Steels

Designation	ASTM, ASME Code Case No. or AISI Type No.	Semi- Fin.	Bars	Angles and Struct. Shapes	Strip	Sheets	Plates	Tub- ing	Ex- truded Shapes	Forg- ings
Carbon Steels										
USS CHAR-PAC	ASTM A 537 ^(a)	X
	ASTM A 201 (Grade A)	X ^(a)
	ASTM A 201 (Grade B)	X ^(a)
	ASTM A 212 (Grade A)	X ^(a)
	ASTM A 212 (Grade B)	X ^(a)
	ASTM A 333 (Grade 1)	X
	ASTM A 333 (Grade 6)	X
	ASTM A 334 (Grade 1)	X
	ASTM A 334 (Grade 6)	X
	ASTM A 442	X
	ASTM A 516 (Grade 55)	X ^(a)
	ASTM A 516 (Grade 60)	X ^(a)
	ASTM A 516 (Grade 65)	X ^(a)
	ASTM A 516 (Grade 70)	X ^(a)
Alloy Steels										
USS "T-1"	ASTM A 517 (Grade F)	X	X	X	..	X	X	X	..	X
	ASME Code Case 1204	X	X
USS 2 1/4% Ni	ASTM A 203 (Grade A)	X	X	X	..	X	X	X	..	X
	ASTM A 203 (Grade B)	X	X	X	..	X	X	X	..	X
	ASTM A 333 (Grade 7)	X
	ASTM A 334 (Grade 7)	X
USS 3 1/2% Ni	ASTM A 203 (Grade D)	X	X	X	..	X	X	X	..	X
	ASTM A 203 (Grade E)	X	X	X	..	X	X	X	..	X
	ASTM A 333 (Grade 3)	X
	ASTM A 334 (Grade 3)	X
USS 9% Ni	ASME Code Case 1308	X	X	X	..	X	X	X	..	X
	ASTM A 353 (Grade A)	X	X	X	..	X	X	X	..	X
	ASTM A 353 (Grade B)	X	X	X	..	X	X	X	..	X
	ASTM A 333 (Grade 8)	X
	ASTM A 334 (Grade 8)	X
Stainless Steels										
USS Stainless	AISI Type Nos. Such As: 301, 302, 304, 304L, etc.	X	X	X	X	X	X	X	X	X

(a) To ASTM A 302 specification.

(b) With modifications.

Note: The size range available in each product and grade of steel can be furnished by the nearest USS Sales Office.



Because missile fuels must remain chemically clean at extremely low temperatures, tanks and related equipment for the storage and handling of liquid oxygen, nitrogen, hydrogen, and helium are fabricated almost exclusively of tough, corrosion-resistant 304 stainless steel. The 28,000-gallon vessels shown here supply liquid oxygen to Atlas and Titan launching sites.

II. Service Considerations

A. Application of Cryogenic Process Equipment

The production and handling problems in low-temperature and cryogenic processes have, until recently, limited the supply and distribution of liquids and gases to a regional basis.

Even today, there are problems and hazards in handling some of these gases and liquids in a pure state. Some commodities are either highly reactive (acetylene and ozone) or extremely toxic (carbon monoxide). As a result, many of these chemicals are normally consumed in the gaseous state at the point of manufacture.

Acetylene is, of course, widely distributed and used throughout the metal fabricating industries as a source of energy for welding and cutting. For such purposes, acetylene is normally partially dissolved in acetone and handled in specially designed cylinders.

One of the major benefits to be derived from handling gases in liquefied form at cryogenic temperatures is the enormous reduction in volume resulting from liquefaction of gas. Savings are achieved because one cubic foot of liquefied gas is equivalent to many hundreds of cubic feet of gas volume at normal pressure and temperature. Consequently, the handling of cryogenic fluids requires less container space with accompanying saving in material, transportation, fabrication, and erection costs.

In the case of some of the low-temperature fluids such as ammonia and

propane, increased densities as well as reduction in pressures provide the economy needed to justify the low-temperature processing.

In the processing of these gases to low temperatures, refrigeration is carried out through one of several variations on the basic thermodynamic cycle, which consists of compression, cooling, expansion, and finally, liquefaction.

Variations on this cycle to take advantage of outside sources of refrigeration may be considered, depending on production rates, temperature of operation, and availability of other and perhaps less expensive cryogenic fluids. The use of nitrogen for precooling hydrogen during its liquefaction, as well as the use of such refrigerant gases as ethane or propane in the manufacture of liquid methane, has some economic justification.

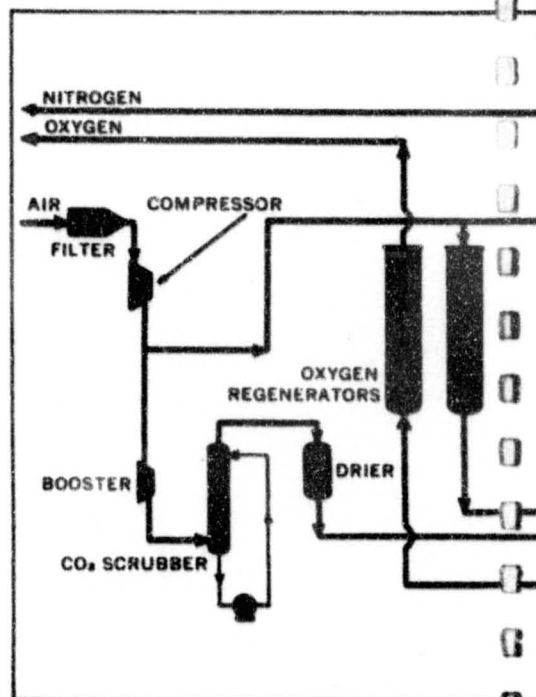
In processing some of the low-temperature fluids down to -75°F , one of the fluorocarbon refrigerant gases may be liquefied and used as a direct heat-exchange medium to liquefy the fluid in question. This type of liquefaction may be particularly useful if the material to be refrigerated has hazardous characteristics, or if "work" done on the fluorocarbon refrigerant may be thermodynamically more efficient than that done on the product actually desired.

For some of the initial stages of low-temperature and cryogenic processing, temperature levels are not as low as those experienced at the liquefaction step in the cycle. In these relatively warmer processing stages, some of the higher strength carbon steels and the lower nickel alloy steels may be economically and efficiently used. In ordinary practice, the steels in these categories are well known and easily chosen for applications in pumps, compressors, and expansion engines associated with low-temperature and cryogenic service.

In still another category, the trouble-

free performance of the stainless and alloy steels in heat exchanger service throughout the process industries is well known. The distillation column (or the low-temperature separation column) may be constructed of alloy or stainless steels because of the combined structural and thermal properties of these steels at low temperatures. In general, cold-box equipment is constructed of stainless steel or alloy steel when minimization of heat leak and product loss through vaporization and/or recycle are important.

An example of the multitude of uses of stainless steels found in air-separation plants can be seen in the schematic flow diagram of the *Air Liquide* low-pressure, air-separation plant (Figure 1). This type of unit is used extensively in the metallurgical and petrochemical indus-



tries, and is used for the production of low-pressure tonnage oxygen of 95-98% purity.

Stainless steels are employed by *Air Liquide* for this particular system in the piping, in the shells for the distillation columns and the heat exchangers, in the heads and tubes, in the regenerators and even in the instrument connection lines, sampling lines and pressure lines.

Stainless steel's ability to be used in conjunction with other materials, its structural strength, its ability to withstand thermal shock, as well as its heat transfer characteristics, make it a superior material capable of performing economically under the most critical operating conditions.

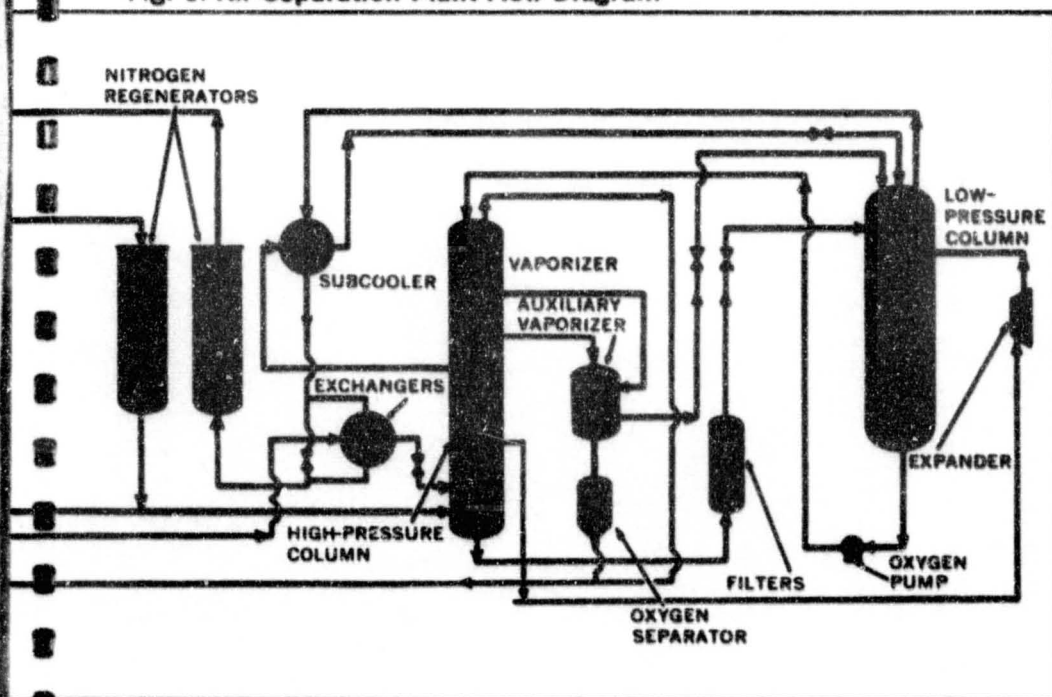
Trouble-free installation on instrument lines, sample lines, and pressure lines is a necessity in providing accu-

rate operating data as well as minimizing maintenance costs in the operations of these atmospheric gas facilities. In typical installations of this type of plant, more than 10 tons of stainless steel are employed for every hundred tons capacity per day for production of oxygen.

In individual components for atmospheric gas liquefaction and separation, stainless steels may be required in heat exchangers, reboilers, and condensers. In these applications, stainless steels have been used alone and in conjunction with copper and other materials depending upon the individual manufacturer's design. Stainless- and alloy-steel piping has provided economic and reliable service in spite of the large temperature and pressure gradients which are sometimes found in these plants.

The appropriate types of steels used

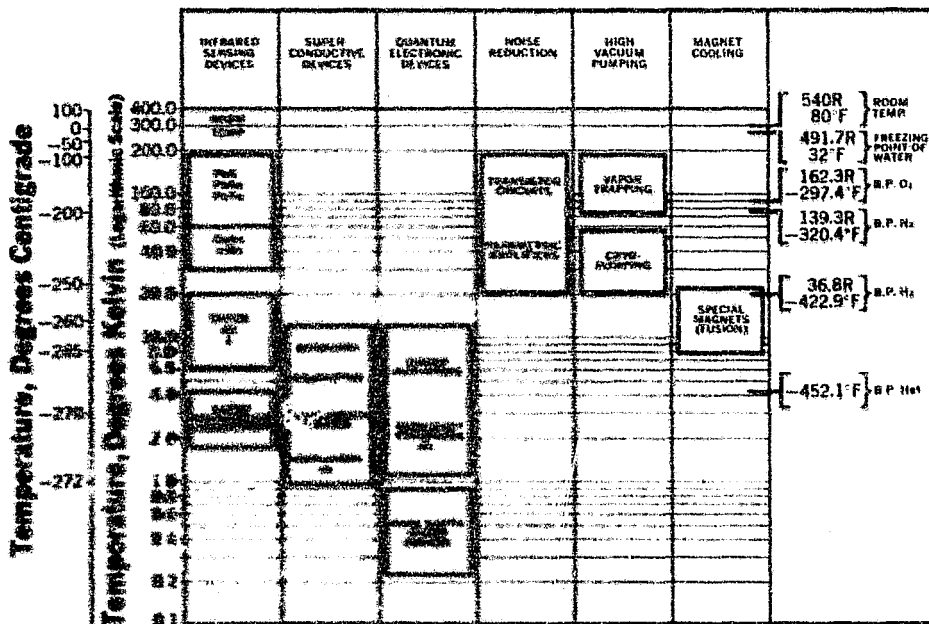
Fig. 1. Air-Separation Plant Flow Diagram



areas of technology, in addition to the propulsion areas, include large segments of the chemical, petrochemical, biological and food-processing industries. In addition, the electronics industry has found a number of new applications for low-temperature technology.

Figure 2 indicates some of these electronic applications. Other new approaches to energy production, such as the magnetohydrodynamic processes, and other areas where high magnetic fields may be involved (perhaps in the fusion reactor area) may also use low-temperature cooling techniques to advantage. All of these end-use areas have their own individual service equipment normally associated with the final use of a cryogenic fluid. For many years to come, however, actual applications will

Figure 2. Low-Temperature Applications in Electronics



involve a gas rather than a low-temperature liquid. Normally, the cryogenic fluid, if received in liquid form, will be vaporized (either through ambient air vaporizers or through the use of heat exchangers employing outside sources of energy). Once the liquid is vaporized, it may be distributed in gaseous form through a pipeline network to the ultimate point of consumption.

If cryogenic liquids are to be employed (such as in certain biological applications, in the freezing of perishable foods, or in the liquid helium applications concerning maser and superconductive devices), special cryogenic equipment must be developed for the ultimate end-use that will both perform the required function economically and efficiently and minimize the loss of the cryogenic fluid through vaporization. The cleanliness, corrosion resistance, and low-temperature performance of the USS Stainless and Alloy Steels make them ideally suited for such end-use equipment.

The illustrations on Page 20 depict erection of an air-separation plant and the fabrication of columns of stainless steel for air-separation plants at the *Air Liquide* manufacturing facilities.

More recent innovations in atmospheric air-separation plant design include the liberal utilization of both 9% nickel steel and stainless steel in Union Carbide Corporation's Linde Division plant at Gary, Indiana. This plant, the largest of its kind in the world, will use USS 9% Nickel Steel in the silica gel traps, regenerators, and the large double-walled container for liquid "back-up" storage. Stainless steel will be used in the high- and low-pressure columns, the shell of the reboiler condenser, the sub-cooler, and most of the piping.

The transportation and distribution of low-temperature and cryogenic gases must be considered in terms of equip-

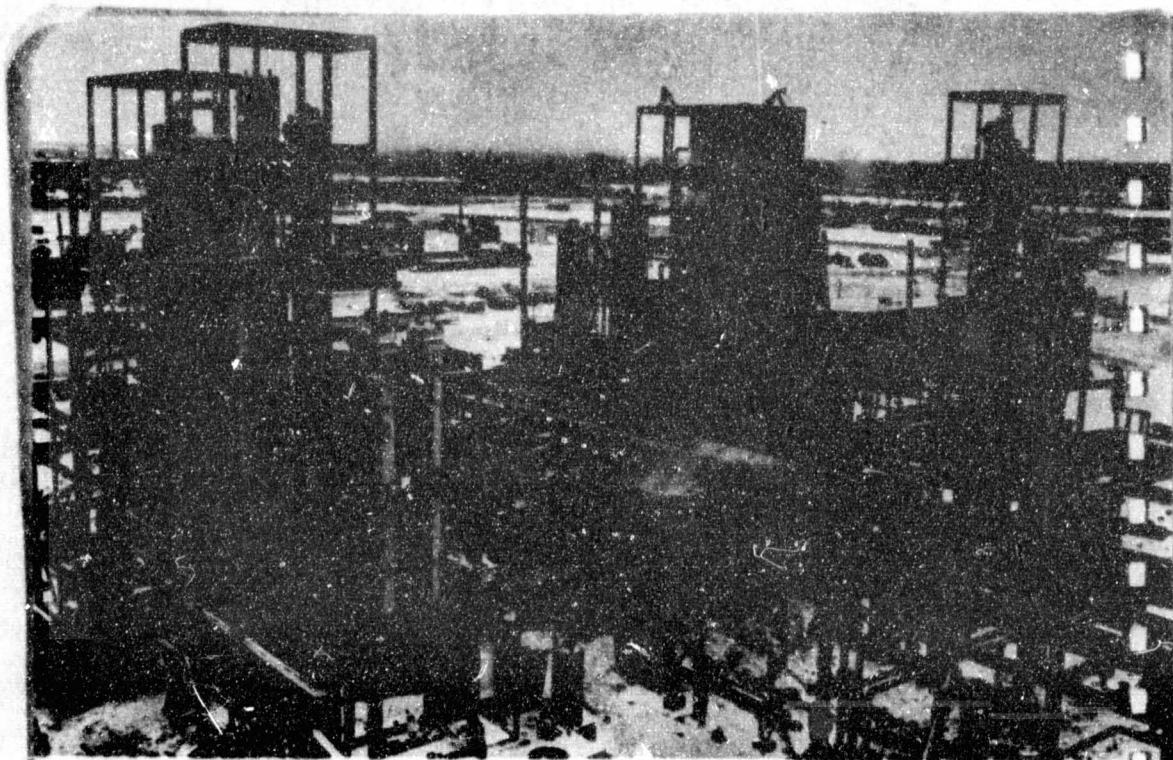
ment use. Normally, large bulk storage facilities are found at the point of production and at central locations for distribution.

Between these points, transportation is usually by truck or rail, although the use of barge and ocean tanker to transport refrigerated propane, refrigerated anhydrous ammonia, and refrigerated methane is becoming more common.

Where the cryogenic fluid is to be transferred via piping, stainless steel, because of its excellent heat transfer properties in terms of minimizing product loss, or 9% nickel steel, with its high strength and excellent performance to -320°F , provide more than adequate service in insulated vacuum-jacketed piping. The lower alloy and the carbon steels perform excellently under less stringent requirements of pressure and temperature.

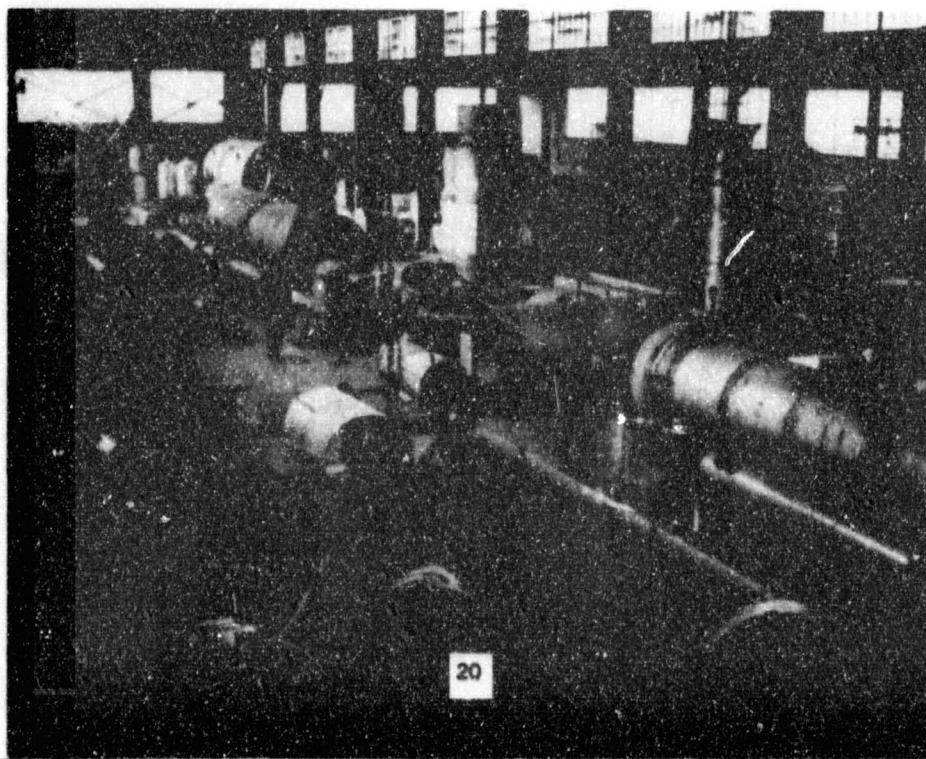
In large, field-erected spheres and cylindrical vessels, the individual choice (in terms of design specifications relative to the ASME and API Codes) will be discussed in following chapters. Stainless steel has, of course, been used at temperatures approaching absolute zero for many years. The recent construction of a 500-psi sphere for liquid hydrogen is only one of many examples where the high quality and economic advantage of steel is justified in cryogenic service.

9% nickel steel is gaining added favor for field-erected cryogenic vessels. One example (Page 21) is a container recently built for hydrogen service at the Brookhaven National Laboratory at Upton, New York. In this service, liquid hydrogen is initially contained in a bubble chamber (-420°F) which may need to be vented quickly in the event of a vacuum failure. A 27-foot-diameter "escape" sphere was fabricated and field-erected to provide for this contingency during experimental work with liquid hydrogen.



A low-temperature gas separation plant under construction at Maitland, Ontario. It was designed by *Air Liquide* in Montreal for Brockville Chemicals Limited.

Fabrication of stainless-steel columns for *Air Liquide* air-separation plants.

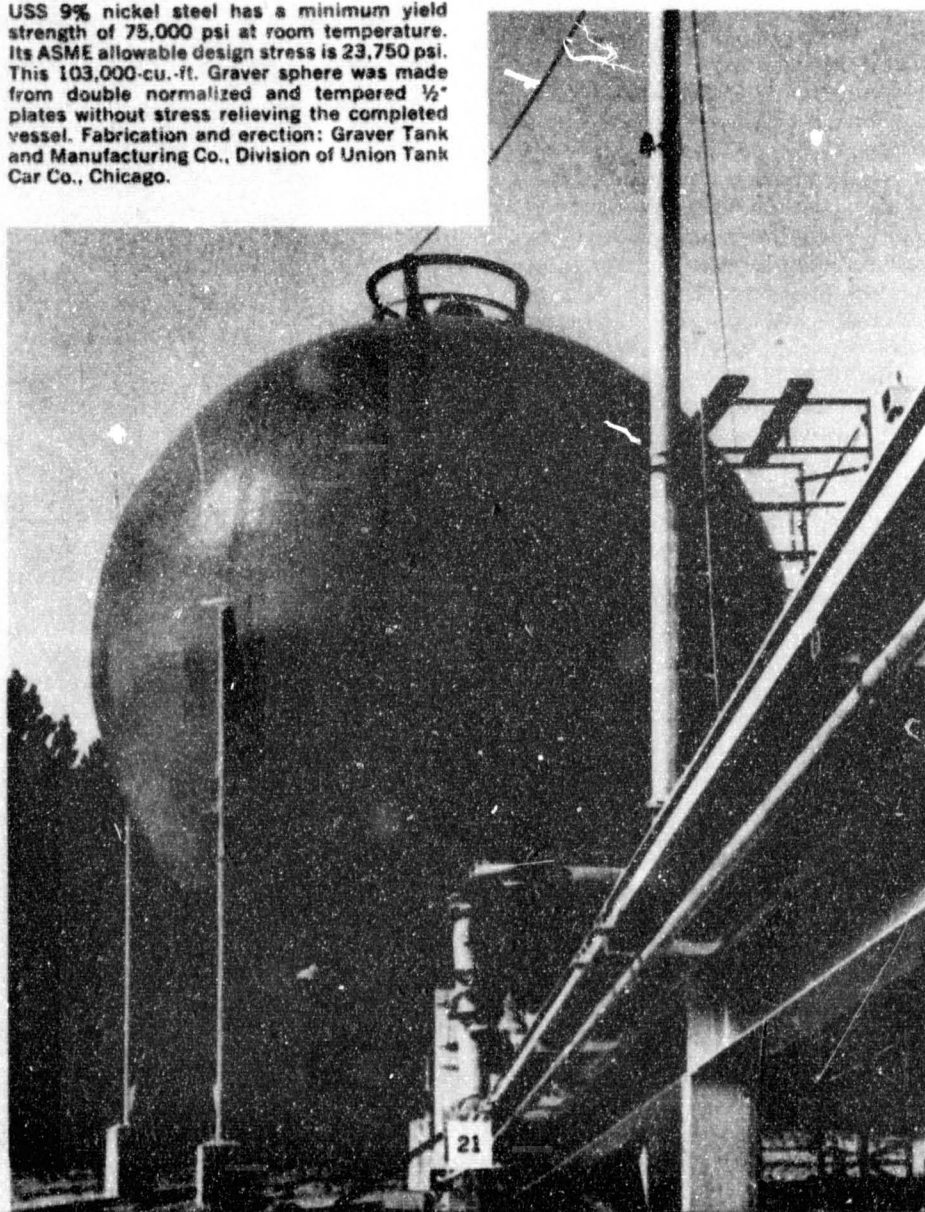


Should the liquid require rapid venting during the tests, the mixture of liquid and gaseous hydrogen would be dumped into the vessel (causing local chilling of the sphere walls), but the extremely tough 9% nickel steel is well adapted to handle this type of thermal shock. For this particular application, the USS 9% Nickel Steel was used because, in the heat-treated condition, it

is strong and ductile at extremely low temperatures without postweld heat treatment. More than 24 tons of one-half inch USS 9% Nickel Steel plates, in the double normalized and tempered condition, were used for this requirement.

Other types of plant storage are characterized by the large field-erected liquid nitrogen storage facility at the Fairless

USS 9% nickel steel has a minimum yield strength of 75,000 psi at room temperature. Its ASME allowable design stress is 23,750 psi. This 103,000-cu.-ft. Graver sphere was made from double normalized and tempered $\frac{1}{2}$ " plates without stress relieving the completed vessel. Fabrication and erection: Graver Tank and Manufacturing Co., Division of Union Tank Car Co., Chicago.



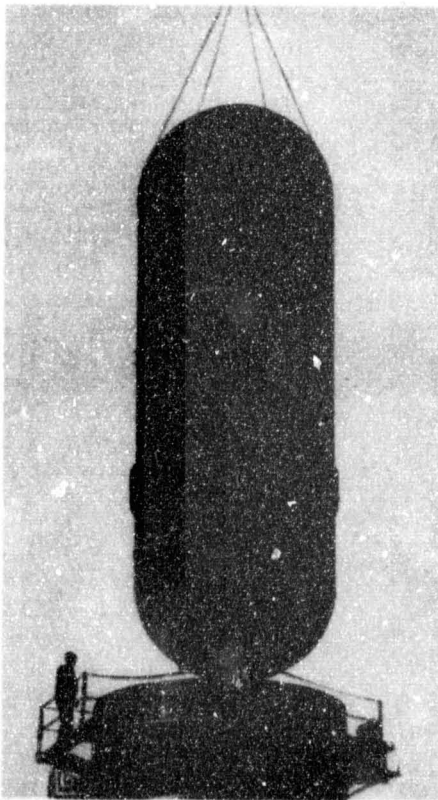
Works of United States Steel Corporation. In this unit, double normalized and tempered USS 9% Nickel Steel plates were utilized for the inner container which was hydrostatically tested to 110 psi. The configuration of most cryogenic containers is that of a tank within a tank, much in the shape of a thermos bottle. Normally, an insulation space is maintained between the two vessels to minimize the heat loss. Where the service requirements become critical in terms of minimizing this heat loss, evacuation of this inner space is economically justifiable.

Maintenance of this vacuum becomes one of the long-term service problems related to a vessel of this nature and can become extremely important in dealing with either the very low-temperature gases or the more expensive cryogenic commodities. In these containers, product loss may occur because of poor or diminishing vacuum resulting from porosity of welds. Completely nonporous welds, 100% X-ray inspected, are desirable for the ultimate in quality performance of vacuum-wall cryogenic containers. The ease with which steels can be welded and the resulting high quality of the welds is well known throughout the cryogenic and process industries. These characteristics, as well as the low rework factors associated with the various steels, make the alloy and stainless steels potential money savers in low-temperature and cryogenic service when compared with nonferrous materials.

In non-ASME Code vessels, such as flat-bottom cylindrical containers with an ellipsoidal top, 100% X-ray quality welding is again important in minimizing potential problems of storage and safety in handling a specific gas or liquid. In these land-based containers, as well as in the shipboard-type designs for liquid methane service, 9% nickel steel has demonstrated its successful application

not only in "Operation Cryogenics"* but in actual service as well. Presently, liquid natural gas storage facilities using 9% nickel steel are being constructed in Africa, France, and the United States.

*Joint tests conducted by The International Nickel Company, Chicago Bridge & Iron, and United States Steel in 1960 to show suitability of 9% nickel steel for cryogenic vessels.



The tank components shown have been assembled at the Fairless Works of United States Steel to hold liquid nitrogen. The vessel has a capacity of 3,750 cubic feet and was designed to meet 1959 ASME code requirements. Nine tons of $\frac{1}{4}$ -inch, double normalized USS 9% nickel steel plates were used for the inner tank shell. The vessel was stress relieved after fabrication and hydrostatically tested at 110 psi. Over-all dimensions are 12' diameter x 37' over-all length for the inner tank which will be enclosed in a 15' x 50' carbon steel outer shell with insulation between the two vessels.

Storage of liquid methane for "peak-shaving" requirements for gas utilities is of increasing interest. Of the alternative techniques for storage of this flammable cryogenic liquid, above-ground 9% nickel steel tankage appears to offer the best combination of reliability and economy. Recent studies indicate that large-scale storage in this type container can be accomplished at a total installed cost near \$6.00 per barrel with possibilities of even lower cost as fabricating technology improves.

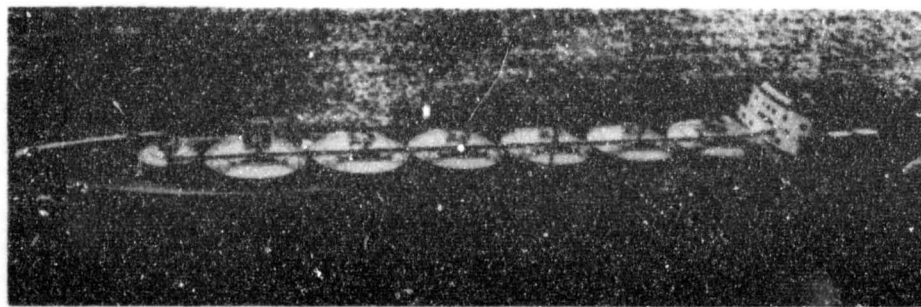
In the shipboard transportation of liquid methane, one must consider that the density of methane is less than that of water. The center of gravity of a methane-carrying ship having steel tanks would be lower in the water than that of a ship using a lighter metal; the ship's stability would be greater with less ballast if it had steel tanks. In this type of specialty tanker, chances are great that the vessel would ride empty on approximately half of its trips. It is essential to consider both the fully loaded as well as the unloaded marine conditions of the ship.

Of particular note is the new liquid methane carrier, the "Beauvais," built

by Gaz de France, which carries liquid methane to France from Algeria in 9% nickel steel tanks. The "Gas Marine" and the "Jules Verne" are two other liquefied-methane tankers with 9% nickel steel tanks.

On the subject of water transportation, products being moved either inland or coastwise in the United States or via ocean liner to overseas ports normally come under the examination and applicable design criteria of the United States Coast Guard. Additionally, unless the vessel is self-insured, the American Bureau of Shipping is concerned with the over-all construction. Rigorous quality standards imposed by the United States Coast Guard are well respected throughout industry in terms of both material requirements and fabricating procedures.

For highway and rail movement, Interstate Commerce Commission regulations apply to the transport of low-temperature and cryogenic fluids. Most of these rules have been developed through the Bureau of Explosives with the assistance of such industry groups as the Compressed Gas Association and the Association of American Railroads.



French methane tanker built by the Seine Maritime Ateliers et Chantiers in Trait. The new French ship, called the "Jules Verne," is equipped with six cylindrical tanks of 9% nickel steel with a 4006 cubic meter capacity.

The tanks are 40 ft. high and 17 ft. in diameter. Nine hundred eighty tons of 9% nickel steel were used in plate thicknesses ranging between 7 mm. and 15 mm. The tanks are used in the vertical position aboard the tanker.

In the tank car area, the forces exerted by the suspension system of the railroad tank car must be considered as well as the severe stresses which a tank car undergoes during normal coupling and uncoupling. Regardless of the internal pressure for which a low-temperature or cryogenic tank car has been designed, the necessity of withstanding forces of acceleration and deceleration of upwards of 8 g's easily justifies the use of steels in cryogenic service.

Also, thermocycling of this equipment can produce severe strains on the material, adding to the rigors under which the materials must perform. Here the high alloy and stainless steels again provide the toughness and thermal stability needed in critical service.

Another factor to consider in the railroad transportation area is the likelihood that some large access openings will be required. Because of the inherent thermal properties of steel, manholes, where required, can be used with a minimum

Transporting cryogenic gases by rail in a "Graver" Cryogenic Tank Car with an inner vessel of Type 304 stainless steel. Graver Tank and Manufacturing Co., Division of Union Tank Car Company built the special car.



amount of additional insulation to prevent heat leakage, compared with the nonferrous materials. In addition, the structural support problems relative to the inner space at the manway area are minimized through the use of steels having high strength at low and cryogenic temperatures.

In over-the-road equipment, most atmospheric gas and liquid hydrogen trailers are normally designed for 25 to 50

psi internal pressure plus a vacuum on the exterior of the inner container. Here again, the inner vessel is potentially subjected to a number of external forces not normally associated with stationary storage containers. The adequate rigidity and high levels of strength, both at room temperature and at cryogenic temperatures, of USS 9% Nickel and Stainless Steels is a valuable asset.

Perhaps to a greater degree than in the stationary storage containers, maintenance of high vacuum levels in mobile evacuated containers is essential to eliminate gas or liquid loss. One of the best ways to assure this is to be certain that containers are fabricated with nonporous welds. Thermal cycling and product loss in cool-down of this type of container are important considerations in the over-all economic performance. Figure 3 (Page 26) shows the relative amounts of heat that must be removed to cool one-pound masses of several metals (9% nickel and stainless steels, copper, and aluminum) from room temperature to various temperatures.

As in all forms of transportation, an increased amount of product hauled at any one time may be of considerable importance in reducing the over-all cost of distribution. The strength requirements established on the vessel can be of prime importance in determining the weight of a given container carrying cryogenic fluids.

The combination of internal supports and stiffening rings and other structural members are often used in this type of vessel. Such structural members can, of course, be of considerable expense, especially if complicated extrusions or structural members are required. Additionally, these members add weight to the container so that over-all weight comparisons of inner tank materials alone cannot be considered.

The over-all design and construction

of the container must be analyzed to give a fair approximation of the performance rendered. Additionally, in over-the-road equipment, shrinkage of the inner vessel as well as the subsequent compaction of insulation may provide additional strain on the vessel as well as increase heat loss in the whole container. Either this heat loss is relieved by adding additional insulation to the container (a relatively expensive proposition both in terms of removing equipment from service and the physical application of the insulation and redrawing of the vacuum on the container) or the user must be content with product loss because of the additional heat transfer.

Relative to the previous discussion, it should be noted that while there are some trailers in liquid nitrogen service capable of hauling more than 7,000 gallons of liquid nitrogen over the road in relatively low-pressure containers, there are also high-pressure propane trailers made of USS "T-1" Constructional Alloy Steel that are capable of hauling 10,000 gallons or more of propane over the highways in many states of this country.

Imaginative design using the high strength and toughness of steels in these low-temperature and cryogenic applications will benefit the fabricators and manufacturers as well as ultimate consumers of liquefied atmospheric gases and other cryogenic fluids by increasing the unit load that can be hauled over the highways.

In addition to the trailers and trucks hauling these products, there are large numbers of smaller cylinders and portable containers used in the transport of liquefied gases. In such containers, heat loss is critical to the performance of the container. The atmospheric gas producers now use a wide variety of cylinders having approximately 3,000 cubic feet of liquid oxygen capacity. Generally speaking, space limitations as well as

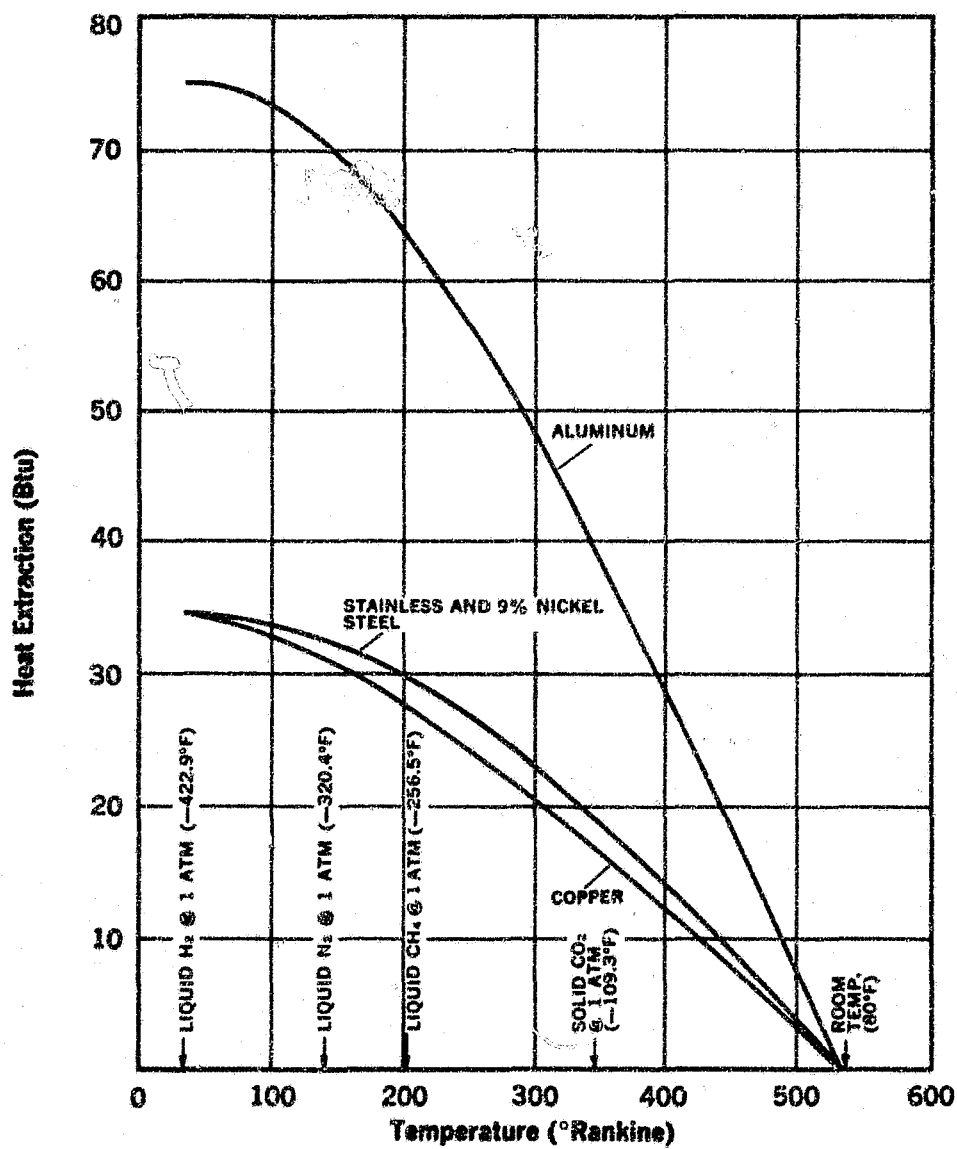


Figure 3. Heat Removal Required to Cool One-Pound Mass of Metal from Room Temperature to Temperature Listed

REFERENCE 13 CONTINUED ON CARD 2

insulation tolerances are so critical that the performance of the ferrous materials relative to their thermal properties favors the use of steels in these cylinders.

Also, the excellent cleanability possible with the stainless steels and low alloy steels makes them highly desirable for these smaller cylinder applications. The smaller types of cylinders are normally considered for liquid hydrogen and liquid helium, particularly in research programs. The cleanliness and low heat leak performance of the steels provide an added plus, both in dollars and actual operating performance, for those desiring the supercold produced by liquid hydrogen and helium.

In numbers, the majority of the bulk storage containers for the low-temperature and cryogenic fluids are shop fabricated. These normally range in sizes from about 200 gallons water capacity up to and in excess of 30,000 gallons water capacity. Many of these, particularly the larger containers, have access openings similar to those sometimes required in tank car service. Where these access openings are required, ferrous materials, from a structural support standpoint, provide a design plus not associated with the nonferrous materials. The size of the individual storage container depends on which cryogenic product is involved, its relative production, and its required delivery schedules to the customer.

In storage vessels, product loss due to high heat transfer rate can be critical, particularly where the vessel is initially oversized in anticipation of increasing use of the cryogenic fluids. Welding must be of the highest quality in order to minimize the loss of vacuum. Porosity can be an acute problem, particularly in dealing with such products as hydrogen and helium. Helium has the ability to diffuse completely through the parent metal of vessels made of certain nonfer-

rous materials. Thus, the over-all economics of the container must consider not only the initial cost (which may be depreciated over a 10- to 15-year life), but also the operating and maintenance costs, both of which may be critical.

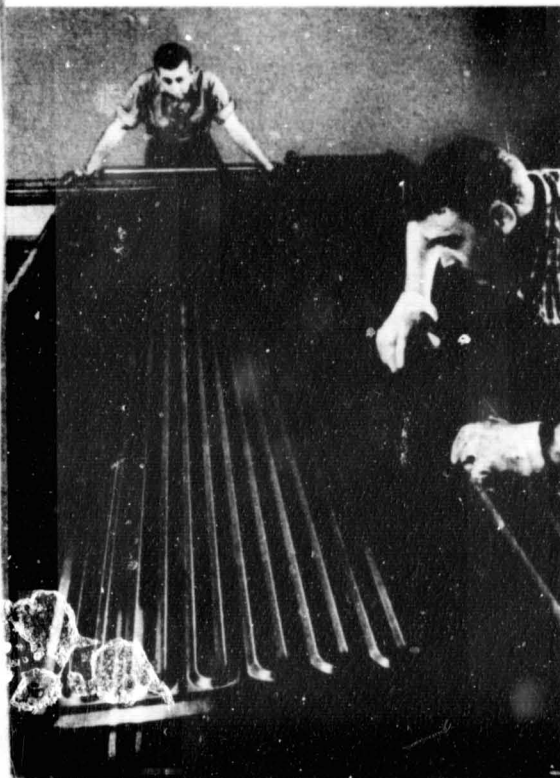
B. Special Design Requirements

The importance of the space and military programs involving low-temperature and cryogenic fluids has been evident for at least a decade. In this period, the Air Force, the National Aeronautics and Space Administration, and a large number of contractors to the government have become involved in the selection and use of low-temperature and cryogenic equipment.

Normally, these applications are not bound by the regulations of the ASME Code, but rather, given pieces of equipment are designed for specific missions or tasks. The cryogenic fluids normally consumed in these applications are involved either in propulsion programs, in life support functions (such as breathing oxygen), or in space simulation equipment.

In the propulsion area, production, distribution, and consuming facilities similar to those in commercial industry have been developed, with many of the facilities being designed and operated by independent outside contracting firms.

In many of these uses, as well as in the end-use functions (such as in missiles and space chambers), not only is design advantage taken of the operating cryogenic properties of materials, but the allowable stresses of materials considered for design may be considered according to entirely different ground rules than those in the ASME Code. Even considering the API standard 620, basing the allowable design strength on 0.3 of



Inspectors test a stainless steel coil heat exchanger used in a cryopump which reproduces the high vacuum of outer space. Stainless steel is specified because it can withstand the low operating temperatures (-443°F) and will not contaminate the gaseous helium used as a cooling medium. Consisting of two embossed sheets resistance-welded to form double-size circulating channels, this application illustrates the excellent forming and welding characteristics of 304 stainless steel.

the tensile or 0.6 of the yield (whichever is lower), 9% nickel steel has a favorable strength-to-weight ratio relative to most of the aluminum alloys considered for cryogenic service; the stainless steels are on an approximately equivalent basis.

Where ultimate strength-to-weight ratios are critical, designs employing austenitic stainless steels, as used in the Titan, Thor, and Atlas cryogenic missile support systems, are well known. In addition, the attractive properties of steel have dictated its use in numerous specific projects using cryogenic equipment such as space environmental chambers, wind tunnels, engine test stands, and experimental aircraft (the RS-70 and X-15). Most of the space chambers are specifically engineered to meet given testing requirements.

The National Aeronautics and Space Administration is conducting a great deal of research and development in the pretesting of parts and components under simulated space conditions before they are actually put in service.

Most space chambers today are individually engineered to test components, engines, solar-activated devices, etc., with each space chamber having a rigorously defined mission. Space chambers may be evacuated either using great amounts of evacuating equipment or lesser amounts of vacuum equipment along with the use of ultra low temperatures which slow molecular movement and reduce the absolute pressure in the space chambers. Either of these methods can provide high levels of vacuum.

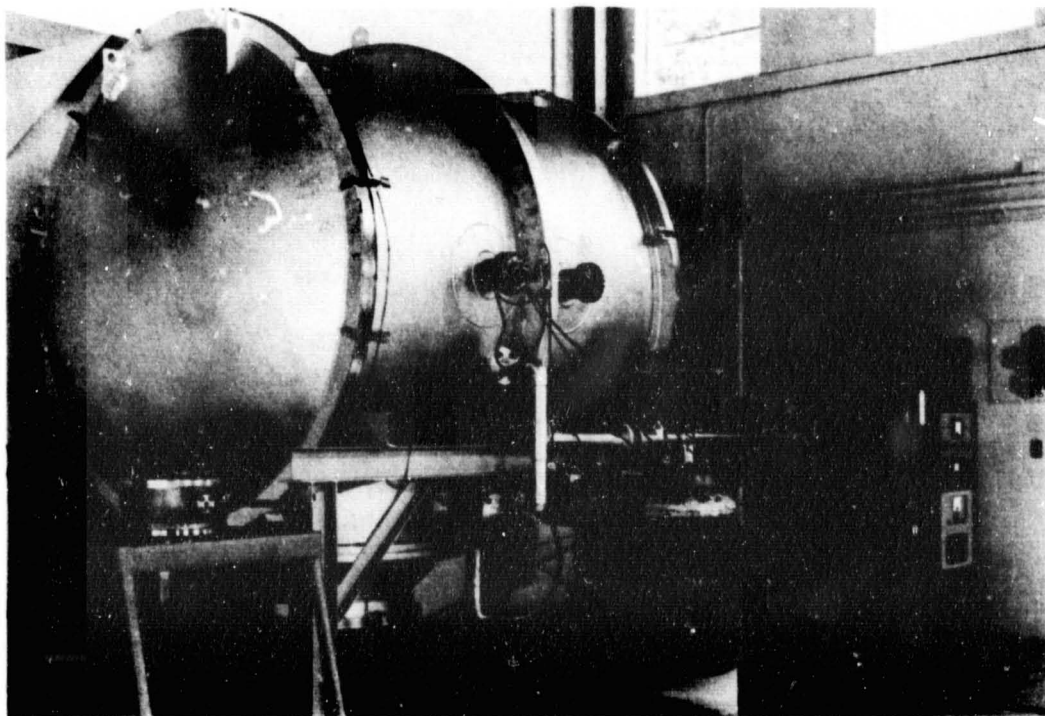
In those areas where low vacuums are desired, liquid nitrogen, hydrogen, or helium are commonly used for cryopumping. Vacuum chambers are now commonly designed to vacuum levels of 10^{-8} or 10^{-10} torr, with experimental space chambers now developed to handle vacuums down to 10^{-15} millimeters of mercury. In these areas, clean-

liness, reflectivity, and emissivity are important properties of materials.

Outgassing, as a result of the above-mentioned properties, and the cleanliness with which the material is fabricated and handled are critical in providing the most serviceable space chamber. The advantages of stainless steels in these areas are described in Chapter III. Where minimization of hydrogen content in the steel is required, degassing techniques have been perfected to reduce the dissolved hydrogen content.

In terms of liquid oxygen and the other atmospheric gases, the requirements of the U. S. Air Force and the other space programs relative to cleanliness have, on the whole, been more rigid than is normally found in com-

PDM Space Chamber built by Pittsburgh-Des Moines Steel Company of Type 304 stainless steel, 8' in diameter and 8' long. The primary use of this chamber will be to evaluate pumps and their components; seals; transition joints; leak percentage; the effects of high vacuums on shrouds; and the use of vacuums in cryogenic tanks. This chamber is cooled by using liquid nitrogen flowing through a shroud.



mercial practice. Although stainless steel is used extensively to meet these critical cleanliness specifications, 9% nickel steel is also being utilized today in similar applications involving cryogenic service.

The reliability which the stainless steels have shown in almost 30 years of cryogenic service with the atmospheric gases is indicative of their ability to perform well at very low temperatures.

For missile and allied ground support equipment, cleaning specifications for liquid-oxygen containers normally limit hydrocarbon content to less than 5 milligrams per liter of cleaning solution in final cleaning. Particle counts are restricted from 0 to 150 microns with specifications generally being under 100 microns and 150 microns as a maximum. With surface finishes rougher than 62 microinches, some difficulty in hydro-

carbon removal might be expected.

As previously noted, for ICBM's the strength-to-weight ratio of the container material is one of the most important design criteria. The stiffness ratio (L/R) is another important design aspect. Most requirements are such that a high yield and tensile strength are desirable at cryogenic temperatures. In an effort to provide these, United States Steel has been assisting in the development of new techniques of forming steels to provide better performance.

The developments of the Mississippi test facility, the Houston operations of the National Aeronautics and Space Administration, as well as the further expansion of both the Cape Kennedy operations and Vandenberg Air Force Base in California, will see a large amount of ground support equipment as

Tanker made of USS "T-1" Steel by Butler Manufacturing Company, Kansas City, Missouri. Operated by E. Brooke Matlack, Inc. When redesigned with "T-1," this tanker

weighed 4,500 pounds less than the old-style twin-barrel models—adding an extra 500 to 700 gallons of propane per trip, depending on the temperature of the cargo.

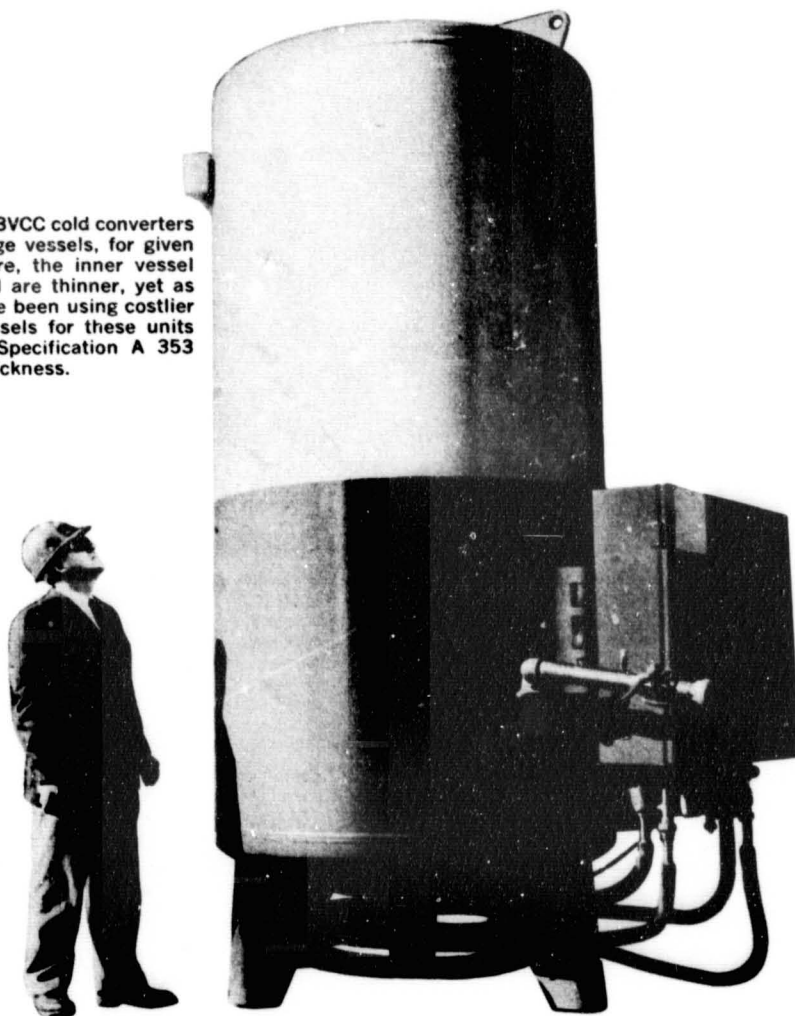


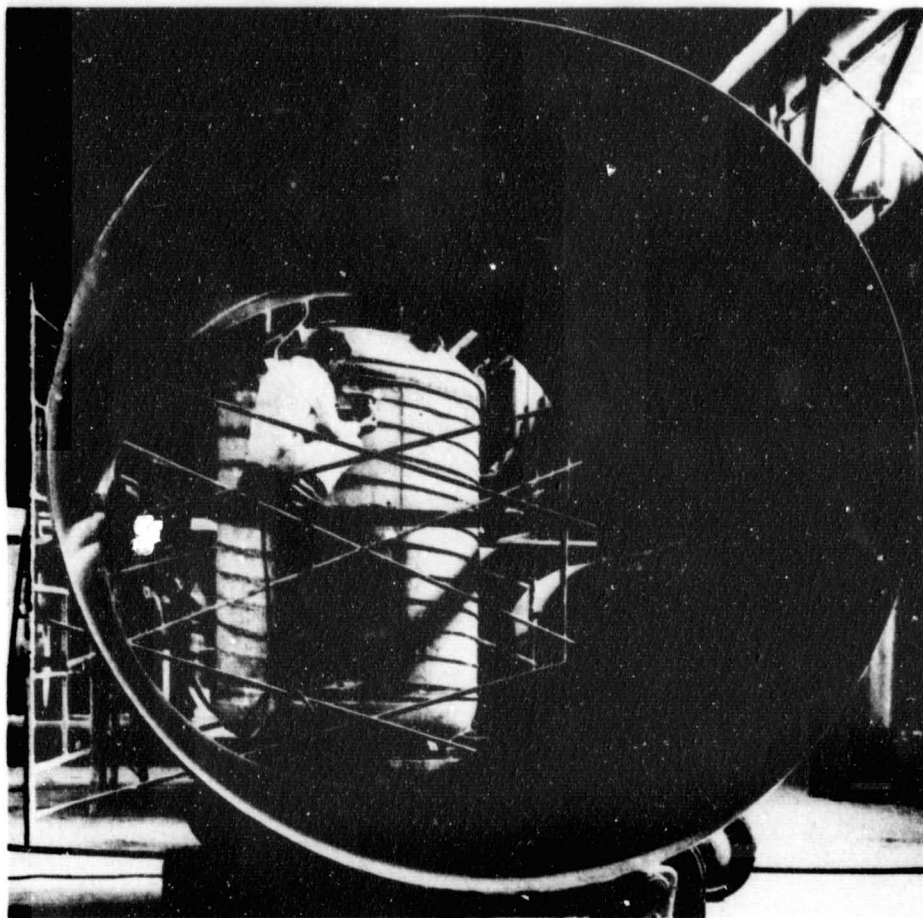
well as fly-away hardware using cryogenic fluids. In most of these areas, the design engineers must balance safety and reliability against the mission and the economics of performing that mission successfully within fixed time tables.

The variety and quality of the family of steels available from United States Steel offer assistance in reaching the goals of our country's space program. United States Steel Corporation has

conducted a great deal of research and development in improving the strengths of the stainless and alloy steels and in the production and development of such steels as the maraging steels, precipitation-hardening stainless steels, USS TENELON steels, and the lower nickel alloy steel grades.

In such units as Linde's 93VCC cold converters and their 150 VST storage vessels, for given pressure and temperature, the inner vessel shells of 9% nickel steel are thinner, yet as strong as they would have been using costlier materials. The inner vessels for these units are designed to ASTM Specification A 353 Grade B, with $\frac{5}{16}$ " wall thickness.





In-fabrication photo shows 1,000-gallon liquid helium (-452°F) Dewar manufactured by CRYENCO for General Dynamics/Astronautics. It shows work being performed on cool-down tube which surrounds a 304 ELC stainless steel inner chamber as seen through the body of the stainless steel outer shell. Complete vacuum jacketed Dewar is mounted on trailer.

C. Gaseous Storage

The original method of handling and distributing most of the atmospheric gases under discussion in this design manual was compression rather than liquefaction. United States Steel has long supplied steels for the fabrication of portable cylinders to distribute and store these compressed gases.

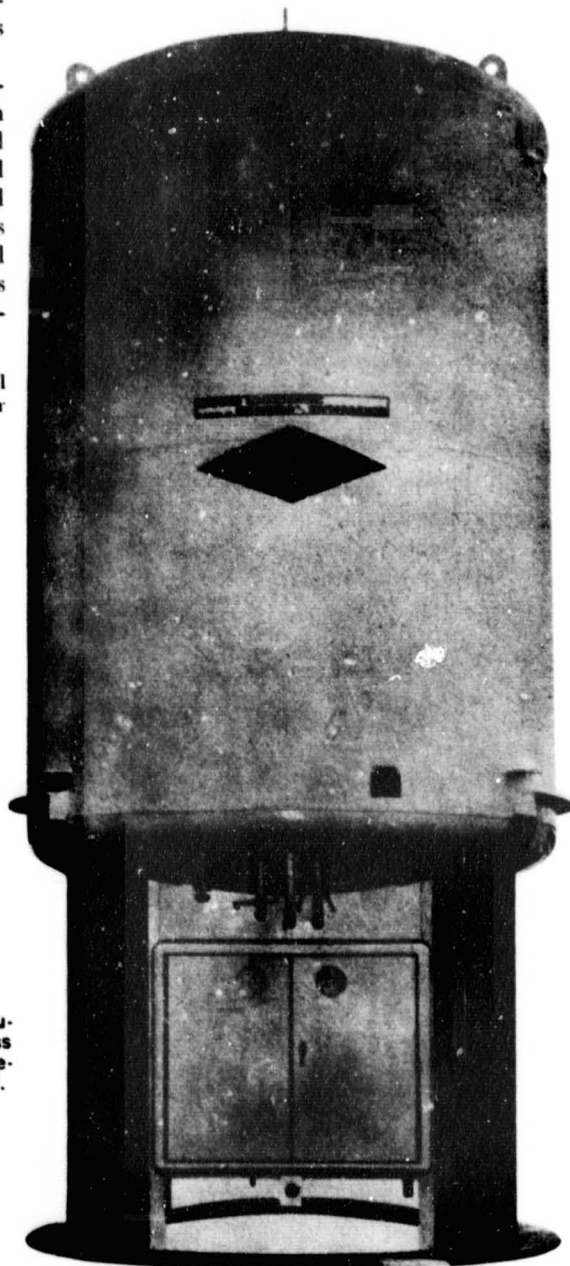
United States Steel's Christy Park Works produces steel high-pressure cylinders for railroad and highway equipment and stationary installations. Re-

cent advances in the development of new steels for these high-pressure pressure vessels have brought about some dramatic reductions in the cost of storage and distribution of these gaseous products.

Newly designed USS seamless pressure vessels can be mounted easily on trailers for the haulage of compressed nitrogen, oxygen, hydrogen, helium and a variety of other gases. In fact, a special trailer design using these pressure vessels was developed by United States Steel to demonstrate how various USS steels and steel products would be economically incorporated in each unit.*

*United States Steel does not build or sell trailers. See your trailer manufacturer for details.

Liquid Carbonic Distributor Station manufactured by Ryan Industries, Inc. It has a gross capacity of 4,800 gallons, with inner shell material being $\frac{1}{2}$ " SA-240, Type 304 stainless steel.



This trailer design is capable of reducing the number of pressure vessels per tube-trailer over conventional designs (utilizing 9 $\frac{5}{8}$ " diameter cylinders) in the order of 7 to 1. In addition to representing a saving in capital cost relative to valves, safety devices and fittings, and mounting attachments, the operation of these trailers allows a greater payload with reduced down time and maintenance.

The large diameter, individual pressure vessels generally have correspondingly thicker walls, thus providing greater protection against impact. Also, they allow a lower center of gravity over conventional tube-trailers, thus providing improved trailer roadability.

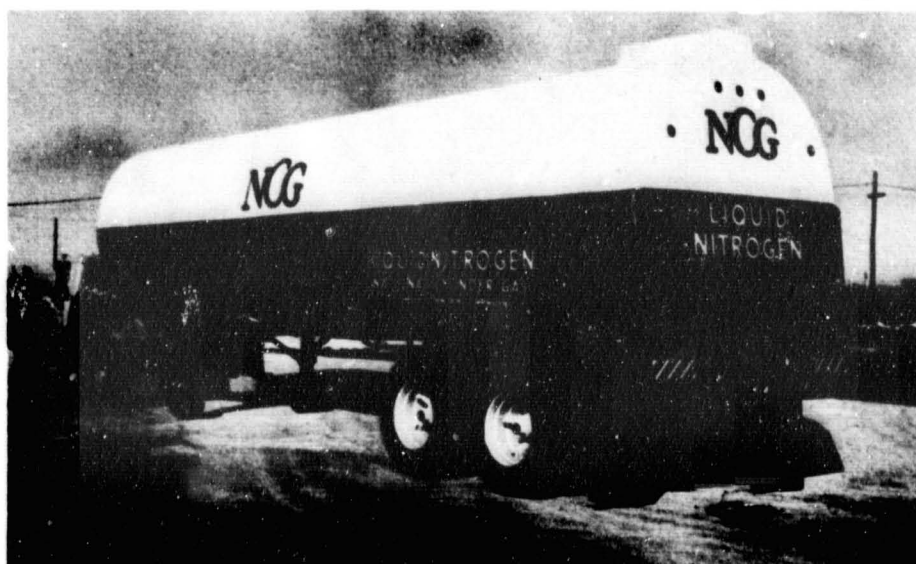
The basic advantage in this design is obtained from the higher mechanical properties of alloy steel with the pres-

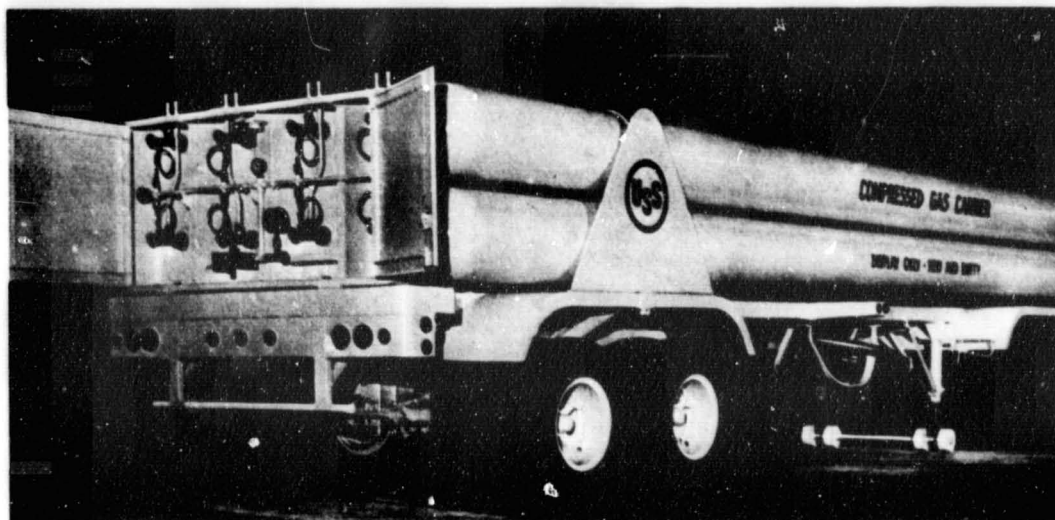
sure vessels being of the seamless type with swaged ends. These cylinders may be obtained under the general class of ICC specifications. With 10% overfill, their design service pressure may be as high as 2,640 psi for inert gases.

The new tube-trailer design, consisting of eight 22" O.D. x 34'4" long seamless pressure vessels, provides an equivalent of 621 cubic feet water volume. With a carrying capacity of over 100,000 cubic feet of helium, such a tube-trailer can be transported across all but two states in this country.

Currently, in states where gross vehicle weights of over 60,000 pounds are permitted, some of these new trailers are operating with a carrying capacity of 128,000 standard cubic feet of helium gas. Such increased capacities may be more than twice as large as the old

A 5,100-gallon liquid nitrogen trailer manufactured by Ryan Industries, Inc., for National Cylinder Gas Division of Chemetron. It has a 12 gage SA-240, Type 304 stainless steel inner vessel to protect its cryogenic cargo.





An over-all rear view of the Rolling Pipeline compressed gas cylinder trailer concept, developed by U. S. Steel, reveals the large capacity carrier's design and the simplicity of the manifold assembly in the rear cabinet. USS Seamless Pressure Vessels reduce the number of cylinders per tube carrier over conventional designs on the order of 7 to 1, which means lower center of gravity for better roadability and fewer valves, safety device connections,

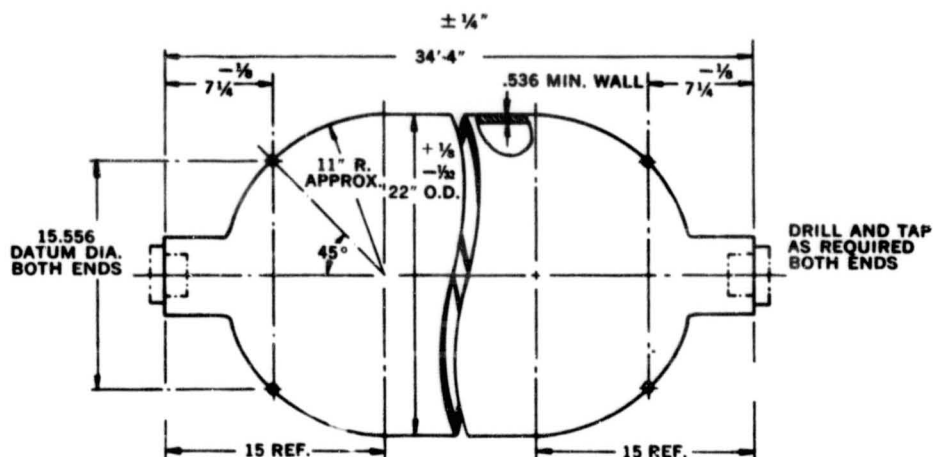
and mounting attachments; this in turn reduces downtime and maintenance.

Rear mountings, in the form of brackets or saddles, are positioned over the center of suspension above the rear wheels. Vertical stay rods bolted through the trailer bed support the cylinders in their brackets, which are tightened to 100 pounds of torque, and six sets of tie rods provide stability against forward or backward motion of the trailer.

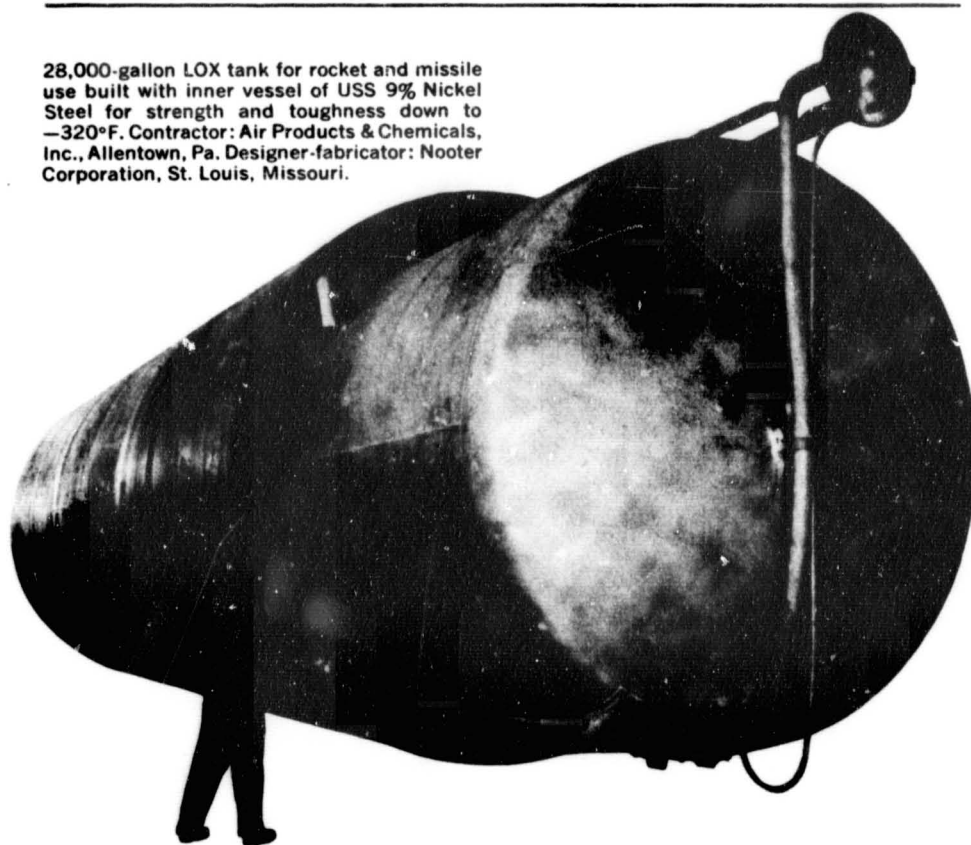
trailers in service for the distribution and handling of these compressed gases.

This new tube-trailer design is another example of United States Steel's interest in providing industrial users of gases and the compressed gas industry with better economic performance in steels. This prototype high-pressure pressure vessel carrier also utilized square and rectangular hot-rolled carbon steel hollow structural tubing in its frame to reduce dead weight, and yet provide the structural strength necessary to support the nearly 18½ tons of cylinders. The details of the manufacture of the pressure vessels as well as the general design of the trailer are shown in the photograph above and in Figure 4 on Page 36.

Figure 4. Twenty-Two-Inch O.D. Trailer Tube



28,000-gallon LOX tank for rocket and missile use built with inner vessel of USS 9% Nickel Steel for strength and toughness down to -320°F. Contractor: Air Products & Chemicals, Inc., Allentown, Pa. Designer-fabricator: Nooter Corporation, St. Louis, Missouri.



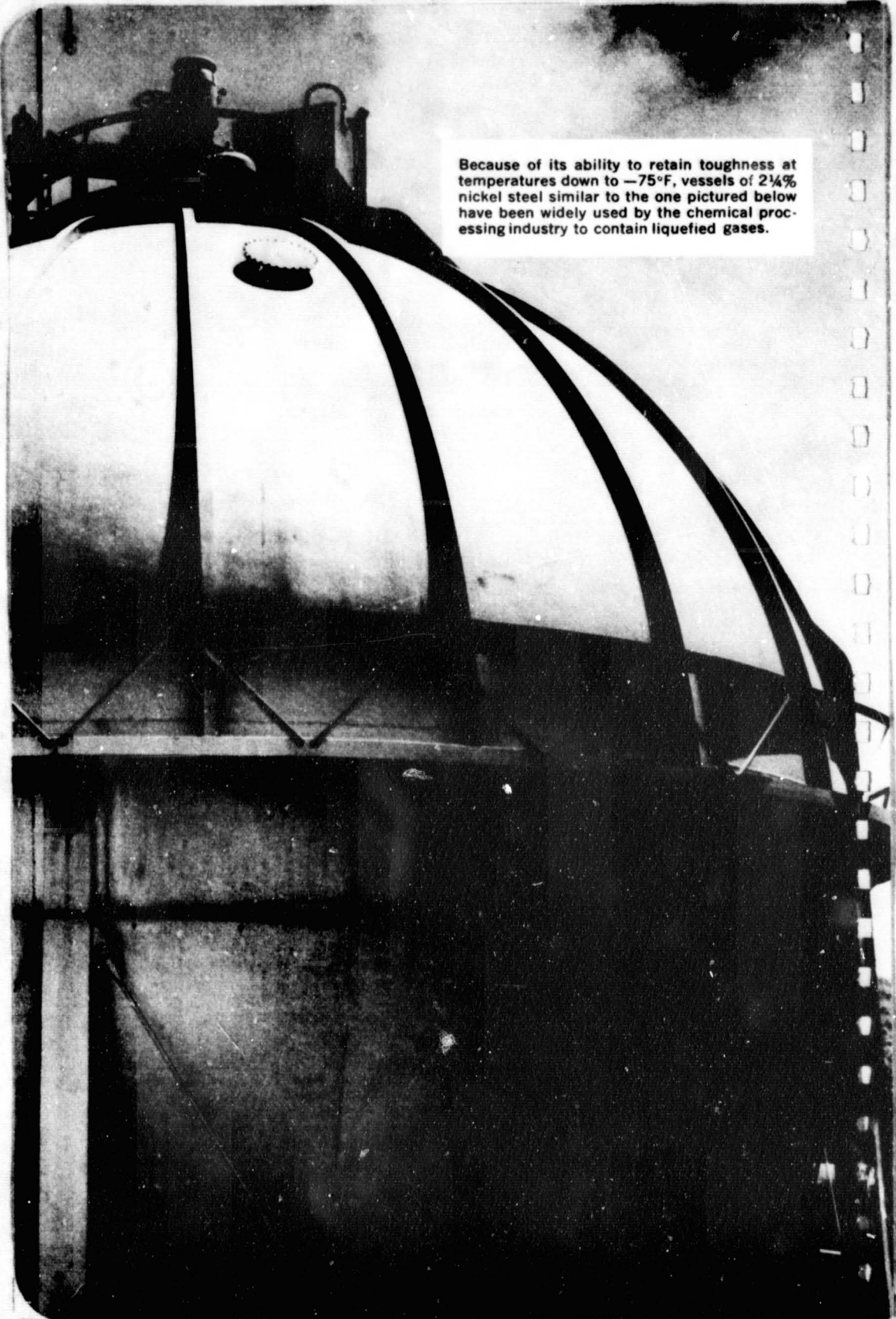
Union Carbide liquid nitrogen refrigerator for storing biologicals has an inner vessel of Type 304 stainless steel.



Regenerator . . . for a new liquid oxygen producing plant has been developed that provides a heat transfer surface of 3,000 sq. ft. per cubic foot of material, which is claimed to be approximately twice the area of the best designs now used in similar applications. Two columns, each containing 15 stainless steel discs, approximately 2 ft. in diameter and $3\frac{1}{2}$ in. high, to exchange heat between incoming high-pressure air and the waste air from the plant, form the regenerator core for a 2-ton per-day liquid oxygen producing plant being developed for the Marine Corps. The entire liquid oxygen producing unit, according to

COSMODYNE CORP., is six times lighter than present units per ton of output. This reduction in weight is said to be achieved by the use of this advanced design core and a common compressor to be used both for the gas turbine cycle and the cryogenic cycle of the plant.

Each disc of the regenerator is made up of flat 0.002 in. sheets of 302 stainless steel that sandwich V-pattern corrugated sheets with a pitch of 0.020 in. and only 0.015 in. high. Stainless steel was found to be most suitable for the application, following a study of various metallic and non-metallic materials, including ceramics, aluminum, lead and copper.



Because of its ability to retain toughness at temperatures down to -75°F , vessels of 2 1/4% nickel steel similar to the one pictured below have been widely used by the chemical processing industry to contain liquefied gases.

III. Materials

A. Fundamental Selection Criteria

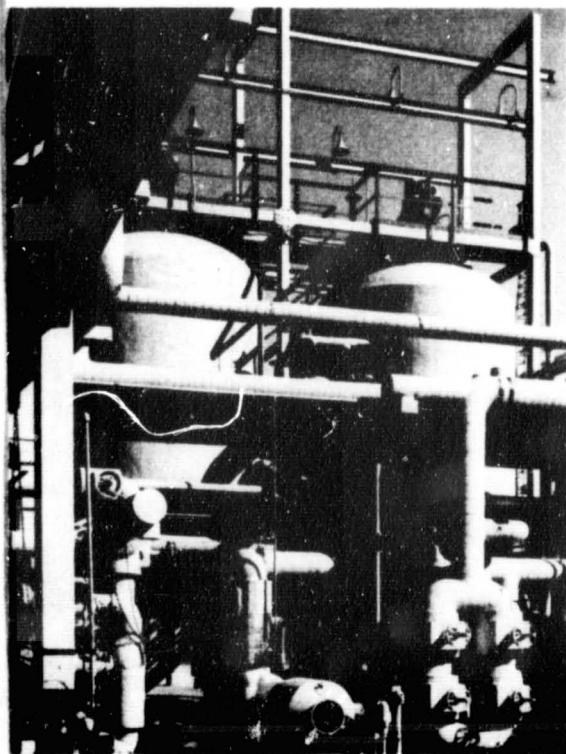
In the selection of metals for low-temperature and cryogenic applications, design engineers should re-evaluate methods of metals selection because certain design parameters take on a greater significance.

Of course, the selection of metals for low-temperature application must be based on many mechanical properties, including the familiar yield and tensile strength, fatigue limit, ductility and toughness. Ductility, the ability of material to deform plastically, and toughness, resistance to brittle failure under specific conditions of stress concentration, must be present in metals that are candidates for use at low or cryogenic temperatures.

However, the final selection may be made on the basis of other properties. Low heat conductivity, low coefficient of thermal expansion and low emissivity are properties that can be used to advantage in storage vessels, vacuum-transfer lines, and other components of low-temperature or cryogenic systems.

Four categories of steel behavior are of practical interest in low-temperature service:

1. The transition from ductile to brittle behavior as a function of temperature;
2. Certain unconventional modes of plastic deformation encountered at very low temperatures;
3. The influence of phase transformations in the crystalline structure on mechanical properties;
4. Ratio of strength in the notched versus unnotched condition.



Outstanding corrosion resistance, together with excellent strength and ductility at temperatures as low as that of liquid helium, have made 304 stainless steel the most widely used material in petrochemical, nuclear, missile, and other cryogenic applications where purity of product is essential.

The choice of a suitable metal is affected by its low-temperature properties, the design in which the material will be employed, and the fabrication process and procedures necessary for construction. The usable temperature limits of each steel are established by its composition and heat treatment.

Of all the metals useful in construction for low-temperature applications, steels remain the most popular because they are the most efficient, most readily available, most versatile and most economical.

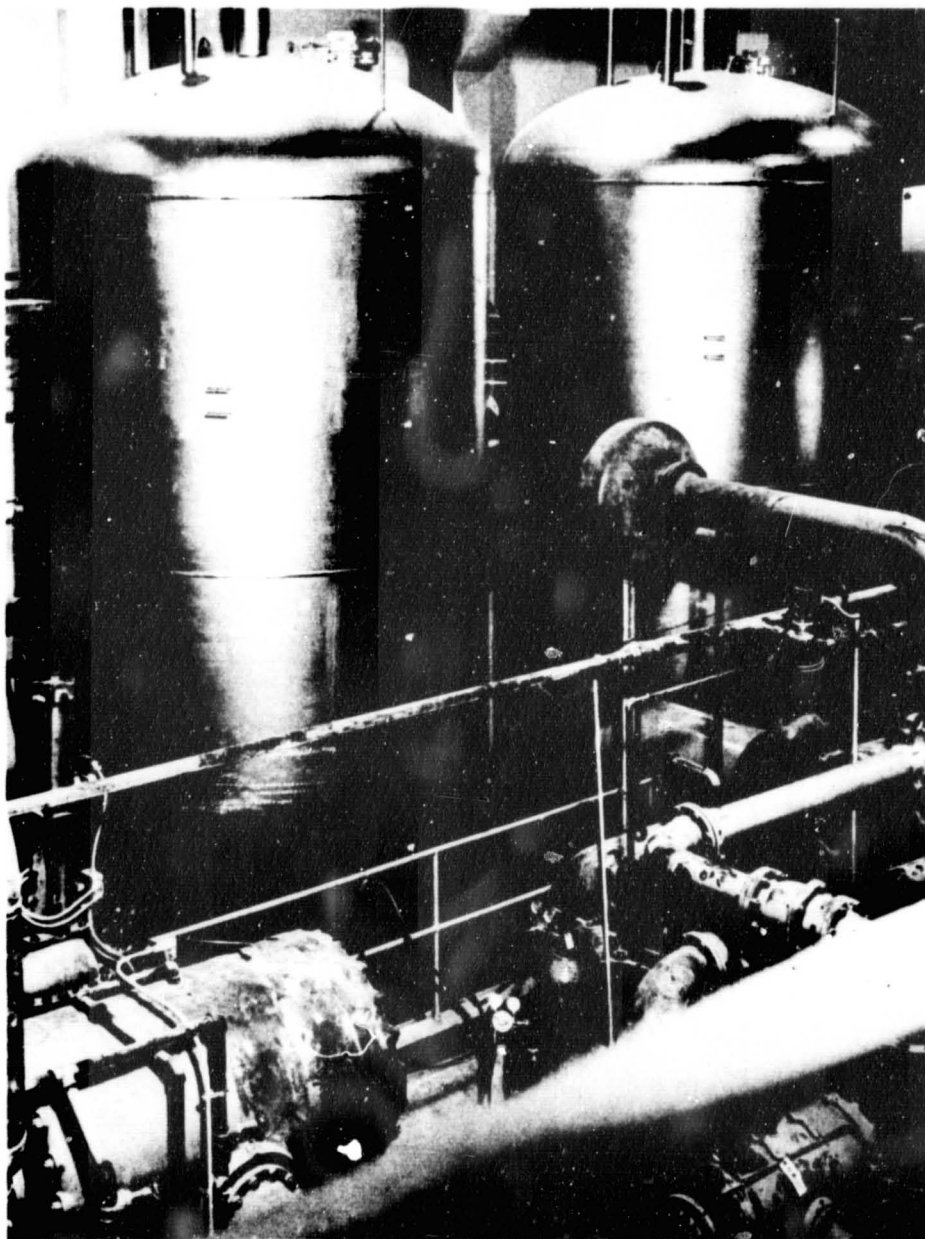
Analysis of the erected costs of vessels and containers fabricated of steel and nonferrous metals indicates that steels, over a very wide range, provide greater economies on the basis of higher design stress and lower unit costs, with no payload or weight penalty, particularly in high yield strength steels.

In addition, as previously noted, all of the steels considered here for low-temperature application are commercially available in a wide variety of forms, although plates for tanks and pressure vessels enjoy the widest range of applications.

The discussion and data presented are therefore directed primarily toward plate steels and are intended to assist the designer and materials engineer in the selection and use of steels for low-temperature and cryogenic service.

The following pages discuss the mechanical properties to be considered for each metal, as well as information on the performance of each.

Austenitic stainless steel (which is nonhardenable by heat treatment) is an excellent material over the entire range of cryogenic applications because of its toughness and high ductility at low temperatures and because it is highly corrosion resistant. In other words, the austenitic stainless steels meet all the requirements for low-temperature serv-



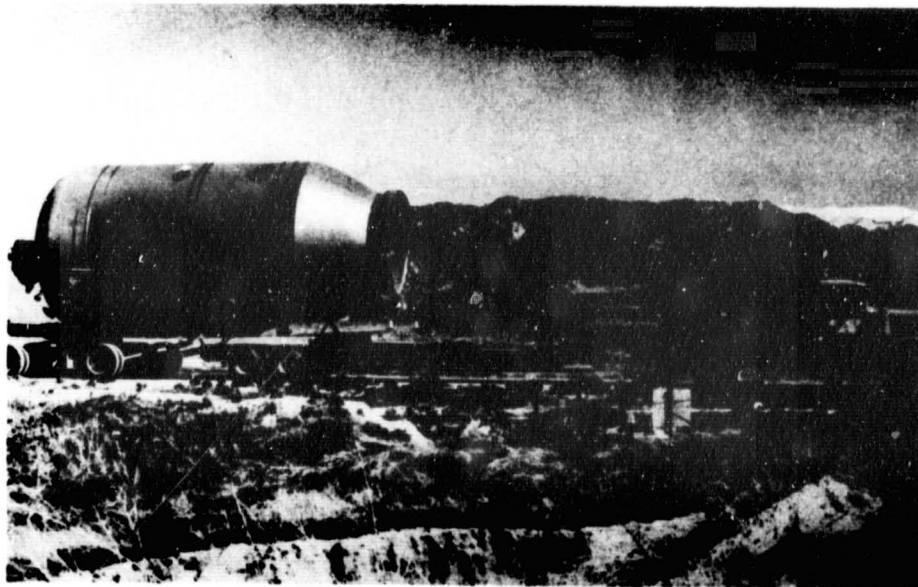
Because of operating temperatures as low as -175°F , low carbon 3½% nickel steel was selected for these brine storage tanks which comprise part of a custom-built refrigeration unit serving high-altitude test facilities at

Wright-Patterson Air Force Base, Dayton, Ohio. The metal's excellent workability is indicated by its use for forged steel tube sheets, pressed steel heads, brine cooler shells, and for all brine piping and fittings.

ice. They remain tough at liquid hydrogen and liquid helium temperatures, and their coefficients of thermal expansion and thermal conductivity are lower than those of nonferrous cryogenic structural materials. Most of these steels show a relatively small increase in yield strength as temperature is lowered, but their tensile strength increases markedly. Ferritic and martensitic stainless steels are not generally recommended for cryogenic use.

In many applications, a wide range from low to high temperatures may occur in a single piece of equipment. Therefore, the properties of metals at elevated temperatures may also be important. All of the steels suggested for low-temperature applications possess good short-time tensile and creep-rupture strengths. The carbon steels and nickel steels are used up to 650°F; some alloy steels are used up to 900°F; and stainless steel is well known for its high-temperature applications up to and exceeding 1500°F.

Because of its excellent resistance to sub-zero embrittlement, 43 tons of 2¼% low carbon nickel steel were used in this jacketed static altitude and controlled temperature test chamber which operates at temperatures ranging from -65°F to 500°F, and simulates conditions at heights up to 75,000 feet.





One of nine vessels built for "Operation Cryogenics"—a series of destruction tests to demonstrate the suitability of 9% nickel steel for very low-temperature use. Six cylindrical vessels like this one (4' diameter x 13' long, $\frac{3}{8}$ " wall thickness) were refrigerated to minus 320°F with liquid nitrogen and pressurized to failure. This is one of two such vessels of quenched and tempered plate, not stress-relieved after welding. Designed for 370 psi internal pressure (equivalent hoop stress in shell: 23,750 psi), the vessel withstood nearly 6 times this stress, bursting at 2,160 psi (132,500 psi hoop stress). Other cylindrical vessels were fabricated of quenched and tempered or of double normalized and tempered material (some with and some without stress relief after fabrication) to compare effect of these operations. All vessels withstood at least four times design stress. All failed in a ductile manner. Impact tests on a rectangular vessel of 9% nickel steel also demonstrated the excellent low-temperature toughness of this steel. Tests were witnessed by designers, users and members of code regulatory bodies.

B. Mechanical Properties

1. Notch Toughness

In general, most engineering structures are subject to stress concentrations under service conditions due to mechanical notches resulting from inadequate design and/or fabricating practices, or from the microstructural variations inherent in polycrystalline metals.

Notch toughness is a property of steel reflected in its resistance to brittle failure under conditions of high stress concentration, such as impact loading in the presence of a notch. This property is a prime requisite of metals intended for low-temperature application, and is vital to selection of materials for storage and transportation of liquefied gases.

The notch toughness of most ferritic steels decreases with decreasing temperatures, and this factor is of critical importance in consideration of these materials for cryogenic applications. The austenitic stainless steels, on the other hand, do not exhibit the marked transition from tough or ductile behavior to brittle behavior with decreasing temperatures.

Various tests have been devised to measure notch toughness: these include the Charpy and Izod notched-bar impact tests, the drop-weight test, the explosion-bulge test, the notched tension test, and others.

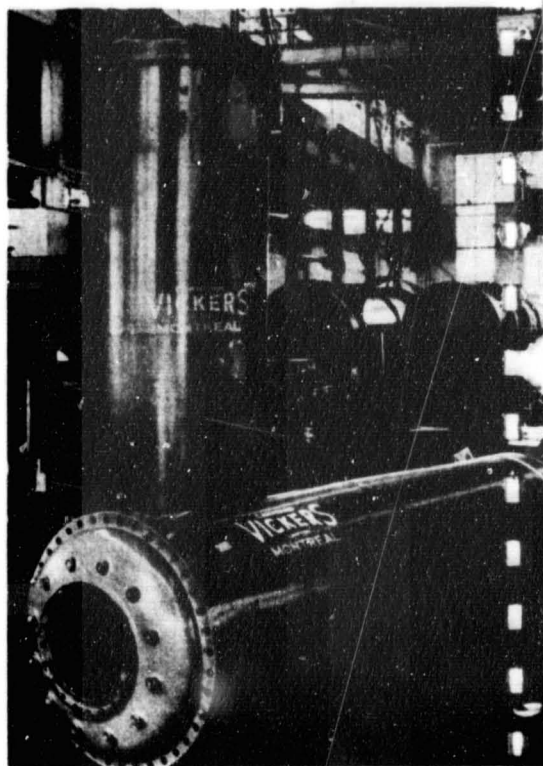
The Charpy notched-bar impact test is widely used to test the toughness of steels intended for low-temperature and cryogenic service. While both the keyhole and the V-notch types of Charpy specimens have been employed and the keyhole test is standard in some specifications, the present preference is for the V-notch type of specimen. Charpy V-notch tests may be employed alone or in conjunction with other tests to evaluate the notch toughness of a given steel for specific low-temperature or cryogenic service conditions.

Figure 5 shows schematically a representation of notch toughness of a steel with respect to an idealized V-notch Charpy performance curve derived from a plot of actual test data. It will be noted that the notch toughness of a steel as measured by the Charpy V-notch test exhibits three behavioral transitions as temperature of testing is decreased.

Because a crack will propagate readily at temperatures higher than those at which a crack will initiate easily, there are at least two different ways of expressing this transition from tough to brittle behavior. One, a ductility transition, indicates the tendency toward crack initiation (NDT, or nil-ductility temperature of the diagram in Figure 5) and the other, a fracture transition

(FTE), indicates the tendency toward crack propagation.

Although there are few direct correlations between performance of a specimen in an impact test and performance of a structure in service, the impact test is used extensively as a guide and, from many years of experience, as a specification tool for materials to be used at low temperatures. For example, ASTM Specification A 300 prescribes minimum impact values for several steels that are



These 9% nickel steel vessels were installed as part of an oxygen-nitrogen reversing regenerator system employed for the commercial production of liquid oxygen used in the flash smelting of copper. Fabricated of $\frac{1}{16}$ " plate, these regenerators were welded with 25-20 stainless steel electrodes. All welds, heat affected zones and base plate easily met minimum keyhole Charpy impact requirements of 15 foot-pounds at -320°F .

used in low-temperature and cryogenic applications.

Since decreasing temperature is one of the major factors affecting toughness, the notch toughness of steels is most conveniently measured by lowering the temperature of notch-test specimens to a point where behavior changes from predominantly ductile to predominantly brittle (NDT). While it varies with the test conditions and criteria employed, this point at which the behavior changes from ductile to brittle is generally expressed in terms of a transition temperature, as indicated in Figure 5.

As previously stated, of the various tests that have been devised to measure toughness, the Charpy notched-bar impact test is used widely for steels in-

tended for low-temperature and cryogenic service. In the Charpy test, the criterion of toughness is frequently an arbitrarily selected minimum value of energy absorbed in breaking the specimen, such as 15 foot-pounds at a designated service temperature, using either a "V" or keyhole type of notch. While a foot-pound energy impact value is used in specifications, an investigator can also employ a selected percentage of fracture appearance, such as 50 per cent shear. The notched-bar impact tests may also be evaluated by measuring the lateral contraction that occurs near the root of the notch in the broken specimens. Lateral expansion of the sides of the impact specimens may also be measured as a criterion, and has been

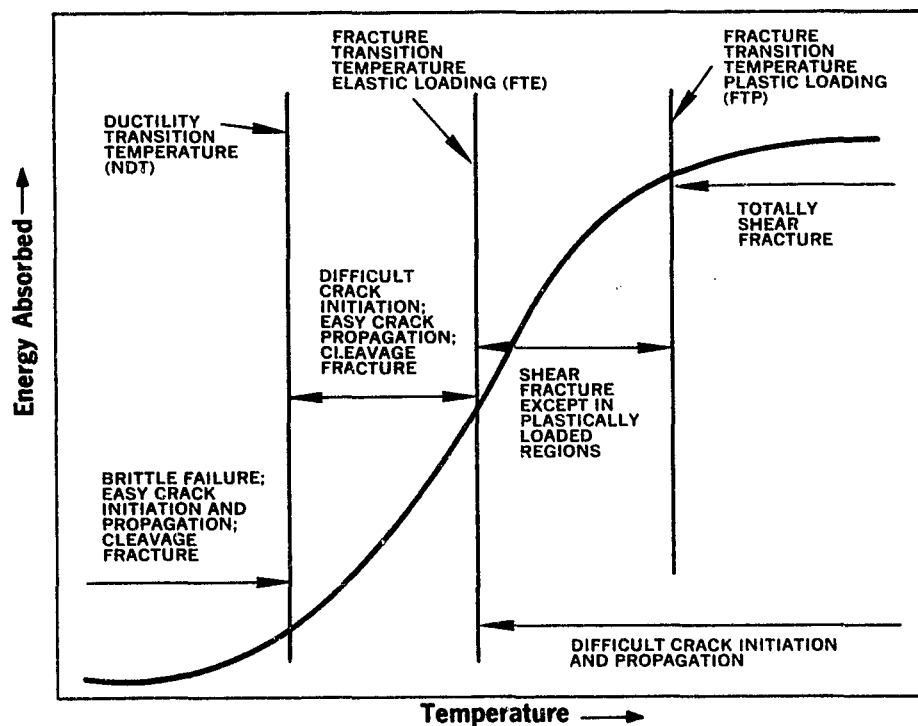


Figure 5. Schematic Representation of Notch Toughness Behavior with Respect to V-notch Charpy Tests.

suggested as a supplemental source of data to be used in conjunction with the drop-weight test.

The drop-weight test, developed by the U. S. Naval Research Laboratory, is a "go—no-go" type of test that determines the temperature below which the capacity of a material to undergo plastic deformation under impact in the presence of a sharp notch is essentially nil. This is referred to as the "nil-ductility temperature" or, abbreviated, NDT. The drop-weight test is covered by a tentative specification of the American Society for Testing and Materials (ASTM E 208-63T). In this test, a weight is dropped onto a plate-like specimen supported at the ends, the point of impact being in the middle of the span. A brittle weld bead on the under or tension side of the plate serves as a crack starter. A stop under the specimen prevents excessive plastic bending so that the specimen remains unbroken unless the material possesses a relatively high degree of brittleness. The NDT is a temperature 10° lower than the lowest duplicate no-break test performance.

The Charpy V-notch test impact-energy absorption at the corresponding nil-ductility temperature also may be determined. However, the impact-energy absorption at a temperature corresponding to NDT in the drop-weight test is dependent upon the composition and metallurgical condition of a given steel, varying from perhaps 5 to 10 foot-pounds in some mild structural steels to as high as 50 to 60 foot-pounds for heat-treated alloy steels.

The explosion-bulge test, also developed by the U. S. Naval Research Laboratory, evaluates primarily the crack-propagation characteristics of materials, which are rated by the test with respect to the nature and extensiveness of deformation and cracks caused by detonating an explosive charge above a plate or

weldment supported on an open die.

For cryogenic service, particularly in the aerospace industry, the notched-to-unnotched tensile ratio has been used as a criterion in the selection of steels. This ratio has been demonstrated to be a useful indicator of the tendency of material to behave in a tough or brittle manner.

As previously stated, many other methods of investigating notch toughness, including the stress-analysis approach, have been developed, but cannot be discussed here.

In evaluating the transition from ductile to brittle behavior, it must be understood that no one transition temperature exists for any steel except under a particular set of conditions and one criterion of toughness.

The hallmarks of ferritic steels for low-temperature service are low carbon content, deoxidation by fine-grain practice, increased alloy content, and heat treatment. Carbon raises the transition temperature while nickel and manganese lower it.

The notch toughness of steel can be improved by grain refinement and by nickel content as shown by the effect of these variables on transition temperature in Figure 6. Heat treatment also improves notch toughness, as will be discussed later in this section.

ASTM A 201 and ASTM A 212 carbon steel grades made to fine-grain practice were for many years the only carbon steels available for use at low-temperature service down to -50°F. Two additional grades covered by ASTM A 442 and four additional grades covered by ASTM A 516 recently have become available. For such low-temperature applications, these carbon steel grades (except the two A 442 grades) are manufactured in flange or firebox quality plate to meet the impact test requirements of ASTM Specification A 300 (which spe-

cifies a Charpy keyhole impact value of 15 foot-pounds at a minimum test temperature of -50°F). A 201, A 212 and A 516 steel plate, to meet the requirements of A 300, are usually furnished in the heat-treated condition, either normalized or normalized and stress relieved. Stress relieving is recommended for plate intended for low-temperature service, particularly in heavy thicknesses. Under certain conditions a "modified" A 201 can be supplied to

meet the specifications of ASTM A 300 at -60°F .

USS "T-1" Constructional Alloy Steel is a quenched and tempered low carbon alloy steel which combines a high yield strength (100,000 psi minimum) with toughness and weldability. This versatile steel has been employed satisfactorily in many vessels for service to -50°F under ASTM A 300 Specifications. The notch toughness of "T-1" Steel has also been evaluated by drop

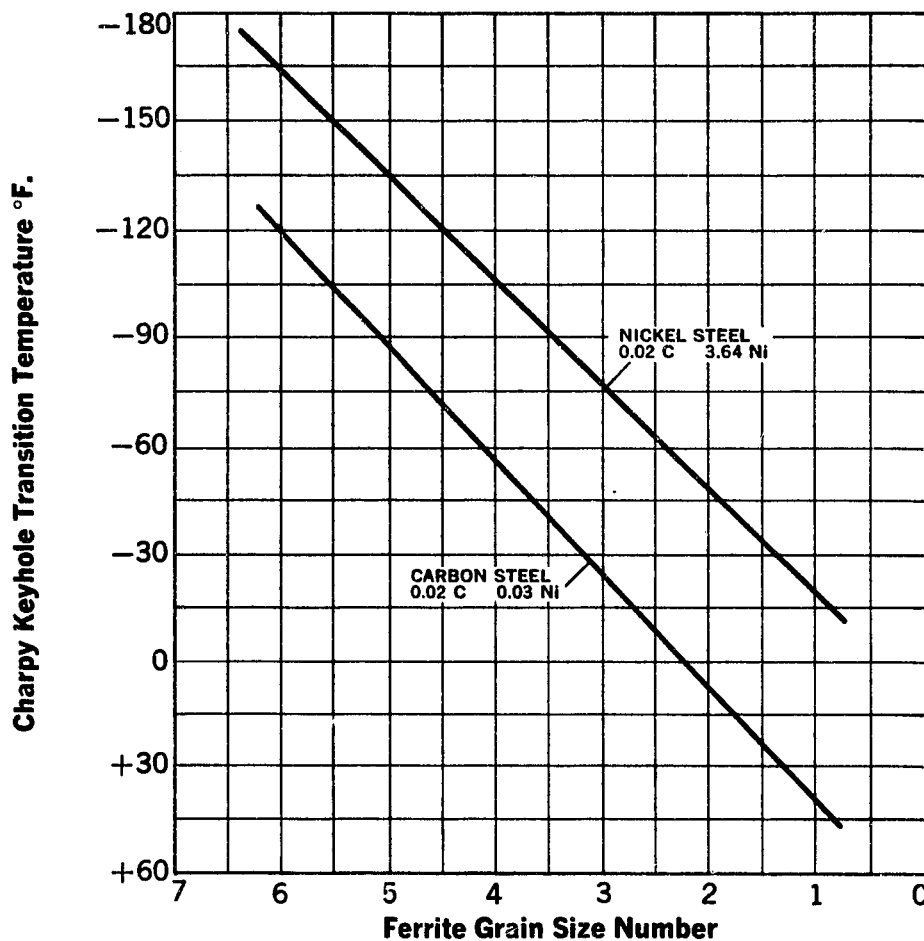


Figure 6. Transition Temperature as a Function of Ferrite Grain Size of a Carbon and a Nickel Steel

weight and explosion bulge tests conducted by the U. S. Naval Research Laboratory. These tests indicate a nil-ductility temperature of -80°F to -90°F and a fracture-arrest transition temperature of -50°F for welded half-inch plate. These results demonstrate the toughness possessed by this steel over a wide range of low temperatures.

The type of electrode used for welding is critical to the proper performance of "T-1" Steel at low temperatures. Table 7 shows the Charpy impact properties of weld metal deposited by a few types of available electrodes.

In the alloy steel, nickel is the most common of the alloying elements used to lower the transition temperature. The general effect on impact value is shown as a function of temperature in Figure 7.

A steel extensively used for a low-temperature service, particularly in the handling of liquid propane at -44°F , and for other applications down to -75°F , is low carbon $2\frac{1}{4}\%$ nickel steel.

This steel, governed by ASTM specification A 203, Grades A and B, is produced to the low-temperature specifications of ASTM A 300, Class 2. Grade B has enjoyed the widest range of applica-

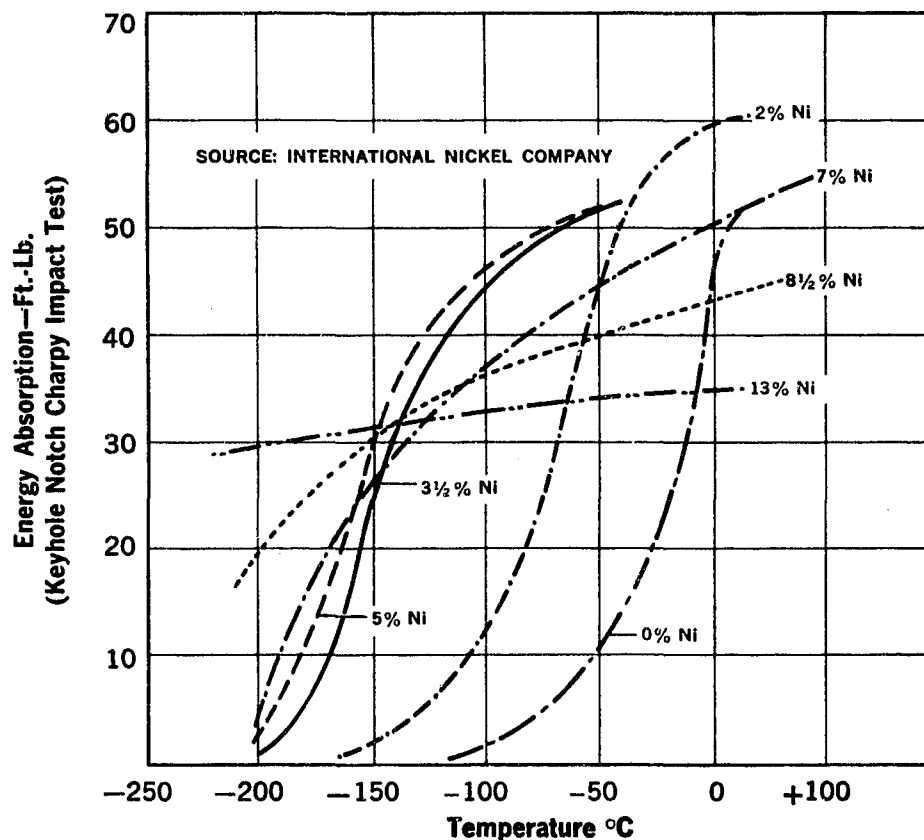


Figure 7. How Nickel Affects Impact Properties

Table 7. Results of Charpy Impact Tests on Weld Metal Joining "T-1" Steel (Butt joints in 1/2-inch and 1-inch thick plates)

Welding Process	Electrode or Wire-Flux Combination	Preheat and Interpass Temp. °F	Condition of Weld Metal	Transition Temperature, °F					Average Energy Absorption, Ft.-Lb.	
				Charpy Keyhole Mid-Envelope	Charpy V-Notch				Charpy Keyhole -50°F	Charpy V-Notch -50°F
					10 Ft.-Lb.	15 Ft.-Lb.	30 Ft.-Lb.	50% Shear Fracture		
Shielded metal-arc	E9015	70	As-welded	-155	-128	-100	-58	-38	Above 28	33
		70	Stress-relieved (1100°F)	-83	33	..
	E11018	70	As-welded	..	-156	-116	-32	-60	..	27
		70	Stress-relieved (1100°F)	..	-96	-52	24	20	..	17
	E12015	70	As-welded	-78	-40	4	..	24	26	10
		70	Stress-relieved (1100°F)	Above +130
Submerged-arc	Linde Oxweld* 100 wire and Unionmelt 709-5 flux	200	As-welded	21
		200	Stress-relieved (1100°F)	18
		300	As-welded	-220	-126	-84	8	6	28	19
		300	Stress-relieved (1100°F)	-160	-52	-12	58	84	24	11
	Lincoln L-61* wire and A0905X10 alloy flux	350	As-welded	-132	-148	-102	-20	-44	20	23
		350	Stress-relieved (1100°F)	..	-56	-28	50	26	..	11
Inert-gas-shielded metal-arc	Airco A632* wire and argon plus 1% oxygen	70	As-welded	-129	-70	..	33	49
		70	Stress-relieved (1100°F)	-5	15	..

*Trademarks of The Linde Co., Division of Union Carbide Corporation, Lincoln Electric Co. and Air Reduction Co.

tions because of its higher ASME maximum allowable design stress (17,500 psi). Grade A has an allowable stress of 16,250 psi. These steels are also covered by SA 203 of the ASME Boiler and Pressure Vessel Code. Typical Charpy impact properties of half-inch 2 1/4% nickel steel plate are shown in Figures 8 and 9. In Figure 8 (Page 50), V-notch transition curves were determined for normalized half-inch and one-inch thick, low carbon 2 1/4% nickel steel plate from a commercial heat. Values plotted in Figure 9 (Page 50) are the results of a series of Charpy keyhole tests on commercial steel plate furnished for pressure vessels to operate at -75°F.

Low carbon 3 1/2% nickel steel has had wide use in land-based facilities for the storage of liquefied gases at temperatures down to -175°F. It is frequently specified for tankage and piping to handle liquid propane, carbon dioxide,

acetylene, ethane, and ethylene. It is governed by ASTM Specification A 203, Grades D and E. Low-temperature requirements are covered by ASTM A 300. Normal expectancy Charpy impact properties of normalized half-inch thick 3 1/2% nickel steel plate are shown in Figures 10 (Page 50) and 11 (Page 51).

The keyhole notch Charpy values are shown in Figure 10 for normalized and tempered 3 1/2% nickel steel, plotted as a scatter band. The curve drawn within the band indicates the median values or normal expectancy at various temperatures. Figure 11 shows similar results for the Charpy V-notch test. Figure 12 shows the effect of heat treatment and plate thickness on impact properties of 3 1/2% nickel steel. Table 8 (Page 51) shows the notch toughness properties of 3 1/2% nickel steel at -150°F for half-inch welded plate.

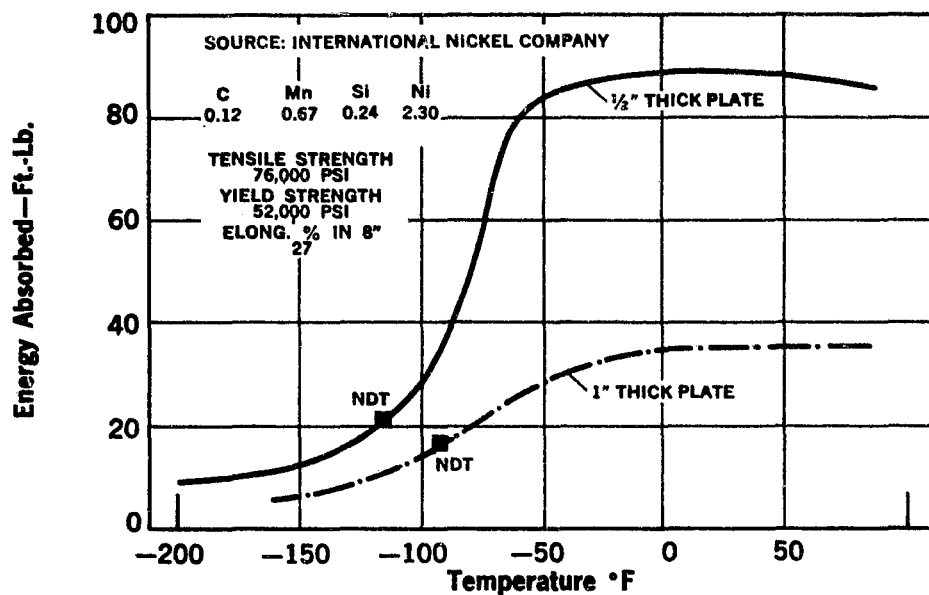


Figure 8. Typical V-Notch Charpy Transition Curves and NDT Temperatures for Normalized 2 1/4% Nickel Steel Plate

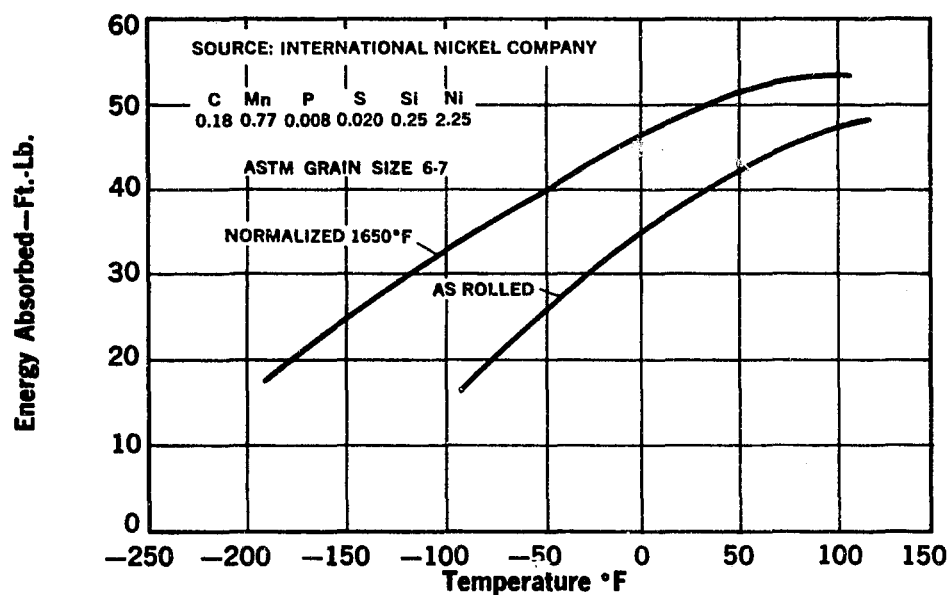


Figure 9. Comparison of Keyhole Charpy Impact Test Results for Normalized and As-Rolled Commercial 1/2-inch Thick Plate of Low Carbon 2 1/4% Nickel Steel

Table 8. Notch-Toughness Properties of 3½% Nickel Alloy Steel at -150°F (½-inch welded plate)*

Condition	Notch Location	Energy Absorbed in Keyhole Charpy Test (Ft.-Lb.)
As-welded	Base Plate	20
	Edge Heat-affected Zone	14
	Middle Heat-affected Zone	16
	Fusion Line	17
	Weld Metal	23
Stress-relieved at 1150°F	Base Plate	28
	Edge Heat-affected Zone	22
	Middle Heat-affected Zone	36
	Fusion Line	36
	Weld Metal	21

*Source: International Nickel Company

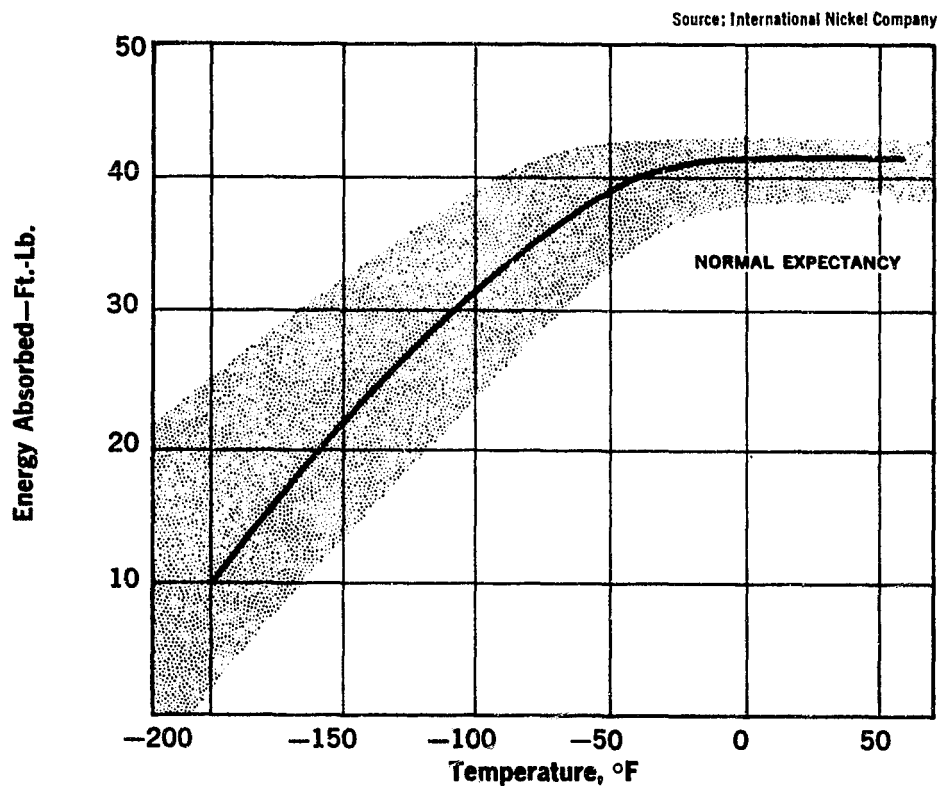


Figure 10. Charpy Keyhole Notch Impact Values for 3½% Nickel Steel (normalized, tempered, ½-inch thick plate)

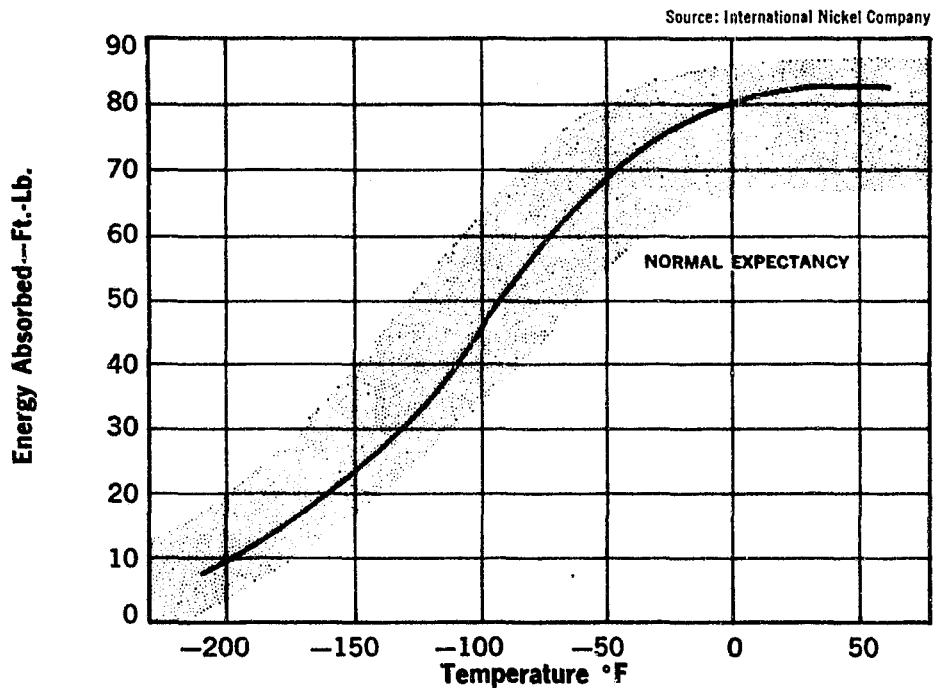


Figure 11. Charpy V-Notch Impact Values for 3½% Nickel Steel (normalized, tempered, ½-inch thick plate)

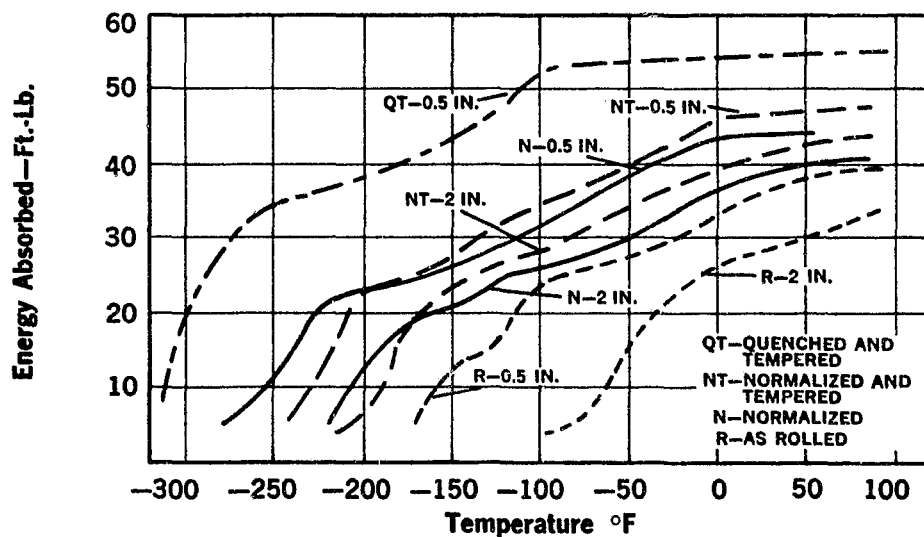


Figure 12. Effect of Heat Treatment and Plate Thickness on Keyhole Notch Charpy Impact Properties of 3½% Nickel Steel Plate (Longitudinal Specimens)

Low carbon 9% nickel steel is a ferritic steel specifically developed to meet the economic and service requirements for cryogenic applications in the atmospheric gas equipment field. It has been used in the construction of various types of equipment for the manufacture and storage of oxygen, nitrogen, argon, liquid methane; the low-temperature separation of helium; and, to a smaller extent, a number of other commodities.

The ASME Boiler and Pressure Vessel Code in 1962 approved Code Case 1308 to permit the use of this steel in construction of vessels without the necessity of postweld heat treatment in thickness to two-inch inclusive. The results of "Operation Cryogenics," carried out at the Fairless Works of United States Steel Corporation in October, 1960, demonstrated the low-temperature suitability of this steel in both the quenched and tempered and the double

normalized and tempered condition. These tests showed the desirability of elimination of postweld heat treatment. This further assisted in the economic acceptability of the steel. Some details of the tests are given in the caption of the illustration on Page 43.

Charpy impact values for 9% nickel, in both the double normalized and tempered and the quenched and tempered condition, are shown in Figures 13 and 14 (Pages 54 and 55). Laboratory test results indicate that the quenched and tempered material has good Charpy V-notch impact values near absolute zero. Based on current research and development results, it is anticipated that 9% nickel steel will be acceptable for welded pressure vessels for liquid hydrogen and liquid helium service. Table 9 shows notch toughness properties of 9% nickel steel test specimens for both the shielded metal-arc and inert-gas-shielded welds.

Table 9. Charpy Impact Test Results on As-Welded ½-inch Thick 9% Nickel Steel Plate (a)

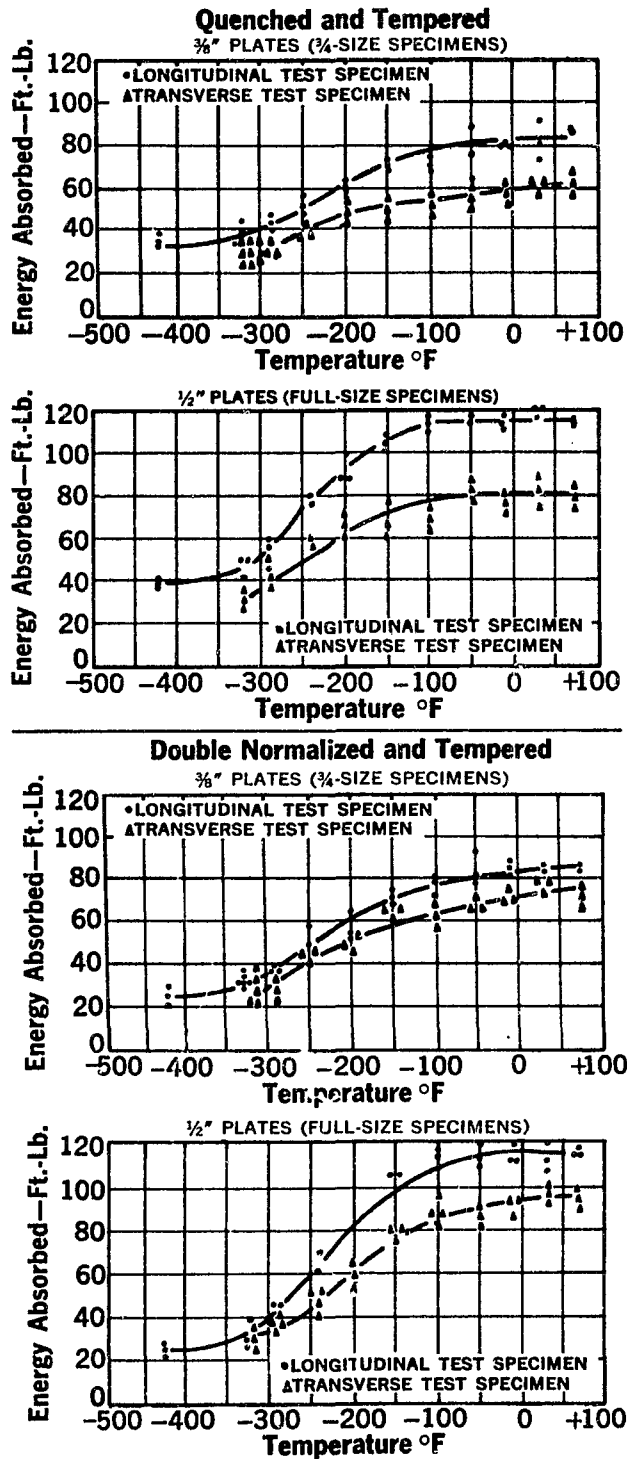
Temperature °F	Location of Notch	Energy Absorbed (Ft.-Lb.)	
		Charpy V-Notch	Charpy Keyhole Notch
75 -320 75 -320	Shielded Metal-Arc Welds* Weld Metal Weld Metal Heat-affected Zone Heat-affected Zone	68-80 60-71 119-127 68-82	33-39 28-34 41-50 29-37
75 -320 75 -320	Inert-Gas-Shielded Metal-Arc Welds† Weld Metal Weld Metal Heat-affected Zone Heat-affected Zone	104-114 96-101 76-104 43-50	59-62 44-52 41-52 22-34

*Metal-arc—Special high nickel chromium covered electrodes with controlled additions of Mn-Cb-Mo to control iron dilution.

†Inert-gas—Special high nickel chromium type wire containing the usual elements with controlled additions of Mn and Ti to reduce sensitivity to iron dilution during welding.

(a) Source: International Nickel Company

Figure 13.
Results of
Charpy V-Notch
Impact Tests
for 9% Nickel Steel



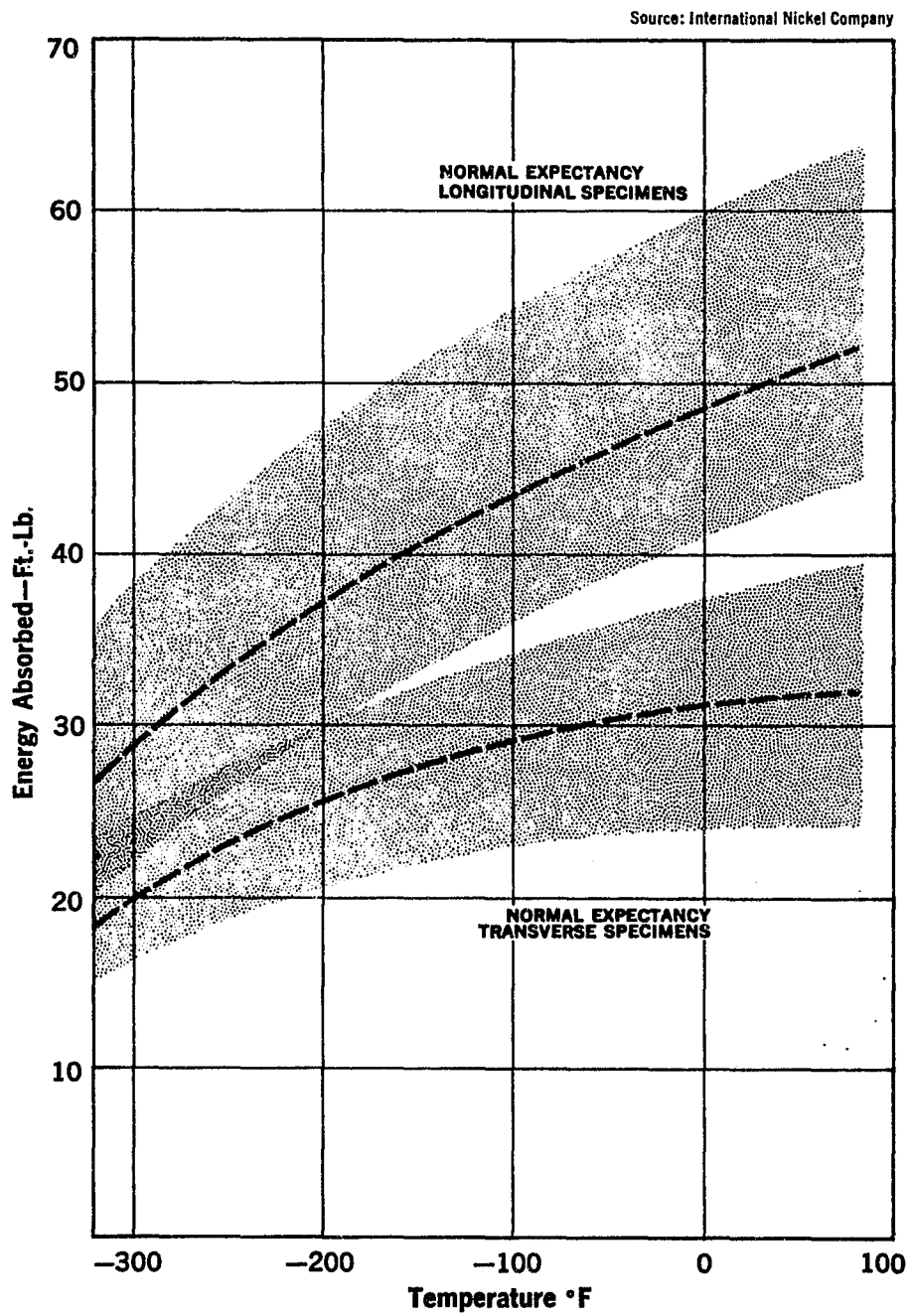


Figure 14. Charpy Keyhole Notch Impact Values for 9% Nickel Steel (double normalized, tempered, plate up to 1-inch thickness)

Table 10. Low-Temperature Impact Properties of Annealed 304 and 304L Stainless Steel

Type	Product Size	Test Temperature °F	Specimen Orientation	Type of Notch	Impact Strength (Ft.-Lb.)
304	3" Plate	-320	Longitudinal	Keyhole	80
304	3" Plate	-320	Transverse	Keyhole	80
304	2½" Plate	-320	Transverse	Keyhole	70
304	½" Plate	-425	Longitudinal	Keyhole	80
304	3½" Plate	-425	Longitudinal	V-notch	91
304	3½" Plate	-425	Transverse	V-notch	85
304L	½" Plate	-320	Longitudinal	Keyhole	73
304L	½" Plate	-320	Transverse	Keyhole	43
304L	3½" Plate	-320	Longitudinal	V-notch	67
304L	3½" Plate	-425	Longitudinal	V-notch	66

Table 10 gives the low-temperature impact properties of annealed 304 and 304L stainless steel. Table 11 shows the retention of impact strength of Type 304 after low-temperature exposures up to one year in duration. This indicates that the steel is relatively insensitive to aging factors. In addition to the excellent performance of the basic material,

welded sections of 304 retain good impact properties as shown in Table 12.

Sensitization, due to intergranular precipitation of chromium carbides, can occur in several types of stainless steel. The severity of sensitization depends upon the carbon content of the steel and the time of exposure to temperatures in the range of about 900 to 1500°F.

Table 11. Low-Temperature Impact Properties of Type 304 after Prolonged Exposure

Type of Steel	Time of Exposure	Test Temperature, °F	Charpy Keyhole Notch Impact Strength (Ft-Lb)
AISI-304	0	-320	85.0
	30 min.	-320	72
	6 mo.	-320	73.0
	12 mo.	-320	75.0

Table 12. Low-Temperature Charpy V-Notch Impact Properties of Inert-Gas-Shielded Metal-Arc Welds in 3½" Type 304 Stainless Steel Plate*

Test Temperature °F	Weld Metal	Heat-Affected Zone Distance from Notch to Fusion Line		
		1/16"	1/8"	1/2"
Type 304				
—320	38.5	51.5	63.0	64.5
—425	22.5	53.0	62.0	60.0
Type 304L				
—320	48.5	58.5	56.0	75.5
—425	45.0	53.0	45.0	64.0

*All values are averages of multiple tests; results are shown in foot-pounds.

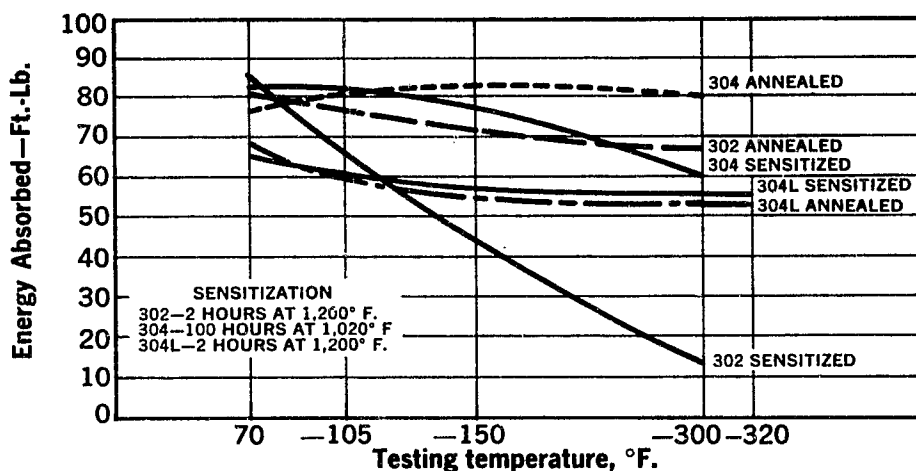


Figure 15. Effect of Sensitization Heat Treatment on Charpy Keyhole Notch Toughness of Annealed Types 302, 304 and 304L Stainless Steels. (V. N. Krivobok, "Properties of Austenitic Stainless Steels at Low Temperatures." NBS Circular 520)

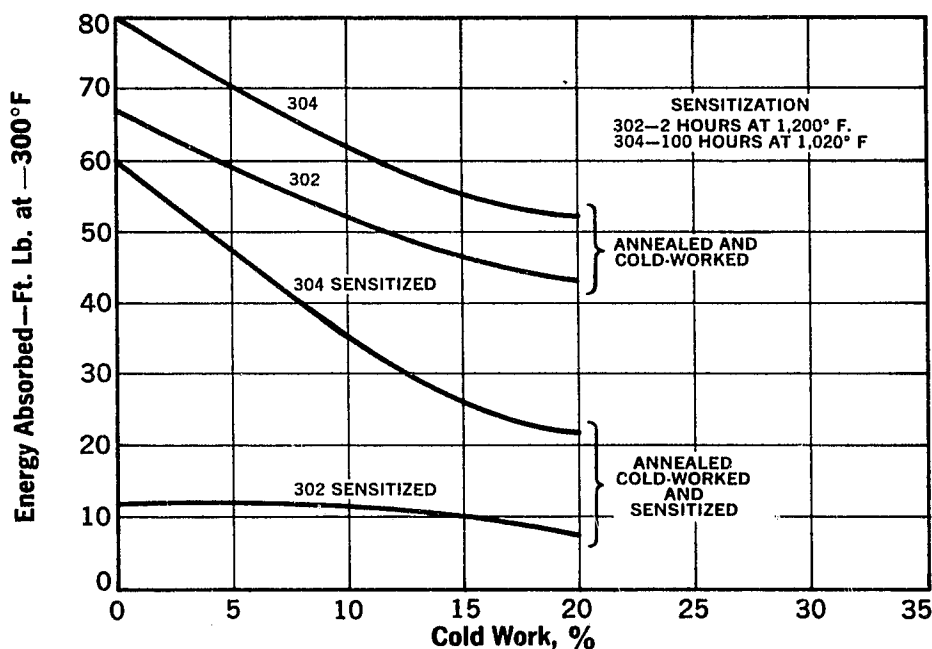


Figure 16. Combined Effect of Cold Work and Sensitization on Charpy Keyhole Notch Toughness of Types 302 and 304 Stainless Steels. (E. H. Schmidt, "Low-Temperature Impact of Annealed and Sensitized 18-8." Metal Progress, Aug. 1950)

Such exposure occurs in the heat-affected area adjacent to welds. Figures 15 and 16 (Page 57) show Charpy key-hole-test values for annealed only, annealed and sensitized, and cold-worked and sensitized Types 302, 304, and 304L stainless steels. In conjunction with Tables 10, 11, and 12, the data in Figure 15 shows that these steels retain good notch toughness at temperatures as low as that of liquid helium, with the exception of sensitized Type 302.

Figure 16 shows that even after substantial cold work after annealing, Types 302 and 304 retain good impact properties. Even after severe sensitization plus cold work, Type 304 has impact strength above the 15 ft.-lb. minimum requirement of the ASME Boiler and Pressure

Vessel Code. Cold-worked and sensitized Type 302, however, shows low impact properties at the -300°F test temperature, as would be expected from the data in Figure 15.

The Astronautics Division of General Dynamics Corporation recently investigated notched-to-unnotched tensile strength as an indication of toughness or resistance to brittleness (see Table 13). This firm's criterion of acceptable performance is that the toughness ratio of notched-to-unnotched must exceed 0.90. Types 301, 302, 304L and 310 stainless steels showed excellent performance in this respect, and stainless steels were selected for Atlas and Centaur propellant tanks.

Table 13. Tensile and Notched Tensile Properties of Cold Rolled Stainless Steel Sheets

Stainless	Test Temperature, $^{\circ}\text{F}$	Yield Strength* psi	Tensile Strength, psi	Elongation, %	Ratio, Notched ($K_t=6.3$) to Unnotched Tensile Strength
Type 301 stainless 60% CR†	78	200,000	224,000	11	1.07
	-100	237,000	253,000	15	0.98
	-320	254,000	323,000	20	0.92
	-423	308,000	335,000	3.5	0.90
Type 301N stainless 60% CR	78	200,000	223,000	12	1.08
	-320	244,000	340,000	18	0.84
	-423	297,000	334,000	12	0.79
Type 302 stainless 60% CR	78	178,000	205,000	3.0	1.08
	-320	228,000	307,000	29	0.92
	-423	249,000	294,000	20	0.95
Type 304L stainless 50% CR	78	158,000	176,000	6.0	1.09
	-100	186,000	198,000	5.0	1.09
	-320	187,000	251,000	33	1.04
	-423	231,000	279,000	1.0	1.09
Type 310 stainless 75% CR	78	157,000	181,000	2.0	1.07
	-100	190,000	204,000	3.0	1.08
	-320	223,000	251,000	10	1.11
	-423	261,000	290,000	5.0	1.12

*0.2% offset.

†CR=cold rolled.

2. Yield and Tensile Strength

Materials used in low-temperature applications must have good yield and tensile strengths at low temperatures. Normally, conventional design properties such as tensile, yield, and fatigue strengths increase at low temperatures—in contrast to the reduction encountered in ductility and impact strength. The modulus of elasticity of metals also gen-

erally increases at low temperatures. However, the designer of code regulated, low-temperature equipment generally must base his calculations on tensile properties at ambient (room) temperature. Table 14 and Figures 17-24 (Pages 60-67) show the pertinent data for these low-temperature steels.

(Continued on Page 68)

Table 14. Summary of Specifications for Low-Temperature and Cryogenic Steels

Designation	Tensile Strength (psi)	Min. Yield Point (psi)	ASME** Allowable Stress (1/4 Tensile Strength)	Elongation in Inches, % Min.		Lowest Usual Service Temperature† (°F)	Where It Is Used
				2	8		
USS CHAR-PAC (A 537) ^b Normalized	70,000 to 90,000	50,000	17,500	..	19	-50	Welded pressure vessels and storage tanks, when weight and strength are not critical. Refrigeration; transport equipment.
Quenched and Tempered	80,000 to 100,000	60,000 ^a	20,000	23	..	-50	
ASTM A 201, Grade A*	55,000 to 65,000	30,000	13,150	28	24	-50	
ASTM A 201, Grade B*	60,000 to 72,000	32,000	15,000	25	22	-50	
ASTM A 212, Grade A*	65,000 to 77,000	35,000	16,250	23	20	-50	Same as above.
ASTM A 212, Grade B*	70,000 to 85,000	38,000	17,500	21	18		
ASTM A 442 Grade 55	55,000 to 60,000	30,000	13,750	28	24		
Grade 60	60,000 to 72,000	32,000	15,000	25	22		
ASTM A 516*	55,000 to 65,000 60,000 to 72,000 65,000 to 77,000 70,000 to 85,000	30,000	13,150	28	24	-50	Same as above.
Grade 55		32,000	15,000	26	22	-50	
Grade 60		35,000	16,250	24	20	-50	
Grade 70		38,000	17,500	22	18	-50	
USS "T-1" Steel (ASTM A 517, Grade F)	115,000 to 135,000	100,000 ^a	28,750†	18	..	-50	Highly stressed pressure vessels. Tank trucks for handling LP gases.
ASTM A 203 (2 1/4% Nickel) Grade A Grade B	65,000 70,000	37,000 40,000	16,250 17,500	25 23	21 19	-75 -75	Tanks, vessels and piping for liquid propane.
ASTM A 203 (3 1/2% Nickel) Grade D Grade E	65,000 70,000	37,000 40,000	16,250 17,500	25 23	21 19	-150 -150	Land-based storage of liquid propane carbon dioxide, acetylene, ethane, and ethylene.
ASME Code Case 1308 (9% Nickel)	100,000 to 120,000	75,000 ^a	23,750‡	22	..	-320	Large tonnage oxygen-producing equipment. Transportation and storage of methane, oxygen, nitrogen and argon.
ASTM A 353 (9% Nickel) Grade A Grade B	90,000 95,000	65,000 ^a 65,000 ^a	22,500 23,750	22 20	..	-320 -320	
ASTM A 240 (Type 304 Stainless Steel) (Type 304L Stainless Steel)	75,000 70,000	30,000 ^a 25,000 ^a	18,750 17,500	-452 -452	

*To ASTM A 300 specification.

**For service applications above +100°F refer to ASME Section VIII, Table UHA-23.

†For service applications above +150°F refer to ASME Code Case 1204.

‡For service applications above +150°F refer to ASME Code Case 1308.

§Service temperatures may be lower if requirements of ASME Section VIII, Par. U.G. 84 are met.

(a) Yield strength (see Table 4, Pages 10 and 11).

(b) With modifications.

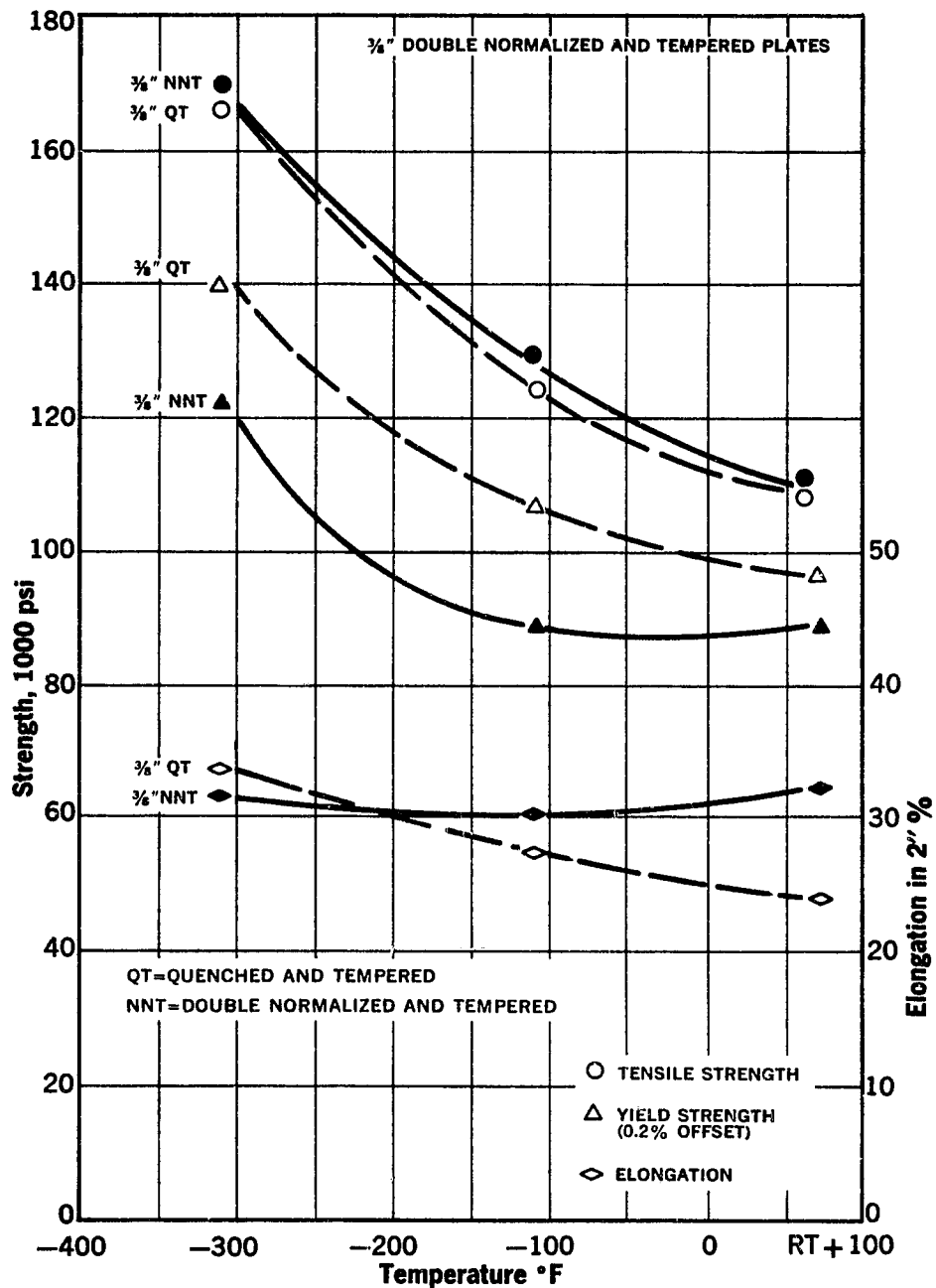


Figure 17. The Effect of Low Temperature on the Strength and Elongation of Double Normalized and Tempered 9% Nickel Steel

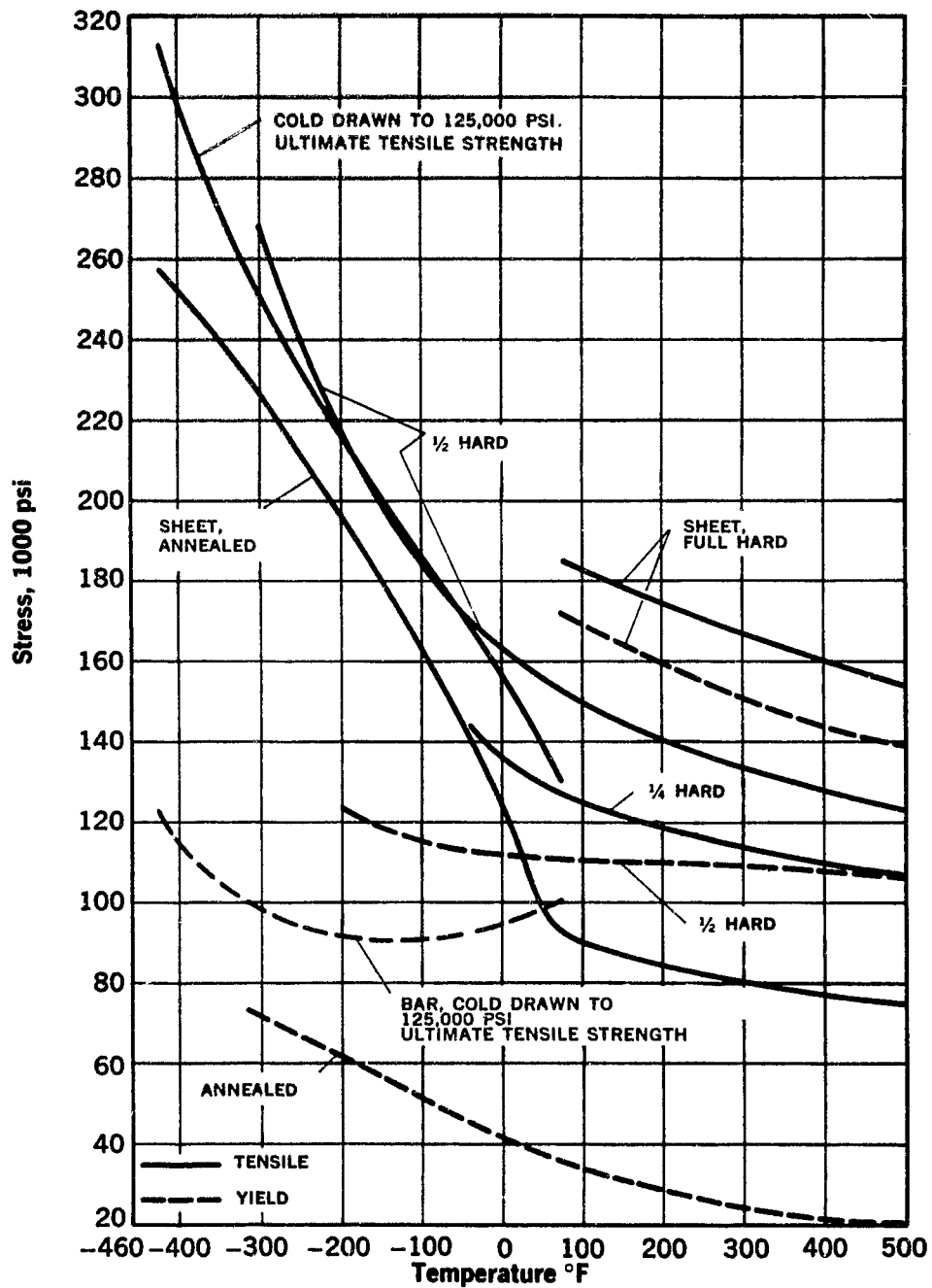


Figure 18. Strength of AISI Type 302 Stainless Steel

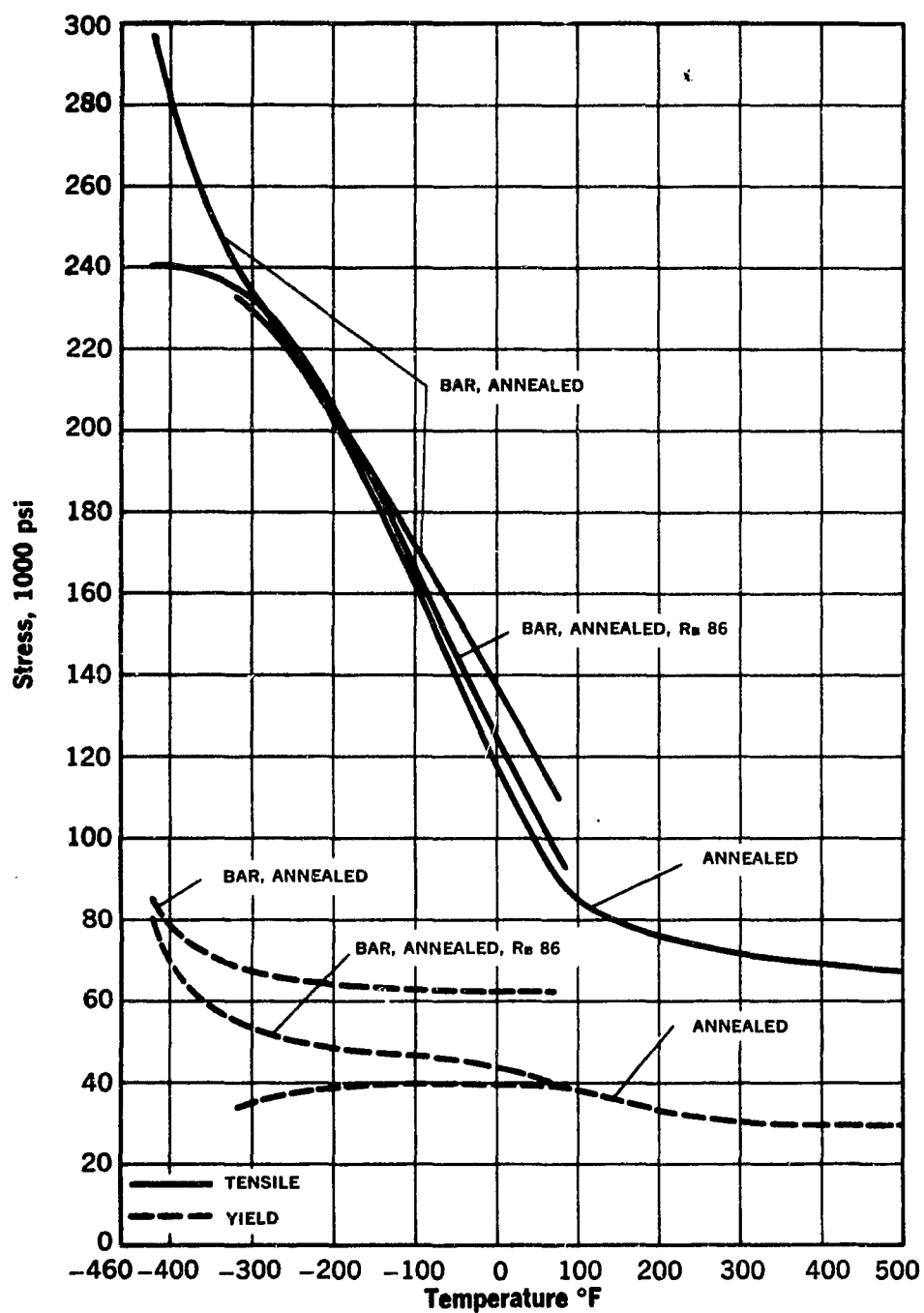


Figure 19. Strength of AISI Type 303 Stainless Steel

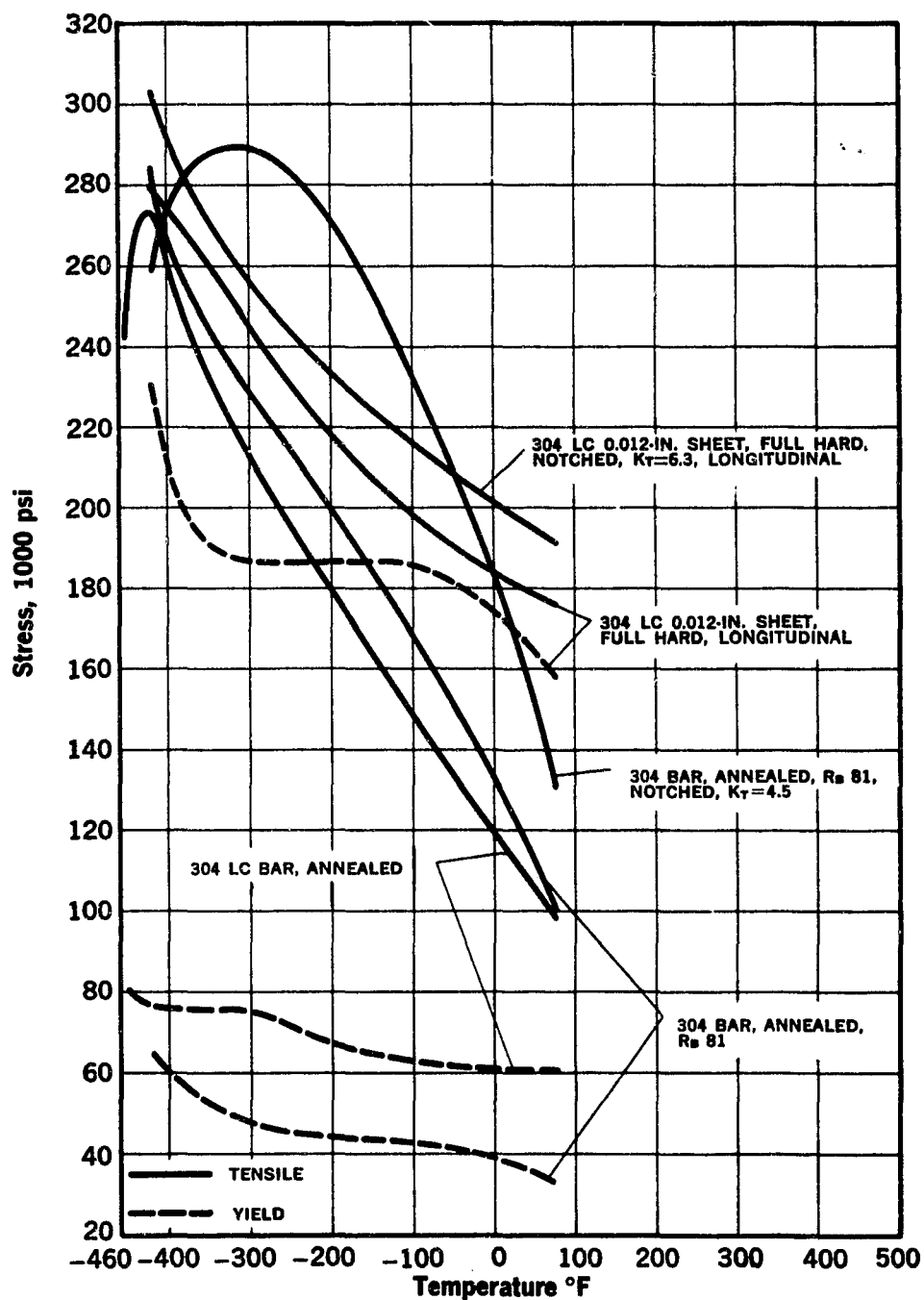


Figure 20. Strength of AISI Type 304 Stainless Steel

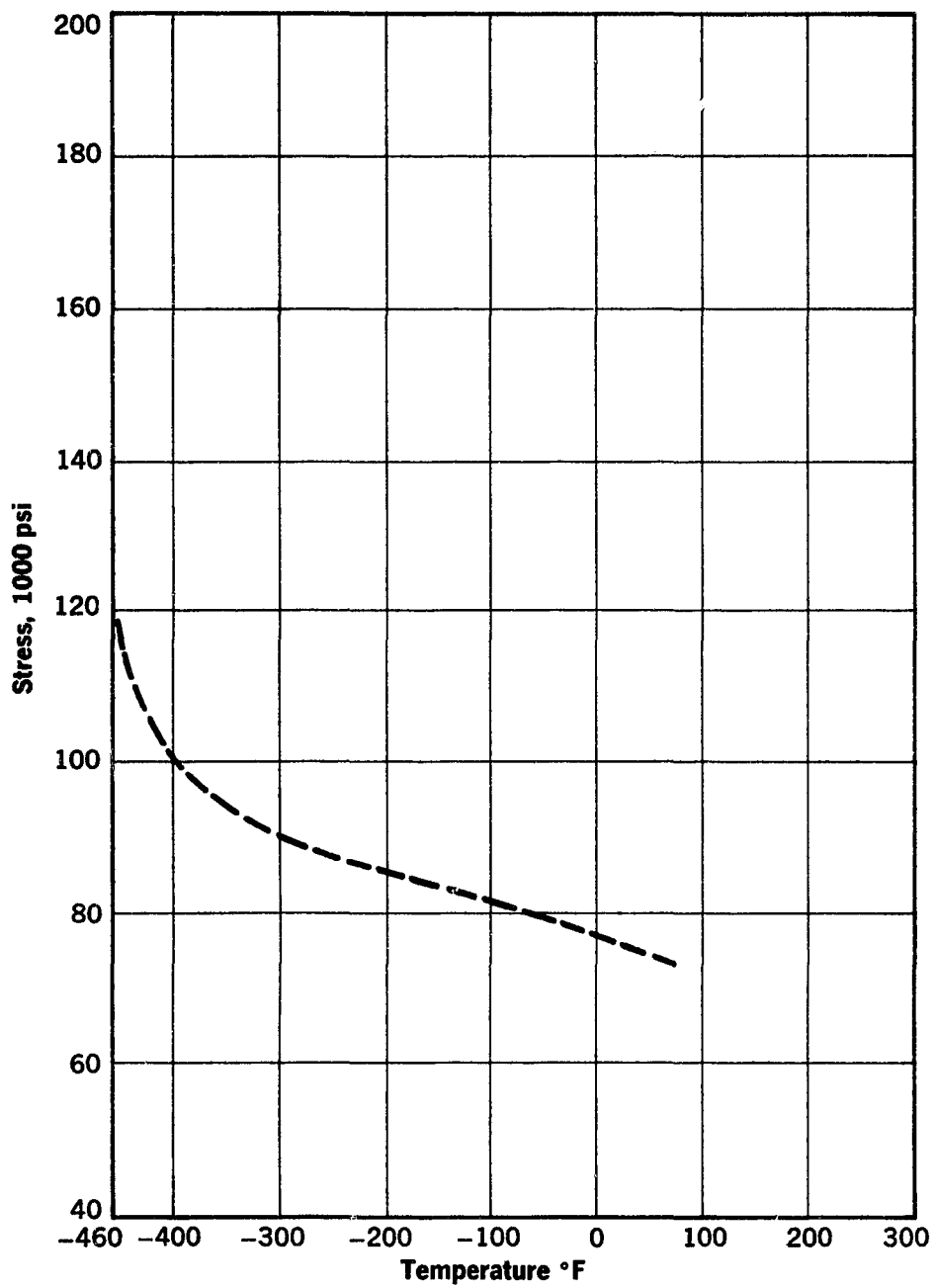


Figure 21. Compressive Yield Strength of AISI Type 304 Stainless Steel

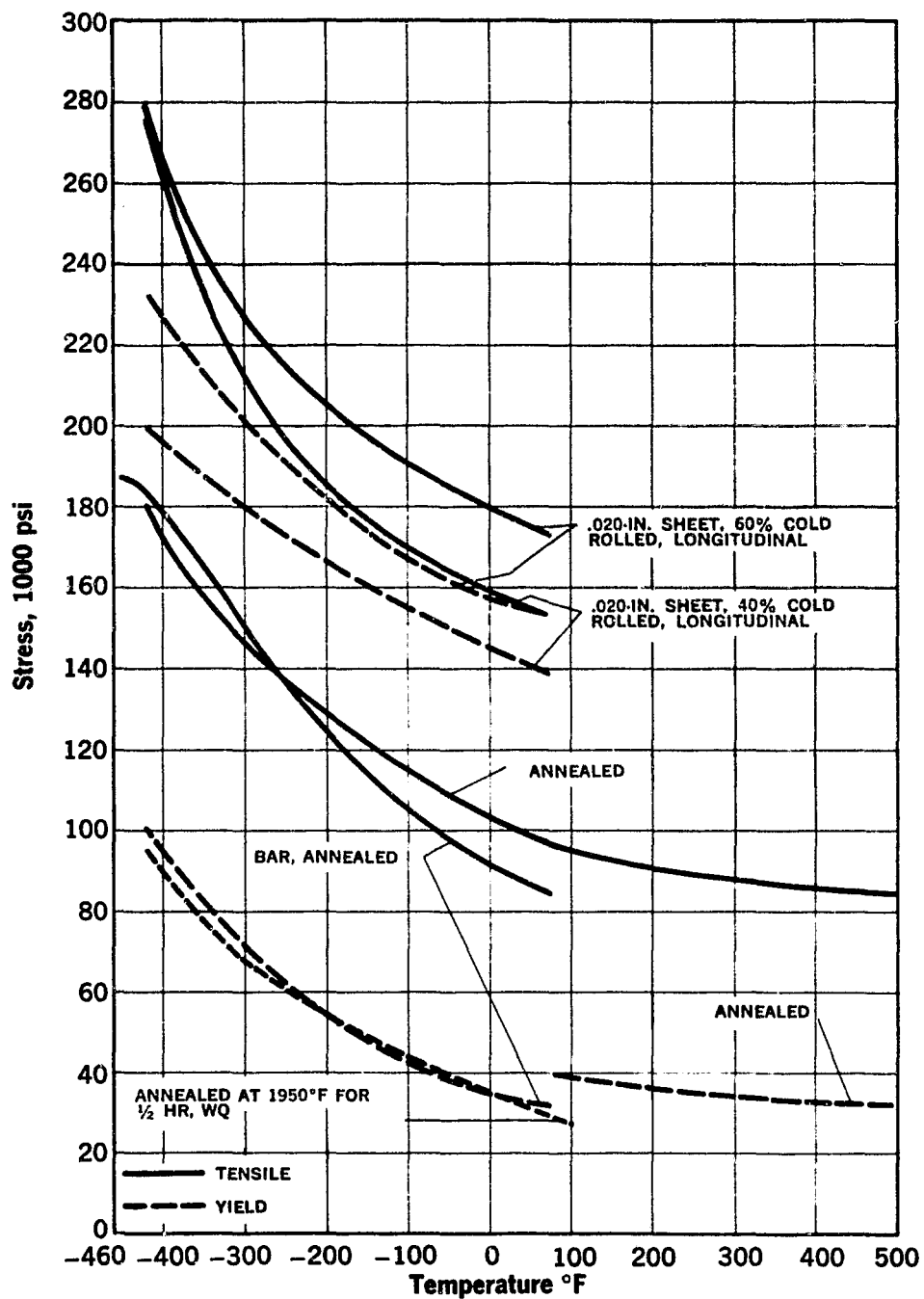


Figure 22. Strength of AISI Type 310 Stainless Steel

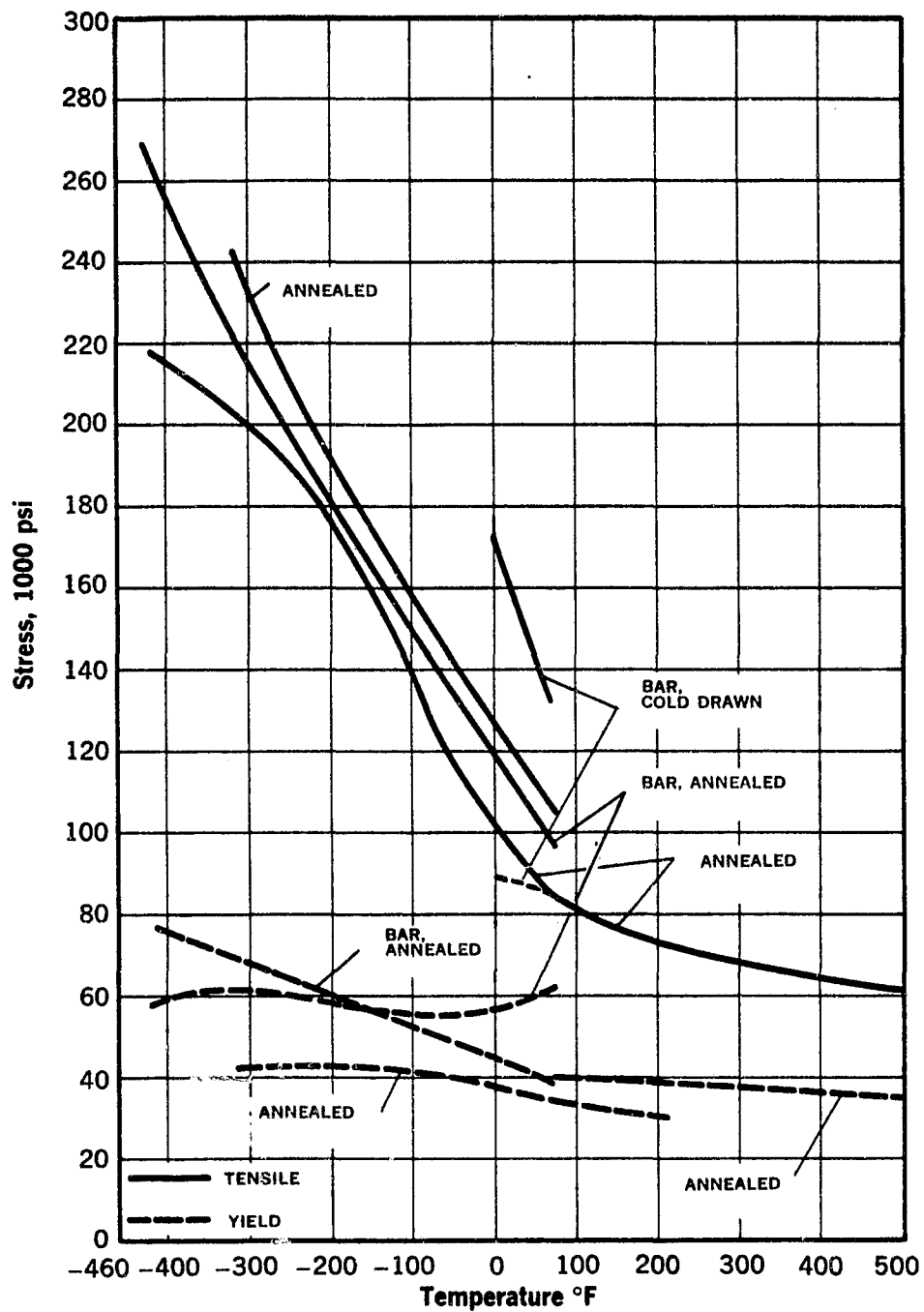


Figure 23. Strength of AISI Type 321 Stainless Steel

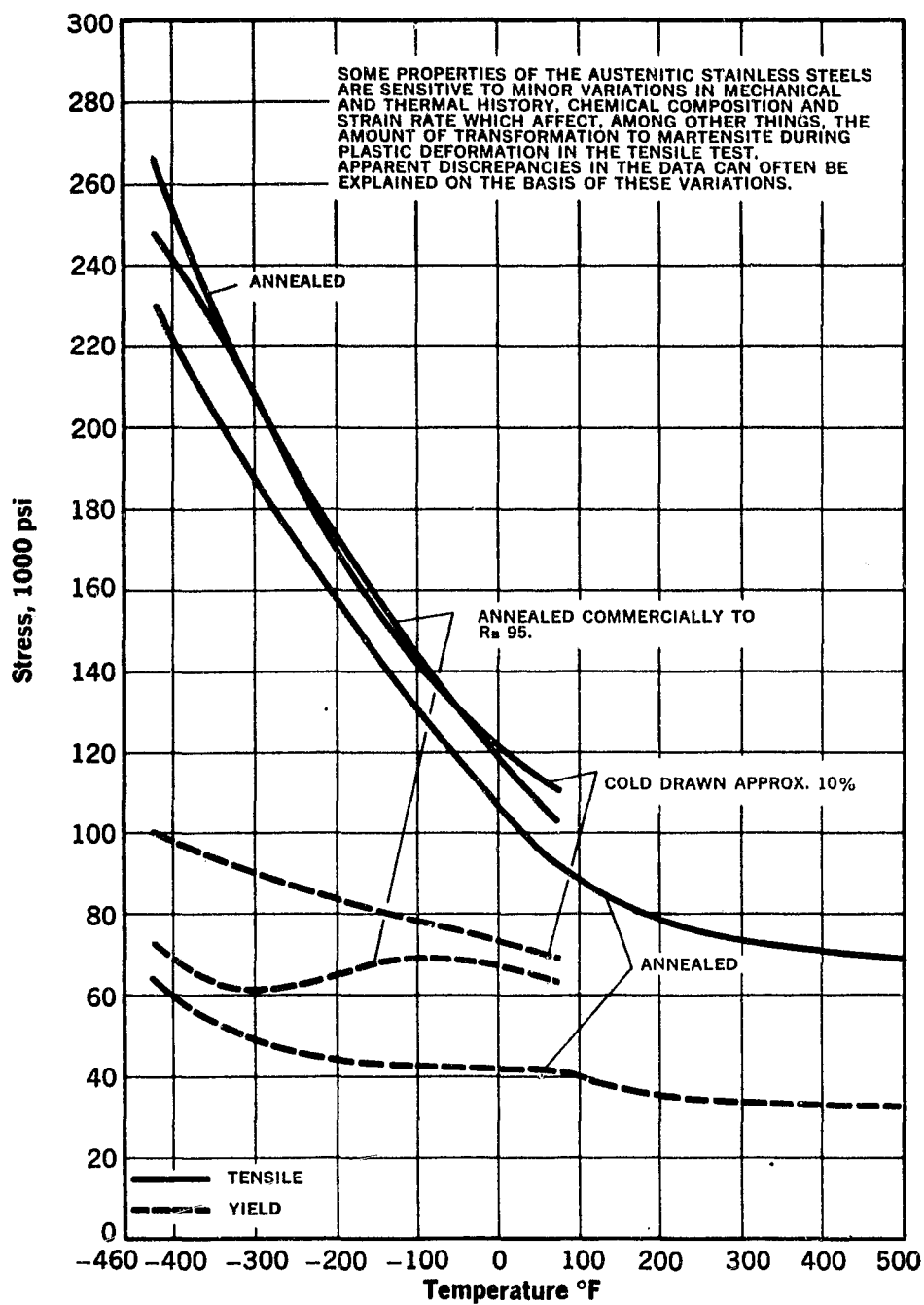


Figure 24. Strength of AISI Type 347 Stainless Steel

(Continued from Page 59)

In non-code work and in certain military and space applications, however, the higher yield and tensile strengths of these steels at low temperatures can be used to good advantage to reduce weight and cost. Data for guidance purposes are given in Figures 17-24.

In the past, testing of various properties at cryogenic temperatures has been accomplished with difficulty and some inaccuracy, particularly at temperatures below the boiling point of liquid nitrogen (-320°F). The Watertown Arsenal Laboratories recently determined the tensile strengths of the 300 series stainless steels to liquid helium temperatures (Figure 25). True stress-strain measurements were made with recently improved and more reliable temperature controls during immersion in liquid helium (at -452°F). The tensile strengths of the 300 series stainless steels generally increase with decreasing temperature. This increase is approximately linear to -350°F , but at -452°F the strengths of several types were slightly lower than would be expected by straight extrapolation from a higher temperature. While ductility decreases with decrease in temperature, the elongation for all the stainless steels is quite adequate for reliable service at temperatures at or near absolute zero (Table 15, Page 70).

3. Fatigue

It is generally recognized that if a structural member is subjected to fluctuating or cyclic stresses, the member may fail even though the maximum stress in the cycle is less than the yield point of the material. This phenomenon is known as fatigue and must be considered when designing structures that are subject to dynamic loads. Examples of applications involving fatigue loadings that are of interest to the cryogenic industry include pumps, vessels that fre-

quently undergo pressure changes, tank trucks, and equipment on board aircraft.

a. Determination of Fatigue Strength

To determine the fatigue strength of a material, specimens of the metal are subjected to alternating stresses that vary between fixed limits of maximum and minimum stress until failure occurs. This procedure is repeated for other specimens at the same ratio of minimum to maximum stress, but at lower stress values. The results of the tests are plotted (like those shown in Figure 26, Page 71) to form an S-N diagram, where S represents the maximum stress in the cycle and N represents the number of cycles required to produce failure. The stress required to produce failure at any given number of cycles is known as the fatigue strength for that number of cycles.

As shown in Figure 26, the fatigue strength decreases as the number of cycles increases, until a stress is reached below which further increases in the number of cycles do not decrease the fatigue strength. This stress is known as the fatigue limit. If the stress is kept below the fatigue limit, the specimen can undergo an infinite number of cycles without failing.

b. Factors Affecting Fatigue Strength

The fatigue strength of any given type of steel depends not only on the number of cycles to which it is subjected, but also depends upon the stress ratio, surface conditions, the stress gradient, the presence of stress concentrations, the temperature, and other factors. The effects of each of these factors will be discussed briefly below.

The stress ratio, R , is defined as the minimum stress divided by the maximum stress. Thus, $R=0$ represents a stress varying from zero to maximum

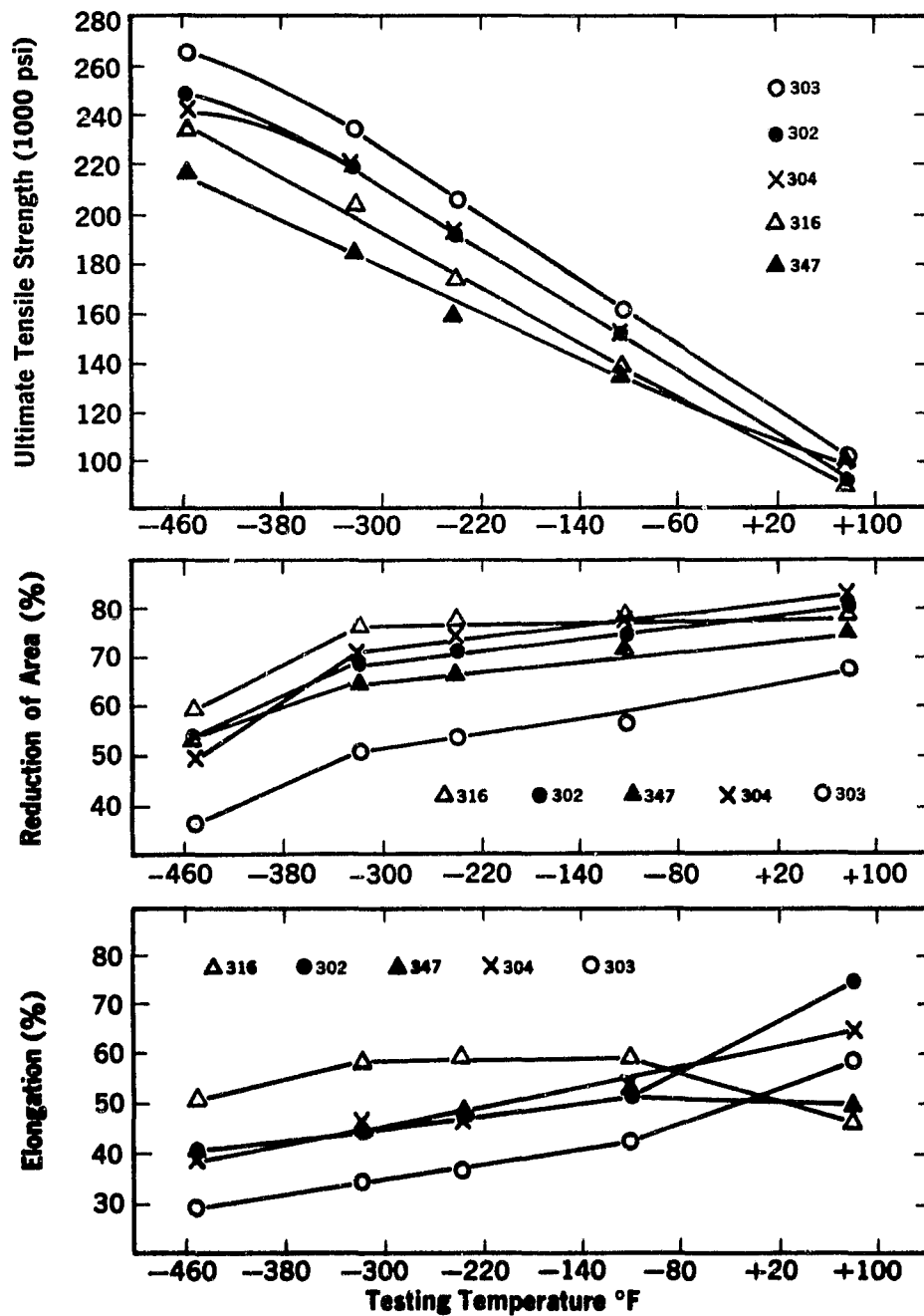


Figure 25. Tensile Strengths of AISI 300 Series Stainless Steels at Various Temperatures

Table 15. Tensile Properties

Testing Temp (°F)	Ultimate Tensile Strength (psi)	Elongation (%)	Reduction of Area (%)	True Stress at Max. Load (psi)	True Strain at Max. Load
AISI 302 Stainless Steel					
R.T.	94,400	75.0	80.7	149,600	0.460
-105	152,400	52.5	73.7	218,700	0.362
-240	191,300	48.0	71.7	262,900	0.318
-320	219,300	46.0	69.5	292,150	0.286
-452	249,500	41.0	54.8	548,500	0.787
AISI 303 Stainless Steel					
R.T.	100,200	59.0	67.4	157,800	0.452
-105	161,500	43.0	56.8	219,900	0.299
-240	206,300	37.0	53.6	266,000	0.254
-320	234,100	35.0	51.5	293,500	0.227
-452	266,500	29.6	37.0	423,600	0.462
AISI 304 Stainless Steel					
R.T.	95,000	65.0	83.4	154,100	0.482
-105	151,100	55.0	77.0	211,800	0.336
-240	193,800	46.0	73.9	264,200	0.308
-320	221,400	46.5	71.8	301,800	0.308
-452	242,500	39.0	49.8	363,400	0.402
AISI 316 Stainless Steel					
R.T.	93,900	47.0	77.5	133,900	0.355
-105	131,500	59.0	78.0	198,800	0.442
-240	161,100	60.0	77.7	256,000	0.462
-320	184,300	59.0	76.2	270,500	0.384
-452	216,400	52.0	59.7	360,200	0.508
AISI 347 Stainless Steel					
R.T.	99,300	50.0	73.0	143,200	0.365
-105	136,600	53.0	72.2	194,700	0.355
-240	172,100	48.0	67.4	238,600	0.327
-320	201,400	46.0	65.5	274,500	0.308
-452	236,400	38.0	54.7	438,000	0.593

in tension, while $R = -1$ represents stress varying between maximum and minimum stresses that are equal in magnitude but opposite in sign. Generally, fatigue strength decreases with decreasing value of R . This effect is shown in Figure 27 for "T-1" Steel tested with alternating axial loads at stress ratios of 0, $-\frac{1}{2}$, and -1 .

Many laboratory tests are conducted on polished specimens while others are conducted on material with surfaces as

received from the rolling mill. The "as received" specimens, because of their rougher surfaces, generally have a lower fatigue strength than polished specimens. Therefore, if fatigue strengths obtained from polished specimens are used as a basis for design, proper allowances must be made for the effects of surface roughness.

Figure 27 (Page 72) also shows the effect of the stress gradient; that is, the manner of stress distribution over the

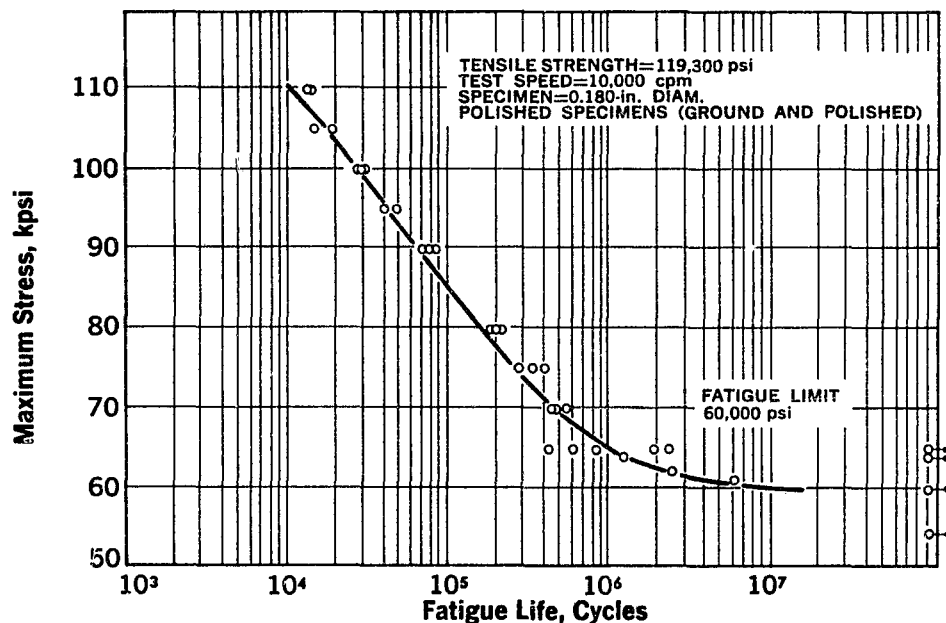


Figure 26. Results of Rotating-Beam Fatigue Tests on USS "T-1" Steel, $R = -1$

cross section. The specimens subjected to alternating axial loads, of course, have stresses that are uniform, whereas the specimens tested as rotating beams have stresses that vary linearly across their thicknesses. As indicated in Figure 27, under the latter stress gradient the specimen has a greater fatigue strength at any given number of cycles than the axially loaded specimen tested at the same stress ratio ($R = -1$). The greatest difference in fatigue strength occurs at the lowest number of cycles.

Stress concentrations, such as are produced by notches, welds, fabrication details, or other abrupt changes in shape, lower the fatigue strength of a given material and, therefore, should be avoided wherever possible. In a fabricated structure, notches that could be avoided often occur, such as punch marks, hammer marks, and weld de-

fects. Other notches may be unavoidable, such as the notch caused by a butt-welded joint with the weld reinforcement in place. Furthermore, fabrication details, such as lugs welded to a member or riveted connections, cause stress concentrations. Where such stress concentrations occur, their effect in lowering fatigue strength must be recognized in design.

Fatigue strength generally increases as the temperature decreases. Therefore, a member stressed at cryogenic temperatures would be expected to have a greater fatigue strength than that indicated by room temperature fatigue tests. For example, the fatigue limit of 9% nickel steel was found to increase by about $\frac{1}{3}$ when tested at -320°F instead of at room temperature. (This data is for polished specimens tested by flexure, $R = -1$. See Table 16, Page 72.)

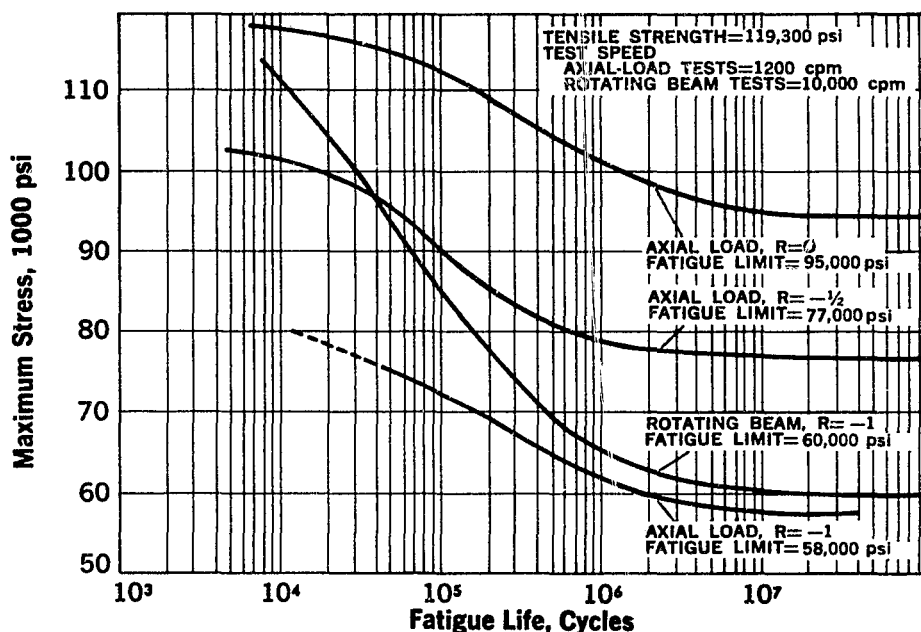


Figure 27. Composite Results of Fatigue Tests on USS "T-1" Steel

c. Design Data

Table 16 gives a compilation of fatigue information for the cryogenic steels. The values are room temperature values, except where otherwise indi-

cated, and contain no safety factors. Additional fatigue information is being determined and will be published when obtained.

Table 16. Fatigue Information for Steels for Low-Temperature and Cryogenic Service

Steel	Stress Ratio	Surface Condition	Fatigue Limit (psi)	Type of Test	Material
USS "T-1" Steel	-1	Polished	58,000	Axial load	0.357-inch diameter bars from 1-inch plates
	-1/2	Polished	77,000	Axial load	
	0	Polished	95,000	Axial load	
	-1	Polished	60,000	Rotating beam	0.180-inch diameter bars from 1-inch plates
	-1	As received	44,000	Axial load	1/4-inch plates
	0	As received	68,000	Axial load	
	+1/2	As received	101,000	Axial load	
2 1/4% Nickel	-1	Polished	45,000	Rotating beam	
3 1/2% Nickel	-1	Polished	49,000	Rotating beam	
9% Nickel	-1	Polished	75,000	Flexure	1/4-inch diameter bars
	-1	Polished	85,000*	Flexure	
	-1	Polished	102,000†	Flexure	

*Testing Temperature = -100°F.

†Testing Temperature = -320°F.

C. Thermal Properties of Low Temperature and Cryogenic Steels

1. Thermal Expansion and Contraction

Thermal expansion can often be an important factor in material selection. The large dimensional changes between ambient and operating temperatures in the cryogenic field can lead to a number of problems in both stationary equipment and in machinery unless proper design consideration is given to thermal expansion and contraction.

This factor is important in sandwich

construction of cryogenic vessels and in double wall vessels that use different materials. In some cases, thermal expansion might influence the decision to make the inner and outer tanks of a cryogenic vessel of the same material. Stainless steel and Invar* are preferred materials for cryogenic transfer lines. Thermal expansion is also an important factor in the selection of welding electrodes and can be a limiting factor in the choice of such an electrode.

In most nonferrous alloys, the coefficients of thermal expansion are consid-

*Trademark of International Nickel Company

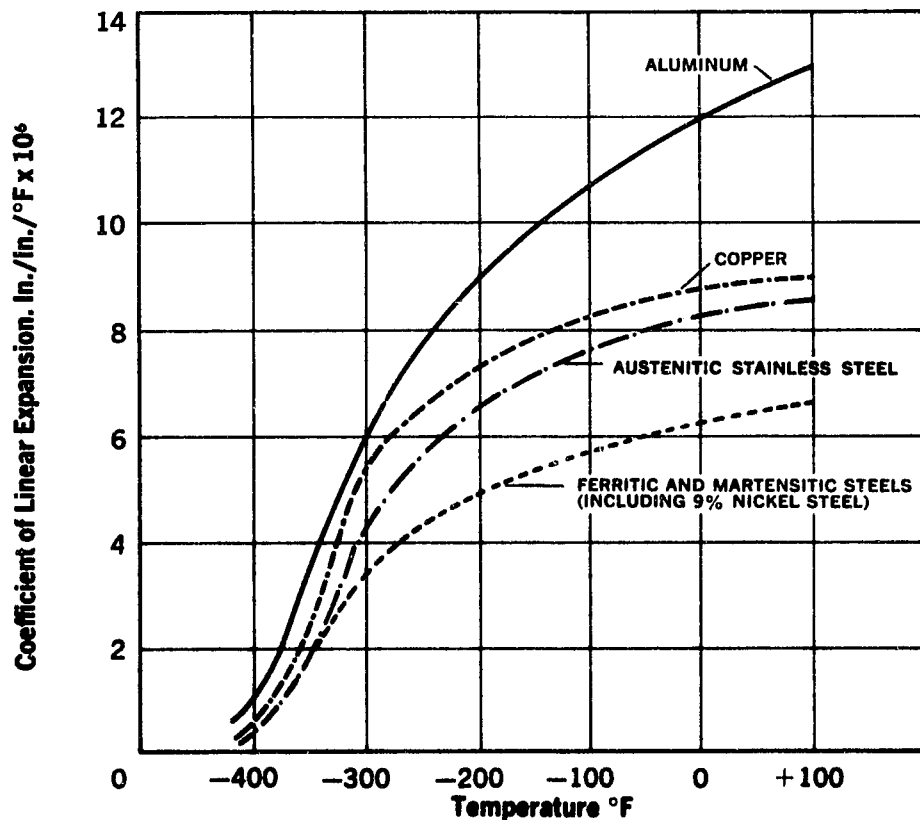


Figure 28. Coefficient of Linear Expansion of Several Materials

Table 17. Selected Thermal Properties of Some Steels
(See also Tables 5A and 5B, Page 12)

3½% Nickel Steel Thermal Expansion Coefficient 0 to +200°F Thermal Conductivity -150°F (mean) +68°F (mean) +200°F (mean) Specific Heat -150 to +80°F +80 to +1000°F	6.15×10^{-6} in./in./°F 214 Btu/in./hr./ft²/°F 253 Btu/in./hr./ft²/°F 270 Btu/in./hr./ft²/°F 0.798 Btu/lb./°F 0.147 Btu/lb./°F
9% Nickel Steel Thermal Expansion Coefficient At room temperature -300 to 0°F (avg.) -300 to +200°F (avg.) at -300°F Thermal Conductivity -320°F -150°F +68°F +200°F Specific Heat -320 to +80°F +80 to +700°F	5.8×10^{-6} in./in./°F 5.3×10^{-6} in./in./°F 5.6×10^{-6} in./in./°F 4.0×10^{-6} in./in./°F 91.3 Btu/in./hr./ft²/°F 169.0 Btu/in./hr./ft²/°F 189.0 Btu/in./hr./ft²/°F 209.0 Btu/in./hr./ft²/°F 0.0878 Btu/lb./°F (avg.) 0.119 Btu/lb./°F (avg.)
304 Stainless Steel Thermal Expansion Coefficient +32 to +212 F 300 to +70 F (mean) +70 to +1000 F (mean) at -300 F Thermal Conductivity 320 F 155 F +70 F +600 F Specific Heat 320 F 150 F +80 F	9.6×10^{-6} in./in./°F 7.3×10^{-6} in./in./°F 10.0×10^{-6} in./in./°F 5.9×10^{-6} in./in./°F 56.4 Btu/in./hr./ft²/°F 90.0 Btu/in./hr./ft²/°F 113.0 Btu/in./hr./ft²/°F 120.0 Btu/in./hr./ft²/°F 0.037 Btu/lb./°F (avg.) 0.088 Btu/lb./°F (avg.) 0.120 Btu/lb./°F (avg.)

erably higher than those for steels as shown in Figure 28 (Page 73). Large dimensional changes can result in dangerous stresses as a result of high coefficients of expansion, and allowance should be made for them in designs. The significance of this fact might be noted in a typical cryogenic container of perhaps 36 feet in length. In such a container, at liquid hydrogen temperatures, stainless steel will contract $1\frac{1}{4}$ inches when cooled from ambient. Aluminum structures will contract almost 2 inches. For cryogenic service, the coefficients of expansion might be more aptly reported as coefficients of contraction since it is primarily the cool-down

that gives the designer major problems.

Type 304 stainless steel has expansion values somewhat higher than the ferritic/martensitic steels but lower than the aluminum alloys. Since the expansion rate for 9% nickel steel and for stainless steel is less than that for aluminum, it is more desirable to use steel in those applications where compaction of insulation in a limited space is important.

Thermal properties of some steels are shown in Table 17 (see also Table 5). Figure 29 compares the thermal contraction of stainless steel and aluminum. Figures 30 to 33 (Pages 76-78) give the thermal expansion properties of various alloy and stainless steels.

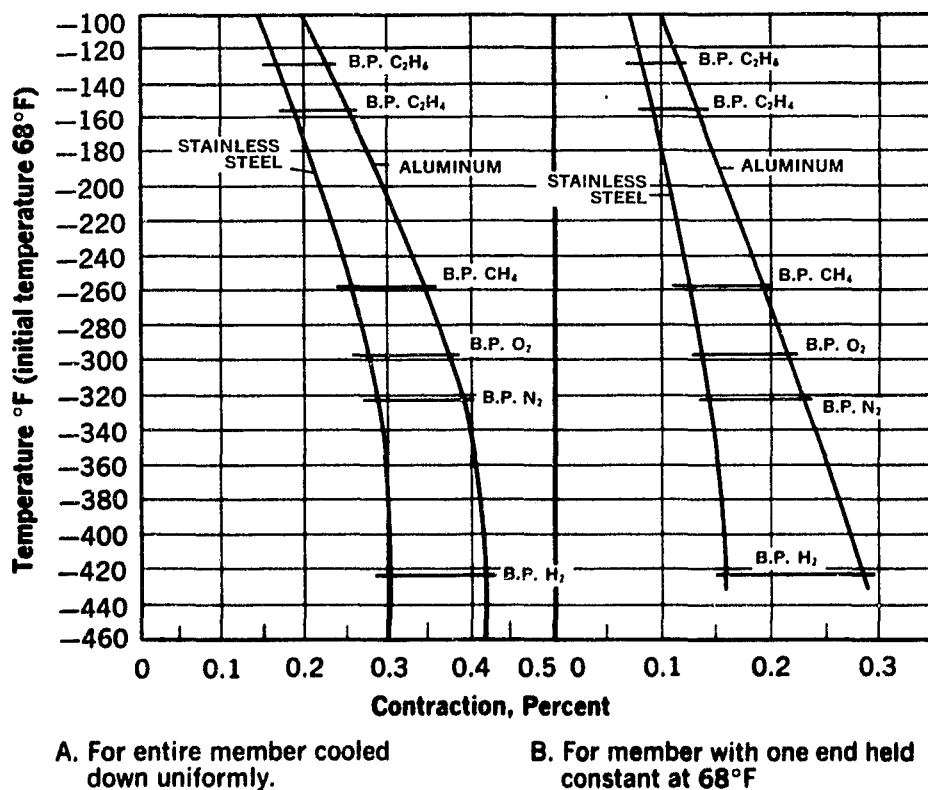


Figure 29. Thermal Contraction from 68°F for Stainless Steel and Aluminum

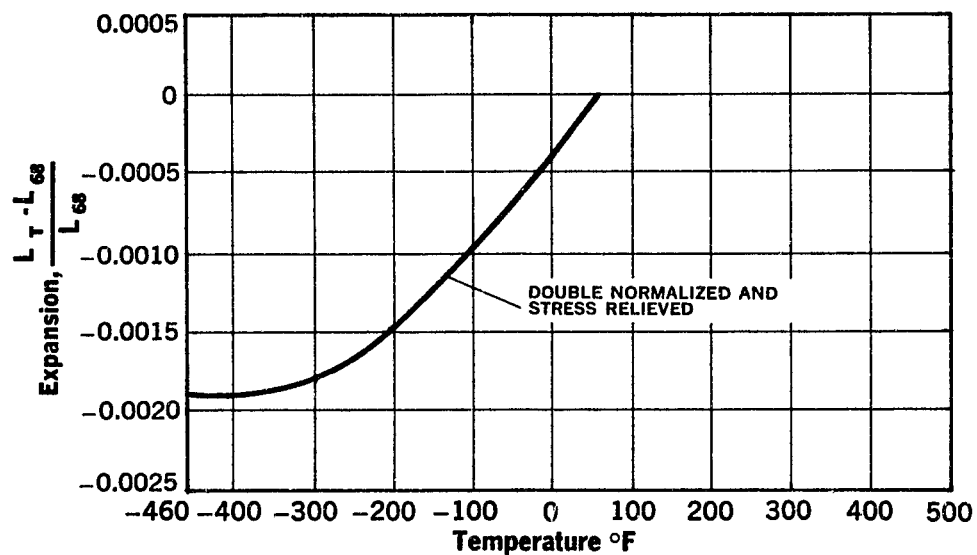


Figure 30. Thermal Expansion of 9% Nickel Steel

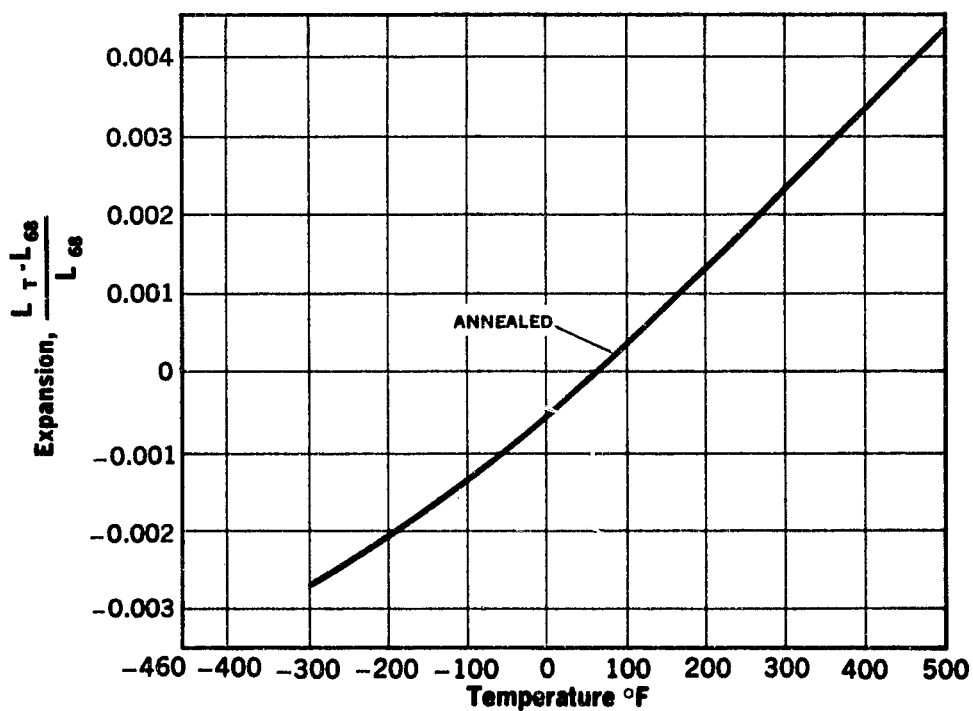


Figure 31. Thermal Expansion of AISI Type 301 Stainless Steel

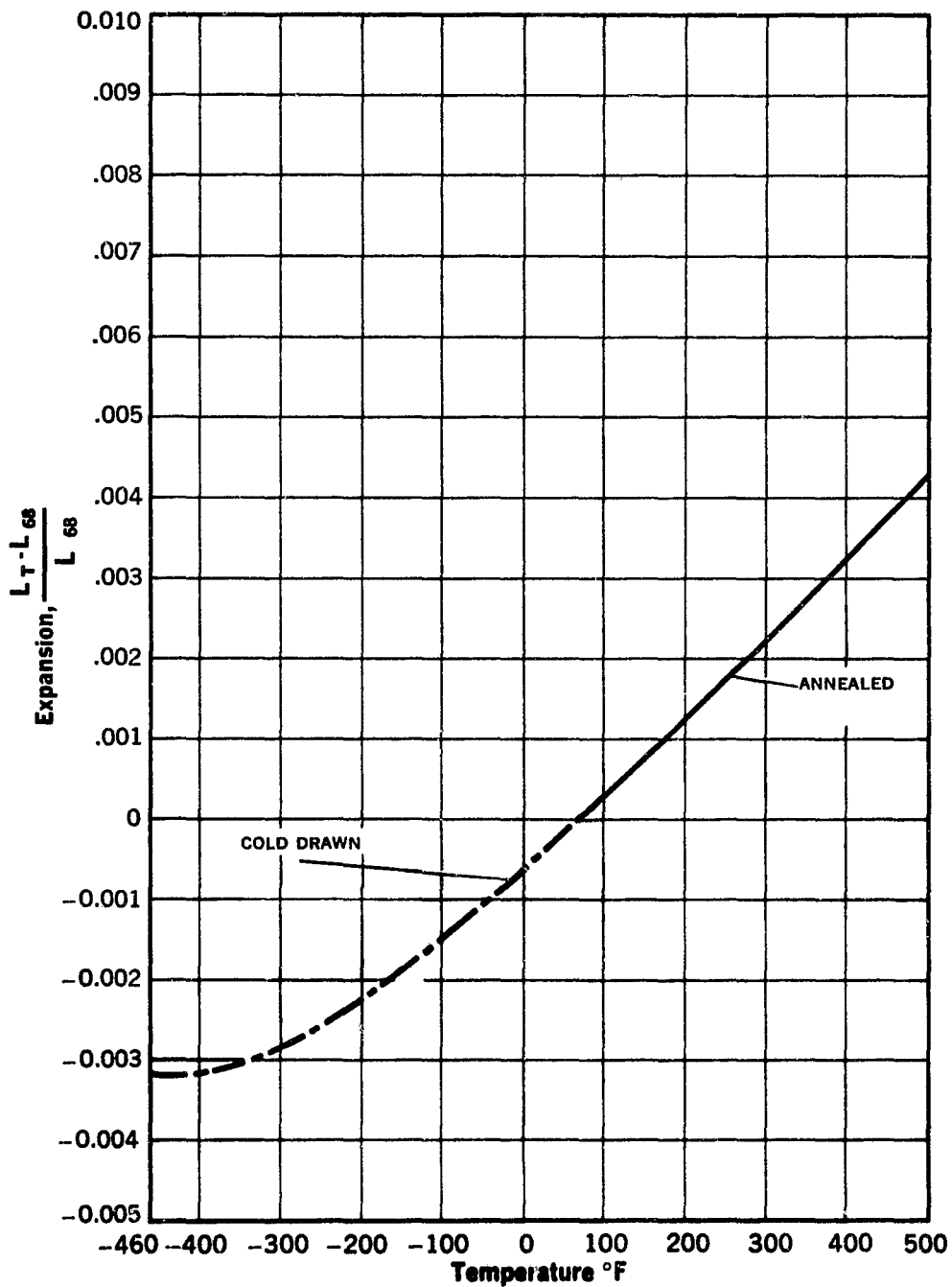


Figure 32. Thermal Expansion of AISI Type 302 Stainless Steel

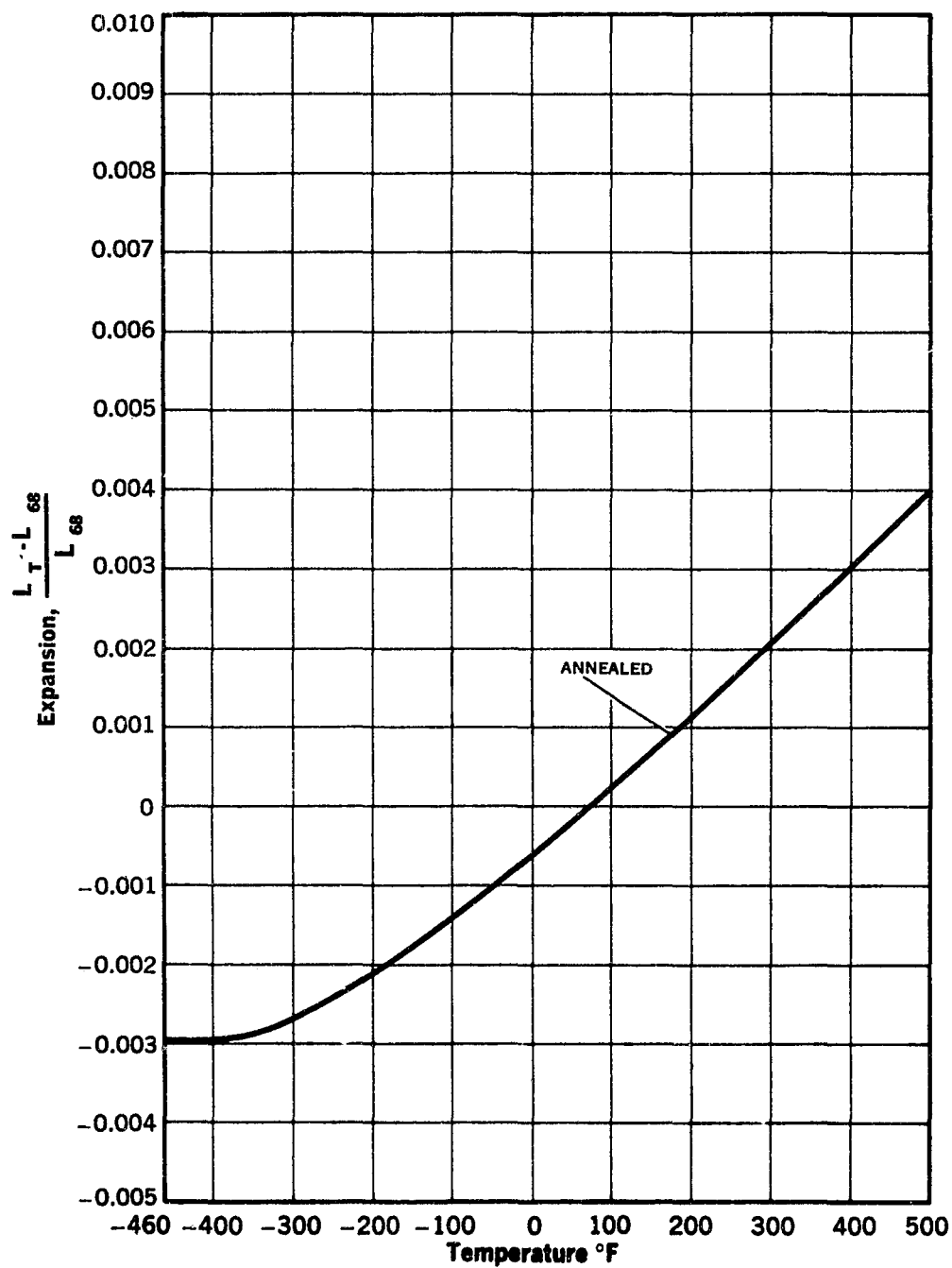


Figure 33. Thermal Expansion of AISI Type 304 Stainless Steel

2. Thermal Conductivity

Thermal conductivity is of considerable importance in the selection of materials for low-temperature applications. For support, piping, sensing lines, etc., design engineers prefer a material with low thermal conductivity. A high conductivity reduces thermal gradients during the initial cool-down but results in much higher heat gains through the piping when the equipment is in service. The levels of thermal conductivity of the family of steels are satisfactory for the vast majority of cryogenic equipment (Tables 5 and 17).

Thermal conductivity is a factor in selecting the materials for supports in small, shop-erected vessels and for plumbing and support equipment. Because of their low thermal conductivity, ferrous materials provide a bonus to the operation of cryogenic equipment. In comparison with most nonferrous materials, steel containers require less insulation to maintain a given heat-leak rate. Thus, insulation costs can be reduced without increasing product loss. Conversely, by raising insulation equivalent to that used in aluminum vessels, product loss can be decreased.

D. Corrosion Resistance

Although the selection of materials of construction for low temperature service is necessarily based primarily on mechanical properties, the corrosion resistance of the materials must also be considered. Corrosion resistance is important for assuring adequate service life and also for minimizing product contamination.

The austenitic stainless steels, of course, afford excellent corrosion resistance in many chemical media, including both strong oxidizing acids and al-

kalis, and are practically immune to atmospheric corrosion in most locations. However, moist chloride environments can cause breakdown of the passive film on stainless steels, resulting in some staining and possible pitting. The alloy steels used for low temperature service, such as the 2¼, 3½, and 9C% nickel steels, although completely resistant to nearly all cryogenic liquids, are inherently less corrosion resistant than the stainless steels, and some corrosion is to be expected with these materials in the atmosphere or in chemical solutions. The addition of up to 12C% nickel to steel, in the absence of chromium, has little effect on corrosion resistance in chemical media, although the nickel does improve the atmospheric resistance somewhat.

Fortunately, because of the low reactivity of most chemicals at low temperatures, corrosion problems resulting from materials in contact with cryogenic liquids have been relatively few. The nickel steels give adequate service, from a corrosion standpoint, in nearly all low temperature applications. An exception is liquid fluorine, for which austenitic stainless steels are more suitable. Because of their excellent resistance to atmospheric corrosion when the equipment is not in use, austenitic stainless steels are also used for systems in which contamination of the cryogenic liquid by solid particles is critical.

In addition to corrosion of equipment by the pure cryogenic liquids, other factors must be considered. For example, moisture in fluorine can drastically increase corrosion. Also, hydrocarbon contaminants on the interior surface of the equipment can react with liquid oxygen or fluorine, causing localized hot spots where the liquids may react rapidly with the metal.

E. Surface Reflectivity and Emissivity

Emissivity is a factor with vacuum-insulated double-wall cryogenic vessels, as opposed to vessels with insulation between the inner and outer vessel walls. Emissivity is more of a factor in selecting materials for cryogenic equipment for space probes than for ICBM's or ground support equipment. It is usually not an important factor in the selection of materials for vessels, because of recent improvements in the insulation materials used between the two walls of cryo-

genic vessels. However, this factor can be important in space and environmental chambers operating at temperatures below -420°F and at high vacuums.

Surface reflectivity and emissivity are functions of surface treatment, finish and cleanliness. Normally, the stainless steels provide the best properties relative to cryogenic applications. 9% nickel steel normally develops an oxide coating. 9% nickel can be polished to meet normal surface reflectivity specifications with the major problem being prevention of the oxide formation when an air atmosphere is permitted in the space chamber.

Table 18. Outgassing Rate for Metallic Materials

A_m = area of sample (cm^2) S_a = pumping speed for air at 25°C (L/sec) K_h = air equivalent outgassing rate after h hr of pumping ($\text{torr-L-sec}^{-1}\text{-cm}^{-2}$) a_h = absolute value of slope of log-log graph of outgassing rate vs. time after h hr of pumping								
Material	A_m	S_a	$10^7 K_h$	a_h	$10^7 K_h$	a_h	$10^7 K_h$	a_h
1. Stainless steel EN 58B (polished, vapor degreased).....	..	1	0.049	1.6	0.014	..
2. Stainless steel.....	65	3.5	1.75	1.1	0.44	0.84	0.21	0.75
3. Stainless steel.....	..	0.7	0.9	0.75	0.3	0.75	0.2	0.75
4. Mild steel.....	65	3.5	5.4	1	1.4	1	0.5	1
5. Mild steel (slightly rusty).....	..	1	6	3.1	0.28	1.5	0.13	1
6. Steel, rusty.....	65	3.5	44	1.4	5.5	1.4	1.6	1.3
7. Iron.....	12	..	4	1	1	1
8. Nickel plated mild steel (polished, vapor degreased).....	..	1	5	2	0.036	1.4	0.01	..
9. Nickel plated steel.....	65	3.5	2.8	2
10. Chrome plated mild steel (polished, vapor degreased).....	..	1	0.1	1	0.023	0.93	0.009	..
11. Aluminum, anodized.....	65	3.5	3.6	0.8	1.1	2.3
12. Aluminum, bright rolled (cleaned in Stergene).....	65	3.5	0.22	1	0.075	1
13. Aluminum.....	12	..	15	1	3.7
14. Duralumin.....	..	0.7	1.7	0.75	0.6	0.75	0.35	0.75
15. Aluminum spray coated mild steel.....	65	0.4	0.6	0.75	0.2	0.75	0.1	0.75
16. Aluminum spray coated mild steel (rusty).....	65	0.4	1.8	0.65	0.8	0.75	0.4	0.75
17. Copper (24 hr at 95 per cent humidity).....	100	0.32	0.2	2
18. Copper.....	12	..	23	1
19. Brass (24 hr at 95 per cent humidity).....	43	0.32	0.15	2.5
20. Brass, cast.....	650	3.5	10	1	2.5	1	1.1	0.75
21. Brass, wave-guide section.....	50	0.3	4	2	0.3	1.4	0.1	1.2
22. Nickel.....	12	..	6	1	1.5	1
23. Nickel.....	12	..	10	1	2.5	1
24. Molybdenum.....	12	..	7	1	1.7	1
25. Tantalum.....	12	..	9	1
26. Zirconium.....	12	..	13	1
27. Tungsten.....	12	..	2	1
28. Silver.....	12	..	6	1

Steel	Total Emissivity (%)
Type 310 stainless (dull finish)	28.4
Type 310 stainless (above sample ground with 1-0 emery)	25.4
Type 302 stainless (#4 finish)	15.3

Recent tests at the U. S. Steel Research Laboratory on Type 310 and Type 302 stainless steels indicate the total emissivity as given in the preceding table.

Concurrent with the importance of reflectivity and emissivity in space chamber applications, outgassing rates and diffusion properties of the various materials may also be important. Practical models of high vacuum systems are now designed to 10^{-9} torr (or less), and some vessels have temperature differentials of more than 1000°F between the inner and outer walls.

Where outgassing is important, Type 301 or Type 304 stainless steels are sometimes preferred. These materials, properly fabricated, will provide dependable service for high vacuum installations. Most outgassing problems can be traced to problems of fabrication and testing rather than to the metal itself.

In a report prepared by B. B. Dayton of Consolidated Vacuum Corporation, Rochester, New York, entitled "Relation Between Size of Vacuum Chamber, Outgassing Rate and Required Pumping Speeds," some relative information on the outgassing rates of various metals has been derived. These data are shown in Table 18, giving both the pumping speed, the outgassing rate constant and the absolute value of slope of the outgassing curve. These constants have been derived for 10^{-7} torr, which is a relatively moderate vacuum.

END OF REFERENCE
13

REFERENCE
14

**VAN HORN, KENT R., ED.: ALUMINUM. VOL. II. DESIGN
AND APPLICATION. AM. SOC. METALS, 1967.**

**THIS REFERENCE IS COPYRIGHTED MATERIAL AND THEREFORE
THE CONTENTS HAVE NOT BEEN REPRODUCED FROM THE TEXT.**

END OF REFERENCE
14

REFERENCE
15

**DEAN, L. E.; AND THOMPSON, W. R.: IGNITION CHARACTERISTICS
OF METALS AND ALLOYS. ARS J. VOL. 31, NO. 7, JULY 1961.**

9 Cohen, C. B. and Reshotko, E., "The Compressible Laminar Boundary Layer with Heat Transfer and Arbitrary Pressure Gradient," NACA Rep. 1294, 1956.

10 Gasley, Jr., C., "Theoretical Evaluation of the Turbulent Skin Friction and Heat Transfer on a Cone in Supersonic Flight," General Electric Co. Rep. R49A0524, 1949.

11 Schlichting, H., *Boundary Layer Theory*, McGraw-Hill Book Co., N. Y., 1955, Ch XXIIc.

12 Welsh, Jr., W. E. and Witte, A. B., "A Comparison of Analytical and Experimental Local Heat Fluxes in Liquid-Propellant Rocket Thrust Chambers," Jet Propulsion Laboratory TR 32-43, California Institute of Technology, Feb. 1 1961.

Ignition Characteristics of Metals and Alloys

L. E. DEAN¹ and
W. R. THOMPSON²

Aerojet-General Corp.
Sacramento, Calif.

The ignition characteristics of engine structural metals and alloys as influenced by the composition and pressure of the ambient atmosphere are of immediate interest to propulsion design engineers. Tubular test sections of the stainless steel, cobalt and nickel alloys, besides aluminum, copper and titanium were resistance heated in controlled atmospheres of oxygen, carbon dioxide and an equal mixture of these gases. Tube and gas temperatures obtained were correlated with color motion picture coverage of the manner in which the tube heated and failed. Stainless steels and cobalt alloys ignited within the melting point range of each material. Nickel alloys did not ignite until the melting point was reached. The rate of combustion increased with oxygen content. Stainless steels with a high nickel content appear most suited for applications at high temperatures in an oxidizing atmosphere.

THE ADVENT of nuclear energy and rocket propulsion has focused attention on the need for a more complete understanding of the mechanisms involved in the high temperature oxidation and ignition of metals in comparatively short time periods. The factors of metal composition and fabrication history, metal temperature and the composition, pressure and superficial velocity of the ambient atmosphere must be considered in any systematic evaluation of such ignition processes. In selecting materials to resist rapid oxidation, however, due emphasis must be given to other necessary metal prerequisites, including high thermal conductivity and tensile strength, low density, high melting point, ease of fabrication, and availability at reasonable cost.

Oxidation Mechanisms

Most metals and alloys, when exposed to an oxidizing atmosphere, undergo a chemical reaction with the oxidizing component of the gas phase, forming an oxide film or scale on

the surface of the metal. The physical and chemical reactions controlling oxidation (e.g., the rate at which the oxide forms and the nature of its bond to the metal surface) are complex functions of a number of variables. These include not only the chemical composition and physical state of the metal surface, and the geometry of the metal object, but also environmental factors (i.e., the chemical composition and fluid-dynamical characteristics of the gaseous environment and the pressure and temperature of the entire system).

Those metals that form a nonporous oxide film which adheres tightly to the base metal are immune to further oxidation. Ignition of the metal will not normally occur unless this protective film is broken. Nickel and aluminum have this desirable characteristic. However, if the oxide film is porous, or does not adhere to the base metal, oxidation will occur. This results in destruction of the metal through complete conversion to the oxide form. Ignition occurs more readily for metals forming such films. Mild steel, molybdenum and titanium have these characteristics. For most common metals, under ambient atmospheric conditions, such oxidation rates are comparatively slow.

Oxidation is an exothermic reaction. For slow rates of oxidation (e.g., the rusting of steel) the heat of reaction at the surface of the metal is dissipated principally by conduction to the bulk of the metal and by convection to the atmosphere. The metal temperature thus remains essentially at the ambient level. If, however the rate of oxidation is so rapid that

Presented at the ARS 15th Annual Meeting, Washington, D. C., Dec. 5-8, 1960.

¹ Head, Physical Research Section, Research and Material Dept., Liquid Rocket Plant. Member ARS.

² Senior Engineer, Advanced Research Div., Azusa, Calif. Member ARS.

* Numbers in parentheses indicate References at end of paper.

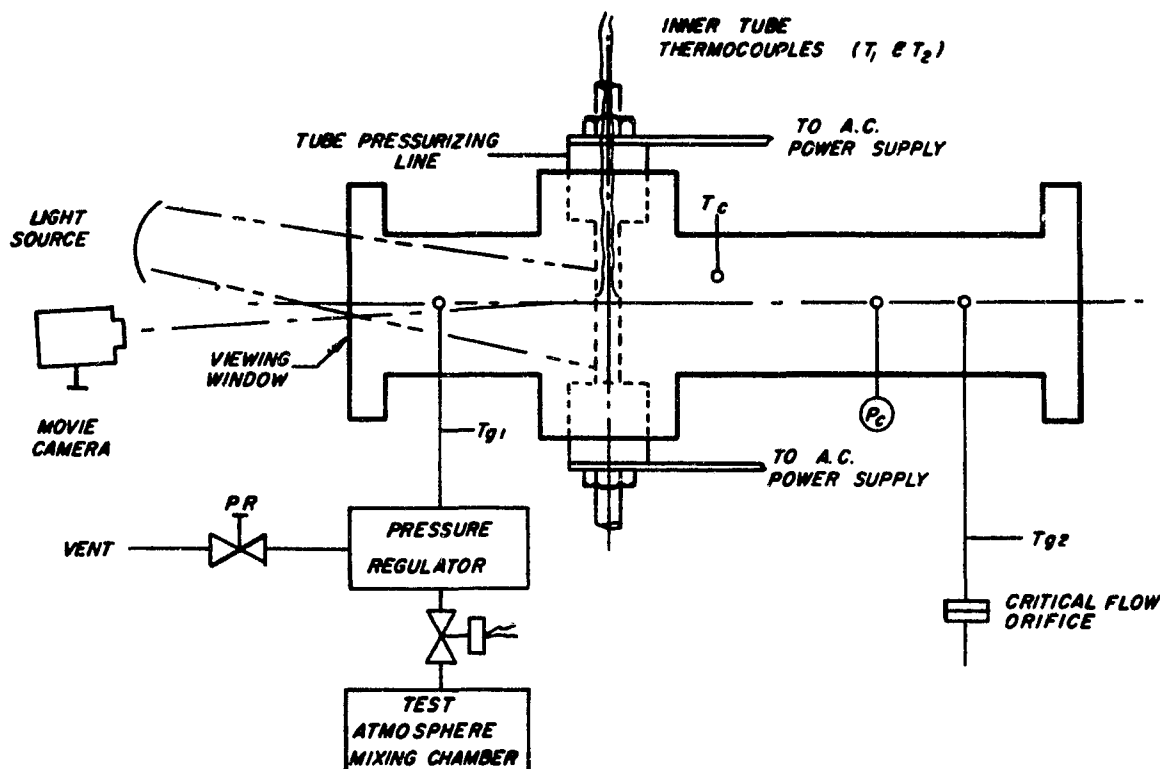


Fig. 1 Schematic of test apparatus

the generated heat cannot be removed from the surface at the same rate, the sensible heat of the surface increases with an accompanying temperature rise. This process continues until ignition of the metal occurs.

The problem of whether ignition, or kindling, of metals occurs below, at or above the melting point of the metal or alloy depends to an appreciable extent on the characteristics of the oxide film and on the overall rate of oxidation. For example, Fassell and co-workers (1) have shown that for magnesium alloys, the ignition temperature decreases as the oxidation rate is increased. The ignition temperatures of pure metals have been studied by Grosse and Conway (2) and by Mellor (3). Considerable data have been obtained by Reynolds (4) concerning the ignition of metals and various alloys in air and in oxygen and helium atmospheres under both stagnant and flowing conditions. In this investigation metal temperatures up to the point of ignition were measured by optical pyrometry. It was found that metals such as carbon steel, Type 410 stainless steel, molybdenum, tantalum, titanium and tungsten would ignite below their melting point. Metals such as Type 302 stainless steel and Inconel X ignited when the metal melted. No ignition occurred when nickel, Inconel and copper were tested in oxygen atmospheres. In general, the rate of burning was found to increase with pressure.

Hill and co-workers (5) reported that titanium, iron, carbon steel and 4130 steel spontaneously ignited in the solid phase (below the melting point) when heated in an atmosphere of oxygen. These metals melted rapidly while burning. Inconel, copper, 18-8 stainless steel, monel and aluminum could not be made to ignite spontaneously at temperatures up to melting with the equipment available. These tests were conducted under both static and flow conditions in air, oxygen and nitrogen atmospheres. Recent work at Aerojet-General (6) on the rates of self-sustaining burning of magnesium in

oxygen (with oxygen pressure and superficial velocity as variables) indicated that the burning rate followed either increased oxygen velocity or increased pressure. The rate controlling step appeared to be the maximum rate of vaporization of the metal at a temperature slightly above its boiling point. The same work contains a critical review and reinterpretation of the Eyring-Zwolinsky theory of metal ignition, based on the experimental data reported in (1). Microscopic intergranular oxidation at the surface of the metal, producing localized hot spots at the metal surface, may result in metal vaporization and ignition.

Description of the Test Apparatus and Testing Procedure

The test technique consisted basically of resistance-heating to destruction tubular specimens of various metals and alloys while surrounded by the test atmosphere at the required pressure. A schematic of the test apparatus is shown in Fig. 1. Tubular sections of the metal to be tested were clamped in the electrodes in a horizontal position in the testing device, parallel to the viewing port at one end of the cylinder. The chamber was pressurized to 50, 300 or 800 psia with either commercial-grade oxygen, carbon dioxide or a 50-50 mixture (by volume) of the two gases. Controlled cross flow of the chamber gas around the test piece to the outside air prevented stagnation of the atmosphere within the apparatus. The metal was then resistance heated by applying alternating current in step-wise increments at a rate so that metal failure occurred within one to two minutes after the initial application of power. Tube and gas temperatures, as well as power inputs, were continuously recorded. Color motion picture photography recorded the manner in which the tube heated and failed.

Test sections were 4 in. lengths of commercial tubing homo-

TEST ATMOSPHERE	
100% O ₂	
50% O ₂ - 50% CO ₂	
100% CO ₂	
100% NITROGEN	
100% HELIUM	

Fig. 2 Effect of atmosphere on kindling of 347 stainless steel (300 psia)

geneous to visual inspection. Tube diameters tested were either 0.500 or 0.375 in., whereas wall thicknesses varied from 0.010 to 0.035 in. It was necessary to machine some samples to obtain wall thicknesses having the desired electrical resistivity for cases where commercial tubing of the desired wall thickness was not available. Two no. 30 gauge chromel-alumel thermocouples were spotwelded or otherwise affixed to the inner tube walls at the midpoint of the tube (platinum-platinum 10% rhodium thermocouples were also used for a limited number of tests). Thermocouple lead wires were led through a 0.25-in. steel tube which was then filled with an epoxy resin to seal the outlet. A bleed orifice calculated to allow the desired gas cross-flow velocity around the test piece was installed downstream of the test chamber. The test atmosphere, prepared in the mixing chamber by pressurizing with the desired gases (using the pressure ratio as indicative of the volume fraction of each gas present), was then admitted to the test fixture at the desired pressure.

Power, controlled through a variable autotransformer, was applied to steel and alloy tubes in increments of approximately 0.25 v at 5-sec. intervals and increments of approximately 0.02 v at 5-sec intervals for the nonferrous test sections. Tests were continued until either tube failure occurred or the maximum voltage output of the transformer was reached. Two hundred individual tests were conducted in this manner.

Experimental Results

Two general series of tests were conducted. Since Type 347 stainless steel has wide application in fabricating propulsion system hardware, the ignition characteristics of this alloy were most intensively studied. More limited testing was performed on samples of the other metals and alloys.

347 Stainless Steel

A complete series of tests were conducted at 50, 300 and 800 psia in atmospheres of oxygen, carbon dioxide and an equal-volume mixture of these gases. Additional tests were made using nitrogen and helium atmospheres at the 300 psia pressure level. Tests were also conducted on the effects of superficial gas cross-flow velocity, rate of heating, and special metal surface treatment.

Effect of gas composition at 300 psia pressure. Failure of the test specimens occurred within the melting point range for all the gas compositions tested. The metal ignited in 100% oxygen and 50% O₂-50% CO₂ atmospheres with partial destruction of the test sections. Test results are shown in Fig. 2.

Effect of gas pressure. No ignition occurred in oxygen at 50 psia. At 300 and 800 psia ignition took place within the melting point range of the alloy, resulting in destruction of the test specimen. The rate of burning and proportion of test section destroyed increased with pressure. No ignition occurred in a carbon dioxide atmosphere. Post-test specimen appearance is shown in Fig. 3.

Effect of other factors. Wide variations in gas cross-flow velocity and in the rate of heating showed that ignition again took place within the melting point range of the metal. In tests where the tube was partially coated with a refractory ceramic, the metal ignited under the coating and burned as the coating flaked off the surface.

Carbon Steel and Other Stainless Steel Alloys

Effects of variations in gas composition and pressure upon the ignition of mild steel and Types 304, 310, 321, 410, AM350 and 17-7 PH stainless steel, comprises the bulk of the steel alloys used in rocket propulsion hardware.

Effect of an oxygen atmosphere. At a pressure of 50 psia, specimen ignition occurred within the melting point range of the metal with exception of Type 410 stainless steel which ignited at a lower temperature. At 800 psia, Type 304 stainless steels ignited at temperatures within the melting point range of the alloy. Ignition of the other metals tested oc-

TEST ATMOSPHERE			
TEST PRESSURE	100% O ₂	50% O ₂ — 50% CO ₂	100% CO ₂
50 PSIA			
300 PSIA			
800 PSIA			

Fig. 3 Typical test results, 347 stainless steel

TEST ATMOSPHERE	100% O ₂	50% O ₂ — 50% CO ₂	100% CO ₂
CARBON STEEL			
17-7 PH			
310 S.S.			
410 S.S.			

Fig. 4 Effect of atmosphere on kindling of iron alloys (300 psia)

TEST ATMOSPHERE	100% O ₂	50% O ₂ — 50% CO ₂	100% CO ₂
NICKEL "X"			
INCONEL "X"			
MONEL			
HASTALLOY "X"			

Fig. 5 Effect of atmosphere on kindling of nickel alloys (300 psia)

occurred at temperatures of 250 to 500 F below their respective melting points. The rate of burning was found to increase with pressure. At 50 psia the carbon steel sample was completely destroyed, whereas about 60 to 80% of the stainless steel test sections were consumed. At the higher pressure levels, essentially all the tubing between the electrodes was destroyed.

Effect of gas composition at 300 psia pressure. Comparison of photographic and instrument data for tubes heated to destruction in 100% O₂, in 100% CO₂, and in an equal-volume mixture of these gases showed that, with the exception of Type 410 stainless steel, each test sample failed at a temperature within the melting point range of the alloy. In an oxygen atmosphere up to 70% of each test section was destroyed due to ignition and combustion of the metal. In the 50% O₂-50% CO₂ mixture, when ignition did occur with carbon steel and Stainless types 347, 410 and AM 350 alloys, only partial destruction of the test specimen resulted. No ignition occurred in the carbon dioxide atmosphere; failure of the tube was due to melting. Test results are shown in Fig. 4.

Nickel Based Alloys

Test sections of six nickel based alloys were tested to destruction. These were Nickel A, Monel, Inconel X, Hastelloy C, Hastelloy R and Hastelloy X.

Effect of an oxygen atmosphere. At the 50 psia pressure level, test sections of these alloys all failed at temperatures within their melting point ranges. However, at 800 psia, both Inconel X and Monel failed at temperatures 250 to 500 F below their respective melting points. No ignition of the metal occurred with Nickel A at 50, 300 or 800 psia. Test sections of Monel, Inconel X, Hastelloy R and Hastelloy X ignited at a gas pressure of 800 psia. The ignition of Inconel X and Monel at the high gas pressure, and of Hastelloy R and Hastelloy X at all pressure levels resulted in partial destruction of the test section.

Effect of gas composition at 300 psia pressure. All test specimens failed at temperatures within their respective melting point ranges. Ignition of Hastelloy R in an oxygen atmosphere resulted in 60% destruction of the test section.

Although ignition occurred in oxygen for samples of Inconel X, Hastelloy C and Hastelloy X, only the portion of the tube immediately adjacent to the severance area was consumed. With the exception of Hastelloy R, no ignition occurred in the 50% O₂-50% CO₂ atmosphere. The appearance of these sections following the tests is shown in Fig. 5.

Cobalt Based Alloys

Two cobalt based alloys were studied in this program. These were Haynes 25 and Multimet.

Effect of an oxygen atmosphere. Ignition of test samples of these two alloys occurred within their respective melting point ranges. The rate of tube destruction increased with gas pressure; at the 50 psia pressure level, 5 to 30% of each test section was consumed after ignition, whereas at higher pressures 50 to 70% of each sample was destroyed.

Effect of gas composition at 300 psia pressure. Metal ignition occurred for both alloys in 100% oxygen with over 70% of each section destroyed. Test specimens of Multimet ignited in the 50-50 mixture of oxygen and carbon dioxide. The remains of the test samples are shown in Fig. 6.

Miscellaneous Metals

Of the nonferrous metals of importance to propulsion system design, aluminum, copper and titanium were selected for testing.

Effect of an oxygen atmosphere. Failure of the aluminum test section was due to melting of the metal with no subsequent ignition. At an oxygen pressure of 50 psia, no ignition occurred for the copper sample; however, at 300 psia ignition occurred and 60% of the test section was destroyed. Ignition of titanium occurred 250 to 1000 F below the melting point of the metal. Test sections were completely destroyed. Even the copper electrodes which held the test section in place

ignited and burned during the test conducted at 300 psia. Titanium was by far the most reactive of all the metals tested.

Effect of gas composition at 300 psia pressure. Failure of the aluminum test sections in oxygen, carbon dioxide and their equal-volume mixture was due solely to melting and subsequent severance of the tube. For copper, ignition and partial destruction was noted for tests conducted in oxygen with no ignition in other gas compositions. Titanium was observed to ignite in all the atmospheres tested. Even in the 100% CO₂ atmosphere the test specimen was completely destroyed at a temperature 250 F below the melting point of the metal. The remains of the samples after testing are shown in Fig. 7.

Discussion of Test Results

Carbon Steel and Stainless Steel Alloys

The ignition temperature of carbon steel in an oxygen atmosphere as reported in (3 and 5) varies from 1700 to 2300 F. In this study, the ignition temperature was found to vary between 2000 to 2700 F, depending upon the pressure. It is probable that the oxide film on the tube's surface, as noted in the motion picture coverage, influenced the ignition characteristics of the test piece.

Stainless steels having an appreciable nickel content may be raised to their melting point before ignition will occur. Alloys such as Type 410 and Type 430, which have no nickel as an alloying element, ignite at temperatures 250 to 300 F below their nominal melting points.

For all the ferrous alloys investigated, the rate of burning increased with increases in gas pressure. Since combustion depends upon a continuous renewal of reactants in the combustion zone, it is obvious that increasing the total oxygen pressure results in a proportionately greater concentration of oxygen molecules available to the flame front. After initial




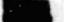


TEST ATMOSPHERE	100 % O ₂	50 % O ₂ — 50 % CO ₂	100 % CO ₂
HAYNES 25			
MULTIMET			

Fig. 6 Effect of atmosphere on kindling of cobalt alloys (300 psia)








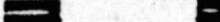

TEST ATMOSPHERE	100 % O ₂	50 % O ₂ — 50 % CO ₂	100 % CO ₂
ALUMINUM			
COPPER			
TITANIUM			

Fig. 7 Effect of atmosphere on kindling of metals (300 psia)

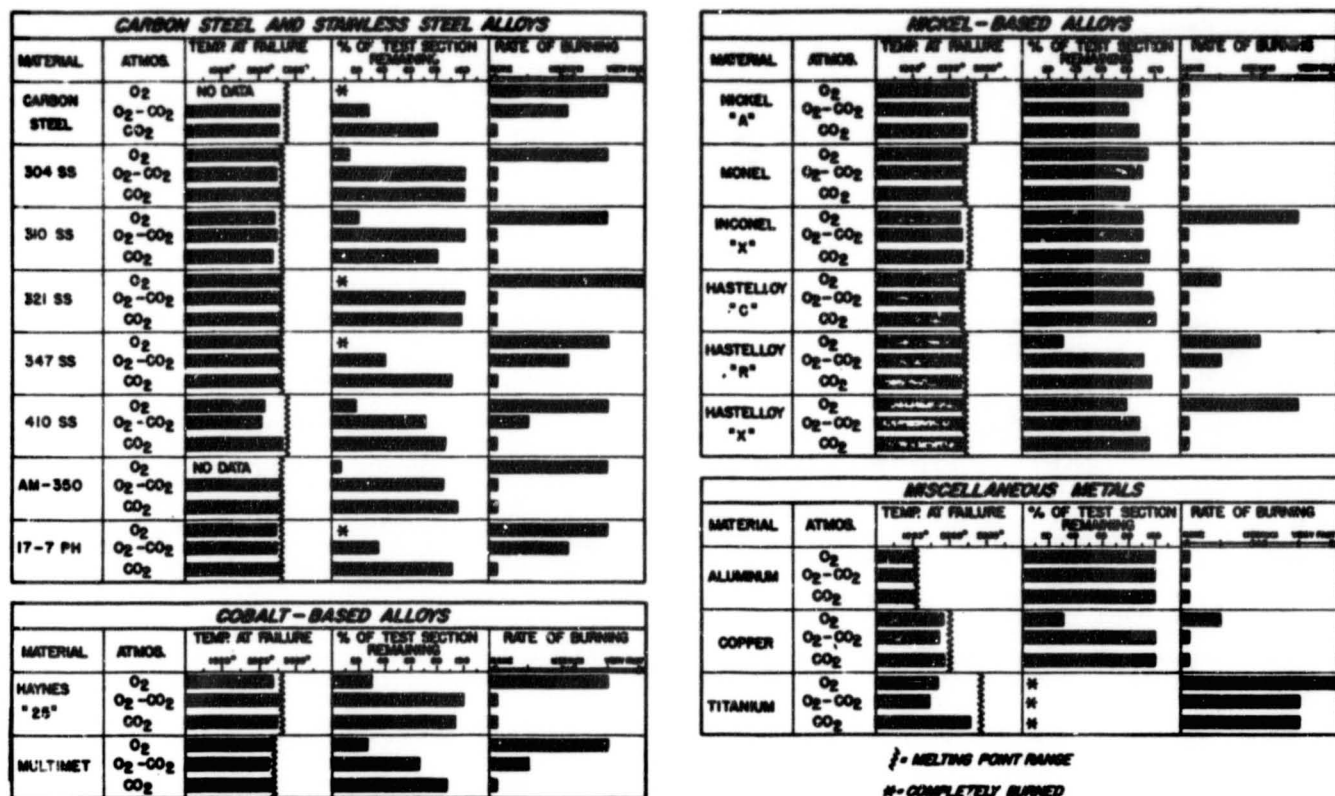


Fig. 8 Test summary in various atmospheres, pressure = 300 psia

ignition, the entire test section was destroyed at the higher pressure levels, whereas the test section was only partially destroyed for low pressure tests.

In atmospheres composed of 50% oxygen-50% carbon dioxide, ignition occurred within the melting point ranges of the particular metals tested (with the exception of Type 410 stainless steel). The rate of burning and the related length of sample consumed during the test decreased with decreasing oxygen concentration. Failure of the test sections in a carbon dioxide atmosphere occurred owing to melting and severance of the tube. No ignition was noted.

Nickel Based Alloys

Test results with Nickel A showed tube failure occurred by tube melting and severance. No ignition or combustion was observed in any test. Reynolds (4) reports similar results with Inconel in an oxygen atmosphere. Apparently a protective nonporous adherent oxide coating forms on the surface of the metal, inhibiting further oxidation.

Inconel X was found to ignite and burn at the 300 and 800 psi pressure levels. Only at the higher pressure did combustion completely destroy the tube. Reynolds also reports ignition and burning with Inconel X in an oxygen atmosphere. The ignition of Inconel X may possibly be attributed to the presence of 2-1/2% titanium in this alloy.

Of the three Hastelloy alloys evaluated, Hastelloy C appears most resistant to oxidation at high temperatures and pressures. Ignition and partial destruction of test sections of Hastelloy R and Hastelloy X occurred at both 300 and 800 psi gas pressure.

No ignition and subsequent combustion of nickel based alloys was noted in either carbon dioxide or 50% oxygen-50% carbon dioxide atmospheres with one exception. Partial destruction of a test section of Hastelloy R was observed for tests in the 50-50 mixture. Again, the ignition may result from the presence of titanium in the alloy.

Cobalt Based Alloys

In an oxygen atmosphere, ignition of the two cobalt based alloys occurred when the metal reached the melting point. The rate of destruction of the test section increased with increasing pressure, with both metals igniting almost explosively at the 800 psia level.

No ignition was observed for Haynes 25 in either carbon dioxide or the oxygen-carbon dioxide mixture at 300 psia, tube failure occurring due to melting. Multimet N-155 melted in the CO₂ atmosphere, whereas partial destruction occurred in the test with the O₂-CO₂ mixture.

Nonferrous Metals

No ignition or burning of the aluminum alloy occurred. Grosse and Conway (2) have shown that aluminum will not ignite until its temperature is raised above the melting point (1800 F). In the present study, evaluation of photo coverage showed that the tube melted and severed with no incandescence or hot spots. The high thermal conductivity allowed heat from the melting zone to be quickly dissipated, lowering the temperature below its kindling point.

Results of this study show that copper ignites at a temperature slightly below its melting point in a 100% oxygen atmosphere and at a pressure of 300 psia, resulting in the destruction of approximately 70% of the test specimen. Ignition of copper may be related to the condition of the oxide film and consequently dependent on the test conditions.

The results indicate that in an oxygen atmosphere, ignition of titanium will take place when the metal temperature exceeds 1500 F. In a carbon dioxide atmosphere, ignition was found to occur at a temperature 250 F below the melting point. It is reported (8 and 9) that titanium will react with carbon dioxide and form titanium dioxide and carbon monoxide. This reaction will occur at a temperature of 1650 F. Reynolds (4) also reports a wide range of temperatures wherein titanium

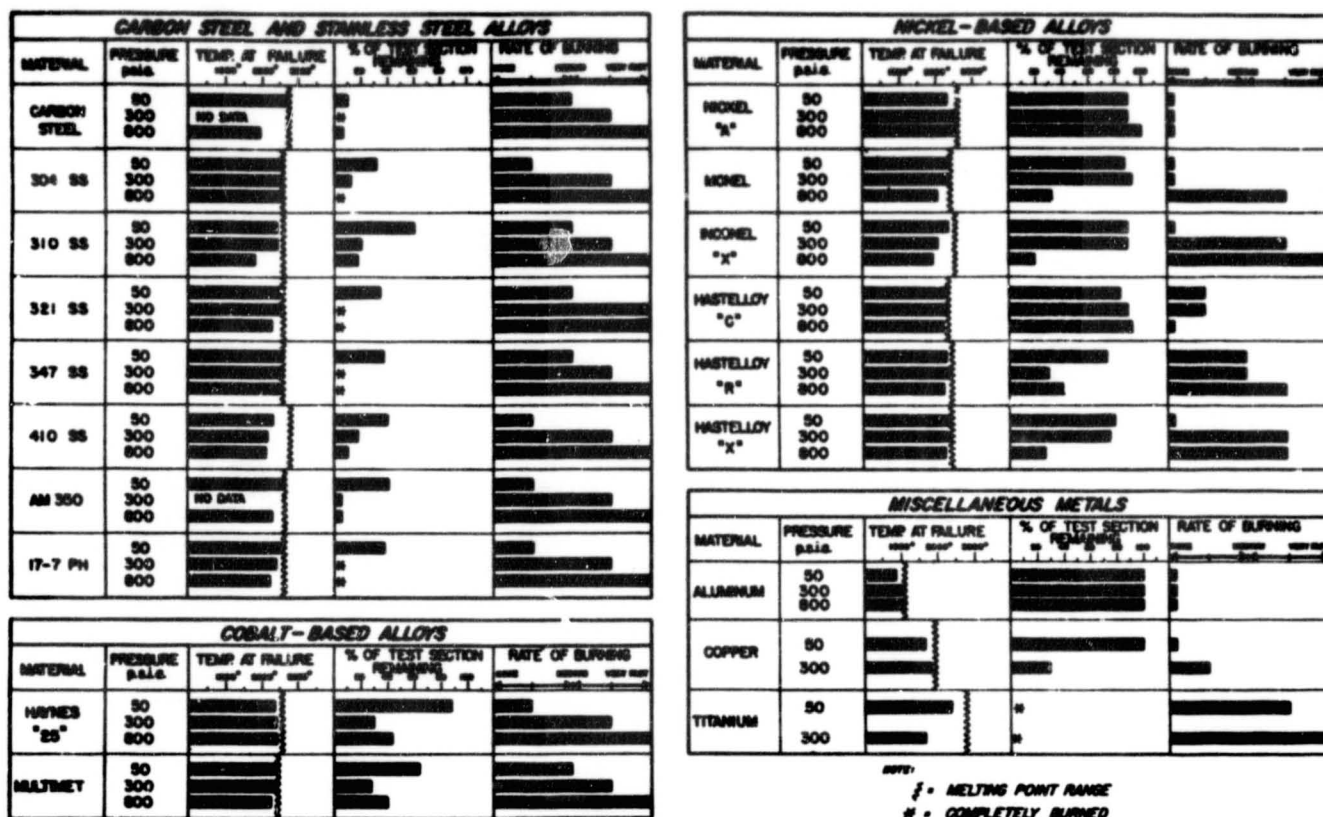


Fig. 9 Test summary in oxygen atmosphere

may ignite. These results indicate that ignition of titanium is also dependent upon the condition of the oxide film and consequently upon the particular testing technique employed. Of all the metals tested, titanium proved to be the most reactive metal at elevated temperatures regardless of the composition of the atmosphere.

Conclusions

The results of this investigation are graphically summarized in Fig. 8, in which the effect of gas composition at a constant pressure is shown, and in Fig. 9, in which the effect of pressure upon tubes in an oxygen atmosphere is noted. The following general conclusions are indicated.

The ignition of stainless steels (containing nickel) occurred within the melting point ranges of the alloys during tests in an oxygen atmosphere. Steel alloys, with no nickel content ignited at temperatures below their melting points. The rates of burning and destruction of the test sections increased with increasing oxygen concentrations.

Most of the nickel based alloys did not ignite until the melting point was reached. Nickel A did not ignite in oxygen, and, whereas ignition was noted for the other alloys at elevated pressures, the rate of burning of Nickel A was generally less severe than that observed for the ferrous based alloys.

Cobalt based alloys ignited at temperatures within their melting point range. The rates of burning were similar to those of the iron based alloys; however, the resulting damage to the test sections was less severe.

Ignition did not occur with the aluminum alloy studied. A copper test section ignited when tested in oxygen at the 300 psia pressure level. Titanium was the most reactive of all the metals tested, and was the only metal which ignited in an atmosphere of carbon dioxide.

From these test results it is concluded that stainless steels with a high nickel content are the most suitable material for the manufacture of such items as rocket engine combustion chambers. This metal is especially adaptable where high temperature environment plus resistance to oxidation reactions are major controlling factors.

References

- 1 Fassell, W. M., Gulbransen, L. B., Lewis, J. R. and Hamilton, J. H., "Ignition Temperatures of Magnesium and Magnesium Alloys," *J. Metals*, vol. 3, March 1940, pp. 522-528.
- 2 Groase, A. V. and Conway, J. B., "Combustion of Metals in Oxygen," *Ind. and Eng. Chem.*, vol. 50, April 1958, pp. 663-672.
- 3 Mellor, J. W., *Treatise on Inorganic and Theoretical Chemistry*, Longmans, Green and Co., N. Y., 1946.
- 4 Reynolds, W. C., "Investigation of Ignition Temperatures of Solid Metals," NASA Tech. Note TN D-182, Oct. 1959.
- 5 Hill, P. R., Adamson, D., Fuland, D. H. and Bressette, W. E., "High-Temperature Oxidation and Ignition of Metals," NACA Rep. L55L23b, Research Mem. RM, March 1956.
- 6 "The Reaction of Metal in Oxidizing Gases at High Temperatures," Aerojet-General Rep. AGC-IDO-28000, Azusa, Calif., April 30, 1957.
- 7 Harrison, P. L., "The Combustion of Titanium and Zirconium," *Seventh Symposium (International) on Combustion*, Butterworths Scientific Publications, London, Eng.
- 8 Sidgwick, N. V., *The Chemical Elements and Their Compounds*, Oxford University Press, N. Y., 1950.
- 9 Moeller, T., *Inorganic Chemistry*, John Wiley and Sons, N. Y., 1952.

END OF REFERENCE
15

REFERENCE

16

**VAN HORN, KENT R., ED.: ALUMINUM. VOL. III. FABRICATION
AND FINISHING. AM. SOC. METALS, 1967.**

**THIS REFERENCE IS COPYRIGHTED MATERIAL AND THEREFORE
THE CONTENTS HAVE NOT BEEN REPRODUCED FROM THE TEXT.**

END OF REFERENCE

16

REFERENCE

17

ANON.: SAE HANDBOOK. SOC. AUTOMOTIVE ENG., 1969.

**THIS REFERENCE IS A COPYRIGHTED HANDBOOK AND THEREFORE
THE CONTENTS HAVE NOT BEEN REPRODUCED FROM THE TEXT.**

END OF REFERENCE

17

REFERENCE
18

KEY, C. F.; AND RIEHL, W. A.: COMPATIBILITY OF MATERIALS WITH LIQUID OXYGEN. NASA TM X-985, 1964.

THIS REFERENCE IS LIMITED IN DISTRIBUTION FOR INTERNAL U.S. GOVERNMENT USE ONLY.

END OF REFERENCE
18

REFERENCE

19

TOULOUKIAN, Y. S.: THERMOPHYSICAL PROPERTIES OF HIGH TEMPERATURE SOLID MATERIALS. VOL. 2. PARTS I AND II, MACMILLIAN CO., 1966.

THIS REFERENCE IS A COPYRIGHTED HANDBOOK AND THEREFORE THE CONTENTS HAVE NOT BEEN REPRODUCED FROM THE TEXT.

END OF REFERENCE
19

REFERENCE

20

HUST, J. G.; POWELL, ROBERT L.; AND WEITZEL, D. H.: THERMAL CONDUCTIVITY, ELECTRICAL RESISTIVITY AND THERMOPOWER OF AEROSPACE ALLOYS FROM 4 TO 300K. REP. 9732, NATIONAL BUREAU OF STANDARDS (NASA CR-108088), JUNE 9, 1969.

THIS REFERENCE IS A COPYRIGHTED HANDBOOK AND THEREFORE THE CONTENTS HAVE NOT BEEN REPRODUCED FROM THE TEXT.

END OF REFERENCE
20

REFERENCE

21

ELDRIDGE, E. A.; AND DEEM, H. W.: REPORT ON PHYSICAL PROPERTIES OF METALS AND ALLOYS FROM CRYOGENIC TO ELEVATED TEMPERATURES. SPEC. TECH. PUBL. NO. 296, ASTM, 1961.

THIS MATERIAL HAS BEEN APPROVED TO BE MADE AVAILABLE FOR THE
TECHNICAL AND SCIENTIFIC COMMUNITY PER LETTER ALBERT L. BATIK
TO JOANNE FOLK DATED OCT. 6, 1972.

REPORT ON
PHYSICAL PROPERTIES
of
METALS AND ALLOYS
from
CRYOGENIC TO ELEVATED TEMPERATURES

Data Compiled by and Issued Under the Auspices of

THE DATA AND PUBLICATIONS PANEL

of

THE ASTM-ASME JOINT COMMITTEE ON
EFFECT OF TEMPERATURE ON THE PROPERTIES OF METALS

Prepared for the Panel by

E. A. ELDRIDGE AND H. W. DEEM

LIBRARY COPY

RETURN TO
LEWIS LIBRARY
CLEVELAND, OHIO

Published by the

AMERICAN SOCIETY FOR TESTING MATERIALS
1916 RACE STREET, PHILADELPHIA 3, PENNSYLVANIA

536.5
E2
C. 4

THIS MATERIAL HAS BEEN APPROVED TO BE MADE AVAILABLE FOR THE
TECHNICAL AND SCIENTIFIC COMMUNITY PER LETTER ALBERT L. BATIK
TO JOANNE FOLK DATED OCT. 6, 1972.

REPORT ON
PHYSICAL PROPERTIES
of
METALS AND ALLOYS
from
CRYOGENIC TO ELEVATED TEMPERATURES

Data Compiled by and Issued Under the Auspices of
THE DATA AND PUBLICATIONS PANEL
of
THE ASTM-ASME JOINT COMMITTEE ON
EFFECT OF TEMPERATURE ON THE PROPERTIES OF METALS

Prepared for the Panel by
E. A. ELDRIDGE AND H. W. DEEM

LIBRARY COPY
DONATED
LEVIN LIBRARY
CLEVELAND, OHIO

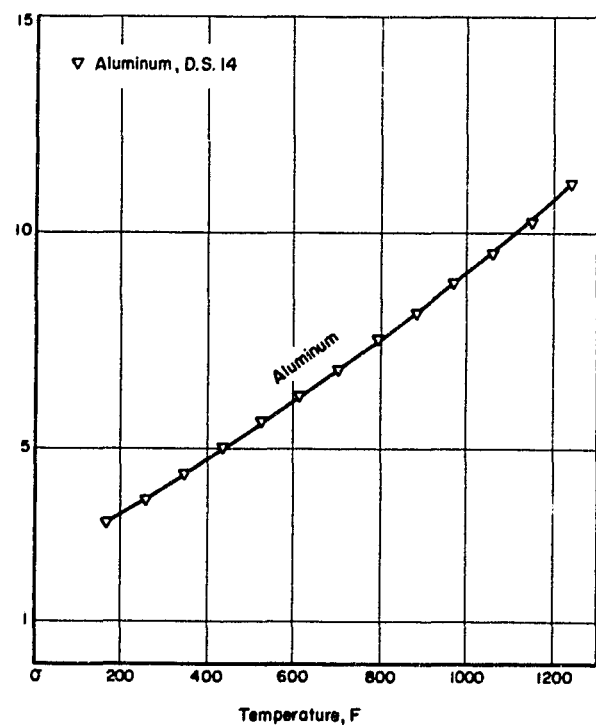
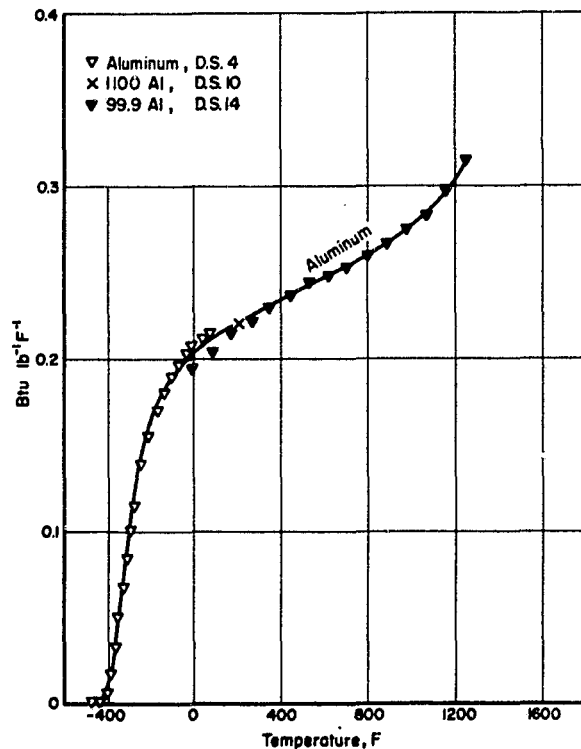
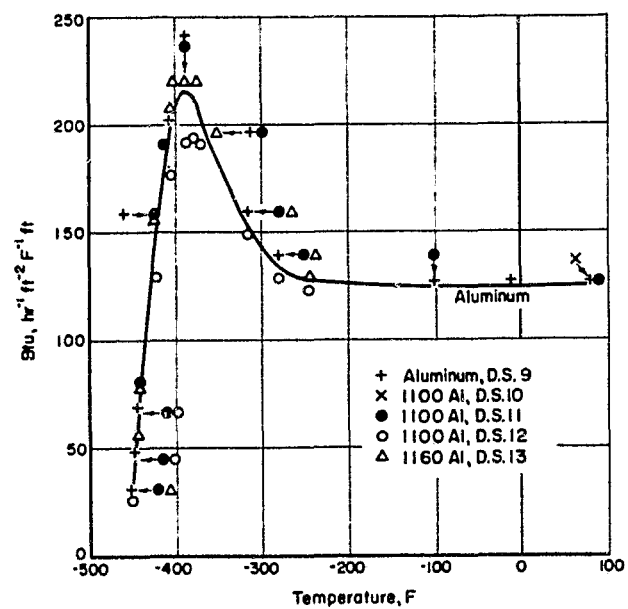
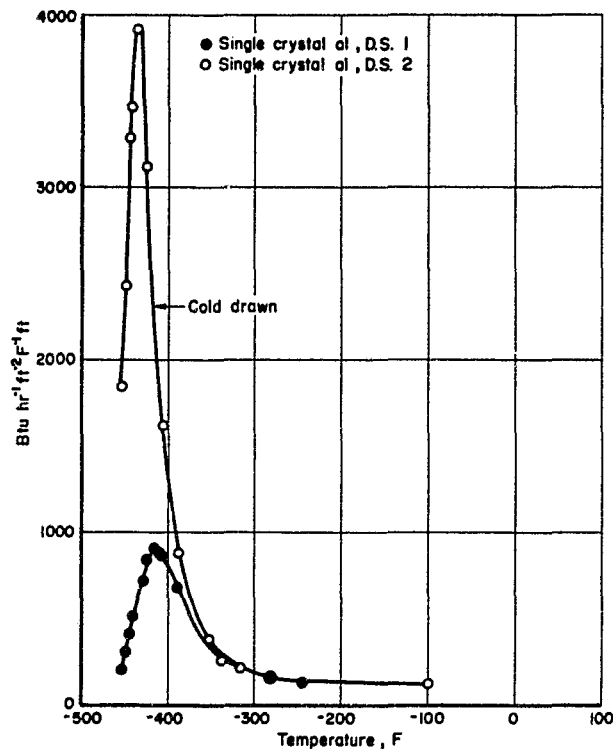
ASTM Special Technical Publication No. 296
List Price: \$4.75
Price to ASTM and ASME Members: \$3.80

Published by the
AMERICAN SOCIETY FOR TESTING MATERIALS
1916 RACE STREET, PHILADELPHIA 3, PA.

CONTENTS

	PAGE
INTRODUCTION	1
ALUMINUM AND ITS ALLOYS	
Aluminum	5
Aluminum-Copper Alloys	9
Aluminum-Magnesium Alloys	16
Aluminum-Manganese Alloys	20
COBALT AND ITS ALLOYS	
Cobalt	25
Cobalt Base Alloys	27
IRON AND ITS ALLOYS	
Iron	35
Alloy Steels	42
Carbon Steels	51
Cast Iron	59
Chromium-Nickel Stainless Steels	62
Ferritic-Chromium Stainless Steels	78
Martensitic-Chromium Stainless Steels	81
Age Hardening Stainless Steels	86
Superalloys	97
Iron Base Alloys	106
MAGNESIUM AND ITS ALLOYS	
Magnesium	115
Magnesium-Aluminum Alloys	118
Magnesium-Manganese Alloys	129
Magnesium-Thorium Alloys	131
Magnesium-Zinc Alloys	136
Magnesium-Zirconium Alloys	139
MOLYBDENUM AND ITS ALLOYS	
Molybdenum	145
Molybdenum Base Alloys	154
NICKEL AND ITS ALLOYS	
Nickel	161
Nickel-Chromium Alloys	167
Nickel-Chromium-Cobalt Alloys	172
Nickel-Chromium-Iron Alloys	181
Nickel-Copper Alloys	191
Nickel-Iron-Chromium-Molybdenum Alloys	196
Nickel Base Alloys	204

ALUMINUM



ASTM-ASME JOINT COMMITTEE ON EFFECT OF
TEMPERATURE ON PROPERTIES OF METALS

6

MATERIAL	Aluminum				HEAT NUMBER			
CHEMICAL COMPOSITION PER CENT								
FORM HEAT TREATMENT								
REFERENCE	Thomas and Mendoza; received from V. J. Johnson, NBS Cryogenic Engineering Laboratory, Boulder, Colorado.							
REMARKS								

ELECTRICAL RESISTIVITY

TEMP, F	MICRONH- CM	TEMP, F	MICRONH- CM	TEMP, F	MICRONH- CM	TEMP, F	MICRONH- CM
-453	0.0065						

ASTM-ASME JOINT COMMITTEE ON EFFECT OF
TEMPERATURE ON PROPERTIES OF METALS

7

MATERIAL	Aluminum				HEAT NUMBER			
CHEMICAL COMPOSITION PER CENT								
FORM HEAT TREATMENT								
REFERENCE	Justi and Schiffers; received from V. J. Johnson, NBS Cryogenic Engineering Laboratory, Boulder, Colorado.							
REMARKS								

ELECTRICAL RESISTIVITY

TEMP, F	MICRONH- CM	TEMP, F	MICRONH- CM	TEMP, F	MICRONH- CM	TEMP, F	MICRONH- CM
-424	0.0045	-435	0.0035				

ASTM-ASME JOINT COMMITTEE ON EFFECT OF
TEMPERATURE ON PROPERTIES OF METALS

8

MATERIAL	Aluminum				HEAT NUMBER			
CHEMICAL COMPOSITION PER CENT								
FORM HEAT TREATMENT								
REFERENCE	Meissner and Voigt; received from V. J. Johnson, NBS Cryogenic Engineering Laboratory, Boulder, Colorado.							
REMARKS								

ELECTRICAL RESISTIVITY

TEMP, F	MICRONH- CM	TEMP, F	MICRONH- CM	TEMP, F	MICRONH- CM	TEMP, F	MICRONH- CM
-320	0.252	-423	0.01875	-451	0.01625	-457	0.01675

ASTM-ASME JOINT COMMITTEE ON EFFECT OF
TEMPERATURE ON PROPERTIES OF METALS

9

MATERIAL	Commercial Pure Aluminum				HEAT NUMBER			
CHEMICAL COMPOSITION PER CENT	Al							
	99							
FORM HEAT TREATMENT								
REFERENCE	Powell, R. L., Hall, W. F. and Roder, H. M., to be published; as found in "A Compendium of the Properties of Materials at Low Temperatures, Phase I", Part II, edited by Victor J. Johnson, NBS Cryogenic Engineering Laboratory, Boulder, Colorado (December, 1959).							

THERMAL CONDUCTIVITY

TEMP, F	BTU HR-1 FT-2 F-1 FT	TEMP, F	BTU HR-1 FT-2 F-1 FT	TEMP, F	BTU HR-1 FT-2 F-1 FT	TEMP, F	BTU HR-1 FT-2 F-1 FT
-453	31.8	-424	159	-352	196	-100	127
-449	48.5	-406	202	-316	159	-10	127
-445	69.3	-388	220	-280	139	80	127
Values interpolated from graph.							

ASTM-ASME JOINT COMMITTEE ON EFFECT OF
TEMPERATURE ON PROPERTIES OF METALS

10

MATERIAL	Aluminum Alloy--1100				HEAT NUMBER			
CHEMICAL COMPOSITION PER CENT	Al							
	99.0							
FORM HEAT TREATMENT	Annealing temperature: 650 F; Hot working temperature range: 500-950 F; Melting temperature range: 1190-1215 F.							
REFERENCE	"Materials in Design Engineering", Materials Selector, edited by H. R. Clauser, Vol 46, No. 4 (September, 1957).							

THERMAL CONDUCTIVITY

TEMP, F	BTU HR-1 FT-2 F-1 FT	TEMP, F	BTU HR-1 FT-2 F-1 FT	TEMP, F	BTU HR-1 FT-2 F-1 FT	TEMP, F	BTU HR-1 FT-2 F-1 FT
77	128						

COEFFICIENT OF LINEAR THERMAL EXPANSION

TEMP RANGE, F	F-1 X 10 ⁶	TEMP RANGE, F	F-1 X 10 ⁶	TEMP RANGE, F	F-1 X 10 ⁶	TEMP RANGE, F	F-1 X 10 ⁶
68-212	13.1						

SPECIFIC HEAT

TEMP, F	BTU LB-1 F-1	TEMP, F	BTU LB-1 F-1	TEMP, F	BTU LB-1 F-1	TEMP, F	BTU LB-1 F-1
212	0.22						

ELECTRICAL RESISTIVITY

TEMP, F	MICRONH-CM	TEMP, F	MICRONH-CM	TEMP, F	MICRONH-CM	TEMP, F	MICRONH-CM
68	2.92						

DENSITY

TEMP, F	LB CU IN-1	TEMP, F	LB CU IN-1	TEMP, F	LB CU IN-1	TEMP, F	LB CU IN-1
Room	0.098						
Data assumed to be at room temperature.							

ASTM-ASME JOINT COMMITTEE ON EFFECT OF TEMPERATURE ON PROPERTIES OF METALS

(11)

MATERIAL	Aluminum--1100 F			HEAT NUMBER			
CHEMICAL COMPOSITION PER CENT							
FORM	As fabricated.						
HEAT TREATMENT							
REFERENCE	Powell, R. L., Hall, W. J., and Roder, H. M., to be published (1958); as found in "A Compendium of the Properties of Materials at Low Temperatures, Phase I", Part II, edited by Victor J. Johnson, NBS Cryogenic Engineering Laboratory Boulder, Colorado (December, 1959).						

THERMAL CONDUCTIVITY

TEMP, F	BTU HR-1 FT-2 F-1 FT	TEMP, F	BTU HR-1 FT-2 F-1 FT	TEMP, F	BTU HR-1 FT-2 F-1 FT	TEMP, F	BTU HR-1 FT-2 F-1 FT
-453	31.2	-442	81.5	-388	220	-280	142
-449	43.9	-424	159	-352	196	-100	127
-445	65.3	-415	191	-316	162	88	127
Values interpolated from graph.							

ASTM-ASME JOINT COMMITTEE ON EFFECT OF TEMPERATURE ON PROPERTIES OF METALS

(12)

MATERIAL	Aluminum -- 1100 Alcoa			HEAT NUMBER			
CHEMICAL COMPOSITION PER CENT	Al	Fe	Si				
	99	0.41	0.22				
FORM							
HEAT TREATMENT	Annealed for 2 hours at 400 C.						
REFERENCE	Cryogenic Engineering Laboratories, National Bureau of Standards, Boulder, Colorado.						
REMARKS	Grain size--longitudinal 0.040 x 0.032 mm, Transverse 0.036 mm, Diamond point hardness - longitudinal - 36, Transverse = 34.						

THERMAL CONDUCTIVITY

TEMP, F	BTU HR-1 FT-2 F-1 FT	TEMP, F	BTU HR-1 FT-2 F-1 FT	TEMP, F	BTU HR-1 FT-2 F-1 FT	TEMP, F	BTU HR-1 FT-2 F-1 FT
-453	26	-424	129	-379	194	-280	129
-447	46	-406	175	-370	191	-244	123
-442	66	-388	192	-316	149		

ELECTRICAL RESISTIVITY

TEMP, F	MICRONH-CM	TEMP, F	MICRONH-CM	TEMP, F	MICRONH-CM	TEMP, F	MICRONH-CM
-453	0.205	-406	0.223	-352	0.34	-280	0.69
-442	0.206	-388	0.25	-316	0.49	80	2.93
-424	0.211	-370	0.29				

ASTM-ASME JOINT COMMITTEE ON EFFECT OF TEMPERATURE ON PROPERTIES OF METALS

(13)

MATERIAL	Aluminum--1160 Alcoa			HEAT NUMBER			
CHEMICAL COMPOSITION PER CENT	Al	Si					
	99	0.13					
FORM							
HEAT TREATMENT	As fabricated.						
REFERENCE	Cryogenic Engineering Laboratories, National Bureau of Standards, Boulder, Colorado.						
REMARKS	Grain size: longitudinal--0.024 x 0.008 mm, transverse--0.012mm Diamond point hardness--longitudinal--45, transverse--44.						

THERMAL CONDUCTIVITY

TEMP, F	BTU HR-1 FT-2 F-1 FT	TEMP, F	BTU HR-1 FT-2 F-1 FT	TEMP, F	BTU HR-1 FT-2 F-1 FT	TEMP, F	BTU HR-1 FT-2 F-1 FT
-453	32	-424	156	-388	220	-316	159
-447	56	-406	208	-379	220	-280	138
-442	80	-398	219	-352	197	-244	129

ASTM-ASME JOINT COMMITTEE ON EFFECT OF TEMPERATURE ON PROPERTIES OF METALS

(14)

MATERIAL	Aluminum			HEAT NUMBER			
CHEMICAL COMPOSITION PER CENT	Al	Si	B				
	99.9	0.05	0.03				
FORM	Slope of initial temp. rise curve in resistance heated wire.						
REFERENCE	Pochapsky, T. E., "Heat Capacity and Resistance Measurements for Aluminum and Lead Wires", ACTA Met. 1, pp. 747-51; as found in WADC Technical Report 58-476, "Thermophysical Properties of Solid Materials" January, 1959, Armour Research Foundation.						
REMARKS	Author estimates accuracy $\pm 5\%$.						

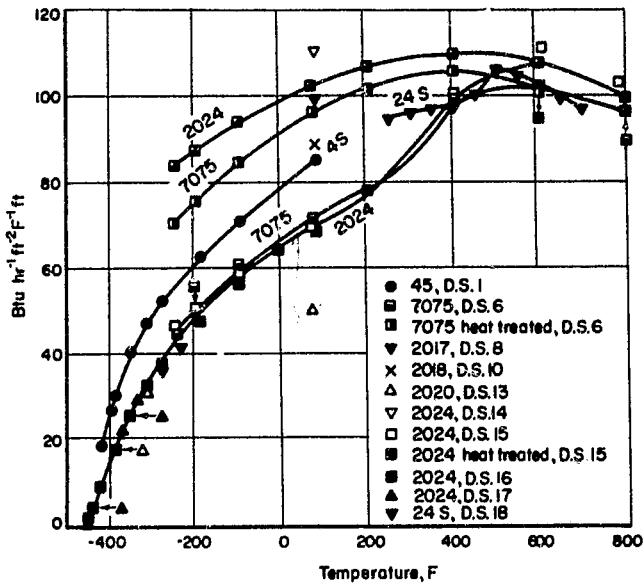
ELECTRICAL RESISTIVITY

TEMP, F	MICRONH-CM	TEMP, F	MICRONH-CM	TEMP, F	MICRONH-CM	TEMP, F	MICRONH-CM
170	3.3	530	5.6	800	7.5	1070	9.5
260	3.8	620	6.2	890	8.1	1160	10.2
350	4.4	710	6.8	980	8.8	1250	11.1
440	5.0						

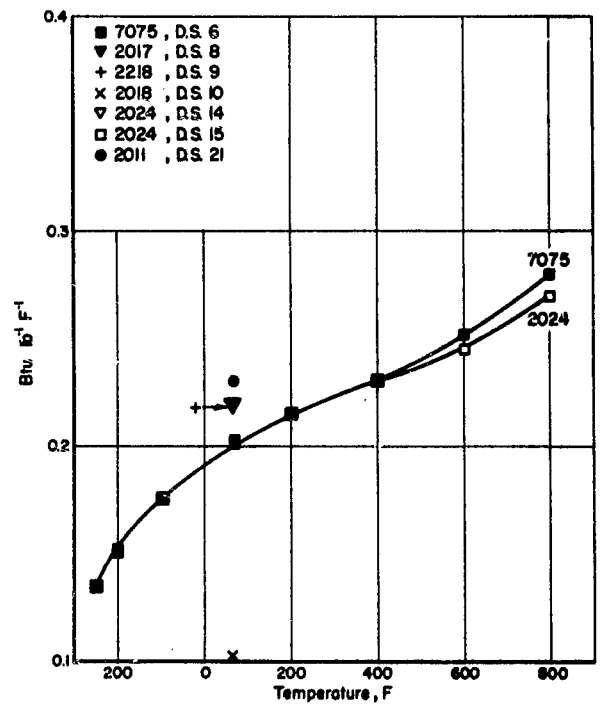
SPECIFIC HEAT

TEMP, F	BTU LB-1 F-1	TEMP, F	BTU LB-1 F-1	TEMP, F	BTU LB-1 F-1	TEMP, F	BTU LB-1 F-1
-10	0.196	350	0.230	710	0.263	1070	0.283
80	0.205	440	0.237	800	0.260	1160	0.257
170	0.214	530	0.244	890	0.267	1250	0.314
260	0.222	620	0.248	980	0.274		

ALUMINUM-COPPER ALLOYS



THERMAL CONDUCTIVITY OF ALUMINUM-COPPER ALLOYS



SPECIFIC HEAT OF ALUMINUM-COPPER ALLOYS

ASTM-ASME JOINT COMMITTEE ON EFFECT OF
TEMPERATURE ON PROPERTIES OF METALS

MATERIAL	Aluminum Alloy--45							HEAT NUMBER
CHEMICAL COMPOSITION PER CENT	Mn	Mg	Fe	Cu	Si	Cr	Ti	Al
	1.20	1.02	0.52	0.16	0.13	0.02	0.02	Bal
								96.93
FORM								
HEAT TREATMENT								
REFERENCE	Powers, R. W., Ziegler, J. B. and Johnston, H. L., TR 264-7, Cryogenics Laboratory, Ohio State University, p. 10 (1951); as found in "A Compendium of the Properties of Materials at Low Temperatures, Phase I", Part II, edited by Victor J. Johnson, NBS Cryogenic Engineering Laboratory, Boulder, Colorado (December, 1959).							

THERMAL CONDUCTIVITY

TEMP, F	BTU HR-1 FT-2 F-1 FT	TEMP, F	BTU HR-1 FT-2 F-1 FT	TEMP, F	BTU HR-1 FT-2 F-1 FT	TEMP, F	BTU HR-1 FT-2 F-1 FT
-419	19.1	-352	40.5	-280	52.6	-100	71.1
-397	27.7	-316	47.4	-190	63.0	80	85.5
-388	30.6						
Values interpolated from graph.							

ASTM-ASME JOINT COMMITTEE ON EFFECT OF
TEMPERATURE ON PROPERTIES OF METALS

MATERIAL	Aluminum Alloy--AMS 4127						HEAT NUMBER
CHEMICAL COMPOSITION PER CENT	Cu	Mg	Cr	Si	Al		
	0.3	1.0	0.25	0.6	Bal		
FORM	Forged						
HEAT TREATMENT	Temper--T6.						
REFERENCE	"Report on Materials for Use at Liquid Hydrogen Temperature", Prepared for the 63rd Annual Meeting of the American Society for Testing Materials.						

COEFFICIENT OF LINEAR THERMAL EXPANSION

TEMP RANGE, F	P-1 X 10 ⁶	TEMP RANGE, F	P-1 X 10 ⁶	TEMP RANGE, F	P-1 X 10 ⁶	TEMP RANGE, F	P-1 X 10 ⁶
78-(-104)	11.8	78-(-320)	10.3	78-(-410)	8.9		

ASTM-ASME JOINT COMMITTEE ON EFFECT OF
TEMPERATURE ON PROPERTIES OF METALS

MATERIAL	Aluminum Alloy--AMS 4212					HEAT NUMBER
CHEMICAL COMPOSITION PER CENT	Cu	Mg	Si	Al		
	1.2	0.5	5.0	Bal		
						6.7
FORM	Sand cast.					
HEAT TREATMENT	Temper--T6.					
REFERENCE	"Report on Materials for Use at Liquid Hydrogen Temperature", Prepared for the 63rd annual meeting of the American Society for Testing Materials.					

COEFFICIENT OF LINEAR THERMAL EXPANSION

TEMP RANGE, F	P-1 X 10 ⁶	TEMP RANGE, F	P-1 X 10 ⁶	TEMP RANGE, F	P-1 X 10 ⁶	TEMP RANGE, F	P-1 X 10 ⁶
78-(-104)	11.2	78-(-320)	9.9	78-(-410)	8.9		

ASTM-ASME JOINT COMMITTEE ON EFFECT OF
TEMPERATURE ON PROPERTIES OF METALS

MATERIAL	Aluminum Alloy--AMS 4281					HEAT NUMBER
CHEMICAL COMPOSITION PER CENT	Si	Cu	Mg	Al		
	5.0	1.2	0.5	Bal		
FORM	Permanent mold cast.					
HEAT TREATMENT	Temper--T6.					
REFERENCE	"Report on Materials for Use at Liquid Hydrogen Temperature", Prepared for the 63rd annual meeting of the American Society for Testing Materials.					

COEFFICIENT OF LINEAR THERMAL EXPANSION

TEMP RANGE, F	P-1 X 10 ⁶	TEMP RANGE, F	P-1 X 10 ⁶	TEMP RANGE, F	P-1 X 10 ⁶	TEMP RANGE, F	P-1 X 10 ⁶
78-(-104)	11.2	78-(-320)	9.9	78-(-410)	9.0		

ASTM-ASME JOINT COMMITTEE ON EFFECT OF
TEMPERATURE ON PROPERTIES OF METALS

MATERIAL	Aluminum Alloy--AMS 4122					HEAT NUMBER
CHEMICAL COMPOSITION PER CENT	Zn	Mg	Cu	Cr	Al	
	5.6	2.5	1.6	0.3	Bal	
FORM	Rolled					
HEAT TREATMENT	Temper--T6.					
REFERENCE	"Report on Materials for Use at Liquid Hydrogen Temperatures", Prepared for the 63rd annual meeting of the American Society for Testing Materials.					

COEFFICIENT OF LINEAR THERMAL EXPANSION

TEMP RANGE, F	P-1 X 10 ⁶	TEMP RANGE, F	P-1 X 10 ⁶	TEMP RANGE, F	P-1 X 10 ⁶	TEMP RANGE, F	P-1 X 10 ⁶
78-(-104)	11.9	78-(-320)	10.7	78-(-410)	9.4		

ASTM-ASME JOINT COMMITTEE ON EFFECT OF
TEMPERATURE ON PROPERTIES OF METALS

MATERIAL	Aluminum Alloy--7075					HEAT NUMBER
CHEMICAL COMPOSITION PER CENT	Zn	Mg	Cu	Cr	Al	
	5.6	2.5	1.6	0.3	Bal	
FORM						
HEAT TREATMENT	Temper--T6.					
REFERENCE	Lucke, C. F. and Deem, H. W., "Thermal Properties of Thirteen Metals", ASTM Special Technical Publication, No. 227.					

THERMAL CONDUCTIVITY

TEMP, F	(1) BTU HR-1 FT-2 F-1 FT	TEMP, F	(2) BTU HR-1 FT-2 F-1 FT
-250	45	-250	71
-200	51	-200	76
-100	60	-100	85
68	72	68	97
200	79	200	102
400	99	400	106
600	102	600	102
800	97	800	97
(1)	As received.		
(2)	After heating above 575 F.		

COEFFICIENT OF LINEAR THERMAL EXPANSION

TEMP RANGE, F	$\alpha \times 10^6$	TEMP RANGE, F	$\alpha \times 10^6$	TEMP RANGE, F	$\alpha \times 10^6$	TEMP RANGE, F	$\alpha \times 10^6$
68-(-250)	9.87	68-(-100)	11.01	68-200	12.35	68-600	14.38
68-(-200)	10.30	68	xx	68-400	13.55	68-800	15.12

SPECIFIC HEAT

TEMP, F	BTU LB-1 F-1	TEMP, F	BTU LB-1 F-1	TEMP, F	BTU LB-1 F-1	TEMP, F	BTU LB-1 F-1
-250	0.137*	-100	0.176	200	0.215	600	0.252
-200	0.152	68	0.201	400	0.230	800	0.280

* Extrapolated.

DENSITY

TEMP, F	LB CU IN-1	TEMP, F	LB CU IN-1	TEMP, F	LB CU IN-1	TEMP, F	LB CU IN-1
-250	0.1023	-100	0.1017	200	0.1006	600	0.0989
-200	0.1022	68	0.1012	400	0.0998	800	0.0980

Calculated from thermal expansion data and measured density of 0.1013 lb in⁻³ at 32 F.

DIFFUSIVITY

TEMP, F	(1) FT ² HR-1	TEMP, F	(2) FT ² HR-1
-250	1.86	-250	2.93*
-200	1.91	-200	2.83
-100	1.94	-100	2.77
68	2.03	68	2.77
200	2.11	200	2.75
400	2.50	400	2.68
600	2.39	600	2.39
800	2.05	800	2.05

(1) As received.
(2) After heating above 575 F.
* Extrapolated.

ASTM-ASME JOINT COMMITTEE ON EFFECT OF TEMPERATURE ON PROPERTIES OF METALS

MATERIAL	Aluminum Alloy--7075					HEAT NUMBER
CHEMICAL COMPOSITION PER CENT	Cr	Mg	Cu	Zn	Al	
	0.3	2.5	1.6	5.6	Bal	

FORM: Sheet (0.025 in.)
HEAT TREATMENT: Temper--T6.
REFERENCE: Welles, V., Schaeffer, G. T., Saule, A., and Sachs, G., "Thermal Cycling Under Constant Load to Low Temperatures of Aluminum and Magnesium Alloys, presented at 63rd Annual Meeting of ASTM, June 26-July 1, 1960.
REMARKS:

COEFFICIENT OF LINEAR THERMAL EXPANSION

TEMP RANGE, F	$\alpha \times 10^6$	TEMP RANGE, F	$\alpha \times 10^6$	TEMP RANGE, F	$\alpha \times 10^6$	TEMP RANGE, F	$\alpha \times 10^6$
68-(-328)	10.0	68-212	13.2	68-392	13.5		

ASTM-ASME JOINT COMMITTEE ON EFFECT OF TEMPERATURE ON PROPERTIES OF METALS

8

MATERIAL	Aluminum Alloy--2017				HEAT NUMBER
CHEMICAL COMPOSITION PER CENT	Cu	Mn	Mg	Al	
	3.5-4.5	0.4-1.0	0.2-0.8	Bal	

FORM: HEAT TREATMENT: Annealing temperature: 775 F; Solution temperature: 940 F.
REFERENCE: "Materials in Design Engineering", Materials Selector, edited by H. R. Clauser, Vol 46, No. 4 (September, 1957) p. 82.
REMARKS:

THERMAL CONDUCTIVITY

TEMP, F	BTU IN-1 FT-2 F-1	TEMP, F	BTU IN-1 FT-2 F-1	TEMP, F	BTU IN-1 FT-2 F-1	TEMP, F	BTU IN-1 FT-2 F-1
77	99.4						

COEFFICIENT OF LINEAR THERMAL EXPANSION

TEMP RANGE, F	$\alpha \times 10^6$	TEMP RANGE, F	$\alpha \times 10^6$	TEMP RANGE, F	$\alpha \times 10^6$	TEMP RANGE, F	$\alpha \times 10^6$
68-212	12.7	68-572	13.9				

SPECIFIC HEAT

TEMP, F	BTU LB-1 F-1	TEMP, F	BTU LB-1 F-1	TEMP, F	BTU LB-1 F-1	TEMP, F	BTU LB-1 F-1
Room	0.22						

Data assumed to be at room temperature.

ELECTRICAL RESISTIVITY

TEMP, F	MICRONH CM	TEMP, F	MICRONH CM	TEMP, F	MICRONH CM	TEMP, F	MICRONH CM
68	3.63						

DENSITY

TEMP, F	LB CU IN-1	TEMP, F	LB CU IN-1	TEMP, F	LB CU IN-1	TEMP, F	LB CU IN-1
Room	0.101						

Data assumed to be at room temperature.

ASTM-ASME JOINT COMMITTEE ON EFFECT OF TEMPERATURE ON PROPERTIES OF METALS

9

MATERIAL	Aluminum Alloy--2218				HEAT NUMBER
CHEMICAL COMPOSITION PER CENT	Cu	Ni	Mg	Al	
	3.5-4.5	1.7-2.3	1.2-1.8	Bal	

FORM: HEAT TREATMENT: Annealing temperature: 775 F; Solution temperature: 950 F; Aging temperature: 460 F.
REFERENCE: "Materials in Design Engineering", Materials Selector, edited by H. R. Clauser, Vol 46, No. 4 (September, 1957) p. 83.
REMARKS:

THERMAL CONDUCTIVITY

TEMP, F	BTU IN-1 FT-2 F-1 FT	TEMP, F	BTU IN-1 FT-2 F-1 FT	TEMP, F	BTU IN-1 FT-2 F-1 FT	TEMP, F	BTU IN-1 FT-2 F-1 FT
77	97.0						

COEFFICIENT OF LINEAR THERMAL EXPANSION

TEMP RANGE, F	$\mu-1 \times 10^6$	TEMP RANGE, F	$\mu-1 \times 10^6$	TEMP RANGE, F	$\mu-1 \times 10^6$	TEMP RANGE, F	$\mu-1 \times 10^6$
68-212	12.4	68-572	13.5				

SPECIFIC HEAT

TEMP, F	BTU LB-1 F-1	TEMP, F	BTU LB-1 F-1	TEMP, F	BTU LB-1 F-1	TEMP, F	BTU LB-1 F-1
Room	0.22						
Data assumed to be at room temperature.							

DENSITY

TEMP, F	LB CU IN-1	TEMP, F	LB CU IN-1	TEMP, F	LB CU IN-1	TEMP, F	LB CU IN-1
Room	0.102						
Data assumed to be at room temperature.							

ASTM-ASME JOINT COMMITTEE ON EFFECT OF
TEMPERATURE ON PROPERTIES OF METALS

10

MATERIAL		HEAT NUMBER					
Aluminum Alloy--2018							
CHEMICAL COMPOSITION PER CENT	Cu	Ni	Mg	Al			
	3.5-	1.7-	0.45-				
	4.5	2.3	0.9	Bal			
FORM							
HEAT TREATMENT Annealing temperature: 775 F; Solution temperature: 950 F; Aging temperature: 340 F.							
REFERENCE "Materials in Design Engineering", Materials Selector, edited by H. R. Clauser, Vol 46, No. 4 (September, 1957) p. 83.							

THERMAL CONDUCTIVITY

TEMP, F	BTU IN-1 FT-2 F-1 FT	TEMP, F	BTU IN-1 FT-2 F-1 FT	TEMP, F	BTU IN-1 FT-2 F-1 FT	TEMP, F	BTU IN-1 FT-2 F-1 FT
77	89.0						

COEFFICIENT OF LINEAR THERMAL EXPANSION

TEMP RANGE, F	$\mu-1 \times 10^6$	TEMP RANGE, F	$\mu-1 \times 10^6$	TEMP RANGE, F	$\mu-1 \times 10^6$	TEMP RANGE, F	$\mu-1 \times 10^6$
68-212	12.4	68-572	13.4				

SPECIFIC HEAT

TEMP, F	BTU LB-1 F-1	TEMP, F	BTU LB-1 F-1	TEMP, F	BTU LB-1 F-1	TEMP, F	BTU LB-1 F-1
Room	0.101						
Data assumed to be at room temperature.							

DENSITY

TEMP, F	LB CU IN-1	TEMP, F	LB CU IN-1	TEMP, F	LB CU IN-1	TEMP, F	LB CU IN-1
Room	0.101						
Data assumed to be at room temperature.							

ASTM-ASME JOINT COMMITTEE ON EFFECT OF
TEMPERATURE ON PROPERTIES OF METALS

11

MATERIAL		HEAT NUMBER					
Aluminum Alloy--514							
CHEMICAL COMPOSITION PER CENT	Si	Mn	Mg	Al			
	3.9-	0.4-	0.2-				
	5.0	1.2	0.8	Bal			
FORM							
HEAT TREATMENT Annealing temperature: 775 F; Solution temperature: 950 F; Aging temperature: 340 F.							
REFERENCE "Materials in Design Engineering", Materials Selector, edited by H. R. Clauser, Vol 46, No. 4 (September, 1957).							
REMARKS Melting temperature range: 950-1180 F.							

THERMAL CONDUCTIVITY

TEMP, F	BTU IN-1 FT-2 F-1 FT	TEMP, F	BTU IN-1 FT-2 F-1 FT	TEMP, F	BTU IN-1 FT-2 F-1 FT	TEMP, F	BTU IN-1 FT-2 F-1 FT
77	111.0						

COEFFICIENT OF LINEAR THERMAL EXPANSION

TEMP RANGE, F	$\mu-1 \times 10^6$	TEMP RANGE, F	$\mu-1 \times 10^6$	TEMP RANGE, F	$\mu-1 \times 10^6$	TEMP RANGE, F	$\mu-1 \times 10^6$
68-212	12.5	68-572	13.6				

SPECIFIC HEAT

TEMP, F	BTU LB-1 F-1	TEMP, F	BTU LB-1 F-1	TEMP, F	BTU LB-1 F-1	TEMP, F	BTU LB-1 F-1
Room	0.22						
Data assumed to be at room temperature.							

ELECTRICAL RESISTIVITY

TEMP, F	MICRON- CM	TEMP, F	MICRON- CM	TEMP, F	MICRON- CM	TEMP, F	MICRON- CM
68	3.45						

DENSITY

TEMP, F	LB CU IN-1	TEMP, F	LB CU IN-1	TEMP, F	LB CU IN-1	TEMP, F	LB CU IN-1
Room	0.101						
Data assumed to be at room temperature.							

ASTM-ASME JOINT COMMITTEE ON EFFECT OF TEMPERATURE ON PROPERTIES OF METALS

12

MATERIAL	Aluminum Alloy--AMS 4135					HEAT NUMBER		
CHEMICAL COMPOSITION PER CENT	Cu	Si	Mn	Mg	Al			
	4.5	0.9	0.8	0.5	Bal			
FORM	Forged.							
HEAT TREATMENT								
REFERENCE	"Report on Materials for Use at Liquid Hydrogen Temperature", Prepared for the 63rd annual meeting of the American Society for Testing Materials.							
REMARKS								

COEFFICIENT OF LINEAR THERMAL EXPANSION

TEMP RANGE, F	F-1 X 10 ⁶	TEMP RANGE, F	F-1 X 10 ⁶	TEMP RANGE, F	F-1 X 10 ⁶	TEMP RANGE, F	F-1 X 10 ⁶
78-(-104)	11.3	78-(-320)	10.1	78-(-410)	8.8		

ASTM-ASME JOINT COMMITTEE ON EFFECT OF TEMPERATURE ON PROPERTIES OF METALS

13

MATERIAL	Aluminum Alloy--2020					HEAT NUMBER		
CHEMICAL COMPOSITION PER CENT	Cu	Li	Mn	Cd	Al			
	4.5	1.1	0.5	0.2	Bal			
FORM	Sheet (0.028 in.)							
HEAT TREATMENT								
REFERENCE	Weiss, V., Schaeffer, G. T., Saule, H., and Sachs, G., "Thermal Cycling Under Constant Load to Low Temperatures of Aluminum and Magnesium Alloys."							
REMARKS								

THERMAL CONDUCTIVITY

TEMP, F	BTU HR-1 FT-2 F-1 FT	TEMP, F	BTU HR-1 FT-2 F-1 FT	TEMP, F	BTU HR-1 FT-2 F-1 FT	TEMP, F	BTU HR-1 FT-2 F-1 FT
68	50.8						

COEFFICIENT OF LINEAR THERMAL EXPANSION

TEMP RANGE, F	F-1 X 10 ⁶	TEMP RANGE, F	F-1 X 10 ⁶	TEMP RANGE, F	F-1 X 10 ⁶	TEMP RANGE, F	F-1 X 10 ⁶
68-(-328)	9.8	68-212	12.8	68-392	13.3		

ELECTRICAL RESISTIVITY

TEMP, F	MICRON CM	TEMP, F	MICRON CM	TEMP, F	MICRON CM	TEMP, F	MICRON CM
68	7.8						

DENSITY

TEMP, F	LB CU IN-1	TEMP, F	LB CU IN-1	TEMP, F	LB CU IN-1	TEMP, F	LB CU IN-1
Room	0.98						
Data assumed to be at room temperature.							

ASTM-ASME JOINT COMMITTEE ON EFFECT OF TEMPERATURE ON PROPERTIES OF METALS

14

MATERIAL	Aluminum Alloy--2024				HEAT NUMBER			
CHEMICAL COMPOSITION PER CENT	Cu	Mg	Mn	Al				
	3.8-4.9	1.2-1.8	0.3-0.9	Bal				
FORM								
HEAT TREATMENT	Annealing temperature: 775 F, Solution temperature: 920 F, Aging temperature: 375 F.							
REFERENCE	"Materials in Design Engineering", Materials Selector, edited by H. R. Clauser, Vol 46, No. 4 (September, 1957).							
REMARKS	Melting temperature range: 935-1180 F.							

THERMAL CONDUCTIVITY

TEMP, F	BTU HR-1 FT-2 F-1 FT	TEMP, F	BTU HR-1 FT-2 F-1 FT	TEMP, F	BTU HR-1 FT-2 F-1 FT	TEMP, F	BTU HR-1 FT-2 F-1 FT
77	111.0						

COEFFICIENT OF LINEAR THERMAL EXPANSION

TEMP RANGE, F	F-1 X 10 ⁶	TEMP RANGE, F	F-1 X 10 ⁶	TEMP RANGE, F	F-1 X 10 ⁶	TEMP RANGE, F	F-1 X 10 ⁶
68-212	12.6	68-572	13.7				

SPECIFIC HEAT

TEMP, F	BTU LB-1 F-1	TEMP, F	BTU LB-1 F-1	TEMP, F	BTU LB-1 F-1	TEMP, F	BTU LB-1 F-1
Room	0.22						
Data assumed to be at room temperature.							

ELECTRICAL RESISTIVITY

TEMP, F	(1) MICRON CM	TEMP, F	(2) MICRON CM
68	3.45	68	5.75
(1) Temper 0,			
(2) Temper 4,			

DENSITY

TEMP, F	LB CU IN-1	TEMP, F	LB CU IN-1	TEMP, F	LB CU IN-1	TEMP, F	LB CU IN-1
Room	0.100						
Data assumed to be at room temperature.							

ASTM-ASME JOINT COMMITTEE ON EFFECT OF
TEMPERATURE ON PROPERTIES OF METALS

15

MATERIAL	Aluminum Alloy--2024				HEAT NUMBER			
CHEMICAL COMPOSITION PER CENT	Al	Cu	Mg					
	93	4.54	1.70					
FORM								
HEAT TREATMENT	Temper--T4.							
REFERENCE	Lucke, C. F. and Deem, H. W., "Thermal Properties of Thirteen Metals", ASTM Special Technical Publication No. 227.							
REMARKS								

THERMAL CONDUCTIVITY

TEMP, F	(1) BTU HR-1 FT-2 F-1 FT		TEMP, F	(2) BTU HR-1 FT-2 F-1 FT	
-250	46		-250	84	
-200	51		-200	88	
-100	59		-100	95	
-68	70		-68	103	
200	78		200	107	
400	100		400	110	
600	108		600	108	
800	100		800	100	
(1) As received.					
(2) After heating above 575 F.					

COEFFICIENT OF LINEAR THERMAL EXPANSION

TEMP RANGE, F	P-1 X 10 ⁶	TEMP RANGE, F	P-1 X 10 ⁶	TEMP RANGE, F	P-1 X 10 ⁶	TEMP RANGE, F	P-1 X 10 ⁶
-250	10.85	-100	11.55	200	13.18	600	14.19
-200	10.97	68	--	400	13.98	800	14.54

SPECIFIC HEAT

TEMP, F	BTU LB-1 F-1	TEMP, F	BTU LB-1 F-1	TEMP, F	BTU LB-1 F-1	TEMP, F	BTU LB-1 F-1
-250	0.135	-100	0.174	200	0.217	600	0.345
-200	0.151	68	0.203	400	0.231	800	0.370

DENSITY

TEMP, F	LB CU IN-3	TEMP, F	LB CU IN-3	TEMP, F	LB CU IN-3	TEMP, F	LB CU IN-3
-250	0.1019	-100	0.1010	200	0.1000	600	0.0983
-200	0.1014	68	0.1006	400	0.0992	800	0.0973
Calculated from thermal expansion and measured density of 0.1006 lb in. ⁻³ at 32°F.							

DIFFUSIVITY

TEMP, F	(1) FT ² HR-1	TEMP, F	FT ² HR-1	TEMP, F	(2) FT ² HR-1	TEMP, F	FT ² HR-1
-250	1.95			-250	3.54		
-200	1.95			-200	3.38		
-100	1.93			-100	3.10		
68	2.00			68	2.51		
200	2.07			200	2.84		
400	2.53			400	2.78		
600	2.61			600	2.61		
800	2.20			800	2.20		
(1) As received.							
(2) After heating above 575 F.							

ASTM-ASME JOINT COMMITTEE ON EFFECT OF
TEMPERATURE ON PROPERTIES OF METALS

16

MATERIAL	Aluminum Alloy--2024				HEAT NUMBER			
CHEMICAL COMPOSITION PER CENT	Al	Cu	Mg	Mn				
	93	4.5	1.5	0.6				
FORM								
HEAT TREATMENT	Solution heat treated.							
REFERENCE	Powell, R. L., Hall, W. J. and Roder, H. M., to be published (1958); as found in "A Compendium of the Properties of Materials at Low Temperatures, Phase I", Part II, edited by Victor J. Johnson, NBS Cryogenic Engineering Laboratory, Boulder, Colorado (December, 1959).							
REMARKS								

THERMAL CONDUCTIVITY

TEMP, F	BTU HR-1 FT-2 F-1 FT	TEMP, F	BTU HR-1 FT-2 F-1 FT	TEMP, F	BTU HR-1 FT-2 F-1 FT	TEMP, F	BTU HR-1 FT-2 F-1 FT
-451	2.37	-424	9.54	-316	33	-100	57
-449	2.83	-388	18	-280	38	-10	64.7
-442	4.80	-352	25.0	-190	48	80	69.3
Values interpolated from graph.							

ASTM-ASME JOINT COMMITTEE ON EFFECT OF
TEMPERATURE ON PROPERTIES OF METALS

17

MATERIAL	Aluminum Alloy--2024 Alcoa				HEAT NUMBER			
CHEMICAL COMPOSITION PER CENT	Al	Cu	Mg					
	93	4.58	1.70					
FORM								
HEAT TREATMENT	Solution heat treated at factory.							
REFERENCE	Cryogenic Engineering Laboratories, National Bureau of Standards, Boulder, Colorado.							
REMARKS								

THERMAL CONDUCTIVITY

TEMP, F	BTU HR-1 FT-2 F-1 FT	TEMP, F	BTU HR-1 FT-2 F-1 FT	TEMP, F	BTU HR-1 FT-2 F-1 FT	TEMP, F	BTU HR-1 FT-2 F-1 FT
-453	1.85	-442	4.80	-370	22.5	-316	32.0
-449	2.83	-424	9.65	-352	25.9	-280	37.1
-442	3.81	-388	18.7	-334	29.2	-234	41.7

ELECTRICAL RESISTIVITY

TEMP, F	MICRON- CM	TEMP, F	MICRON- CM	TEMP, F	MICRON- CM	TEMP, F	MICRON- CM
4	3.10	20	3.10	70	5.34	300	5.8
10	3.10	40	3.17	100	5.61		

ASTM-ASME JOINT COMMITTEE ON EFFECT OF
TEMPERATURE ON PROPERTIES OF METALS

18

MATERIAL	Aluminum Alloy--24S				HEAT NUMBER			
CHEMICAL COMPOSITION PER CENT	Cu	Mg	Mn	Al				
	4.5	1.5	0.6	Bal				
FORM								
HEAT TREATMENT								
REFERENCE	Evans, J. E., Jr., Lewis Flight Propulsion Laboratory, "Thermal Conductivity of 14 Metals and Alloys Up to 1100 F". NACA Research Memorandum CRME50L07 (Mar 2, 1951).							

THERMAL CONDUCTIVITY

TEMP, F	BTU HR-1 FT-2 F-1 FT	TEMP, F	BTU HR-1 FT-2 F-1 FT	TEMP, F	BTU HR-1 FT-2 F-1 FT	TEMP, F	BTU HR-1 FT-2 F-1 FT
250	95.5	400	98.4	550	105	650	99.8
300	96.5	450	101	600	102.5	700	97.4
350	97.5	500	106.8				

ASTM-ASME JOINT COMMITTEE ON EFFECT OF
TEMPERATURE ON PROPERTIES OF METALS

19

MATERIAL	Aluminum Alloy--24S				HEAT NUMBER			
CHEMICAL COMPOSITION PER CENT	Cu	Mg	Mn	Al				
	4.5	1.5	0.6	Bal				
FORM								
HEAT TREATMENT								
REFERENCE	General Electric Company, Handbook No. 1.							
REMARKS	Nominal Composition taken from DMIC Memo 42.							

COEFFICIENT OF LINEAR THERMAL EXPANSION

TEMP RANGE, F	F-1 X 10 ⁶	TEMP RANGE, F	F-1 X 10 ⁶	TEMP RANGE, F	F-1 X 10 ⁶	TEMP RANGE, F	F-1 X 10 ⁶
100	12.12	300	13.14	400	13.40	500	13.58
200	12.77						

ASTM-ASME JOINT COMMITTEE ON EFFECT OF
TEMPERATURE ON PROPERTIES OF METALS

20

MATERIAL	Aluminum Alloy--AMS 4120				HEAT NUMBER			
CHEMICAL COMPOSITION PER CENT	Cu	Mg	Mn	Al				
	4.5	1.5	0.6	Bal				
FORM	Rolled							
HEAT TREATMENT								
REFERENCE	"Report on Materials for Use at Liquid Hydrogen Temperature", Prepared for the 63rd annual meeting of the American Society for Testing Materials.							

COEFFICIENT OF LINEAR THERMAL EXPANSION

TEMP RANGE, F	F-1 X 10 ⁶	TEMP RANGE, F	F-1 X 10 ⁶	TEMP RANGE, F	F-1 X 10 ⁶	TEMP RANGE, F	F-1 X 10 ⁶
78-(-104)	11.9	78-(-320)	10.4	78-(-410)	9.1		

ASTM-ASME JOINT COMMITTEE ON EFFECT OF
TEMPERATURE ON PROPERTIES OF METALS

21

MATERIAL	Aluminum Alloy--2011				HEAT NUMBER			
CHEMICAL COMPOSITION PER CENT	Cu	Pb	Bi	Al				
	5.0-6.0	0.2-0.6	0.2-0.6	Bal				
FORM								
HEAT TREATMENT	Annealing temperature: 775 F; Solution temperature: 950 F; Aging temperature: 320 F.							
REFERENCE	"Materials in Design Engineering", Materials Selector, edited by H. R. Clauser, Vol 46, No. 4 (September, 1957) p. 82.							
REMARKS	Melting temperature range: 995-1190 F.							

THERMAL CONDUCTIVITY

TEMP, F	BTU HR-1 FT-2 F-1 FT	TEMP, F	BTU HR-1 FT-2 F-1 FT	TEMP, F	BTU HR-1 FT-2 F-1 FT	TEMP, F	BTU HR-1 FT-2 F-1 FT
77	81.7						

COEFFICIENT OF LINEAR THERMAL EXPANSION

TEMP RANGE, F	F-1 X 10 ⁶	TEMP RANGE, F	F-1 X 10 ⁶	TEMP RANGE, F	F-1 X 10 ⁶	TEMP RANGE, F	F-1 X 10 ⁶
68-212	12.8	68-572	13.9				

SPECIFIC HEAT

TEMP, F	BTU LB-1 F-1	TEMP, F	BTU LB-1 F-1	TEMP, F	BTU LB-1 F-1	TEMP, F	BTU LB-1 F-1
Room	0.23						
Data assumed to be at room temperature.							

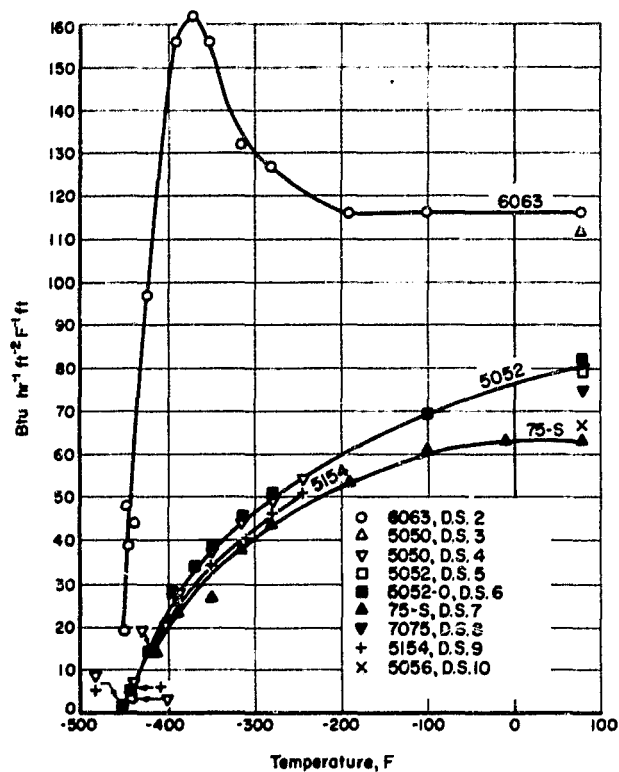
ELECTRICAL RESISTIVITY

TEMP, F	MICROHM- CM	TEMP, F	MICROHM- CM	TEMP, F	MICROHM- CM	TEMP, F	MICROHM- CM
68	4.31						

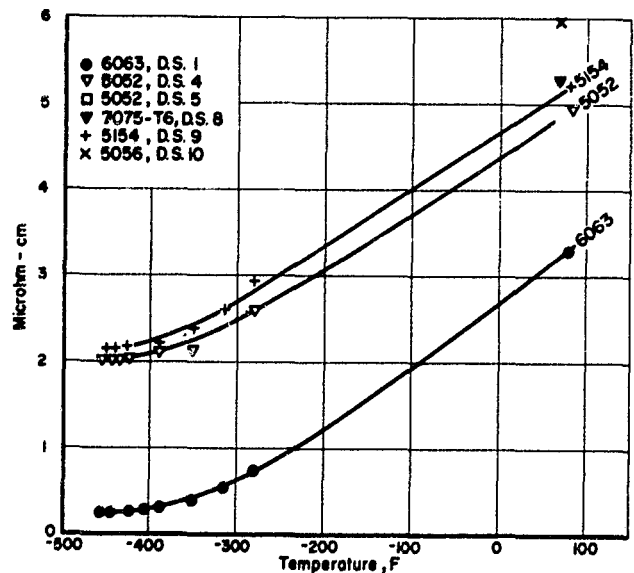
DENSITY

TEMP, F	LB CU IN-3	TEMP, F	LB CU IN-3	TEMP, F	LB CU IN-3	TEMP, F	LB CU IN-3
Room	0.102						
Data assumed to be at room temperature.							

ALUMINUM-MAGNESIUM ALLOYS



THERMAL CONDUCTIVITY OF ALUMINUM-MAGNESIUM ALLOYS



ELECTRICAL RESISTIVITY OF ALUMINUM-MAGNESIUM ALLOYS

ASTM-ASME JOINT COMMITTEE ON EFFECT OF
TEMPERATURE ON PROPERTIES OF METALS

1

MATERIAL Aluminum--6063 Alcoa				HEAT NUMBER			
CHEMICAL COMPOSITION PER CENT	Al	Mg	Si				
	98.5	0.38	0.65				
FORM HEAT TREATMENT Factory heat treated,							
REFERENCE Cryogenic Engineering Laboratories, National Bureau of Standards, Boulder, Colorado,							
REMARKS Grain size: longitudinal--0.052 x 0.048 mm, transverse--0.052 mm Diamond point hardness: longitudinal--71, transverse--64.							

ELECTRICAL RESISTIVITY

TEMP, F	MICRON- CM	TEMP, F	MICRON- CM	TEMP, F	MICRON- CM	TEMP, F	MICRON- CM
-453	0.278	-406	0.302	-316	0.56		
-445	0.278	-388	0.323	-280	0.76		
-424	0.284	-352	0.416	80	3.33		

ASTM-ASME JOINT COMMITTEE ON EFFECT OF
TEMPERATURE ON PROPERTIES OF METALS

2

MATERIAL Aluminum Alloy--6063				HEAT NUMBER			
CHEMICAL COMPOSITION PER CENT	Al	Mg	Si				
	98.5	0.7	0.4				
FORM HEAT TREATMENT As fabricated							
REFERENCE Powell, R. L., Hall, W. J. and Roder, H. M., to be published (1958); as found in "A Compendium of the Properties of Materials at Low Temperatures, Phase I", Part II, edited by Victor J. Johnson, NBS Cryogenic Engineering Laboratory, Boulder, Colorado (December, 1959).							

THERMAL CONDUCTIVITY

TEMP, F	BTU HR-1 FT-2 F-1 FT	TEMP, F	BTU HR-1 FT-2 F-1 FT	TEMP, F	BTU HR-1 FT-2 F-1 FT	TEMP, F	BTU HR-1 FT-2 F-1 FT
-453	19.6	-424	97.0	-352	156	-190	116
-449	48.0	-388	156.0	-316	132	-100	116
-445	39.2	-370	162.0	-280	127	80	116+
-442	44.5						
Values interpolated from graph,							

ASTM-ASME JOINT COMMITTEE ON EFFECT OF
TEMPERATURE ON PROPERTIES OF METALS

3

MATERIAL Aluminum Alloy--5050				HEAT NUMBER			
CHEMICAL COMPOSITION PER CENT	Mg	Al					
	1.0- 1.8	Bal					
FORM HEAT TREATMENT Annealing temperature: 650 F.							
REFERENCE "Materials in Design Engineering", Materials Selector, edited by H. R. Clauser, Vol 46, No. 4 (September, 1957).							
REMARKS Melting temperature range: 1160-1205 F.							

THERMAL CONDUCTIVITY

TEMP, F	BTU HR-1 FT-2 F-1 FT	TEMP, F	BTU HR-1 FT-2 F-1 FT	TEMP, F	BTU HR-1 FT-2 F-1 FT	TEMP, F	BTU HR-1 FT-2 F-1 FT
77	111						

COEFFICIENT OF LINEAR THERMAL EXPANSION

TEMP RANGE, F	F-1 X 10 ⁶	TEMP RANGE, F	F-1 X 10 ⁶	TEMP RANGE, F	F-1 X 10 ⁶	TEMP RANGE, F	F-1 X 10 ⁶
68-212	13.2	68-572	14.2				

SPECIFIC HEAT

TEMP, F	BTU LB-1 F-1	TEMP, F	BTU LB-1 F-1	TEMP, F	BTU LB-1 F-1	TEMP, F	BTU LB-1 F-1
212	0.22						

DENSITY

TEMP, F	LB CU IN-1	TEMP, F	LB CU IN-1	TEMP, F	LB CU IN-1	TEMP, F	LB CU IN-1
Room	0.097						
Data assumed to be at room temperature.							

ASTM-ASME JOINT COMMITTEE ON EFFECT OF
TEMPERATURE ON PROPERTIES OF METALS

4

MATERIAL Aluminum Alloy--5052 Alcoa				HEAT NUMBER			
CHEMICAL COMPOSITION PER CENT	Al	Mg	Cr				
	97	2.46	0.22				
FORM HEAT TREATMENT Annealed for 2 hours at 400 C.							
REFERENCE Cryogenic Engineering Laboratories, National Bureau of Standards, Boulder, Colorado.							

THERMAL CONDUCTIVITY

TEMP, F	BTU HR-1 FT-2 F-1 FT	TEMP, F	BTU HR-1 FT-2 F-1 FT	TEMP, F	BTU HR-1 FT-2 F-1 FT	TEMP, F	BTU HR-1 FT-2 F-1 FT
-453	2.60	-424	14.5	-352	37.7	-280	49.8
-447	4.74	-406	21.7	-316	44.6	-244	54.3
-442	6.93	-388	28.0				

ELECTRICAL RESISTIVITY

TEMP, F	MICRON- CM	TEMP, F	MICRON- CM	TEMP, F	MICRON- CM	TEMP, F	MICRON- CM
-453	2.05	-442	2.05	-388	2.11	-280	2.66
-449	2.05	-424	2.06	-352	2.19	80	4.95

ASTM-ASME JOINT COMMITTEE ON EFFECT OF
TEMPERATURE ON PROPERTIES OF METALS

5

MATERIAL	Aluminum--5052			HEAT NUMBER			
CHEMICAL COMPOSITION PER CENT	Mg	Cu	Al				
	2.2-	0.15-					
	2.8	0.35	Bal				
FORM							
HEAT TREATMENT	Annealing temperature: 650 F. Hot working temperature range: 500-950 F.						
REFERENCE	"Materials in Design Engineering", Materials Selector, edited by H. R. Clauser, Vol 46, No. 4 (September, 1957) p. 81.						
REMARKS	Melting temperature range: 1100-1200 F.						

THERMAL CONDUCTIVITY

TEMP, F	BTU HR-1 FT-2 F-1 FT	TEMP, F	BTU HR-1 FT-2 F-1 FT	TEMP, F	BTU HR-1 FT-2 F-1 FT	TEMP, F	BTU HR-1 FT-2 F-1 FT
77	79.2						

COEFFICIENT OF LINEAR THERMAL EXPANSION

TEMP RANGE, F	F-1 X 10 ⁶	TEMP RANGE, F	F-1 X 10 ⁶	TEMP RANGE, F	F-1 X 10 ⁶	TEMP RANGE, F	F-1 X 10 ⁶
68-212	13.2	68-572	14.3				

SPECIFIC HEAT

TEMP, F	BTU LB-1 F-1	TEMP, F	BTU LB-1 F-1	TEMP, F	BTU LB-1 F-1	TEMP, F	BTU LB-1 F-1
212	0.22						

ELECTRICAL RESISTIVITY

TEMP, F	MICRON- CM	TEMP, F	MICRON- CM	TEMP, F	MICRON- CM	TEMP, F	MICRON- CM
68	4.93						

DENSITY

TEMP, F	LB CU IN-3	TEMP, F	LB CU IN-3	TEMP, F	LB CU IN-3	TEMP, F	LB CU IN-3
Room	0.097						
Data assumed to be at room temperature.							

ASTM-ASME JOINT COMMITTEE ON EFFECT OF
TEMPERATURE ON PROPERTIES OF METALS

6

MATERIAL	Aluminum Alloy--505 2-0			HEAT NUMBER			
CHEMICAL COMPOSITION PER CENT	Al	Mg	Cu				
	97	2.5	0.25				
FORM							
HEAT TREATMENT	Annealed.						
REFERENCE	Powell, R. L., Hall, W. J. and Roder, H. M., to be published (1958); as found in "A Compendium of the Properties of Materials at Low Temperatures, Phase I", Part II, edited by Victor J. Johnson, NBS Cryogenic Engineering Laboratory, Boulder, Colorado (December, 1959).						

THERMAL CONDUCTIVITY

TEMP, F	BTU HR-1 FT-2 F-1 FT	TEMP, F	BTU HR-1 FT-2 F-1 FT	TEMP, F	BTU HR-1 FT-2 F-1 FT	TEMP, F	BTU HR-1 FT-2 F-1 FT
-453	2.83	-442	6.88	-370	34.0	-280	50.8
-449	4.04	-424	14.4	-352	38.7	-100	69.3
-445	5.37	-388	28.9	-316	45.6	80	82.0
Values interpolated from graph.							

ASTM-ASME JOINT COMMITTEE ON EFFECT OF
TEMPERATURE ON PROPERTIES OF METALS

7

MATERIAL	Aluminum Alloy--75-S						HEAT NUMBER	
CHEMICAL COMPOSITION PER CENT	Zn	Mg	Cu	Cr	Mn	Al		
	5.5	2.5	1.5	0.3	0.2	Bal		
FORM								
HEAT TREATMENT								
REFERENCE	Powell, R. L., Hall, W. J. and Roder, H. M., to be published (1958); as found in "A Compendium of the Properties of Materials at Low Temperatures, Phase I", Part II, edited by Victor J. Johnson, NBS Cryogenic Engineering Laboratory, Boulder, Colorado (December, 1959).							

THERMAL CONDUCTIVITY

TEMP, F	BTU HR-1 FT-2 F-1 FT	TEMP, F	BTU HR-1 FT-2 F-1 FT	TEMP, F	BTU HR-1 FT-2 F-1 FT	TEMP, F	BTU HR-1 FT-2 F-1 FT
-424	--	-352	31.8	-190	53.7	-10	63.6
-415	14.4	-316	38.7	-100	60.1	80	63.6+
-388	23.7						
Values interpolated from graph.							

ASTM-ASME JOINT COMMITTEE ON EFFECT OF
TEMPERATURE ON PROPERTIES OF METALS

8

MATERIAL	Aluminum--7075					HEAT NUMBER	
CHEMICAL COMPOSITION PER CENT	Zn	Mg	Cu	Cr	Al		
	5.6	2.5	1.6	0.3	Bal		
FORM	Sheet (0.025 in.),						
HEAT TREATMENT							
REFERENCE	Weiss, V., Schaeffer, G. T., Saule, A. and Sachs, G., "Thermal Cycling under Constant Load to Low Temperatures of Aluminum and Magnesium Alloys".						
REMARKS							

10

MATERIAL				Aluminum Alloy--5056				HEAT NUMBER			
CHEMICAL COMPOSITION PER CENT	Mg	Mn	Cr	Al							
	4.7-	0.05-	0.05-								
	5.6	0.20	0.20	Bal							
FORM											
HEAT TREATMENT											
Annealing temperature: 650 F, Hot working temperature range: 500-950 F.											
REFERENCE											
"Materials in Design Engineering", Materials Selector, edited by H. R. Clauser, Vol 46, No. 4 (September, 1957).											
REMARKS											
Melting temperature range: 1055-1180 F.											

THERMAL CONDUCTIVITY

[illegible]

COEFFICIENT OF LINEAR THERMAL EXPANSION

TEMP RANGE, F	$F^{-1} \times 10^6$	TEMP RANGE, F	$F^{-1} \times 10^6$	TEMP RANGE, F	$F^{-1} \times 10^6$	TEMP RANGE, F	$F^{-1} \times 10^6$
68-212	13.4	68-572	14.5				

SPECIFIC HEAT

TEMP, F	BTU LB-1 F-1	TEMP, F	BTU LB-1 F-1	TEMP, F	BTU LB-1 F-1	TEMP, F	BTU LB-1 F-1
212	0.22						

ELECTRICAL RESISTIVITY

TEMP. F	MICRONH- CM			TEMP. F	MICRONH- CM		
68	5.94 (1)			68	6.39 (2)		
(1) Annealed				(2) Hard			

DENSITY

[illegible]

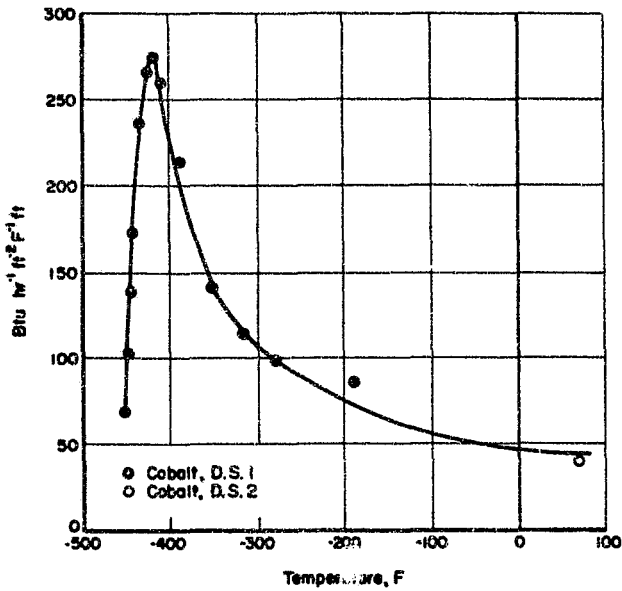
REFERENCE 21 CONTINUED ON CARD 3

REFERENCE 21
PAGE 22 BLANK

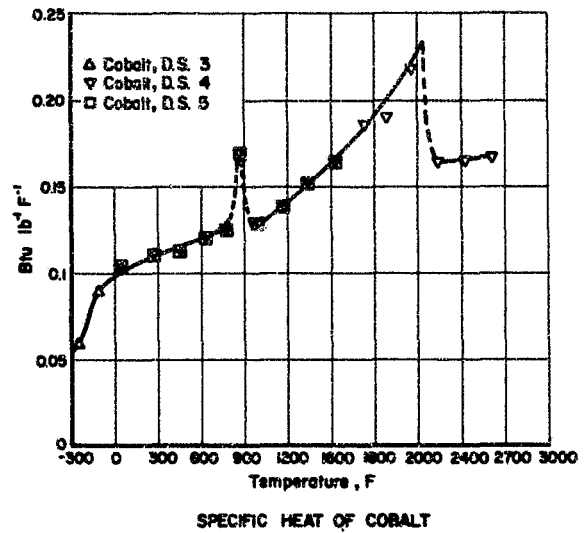
COBALT AND ITS ALLOYS

REFERENCE 21
PAGE 24 BLANK

COBALT



THERMAL CONDUCTIVITY OF COBALT



SPECIFIC HEAT OF COBALT

ASTM-ASME JOINT COMMITTEE ON EFFECT OF
TEMPERATURE ON PROPERTIES OF METALS

1

MATERIAL	Cohalt	HEAT NUMBER					
CHEMICAL COMPOSITION PER CENT	Co						
	99.9						
FORM							
HEAT TREATMENT	Annealed.						
REFERENCE	White, G. K., Woods, S. B., Canadian Journal of Physics, 35, (1957) pp. 656-665; as found in "A Compendium of Properties of Materials at Low Temperatures, Phase I", Part II, edited by Victor J. Johnson, NBS Cryogenic Engineering Laboratory, Boulder, Colorado (December, 1959).						

ASTM-ASME JOINT COMMITTEE ON EFFECT OF
TEMPERATURE ON PROPERTIES OF METALS

2

MATERIAL		Cobalt				HEAT NUMBER			
CHEMICAL COMPOSITION PER CENT	Co								
	99.9								
TEST									
HEAT TREATMENT									
REFERENCE	"Materials in Design Engineering", Materials Selector, edited by H. R. Clauser, Vol 46, No. 4 (Sept. 57), p 84.								
REMARKS	Melting point, F: 2723.								

THERMAL CONDUCTIVITY

[illegible]

COEFFICIENT OF LINEAR THERMAL EXPANSION

[illegible]

Thermal Conductivity

[illegible]

DENSITY

[illegible]ASTM-AIME JOINT COMMITTEE ON EFFECT OF
TEMPERATURE ON PROPERTIES OF METALS

MATERIAL	Cobalt	HEAT NUMBER						
	Co	Fe	Cu	Ni	S	Mn		
CHEMICAL COMPOSITION PER CENT	96.95	2.50	0.26	0.20	0.08	0.01		
FURNACE								
HEAT TREATMENT								
REFERENCE	Clusings, Keane, Schachinger, and Liselotte, "Results of Low-Temperature Research IX. The Atomic Heat of Cobalt Between 15 and 270 K", Z. Naturforsch., Vol 17a, pp. 185-91 (Germany); as found in WADC Technical Report 58-476.							
REMARKS								

SPECIFIC HEAT

[illegible]ASTM-A5WE JOINT COMMITTEE ON EFFECT OF
TEMPERATURE ON PROPERTIES OF METALS

MATERIAL	Cobalt	HEAT NUMBER
CHEMICAL COMPOSITION PER CENT	Co - Fe	
	99.95 0.05	
FORM		
HEAT		
TREATMENT		
REFERENCE	Jzege, F. M., Rosenbahr E., and Aulthoff, A. J., "Exact Determination of Specific Heats at High Temperatures, XII. Specific Heat, Electrical Resistance and Thermoelectric Power of Cobalt", Rec. Tran. Chim., Vol 59, pp. 831-56 (France); as found in WADC Technical Report 58-476.	

SPECIFIC HEAT

T_{MP} , °F	STU LS-1 $\rho=1$	T_{MP} , °F	STU LS-1 $\rho=1$	T_{MP} , °F	STU LS-1 $\rho=1$	T_{MP} , °F	STU LS-1 $\rho=1$
260	0.112	895	0.161*	1520	0.164	2240	0.166**
440	0.116	970	0.128	1760	0.177	2420	0.167
620	0.121	1160	0.139	1890	0.190	2500	0.168
800	0.125	1340	0.152	2060	0.220		

* Discontinuity due to $d \rightarrow B$ transformation.

** Discontinuity due to Curie point.

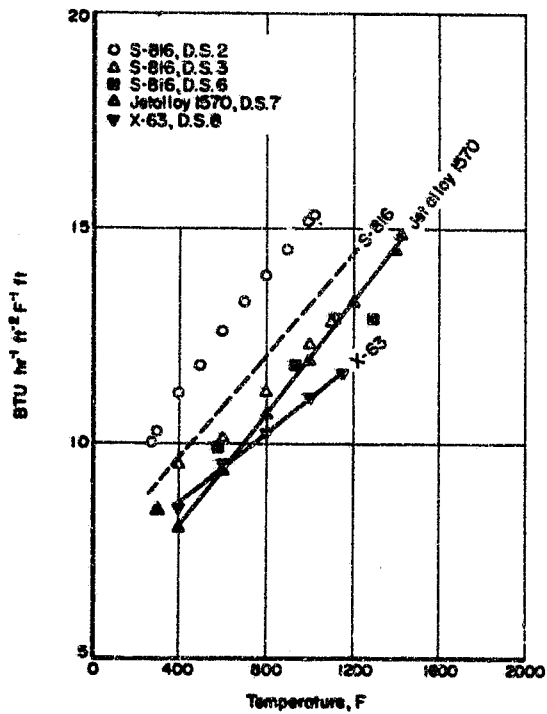
ASTM-AIME JOINT COMMITTEE ON EFFECT OF
TEMPERATURE ON PROPERTIES OF METALS

MATERIAL		HEAT INDEX									
CHEMICAL COMPOSITION PER CENT	IMPURE	Co									
	<0.01	Fe									
FORM											
HEAT TREATMENT											
REFERENCE	Armstrong, L. D., and Grayson-Smith, H., "High-Temperature Calorimetry. I-A new Adiabatic Calorimeter. II-Atomic Heats of Chromium, Manganese, and Cobalt between 0 and 850°", <i>Am. Jour. Research</i> , Vol 28A, p 44-50, 51-59 (Canada). Data found in WADC Technical Report 58-476.										

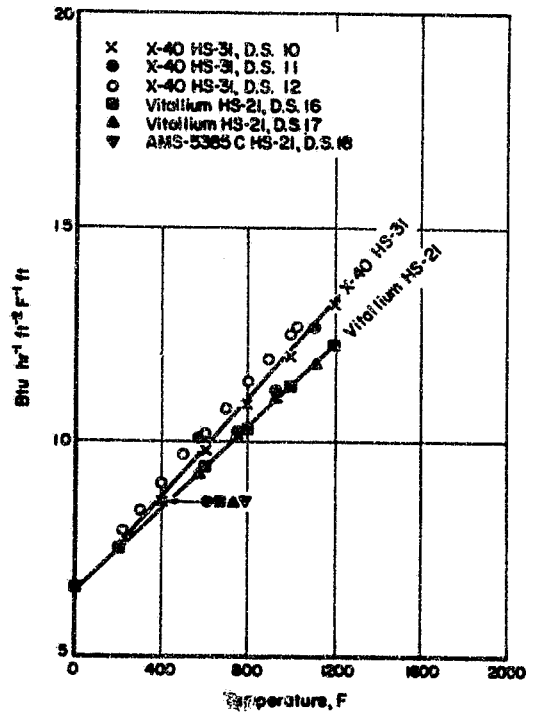
SPECIFIC HEAT

[illegible]

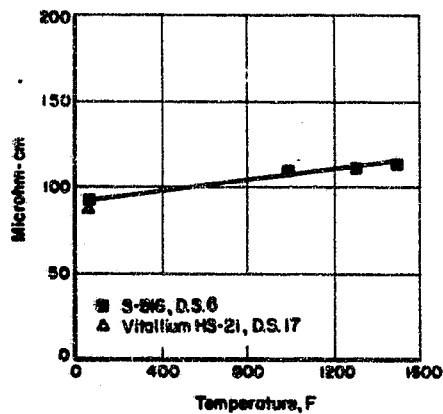
COBALT BASE ALLOYS



THERMAL CONDUCTIVITY OF COBALT BASE ALLOYS



THERMAL CONDUCTIVITY OF COBALT BASE ALLOYS



ELECTRICAL RESISTIVITY OF COBALT BASE ALLOYS

ASTM-ASME JOINT COMMITTEE ON EFFECT OF
TEMPERATURE ON PROPERTIES OF METALS

1

MATERIAL	Haynes Alloy No. 36						HEAT NUMBER			
	Cr	W	Ni	Fe max.	C	Co				
CHEMICAL COMPOSITION PER CENT	18.5	15	10	2.0	0.40	Bal				
FORM										
HEAT TREATMENT										
REFERENCE	Haynes Stellite Company									

DENSITY

TEMP, F	LB CU IN-1	TEMP, F	LB CU IN-1	TEMP, F	LB CU IN-1	TEMP, F	LB CU IN-1
Room	0.326						

ASTM-ASME JOINT COMMITTEE ON EFFECT OF
TEMPERATURE ON PROPERTIES OF METALS

2

MATERIAL	Cobalt--S 816									HEAT NUMBER			
	Cr	Ni	Mo	W	Cb	Fe	Mn	Si	C				
CHEMICAL COMPOSITION PER CENT	20	20	4	4	4	3	1.2	0.1	0.38				
FORM													
HEAT TREATMENT													
REFERENCE	Evans, E., Jr., "Thermal Conductivity of 14 Metals and Alloys Up to 1100 F", Lewis Flight Propulsion Laboratory, NACA Research Memorandum Rm E 501.07 (March, 1951).												
REMARKS	Nominal composition found in DMIC Memo 42.												

THERMAL CONDUCTIVITY

TEMP, F	BTU IN-1 FT-2 F-1 FT	TEMP, F	BTU IN-1 FT-2 F-1 FT	TEMP, F	BTU IN-1 FT-2 F-1 FT	TEMP, F	BTU IN-1 FT-2 F-1 FT
275	10	500	11.8	800	13.9	1000	15.2
300	10.2	600	12.6	900	14.5	1025	15.3
300	11.1	700	13.3				
Interpolated data taken from a heat curve.							

ASTM-ASME JOINT COMMITTEE ON EFFECT OF
TEMPERATURE ON PROPERTIES OF METALS

3

MATERIAL	Cobalt--S 816									HEAT NUMBER			
	Ni	Cr	Mo	W	Cb	Fe	Mn	Si	C				
CHEMICAL COMPOSITION PER CENT	20	20	4	4	4	3	1.2	0.4	0.38				
FORM													
HEAT TREATMENT													
REFERENCE	Materials Data Book No. 1, General Electric Company.												

THERMAL CONDUCTIVITY

TEMP, F	BTU IN-1 FT-2 F-1 FT	TEMP, F	BTU IN-1 FT-2 F-1 FT	TEMP, F	BTU IN-1 FT-2 F-1 FT	TEMP, F	BTU IN-1 FT-2 F-1 FT
300	8.4	600	10.1	1000	12.2	1100	12.9
400	9.5	800	11.2				

ASTM-ASME JOINT COMMITTEE ON EFFECT OF
TEMPERATURE ON PROPERTIES OF METALS

4

MATERIAL	Cobalt--S 816									HEAT NUMBER			
	Co	Ni	Cr	Cb	Mo	W	Fe	Mn	Si				
CHEMICAL COMPOSITION PER CENT	43.70	20.23	19.5	4.06	3.93	3.45	2.95	0.58	0.54				
FORM	1/2" dia. bar.												
HEAT TREATMENT													
REFERENCE	U. S. Naval Engineering Experiment Station.												
REMARKS	Absolute method, Lertz Dilatometer, heating rate: 5.0 or 5.6 F per minute.												

COEFFICIENT OF LINEAR THERMAL EXPANSION

TEMP RANGE, F	$\alpha \times 10^6$	TEMP RANGE, F	$\alpha \times 10^6$	TEMP RANGE, F	$\alpha \times 10^6$	TEMP RANGE, F	$\alpha \times 10^6$
100-500	7.6	100-1000	8.8	100-1600	9.8		

ASTM-ASME JOINT COMMITTEE ON EFFECT OF
TEMPERATURE ON PROPERTIES OF METALS

5

MATERIAL	Cobalt and Mixed Base Alloys--S 816									HEAT NUMBER			
	Ni	Cr	Mo	W	Cb	Fe	Mn	Si	C				
CHEMICAL COMPOSITION PER CENT	20	20	4	4	4	3	1.2	0.4	0.38				
FORM													
HEAT TREATMENT													
REFERENCE	Materials and Methods Manual No. 115, "Metals for Short Time Service at High Temperatures", by A. Levy (April 1955), p. 121.												
REMARKS	Melting point--2400°F. Nominal composition taken from DMIC Memo 42.												

COEFFICIENT OF LINEAR THERMAL EXPANSION

TEMP RANGE, F	$\alpha \times 10^6$	TEMP RANGE, F	$\alpha \times 10^6$	TEMP RANGE, F	$\alpha \times 10^6$	TEMP RANGE, F	$\alpha \times 10^6$
70-600	6.5	70-1000	7.1	70-1400	7.7	70-1800	8.3
70-800	6.9	70-1200	7.4	70-1600	8.0		

DENSITY

TEMP, F	LB CU IN-1	TEMP, F	LB CU IN-1	TEMP, F	LB CU IN-1	TEMP, F	LB CU IN-1
Room	0.313						
Data assumed to be at room temperature.							

ASTM-ASME JOINT COMMITTEE ON EFFECT OF
TEMPERATURE ON PROPERTIES OF METALS

6

MATERIAL	Cobalt--S 816									HEAT NUMBER			
	Co	Ni	Cr	W	Cb	Mo	Fe	Mn	Si				
CHEMICAL COMPOSITION PER CENT	41.71	20.65	19.88	4.20	4.13	3.76	3.38	1.32	0.56				
FORM													
HEAT TREATMENT													
REFERENCE	Allegheny Ludlum Steel Corporation.												
REMARKS	Rolled or forged from 2100-2250 F. Solution: 2150-2250 hr W.Q. Aged 1400-1500 F - 16 hr air. Excellent corrosion resistance to 1500 F.												

THERMAL CONDUCTIVITY

TEMP. F	BTU HR-1 FT-2 F-1 FT	TEMP. F	BTU HR-1 FT-2 F-1 FT	TEMP. F	BTU HR-1 FT-2 F-1 FT	TEMP. F	BTU HR-1 FT-2 F-1 FT
302	8.82	932	11.8	1112	12.9	1292	12.9
572	9.92						

COEFFICIENT OF LINEAR THERMAL EXPANSION

TEMP. RANGE, F	$\alpha \times 10^6$	TEMP. RANGE, F	$\alpha \times 10^6$	TEMP. RANGE, F	$\alpha \times 10^6$	TEMP. RANGE, F	$\alpha \times 10^6$
68-572	6.6	68-932	7.1	68-1292	7.5	68-1652	8.0
68-752	6.9	68-1112	7.2	68-1472	7.8	68-1832	8.3

SPECIFIC HEAT

TEMP. F	BTU LB-1 F-1	TEMP. F	BTU LB-1 F-1	TEMP. F	BTU LB-1 F-1	TEMP. F	BTU LB-1 F-1
77-572	0.0940-10	77-932	0.10	77-1292	0.12		

ELECTRICAL RESISTIVITY

TEMP. F	MICRON- CM	TEMP. F	MICRON- CM	TEMP. F	MICRON- CM	TEMP. F	MICRON- CM
81	93.0	990	109.3	1302	111.4	1505	113.0

DENSITY

TEMP. F	LB CU IN-3	TEMP. F	LB CU IN-3	TEMP. F	LB CU IN-3	TEMP. F	LB CU IN-3
Room	0.313						

ASTM-ASME JOINT COMMITTEE ON EFFECT OF
TEMPERATURE ON PROPERTIES OF METALS

MATERIAL		HEAT NUMBER							
		Ni	Cr	W	Ti	Fe	C	Co	
CHEMICAL COMPOSITION PER CENT		28	20	7	4	2	0.2	Bal	
FORM HEAT TREATMENT									
REFERENCE		Research Lab, General Electric Company.							
REMARKS		Nominal composition found in DMIC Memo 42.							

THERMAL CONDUCTIVITY

TEMP. F	BTU HR-1 FT-2 F-1 FT	TEMP. F	BTU HR-1 FT-2 F-1 FT	TEMP. F	BTU HR-1 FT-2 F-1 FT	TEMP. F	BTU HR-1 FT-2 F-1 FT
400	8.08	800	10.65	1200	13.25	1425	14.87
600	9.37	1000	11.96	1400	14.54		

COEFFICIENT OF LINEAR THERMAL EXPANSION

TEMP. RANGE, F	$\alpha \times 10^6$	TEMP. RANGE, F	$\alpha \times 10^6$	TEMP. RANGE, F	$\alpha \times 10^6$	TEMP. RANGE, F	$\alpha \times 10^6$
300	7.883	600	7.932	1000	8.130	1400	8.725
400	7.895	800	7.995	1200	8.373	1575	9.145
Assumed to be instantaneous coefficients.							

ASTM-ASME JOINT COMMITTEE ON EFFECT OF
TEMPERATURE ON PROPERTIES OF METALS

MATERIAL		HEAT NUMBER							
		Co	Cr	Ni	Mo	Fe	Al	C	
CHEMICAL COMPOSITION PER CENT		56.50	22.00	10.00	6.00	2.00	1.25	0.40	
FORM HEAT TREATMENT		Cast							
REFERENCE		Materials Data Bk I, General Electric Company, Thompson Lab.							
REMARKS		Nominal composition found in DMIC Memo 42.							

THERMAL CONDUCTIVITY

TEMP. F	BTU HR-1 FT-2 F-1 FT	TEMP. F	BTU HR-1 FT-2 F-1 FT	TEMP. F	BTU HR-1 FT-2 F-1 FT	TEMP. F	BTU HR-1 FT-2 F-1 FT
400	8.48	800	10.27	1000	11.07	1150	11.65
600	9.47						

ASTM-ASME JOINT COMMITTEE ON EFFECT OF
TEMPERATURE ON PROPERTIES OF METALS

MATERIAL		HEAT NUMBER							
		Co	Cr	Ni	Mo	W	Cb-Ta	Fe	Al
CHEMICAL COMPOSITION PER CENT		43.00	25.00	20.00	4.00	2.30	2.00	2.00	0.90
		C	S	P					
		0.30	0.02	0.02					
FORM HEAT TREATMENT									
REFERENCE		Allegheny Ludlum Steel Corporation.							
REMARKS		Rolled or forged from 1800 to 2250 F.							

COEFFICIENT OF LINEAR THERMAL EXPANSION

TEMP. RANGE, F	$\alpha \times 10^6$	TEMP. RANGE, F	$\alpha \times 10^6$	TEMP. RANGE, F	$\alpha \times 10^6$	TEMP. RANGE, F	$\alpha \times 10^6$
122-212	6.7	122-752	7.9	122-1472	8.8	122-1832	8.9
122-392	7.1	122-1112	8.5				
Heat treatment: 2250 F--1 hr W.Q.; 2250 F--1 hr W.Q. + 1400--16 hr air.							

COEFFICIENT OF LINEAR THERMAL EXPANSION

TEMP. RANGE, F	$\alpha \times 10^6$	TEMP. RANGE, F	$\alpha \times 10^6$	TEMP. RANGE, F	$\alpha \times 10^6$	TEMP. RANGE, F	$\alpha \times 10^6$
122-212	6.1	122-752	7.8	122-1472	8.8	122-1832	9.3
122-392	7.2	122-1112	8.1				
Heat treatment: 2250 F--1 hr W.Q.; 2250 F--1 hr W.Q. + 1400--16 hr air.							

DENSITY

TEMP, F	LB CU IN-1	TEMP, F	LB CU IN-1	TEMP, F	LB CU IN-1	TEMP, F	LB CU IN-1
Room	0.503						
Data assumed to be at room temperature. Heat treatment solution: 2250-2275 - water quenched - age 1400 F - 16 hour - air.							

ASTM-ASME JOINT COMMITTEE ON EFFECT OF TEMPERATURE ON PROPERTIES OF METALS

(10)

MATERIAL	Cobalt Alloy--X-40 (Stellite 31)					HEAT NUMBER	
CHEMICAL COMPOSITION PER CENT	Cr	Ni	Mo	Fe	Co		
	23.06	10.00	7.00	1.00	Bal		
FORM	Cast						
HEAT TREATMENT							
REFERENCE	Materials Data Bk. 1, General Electric Company, Thomson Lab.						
REMARKS	Nominal composition obtained from DMIC Memo 42.						

THERMAL CONDUCTIVITY

TEMP, F	BTU IN-1 FT-2 P-1 FT	TEMP, F	BTU IN-1 FT-2 P-1 FT	TEMP, F	BTU IN-1 FT-2 P-1 FT	TEMP, F	BTU IN-1 FT-2 P-1 FT
400	8.62	800	10.90	1000	12.93	1200	13.17
600	9.77						
Interpolated data from curve.							

COEFFICIENT OF LINEAR THERMAL EXPANSION

TEMP RANGE, F	F-1 X 10 ⁶	TEMP RANGE, F	F-1 X 10 ⁶	TEMP RANGE, F	F-1 X 10 ⁶	TEMP RANGE, F	F-1 X 10 ⁶
200	21.5	600	24.2	1000	26.8	1400	32.4
400	22.9	800	25.5	1200	28.1		
Values interpolated from curve and assumed to be instantaneous coefficients.							

ASTM-ASME JOINT COMMITTEE ON EFFECT OF TEMPERATURE ON PROPERTIES OF METALS

(11)

MATERIAL	Cobalt Alloy--X-40 (Stellite 31)					HEAT NUMBER	
CHEMICAL COMPOSITION PER CENT	Cr	Ni	W	C	Co		
	25.5	10.5	7.5	0.05	Bal		
FORM							
HEAT TREATMENT							
REFERENCE	Haynes Stellite Company.						
REMARKS	Investment cast alloy. As cast - Rockwell C 34 maximum. Aged 50 hrs at 1500 F - Rockwell C 42 maximum.						

THERMAL CONDUCTIVITY

TEMP, F	BTU IN-1 FT-2 P-1 FT	TEMP, F	BTU IN-1 FT-2 P-1 FT	TEMP, F	BTU IN-1 FT-2 P-1 FT	TEMP, F	BTU IN-1 FT-2 P-1 FT
392	8.38	792	10.2	932	11.2	1112	12.7
572	10.1						

COEFFICIENT OF LINEAR THERMAL EXPANSION

TEMP RANGE, F	F-1 X 10 ⁶	TEMP RANGE, F	F-1 X 10 ⁶	TEMP RANGE, F	F-1 X 10 ⁶	TEMP RANGE, F	F-1 X 10 ⁶
70-600	7.84	70-1000	8.39	70-1500	9.19	70-1600	9.19
70-800	8.08	70-1200	8.75				

SPECIFIC HEAT

TEMP, F	BTU LB-1 F-1	TEMP, F	BTU LB-1 F-1	TEMP, F	BTU LB-1 F-1	TEMP, F	BTU LB-1 F-1
Room	0.0981						
Data assumed to be at room temperature.							

DENSITY

TEMP, F	LB CU IN-1	TEMP, F	LB CU IN-1	TEMP, F	LB CU IN-1	TEMP, F	LB CU IN-1
Room	0.315						
Data assumed to be at room temperature.							

ASTM-ASME JOINT COMMITTEE ON EFFECT OF TEMPERATURE ON PROPERTIES OF METALS

(12)

MATERIAL	Cobalt Alloy--X-40 (Stellite 31)					HEAT NUMBER	
CHEMICAL COMPOSITION PER CENT	Cr	Ni	Fe	C	Co		
	25.5	10.5	2.0	0.53	Bal		
FORM							
HEAT TREATMENT							
REFERENCE	Jesse E. Evans, Jr., "Thermal Conductivity of 14 Metals and Alloys up to 1100 F", Lewis Flight Propulsion Lab, NACA Research Memorandum RME 50L07 (March 51).						

THERMAL CONDUCTIVITY

TEMP, F	BTU IN-1 FT-2 P-1 FT	TEMP, F	BTU IN-1 FT-2 P-1 FT	TEMP, F	BTU IN-1 FT-2 P-1 FT	TEMP, F	BTU IN-1 FT-2 P-1 FT
220	7.9	500	9.7	800	11.4	1000	12.5
300	8.4	600	10.2	900	11.9	1020	12.65
400	9.1	700	10.8				

ASTM-ASME JOINT COMMITTEE ON EFFECT OF TEMPERATURE ON PROPERTIES OF METALS

(13)

MATERIAL	Cobalt Alloy--HS-23							
CHEMICAL COMPOSITION PER CENT	Co	Cr	W	Mn	Fe	Si	C	Mo
	65.12	26.57	5.08	0.04	0.71	0.68	0.56	0.32
FORM								
HEAT TREATMENT								
REFERENCE	U. S. Naval Engineering Experiment Station.							
REMARKS	Absolute method, Leitz Dilatometer, Heating rate: 5.0° or 5.6° per minute.							

COEFFICIENT OF LINEAR THERMAL EXPANSION

TEMP RANGE, F	F-1 X 10 ⁶	TEMP RANGE, F	F-1 X 10 ⁶	TEMP RANGE, F	F-1 X 10 ⁶	TEMP RANGE, F	F-1 X 10 ⁶
100-500	7.5	100-1000	8.3	100-1600	9.1		

ASTM-ASME JOINT COMMITTEE ON EFFECT OF
TEMPERATURE ON PROPERTIES OF METALS

14

MATERIAL	Cobalt Alloy--HS-27								HEAT NUMBER
CHEMICAL COMPOSITION PER CENT	Co	Ni	Cr	Mo	Mn	Si	Fe	C	
	33.85	30.91	26.40	6.14	1.02	1.0	0.97	0.5	
FORM									
HEAT TREATMENT									
REFERENCE	U. S. Naval Engineering Experiment Station.								
REMARKS	Absolute method, Leitz Dilatometer. Heating rate: 5.0° or 5.6° per minute.								

COEFFICIENT OF LINEAR THERMAL EXPANSION

TEMP. RANGE, F	F-1 X 10 ⁶	TEMP. RANGE, F	F-1 X 10 ⁶	TEMP. RANGE, F	F-1 X 10 ⁶	TEMP. RANGE, F	F-1 X 10 ⁶
100-500	7.3	100-1000	7.7	100-1600	8.7		

ASTM-ASME JOINT COMMITTEE ON EFFECT OF
TEMPERATURE ON PROPERTIES OF METALS

15

MATERIAL	Cobalt Alloy--HS-27								HEAT NUMBER
CHEMICAL COMPOSITION PER CENT	Co	Ni	Cr	Mo	Mn	Si	C	Fe	
	32.0	32.0	25.0	6.5	1.0	0.4	0.2	Bal	
FORM									
HEAT TREATMENT									
REFERENCE	U. S. Naval Engineering Experiment Station.								
REMARKS	Absolute method, Leitz Dilatometer, heating rate: 5.0 or 5.6 F per minute.								

COEFFICIENT OF LINEAR THERMAL EXPANSION

TEMP. RANGE, F	F-1 X 10 ⁶	TEMP. RANGE, F	F-1 X 10 ⁶	TEMP. RANGE, F	F-1 X 10 ⁶	TEMP. RANGE, F	F-1 X 10 ⁶
100-500	7.7	100-1000	8.1	100-1600	9.1		

ASTM-ASME JOINT COMMITTEE ON EFFECT OF
TEMPERATURE ON PROPERTIES OF METALS

16

MATERIAL	Cobalt Alloy--Vitalium (HS-21)								HEAT NUMBER
CHEMICAL COMPOSITION PER CENT	Cr	Mo	Fe	N	C	Co			
	27	5.5	3.0	2.75	0.25	Bal			
FORM									
HEAT TREATMENT									
REFERENCE	Thomson Lab Data, General Electric Company.								

THERMAL CONDUCTIVITY

TEMP, F	BTU HR-1 FT-2 P-1 FT	TEMP, F	BTU HR-1 FT-2 P-1 FT	TEMP, F	BTU HR-1 FT-2 P-1 FT	TEMP, F	BTU HR-1 FT-2 P-1 FT
0	6.58	400	8.50	800	10.34	1200	12.24
200	7.32	600	9.40	1000	11.30		

ASTM-ASME JOINT COMMITTEE ON EFFECT OF
TEMPERATURE ON PROPERTIES OF METALS

17

MATERIAL	Cobalt Alloy--Vitalium (Stellite 21)								HEAT NUMBER
CHEMICAL COMPOSITION PER CENT	Cr	Mo	Fe	N	C	Co			
	27	5.5	3.0	2.75	0.25	Bal			
FORM	Investment Cast Alloy.								
HEAT TREATMENT									
REFERENCE	Haynes Stellite Company.								
REMARKS	As cast Rockwell C 34 maximum. Aged 50 hrs, at 1475 F - Rockwell C 45 maximum.								

THERMAL CONDUCTIVITY

TEMP, F	BTU HR-1 FT-2 P-1 FT	TEMP, F	BTU HR-1 FT-2 P-1 FT	TEMP, F	BTU HR-1 FT-2 P-1 FT	TEMP, F	BTU HR-1 FT-2 P-1 FT
392	8.42	752	10.1	932	11.0	1112	11.8
572	9.45						

COEFFICIENT OF LINEAR THERMAL EXPANSION

TEMP. RANGE, F	F-1 X 10 ⁶	TEMP. RANGE, F	F-1 X 10 ⁶	TEMP. RANGE, F	F-1 X 10 ⁶	TEMP. RANGE, F	F-1 X 10 ⁶
70-600	7.83	70-1000	8.18	70-1500	8.68	70-1600	8.72
70-800	7.96	70-1200	8.38				

SPECIFIC HEAT

TEMP, F	BTU LB-1 F-1	TEMP, F	BTU LB-1 F-1	TEMP, F	BTU LB-1 F-1	TEMP, F	BTU LB-1 F-1
Room	0.1006						
Data assumed to be at room temperature.							

ELECTRICAL RESISTIVITY

TEMP, F	MICRON- OHM CM	TEMP, F	MICRON- OHM CM	TEMP, F	MICRON- OHM CM	TEMP, F	MICRON- OHM CM
Room	34.4						
Data assumed to be at room temperature.							

DENSITY

TEMP, F	LB CU IN-1	TEMP, F	LB CU IN-1	TEMP, F	LB CU IN-1	TEMP, F	LB CU IN-1
Room	0.299						
Data assumed to be at room temperature.							

END OF REFERENCE

21

REFERENCE

22

COSTON, R. M.: HANDBOOK OF THERMAL DESIGN DATA FOR MULTILAYER INSULATION SYSTEMS. VOL. II. REP. LMSC-A847882, VOL. II, LOCKHEED MISSILES AND SPACE CO. (NASA CR-87485), JUNE 25, 1967.

25 JUNE 1967

LMSC-A847882, Vol. II

HANDBOOK OF THERMAL DESIGN DATA FOR MULTILAYER INSULATION SYSTEMS

FINAL REPORT, VOLUME II
OF
HIGH-PERFORMANCE INSULATION THERMAL DESIGN CRITERIA
NAS 8-20353

CRYOGENIC STAGE PROGRAMS



Prepared For
GEORGE C. MARSHALL SPACE FLIGHT CENTER
HUNTSVILLE, ALABAMA

Prepared By
R. M. COSTON, PROJECT MANAGER,
CRYOGENIC STAGE PROGRAMS

67-34910
(ACCESSION NUMBER)
180
(PAGES)
CR-87485
(NASA CR OR TNX OR AD NUMBER)

(THRU)

(CODE)

(CATEGORY)

Lockheed

MISSILES & SPACE COMPANY

A GROUP DIVISION OF LOCKHEED AIRCRAFT CORPORATION

SUNNYVALE, CALIFORNIA

2. METALS

The thermal effectiveness of a multilayer insulation system is influenced by the type and quantity of structural, plumbing, and electrical line penetrations through the insulation to the propellant tank. The selection of materials for fabricating these penetrations depends on structural properties, thermal properties, cost, and ease of fabrication. This section of the Handbook provides pertinent design data for metals used in most of the insulation penetrations.

The metals selected for reporting are those which exhibit good low-temperature structural properties. Where data for a specific metal are not available, data for similar metals are provided. Data for high-purity metals are presented, also, for reference purposes. The data presented include density, linear thermal expansion, thermal conductivity, specific heat, and emissivity.

Density of Metals

The aluminum alloys shown are normally used for propellant tanks, the stainless steels for plumbing lines, and the titanium alloys for tank support structures.

Table 2-1

DENSITY OF METALS

Metals	Density at 75°F	
	lb/in. ³	lb/ft ³
ALUMINUM	0.097	168
2024	0.100	173
2219	0.102	176
6061	0.098	169
7039	0.099	171
7075	0.101	175
STAINLESS STEELS		
301	0.286	494
304	0.29	—
316	0.29	—
347	0.29	—
TITANIUM	0.163	281
5A1 2.5Sn	0.162	280
6A1 4V	0.161	278

Linear Thermal Expansion of Metals as a Function of Temperature

Certain curves were adjusted slightly so that zero percent expansion falls at 538° R. This shift does not affect the relative value of thermal expansion between two temperatures.

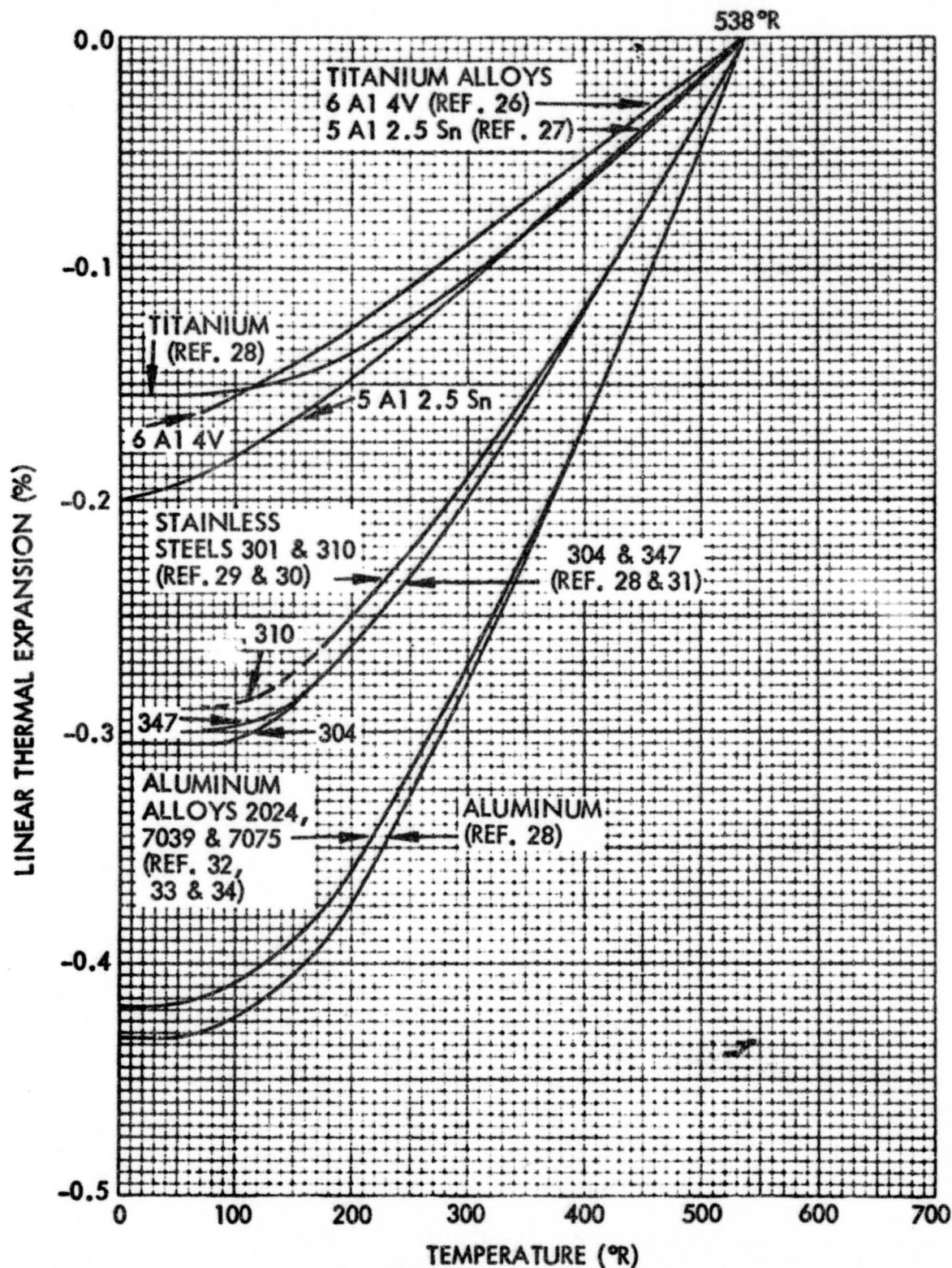


Fig. 2-1 Linear Thermal Expansion of Metals as a Function of Temperature

Thermal Conductivity of Metals as a Function of Temperature

The thermal conductivity of 7075-T6 aluminum in the annealed condition is higher than for the same material in the tempered condition. This characteristic is typical of an alloy after annealing.

The thermal conductivity of four commercial titanium alloys and several stainless alloys have been included in a separate figure for clarity. The titanium alloys are alloyed as follows:

4A1-3Mo-1V - 4.4% Al, 1.0% V, 3.0% Mo, 0.1% Fe, 0.03% C, 0.011% N

2.5A1-16V - 2.75% Al, 14.95% V, 0.21% Fe, 0.03% C, 0.015% N

6A1-4V - 5.89% Al, 3.87% V, 0.15% Fe, 0.02% C, 0.015% N

13V-11Cr-3A1 - 3.5% Al, 13.9% V, 10.4% Cr, 0.25% Fe, 0.04% C, 0.025% N

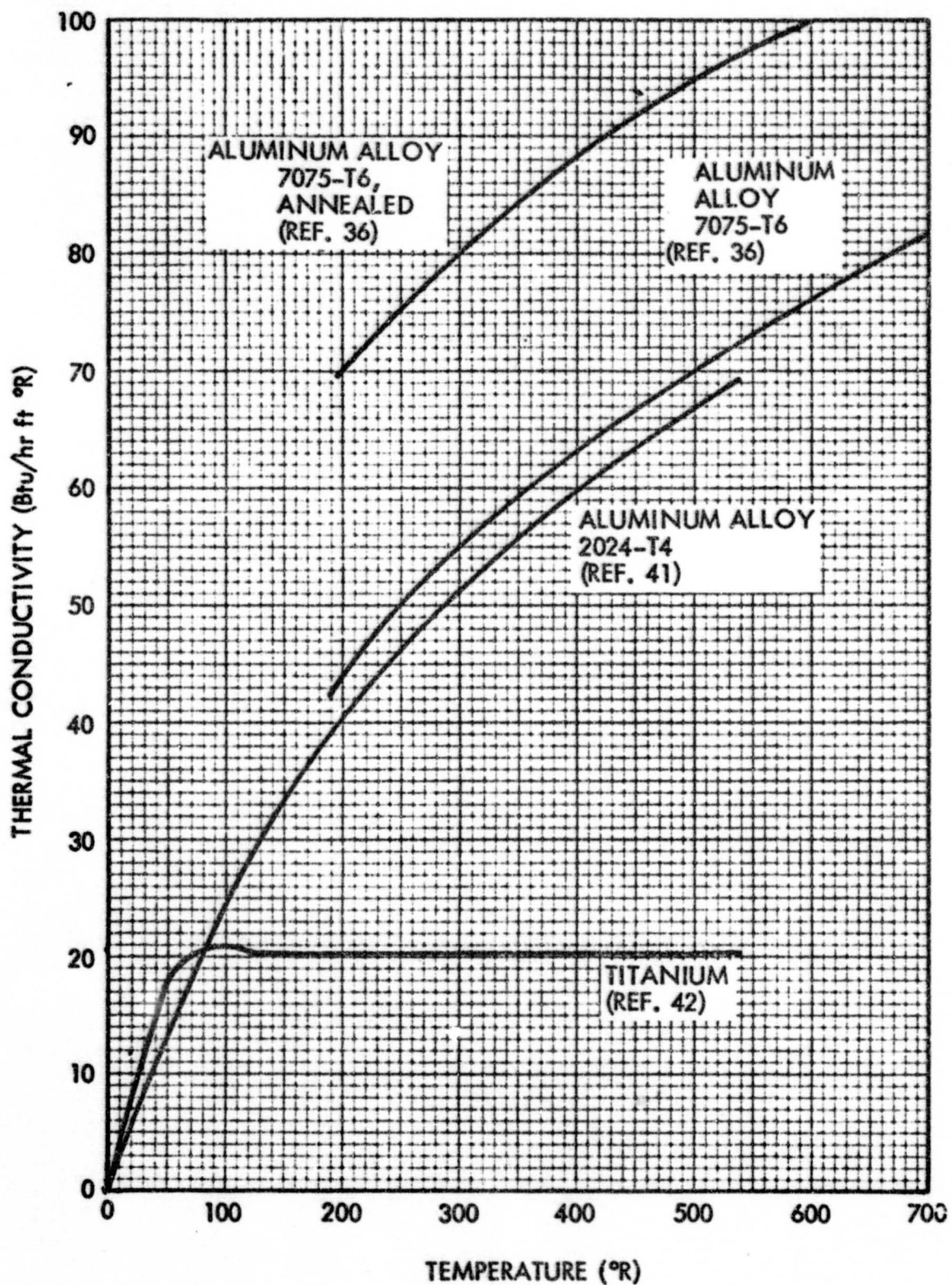


Fig. 2-2 Thermal Conductivity of Metals as a Function of Temperature

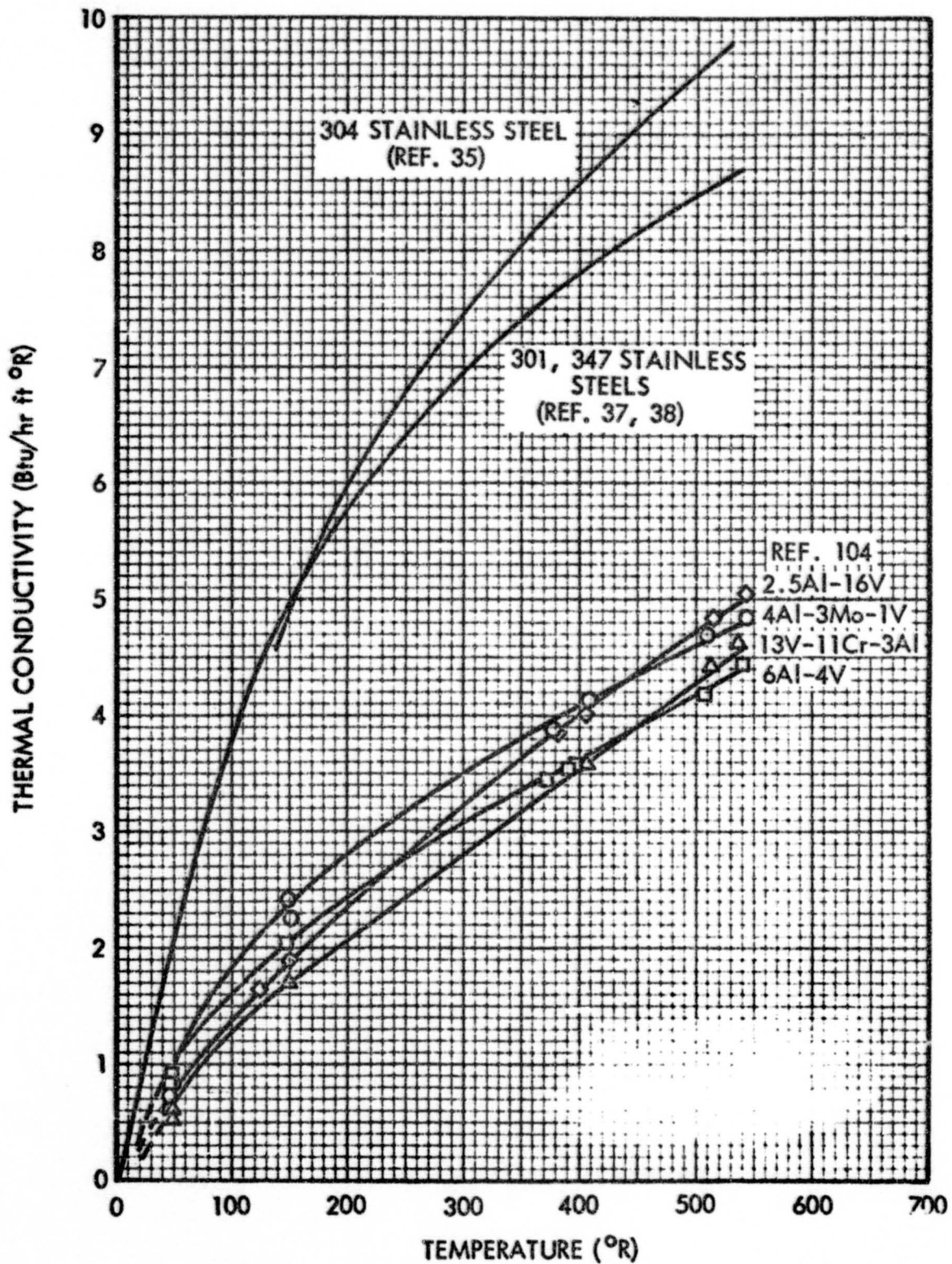


Fig. 2-3 Thermal Conductivity of Titanium Alloys as a Function of Temperature

Thermal Conductivity Integrals of Metals

The thermal conductivity integrals for metallic solids are presented in this section as a function of temperature. The thermal conductivity integral is defined from the Fourier Equation for steady unidirectional heat conduction as follows:

$$Q = kA \cdot \frac{dT}{dx}$$

where

Q = Rate of heat conduction, negative in the direction of increasing length

k = Thermal conductivity

A = Cross-sectional area of the heat conduction path, normal to the direction of heat flow

$\frac{dT}{dx}$ = Temperature gradient along the path at the section under consideration

T = Temperature

x = Length

For a constant cross-sectional area the Fourier Equation becomes

$$Q \frac{L}{A} = \int_{T_1}^{T_2} k dT$$

where T_1 and T_2 are the temperatures at any two points along the path of heat flow, and L is the distance between these two points.

The thermal conductivity integrals plotted in this section as function of temperature are values of

$$\int_{T_0}^{T_L} k dT$$

where T_o and T_L are temperatures along a heat flow path communicating between heat reservoirs at $T_o = 7.2^\circ R$ and T_L at length L , for T_o . The heat flow along a conductor of constant cross-section A , through length L , may then be determined from the difference of the thermal conductivity integrals

$$Q \frac{L}{A} = \int_{T_1}^{T_2} k dT = \int_{T_o}^{T_2} k dT - \int_{T_o}^{T_1} k dT$$

In order to extend the usefulness and accuracy of the data presented, temperature scales have been expanded and data have been plotted on a series of graphs to cover the entire temperature range of interest.

Thermal Conductivity Integrals of Pure Aluminum
as a Function of Temperature

Aluminum I - 99.996% pure, single crystal (ALCOA)
99.99% pure, cold drawn (ALCOA)

Aluminum II - 99% commercial pure (ALCOA) drawn

All data were obtained from Ref. 104.

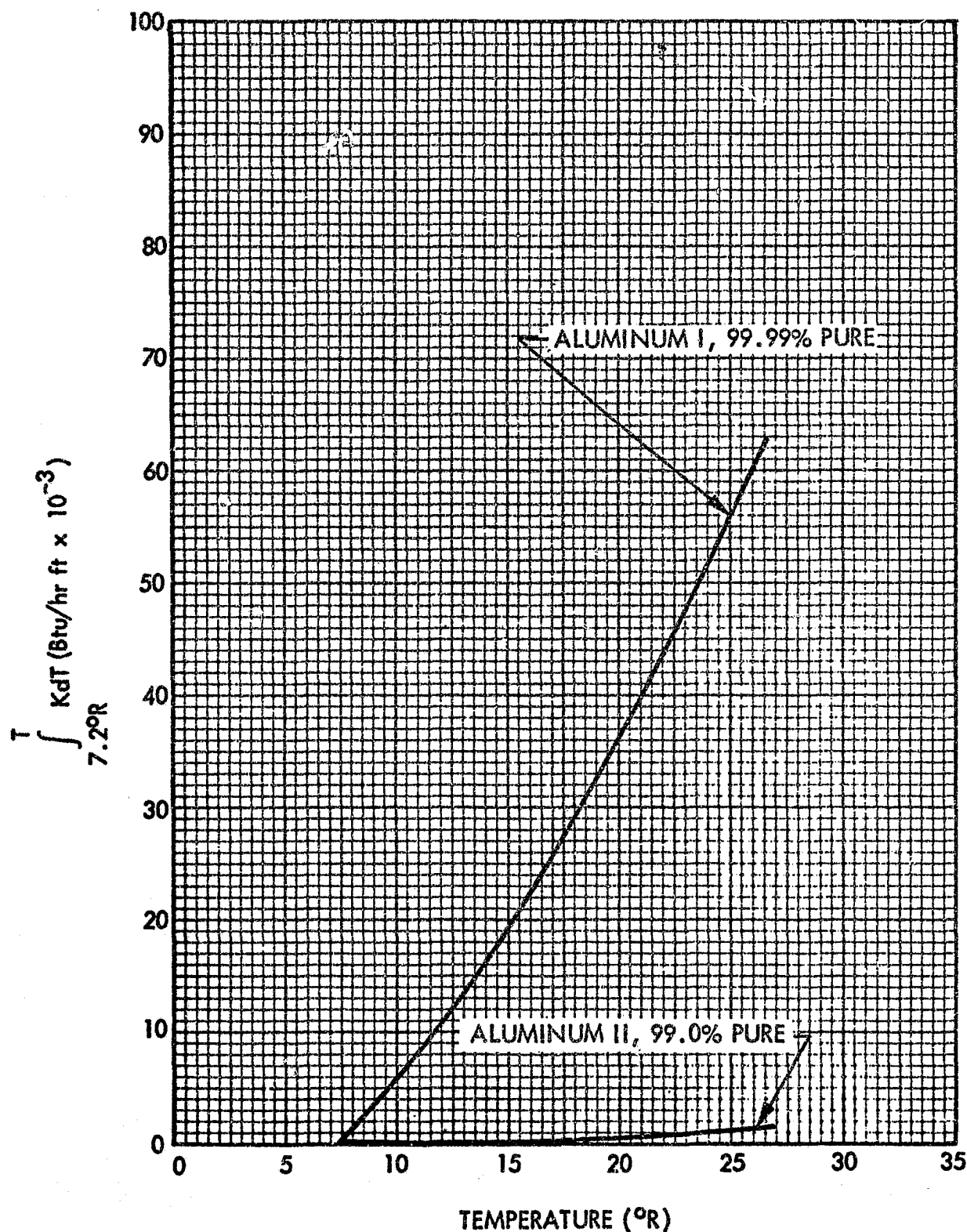


Fig. 2-4(a) Thermal Conductivity Integrals of Pure Aluminum as a Function of Temperature

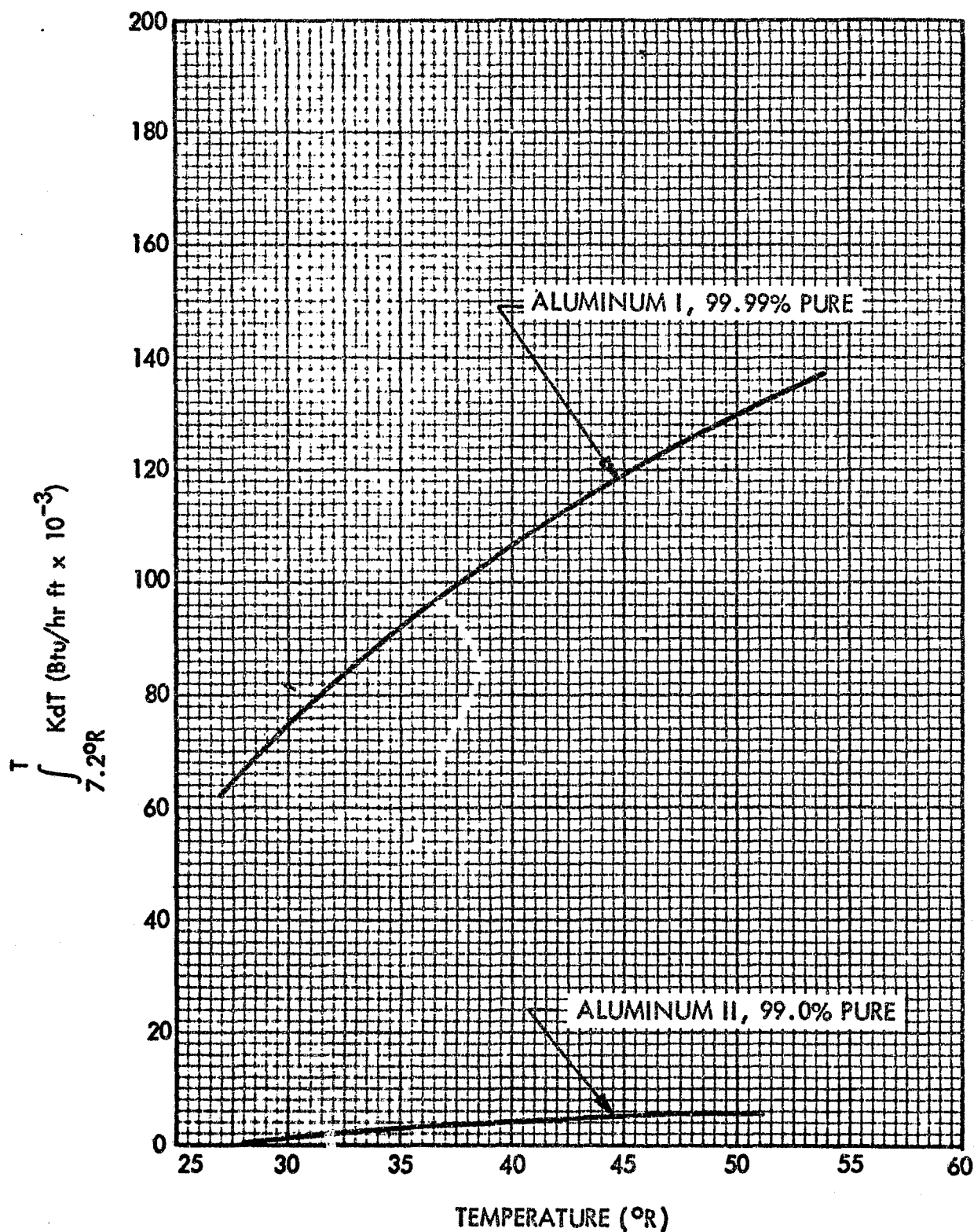


Fig. 2-4(b) Thermal Conductivity Integrals of Pure Aluminum as a Function of Temperature

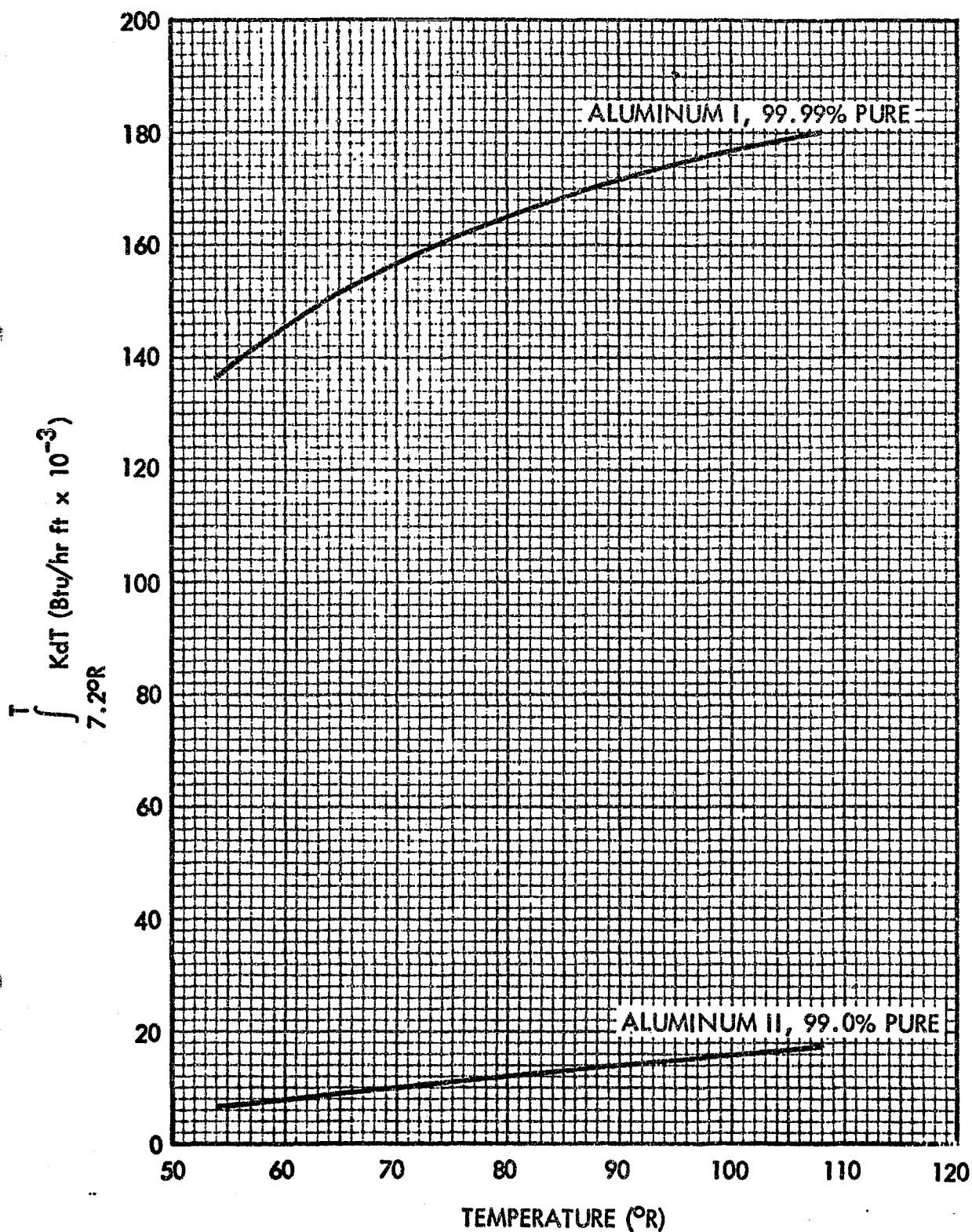


Fig. 2-4(c) Thermal Conductivity Integrals of Pure Aluminum as a Function of Temperature

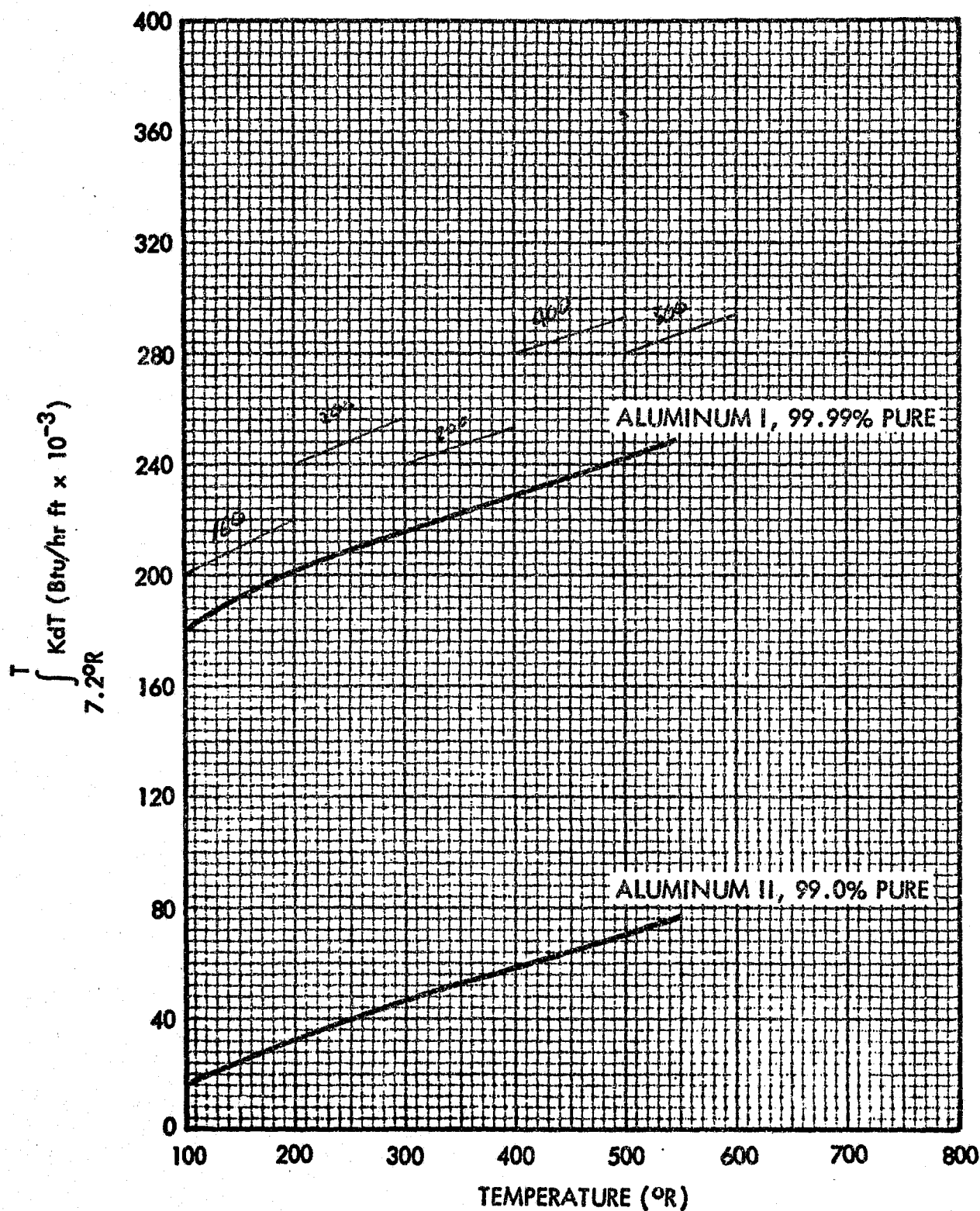


Fig. 2-4(d) Thermal Conductivity Integrals of Pure Aluminum as a Function of Temperature

Thermal Conductivity Integrals of Various Aluminum Alloys
as a Function of Temperature

The alloys cited in the graphs are composed of the various elements as follows:

1100-F - ALCOA, 99% pure aluminum as fabricated

6063-T5 - ALCOA, 0.4% Si, 0.7% Mg, 98.5% Al, as fabricated

3003-F - ALCOA, 1.2% Mn, 98.5% Al, as fabricated

4S - 0.16% Cu, 1.02% Mg, 1.20% Mn, 0.52% Fe, 0.13% Si, 0.02% Cr, 0.02% Ti

5052-O - 0.25% Cr, 2.5% Mg, 97% Al, annealed

5154-O - 0.25% Cr, 3.5% Mg, 96% Al, annealed

75-S - 1.5% Cu, 5.5% Zn, 2.5% Mg, 0.2% Mn, 0.3% Cr

2024-T4 - 0.6% Mn, 1.5% Mg, 4.5% Cu, 93% Al, solution heat treated

All data were obtained from Ref. 104

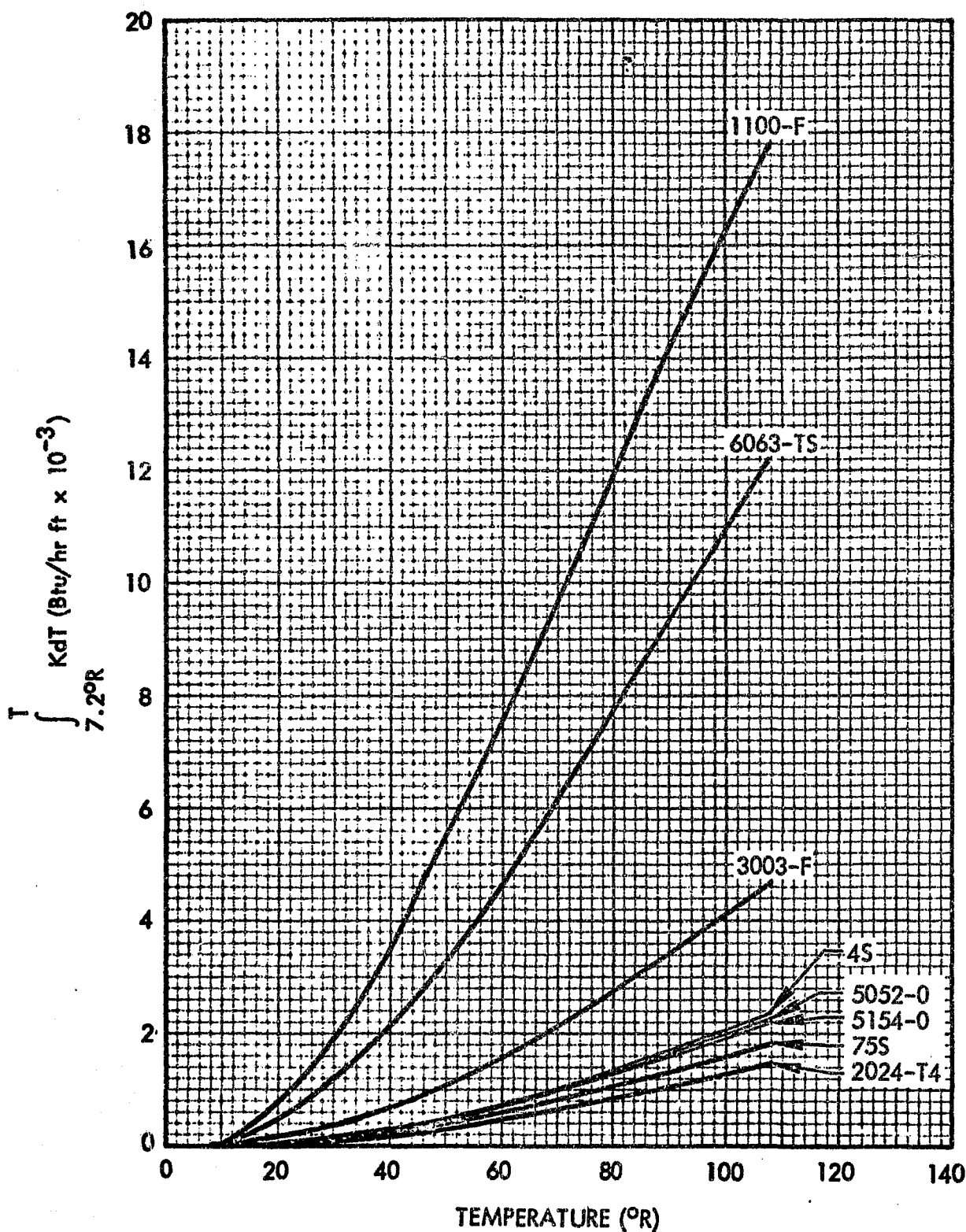


Fig. 2-5(a) Thermal Conductivity Integrals of Various Aluminum Alloys as a Function of Temperature

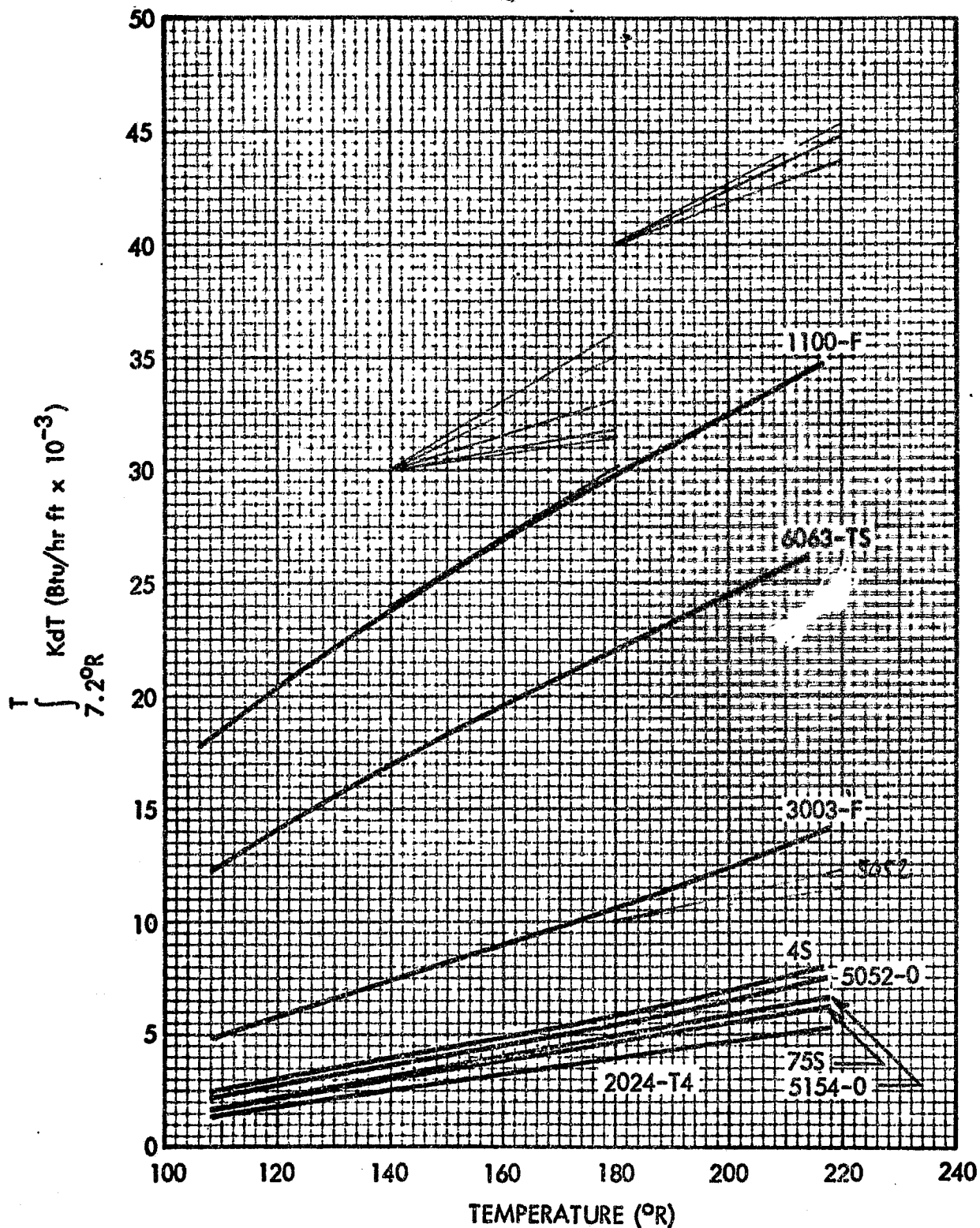


Fig. 2-5(b) Thermal Conductivity Integrals of Various Aluminum Alloys as a Function of Temperature

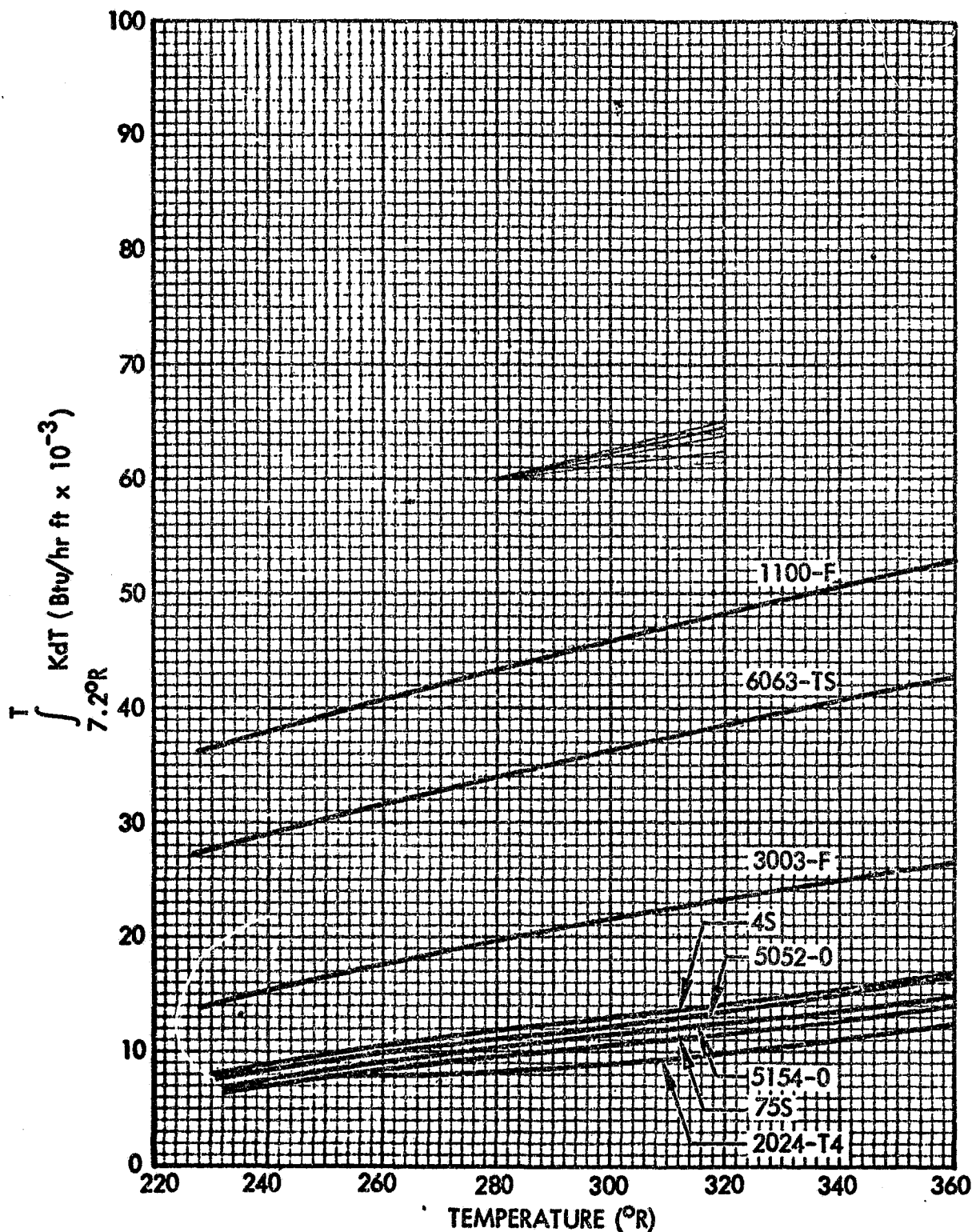


Fig. 2-5(c) Thermal Conductivity Integrals of Various Aluminum Alloys as a Function of Temperature

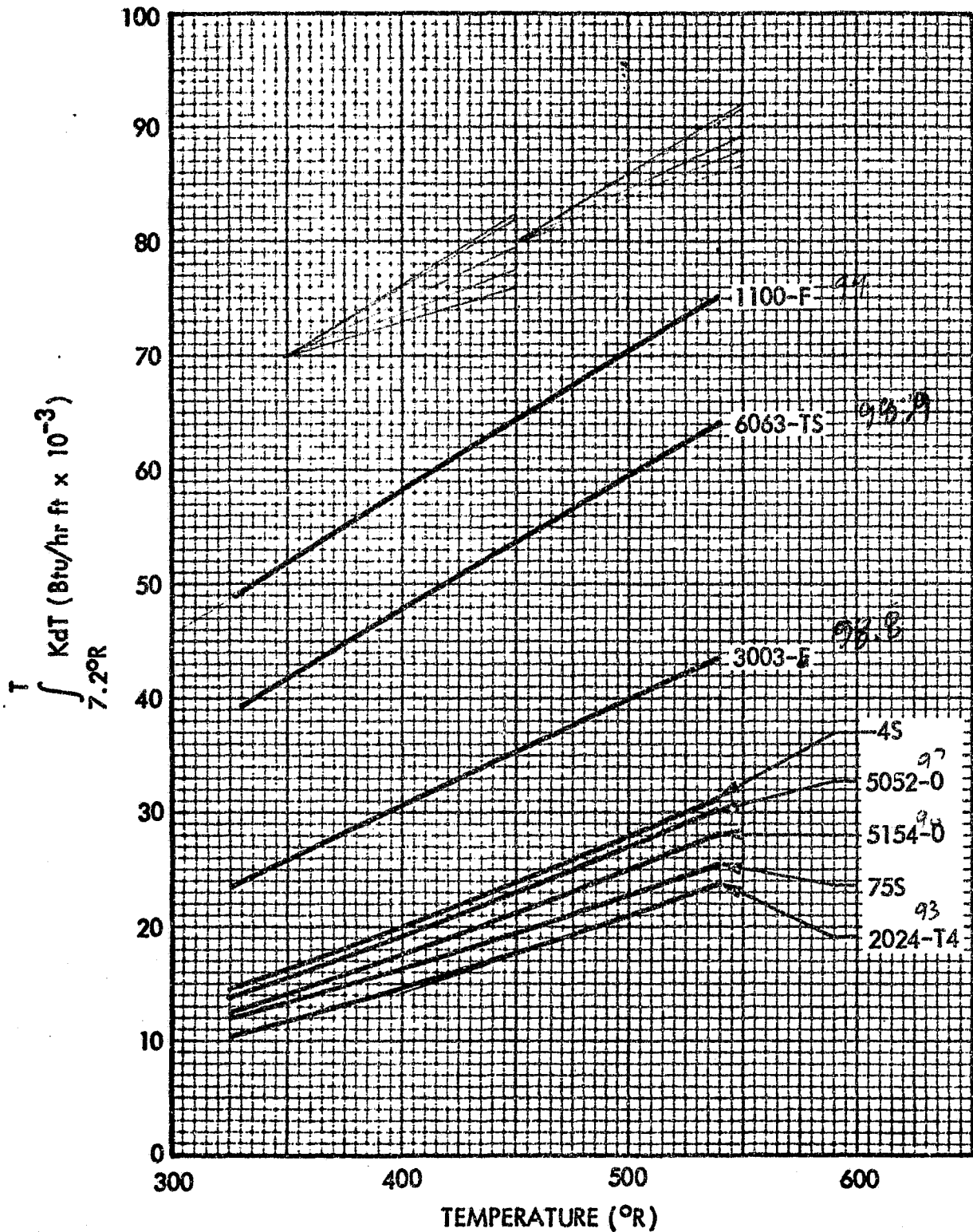


Fig. 2-5(d) Thermal Conductivity Integrals of Various Aluminum Alloys as a Function of Temperature

12
135x
590
5400
675
72900

Thermal Conductivity Integrals of Titanium
as a Function of Temperature

Titanium - 99.99% pure, single crystal, Associates Electric Industries

Titanium Alloy - Rem-Cru, RC 130-B, 4.7% Mn, 3.99% Al, 0.14% C

All data were obtained from Ref. 104.

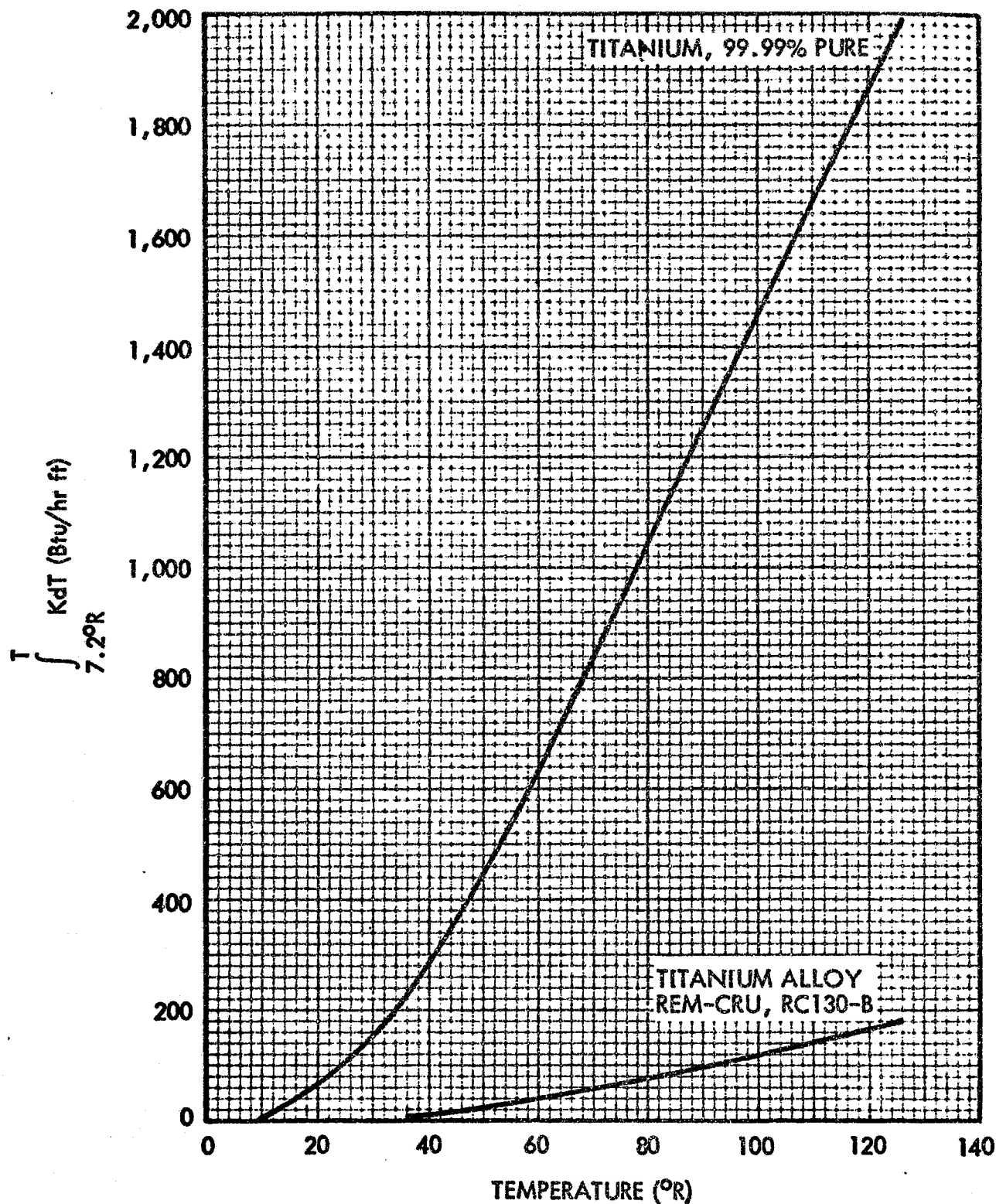


Fig. 2-6(a) Thermal Conductivity Integrals of Titanium as a Function of Temperature

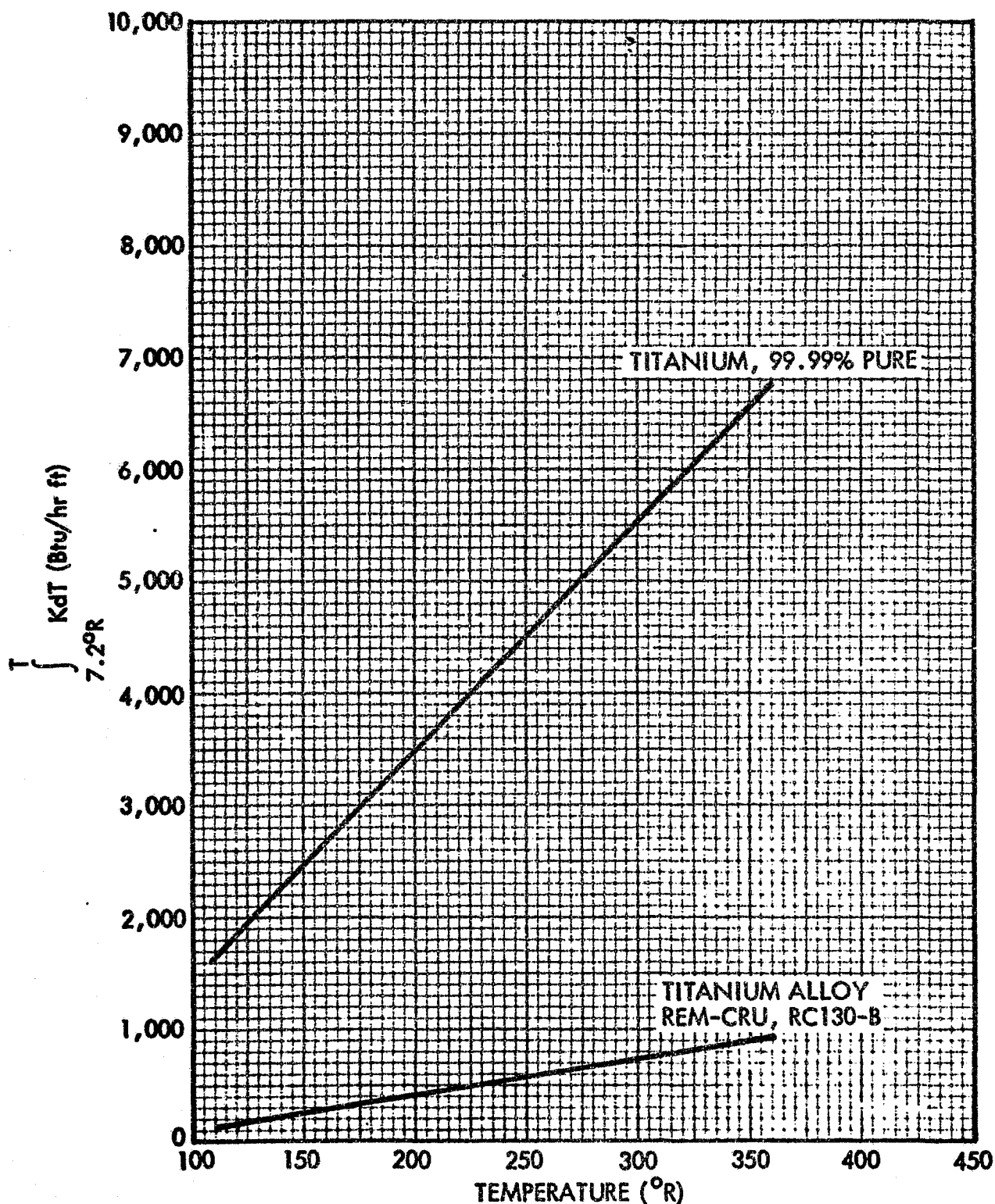


Fig. 2-6(b) Thermal Conductivity Integrals of Titanium as a Function of Temperature

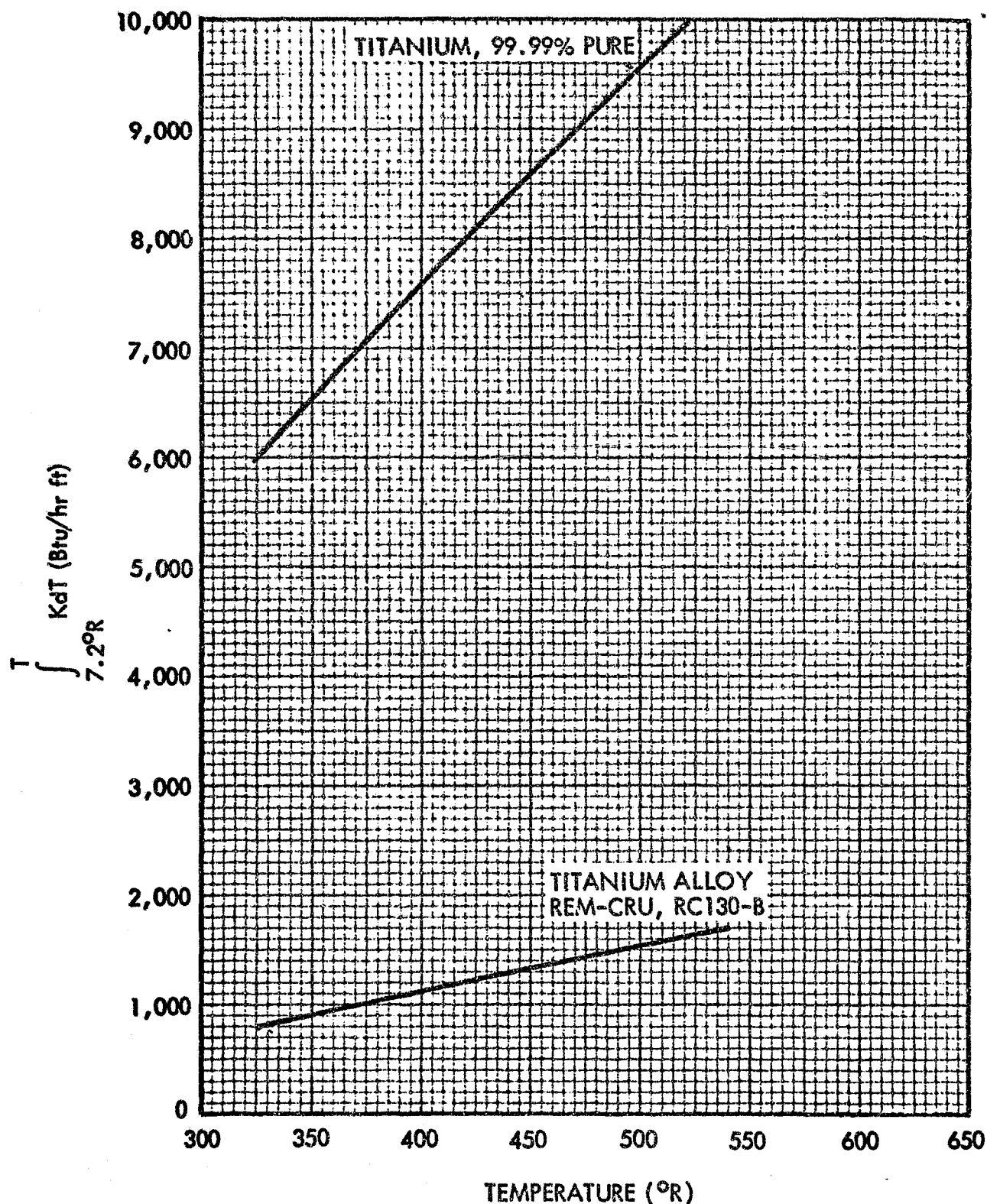


Fig. 2-6(c) Thermal Conductivity Integrals of Titanium as a Function of Temperature

Thermal Conductivity Integrals of Several Commercial Titanium

Alloys

4Al-3Mo-1V - 4.4% Al, 1.0% V, 3.0% Mo, 0.1% Fe, 0.03% C, 0.011% N

2.5Al-16V - 2.75% Al, 14.95% V, 0.21% Fe, 0.03% C, 0.015% N

6Al-4V - 5.89% Al, 3.87% V, 0.15% Fe, 0.02% C, 0.015% N

13V-11Cr-3Al - 3.5% Al, 13.9% V, 10.4% Cr, 0.25% Fe, 0.04% C, 0.025% N

All data were obtained from Ref. 105.

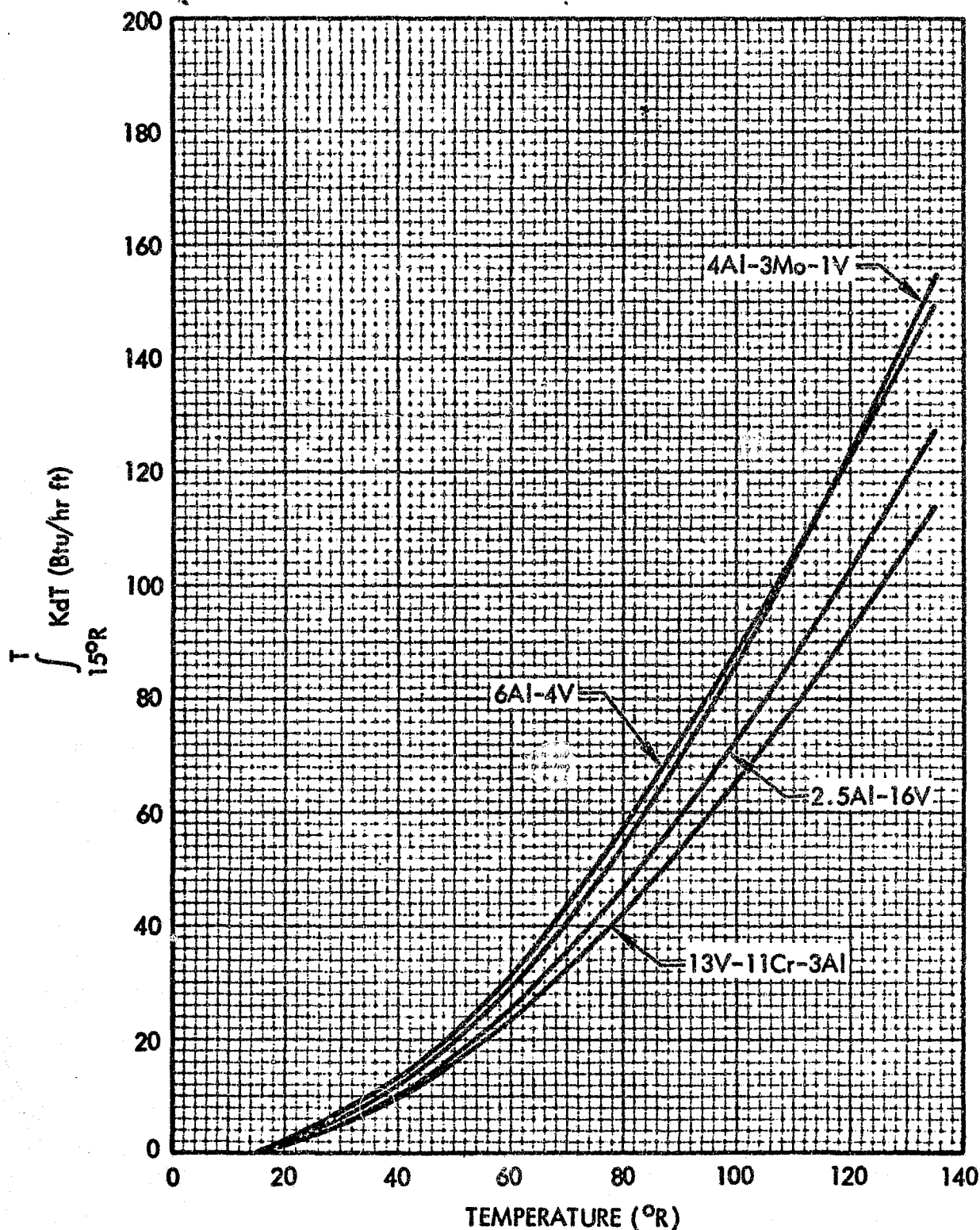


Fig. 2-7(a) Thermal Conductivity Integrals of Several Commercial Titanium Alloys

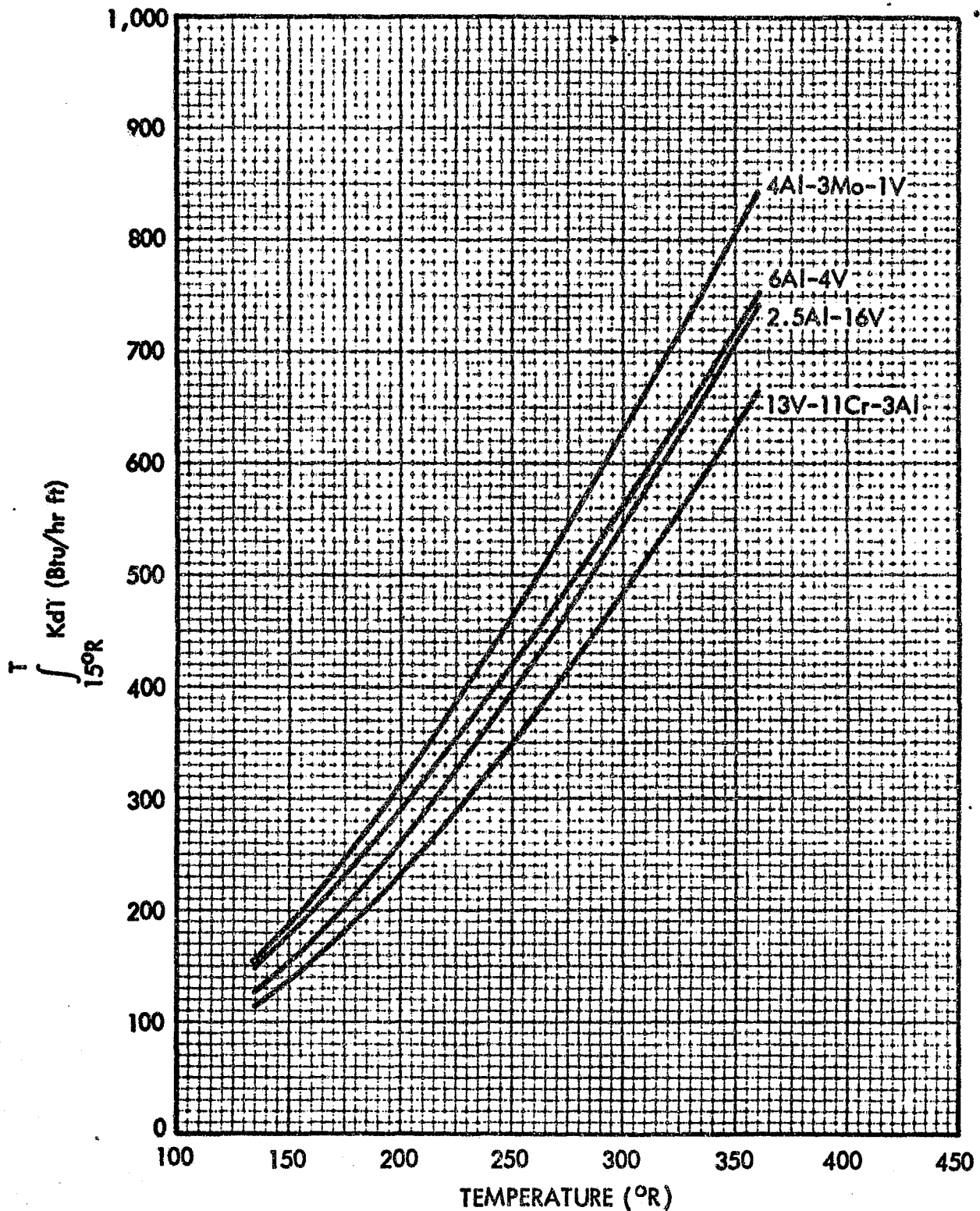


Fig. 2-7(b) Thermal Conductivity Integrals of Several Commercial Titanium Alloys

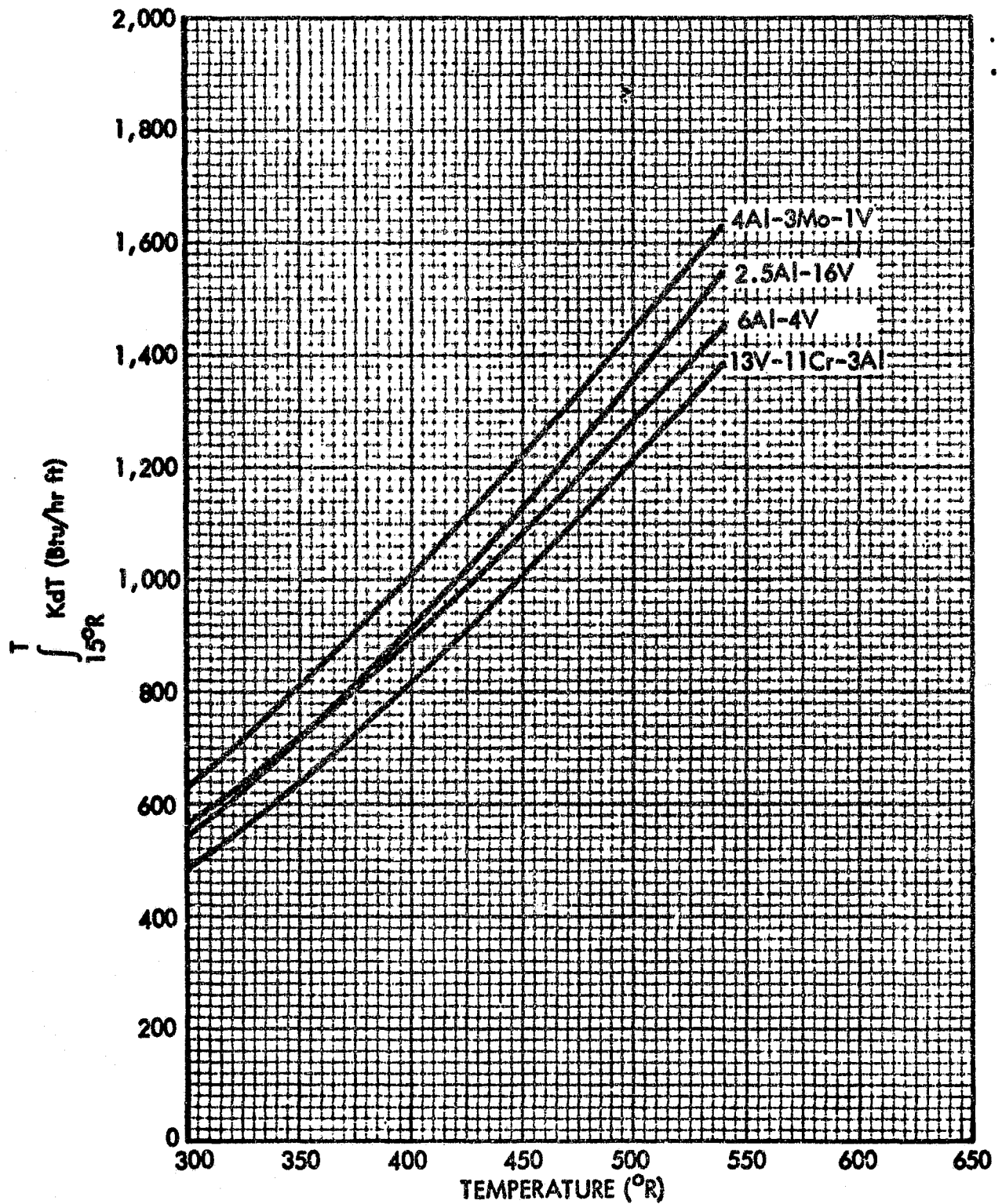


Fig. 2-7(c) Thermal Conductivity Integrals of Several Commercial Titanium Alloys

Thermal Conductivity Integrals of Ferrous Alloys
as a Function of Temperature

410 - 12.6% Cr, 0.36% Si, 0.32% Mn, 0.12% Ni, 0.09% C, 0.06% Cu, 0.03% N,
0.01% P

Stainless - Average value for close curves of types 303, 304, 316, 347, and
"stainless" as compiled in NBS Circular 556

All data were obtained from Ref. 104.

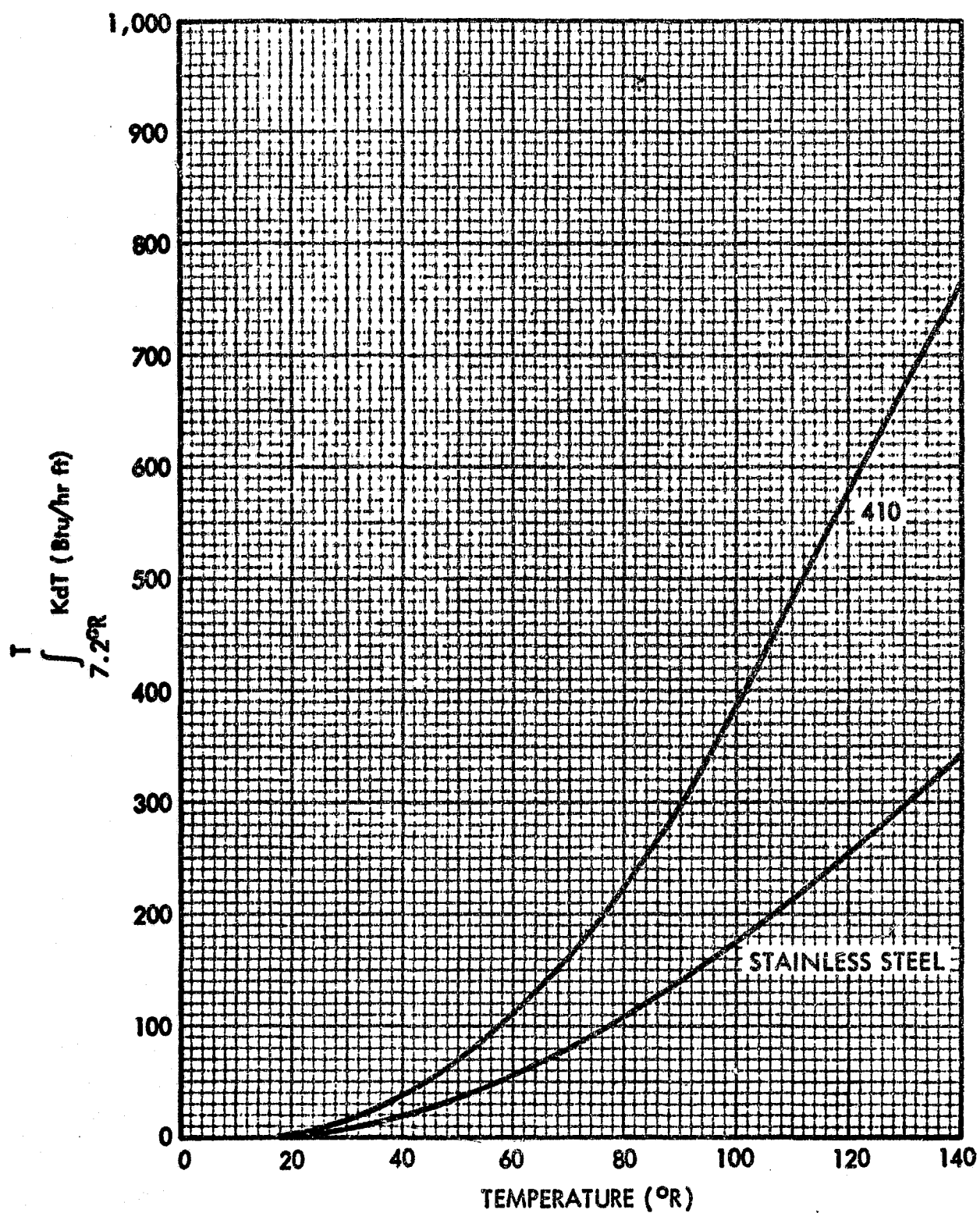


Fig. 2-8(a) Thermal Conductivity Integrals of Ferrous Alloys as a Function of Temperature

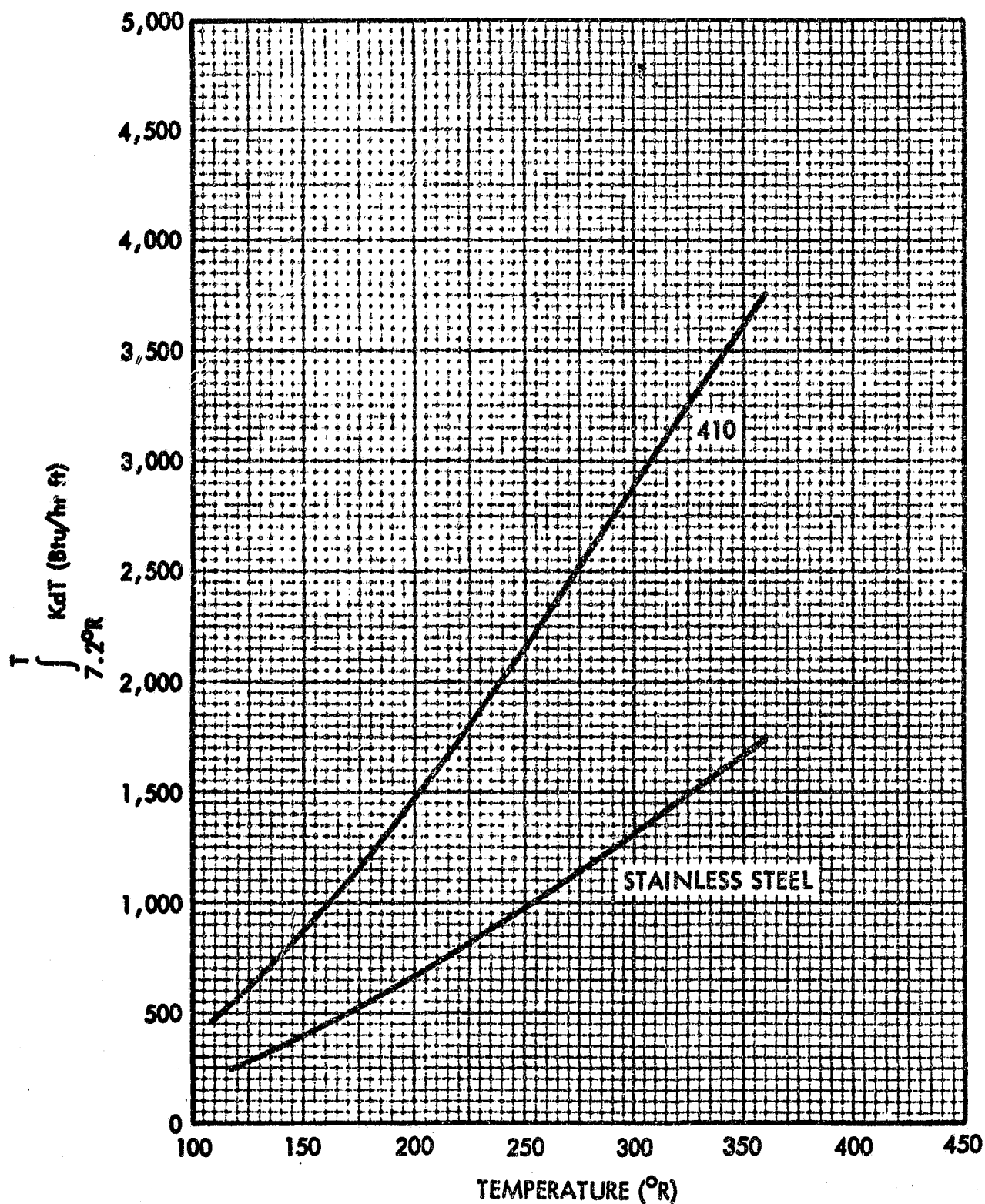


Fig. 2-8(b) Thermal Conductivity Integrals of Ferrous Alloys as a Function of Temperature

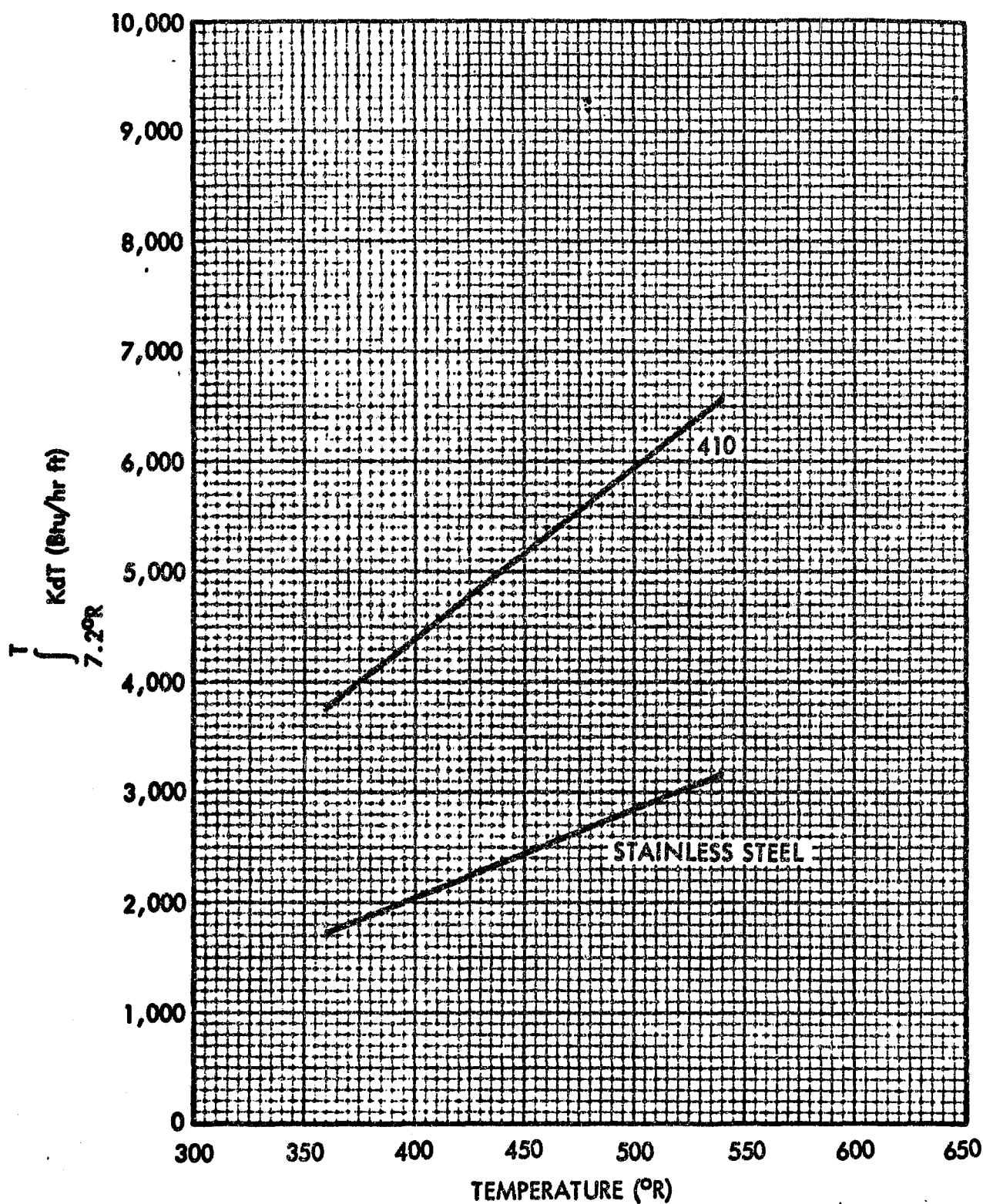


Fig. 2-8(c) Thermal Conductivity Integrals of Ferrous Alloys as a Function of Temperature

Specific Heat of Metals as a Function of Temperature

The stainless-steel alloys 316 and 347 are classified as 18-8 austenitic stainless steels. These contain 18 percent chromium and 8 percent nickel.

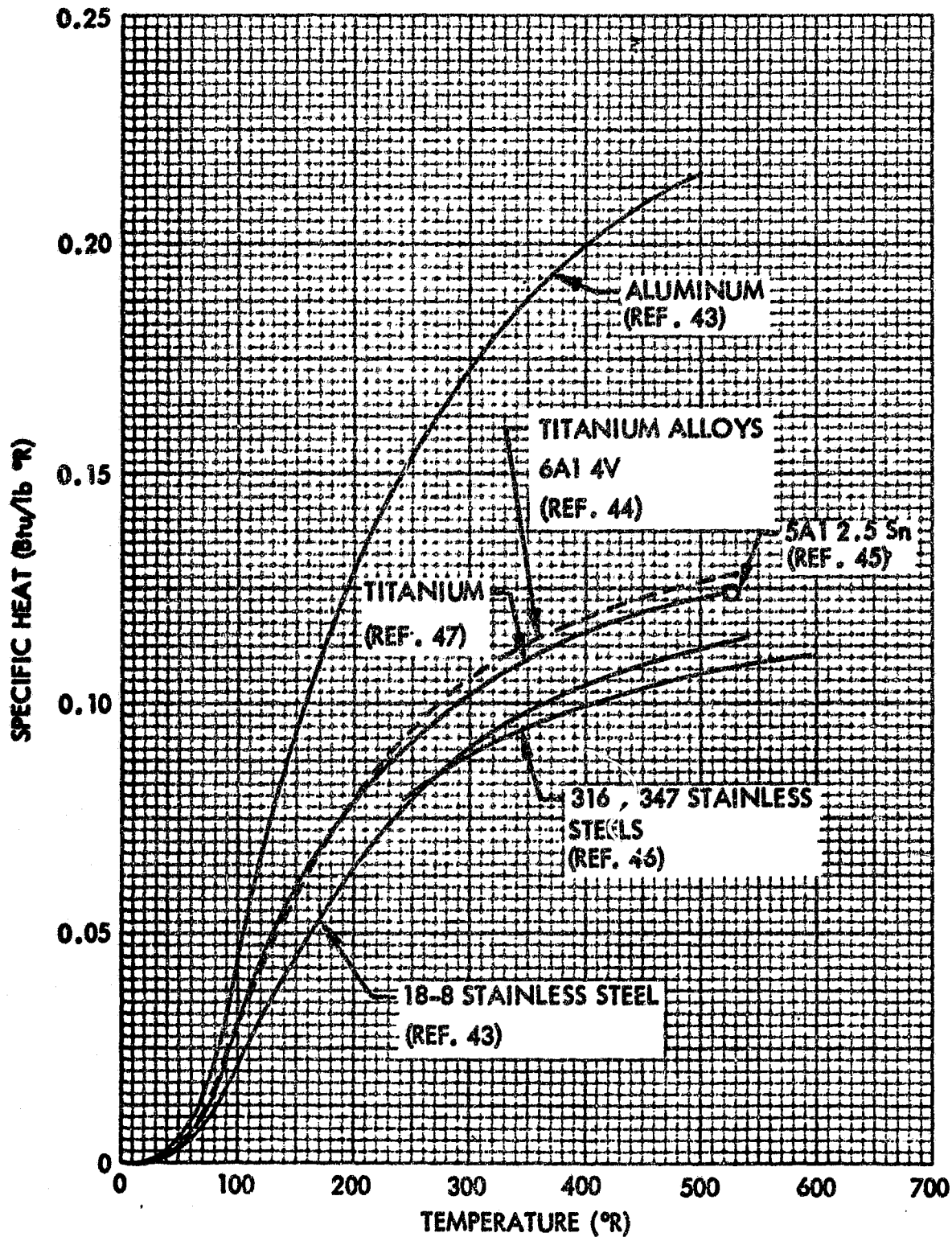


Fig. 2-9 Specific Heat of Metals as a Function of Temperature

Emittance of Metals as a Function of Temperature

Values of emittance depend markedly on the type of material, surface roughness, degree of oxidation, and temperature.

The No. 1 finish requires a 15- μ in. rms surface; the No. 8 finish requires a 2- μ in. rms surface.

The data for 2024 and 7075 aluminum alloy apply to "clean and smooth surfaces scrubbed with soap, washed with water, dried, wiped with toluene and then with alcohol", according to Refs. 48 and 49.

The data for 347 stainless steel apply to a surface cleaned as noted above.

Fig. 2-11 shows the variation of emittance with temperature for chemically cleaned copper and 1/4-mil thick aluminum foil. The aluminum foil is typical of that found in some multilayer insulation composites.

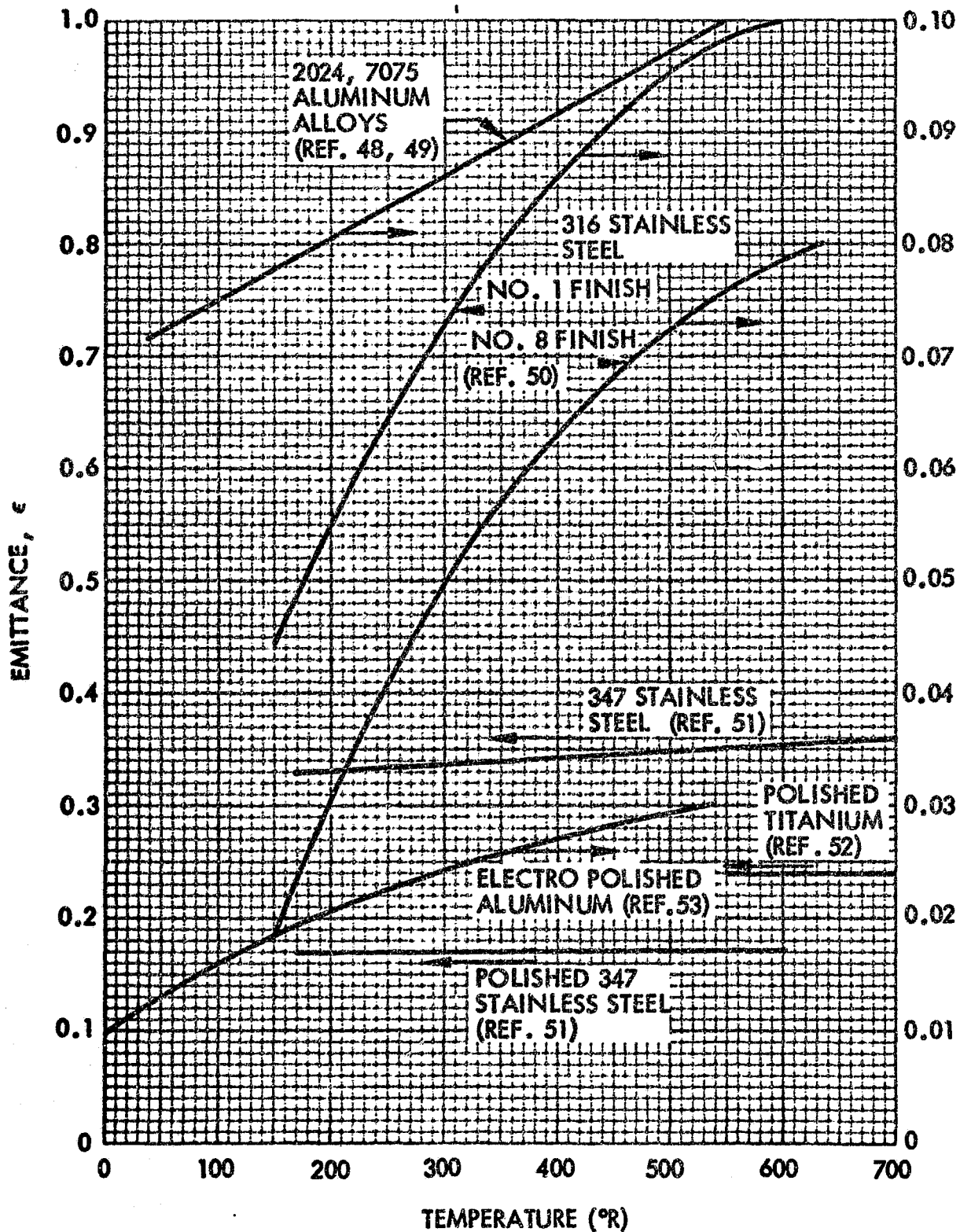


Fig. 2-10 Emittance of Metals as a Function of Temperature

2-51

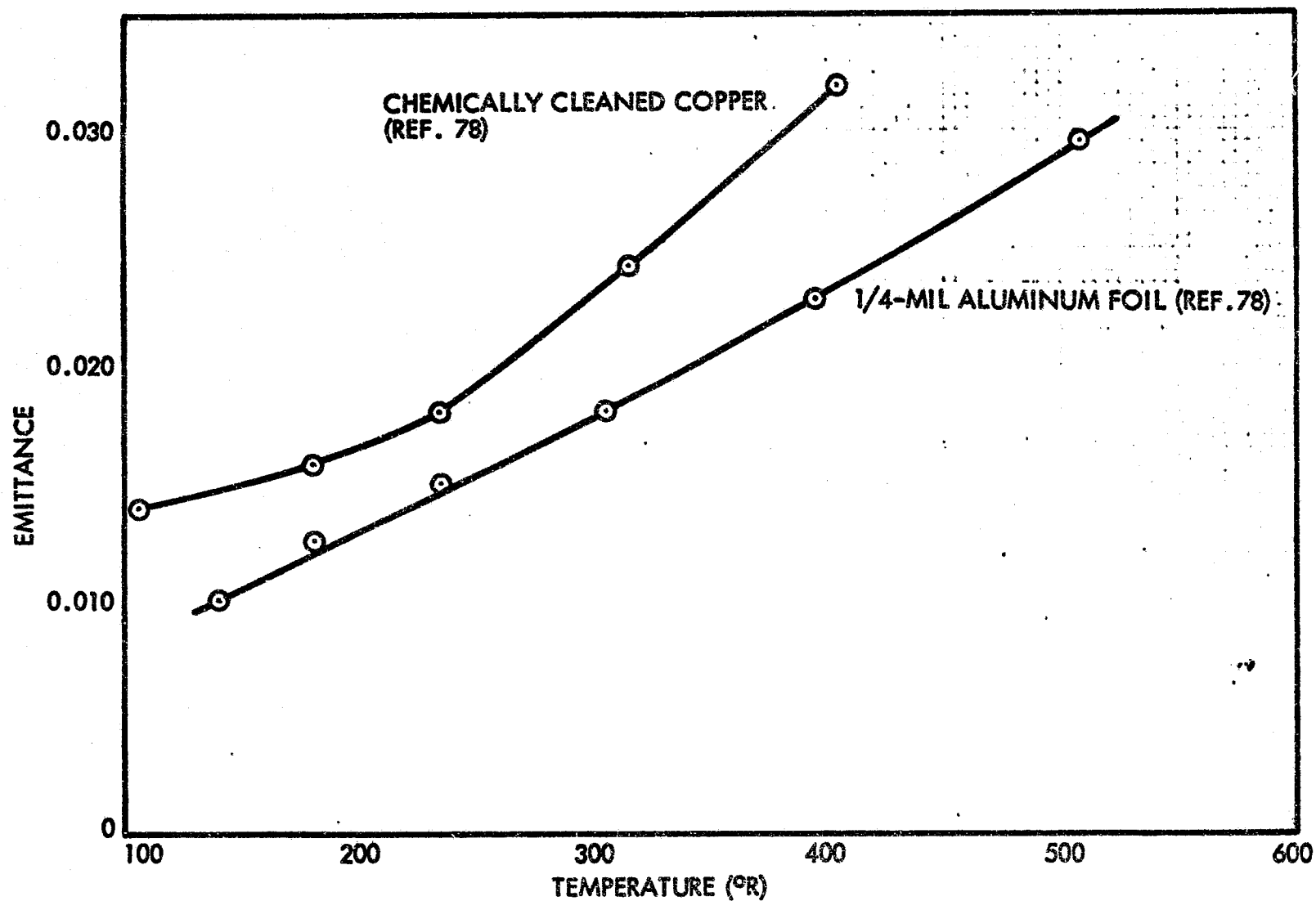


Fig. 2-11 Emissivity of Chemically Cleaned Copper and 1/4-mil Thick Aluminum Foil as a Function of Temperature

END OF REFERENCE

22

REFERENCE

23

SCHWARTZBERG, FRED H.; OSGOOD, SAMUEL H.; BRYANT, CAROL; AND KNIGHT, MARVIN: CRYOGENIC MATERIALS DATA HANDBOOK. REP. AFML-TDR-64-280, AIR FORCE MATERIALS LAB., VOL. I (AD-713619) -- SECTIONS A, B, AND C, JULY 1970.

31-0-0
AD 713 619

CRYOGENIC MATERIALS DATA HANDBOOK (REVISED).
VOLUME I SECTIONS A, B, C. ↑

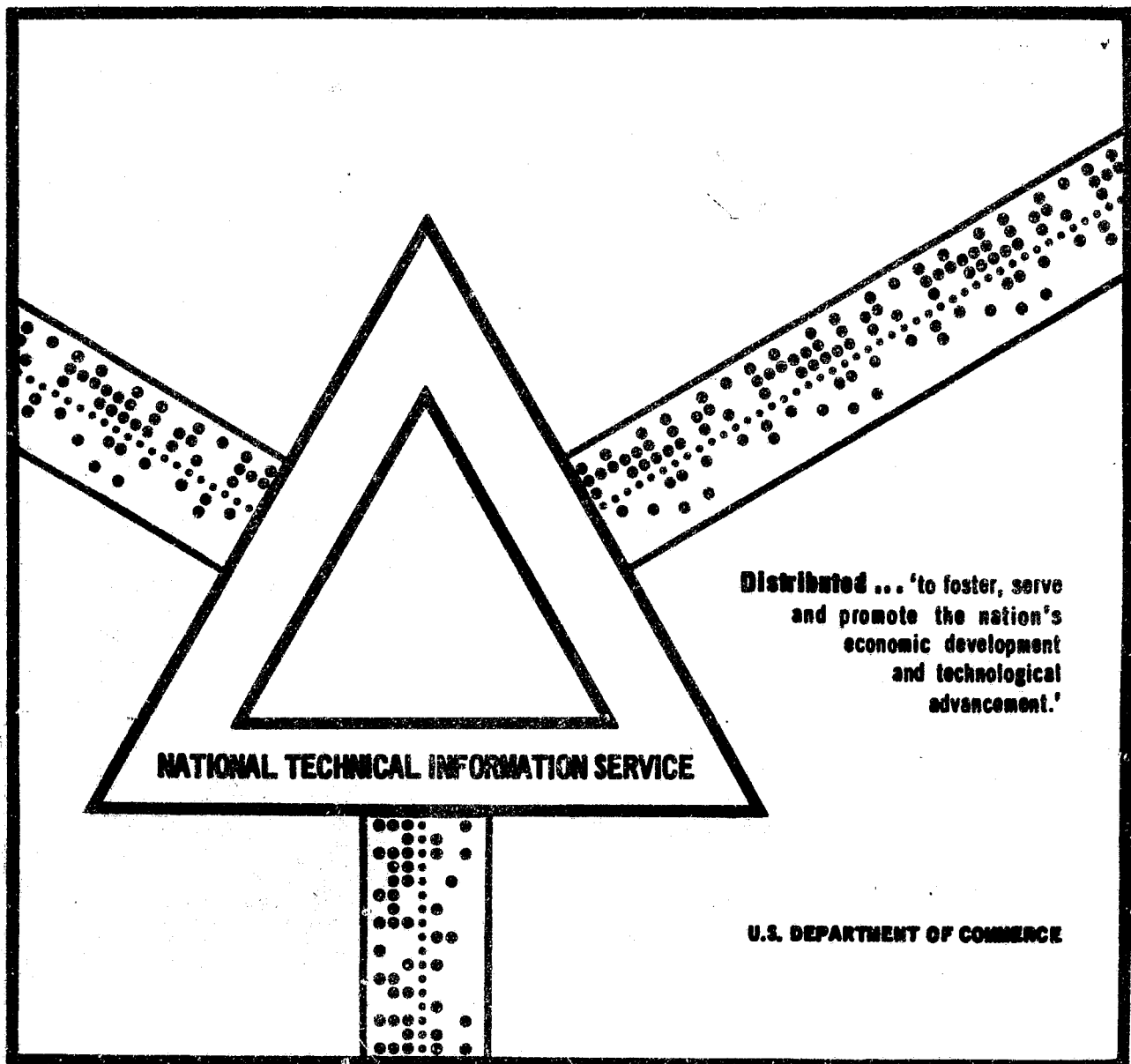
Fred R. Schwartzberg et al

Martin Marietta Corporation
Denver, Colorado

July 1970

LEWIS RESEARCH CENTER
Aerospace Safety Research
and Data Institute
JAN 30 1971

CLEVELAND, OHIO



**AFML-TDR-64-280
VOLUME I (REVISED 1970)**

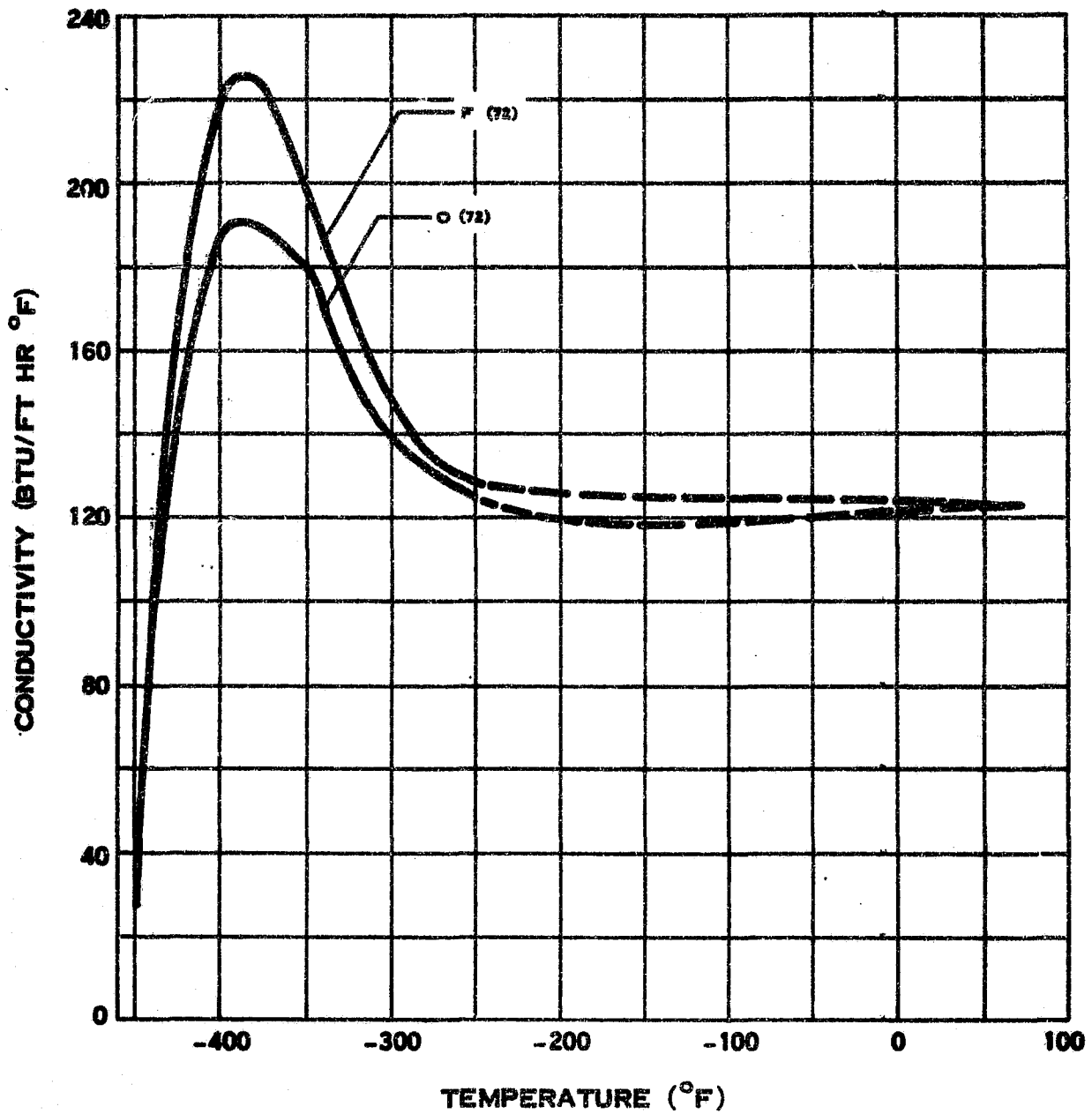
CRYOGENIC MATERIALS DATA HANDBOOK

**VOLUME I
SECTIONS A, B, C**

**F. R. SCHWARTZBERG, et al
MARTIN MARIETTA CORPORATION
COMPILER
M. KNIGHT
AIR FORCE MATERIALS LABORATORY**

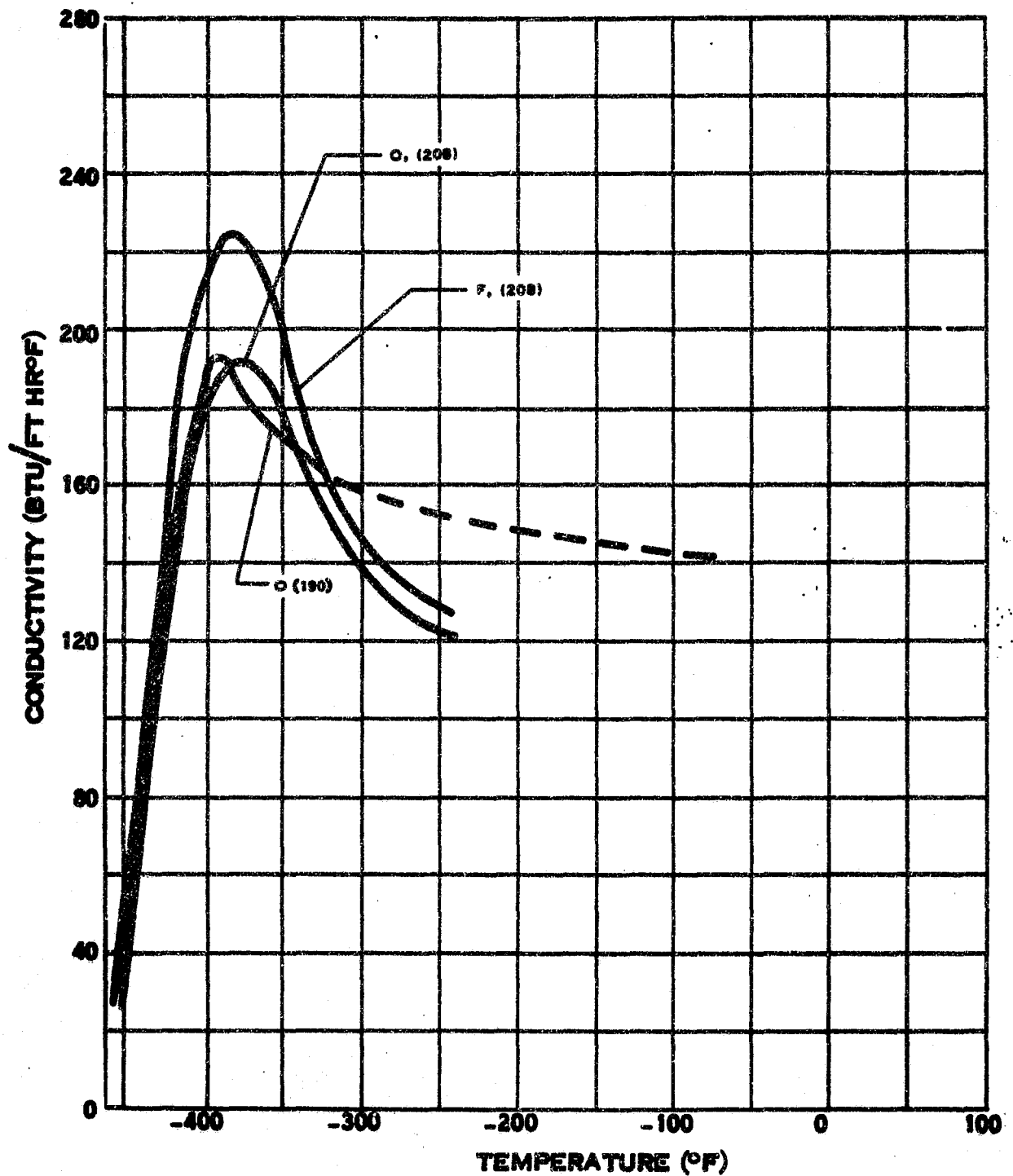
**This document has been approved for public release
and sale; its distribution is unlimited.**

A.1.v



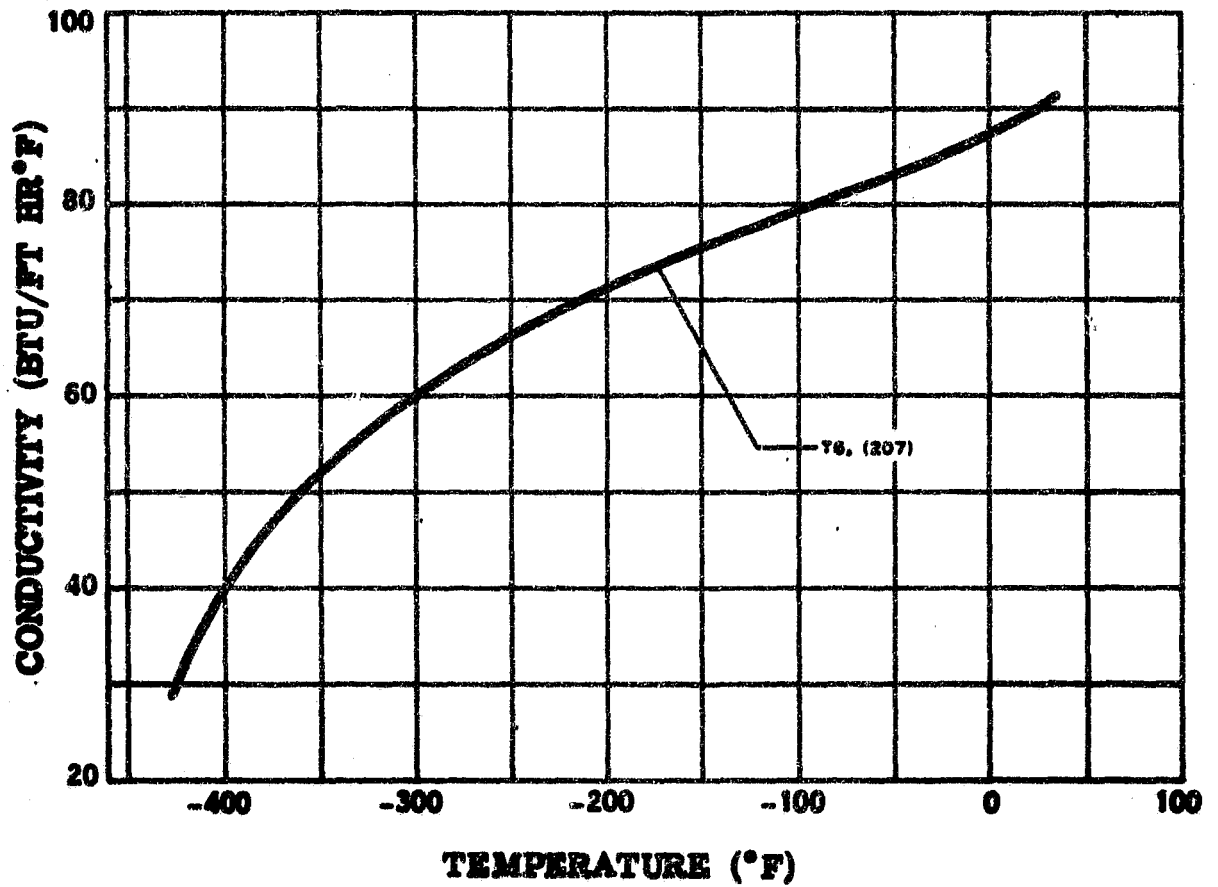
THERMAL CONDUCTIVITY OF 1100 ALUMINUM

A.1.v-1



THERMAL CONDUCTIVITY OF 1100 ALUMINUM

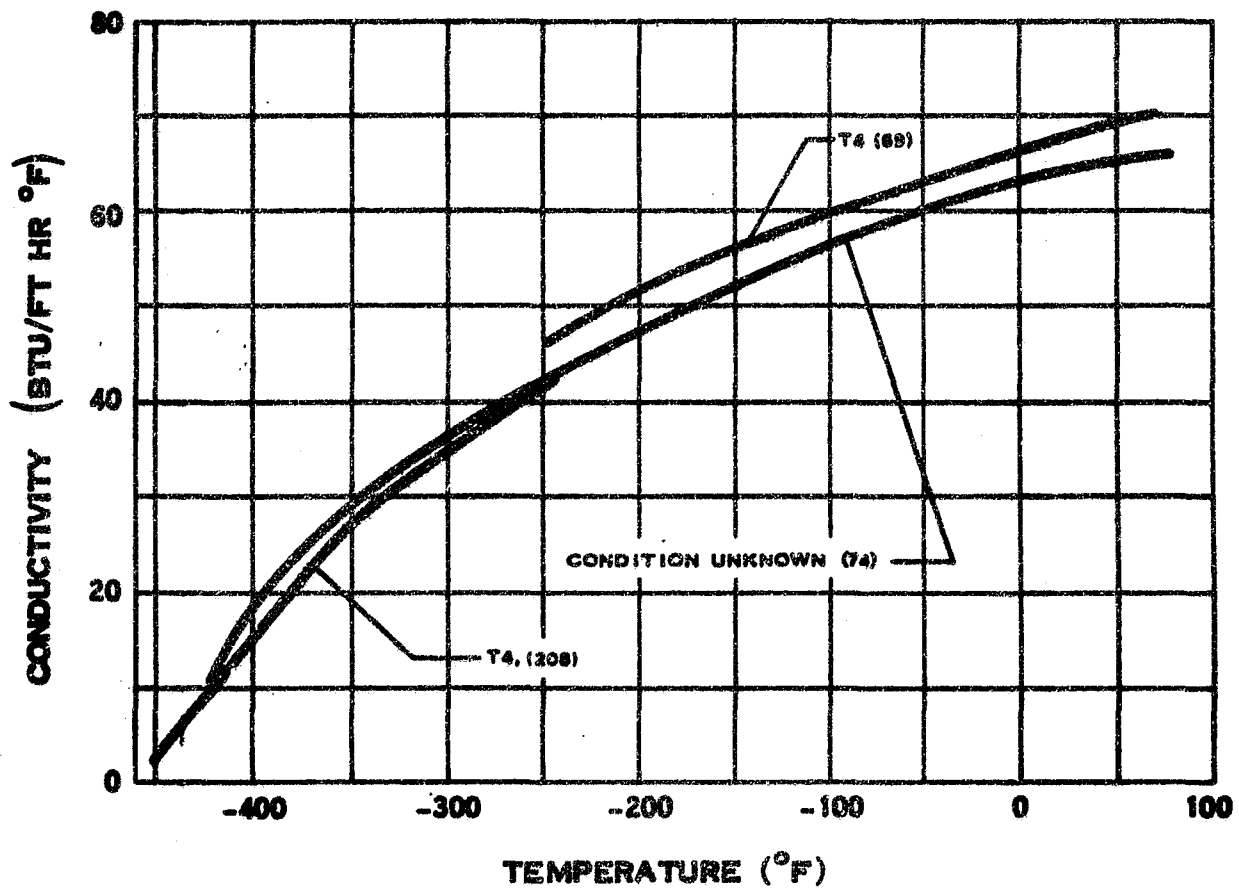
A.2.v



THERMAL CONDUCTIVITY OF 2014 ALUMINUM

(6-66)

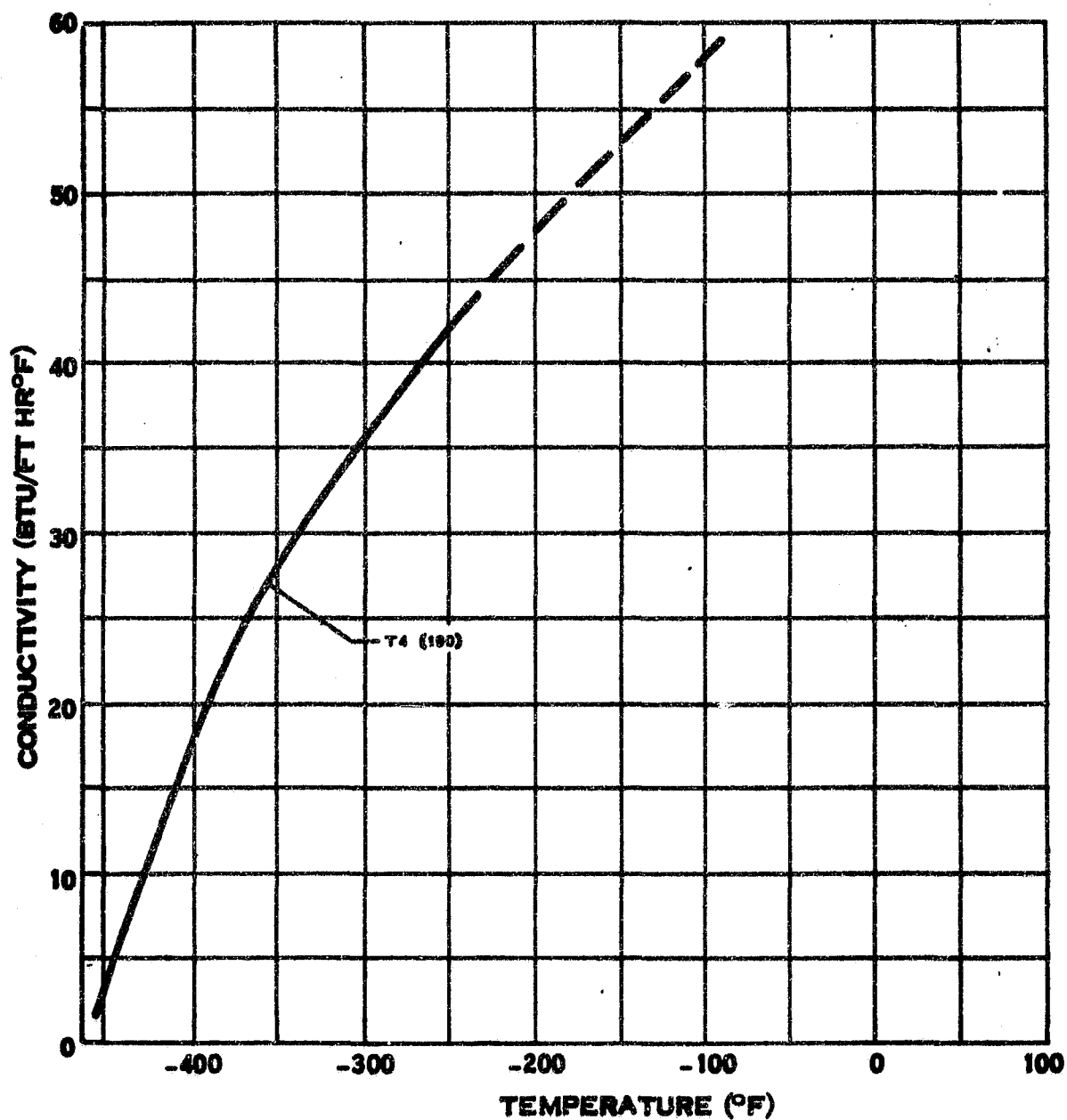
A.4.v



THERMAL CONDUCTIVITY OF 2024 ALUMINUM

(8-68)

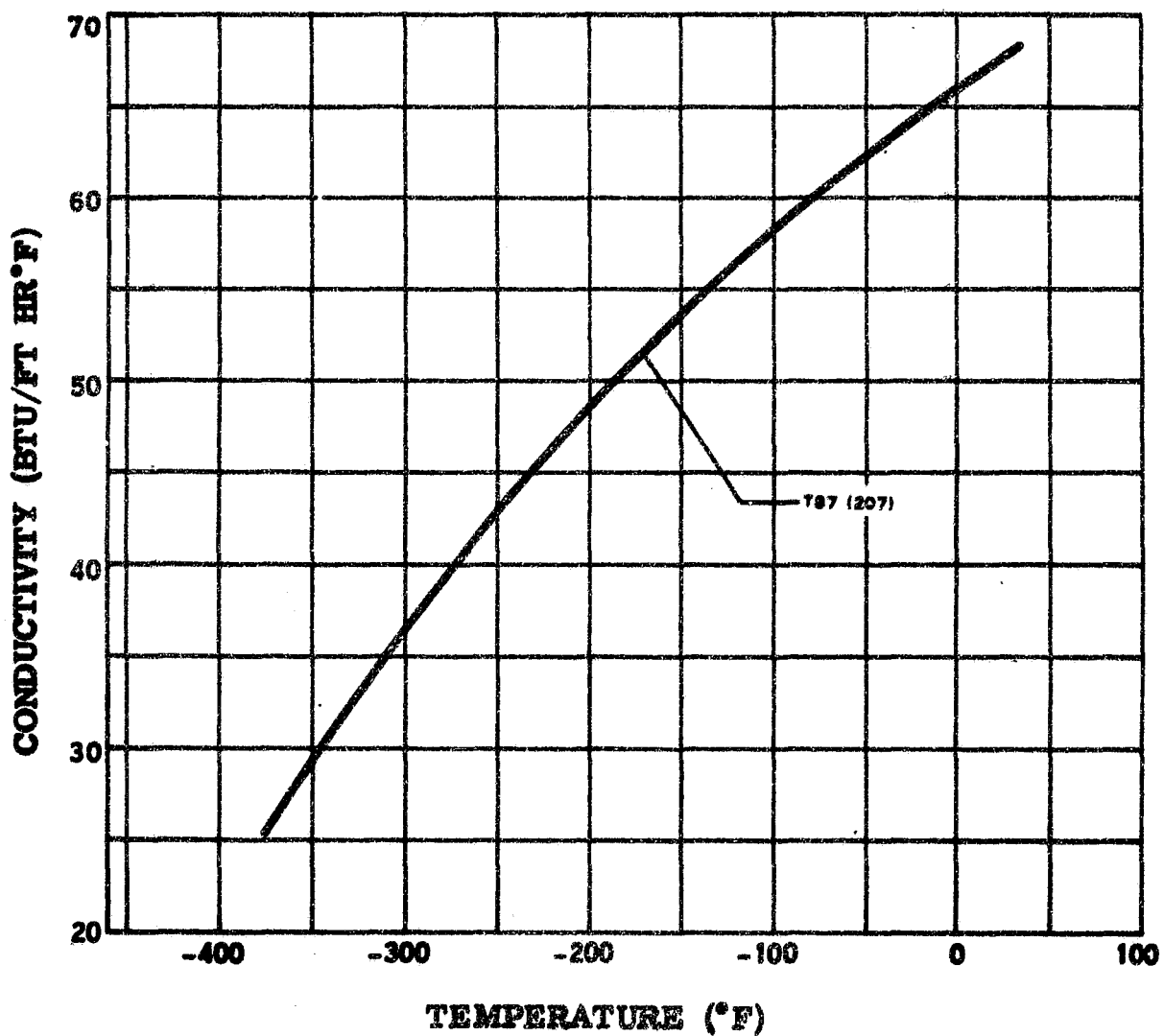
A.4.v-1



THERMAL CONDUCTIVITY OF 2024 ALUMINUM

(6-88)

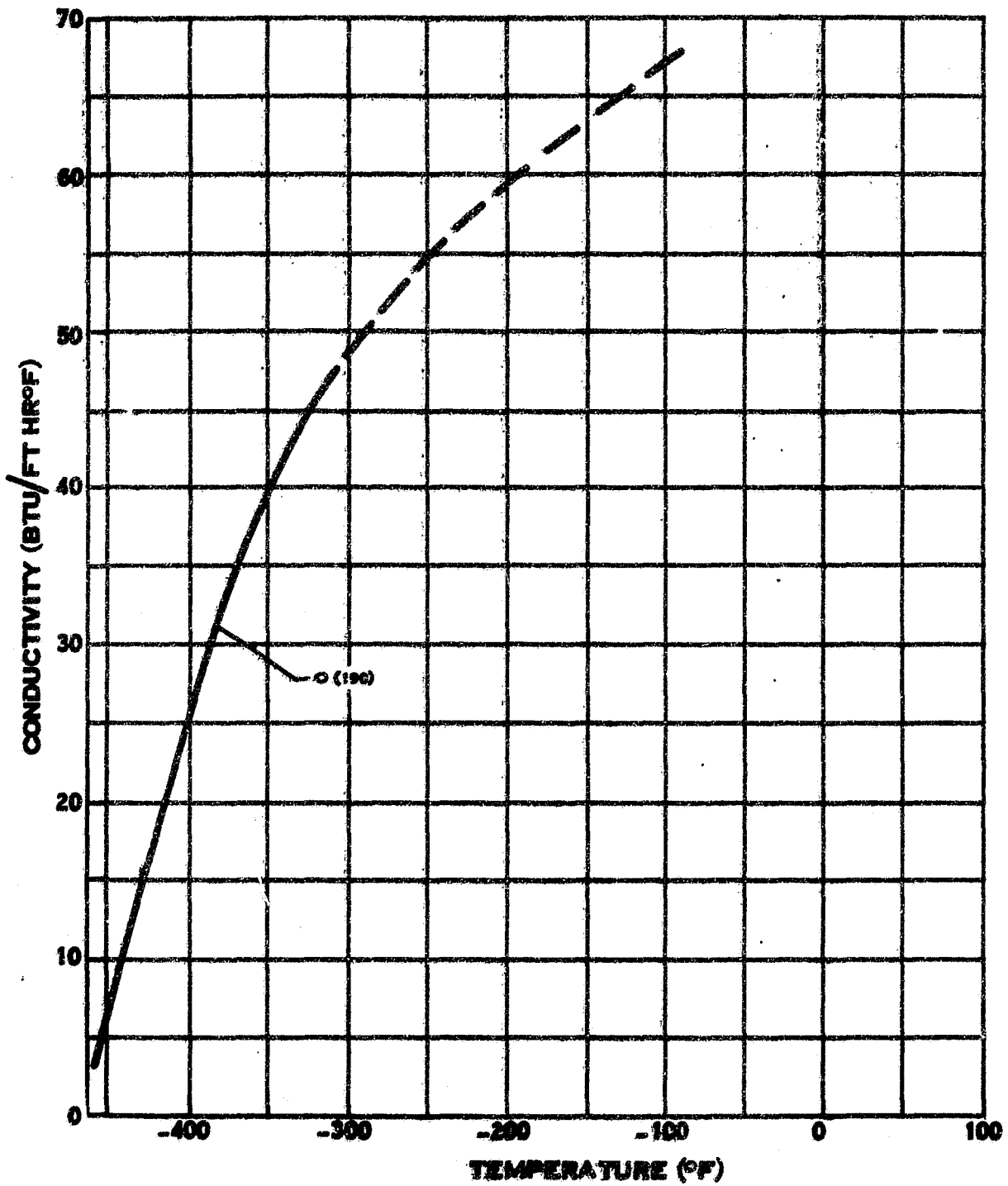
A.5.v



THERMAL CONDUCTIVITY OF 2219 ALUMINUM

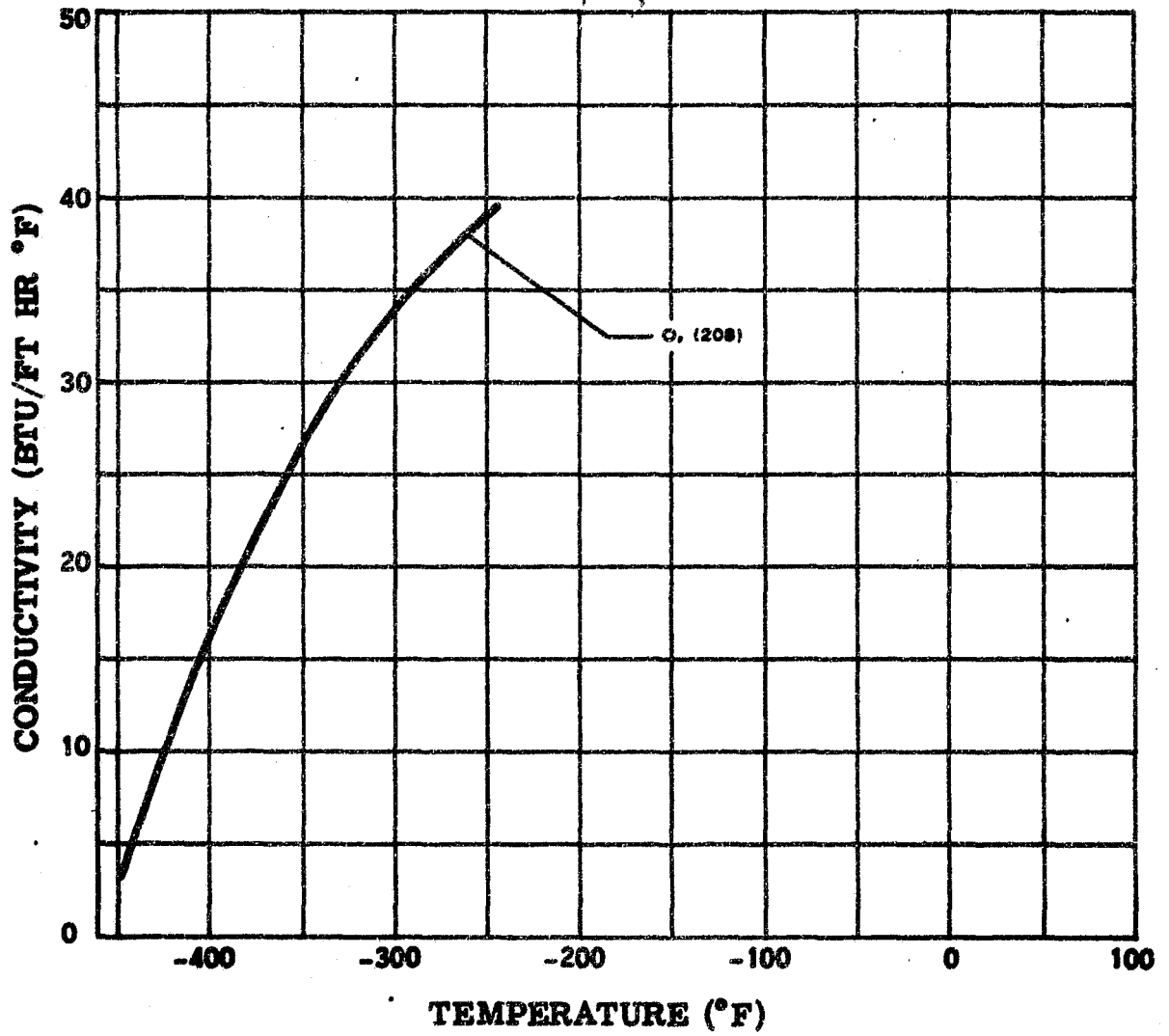
(6-68)

A.8.v



THERMAL CONDUCTIVITY OF 5052 ALUMINUM

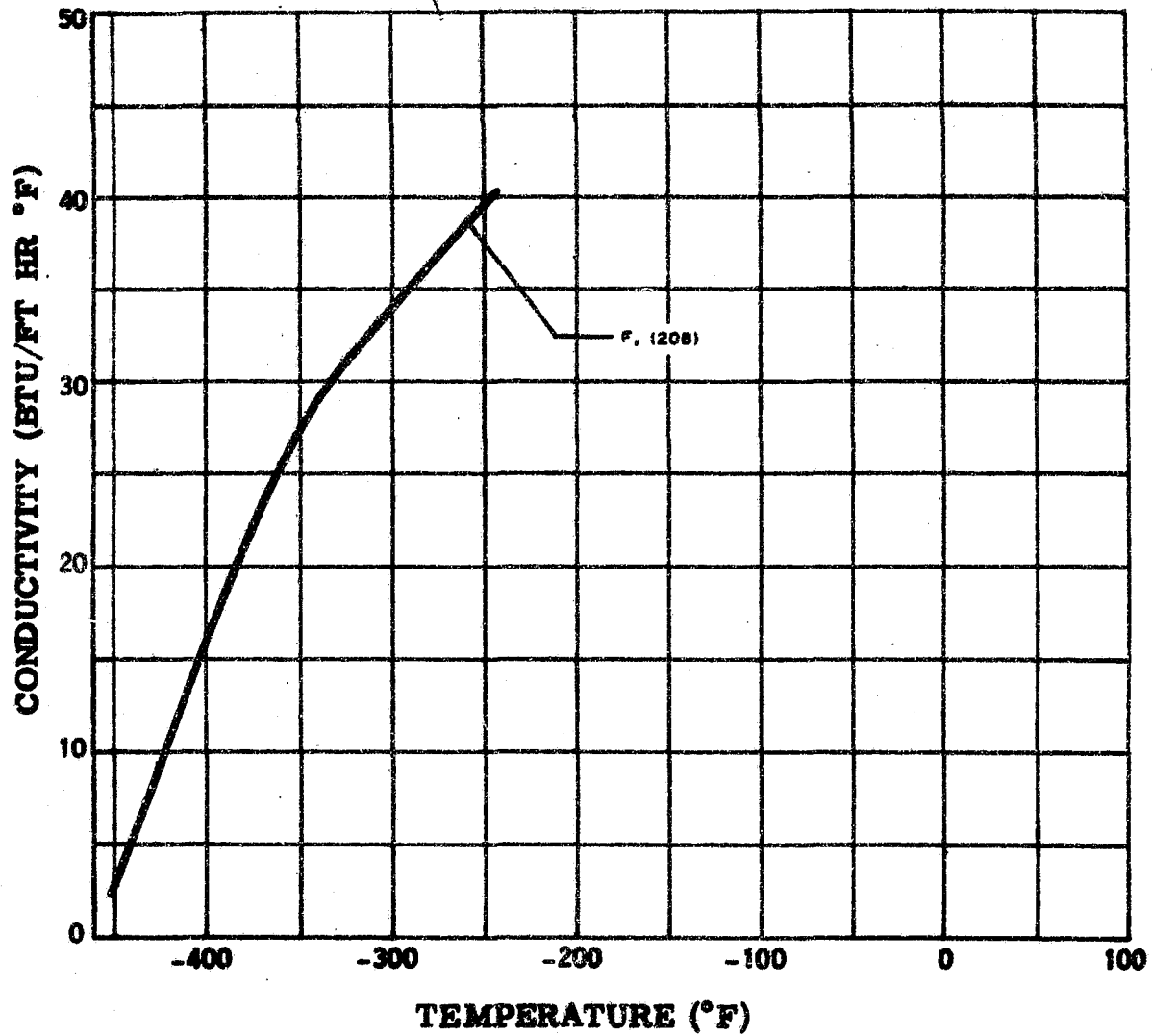
A.9.v



THERMAL CONDUCTIVITY OF 5083 ALUMINUM

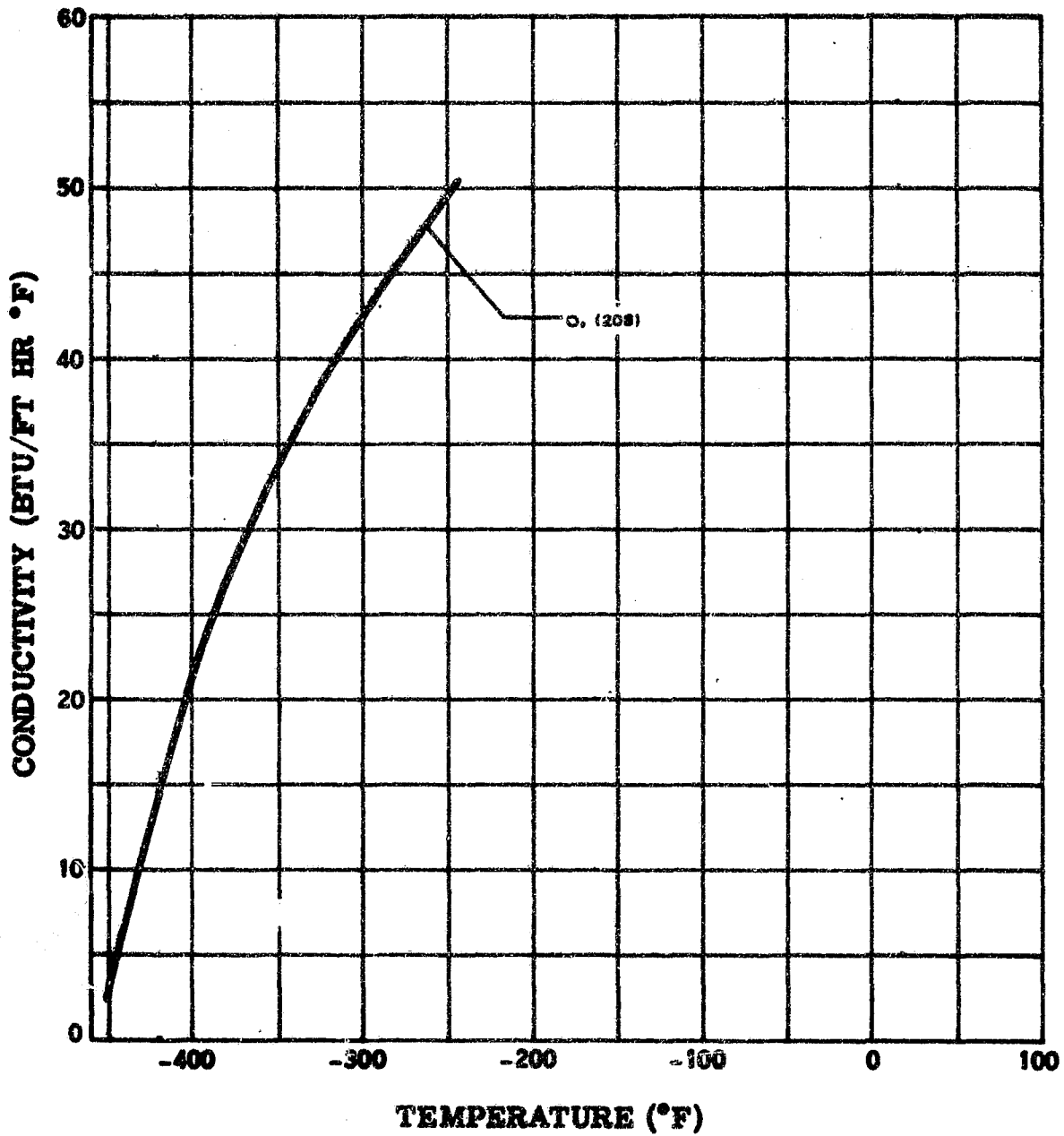
(6-68)

A.10.v



THERMAL CONDUCTIVITY OF 5083 ALUMINUM

A.11.v



THERMAL CONDUCTIVITY OF 5154 ALUMINUM

REFERENCE

23

SCHWARTZBERG, FRED H.; OSGOOD, SAMUEL H.; BRYANT, CAROL; AND KNIGHT, MARVIN: CRYOGENIC MATERIALS DATA HANDBOOK. REP. AFML-TDR-64-280, AIR FORCE MATERIALS LAB., VOL. II (AD-713620) -- SECTIONS D, E, F, G, H, AND I, JULY 1970.

3.1-0-0

AD 713 620

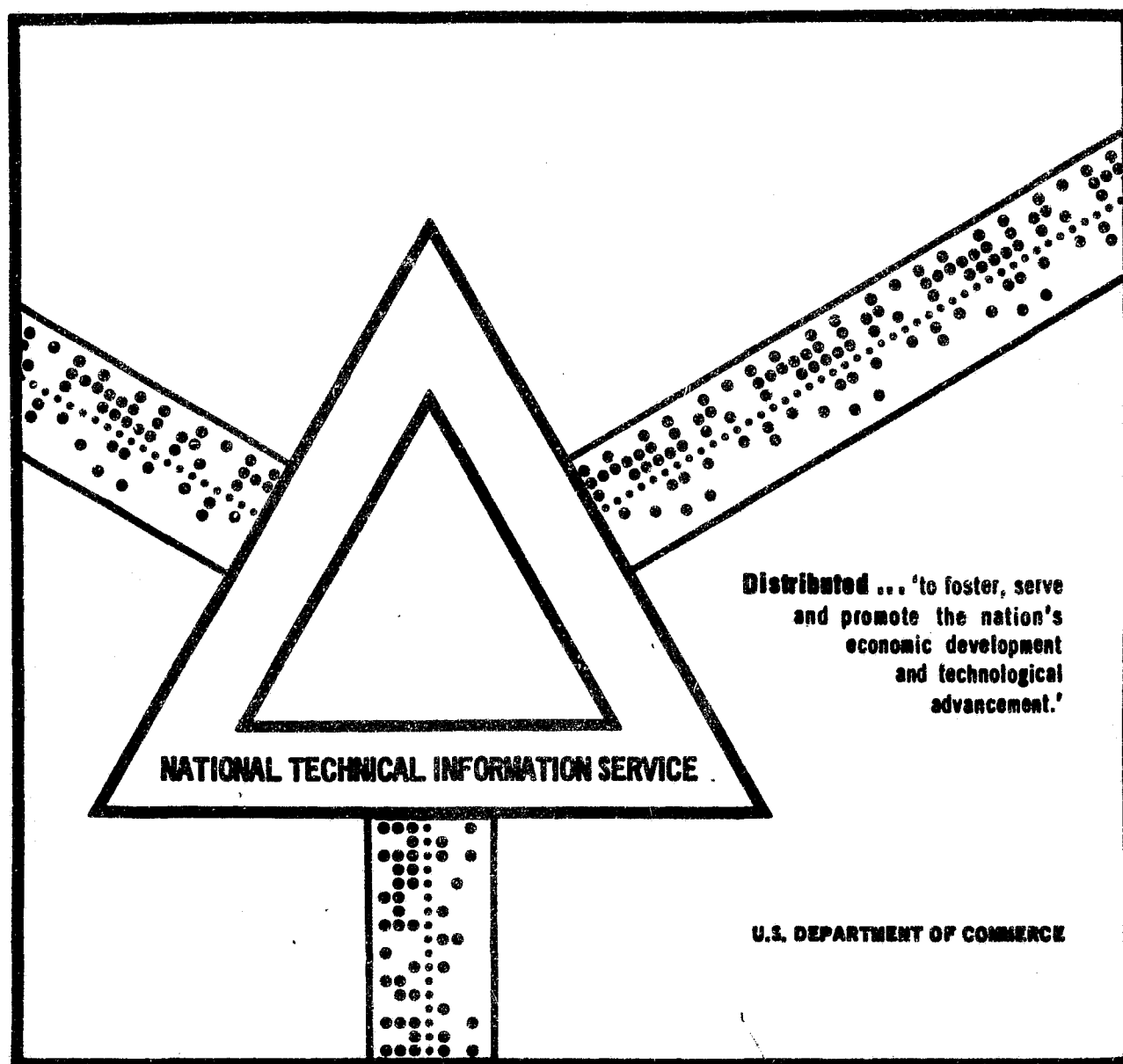
CRYOGENIC MATERIALS DATA HANDBOOK (REVISED)
VOLUME II, SECTIONS D, E, F, G, H, AND I

Fred H. Schwartzberg et al

Martin Marietta Corporation
Denver, Colorado

July 1970

LEWIS RESEARCH CENTER
Aerospace Safety Research
and Data Institute
JAN 3 1971
CLEVELAND, OHIO



AFML-TDR-64-280
VOLUME II (REVISED 1970)

CRYOGENIC MATERIALS DATA HANDBOOK

VOLUME II

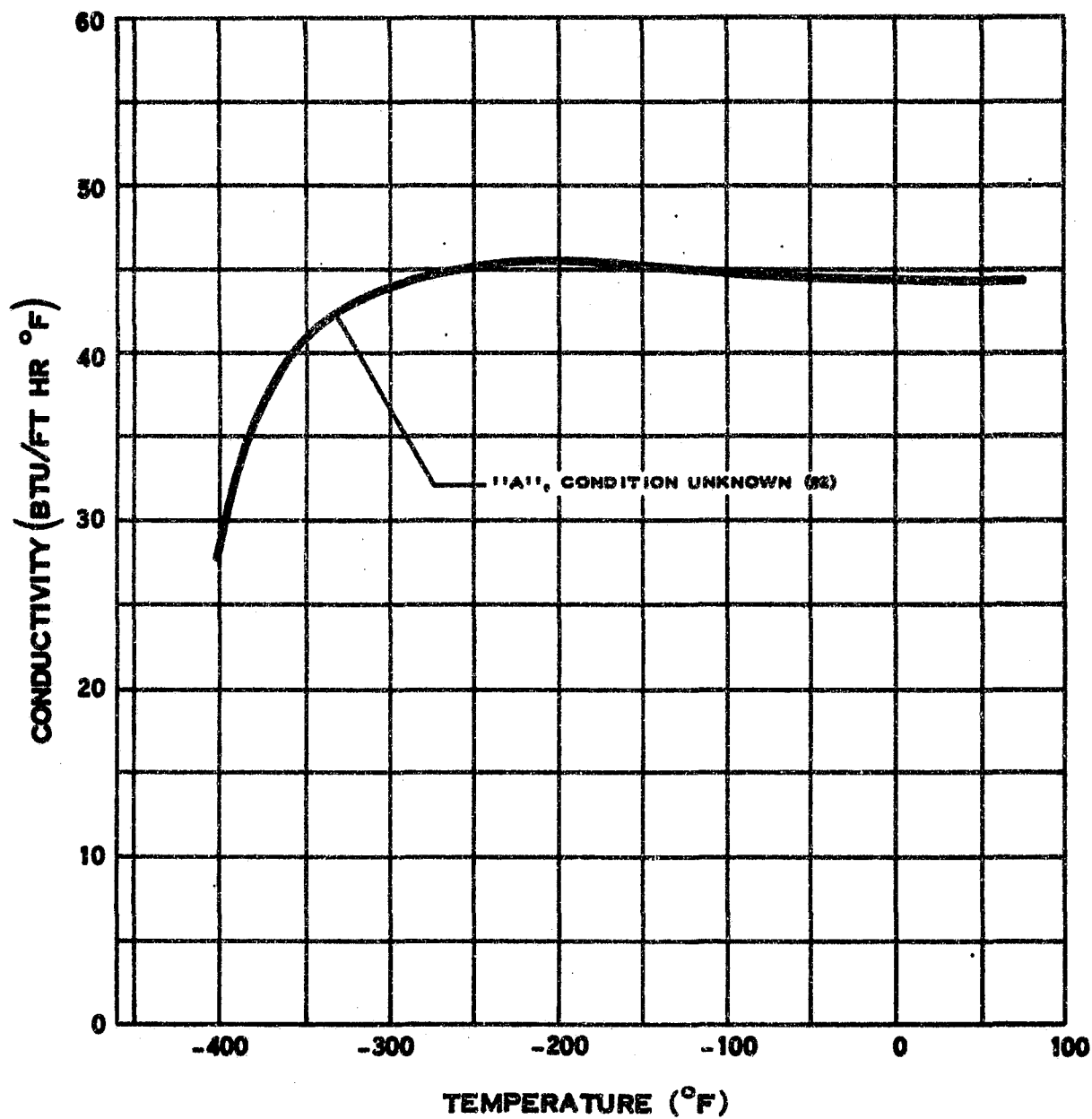
SECTIONS D, E, F, G, H AND I

S. R.
F. R. SEWARTZ, et al
MARTIN MARIETTA CORPORATION

COMPILER
M. KNIGHT
AIR FORCE MATERIALS LABORATORY

**This document has been approved for public release
and sale; its distribution is unlimited.**

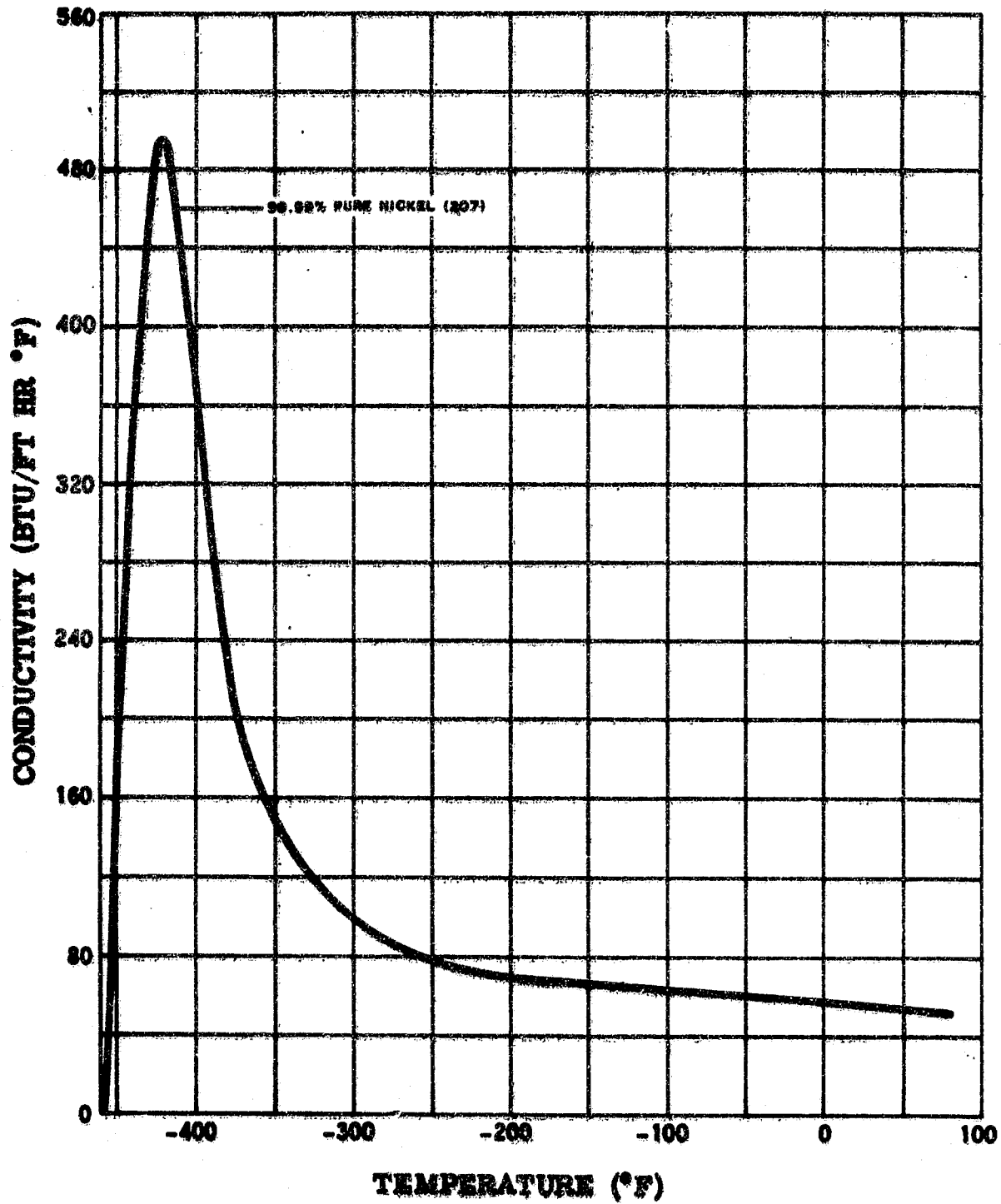
D.1.v



THERMAL CONDUCTIVITY OF NICKEL

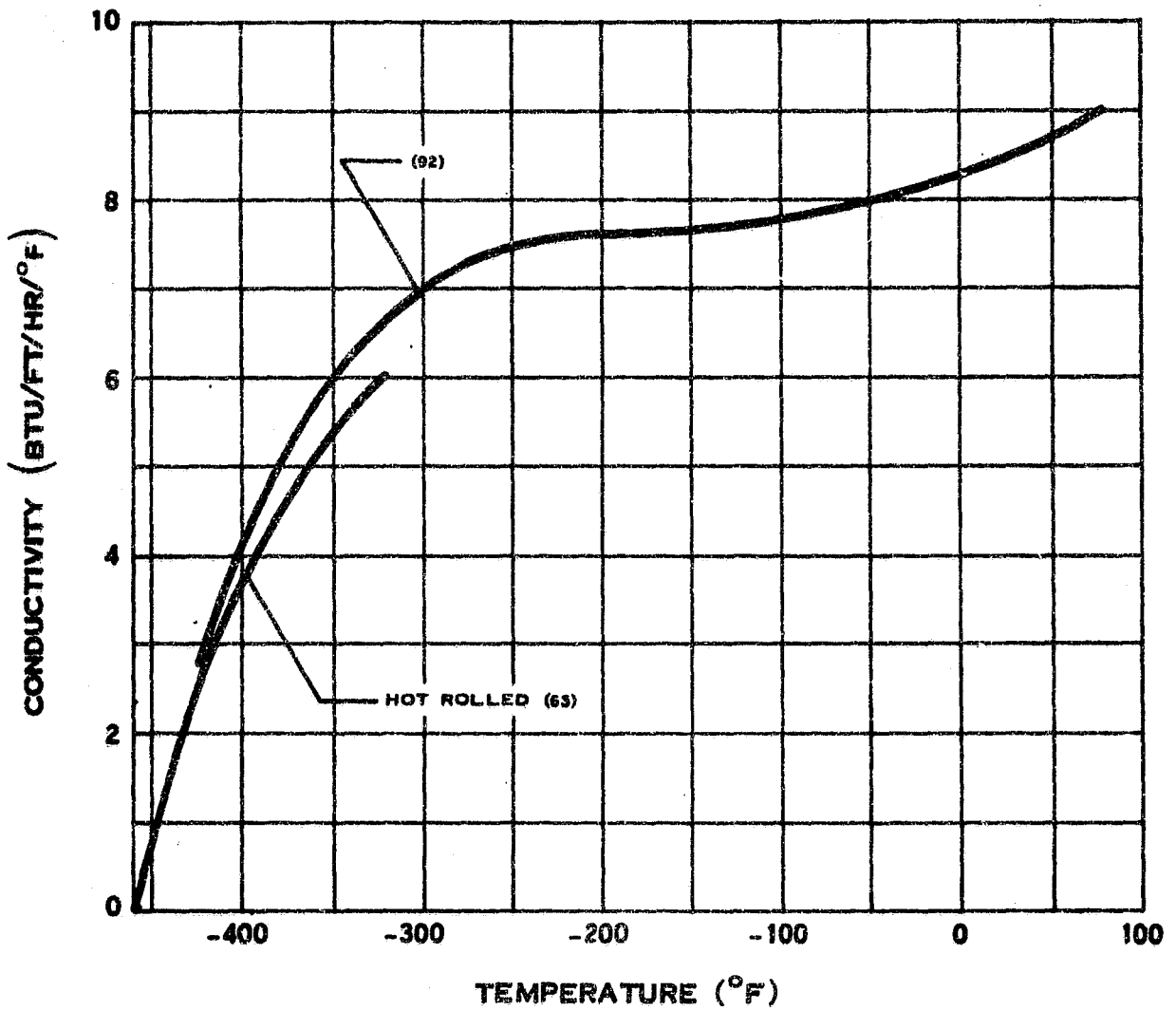
(7-84)

D.1.v-1



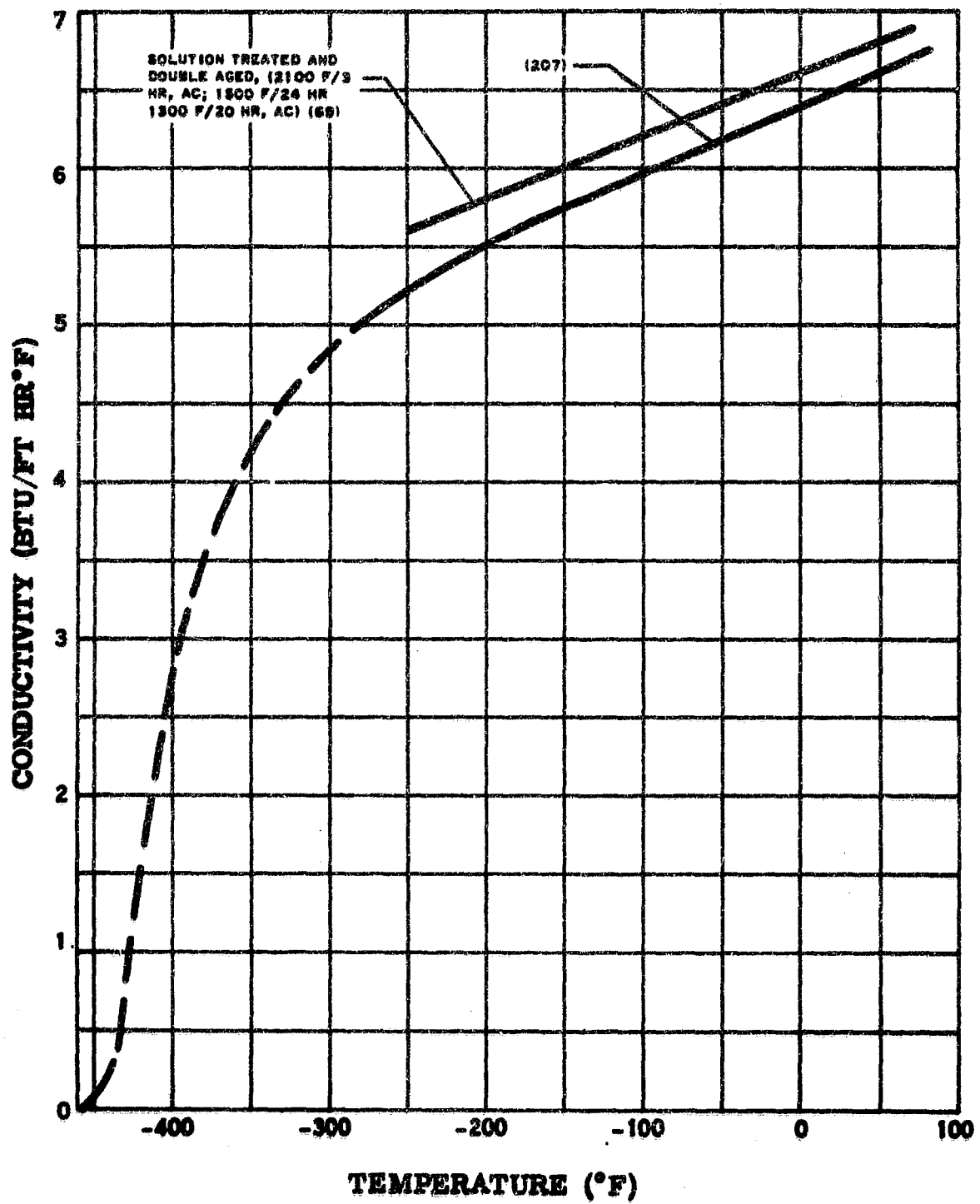
THERMAL CONDUCTIVITY OF NICKEL

D.2.v



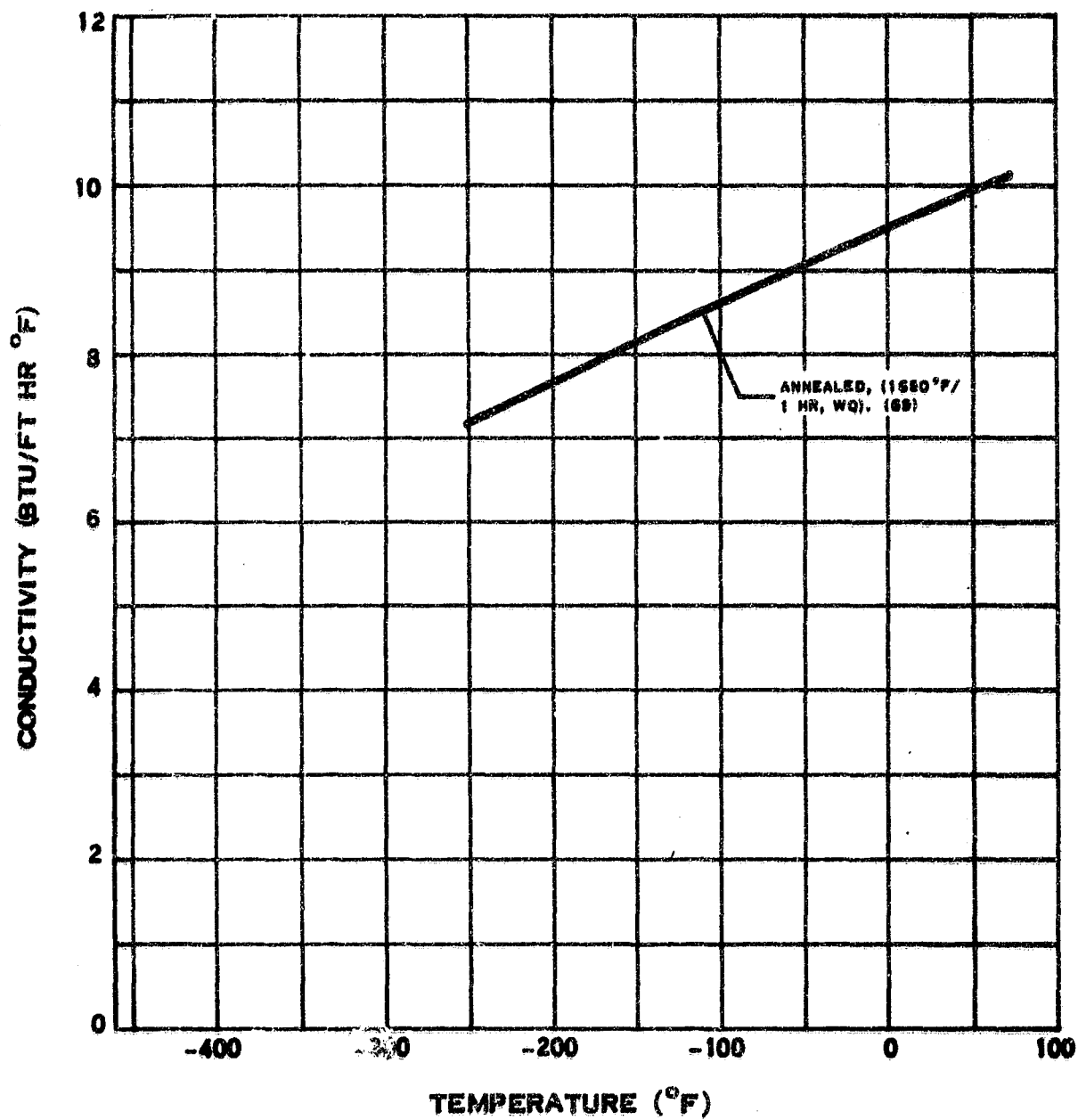
THERMAL CONDUCTIVITY OF INCONEL

D.3.v



THERMAL CONDUCTIVITY OF INCONEL X

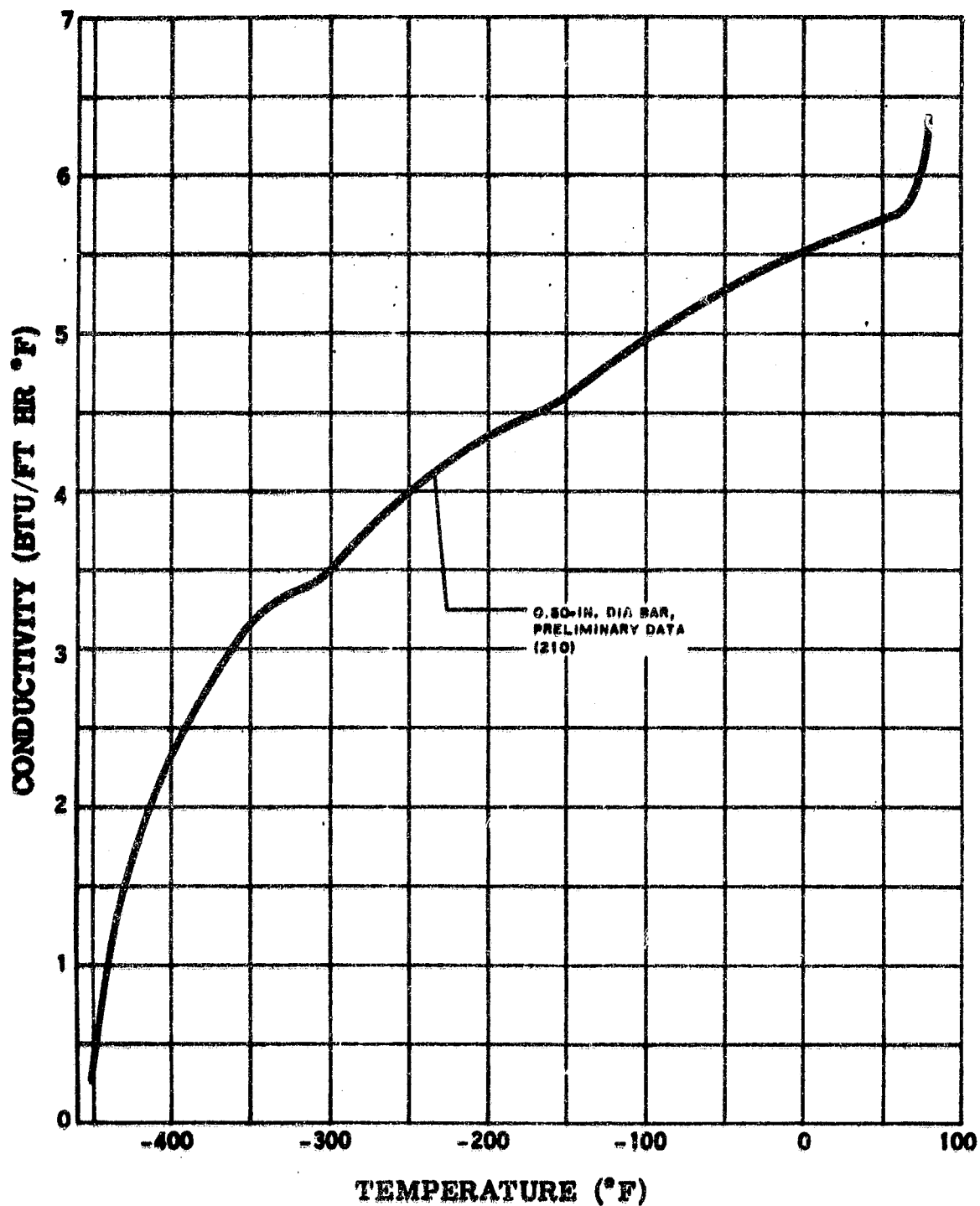
D.4.v



THERMAL CONDUCTIVITY OF K MONEL

(5-58)

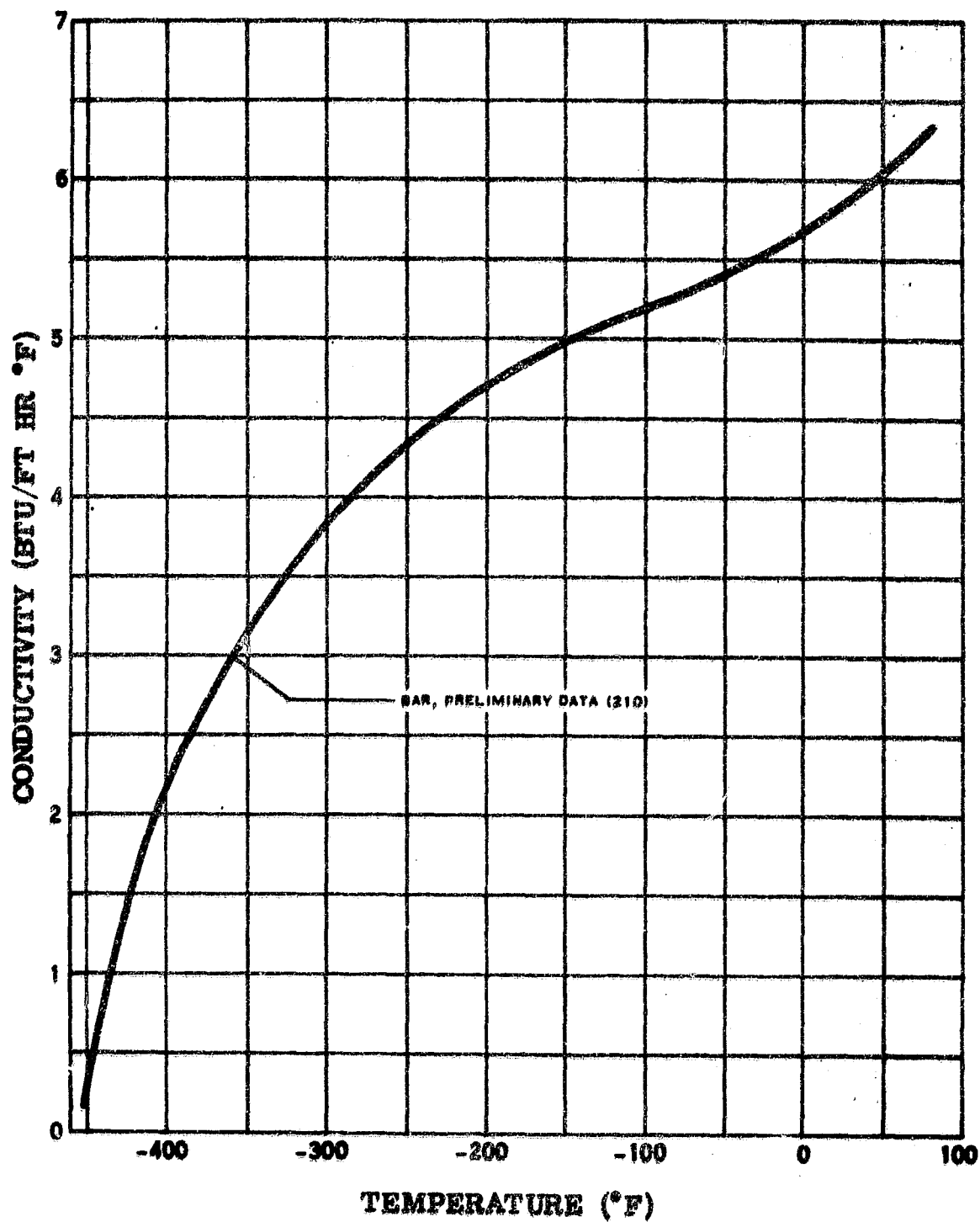
D.8.v



THERMAL CONDUCTIVITY OF HASTELLOY X

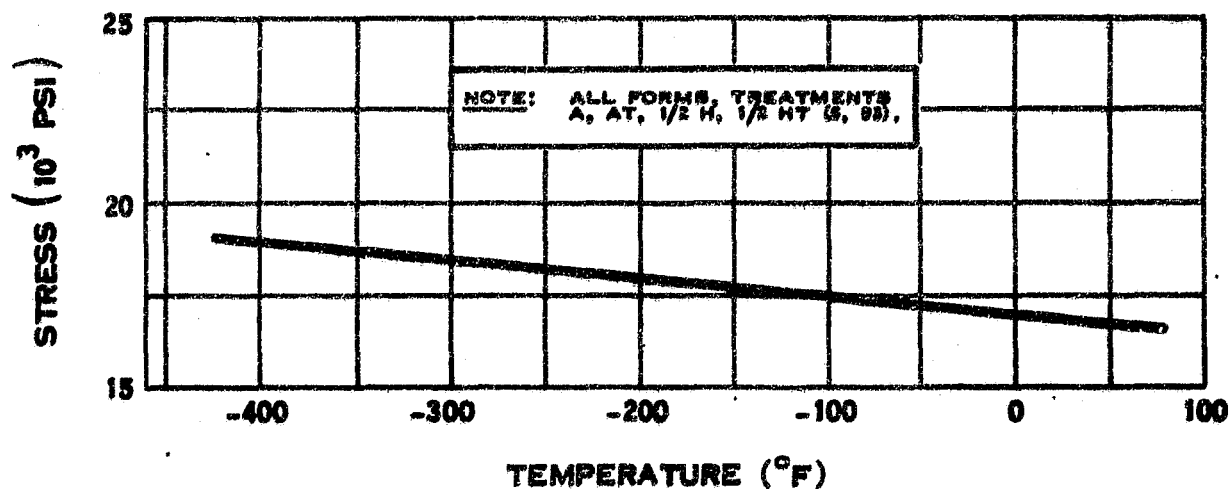
(8-66)

D.13.v

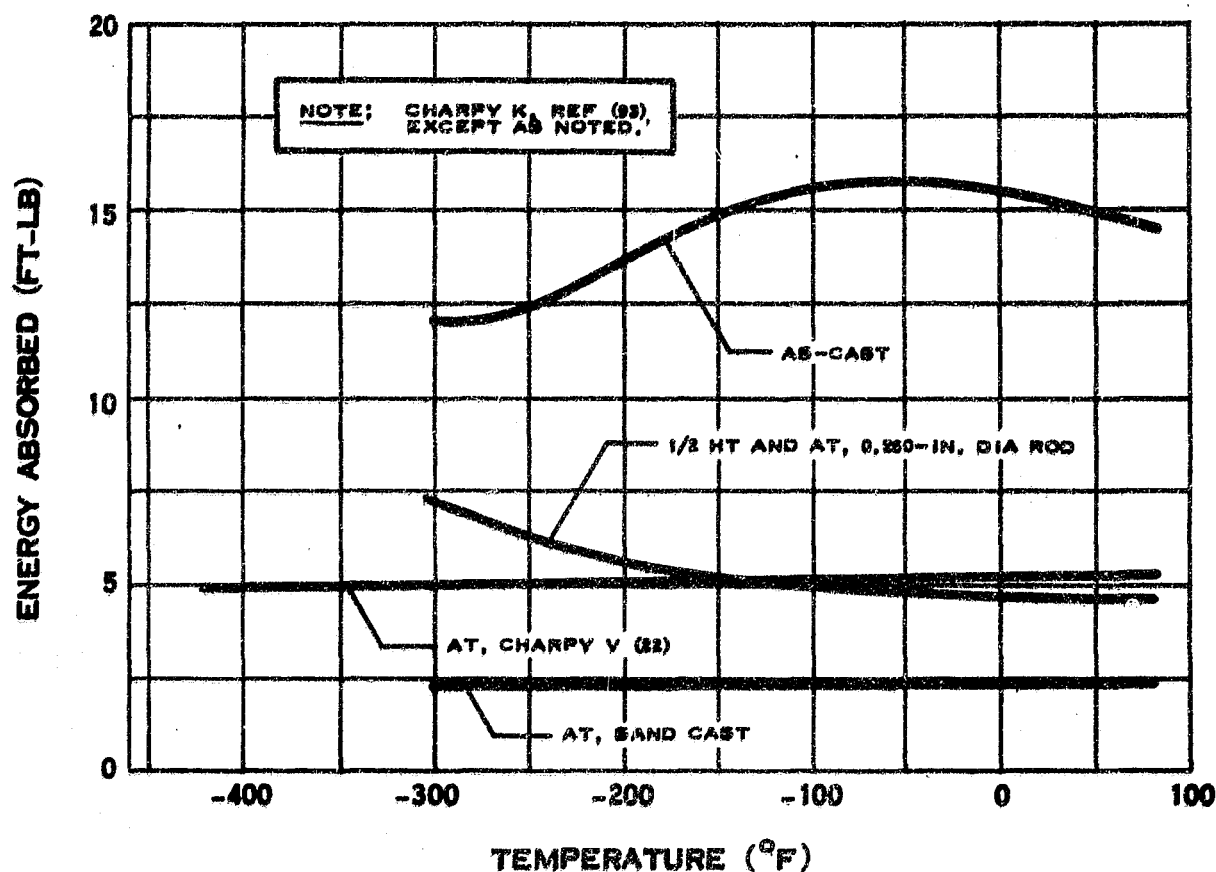


THERMAL CONDUCTIVITY OF INCONEL 718

F.2.11



MODULUS OF ELASTICITY OF BERYLLIUM COPPER



IMPACT STRENGTH OF BERYLLIUM COPPER

END OF REFERENCE
23

REFERENCE

24

**VAN HORN, KENT R., ED.: ALUMINUM. VOL. I. PROPERTIES,
PHYSICAL METALLURGY AND PHASE DIAGRAMS. AM. SOC.
METALS, 1967.**

**THIS REFERENCE IS COPYRIGHTED MATERIAL AND THEREFORE
THE CONTENTS HAVE NOT BEEN REPRODUCED FROM THE TEXT.**

END OF REFERENCE
24

REFERENCE

25

**ROSENBERG, SAMUEL J.: NICKEL AND ITS ALLOYS. MONOGRAPH
106, NATIONAL BUREAU OF STANDARDS, MAY 1968.**

NBS MONOGRAPH 106

Nickel and Its Alloys

**U.S. DEPARTMENT OF COMMERCE
NATIONAL BUREAU OF STANDARDS**

620.18
R813
c.4

UNITED STATES DEPARTMENT OF COMMERCE • C. R. Smith, *Secretary*

NATIONAL BUREAU OF STANDARDS • A. V. Astin, *Director*

Nickel and Its Alloys

Samuel J. Rosenberg

Institute for Materials Research
National Bureau of Standards
Washington, D.C. 20234



LIBRARY COPY
RETURN TO
LEWIS LIBRARY
CLEVELAND, OHIO

National Bureau of Standards Monograph 106

Issued May, 1968

(Supersedes NBS Circular 592)

For sale by the Superintendent of Documents, U.S. Government Printing Office
Washington, D.C., 20402 - Price \$1.25

ing in table 26. For electrolytic etching, Inconel alloy 600 is used as the cathode and where water is indicated, tap water is used. Additional useful reagents are given by Smithells [405].

The microstructure of high-purity nickel is shown in figure 49.



FIGURE 49. Microstructure of high-purity nickel (Nickel 200) as forged. Etched with $\text{NaCN} - (\text{NH}_4)_2\text{S}_2\text{O}_8$. a. $\times 100$. b. $\times 500$.

2.7. Uses of Nickel

Topics discussed in this section include the production of nickel coatings by various procedures and the end uses of nickel-plated and solid-nickel objects.

a. Coatings

(1) *Electroplating.* Nickel is one of the most important metals applied by electrodeposition [406]. Nickel electrodeposits are used extensively as a foundation for a highly lustrous finish on many manufactured metallic articles. Protection of the basis metal and permanence of a stain-free surface are the primary requisites of such decorative coatings. These are obtained by an adequate thickness of nickel and a comparatively thin layer of chromium over it. Nickel coatings alone are also used industrially to protect the basis metal from corrosion or to prevent contamination of a chemical product. Although surface improvement and corrosion resistance are the principal objectives of nickel electroplating, it is also used for building up worn parts [407] and for electroforming of printing plates, tubes, and many other articles [408,409]. Williams [410] reported that steel sheet or plate up to 80 in wide and up to 20 ft long can be coated with 0.006 to 0.020 in of nickel by electroplating. Nickel electroplating was originally used on iron, steel, and copper alloys but has been extended to zinc-base die castings, aluminum, magnesium, and many other metals and plastics. An undercoat of copper is frequently employed to create a better surface for the deposition of nickel and the good appearance and tarnish resistance of the nickel coating may be further improved, for particular applications, by a final coating of other metals, including gold.

According to Gray [335], the history of electroplating goes back to the production of the first good nickel plate by Boettger in 1843, obtained from a bath containing nickel and ammonium sulfates. Adams [411] in 1869 was probably the first to do nickel plating on a truly commercial basis, thereby establishing electroplating as one of the major consumers of nickel. Developments in nickel electroplating led to the installation in about 1890 of electrolytic refining in the production of nickel, and this in turn contributed to the further improvement of nickel electroplating by supplying better anode material. Developments in electroplating have been rapid since early in the present century, with improved baths that permitted plating at high speeds, with improved understanding and control of operating variables and the use of addition agents, and with the development of improved and auto-

TABLE 26. Microetching of nickel and some nickel-base alloys

Alloy	Solution	Voltage (volts)	Time	Remarks
Nickel and Monel alloys.....	H ₃ PO ₄ 20 ml H ₂ O 80 ml	20	10-15 sec	General structure.
	NaCN 10 ml (NH ₄) ₂ S ₂ O ₈ 10 ml H ₂ O 20 ml			Swab: The NaCN and (NH ₄) ₂ S ₂ O ₈ additions are made from 20% stock solutions.
Inconel alloy 600.....	HNO ₃ 5 ml	10	5-10 sec	
Inconel alloy X-750.....	Methanol 95 ml			
	HCl 30 ml HNO ₃ 10 ml CuCl ₂ Saturated			Swab: Let stand 5 min before using, good for Inconel alloy 600 but not Inconel alloy X-750.
Inconel alloy 700.....	HNO ₃ 20 ml Methanol 80 ml	30	15-30 sec	
	HCl 92 ml HNO ₃ 3 ml H ₂ SO ₄ 5 ml			Swab: Add H ₂ SO ₄ last and slowly.
Inconel alloy 625.....	HCl·H ₂ O ₂ 10 ml HCl 3 drops H ₂ O 90 ml	3-4	10-20 sec	This alloy is difficult to etch but one of these two solutions should work for most conditions of heat treatment.
	H ₂ SO ₄ 47 ml HNO ₃ 41 ml H ₃ PO ₄ 12 ml	5-10	2-10 sec	
Inconel alloy 718.....	CrO ₃ 5 gm H ₂ O 100 ml	10	7-10 sec	Dip in 100 ml HNO ₃ +4 drops of HF to remove the stain.
	CrO ₃ 25 gm H ₂ O 7 ml HC ₂ H ₃ O ₂ 133 ml	10	5-15 sec	To dissolve the CrO ₃ , the solution should be heated in hot water only. Add HC ₂ H ₃ O ₂ last. No staining.
	HCl 50 ml HNO ₃ 10 ml Glycerin 10 ml			Swab.
Inconel alloy 800.....	Glycerin 20 ml HCl 20 ml HNO ₃ 10 ml			Swab or immerse and stir.
	Oxalic 20 ml H ₂ O 80 ml	10	10-15 sec	Oxalic is mixed from a 20% stock solution.
Inconel alloy 825.....	Oxalic 10 ml H ₂ O 90 ml	10	5-10 sec	Oxalic is mixed from a 20% stock solution.
Nickels and Monel alloys.....	HNO ₃ 50 ml HC ₂ H ₃ O ₂ 50 ml		2-6 sec	Good for grain size determinations, tends to pit.
High purity Nickel.....	HNO ₃ 20 ml HF 3 ml		1-3 sec	Good for grain size determination, tends to pit.
Inconel alloys.....	HNO ₃ 20 ml HF 3 ml		1-3 sec	Good for grain size determination, tends to pit. Rinse sample thoroughly.

matic equipment for conducting the operations [412,413].

Since 1915, the rate of development of nickel plating has been quite rapid. Among the highlights are high-speed plating, begun by Watts with his famous "Watts bath" [414]; control quality of deposits, first emphasized by Watts and DeVerter [415]; accurate pH control, introduced by Thompson [416]; low pH baths, suggested by Phillips [417]; commercial introduction of modern bright nickel plating begun by Schlotter [418] and the many later developments of it; design of baths for deposition of leveling, semibright and bright nickel coatings; growing appreciation of the importance of high-purity electrolytes and of high ductility and low stress in deposits; and the development of automatic plating equipment that makes possible today's high production rates and low costs.

According to Pinner, Knapp, and Diggin [406] a survey of recent information shows

that the composition of the modern Watts bath can be represented reasonably well by the following:

Nickel sulfate (NiSO₄ · 7H₂O) 240-340 g/l
Nickel chloride (NiCl₂ · 6H₂O) 30- 60 g/l
Boric acid (H₃BO₃) 30- 40 g/l

An all-chloride bath was developed by Blum and Kasper [419]. The better-buffered half-chloride, half-sulfate bath of Pinner and Kinnaman [420] has advantages of both the Watts and the high-chloride baths and has been found to be especially suitable for high-speed plating.

Information of value on the electroplating of nickel is contained in several publications of The International Nickel Company, Inc., [421,422,423,424,425].

Improvements in the nickel anode material have kept pace with improvements in the bath and in the operating procedure. Nickel con-

TABLE 27. Examples of industrial nickel-plating baths and operating conditions

	Watts bath		All chloride bath	Intermediate bath	Hard plating bath	Special purpose bath	Nickel sulfamate bath	Sulfate bath
	(High pH)	(Low pH)						
Nickel sulfate.....oz/gal	32	44		24	24	16		38.5
Sodium sulfate.....oz/gal								3.2
Nickel sulfamate.....oz/gal							60	
Nickel chloride.....oz/gal	6	8	40	23			1.0	
Ammonium chloride.....oz/gal					3.3	2		
Boric acid.....oz/gal					4.0	2		
pH.....	4.5 to 6.0	1.5 to 4.5	4	5.3	5.0 to 5.5	5.0 to 5.5	5	4.5
Temperature.....°F	115 to 180	115 to 140	2.0	1.5	110 to 140	Room	110	2.5
Current density.....Amp/ft ²	20 to 100	25 to 100	25 to 100	100	25 to 80	5 to 10	50	20 to 30

taining up to 10 percent of impurities was acceptable as an anode material in the early baths. The development of the Watts bath, containing chlorides, permitted the use of the 99-percent, chill-cast nickel anode, and later, of the 99-percent, rolled anode that contained small amounts of nickel oxide for depolarizing purposes. A later development, for particular applications, was the cast or rolled carbon-silicon-nickel anode, which under some conditions forms an adherent, porous, carbon-silica film that acts as a bag. Anodes cut from electrolytic nickel sheet have been used to a limited extent, and several patents have been issued for introducing sulfur into nickel anodes to promote corrosion of the anodes.

Several special baths are cited by Gray [335]. In addition, references to the use of sulfamate [425a], fluoroborate [426,427], and pyrophosphate [428] baths, and to the electrodeposition of nickel from molten salt baths [429] have been noted. The brightening action of cadmium salts has long been known, and a great number of organic addition agents have been proposed and used to control the surface appearance (brightness) of the deposit, and sometimes for other reasons [335,430,431]. A black nickel deposit, containing nickel sulfide, can be obtained [432]. Indira et al. [433] described a solution for black nickel plating and showed that a high sulfur content was a prerequisite for achievement of jet-black coatings. Wesley and Knapp [434] patented a method of black nickel plating. McCarthy [435] described the production of various colors on several basis metals using a black nickel plating electrolyte. Wesley [436] reported the production of malleable sheets up to 6 mm thick of nickel that contained only 34 ppm of detectible impurities, by electrodeposition from a purified nickel chloride-boric acid solution, using iridium-platinum electrodes.

Electroplating on aluminum requires special treatment because of interference by the surface oxide film, but procedures have been developed for plating nickel directly on aluminum [437,438,439,440,441,442,443,444]. Likewise, special treatments have been developed so that nickel can be plated on beryllium [445],

on magnesium [446,447], on molybdenum [448,449], on titanium [450], on uranium [451], on zinc [452], and on zirconium [453]. Numerous processes have been developed for the plating of nickel alloys. A review of recent developments in nickel plating was written by Castell [454].

Examples of industrial nickel-plating baths and operating conditions are shown in table 27, without reference to brightening agents and other possible additions. In many industrial operations, the nickel plating may be applied over an undercoat of copper and may be followed by a final thin coating of chromium. Recommended practice for the preparation of nickel for electroplating with nickel is discussed in ASTM Specification B 343-60T. The requirements of ASTM Specifications for minimum thickness of coatings for service conditions of varying severity are summarized in table 28. More recent ASTM specifications are being issued; however these specifications will adhere to the same standards.

The physical and mechanical properties of electroplated nickel are affected by the composition of the bath, by all the variables in bath operation, and by the presence of metallic and gaseous impurities. These effects have been reviewed in many articles [455,456,457, 458]. The mechanical properties of nickel deposits for engineering uses are summarized in table 29.

TABLE 28. ASTM standards for nickel coatings

	Thickness of coating, in (min)			
	Type D	Type F	Type K	Type Q
On steel (ASTM A 166-61T)				
Copper plus nickel.....	0.0020	0.0012	0.00075	0.00040
Nickel (if copper is used).....	.00100	.00060	.00040	.00020
Chromium (if required).....	.000010	.000010	.000010	.000010
On copper and its alloys (ASTM B 141-55)				
Nickel.....		.00050	.00030	.00010
Chromium (if required).....		.000010	.000010	.000010
On zinc and its alloys (ASTM B 142-61)				
Copper plus nickel.....	.0020	.0012	.00075	.00050
Copper.....	.00020	.00020	.00020	.00020
Final nickel.....	.0010	.00050	.00030	.00030
Chromium (if required).....	.000010	.000010	.000010	.000010

TABLE 29. Mechanical properties of nickel deposits for engineering uses [459]

Type of bath	Watts, low pH		Chloride		Hard, as plated	Sulfamate, as plated
	As plated	Annealed	As plated	Annealed		
Tensile strength, psi	63,000	50,000	100,000	58,000	155,000	50,000
Elongation, % in 1 in.	31	50	21	48	6	10
Vickers hardness numbers	137	63	240	81	400	200
Rockwell hardness	75 B	17 B	99 B	35 B	42 B	

Hammond [458] noted that nickel plating may involve risk of hydrogen embrittlement in steels of 180,000 psi or higher, but that this may be obviated by low-temperature baking after plating. Beck and Jankowsky [460] reported that hydrogen embrittlement of 4340 steel induced by chromium plating was substantially reduced by an undercoat of Watts-type nickel.

In addition to electroplates of nickel alone, baths and operating conditions have been developed for the deposition of nickel alloys. Some of these are nickel-aluminum [461], nickel-boron [462], nickel-chromium [463], nickel-cobalt [464], nickel-iron [465], nickel-molybdenum [466], nickel-phosphorus [467], nickel-rhenium [468], nickel-tin [469], and nickel-zinc [470]. Some ternary alloys that have been plated are nickel-iron-chromium [471] and nickel-cobalt-copper [472]. Couch et al. [473] patented the production of nickel-aluminide coatings.

The various processes used for plating nickel are described in a booklet by The International Nickel Company, Inc. [474].

(2) *Electroless plating.* Brenner and Riddell [475] described a process developed at the National Bureau of Standards in 1946 for the deposition of nickel from an ammoniacal solution containing hypophosphite by chemical reduction. The following year the process was expanded to include deposition of nickel from acid solutions and the deposition of cobalt from both alkaline and acid solutions. Reduction of nickel salts by hypophosphite had been long known as a chemical reaction, but Brenner and Riddell were the first to develop a controlled autocatalytic reaction to produce a sound, coherent metallic coating that could be built up to appreciable thicknesses. The coatings contain up to 6 or 7 percent of phosphorus, probably in the form of finely dispersed phosphides. As deposited, the coatings have a Vickers hardness number as high as 700, but heating at elevated temperatures reduces the hardness, and heating for at least 4 hr at 725 to 800 °C converts the plated coating into an iron-nickel alloy [476]. The deposits are somewhat less magnetic, but are similar to electrodeposited nickel in resistance to rusting as indicated by

the salt spray test. The electroless process has three advantages over electroplating:

1. Coatings deposit with uniform thickness in recesses as well as on exposed surfaces.
2. There is no buildup of coating on points or edges.
3. No electrical equipment is required.

Electroless nickel plating can be deposited directly upon surfaces that catalyze the reaction, for example, on aluminum, cobalt, copper, gold, iron, nickel, palladium, platinum, and silver. A method of electroless nickel plating of magnesium and thorium was patented by Puls and Vincent [477] and electroless nickel plating of beryllium was described by Roberts [478]. Titanium, zirconium, and hafnium have also been chemically plated with nickel [479]. Semiconductors, such as graphite and silicon carbide, may be electroless plated by touching the semiconductor with a piece of aluminum or steel to start the reaction, and nonconductors, such as glass, plastics, and ceramics, may be electroless plated after dipping in palladium solution or being otherwise treated to form an absorbed film of palladium or a palladium compound. However, cadmium, manganese bronze, lead and its alloys, and silicon cannot be electroless plated, according to Panchenko and Krokhina [480].

The compositions of various baths for electroless nickel plating and the operating procedures have been described by Krieg [481] and by Aitken [482].

Patents for the electroless deposition of nickel-boron [483] and nickel-vanadium [484] alloys have been issued.

The history of the electroless plating process was reviewed by Brenner [485]. MacLean and Karten [486] reported that small fuse parts with deep blind holes could be plated with 0.1 mil of nickel. Rich [487] reported that the use of ultrasonic vibrations from stainless steel transducers increased the rate of electroless nickel plating. Gutzeit and Landon [488] described operations of a large-scale, electroless, custom plating shop. Chinn [489] reviewed the subject of electroless plating and cited numerous examples of its practical use.

(3) *Electroforming.* Nickel electroforming, accomplished by the use of electroplating processes, is defined as the production or the reproduction of articles by electrodeposition upon a mandrel or mold that is subsequently separated from the deposit. It is a low-cost production method for forming complex assemblies or intricate internal contoured shapes which require high dimensional accuracy and smooth surface finish. The process is sometimes referred to as "cold casting." Inasmuch as the electrodeposit that constitutes an electroformed article is used as a separate structure, its mechanical properties are a matter of major importance.

Nickel ordinarily is electroformed in a Watts-type solution or a nickel sulfamate bath, such as shown in table 30. The pH of all nickel solutions should be maintained within a relatively narrow range of about 0.5 unit for good control of physical and mechanical properties, but a relatively low pH of about 3 is preferred for some applications, whereas a pH of 4 to 4.5 is preferred for others.

TABLE 30. Composition and operating conditions for two nickel electroforming baths [490]

	Watts bath	Sulfamate bath
Nickel sulfate or sulfamate	30 to 50 oz/gal * 44	30 to 50 oz/gal * 50
Nickel chloride	4 to 8 * 6	0.4 to 0.8 * 0.6
Nickel	10 to 12 * 11	8 to 14 * 10
Boric acid	4 to 6 * 5	4 to 6 * 4
pH	2.0 to 4.5	3.5 to 4.2
Temperature	115 to 140 °F	80 to 140 °F
Current density	25 to 50 A/ft ²	20 to 150 A/ft ²

* Typical or average operating condition.

The structure and properties of electroformed nickel (or alloy) depend on electrodeposition conditions as follows: kind and concentration of the nickel salts, concentration of chloride or other anion employed for assisting the dissolution of anodes, pH of the solution, impurity concentrations, solution temperature, cathode current density, kind and amount of solution agitation, and interrelation of these factors. The kind and concentration of organic chemical agents added to the electrodeposition solution for avoiding pitting, reducing stress, or refining the grain structure frequently have profound effects on properties.

Kura et al.[491], in a review of the literature, gave the following ranges for the physical and mechanical properties of electroformed nickel:

Density	0.321 to 0.327 lb/in. ³
Modulus of elasticity	23,000,000 to 28,000,000 psi
Coefficient of linear expansion near room temperature	3.1 to 6.3 microinch/°F
Ultimate tensile strength	55,000 to 215,000 psi
Yield strength	32,000 to 128,000 psi
Elongation in 2 in.	2 to 27 percent

These authors noted that as a rule, an increase was observed in the tensile and yield strengths for electroformed nickel, and a decrease in ductility was evident when the temperature for the electrodeposition bath was lowered. They note further that, of the various baths used for electroforming, stronger nickel with a higher yield strength was obtained with the nickel chloride and nickel sulfamate solution than with any other. Modern electroforming solutions were discussed by Diggin

[492] and the physical and mechanical properties of electroformed nickel at both elevated and subzero temperatures were reported by Sample and Knapp [493].

Electroforming is particularly applicable to the manufacture of phonograph record stampers [494], printing plates [495], screens [496], etc. Even pressure vessels have been electroformed [497].

(4) *Nickel cladding.* Nickel cladding, like electroplating, supplies corrosion resistant, nickel-surfaced material that is cheaper than solid metal. In this process the cladding metal is pressure welded to one or both sides of an open-hearth steel slab in a rolling mill at about 2,200 °F. If the bonding surfaces have been properly cleaned and protected during heating, excellent bonding through the formation of an iron-nickel solid solution is accomplished during hot reduction to between one-eighth and one-sixteenth of the original thickness.

The ratio of cladding material to the base plate is usually expressed as a percentage of the total thickness of the plate. For example, a 1/2-in plate clad 10 percent on one side only consists of about 0.45 in of steel and 0.05 in of nickel; clad 10 percent on both sides, it would be 0.40 in of steel and 0.05 in of nickel on each side. When both sides are clad, the same thickness of nickel usually is applied to each side, but different thicknesses on the two sides may be developed if desired. Nickel-clad steels are regularly supplied with 5-, 10-, 15-, or 20-percent cladding on a 55,000-psi minimum tensile strength steel as base material. According to Theisinger and Huston [498], nickel cladding does not affect the mechanical properties of the clad material, as illustrated by the following data of 1/2-in steel with and without 10-percent nickel cladding.

	Tensile strength	Yield point	Elongation in 8 in	Reduction in area
	psi	psi	%	%
Clad	60,600	40,400	30.0	57.2
Plate	60,800	40,200	30.5	59.0

A relatively new process for metallurgically bonding a pore-free coating onto mild steel consists of applying carbonyl nickel powder in slurry form directly to the surface of a moving strip of hot rolled steel [498a]. The slurry is then dried and sintered to a porous nickel layer which is densified to a nonporous coat by passing between the rolls of a hot compaction mill. Nominal nickel coating thicknesses on the order of 0.0005 to 0.0025 in have been achieved after cold rolling.

Metals have also been clad with nickel by explosive bonding techniques.

Cladding is not restricted to the use of nickel only. Steel may be clad with Monel alloy 400, Inconel alloy 600, stainless steel, etc. In welding the clad surface of a plate, a covered electrode of approximately the same composition as the cladding is used. ASTM Specification A265-62 covers nickel and nickel-base alloy clad steel plate.

(5) *Sprayed and vapor-deposited coatings.* Protective coatings of nickel or of nickel alloys may be applied by metal-spray processes, which are particularly adapted for coating large objects of irregular shape [499]. Pure nickel can be sprayed with either a wire or powder gun. Nickel alloys are usually sprayed in a powder gun because they are more readily available in powder form. After spraying, the material is fused to form a metallurgical bond with the base material, which may be steels, irons, nickel and nickel alloys, copper and copper alloys, and refractory alloys. A self-bonding material that does not have to be fused after spraying is nickel aluminide, which has been described by Sheppard [500]. Kura et al. [491] summarized the process of metal spraying of nickel and its alloys. A patent for obtaining a smooth uniform coating of nickel by spraying with an aqueous solution was issued to Carlson and Prymula [501].

Chemical vapor deposition (CVD) is accomplished by causing gaseous molecules to react chemically at, or near, a heated surface under conditions such that one, and only one, of the reaction products is a solid and is deposited on the heated surface. As the reaction continues, atoms (or molecules) are added to the growing metal lattice one at a time. Such a procedure has been called a "molecular forming" process. Considerable detail concerning the mechanism of deposition at low pressures and the properties of nickel coatings was given by Owen [502]. Nickel can also be vapor deposited by electron beam β rays.

Nickel can be deposited by the thermal decomposition of nickel carbonyl, of nickel acetylacetonate, or by the hydrogen reduction of nickel chloride. According to Owen [503], nickel carbonyl is used because it is highly volatile. The plating temperature is under 250 °C and rates of deposition as fast as 0.030 in/hr are achieved without difficulty.

Tewes et al. [504] studied four potential catalytic agents and found that the use of the hydrogen sulfide/oxygen catalytic mixture achieved the same plating rate at 100 °C as was obtained at 150 °C without a catalyst.

The strength of vapor-deposited nickel films of 700 to 4360 Å thickness was studied by D'Antonio et al. [505], who concluded that a significant contribution to the high strength of thin metal films can be attributed to the vapor-deposition process which, owing to its severe quenching effect, is believed to promote

the formation of many point defects which inhibit the motion of dislocations.

Recent developments in the technique of nickel plating from the vapor of nickel carbonyl have been reviewed by Owen [506].

Gas plating of nickel has been used to coat synthetic fibers such as nylon, rayon, glass, etc. [507,508,509]. The protection afforded uranium by the thermal decomposition of nickel-carbonyl vapor was reported by Owen [510] to be considerably superior to electrodeposited coatings of the same thickness.

According to Cummins [511], the addition of ammonia gas to nickel carbonyl plating gas results in the production of nickel-containing films of relatively high electrical resistance. These coatings are applied to the preparation of electrical resistance units.

Breining [512] obtained a patent on the deposition of nickel-phosphorus alloys by gas plating.

b. Nickel Powders

By varying the conditions of electrodeposition, nickel may be deposited as a powder rather than as a continuous plate [513,514,515,516]. Nickel powder has been produced by electrolysis of fused salts [517], grinding of sulfurized nickel shot, hydrogen reduction of nickel oxide, and in the ammonia-leach process for the recovery of nickel from its ores [518], but the principal production of nickel powder for powder metallurgy uses is by decomposition of nickel carbonyl or by the ammonia-leach process. Various types of carbonyl-nickel powders are also available [519]. The properties of sintered carbonyl nickel powder compacts were reported by Prill and Upthegrove [520].

Nickel powder may be used by itself to form all-nickel parts, or in combination with other metal powders to produce alloys or compounds [45,521,522,523,524]. Pure nickel strip can be produced from powder [525,526,527,527a].

Carbonyl nickel powders of irregular particle shape and low bulk density are used in the production of porous nickel electrodes for nickel-cadmium storage batteries and hydrogen-oxygen fuel cells employing alkaline electrolytes [528,529,530,530a,530b].

Nickel powder parts are particularly valuable in the field of electronics, and controlled-expansion and magnetic alloys formed by powder-metallurgy techniques have advantages over melted metal [531]. Cathode-base materials for the electron tube industry have been made by the powder rolling of nickel powder with controlled alloy additions to achieve unusual combinations of properties, such as electrical passivity and mechanical strength at high temperature [531a]. Nickel-silver con-

END OF REFERENCE
25

REFERENCE

26

KEUHL, K. K.; AND ZWILLENBERG, M. L.: INVESTIGATION OF THE IGNITION AND COMBUSTION OF METAL WIRES. REP. F910336-24, UNITED AIRCRAFT RESEARCH LAB. (NASA CR-89788), MAY 1967.

PAGES WERE NOT REPRODUCED FROM THIS REPORT.

END OF REFERENCE
26

REFERENCE

27

**BROWNING, ETHEL: TOXICITY OF INDUSTRIAL METALS. SECOND
ED., BUTTERWORTHS & CO., 1969.**

**THIS REFERENCE IS COPYRIGHTED MATERIAL AND THEREFORE
THE CONTENTS HAVE NOT BEEN REPRODUCED FROM THE TEXT.**

END OF REFERENCE
27

CONTINUED ON CARD 4

REFERENCE

28

**REYNOLDS, W. C.: INVESTIGATION OF IGNITION TEMPERATURES
OF SOLID METALS. NASA TN D-182, 1959.**

MAR 2 71

2.1-0-1

NASA TN D-182

NASA TN D-182

REF. (2)



COPY 3

TECHNICAL NOTE
D-182

INVESTIGATION OF IGNITION TEMPERATURES OF SOLID METALS

By W. C. Reynolds

Stanford University

LIBRARY COPY

MAR 2 1971

**LEWIS LIBRARY, NASA
CLEVELAND, OHIO**

NATIONAL AERONAUTICS AND SPACE ADMINISTRATION
WASHINGTON

October 1959

NATIONAL AERONAUTICS AND SPACE ADMINISTRATION

TECHNICAL NOTE D-182

INVESTIGATION OF IGNITION TEMPERATURES OF SOLID METALS

By W. C. Reynolds

SUMMARY

C-477

The ignition temperature of a solid metal is related through a thermal definition of ignition to the rate of oxidation and to the radiation and convection heat-transfer parameters. The mechanisms of oxidation are reviewed and the factors which influence ignition temperatures are discussed. Reasonable agreement between theoretical and experimental ignition temperatures is demonstrated. Experimental ignition temperatures for several metals are presented.

INTRODUCTION

For many years the maximum safe operating temperatures for metals have been determined from strength considerations. However, some metals have been known to ignite and burn at what would normally be structurally safe temperatures. It seems, then, that failure by ignition and burning may, in some cases, precede failure by structural weakening with temperature and that the possibility of ignition must be considered in the design of high-temperature metal apparatus.

The advent of high-speed flight has brought about increased interest in the problem of metal ignition. At flight speeds typical of modern aircraft and missiles, aerodynamic heating causes extremely high skin temperatures. The danger of ignition is increased in regions behind shock waves where temperatures and pressures are exceptionally high. Other fields where metal ignition is of interest include the design of gas turbines, high-temperature furnaces, gas-cooled nuclear reactors, and rocket motors.

Obviously there are many factors which enter into the problem of ignition and burning. The mechanisms involved are entirely different, and the distinction between ignition and burning must be kept clear. Ignition is brought about by the exothermal oxidation reaction between the solid metal and its gaseous environment. Consequently, it is believed that the phenomenon of ignition is quite closely related to the relatively slow oxidation that occurs on all metals at low temperatures ("rusting"). Burning, on the other hand, may proceed by any of

several mechanisms. It may be a surface reaction, that is, a further extension of the rusting process; the burning of many metals, notably magnesium, is a vapor-phase reaction and occurs at some distance from the surface. It is conceivable that a body could ignite but not burn, the ignition (rise in temperature) leading simply to melting. This investigation is concerned primarily with the problem of ignition. However, it is impossible to divorce completely ignition from burning, and so some attention has been given to the latter phenomenon also.

Very little information regarding the ignition of metals is available. However, a great deal of information is known about the oxidation of metals. It is not unreasonable to expect that the heat generated in the oxidation reaction prior to ignition could be calculated from oxidation data extrapolated to temperatures near ignition. Under this assumption an ignition temperature may be defined and calculated. For metals where the extrapolation is not made over too large a temperature difference, reasonable agreement between calculated and experimental ignition temperatures can be obtained. The effect of varying the environmental conditions can then be studied. A great deal is known about the mechanisms of oxidation, and thus a study of these mechanisms gives considerable insight into the ignition problem.

The primary objective of this investigation is to study the effects of important environmental parameters on the ignition temperatures of solid metals. Considerable effort has been devoted to the study of the mechanisms of oxidation and to the relation of these phenomena to ignition. Thus, the investigation is primarily one of a theoretical nature, but a certain amount of data has been gathered to confirm and supplement the knowledge of the ignition mechanisms. Since one of the most important applications of this research is in the high-speed flight problem, special attention has been given to metals of interest in aircraft construction. It is difficult to produce flight conditions of this nature in the laboratory, and therefore attention has been given to the manner in which flight conditions (flow velocity, gas pressure and temperature, heat transfer, etc.) influence the oxidation rate and the ignition temperatures.

The present investigation was carried out at Stanford University under the sponsorship and with the financial assistance of the National Advisory Committee for Aeronautics.

SYMBOLS

- A action constant, $g/cm^2\text{-sec}$ or $g^2/cm^4\text{-sec}$; area, cm^2 or ft^2 ;
 constant, dimensional as defined where used
- a constant

B	constant, dimensional as defined where used
C	constant, dimensional as defined where used; thermal capacitance, cal/°K or Btu/°F
C_a	number of activated adsorption sites, 1/cm ²
D	diffusion coefficient, cm ² /sec; diameter, cm, ft, or in.
E	activation energy, cal/mole; constant, dimensional as defined where used
F	Faraday's constant, 96,500 coulombs/(g equivalent)
F^*	Faraday's constant, 23,066 cal/volt
\mathcal{F}	dimensionless factor, defined where used
f	dimensionless factor, defined where used
h	heat-transfer coefficient, cal/sec-cm ² -°C or Btu/hr-ft ² -°F
\hbar	Planck's constant, 6.624×10^{-27} erg sec
K	rate constant, g/(cm ² -sec) or g ² /(cm ⁴ -sec)
ι	electrical conductivity of a single mode, 1/ohm-cm
M	Mach number
m	mass of molecule or atom, g
\mathcal{m}	factor, defined where used
N_{Re}	Reynolds number
N_o	Avogadro's number, 6.023×10^{23} per mole
n	constant; molecular concentration per unit volume, molecules/cm ³
p	pressure, dynes/cm ² , atm, or lb/ft ²
Q	heat of reaction per gram of oxygen, cal/g
q"	heat-transfer rate per unit area, cal/sec-cm ² or Btu/hr-ft ²
R	universal gas constant, 1.986 cal/mole

4

r	ratio of volume of oxide to volume of metal
T	absolute temperature, °K or °R
V	volume, cm ³
v	velocity of molecular reaction, molecules/sec
W	molecular weight
w	weight of oxygen reacted with metal, g
x	coordinate, cm
z	atomic weight of oxide, g/mole
α	factor, defined where used
Γ	rate of molecular diffusion per unit area, molecules/cm ² -sec
γ	ratio of mass of oxide to mass of oxygen forming it
δ	thickness of oxide film, cm; thickness of boundary layer, cm or in.
ε	emissivity
θ	time, sec
κ	Boltzmann's constant, 1.380×10^{-16} erg/°K
λ	free molecular path, cm
λ _m	mean free molecular path, cm
ξ	coordinate, cm
ρ	density, g/cm ³ or lb/ft ³
σ	Stefan-Boltzmann constant, 13.77×10^{-13} cal/cm ² -sec-°K ⁴ or 17.13×10^{-12} Btu/hr-ft ² -°R ⁴ ; molecular or atomic diameter, cm
τ	transference numbers for electrical conductivity
η	pyrophoricity
η _l	linear pyrophoricity, $\frac{A_l Q}{4\sigma\epsilon} \left(\frac{R}{E_l} \right)^4$

- η_p parabolic pyrophoricity, $\frac{A_p Q}{8\sigma\epsilon\delta\rho_{\text{oxide}}\gamma}\left(\frac{R}{E_p}\right)^4$
- h^* term characterizing convection heat transfer
- h_l^* linear heat transfer, $\frac{h}{A_l Q} \frac{E_l}{R}$
- h_p^* parabolic heat transfer, $\frac{2h\delta\rho_{\text{oxide}}\gamma}{A_p Q} \frac{E_p}{R}$
- T^* ignition temperature
- T_l^* linear ignition temperature, RT_{ig}/E_l
- T_p^* parabolic ignition temperature, RT_{ig}/E_p

Subscripts:

- o refers to ambient (T_o denotes recovery temperature), or denotes heating independent of temperature
- 1 refers to oxygen in the gaseous environment, or defined where used
- 2 refers to inert gases in the environment, or defined where used
- 3 refers to oxide vapor
- ∞ refers to ambient or environment
- A refers to anion
- C refers to cation
- e refers to electron
- ig used to denote ignition temperature
- iso isothermal
- l refers to linear oxidation

m	refers to metal
ox	refers to oxidation
oxide	refers to oxide
p	refers to parabolic oxidation
s	used to denote surface temperature
sat	saturated

RELATION BETWEEN IGNITION TEMPERATURE AND OXIDATION RATE

Thermal Definition of Ignition

Before any sensible approach to the problem of solid-body ignition can be made, the ignition temperature must be defined. Generally, ignition is said to occur when the body temperature rises spontaneously and a self-propagating reaction occurs at some elevated temperature. Evidently, thermal stability is involved, and the definition of ignition must be obtained through energy considerations. An energy balance on an object of arbitrary shape results in a complex partial-differential equation, the solution of which describes the temperature-time history of every point in the object. Ignition will occur when, at some point in the object, the temperature starts to rise rapidly, that is, when the heating effect of the exothermal oxidation reaction overcomes the conduction, convection, and radiation cooling. A general definition of ignition, even in the case of simple shapes, involves the solution of the highly non-linear energy equation and is impractical. If the conduction terms in the energy equation are momentarily overlooked, an analysis can be made, and the ignition temperature can be expressed mathematically. Such an analysis then allows an examination of how the ignition temperature depends on environmental conditions. The trends thus indicated should be similar to those applying to more complex systems. Such a simple analysis is therefore of great value, but the assumptions involved must be remembered.

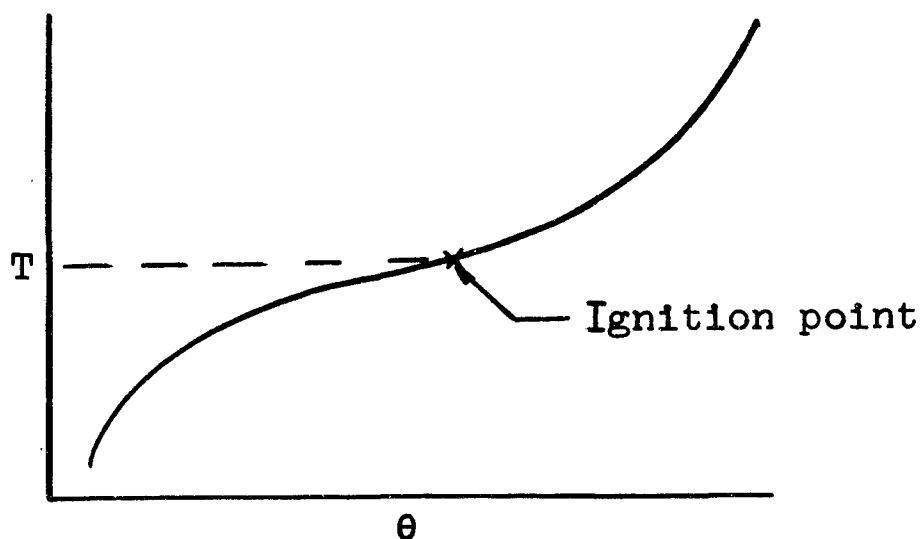
The thermal definition of ignition introduced here is based on an energy balance on an oxidizing isothermal body of arbitrary shape, cooled by convection and radiation. If it is assumed that the heat generated in the reaction may be treated as a heat addition at the surface and that the oxidation, convection, and radiation heat-transfer rates are uniform over the surface, an energy balance on the isothermal body gives

$$\frac{C}{A} \frac{dT}{dt} = q_{ox}'' - h(T - T_0) - \sigma \epsilon (T^4 - T_\infty^4) + q_0'' = \phi(T) \quad (1)$$

where q_0'' is any heat input independent of the body temperature. Note that the rate of change of the body temperature is a function of the temperature and several environmental parameters assumed to be constants. Note that the same equation would apply if the convection and radiation heat-transfer terms were treated as heating rather than cooling terms.

The temperature-time history of the body can be found by integration of equation (1). If the temperature tends to increase in time and the environmental parameters are constant, the body will eventually reach a "steady-state" condition under which the heat input due to oxidation (and perhaps electrical energy) is balanced by the convective and radiation cooling. For most metals, as the temperature increases, the reaction rate increases nearly exponentially and, therefore, q_{ox}'' is usually a rather rapidly increasing function of temperature. This tends to be offset by the increase in the convective and radiation cooling with increasing temperature. Under normal conditions the temperature will rise at a decreasing rate to the point at which the heat inputs are exactly balanced by the cooling, and the body will remain at this steady-state temperature indefinitely. However, if the temperature reaches a point at which further increase in temperature will result in an increase in the oxidation heat input larger than the increase in cooling, the body temperature will then continue to rise at an increasing rate and no steady-state condition will be reached. It appears, then, that there is a maximum steady-state temperature at which the body can exist indefinitely. This temperature is seen to be a function of the environmental conditions. If, in the course of a thermal transient, the temperature should exceed this limit, then the temperature would continue to rise until melting or full-scale combustion phenomena occurred. This maximum stable steady-state temperature will henceforth be called the ignition temperature. Note that ignition as defined here is not necessarily followed by burning; melting produced by the temperature rise due to oxidation could alter the oxidation characteristics sufficiently to prevent further temperature rise to the point of vaporization and actual combustion.

On the basis of the foregoing arguments, the ignition temperature is seen to be equivalent to the temperature at which the body temperature begins to increase at an increasing rate. This may be expressed mathematically as the temperature at which $dT/d\theta$ is a minimum, as seen in the following sketch:



The ignition temperature can be found as a function of the environmental and oxidation parameters by requiring that the derivative of equation (1) with respect to temperature vanish. The resulting defining equation for the ignition temperature is

$$\left[\frac{d}{dT} (q''_{ox}) \right]_{T=T_{ig}} - h - 4\sigma\epsilon T_{ig}^3 = 0 \quad (2)$$

It should be noted that, for ignition to occur, $dT/d\theta$ must be positive at the ignition temperature, and the dependence of the oxidation rate on temperature must be positive and stronger than that of the dominating cooling term. It is extremely interesting that, unless the oxidation rate depends on ambient temperature, the ignition temperature is independent of ambient temperature.

Oxidation-Rate Equations

In general, the oxidation behavior of technically important metals can be classified as either linear or parabolic and correlated by equations of the form

$$w = A_1 e^{-E_1/RT} \theta = K_1 \theta \quad (3)$$

for linear oxidation and

$$w^2 = A_p e^{-E_p/RT} \theta = K_p \theta \quad (4)$$

for parabolic oxidation. In these empirical fits to observed data, w is the weight of oxygen per unit of surface area that has reacted with the metal in time θ ; K is referred to as the rate constant; E is referred to as the activation energy; and A is referred to as the action constant. The constants A and E , in general, depend on environmental conditions and may even be functions of the metal temperature. The constants are obtained from experimental data by plotting the logarithm of K against $1/T$; E is first determined from the slope of a line through the data points, and then A is easily calculated. Since the exponent E/RT is usually relatively high (10 to 80), any small error in E due to fitting a straight line through experimental points causes a large error in A . Even the most careful experimenters in the field of metal oxidation estimate the uncertainty in their activation energies as $\pm 5,000$ calories in about 40,000 calories, and thus the uncertainty in A may be an order of magnitude. This high uncertainty in the oxidation constants limits any quantitative attempt to predict ignition temperatures from experimental oxidation data. Nevertheless, by studying the manner in which these constants depend on environmental conditions, a great deal can be learned about how ignition temperatures depend on environment. Experimental values of A and E for a number of metals are given in table 1. These data are taken largely from reference 2.

The rate of heat generation per unit area is obtained by differentiating equations (3) or (4) with respect to time and multiplying by the heat of reaction per gram of oxygen. This yields

$$q''_{ox} = QA_l e^{-E_l/RT} \quad (5)$$

for linear oxidation and

$$q''_{ox} = \frac{QA_p}{2\delta\rho_{oxide}} e^{-E_p/RT} \quad (6)$$

for parabolic oxidation.

The introduction of equation (5) into equation (2) allows expression of the ignition temperature for linearly oxidizing metals in the following explicit form:

$$e^{-1/T_l^*} = \frac{(T_l^*)^5}{\eta_l} + h_l^* (T_l^*)^2 \quad (7)$$

where

$$T_l^* = T_{lg} R / E_l$$

$$\eta_l = \frac{A_l Q}{4 \sigma \epsilon} \left(\frac{R}{E_l} \right)^4$$

$$h_l^* = \frac{h}{A_l Q} \frac{E_l}{R}$$

Similarly, upon substitution of equation (6) into equation (2) there results the following expression for the ignition temperature of parabolically oxidizing metals:

$$e^{-1/T_p^*} = (1/\eta_p)(T_p^*)^5 + h_p^*(T_p^*)^2 \quad (8)$$

where

$$T_p^* = T_{lg} R / E_p$$

$$\eta_p = \frac{A_p Q}{8 \sigma \epsilon \rho_{\text{oxide}} \gamma} \left(\frac{R}{E_p} \right)^4$$

$$h_p^* = \frac{2 h \delta \rho_{\text{oxide}} \gamma}{A_p Q} \frac{E_p}{R}$$

Since equations (7) and (8) are of the same form, a single set of curves may be used to represent the solution of both. Figure 1 shows the dimensionless ignition temperature T^* plotted against η with h as a parameter. Hereafter η will be referred to as the pyrophoricity; note that materials having high pyrophoricities will have relatively low ignition temperatures. Note also that the effect of an increase in the rate of convective heat transfer, either heating or cooling, will tend to give higher ignition temperatures. This result is quite surprising and as yet has not been supported or repudiated by experimental data. It must be remembered that the oxidation-rate constants A and E may depend on environmental conditions, in which case the ignition temperature is said to depend indirectly on environment.

MECHANISMS OF METAL OXIDATION

C-477

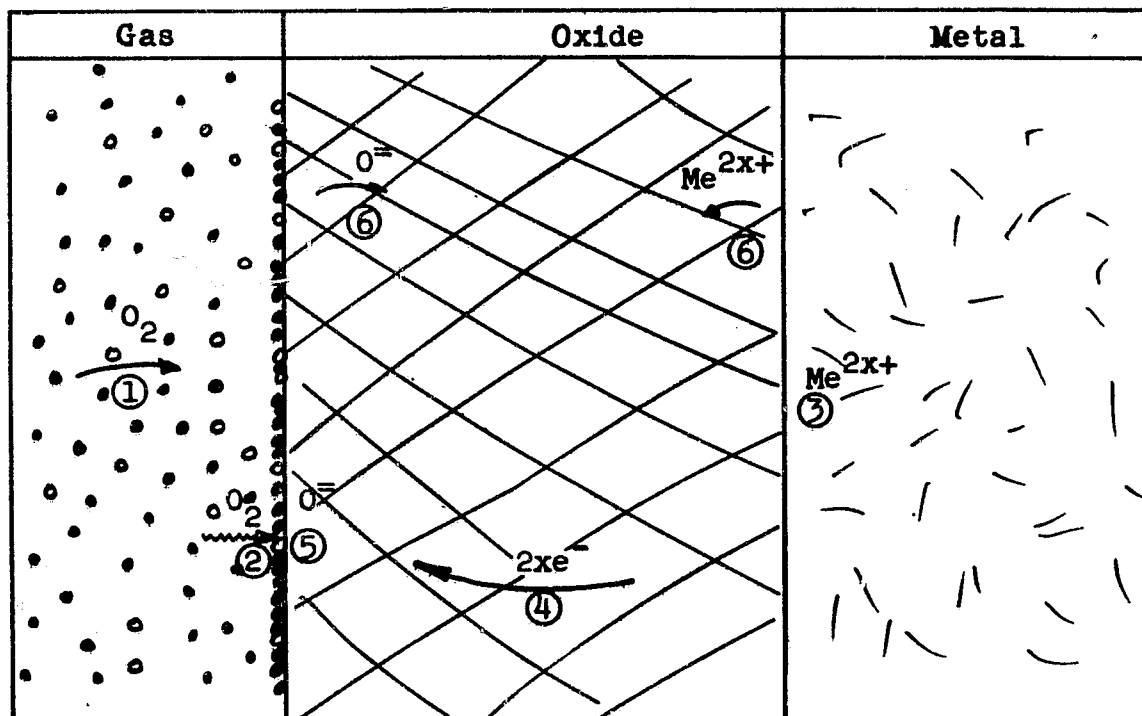
In order to investigate the manner in which the ignition temperature depends on environmental conditions, it is necessary to understand the mechanisms of the oxidation reaction. It is well known that the oxidation reaction proceeds by a series of steps, the slowest of which controls the overall rate of reaction. By comparison of the relative rates of occurrence of these steps it appears that only three of these may be slow enough to be rate controlling: namely, (1) the rate of transport of oxygen to the reacting surface, (2) the rate of adsorption of oxygen molecules at the surface, and (3) the rate of diffusion of ions in the oxide. Analysis indicates that, if the oxygen transport rate controls the reaction, the surface will become oxygen starved, and the body will not ignite. Such a situation might occur on an aircraft flying at extremely high altitudes or on a body sitting in very still air. The oxidation of some metals, notably magnesium and magnesium alloys, is believed to be controlled by the rate of oxygen adsorption. The rate of adsorption is not influenced by ambient pressure, except at extremely low pressures; at low pressures the oxidation rate is decreased, resulting in an increase in the ignition temperature. In continuum flows the adsorption rate is practically independent of the ambient temperature, but in noncontinuum flows the adsorption rate may be very strongly influenced by the gas temperature, being accelerated when the ambient temperature exceeds the body temperature. At low temperatures the oxidation of most metals is controlled by the rate of diffusion of ions in the oxide lattice. Generally, the oxidation rate is independent of ambient temperature and only mildly dependent on the ambient pressure but it may either increase or decrease with increased pressure, depending on the particular mechanism of ion diffusion involved. The rate of ion diffusion varies inversely as the thickness of the oxide scale. Thus it is possible that the removal of the bulk of the oxide scale by the drag of airflow over the surface may substantially increase the oxidation rate and thus lower the ignition temperature.

The mechanisms which govern the oxidation of a given metal will depend on the environment; for example, the rate of oxygen transport will certainly control the oxidation of the skin of a missile flying at 500,000 feet, whereas the sea-level oxidation rate will be controlled by either adsorption or ion diffusion, depending on the relative rates of these two processes.

The mechanisms of oxidation, the rates of oxidation, and the influence of environmental conditions of each are summarized in table 2.

Steps in Oxidation Reaction

For the purposes of this discussion, a simple model of a pure metal Me having valence $2x+$ and forming a single oxide MeO_x is used. This model is shown as follows (the various steps in the reaction are numbered):



The black dots represent oxygen molecules, and the small circles represent molecules of inert gas present in the gaseous environment. The $2xe^-$ indicates the number of electrons transferred in the ionization of stoichiometric amounts of metal and oxygen.

The steps which occur in the oxidation reaction are numbered and are as follows:

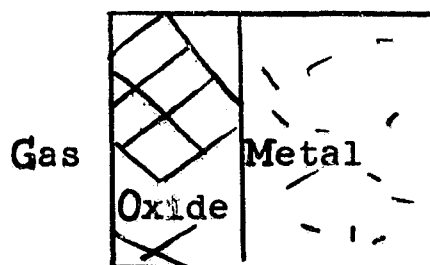
(1) Oxygen molecules are transported to the gas-oxide interface by forced or natural diffusion through the inert gas molecules.

(2) Oxygen molecules whose energy exceeds a certain level are adsorbed by the surface of the oxide.

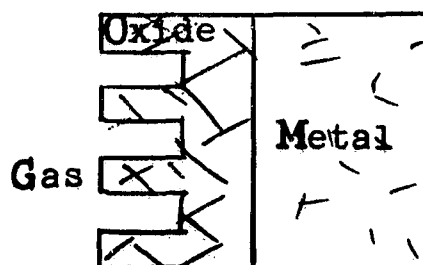
- (3) Metal atoms ionize at the metal-oxide interface.
- (4) The electrons given up by the metal atoms diffuse through the oxide lattice to the gas-oxide interface.
- (5) The oxygen molecules dissociate, and oxygen atoms are ionized by the electrons.
- (6) The oxygen and metal ions diffuse in the oxide lattice, meeting and falling into place in the crystal structure.

Each of these steps will be discussed in detail subsequently. It must be remembered that this is an extremely simple model for analysis and many complicating factors may enter. For example, if the oxide is porous, the gas may attack the metal directly in places and thus two parallel paths for the oxidation may exist; the formation of blisters may inhibit the reaction; several oxides may be formed; and impurities or alloying elements may influence the oxidation. These complicating factors are discussed rather thoroughly in reference 2.

Of particular interest in the study of oxidation mechanisms is the ratio of the volume of the oxide to the volume of the base metal from which it is formed, $V_{\text{oxide}}/V_m = r$. It would seem that for $r < 1$ the oxide could not completely cover the metal surface, and a porous oxide surface would be formed. On the other hand, if r is greater than unity the oxide would tend to be pushed away from the surface, possibly allowing the formation of blisters. It would be expected that the porous oxide would be the less protective of the two types and that differences in the rate-controlling mechanisms may exist. Simplified models for the two types of oxide are shown below. Note that the porous oxide is shown to have a thin layer covering the entire metal surface.



Nonporous
($r > 1$)



Porous
($r < 1$)

It has been observed that metals which oxidize in the parabolic manner generally form nonporous oxides, that is, $r > 1$. Moreover, metals that oxidize in the linear manner form porous oxides, $r < 1$. The reasons for this difference are not well understood. It is generally believed that diffusion through the oxide film governs the parabolic type of reactions, but there is considerable difference of opinion as to the rate-controlling step in linear oxidation. Two viewpoints that appear plausible are (1) that the rate of oxygen adsorption is the slowest step, since the film is so thin, and (2) that diffusion through a constant-thickness thin film at the roots of the pores controls the reaction.

Transport of Oxygen to Gas-Oxide Interface

As oxygen molecules are adsorbed by the oxide close to the gas-oxide interface, new molecules must be brought close to the oxide if the reaction is to be continuous. If a thermal boundary layer is formed over the surface, the temperature variation within several hundred mean free paths from the surface is essentially zero. Since nearly all the oxygen molecules which come in contact with the surface come from a region within a very few mean free paths of the surface, the gas which is transported to the surface may be considered as being at the surface temperature, regardless of the ambient temperature.

If the environment consists of pure oxygen, the rate of molecular interaction with the surface is given by kinetic theory (ref. 3) as

$$\frac{dw}{d\theta} = p \sqrt{\frac{1}{2\pi(R/W_1)T}} \quad (9)$$

where p is the oxygen pressure, W_1 is the molecular weight of oxygen, and T is the surface temperature. By inserting numerical values, it may be shown that the rate of interaction of oxygen $dw/d\theta$ is many orders of magnitude larger than observed weight gains for oxidation of metals. Moreover, the rate of interaction decreases with temperature; this temperature effect is opposite to that exhibited by metals and does not lead to an ignition condition. On the basis of these arguments it is concluded that oxygen transport does not control the rate of oxidation of metals if the environment is pure oxygen and the pressure is not too low.

If the environment contains nonreacting gases such as does air, then, as oxygen molecules are adsorbed at the surface, other oxygen molecules must diffuse through the inert gases to replace them. If the molecules are not replaced faster than they are adsorbed, the surface will become starved of oxygen, and the rate of diffusion of oxygen molecules through the inert gas to the surface would control the rate

of oxidation. The rate of oxygen-molecule diffusion through the inert gas is given by (see ref. 3)

$$\Gamma_1 = \frac{n}{n_2} D \frac{dn_1}{dx} \quad (10)$$

where n_1 is the oxygen concentration and n_2 is the inert gas concentration in molecules per unit volume ($n = n_1 + n_2$), D is the diffusion coefficient, and x is measured from the surface. The diffusion constant D may be calculated from kinetic theory (ref. 3) as

$$D = \left[\frac{3}{2\sqrt{2}\pi (\sigma_1 + \sigma_2)^2 n} \right] \left(\frac{W_1 + W_2}{W_1 W_2} RT \right)^{1/2} \quad (11)$$

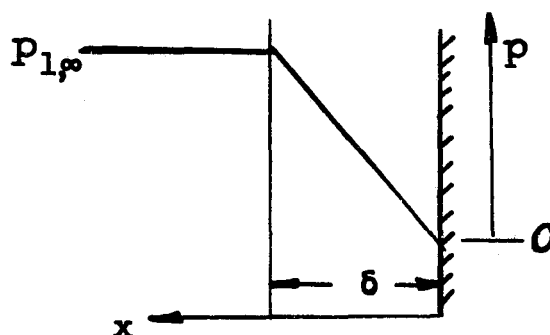
where W and σ represent the molecular weight and diffusion cross section of the respective constituents. From the perfect-gas equation of state,

$$p = n\kappa T \quad (12)$$

From consideration of the above relationships the rate of oxygen mass diffusion may be written as

$$\frac{dw}{d\theta} = \left[\frac{3m_1}{p_2^2 2\sqrt{2}\pi (\sigma_1 + \sigma_2)^2} \right] \left(\frac{W_1 + W_2}{W_1 W_2} RT \right)^{1/2} \frac{dp_1}{dx} \quad (13)$$

where p_1 and p_2 are the partial pressures of the oxygen and the inert gas, respectively, in the environment. For a first approximation, it may be assumed that the variation in the partial pressure of oxygen occurs in a finite region near the surface, varying from $p_{1,\infty}$ in the environment to zero at the surface. For steady diffusion $dw/d\theta$ is constant, and thus the partial pressure varies linearly from the surface as shown by the following sketch:



For this first approximation

$$\frac{dp_1}{dx} = \frac{p_{1,\infty}}{\delta} \quad (14)$$

δ is essentially proportional to the boundary-layer thickness, or inversely proportional to $\sqrt{N_{Re}}$ for a laminar layer. (If natural convection exists, δ will vary as the fourth root of the Grashof number.) The diffusion cross sections σ_1 and σ_2 are essentially constant. Thus, approximately,

$$\frac{dw}{d\theta} = \text{Constant} \frac{p_{1,\infty}}{p_2} \sqrt{T} \sqrt{N_{Re}} \quad (15)$$

This relationship shows the behavior of the rate of oxygen transport to the surface in a mixed-gas environment. It is seen that as the oxygen concentration becomes very small relative to the concentration of the inert gases, the rate of transport becomes very small and could conceivably be the oxidation-rate-controlling process. However, the oxidation reaction could not lead to ignition because of the very mild dependence on temperature. It therefore appears that if ignition does occur, the rate of oxygen transport is not the rate-controlling step.

The possibility that metals can be oxygen starved can be investigated by order-of-magnitude calculations. As an example, the rates of transport in air can be compared with measured oxidation rates for iron. The comparison indicates that transport does not control the reaction rate at low temperatures but may be controlling at high temperatures. For the purposes of these calculations it will be assumed that the thickness of the starved layer is 0.1 centimeter and that the partial pressure of the oxygen in the environment is 0.2 atmosphere. The diffusion coefficient for oxygen in air at 32° F is given in reference 4 as 0.178 cm²/sec. Equation (11) indicates that the diffusion coefficient varies as the 3/2 power of the absolute temperature; thus, at 932° F, $D = 0.278$ cm²/sec, and at 2,192° F, $D = 2.23$ cm²/sec. The partial oxygen densities at these temperatures are 1.10 and 0.528×10^{-4} g/cm³, respectively. Thus, the transport rates are

$$\frac{dw}{d\theta} = D \frac{dp}{dx} \approx 0.278 \frac{1.10 \times 10^{-4}}{0.1} = 3.1 \times 10^{-4} \text{ g/cm}^2\text{-sec}$$

at 932° F and

$$\frac{dw}{d\theta} \approx 2.2 \frac{0.528 \times 10^{-4}}{0.1} = 1.2 \times 10^{-4} \text{ g/cm}^2\text{-sec}$$

at 2,192° F. Using the oxidation-rate constants of table 1 and assuming an oxide film thickness of 0.01 centimeter, the rate of oxidation of iron may be calculated as

$$\frac{dw}{d\theta} = 6.6 \times 10^{-7} \text{ g/cm}^2\text{-sec}$$

at 932° F and as

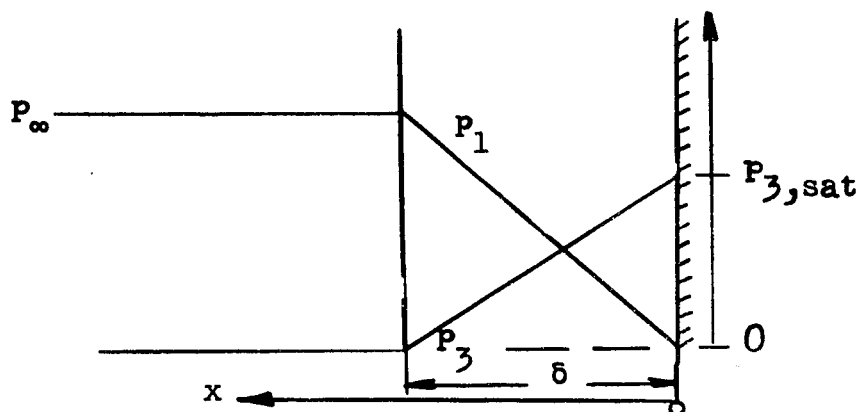
$$\frac{dw}{d\theta} = 1.6 \times 10^{-4} \text{ g/cm}^2\text{-sec}$$

at 2,192° F. It is seen that the transport rate at 932° F is several orders of magnitude larger than the observed oxidation rates, but at 2,192° F the transport rate may indeed be rate controlling. It seems, that transport of this type may be rate controlling at high temperatures, and thus a metal surface might become oxygen starved in air. Flow velocity would then be an extremely important parameter in the oxidation and ignition phenomena.

In the foregoing discussions it was assumed that the vapor pressures of the metals and their oxides are negligible at temperatures below ignition. This is generally true for most metals. However, certain metals and oxides, notably magnesium, molybdenum trioxide, and tungsten dioxide, have extremely high vapor pressures. The dependency of vapor pressure on temperature can usually be represented by empirical equations of the form

$$p_3 = Be^{-C/T} \quad (16)$$

Consider first the case where the vapor pressure of the oxide is high and the environment contains only oxygen. For the purpose of this discussion it will be assumed that, since the oxide vapor is continually being carried away by the boundary layer over the surface, the concentration of the vapor varies from saturation at the surface to zero at some finite distance from the surface. This distance might correspond to the thickness of the boundary layer over the surface. Oxygen must diffuse through the oxide vapor to reach the surface, and thus the oxygen concentration may be assumed to vary from zero at the surface to its free-stream value. Under these relatively simple assumptions the oxide and oxygen concentrations would appear as shown in the following sketch:



Under the assumptions of simple kinetic theory (ref. 3) the rate of mass diffusion may be written as

$$\frac{dw}{d\theta} = \left[\frac{3m_1}{2\sqrt{2\pi}(\sigma_1 + \sigma_3)^2 P_\infty} \right] \left(\frac{w_1 + w_3}{w_1 w_3} RT \right)^{1/2} \frac{dp_1}{dx} \quad (17)$$

Since the rate of diffusion is constant, the partial pressure of the oxygen is a linear function of x . Then assuming that the partial pressure of the vapor is zero at $x = \delta$ and is saturated at $x = 0$,

$$\frac{dp_1}{dx} = \frac{p_{3,sat}}{\delta} \quad (18)$$

δ will be a function of the external flow field, and if a laminar boundary layer exists, δ will vary approximately inversely as the square root of the free-stream Reynolds number; if free convection persists, δ will vary essentially inversely as the fourth root of the Grashof number and thus will be a function of the difference between the temperatures of the surface and the environment. Thus,

$$\frac{dw}{d\theta} = \frac{\text{Constant} \sqrt{N_{Re}} (e^{-C/T}) \sqrt{T}}{P_\infty} \quad (19)$$

This equation shows the general behavior of the oxidation of metals where the rate of oxidation is controlled by the rate of diffusion of oxygen through oxide vapor. It is seen that oxidation of this nature could lead to ignition and that the rate of oxidation could be markedly increased by subjecting the body to a high-velocity oxygen flow. Should the flow velocity become too great, the control of the oxidation reaction might revert to one of the slower steps in the process. On the other hand, if the body were placed in a quiescent environment at approximately

the surface temperature, the rate of oxidation would become extremely small, and the ignition temperature would be raised considerably.

The case of oxidation controlled by the diffusion of oxygen through a metal vapor film cannot be handled simply. In general, metals of technical importance do not have high vapor pressures, and thus their oxidation rates are not controlled by such a process.

The rate of oxygen transport has been compared with observed oxidation rates at various speeds and altitudes. For this comparison the transport rates were calculated from equation (9) using the partial pressure of oxygen behind a normal shock wave and the stagnation temperature; thus the transport rates are higher than if diffusion through inert gases was considered. The results of these calculations are shown in figure 2. The stagnation temperatures are shown also, and typical metal oxidation rates (for titanium) are added for comparison purposes. Note that at low altitudes the transport rates are several orders of magnitude larger than oxidation rates, and thus transport of this type is definitely not rate controlling under such conditions. At higher altitudes, however, the transport rates are of the same order of magnitude as sea-level oxidation rates, and transport may well be the rate-controlling mechanism. But the transport rate decreases with temperature and thus cannot lead to ignition.

Adsorption of Oxygen Molecules

When an oxygen molecule comes close to the oxide surface it must pass over an "energy hill" if it is to be adsorbed by the surface. Only a small fraction of the molecules coming close to the surface have enough energy to pass this barrier, and thus only a small fraction are adsorbed. Adsorption is believed to occur only at activated sites on the surface. If the pressure of the gaseous reactant is not too low the surface will be covered by a monomolecular layer of adsorbed molecules, and the adsorption is said to be kinetically of zero order.

The rate of zero-order adsorption is given in reference 5 as

$$v = C_a \frac{\kappa T_s}{h} e^{-E/RT_s} \quad (20)$$

where v is the number of molecules adsorbed per unit time, C_a is the number of activated adsorption sites, E is the activation energy representative of the minimum energy a molecule must have to pass over the potential energy barrier, T_s is the surface (and gas) temperature, and κ , h , and R are Boltzmann's constant, Planck's constant, and the gas constant, respectively.

The weight rate of adsorption is therefore

$$\frac{dw}{d\theta} = v \frac{W_1}{N_0} = C_a \frac{\kappa T_s W_1}{N_0 R} e^{-E/RT_s} \quad (21)$$

where W_1 is the molecular weight of oxygen, and N_0 is Avogadro's number. Note that the rate of adsorption is independent of pressure and is invariant with time. Note also that equation (21) is of the form (over small temperature ranges)

$$\frac{dw}{d\theta} = A_1 e^{-E_1/RT_s} \quad (22)$$

characteristic of metals oxidizing in a linear manner. By comparing the theoretical frequency factor ($C_a \kappa T_s W_1 / R N_0$) with the experimental constant A_1 , some definite conclusions can be drawn concerning the possibility of adsorption as the rate-controlling mechanism for linear oxidation. For the purpose of this comparison C_a is taken as f times number of oxide molecules per unit area, where f is a roughness factor defined by

$$f = \frac{\text{True surface area}}{\text{Projected area}}$$

In the calculations for this comparison f was taken as 25.

Metal	Oxide	T_s , $^{\circ}F$	$C_a \kappa T_s W_1 / R N_0$, g/cm ² -sec	A_1 , g/cm ² -sec
Mg	MgO	932	26.4×10^6	1.7×10^6
Ti	TiO ₂	1,652	48.5	400
Ca	CaO	932	18.0	.078
U	U ₃ O ₈	572	20.5	7
Ce	CeO ₂	572	15.0	.4

Except for magnesium, the theoretical frequency factors are several orders of magnitudes larger than the observed values of A_1 , and it does not seem possible that adsorption could be the rate-controlling mechanism. However, the agreement for magnesium is close enough to admit the possibility that adsorption is rate determining for magnesium; in fact, an f of 1.6 would give exact agreement. On the basis of the comparison in the preceding table it can be concluded that adsorption

is one step that may control linear oxidation, but certainly not the only one.

It must be remembered that C_a represents the number of adsorption sites available for oxygen molecules. If the environment is a mixture of oxygen and nonreacting gases, it would seem that some sites would be occupied by the inert molecules. It would be expected, for example, that the number of oxygen adsorption sites in air would be approximately 21 percent of the total number of sites. Thus, if adsorption were indeed the rate-controlling step the oxidation rate would vary directly with the percentage of oxygen in the environment. This behavior might be used to help identify the rate-controlling step for linear oxidation.

If the surface is only sparsely covered with adsorbed molecules, the reaction is said to be kinetically of first order. In this case the rate of adsorption is directly proportional to the oxygen concentration in the environment. It is doubtful that metal oxidations are first order because of the high affinity of oxygen for metals. The first-order reaction, which is considerably more involved than the zero-order adsorption, is discussed in reference 5. Expressions similar to equation (20) may be derived but will not be presented here; it is felt that at the extremely low pressures which are required for first-order reactions the reaction will be limited by the rate of oxygen transport, and adsorption will not be rate controlling.

The adsorption rate predicted by equation (20) is based on the assumption that the gas adsorbed at the surface is essentially at the surface temperature. If, however, the mean free path is of the order of magnitude of the boundary-layer thickness, the molecules which approach the surface may have quite different energies. The higher energy molecules are adsorbed more easily than the colder molecules, and thus any temperature distribution in a thin boundary layer of this type may have a profound influence on the adsorption rate. The activation energy E represents the energy a molecule must have in order to be adsorbed; T_s represents the surface and mean molecular temperature. If the mean temperature of gas molecules is some higher temperature T , then the adsorption rate will be greater by

$$F = \frac{\text{Fraction of molecules from a group at mean temperature } T \text{ which have energies exceeding } E}{\text{Fraction of molecules from a group at mean temperature } T_s \text{ which have energies exceeding } E}$$

The fraction of molecules from a group at a given temperature which have energies exceeding a given value is (see ref. 3)

$$f_{\text{Energy} > E} = \frac{2}{\sqrt{\pi}} \sqrt{\frac{E}{RT}} e^{-E/RT} + 1 - \phi(\sqrt{E/RT}) \quad (23)$$

where

$$\phi(x) = \frac{2}{\sqrt{\pi}} \int_0^x e^{-x^2} dx$$

It may be shown that for large values of x ,

$$1 - \phi(x) \approx \frac{1}{\sqrt{\pi}} \frac{e^{-x^2}}{x} \left(1 - \frac{1}{2x^2} + \dots \right)$$

Thus, equation (23) is of the form

$$f_{\text{Energy} > E} = \frac{2}{\sqrt{\pi}} x e^{-x^2} + \frac{1}{\sqrt{\pi}} \frac{e^{-x^2}}{x} \left(1 - \frac{1}{2x^2} + \dots \right)$$

where $x^2 = E/RT$. For metals, $10 < E/RT < 50$, and thus, approximately,

$$f_{\text{Energy} > E} \approx \frac{2}{\sqrt{\pi}} \frac{E}{RT} e^{-E/RT} \quad (24)$$

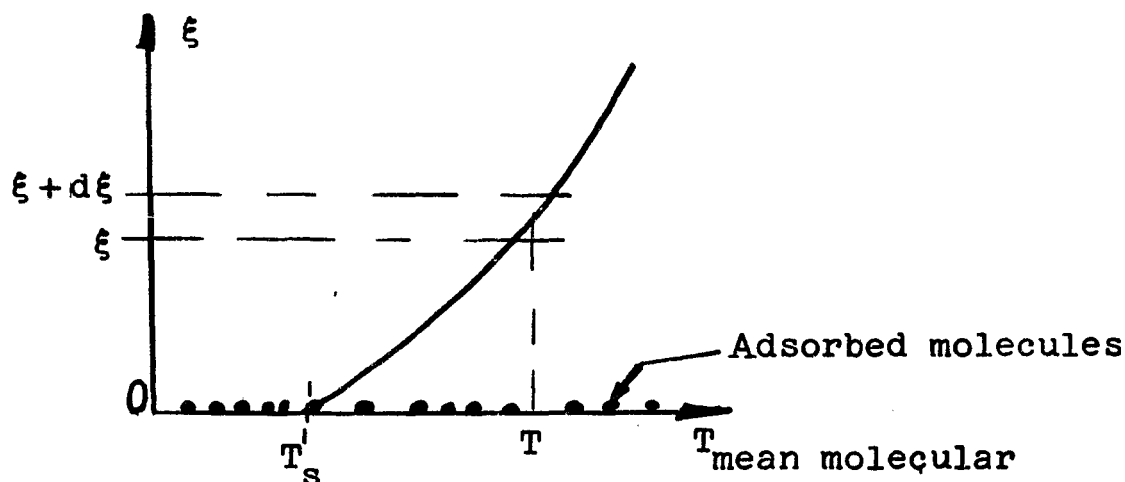
Thus,

$$\mathcal{F} \approx \frac{\frac{2}{\sqrt{\pi}} \sqrt{\frac{E}{RT}} e^{-E/RT}}{\frac{2}{\sqrt{\pi}} \sqrt{\frac{E}{RT_s}} e^{-E/RT_s}} = \frac{1}{\sqrt{(T/T_s)}} e^{\frac{E}{RT_s} \left[1 - \frac{1}{(T/T_s)} \right]} \quad (25)$$

The rate of adsorption of molecules whose mean temperature is T by a surface at temperature T_s may therefore be written as

$$\frac{dw}{d\theta} = \left(\frac{dw}{d\theta} \right)_{\text{iso}} \cdot \mathcal{F} \approx \left(\frac{dw}{d\theta} \right)_{\text{iso}} \sqrt{\frac{T_s}{T}} e^{\frac{E}{RT_s} \left[1 - \frac{1}{(T/T_s)} \right]} \quad (26)$$

This analysis may be extended to the situation where there is a temperature variation near the surface. Suppose, for example, that the surface is cool relative to its environment and that a boundary layer of sorts is formed over the surface. The variation of mean molecular temperature away from the surface might be somewhat as shown in the following sketch:



The mean temperature of the molecules in a region between ξ and $\xi + d\xi$ away from the surface is represented by $T(\xi)$. Because of the distribution of molecular free paths, most of the molecules which are adsorbed at the surface come from regions quite close to the surface. The probability that any given adsorbed molecule came from the region $d\xi$ is (ref. 3)

$$P(\xi) = \frac{1}{\lambda_m} e^{-\xi/\lambda_m} d\xi \quad (27)$$

where λ_m is the mean free path. The rate of adsorption of molecules from the interval $d\xi$ is therefore

$$\begin{aligned} \left(\frac{dw}{d\theta}\right)_{d\xi} &= \left(\frac{dw}{d\theta}\right)_{iso} \sqrt{\frac{T_s}{T}} e^{\frac{E}{RT_s} \left[1 - \frac{T_s}{T(\xi)}\right]} \frac{1}{\lambda_m} e^{-\xi/\lambda_m} d\xi \\ &= \left(\frac{dw}{d\theta}\right)_{iso} d\mathcal{M} \end{aligned} \quad (28)$$

If it is assumed that the temperature distribution does not appreciably influence λ_m , the total rate of adsorption of molecules from all distances is

$$\frac{dw}{d\theta} = \left(\frac{dw}{d\theta}\right)_{iso} \mathcal{M} \quad (29)$$

where

$$m = \int_0^{\infty} \sqrt{\frac{T_s}{T(\xi)}} e^{\frac{E}{RT_s} \left[1 - \frac{T_s}{T(\xi)} \right]} e^{-\xi/\lambda_{md}(\xi/\lambda_m)} d\xi \quad (30)$$

The factor m represents the increase in adsorption rate due to the temperature variation away from the surface.

To illustrate the influence of ambient temperature on adsorption rates, equation (30) has been integrated for a linear temperature variation. The results are shown in figure 3. The $a = 0$ situation corresponds to a free molecule flow, and the $a = \infty$ situation represents a thick boundary layer or continuum flow. Note that the ambient temperature can have an appreciable influence in noncontinuum flows, with high temperatures increasing adsorption rates by several orders of magnitude.

Another manner in which high ambient temperatures can influence the rate of adsorption is through dissociation. If the gas surrounding the surface consists of atoms rather than molecules, the mean free path is longer and more higher energy atoms (which originate far from the surface) reach the surface. This effect is compounded by the relative ease with which atoms (compared with molecules) are adsorbed. The result may be a rather substantial increase in the adsorption rate.

Ionization of Oxygen Molecules and Metal Atoms

Very little can be said about the rates of ionization. It is generally believed that ionization rates are much faster than rates of diffusion even through extremely thin films. It would seem that the rates of ionization would not depend upon the thickness of the oxide film and thus would be invariant with time. This means that ionization could not be the rate-controlling step in oxidation that occurs in a time-dependent manner (parabolic oxidation), which indicates that ionization rates are faster than diffusion rates with the possible exception of extremely thin films. Some experiments with ionized gas have been made, and no increase in the reaction rate was observed. Although it cannot be definitely said that ionization rates do not control the linear-type oxidations, it is believed that this is true.

Diffusion of Ions and Electrons

The rate of ion diffusion in oxides has been related to the electrical conductivity by Wagner in reference 6. Electrical charge can be transferred by transfer of ions or electrons which move through the oxide lattice. Most of the metal oxides and nitrides exhibit electronic, as well as ionic, conductivity and are generally classed as semiconductors.

The transference numbers of the cations, anions, and electrons are defined by

$$\tau_A = \frac{l_A}{l_A + l_C + l_e}$$

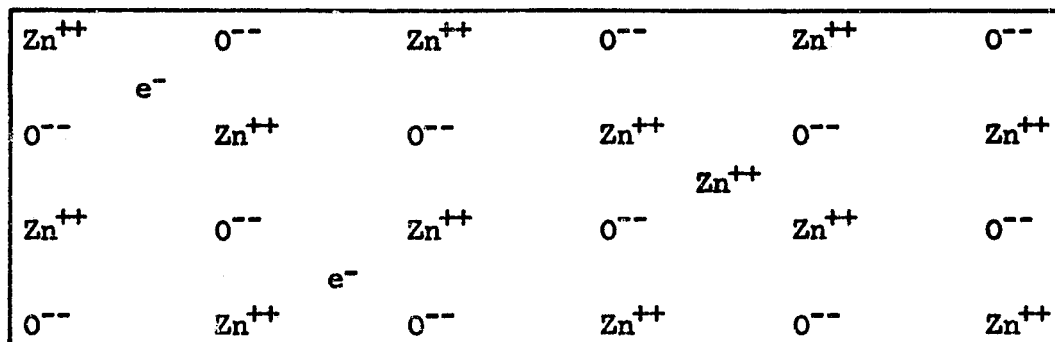
$$\tau_C = \frac{l_C}{l_A + l_C + l_e}$$

$$\tau_e = \frac{l_e}{l_A + l_C + l_e}$$

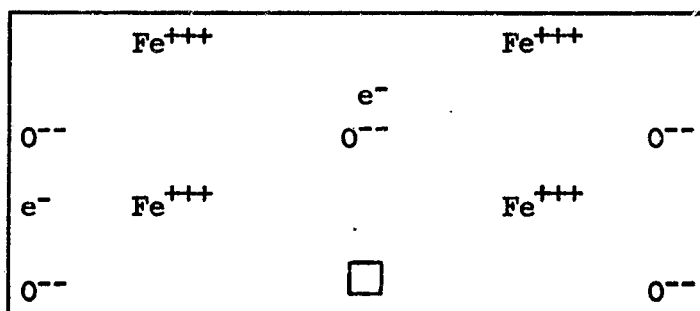
where l_C , l_A , and l_e represent portions of the conductivity, or the respective mobilities, of the cation, anion, and electron.

Thus τ_A , τ_C , and τ_e represent the fractions of the electrical conduction due to transfer of cations, anions, and electrons.

If an excess of metal ions (cations) exists, two conduction mechanisms are possible, and they are referred to as "metal excess semiconduction" and "anion deficit semiconduction." In metal excess semiconductors, metal ions and electrons appear interstitially in the lattice, and conduction occurs by migration of cations and electrons. Thus the transference number τ_A is negligible; τ_C is also small, but is of importance. In the anion deficit semiconductor, anions are missing from their respective lattice sites, and electrons are distributed interstitially. Conduction occurs by migration of anions between the defects and electrons in the lattice. Thus τ_C is negligible, and τ_A is small but important. Experimentally it is found that the conductivity of both of these two types of metal excess semiconductors decreases with increased pressure of the negative component (i.e., oxygen). For the first type this is believed to be caused by increased migration of the interstitial cations to new lattice sites at the edge of the crystal, which causes an impoverishment of the interstitial electrons. For the anion deficit semiconductor, an increase in pressure of the negative component causes some of the defects to be filled, reducing the conductivity. Models of these two types of semiconductors are shown as follows:

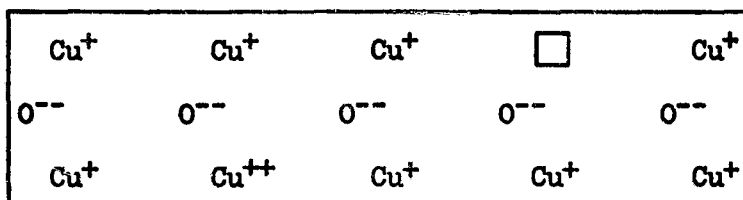


Metal Excess Semiconductor

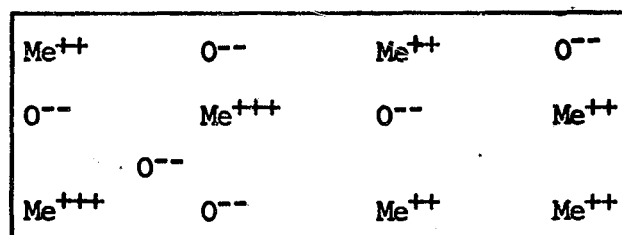


Anion Deficit Semiconductor

If an excess of anions (oxygen ions) exists, two conduction mechanisms are possible, and they are referred to as metal deficit semiconduction and anion excess semiconduction. In metal deficit semiconductors, the cation lattice contains some vacant sites, and electric neutrality is established by the formation of cations of higher valence (termed electron defect). Conduction occurs by electron exchange between cations of different valence and cation migration in the vacant lattice sites. Thus, τ_A is negligible, and τ_C is small but important. In anion excess semiconductors, anions are distributed interstitially, and electric neutrality is maintained by electron defect. Conduction occurs by interchange of electrons between the cations of different valence and anion migration in the interstitial spaces. Thus τ_C is negligible, and τ_A is small but important. It is experimentally found that the conductivity of both of these two types of anion excess semiconductors increases with increased pressure of the negative element (oxygen). For the first type this is said to be due to cation migration to the surface of the crystal leaving more vacant lattice sites and causing more electron defects. For the second type this could be attributed to an increase in the number of interstitial anions, which in turn causes more electron defects. Models for these two types of semiconductors are shown as follows:



Metal Deficit Semiconductor



Anion Excess Semiconductor

Wagner, reference 6, has derived an expression for the rate of oxidation in terms of the specific electrical conductivity of the film, the transference numbers of the anions, cations, and electrons, and the free energy decrease of the oxidation reaction. All these quantities can be measured independently, and thus his analysis can be and has been verified experimentally. It is assumed in the analysis that the transport of both ions and electrons through an oxidation layer is fundamentally the same as current flow in a cell. The film provides both the electrolyte by virtue of ionic transport and the external circuit because of electronic conduction. The electromotive force of the cell is assumed to be the decrease in free energy of the reaction. Wagner's analysis leads to

$$\frac{dw}{d\theta} = \frac{z}{\gamma} \frac{(\tau_A + \tau_C)\tau_e}{F\delta} \frac{nRT}{2F^*} (p_1^{1/n} - p_m^{1/n}) B e^{-E/RT} \quad (31)$$

Note that this equation has the form, over limited temperature ranges,

$$\frac{dw}{d\theta} = \frac{\text{Constant}}{w} e^{-\text{Constant}/RT} \quad (32)$$

which in turn leads to an equation of the form

$$w^2 = \text{Constant} e^{-\text{Constant}/RT} = K_p \theta \quad (33)$$

which is found experimentally to be characteristic of the oxidation of many metals.

It is seen from this analysis that the dependence of the oxidation rate on pressure may be either positive or negative, depending on the semiconduction characteristics of the oxide film. For most metals, this dependence is extremely slight, at least where diffusion is known to be rate controlling. The oxidation rate of copper, for example, varies about as the $1/7$ power of the oxygen pressure; the oxidation of zinc varies about as the $-1/6$ power of pressure.

When an oxygen molecule strikes the surface, it assumes an energy level essentially equivalent to the surface temperature. Ionization and diffusion will then occur at exactly the same rate as if the mean molecular temperature in the gaseous environment were equal to the surface temperature. If dissociation occurs, atoms striking the surface will also assume the surface temperature, and since, in general, atoms are ionized easier than molecules, it might be suspected that the rates of ionization will be faster with dissociation. This is of no consequence since ionization is not important as a rate-controlling step. Thus it appears that the ambient temperature does not influence oxidation where diffusion is the rate-controlling step.

For most metals of technical importance the rate of ion diffusion varies only slightly with pressure. Figure 4 shows the order of magnitude of the influence of flight conditions on diffusion rates for metals where the diffusion rate varies as the $1/7$ power of (stagnation) pressure. Note that the influence of pressure is relatively small, especially at Mach numbers which would be practical at any altitude. The influence of pressure on the ignition temperature will be slight, with low pressures giving higher ignition temperatures for metals whose oxides are metal deficit semiconductors and lower ignition temperatures for metal excess semiconductors. The mechanism of ion diffusion in the oxide is therefore of importance in determining how ignition temperatures (diffusion controlled) vary with flight conditions.

If the flow over the surface causes the oxide to be blown away, the oxidation will proceed at essentially a constant rate (at any temperature). The partial removal of oxide may increase the rate of diffusion to the point where some other mechanism becomes rate controlling, and thus oxidation data obtained in still air would not apply. This is one of the more important considerations regarding ignition in flight and needs to be studied more carefully.

EXPERIMENTAL RESULTS

The objectives of the experimental part of this investigation were to obtain ignition temperatures for a number of technically important metals and alloys and to support the postulated ignition theory.

Ignition temperatures for a number of metals are presented in table 3. In general, it was observed that the ignition temperatures were relatively independent of the oxygen concentration in the environment; this observation is in agreement with the theories for oxidation controlled by adsorption or diffusion. The ignition temperatures were not appreciably influenced by high-velocity airflow over the oxidizing surface; this indicates either that the airflow was not able to blow away the oxide scale to any appreciable extent or that the removal had little effect on the ignition temperature. The high-velocity airflow should tend to give higher convection coefficients, which should, in turn, lead to higher ignition temperatures according to the theory. However, the increase in the ignition temperatures predicted by the theory is only of the order of 20° to 50° F, and thus it is difficult to determine if there were such an increase. The high-velocity tests therefore neither confirm nor contradict the effect of convection predicted by the theory. The shape of the body seemed to be unimportant, at least in the range of conditions obtainable. Thus, the use of an isothermal body as a basis for analysis may not be too bad, except under more extreme circumstances.

In general, the experimental observations and the theory of ignition are in reasonable agreement, and the behavior of actual ignition temperatures with environmental conditions is predicted quite adequately by the theory.

Apparatus and Procedures

The experimental part of this investigation consisted of three phases. In the first phase several metals were heated electrically in a specially constructed container in which controlled environments could be maintained. The temperature of the samples was raised until ignition or melting occurred, and the failure temperature was measured with an optical pyrometer. In the second phase metals were heated electrically in a jet of air at a Mach number of 1.25, and failure temperatures were observed optically. In the third phase calcium models of various shapes were placed in a hot airstream, and ignition temperatures were measured with thermocouple circuits.

The pressure tank and control console used in the first phase are shown in figures 5 and 6. The models were strips or wires of various dimensions and were abraded prior to testing to remove all oxide scale. Air or oxygen pressures of up to 8 atmospheres could be maintained in the tank. A quartz window and mirror train allowed observation with the optical pyrometer. The temperature at which the model temperature started to increase rapidly was recorded as the ignition temperature; in some cases the models simply melted, and the observed melting point was recorded. The observed temperatures were corrected for adsorption

by the window and mirror train but were not corrected for the fact that the target was not a true black body. The temperatures reported are therefore "brightness" temperatures and are lower than the true temperatures. In each case the uncertainty in temperature was estimated and recorded.

The free-jet wind-tunnel installation used in the second phase is shown in figure 7. The discharge area is 0.760 square inch, and stagnation temperatures up to 180° F may be obtained. A typical model is shown suspended between the electrodes. The technique for measuring the ignition temperatures was the same as that used in the pressure tank, except that no correction for a mirror train was required.

The high-temperature-air supply used in the third phase is shown in figure 8. Air was heated electrically by a series of Nichrome screens, and temperatures up to 1,850° F at 100 ft/sec could be obtained. The discharge area was 1 square inch. The models were calcium cones of various shapes with iron-constantan thermocouples mounted in the tips. Immediately prior to testing, the models were abraded to remove the oxide scale, and the points were sharpened. The air temperature was then increased slowly, and the model temperature recorded on a fast response millivoltmeter. When ignition occurred the model temperature rose rapidly, and the ignition temperature was well defined by a sharp break in the temperature-time curve.

Test Results

The experiments in the pressure tank were performed to determine the effect of the environmental pressure on the ignition temperature. In no case was any appreciable effect observed, and this is in agreement with the mechanisms and thermal definition of ignition. The observed melting points are in agreement with the well-known values. There is some scatter in the data, and this may be due to time dependencies of the oxidation rate, although effort was made to have the warmup time of all models the same. Models of various thicknesses were tested, and no effect of thickness was observed. Since the rate of burning after ignition was considerably greater with oxygen than with air, the ignition temperature was better defined with oxygen, and thus the data obtained using oxygen are probably more accurate. No appreciable difference between the ignition temperatures in air and oxygen was observed, which indicates that diffusion in the oxide controlled the reaction.

The experiments in the supersonic jet were performed to study the effect of flow velocity. It was expected that the thickness of the oxide film might be reduced by the flow, thus lowering the ignition temperature. No appreciable effect of the jet was observed.

Unfortunately, the convection conductances were not high enough so that the effect of convection heat transfer predicted by the analysis could be checked.

The experiments in the hot airstream were performed to study the effect of shape. Calcium was chosen as the test metal because it has an ignition temperature in the range of the temperatures producible in the jet, because it is known to oxidize in a time-independent manner, and because it has reasonably good strength characteristics in the range of ignition. Magnesium was tried at first, but the models sagged before ignition and thus were useless for a study of the shape effect. Cones having included angles of from 20° to 180° and base diameters of $3/8$ inch were tested at approximately 85 ft/sec, and no appreciable effect of shape was observed. Ignition was seen to occur first at the very tip of the models and then to propagate to the afterbody. In a few seconds the entire model was consumed. The possibility of a shape effect cannot be ruled out entirely, because it is probable that the shape effect will be more pronounced at more rapid heating rates.

Table 3 presents a summary of ignition temperatures of solid metals obtained under static conditions. The data of a number of other investigators are included. The results of the pressure tank and supersonic wind-tunnel tests of this investigation are presented in tables 4 to 23 and in figures 9 to 17. The results of the shape-effect experiments are presented in table 24.

Comparison of Predicted and Experimental

Ignition Temperatures

The experimental ignition temperatures for a number of metals are compared with the ignition temperatures predicted by the thermal definition of ignition in figure 18. In this comparison the oxidation data of table 1 and the heats of formation of table 25 were used. In addition, the comparison is made for several magnesium alloys. The oxidation data for these comparisons for magnesium were taken from reference 7 and the ignition-temperature data were taken from reference 8, and both are summarized in table 26.

In figure 18 the experimental data are compared with the curve for $h^* = 0$; this is reasonable for a qualitative comparison, since the ignition temperatures were all measured in quiescent environments. It must be remembered that the uncertainty in the oxidation rate constants is extremely high and thus the comparison cannot be too quantitative. It is felt that the agreement of the data with the theoretical ignition temperatures is satisfactory, and thus the postulate of a direct relation between oxidation and ignition, and all consequences thereof, is correct.

CONCLUDING REMARKS

A simplified definition of ignition has been developed from an energy balance on an isothermal body. The conclusions regarding the effects of environmental factors on the ignition temperature are thus restricted to situations where internal temperature gradients are relatively small, but more drastic shapes may well produce substantial departures from the predicted behavior. The simple analysis, and consideration of the oxidation mechanisms, indicate that the ignition temperature is essentially independent of ambient temperature and pressure, except insofar as these items influence convective heat transfer. The dependence of the ignition temperature on convection and radiation heat-transfer rate predicted by the analysis is extremely interesting. It is found that the ignition temperature depends only on the magnitude of these transfers and not upon their direction, with higher heating or cooling rates giving higher ignition temperatures. No data are available either to substantiate or to repudiate this result. Under certain circumstances the ignition temperature depends on the thickness of the oxide scale covering the surface, and thus any factors which might tend to reduce the scale thickness are important. The available data are in reasonably good agreement with the postulated mechanisms and the thermal definition of ignition.

Stanford University,
Stanford, Calif., June 15, 1957.

REFERENCES

1. Hill, Paul R., Adamson, David, Foland, Douglas H., and Bressette, Walter E.: High-Temperature Oxidation and Ignition of Metals. NACA RM L55L23b, 1956.
2. Kubaschewski, O., and Hopkins, B. E.: Oxidation of Metals and Alloys. Butterworths Sci. Pub. (London), 1953.
3. Kennard, Earle H.: Kinetic Theory of Gases. McGraw-Hill Book Co, Inc., 1938.
4. Hodgman, Charles D., ed.: Handbook of Chemistry and Physics. Thirty-six ed., Chemical Rubber Pub. Co., 1954-1955.
5. Glasstone, Samuel, Laidler, Keith J., and Eyring, Henry: The Theory of Rate Processes. First ed., McGraw-Hill Book Co., Inc., 1941.
6. Wagner, C.: Beitrag zur Theorie des Anlaufvorgangs. Zeitschr. f. phys. Chem., Abt. B, Bd. 21, July 1933, pp. 25-41.
7. Leontis, T. E., and Rhines, F. N.: Rates of High-Temperature Oxidation of Magnesium and Magnesium Alloys. Tech. Pub. No. 2003, Am. Inst. Mining and Metallurgical Eng., Feb. 1946.
8. Fassell, W. Martin, Jr., Gulbransen, Leonard B., Lewis, John R., and Hamilton, J. Hugh: Ignition Temperatures of Magnesium and Magnesium Alloys. Jour. Metals, vol. 3, no. 7, July 1951, pp. 522-528.
9. Conway, J. B., and Kirshenbaum, M. S.: Ninth Progress Report. Contract N9-ONR-87301, Res. Inst. of Temple Univ., Jan. 1, 1954.
10. Loriaers, Jean: Sur l'oxydation de l'uranium métallique. Comptes Rendus, t. 234, no. 1, Jan. 2, 1952, pp. 91-93.
11. Loriaers, Jean: Sur l'oxydation du cérium et du lanthane. Comptes Rendus, t. 229, no. 11, Sept. 12, 1949, pp. 547-549.

C-477

TABLE 1

OXIDATION DATA FOR METALS

Metal	Primary oxide	Gas	Pressure, mm. Hg	Temperature range, °F	A_p , g^2/cm^4 -sec	A_l , g/cm^2 -sec	E_p or E_l , cal/mole
Be	BeO	O ₂	100	840 to 970	0.22	-----	62,000
	BeO	O ₂	76	350 to 700	1.8×10^{-12}	-----	8,500
	BeO	O ₂	76	750 to 950	3.5×10^{-3}	-----	50,300
Mg	MgO	O ₂	760	475 to 575	-----	1.7×10^6	50,500
Ca	CaO	O ₂	760	600	-----	.2	19,600
Th	ThO ₂	O ₂	450	250 to 350	.073	-----	31,000
	ThO ₂	O ₂	210	350 to 450	-----	.078	22,000
	ThO ₂	O ₂	210	450	-----	10.9	25,600
Ti	Rutile	O ₂	76	400 to 600	2.0×10^{-5}	-----	29,300
	Rutile	O ₂	760	650 to 830	-----	400	40,000
	Rutile	O ₂	760	830 to 950	-----	5	47,000
Zr	ZrO ₂	O ₂	76	200 to 425	2.9×10^{-7}	-----	18,200
	ZrO ₂	O ₂	74	600 to 920	2.4×10^{-3}	-----	32,000
V	V ₂ O ₅	O ₂	76	400 to 600	1.3×10^{-3}	-----	30,700
Nb	NbO	O ₂	76	200 to 375	2.6×10^{-5}	-----	27,400
Ta	Ta ₂ O ₅	O ₂	76	250 to 450	3.5×10^{-4}	-----	27,400
		O ₂	760	1,250	65	-----	43,700
Cr	Cr ₂ O ₃	O ₂	76	700 to 900	31.5	-----	66,300
Mo	MoO ₃	O ₂	76	350 to 450	3.55×10^{-2}	-----	36,500
W	WO ₃	O ₂	76	400 to 840	5.1×10^3	-----	54,000
Mn	Mn ₃ O ₄	Air		400 to 1,000	1.95×10^{-3}	-----	28,300
Fe	FeO	Air		500 to 1,100	.37	-----	33,000
Co	CoO	O ₂	76	200 to 400	2.0×10^{-5}	-----	23,400
		O ₂	76	300 to 600	3.0×10^{-6}	-----	22,200
		Air		400 to 625	3.0×10^{-6}	-----	22,200
Ni	NiO	Air		625 to 1,100	.56	-----	44,100
		Air		750 to 1,240	3.2×10^{-2}	-----	45,000
Cu	Cu ₂ O	Air		300 to 550	1.5×10^{-5}	-----	20,140
	CuO	Air		550 to 900	.266	-----	37,700
Al	Al ₂ O ₃	O ₂	76	350 to 475	$2 - 7.5 \times 10^{-8}$	-----	22,800
Pb	PbO	Air		100 to 300	.009	-----	24,200
Ce	Ce ₂ O ₃ , CeO ₂	Air	760	300	-----	.4	7,000
U	U ₃ O ₈			300	-----	7	18,400

TABLE 2

SUMMARY OF POSSIBLE OXIDATION-RATE-CONTROLLING MECHANISMS
SHOWING THE INFLUENCE OF ENVIRONMENTAL FACTORS

Mechanism	Simplified rate formula	Remarks
Transport mechanisms:		
Molecular collision in pure oxygen	$\frac{dw}{d\theta} = \text{Constant } p/\sqrt{T}$	Will not lead to ignition
Oxygen diffusion through nonreacting gas	^a $\frac{dw}{d\theta} = \text{Constant } \frac{p_{\infty}}{p_1} \sqrt{T} \sqrt{N_{Re}}$	Will not lead to ignition; may depend somewhat on T_{∞}
Oxygen diffusion through oxide vapor	^a $\frac{dw}{d\theta} = \text{Constant } \frac{\sqrt{T}}{p_{\infty}} \sqrt{N_{Re}} e^{-C/T}$	May depend somewhat on T_{∞} ; known to be rate controlling for molybdenum
Reaction in metal vapor film		Extremely rapid reaction, but not common in technically important metals below the ignition temperature
Adsorption of oxygen at gas-oxide interface	$\frac{dw}{d\theta} = \text{Constant } \frac{p_{O_2}}{p_{\infty}} T e^{-E/RT}$	Believed to be rate controlling for magnesium; independent of flow velocity
Ionization of oxygen and metal		Not believed to be rate controlling for metals
Diffusion mechanisms:		
Cation excess semiconductors	$\frac{dw}{d\theta} = \frac{\text{Constant}}{\delta} (p_{O_2})^{-1/n} e^{-E/RT}$	Usually only slightly decreasing with oxygen pressure; independent of flow velocity (example: ZnO)
Anion excess semiconductors	$\frac{dw}{d\theta} = \frac{\text{Constant}}{\delta} (p_{O_2})^{1/n} e^{-E/RT}$	Usually only slightly increasing with oxygen pressure; independent of flow velocity (example: Cu ₂ O)

^aBelow some limit the oxidation rate will be independent of Reynolds number;
 $\sqrt{N_{Re}}$ holds for the laminar boundary layer.

TABLE 3

IGNITION TEMPERATURES OF SOLID METALS

Metal	Ignition temperature, °F	Source	Gas	Pressure, atm
Mild steel	2,240 to ^a 2,330	(b)	Air, (c)	1 to 7
W	2,270 to ^a 2,350	(b)	Air, (c)	1 to 7
Ta	2,260 to ^a 2,340	(b)	Air, (c)	1 to 7
Ti alloys:				
RC-70	2,880 to ^a 2,960	(b)	Air, O ₂	1 to 7
RS-70	2,890 to ^a 2,940	(b)	Air, O ₂	1 to 7
RS-110-A	2,860 to ^a 2,910	(b)	(d), O ₂	1 to 7
RS-110-BX	2,850 to ^a 2,920	(b)	(d), O ₂	1 to 7
Stainless steels:				
430	2,460 to ^a 2,490	(b)	(d), O ₂	1 to 7
302	(e)	(b)	Air, O ₂	1 to 7
Cu	(e)	(b)	Air, O ₂	1 to 7
Ni	(e)	(b)	Air, O ₂	1 to 7
Ni alloys:				
Inconel	(e)	(b)	Air, O ₂	1 to 7
Inconel X	(e)	(b)	Air, O ₂	1 to 7
Be alloys:				
Berylco 10	1,750 to 1,760	(b)	Air, O ₂	1 to 7
Berylco 25	(e)	(b)	Air, O ₂	1 to 7
Mg	1,171	ref. 6	O ₂	1 to 10
Mg alloys:				
20% Al	936	ref. 7	O ₂	1
70% Zn	1,004	ref. 7	O ₂	1
25% Ni	934	ref. 7	O ₂	1
20% Sb	1,099	ref. 7	O ₂	1
63% Al	862	ref. 7	O ₂	1
Fe	1,706	ref. 9	O ₂	1
Sr	1,328	ref. 9	O ₂	1
Ca	1,022	ref. 9	O ₂	1
Th	932	ref. 9	O ₂	1
Ba	347	ref. 9	O ₂	1
Mo	1,400	ref. 9	O ₂	1
U	608	ref. 10	O ₂	1
Ce	608	ref. 11	O ₂	1
Al	(e)	ref. 9	O ₂	1
Zn	(e)	ref. 9	O ₂	1
Pb	(e)	ref. 9	O ₂	1
Sn	(e)	ref. 9	O ₂	1
Bi	(e)	ref. 9	O ₂	1
Li	(e)	ref. 9	O ₂	1
Cd	(e)	ref. 9	O ₂	1
Na	(e)	ref. 9	O ₂	1
K	(e)	ref. 9	O ₂	1

^aBrightness temperature.^bPresent investigation.^cNot tested in oxygen, but probably ignites in oxygen at about the same temperature.^dDoes not ignite in air.^eMelts before igniting.

TABLE 4

TANK TESTS WITH MILD STEEL

Run	Model specifications		Gas	Pressure, atm	Ambient temperature, °F	Humidity, $\frac{\text{lb H}_2\text{O}}{\text{lb air}}$	Power at failure, w	Brightness ignition temperature, °F
	Length, in.	Diameter, in.						
1	2	0.080	Air	1	74	0.006	^a 160	2,330 ± 20
2	2	.080	Air	1	74	.006	----	2,320 ± 20
3	2	.080	Air	1	74	.006	----	2,240 ± 20
4	2	.080	Air	1	74	.006	----	2,280 ± 20
5	2	.080	Air	1	75	.006	----	2,260 ± 20
6	2	.080	Air	2	75	.006	----	2,340 ± 20
7	2	.080	Air	2	75	.006	----	2,280 ± 20
8	2	.080	Air	2	72	.006	----	2,330 ± 20
9	2	.080	Air	2	76	.006	----	2,380 ± 20
10	2	.080	Air	2	76	.006	----	2,330 ± 20
11	2	.080	Air	3	77	.006	----	2,310 ± 20
12	2	.080	Air	3	77	.006	----	2,280 ± 20
13	2	.080	Air	3	77	.006	----	2,290 ± 20
14	2	.080	Air	3	77	.006	----	2,300 ± 20
15	2	.080	Air	5	78	.006	----	2,330 ± 20
16	2	.080	Air	5	78	.006	----	2,280 ± 20
17	2	.080	Air	5	79	.006	----	2,320 ± 20
18	2	.080	Air	8	79	.006	----	2,300 ± 20
19	2	.080	Air	8	78	.006	----	2,320 ± 20
20	2	.080	Air	8	78	.006	----	2,310 ± 20

^aNominal.

TABLE 5

TANK TESTS WITH TUNGSTEN

Run	Model specifications		Gas	Pressure, atm	Ambient temperature, °F	Humidity, $\frac{\text{lb H}_2\text{O}}{\text{lb air}}$	Power at failure, w	Brightness ignition temperature, °F
	Length, in.	Diameter, in.						
1	2	0.036	Air	1	74	0.006	^a 60	2,340 ± 20
2	2	.036	Air	1	74	.006	---	2,350 ± 20
3	2	.036	Air	2	74	.006	---	2,300 ± 20
4	2	.036	Air	2	74	.006	---	2,280 ± 20
5	2	.036	Air	3	74	.006	---	2,280 ± 20
6	2	.036	Air	3	74	.006	---	2,270 ± 20
7	2	.036	Air	4	74	.006	---	2,370 ± 20
8	2	.036	Air	5	74	.006	---	2,340 ± 20
9	2	.036	Air	5	74	.006	---	2,370 ± 20
10	2	.036	Air	6	74	.006	---	2,280 ± 20
11	2	.036	Air	6	74	.006	---	2,340 ± 20
12	2	.036	Air	7	74	.006	---	2,340 ± 20
13	2	.036	Air	7	74	.006	---	2,300 ± 20

^aNominal.

TABLE 6

TANK TESTS WITH TANTALUM

Run	Model specifications			Gas	Pressure, atm	Ambient temperature, °F	Humidity, $\frac{\text{lb H}_2\text{O}}{\text{lb air}}$	Power at failure, w	Brightness ignition temperature, °F
	Length, in.	Width, in.	Thickness, in.						
1	1	1/4	0.02	Air	1	74	0.006	^a 100	2,300 ± 20
2	1	1/4	.02	Air	1	74	.006	----	2,260 ± 20
3	1	1/4	.02	Air	2	74	.006	----	2,330 ± 20
4	1	1/4	.02	Air	2	74	.006	----	2,310 ± 20
5	1	1/4	.02	Air	3	74	.006	----	2,320 ± 20
6	1	1/4	.02	Air	3	74	.006	----	2,260 ± 20
7	1	1/4	.02	Air	4	74	.006	----	2,340 ± 20
8	1	1/4	.02	Air	4	74	.006	----	2,340 ± 20
9	1	1/4	.02	Air	4	74	.006	----	2,300 ± 20
10	1	1/4	.02	Air	4	74	.006	----	2,310 ± 20
11	1	1/4	.02	Air	5	74	.006	----	2,280 ± 20
12	1	1/4	.02	Air	5	74	.006	----	2,300 ± 20
13	1	1/4	.02	Air	6	74	.006	----	2,320 ± 20
14	1	1/4	.02	Air	6	74	.006	----	2,280 ± 20
15	1	1/4	.02	Air	7	74	.006	----	2,290 ± 20
16	1	1/4	.02	Air	7	74	.006	----	2,290 ± 20
17	1	1/4	.02	Air	8	74	.006	----	2,320 ± 20
18	1	1/4	.02	Air	8	74	.006	----	2,330 ± 20

^aNominal.

TABLE 7

04

TANK TESTS WITH TITANIUM RC-70

Run	Model specifications			Gas	Pressure, atm	Ambient temperature, °F	Humidity, $\frac{\text{lb H}_2\text{O}}{\text{lb air}}$	Power at failure, w	Brightness ignition temperature, °F
	Length, in.	Width, in.	Thickness, in.						
1	1.5	1/8	0.020	O ₂	1	70	-----	101	2,930 ± 30
2	1.5	1/8	.020	O ₂	1	70	-----	114	2,880 ± 30
3	1.5	1/4	.067	O ₂	2	70	-----	1,150	2,940 ± 30
4	1.5	1/8	.067	O ₂	3	70	-----	460	2,910 ± 20
5	1.5	1/8	.040	O ₂	4	70	-----	295	2,890 ± 20
6	1.5	1/8	.040	O ₂	4	70	-----	300	2,930 ± 20
7	1.5	1/4	.067	O ₂	5	70	-----	1,220	2,930 ± 20
8	1.5	1/8	.010	O ₂	6	70	-----	-----	2,895 ± 20
9	1.25	1/4	.067	O ₂	7	70	-----	840	2,900 ± 30
10	1.5	1/4	.067	O ₂	7	70	-----	940	2,880 ± 30
11	1.5	1/4	.010	Air	1	63	0.0080	-----	2,910 ± 20
12	1.5	1/4	.010	Air	2	63	.0080	-----	2,900 ± 30
13	1.5	1/4	.010	Air	3	63	.0080	-----	2,910 ± 20
14	1.5	1/4	.010	Air	4	63	.0080	-----	2,890 ± 30
15	1.5	1/4	.010	Air	5	63	.0080	-----	2,920 ± 20
16	1.5	1/4	.010	Air	6	63	.0080	-----	2,940 ± 20
17	1.5	1/4	.010	Air	7	63	.0080	-----	2,920 ± 20
18	1.5	1/4	.067	He	1	63	-----	-----	^a 3,010 ± 20

^aMelted.

TABLE 8

WIND-TUNNEL TEST OF TITANIUM RC-70

Run	Model specifications			Mach number	Humidity of jet, lb H ₂ O lb dry air	Stagnation temperature, °F	Power at failure, w	Brightness ignition temperature, °F
	Length, in.	Width, in.	Thickness, in.					
1	1.88	0.138	0.067	1.25	0.00184	163	1,670	2,950 ± 10
2	1.88	.202	.067	1.25	.00184	197	1,800	2,880 ± 20
3	1.88	.237	.067	1.25	.00184	163	2,210	2,950 ± 20
4	1.88	.237	.067	1.25	.00184	140	1,900	2,960 ± 20

TABLE 9

TANK TESTS WITH TITANIUM RS-70

Run	Model specifications			Gas	Pressure, atm	Ambient temperature, °F	Humidity, lb h ₂ O lb dry air	Power at failure, w	Brightness ignition temperature, °F
	Length, in.	Width, in.	Thickness, in.						
1	1.5	3/16	0.025	O ₂	1	71	-----	311	2,920 ± 20
2	1.5	3/16	.025	O ₂	3	71	-----	281	2,940 ± 10
3	1.5	3/16	.025	O ₂	4	71	-----	307	2,920 ± 20
4	1.5	3/16	.025	O ₂	5	71	-----	285	2,940 ± 10
5	1.5	3/16	.025	O ₂	6	71	-----	307	2,930 ± 20
6	1.5	3/16	.025	O ₂	7	71	-----	281	2,890 ± 20
7	1.5	3/16	.025	Air	1	73	0.0062	298	2,930 ± 30
8	1.5	3/16	.025	Air	1	73	.0062	304	2,970 ± 30
9	1.5	3/16	.025	Air	1	73	.0062	298	3,000 ± 30
10	1.5	3/16	.025	Air	3	73	.0062	298	3,010 ± 30
11	1.5	3/16	.025	Air	5	73	.0062	298	2,930 ± 30
12	1.5	3/16	.025	Air	7	73	.0062	310	2,960 ± 30

TABLE 10

WIND-TUNNEL TESTS OF TITANIUM RS-70

Run	Model specifications			Mach number	Humidity of jet, lb H_2O <u>lb dry air</u>	Stagnation temperature, $^{\circ}F$	Brightness ignition temperature, $^{\circ}F$
	Length, in.	Width, in.	Thickness, in.				
1	1.88	0.188	0.025	1.25	0.00184	105	2,950 \pm 30
2	1.88	.188	.025	1.25	.00184	105	2,940 \pm 30

TABLE 11

TANK TESTS WITH TITANIUM RS-110-A

Run	Model specifications			Gas	Pressure, atm	Ambient temperature, °F	Humidity, lb H ₂ O lb dry air	Power at failure, w	Brightness ignition temperature, °F
	Length, in.	Width, in.	Thickness, in.						
1	1.5	3/16	0.025	O ₂	1	71	-----	282	2,890 ± 20
2	1.5	3/16	.025	O ₂	3	71	-----	300	2,890 ± 30
3	1.5	3/16	.025	O ₂	5	71	-----	331	2,890 ± 10
4	1.5	3/16	.025	O ₂	7	71	-----	328	2,910 ± 20
5	1.5	3/16	.025	O ₂	8	71	-----	307	2,860 ± 20
6	1.5	3/16	.025	Air	1	73	0.0081	288	^a 3,260 ± 100
7	1.5	3/16	.025	Air	1	73	.0081	260	^a 3,260 ± 50
8	1.5	3/16	.025	Air	3	73	.0081	325	^a 3,110 ± 50
9	1.5	3/16	.025	He	1	70	-----	330	^a 3,040 ± 50

^aMelted.

TABLE 12

WIND-TUNNEL TESTS OF TITANIUM RS-110-A

Run	Model specifications			Mach number	Humidity of jet, lb H ₂ O lb dry air	Stagnation temperature, °F	Brightness ignition temperature, °F
	Length, in.	Width, in.	Thickness, in.				
1	1.88	0.188	0.025	1.25	0.00184	140	^a 2,760 ± 30
2	1.88	.188	.025	1.25	.00184	140	^a 2,720 ± 30
3	1.88	.188	.010	1.25	.00184	140	^a 3,040 ± 30
4	1.88	.188	.010	1.25	.00184	140	^a 3,060 ± 30

^aMelted.

TABLE 13

TANK TESTS WITH TITANIUM RS-110-BX

Run	Model specifications			Gas	Pressure, atm	Ambient temperature, °F	Humidity, lb H ₂ O lb dry air	Power at failure, w	Brightness ignition temperature, °F
	Length, in.	Width, in.	Thickness, in.						
1	1.5	3/16	0.025	O ₂	1	70	-----	248	2,910 ± 20
2	1.5	3/16	.025	O ₂	1	70	-----	260	2,850 ± 20
3	1.5	3/16	.025	O ₂	3	70	-----	272	2,920 ± 20
4	1.5	3/16	.025	O ₂	5	70	-----	265	2,900 ± 20
5	1.5	3/16	.025	O ₂	7	70	-----	282	2,890 ± 20
6	1.5	3/16	.025	O ₂	8	70	-----	300	2,890 ± 20
7	1.5	3/16	.025	Air	1	70	0.0075	264	^a 3,280 ± 50
8	1.5	3/16	.025	Air	1	68	-----	---	^a 3,150 ± 30
9	1.5	3/16	.025	Air	1	68	-----	---	^a 3,040 ± 30
10	1.5	3/16	.025	Air	5	70	.0075	306	^a 3,050 ± 50
11	1.5	3/16	.025	Air	8	70	.0075	278	^a 3,270 ± 50

^aMelted.

TABLE 14

WIND-TUNNEL TESTS OF TITANIUM RS-110-BX

Run	Model specifications			Mach number	Humidity of jet, lb H ₂ O lb dry air	Stagnation temperature, °F	Brightness ignition temperature, °F
	Length, in.	Width, in.	Thickness, in.				
1	1.88	0.188	0.025	1.25	0.00184	140	2,940 ± 20
2	1.88	.188	.025	1.25	.00184	140	2,880 ± 20
3	1.88	.188	.025	1.25	.00184	140	2,830 ± 20
4	1.88	.188	.025	1.26	.00184	140	2,850 ± 20
5	1.88	.188	.025	1.25	.00184	140	3,050 ± 20
6	1.88	.188	.010	1.25	.00184	140	2,930 ± 20
7	1.88	.188	.010	1.25	.00184	140	2,910 ± 20
8	1.88	.188	.010	1.25	.00184	140	2,950 ± 20
9	1.88	.188	.010	1.25	.00184	140	2,950 ± 20
10	1.88	.188	.010	1.25	.00184	140	2,930 ± 20

TABLE 15

TANK TESTS WITH STAINLESS STEEL 430

Run	Model specifications			Gas	Pressure, atm	Ambient temperature, °F	Humidity, lb H ₂ O lb dry air	Power at failure, w	Brightness ignition temperature, °F
	Length, in.	Width, in.	Thickness, in.						
1	1.75	3/16	0.025	O ₂	1	67	-----	243	2,470 ± 20
2	1.75	3/16	.025	O ₂	1	67	-----	233	2,490 ± 20
3	1.75	3/16	.025	O ₂	3	67	-----	223	2,480 ± 20
4	1.75	3/16	.025	O ₂	5	67	-----	205	2,460 ± 20
5	1.75	3/16	.025	O ₂	5	67	-----	205	2,470 ± 20
6	1.75	3/16	.010	O ₂	7	67	-----	---	2,480 ± 20
7	1.75	3/16	.025	Air	1	67	0.0065	261	^a 2,670 ± 30
8	1.75	3/16	.025	Air	1	67	.0065	284	^a 2,680 ± 30
9	1.75	3/16	.025	Air	4	67	.0065	244	^a 2,710 ± 30
10	1.75	3/16	.025	Air	7	67	.0065	294	^a 2,720 ± 30

^aMelted.

TABLE 16

WIND-TUNNEL TEST OF STAINLESS STEEL 430

Run	Model specifications			Mach number	Humidity of jet, lb H ₂ O lb dry air	Stagnation temperature, °F	Brightness ignition temperature, °F (a)
	Length, in.	Width, in.	Thickness, in.				
1	1.88	0.188	0.025	1.25	0.00184	110	2,730 ± 20
2	1.88	.188	.025	1.25	.00184	107	2,780 ± 40

^aModel melted.

TABLE 17

TANK TESTS WITH STAINLESS STEEL 302

Run	Model specifications			Gas	Pressure, atm	Ambient temperature, °F	Humidity, lb H ₂ O lb dry air	Power at failure, w	Brightness ignition temperature, °F (a)
	Length, in.	Width, in.	Thickness, in.						
1	1.5	3/16	0.025	O ₂	1	71	-----	254	2,600 ± 30
2	1.5	3/16	.025	O ₂	1	71	-----	259	2,550 ± 30
3	1.5	3/16	.025	O ₂	3	71	-----	255	2,500 ± 20
4	1.5	3/16	.025	O ₂	5	71	-----	266	2,520 ± 20
5	1.5	3/16	.025	O ₂	7	71	-----	255	2,520 ± 20
6	1.5	3/16	.025	O ₂	8	71	-----	247	2,510 ± 20
7	1.5	3/16	.025	Air	1	71	0.0050	292	2,550 ± 20
8	1.5	3/16	.025	Air	1	71	.0050	320	2,510 ± 20
9	1.5	3/16	.025	Air	3	71	.0050	296	2,550 ± 20
10	1.5	3/16	.025	Air	5	71	.0050	289	2,540 ± 20
11	1.5	3/16	.025	Air	8	71	.0050	310	2,590 ± 20

^aModel melted.

TABLE 18

TANK TESTS WITH COPPER

Run	Model specifications		Gas	Pressure, atm	Ambient temperature, °F	Humidity, lb H ₂ O / lb dry air	Power at failure, w	Brightness ignition temperature, °F (a)
	Length, in.	Diameter, in.						
1	1.75	0.020	O ₂	1	63	-----	27.3	1,880 ± 20
2	1.75	.020	O ₂	1	63	-----	25.4	1,860 ± 20
3	1.75	.020	O ₂	2	63	-----	27.3	1,870 ± 10
4	1.75	.020	O ₂	4	63	-----	25.3	1,865 ± 10
5	1.75	.020	O ₂	6	63	-----	27.3	1,860 ± 20
6	1.75	.020	O ₂	8	63	-----	28.3	1,860 ± 20
7	1.75	.020	Air	1	63	0.0086	27.3	1,865 ± 10
8	1.75	.020	Air	2	63	.0086	27.3	1,880 ± 20
9	1.75	.020	Air	4	63	.0086	28.3	1,860 ± 10
10	1.75	.020	Air	6	63	.0086	26.1	1,880 ± 20
11	1.75	.020	Air	8	63	.0086	26.3	1,850 ± 20
12	1.75	.020	He	1	71	-----	-----	1,830 ± 15

^aModel melted.

TABLE 19

TANK TESTS WITH NICKEL

Run	Model specifications			Gas	Pressure, atm	Ambient temperature, °F	Humidity, lb H ₂ O lb dry air	Power at failure, w	Brightness ignition temperature, °F (a)
	Length, in.	Width, in.	Thickness, in.						
1	1.5	3/16	0.025	O ₂	1	71	-----	234	2,540 ± 20
2	1.5	3/16	.025	O ₂	3	71	-----	246	2,550 ± 20
3	1.5	3/16	.025	O ₂	5	71	-----	234	2,545 ± 20
4	1.5	3/16	.025	O ₂	7	71	-----	256	2,545 ± 20
5	1.5	3/16	.025	O ₂	8	71	-----	250	2,550 ± 20
6	1.5	3/16	.025	Air	1	71	0.0050	226	2,540 ± 20
7	1.5	3/16	.025	Air	4	71	.0050	252	2,550 ± 20
8	1.5	3/16	.025	Air	6	71	.0050	250	2,540 ± 20
9	1.5	3/16	.025	He	1	71	-----	---	2,400 ± 15

^aModel melted.

TABLE 20

TANK TESTS WITH INCONEL

Run	Model specifications			Gas	Pressure, atm	Ambient temperature, °F	Humidity, lb H ₂ O lb dry air	Power at failure, w	Brightness ignition temperature, °F (a)
	Length, in.	Width, in.	Thickness, in.						
1	1.5	3/16	0.018	O ₂	1	69	-----	281	2,550 ± 20
2	1.5	3/16	.018	O ₂	1	69	-----	268	2,520 ± 20
3	1.5	3/16	.018	O ₂	3	69	-----	281	2,520 ± 20
4	1.5	3/16	.018	O ₂	5	69	-----	297	2,550 ± 20
5	1.5	3/16	.018	O ₂	7	69	-----	281	2,560 ± 20
6	1.5	3/16	.018	O ₂	8	69	-----	277	2,520 ± 20
7	1.5	3/16	.018	Air	1	69	0.0069	248	2,520 ± 20
8	1.5	3/16	.018	Air	1	69	.0069	273	2,520 ± 20
9	1.5	3/16	.018	Air	4	69	.0069	281	2,520 ± 20
10	1.5	3/16	.018	Air	7	69	.0069	281	2,530 ± 20
11	1.5	3/16	.018	He	1	71	-----	---	2,550 ± 15

^aModel melted.

TABLE 21

TANK TESTS WITH INCONEL X

Run	Model specifications			Gas	Pressure, atm	Ambient temperature, °F	Humidity, lb H ₂ O lb dry air	Power at failure, w	Brightness ignition temperature, °F (a)
	Length, in.	Width, in.	Thickness, in.						
1	1.5	3/16	0.025	O ₂	1	69	-----	284	2,500 ± 30
2	1.5	3/16	.025	O ₂	1	69	-----	277	2,500 ± 30
3	1.5	3/16	.025	O ₂	3	69	-----	298	2,550 ± 30
4	1.5	3/16	.025	O ₂	5	69	-----	302	2,560 ± 30
5	1.5	3/16	.025	O ₂	7	69	-----	295	2,530 ± 40
6	1.5	3/16	.025	O ₂	8	69	-----	307	2,510 ± 40
7	1.5	3/16	.025	Air	1	69	0.0072	284	2,455 ± 30
8	1.5	3/16	.025	Air	4	69	.0072	295	2,460 ± 30
9	1.5	3/16	.025	Air	7	69	.0072	288	2,480 ± 30
10	1.5	3/16	.025	He	1	72	-----	---	2,550 ± 15

^aModel melted.

TABLE 22

TANK TESTS WITH BERYLCO 25

Run	Model specifications			Gas	Pressure, atm	Ambient temperature, °F	Humidity, lb H ₂ O lb dry air	Brightness ignition temperature, °F (a)
	Length, in.	Width, in.	Thickness, in.					
1	1.5	3/16	0.007	O ₂	1	70	0.006	1,580
2	1.5	3/16	.007	O ₂	1	70	.006	1,600
3	1.5	3/16	.007	O ₂	3	70	.006	1,600
4	1.5	3/16	.007	O ₂	5	70	.006	1,595
5	1.5	3/16	.007	O ₂	7	70	.006	1,600
6	1.5	3/16	.007	Air	1	70	.006	1,600
7	1.5	3/16	.007	Air	4	70	.006	1,580
8	1.5	3/16	.007	Air	7	70	.006	1,585

^aModel melted.

TABLE 23

TANK TESTS WITH BERYLCO 10

Run	Model Specifications			Gas	Pressure, atm	Ambient temperature, °F	Humidity, lb H ₂ O lb dry air	Brightness ignition temperature, °F
	Length, in.	Width, in.	Thickness, in.					
1	1.5	1/4	0.015	O ₂	1	70	-----	1,750
2	1.5	1/4	.015	O ₂	1	70	-----	1,755
3	1.5	1/4	.015	O ₂	3	70	-----	1,750
4	1.5	1/4	.015	O ₂	5	70	-----	1,755
5	1.5	1/4	.015	O ₂	7	70	-----	1,750
6	1.5	1/4	.015	Air	1	70	0.007	1,760
7	1.5	1/4	.015	Air	4	70	.007	1,760
8	1.5	1/4	.015	Air	7	70	.007	1,755

TABLE 24

RESULTS OF SHAPE EFFECT RUNS WITH CALCIUM CONES^a

Run	Included angle, deg	Base diameter, in.	Air temperature, °F	Air velocity, ft/sec	Ignition temperature, °F
1	180	3/8	1,820	83	1,356
2	180	3/8	1,825	60	1,365
3	90	3/8	1,850	75	1,370
4	20	3/8	1,560	84	1,360
5	20	3/8	1,620	66	1,360
6	10	3/8	1,770	81	1,345
7	10	3/8	1,600	86	1,320
8	10	3/8	1,630	84	1,320
9	10	3/8	1,630	83	1,355

^a99-percent pure calcium, turned from castings.

TABLE 25

PROPERTIES OF SOME METALS AND THEIR OXIDES

Metal	Oxide	Metal melting point, °C	Oxide melting point, °C	Volume ratio	Oxide density, g/cm ³	γ , g oxide g O ₂	Heat of formation (18° C), cal/mole of oxide	Heat of reaction (18° C), cal/g of O ₂
Be	BeO	1,278	2,520	1.68	3.01	1.562	^a -66,000	^a 4,120
Mg	MgO	651	2,800	.81	3.58	2.52	-145,760	4,080
Ca	CaO	842	2,570	.64	3.37	3.44	-151,700	9,160
Th	ThO ₂	1,845	2,950	1.35	10.03	8.25	-330,950	10,320
Ti	TiO ₂	1,800	1,860	1.73	4.26	2.49	-217,000	6,680
Zr	ZrO ₂	1,900	2,715	1.45	5.6	3.85	-178,700	5,580
V	V ₂ O ₅	1,710	660	3.19	3.36	2.27	-437,200	5,560
Nb	NbO	1,950	-----	1.37	6.27	6.80	^a -100,000	^a 6,300
Ta	Ta ₂ O ₅	^b 3,027	1,470	2.54	8.74	5.52	-500,120	6,270
Cr	Cr ₂ O ₃	1,890	2,440	2.07	5.2	3.17	-267,390	5,570
Mo	MoO ₃	2,620	795	3.24	4.50	3.00	-174,000	3,650
W	WO ₃	3,370	1,470	3.35	7.16	4.80	-151,400	3,970
Mn	Mn ₂ O ₃	1,260	1,580	2.15	4.86	3.58	-327,810	5,130
Fe	FeO	1,535	1,371	.63	5.7	2.24	-64,040	2,000
	Fe ₂ O ₃	1,535	1,565	2.14	5.24	3.32	-190,900	3,960
	Fe ₃ O ₄	1,535	1,457	2.10	5.18	3.62	-265,950	4,150
Co	CoO	1,495	1,810	1.86	6.0	4.68	-57,490	3,600
Ni	NiO	1,455	1,960	1.65	7.45	4.67	-57,380	3,580
Cu	CuO	1,083	1,030	1.72	6.40	4.97	-31,800	1,980
Al	Al ₂ O ₃	660	2,020	1.45	3.9	2.12	-339,050	7,060
Pb	PbO	327	885	1.26	9.53	13.95	-52,473	3,280
Ce	Ce ₂ O ₃	640	1,692	1.16	7.0	6.85	-150,000	3,130
U	CeO ₂	640	3,000	1.22	7.3	10.78	-234,900	14,550
	U ₃ O ₈	^b 1,133	1,540	2.66	8.30	6.58	-845,170	6,600

^aUnreliable data.^bDissociates.

TABLE 26

OXIDATION AND IGNITION DATA OF MAGNESIUM ALLOYS

[Data obtained from references 7 and 8]

Alloy metal, percent by weight	A_i , g/cm ² -sec	E_i , cal/mole	T_{ig} , °F
1.78% Al	2.5×10^4	42,700	1,105
3.81% Al	3.1×10^3	38,600	1,065
7.23% Al	7.5×10^8	54,700	1,018
9.12% Al	1.1×10^{16}	74,500	990
1.54% Zn	3.1×10^6	50,000	1,076
3.28% Zn	2.7×10^1	31,500	1,045
3.83% Ag	1.1×10^7	52,600	1,049
3.78% Sn	3.3×10^1	31,600	1,112
3.86% In	2.3×10^5	46,600	1,148
4.18% Cd	1.7×10^6	50,500	1,148
3.94% Pb	7.5×10^6	51,600	1,112
.49% Ni	9.7×10^4	42,000	1,085
.23% Cu	6.6×10^5	44,800	1,148

C-477

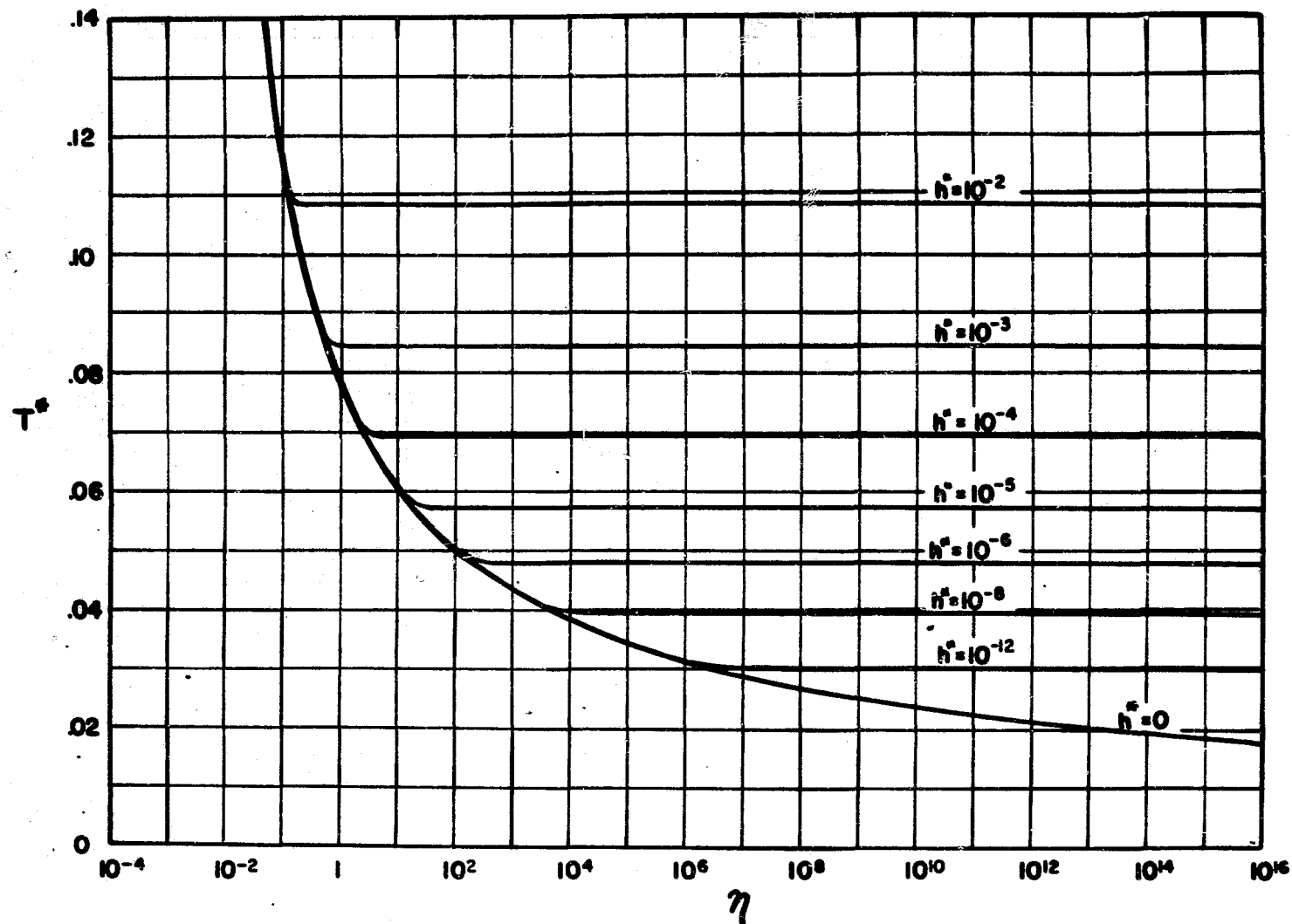


Figure 1.- Curves for prediction of ignition temperatures from oxidation data.

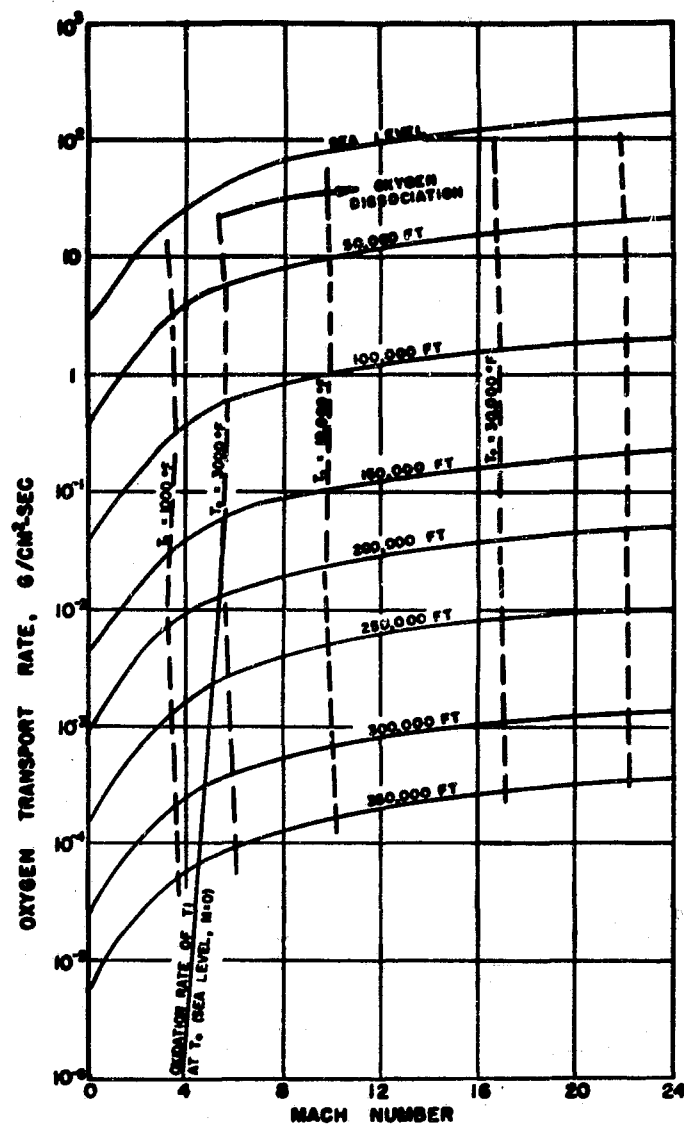


Figure 2.- Oxygen transport rate behind a normal shock wave.

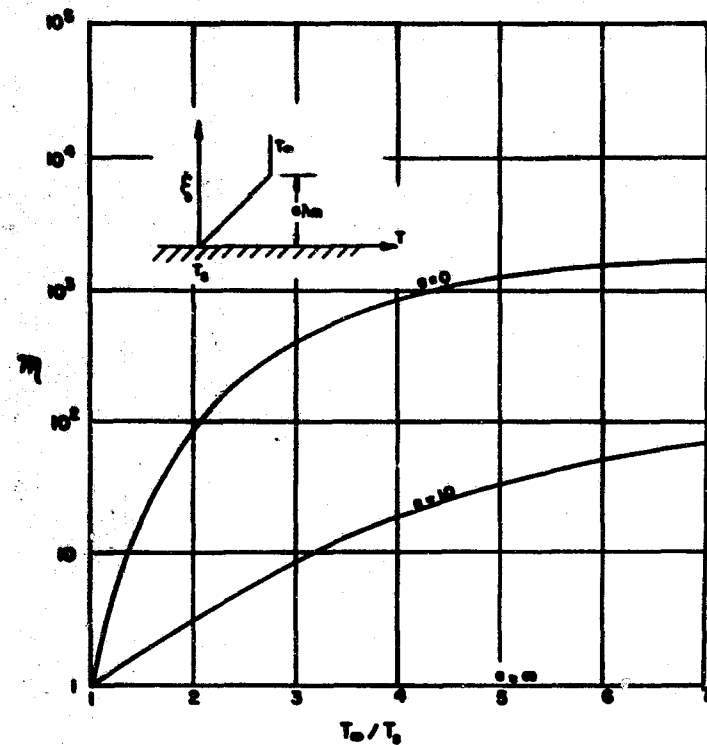


Figure 3.- Dependence of adsorption rate on temperature variation near surface.

$$\frac{E}{RT_s} = 10; \frac{dw}{d\theta} = \eta \left(\frac{dw}{d\theta} \right)_{iso}$$

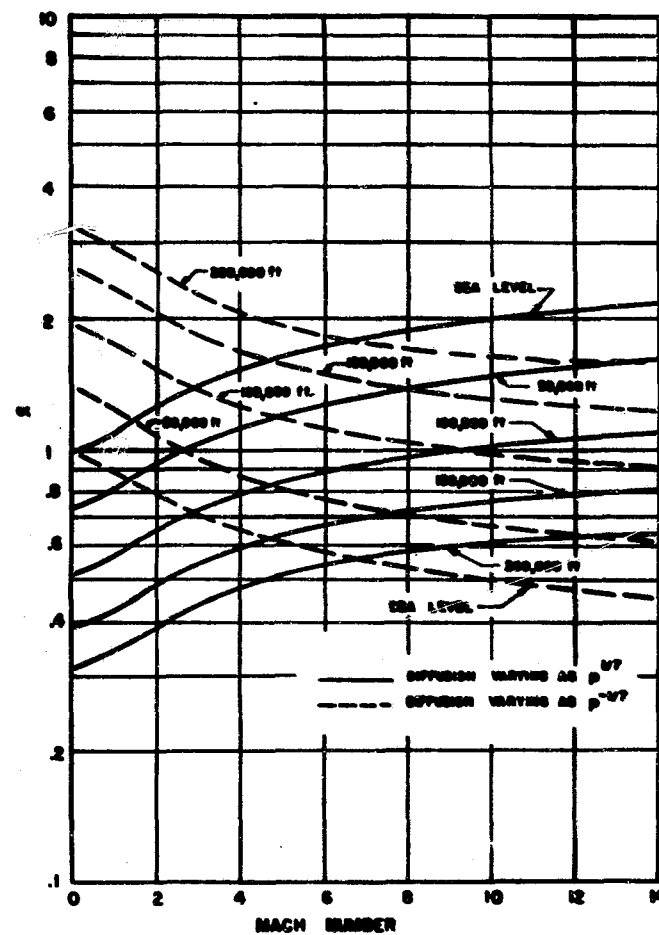
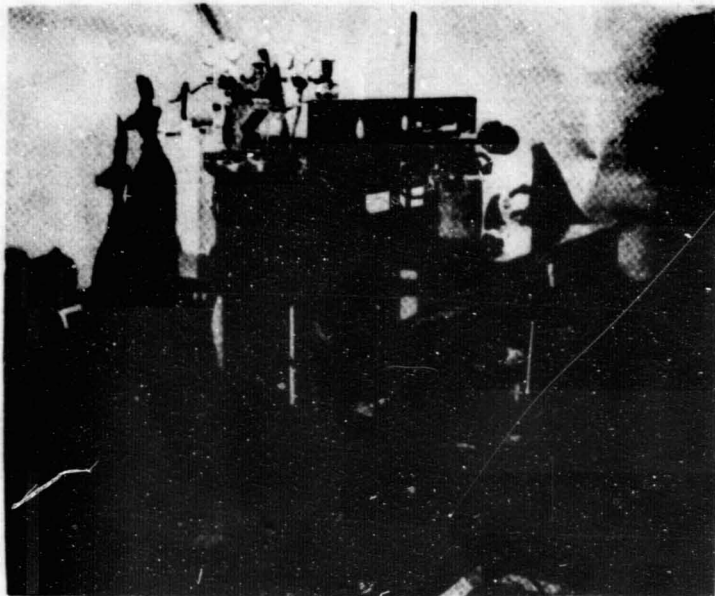
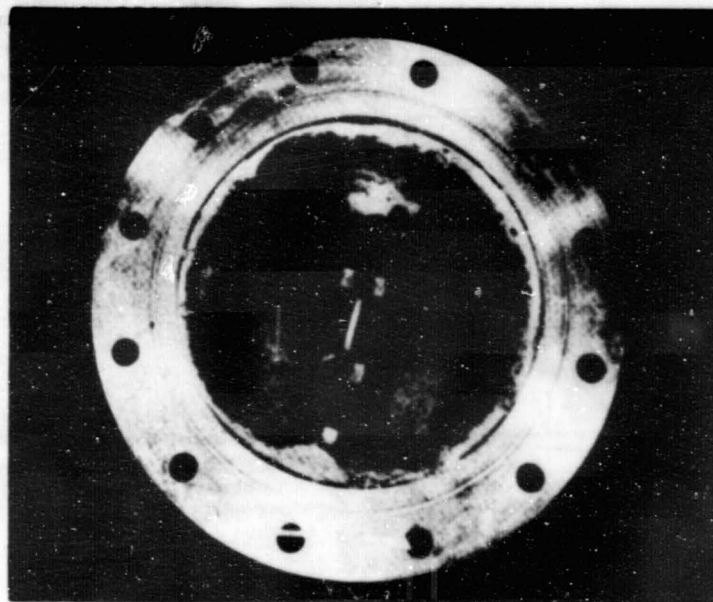


Figure 4.- Effect of flight conditions on rates of diffusion through oxide film.

$$\frac{dw}{d\theta} = \alpha \left(\frac{dw}{d\theta} \right)_{sea\ level, M=0}$$



L-58-100a
Figure 5.- Pressure tank and control console.



L-58-101a
Figure 6.- Inside of pressure tank.

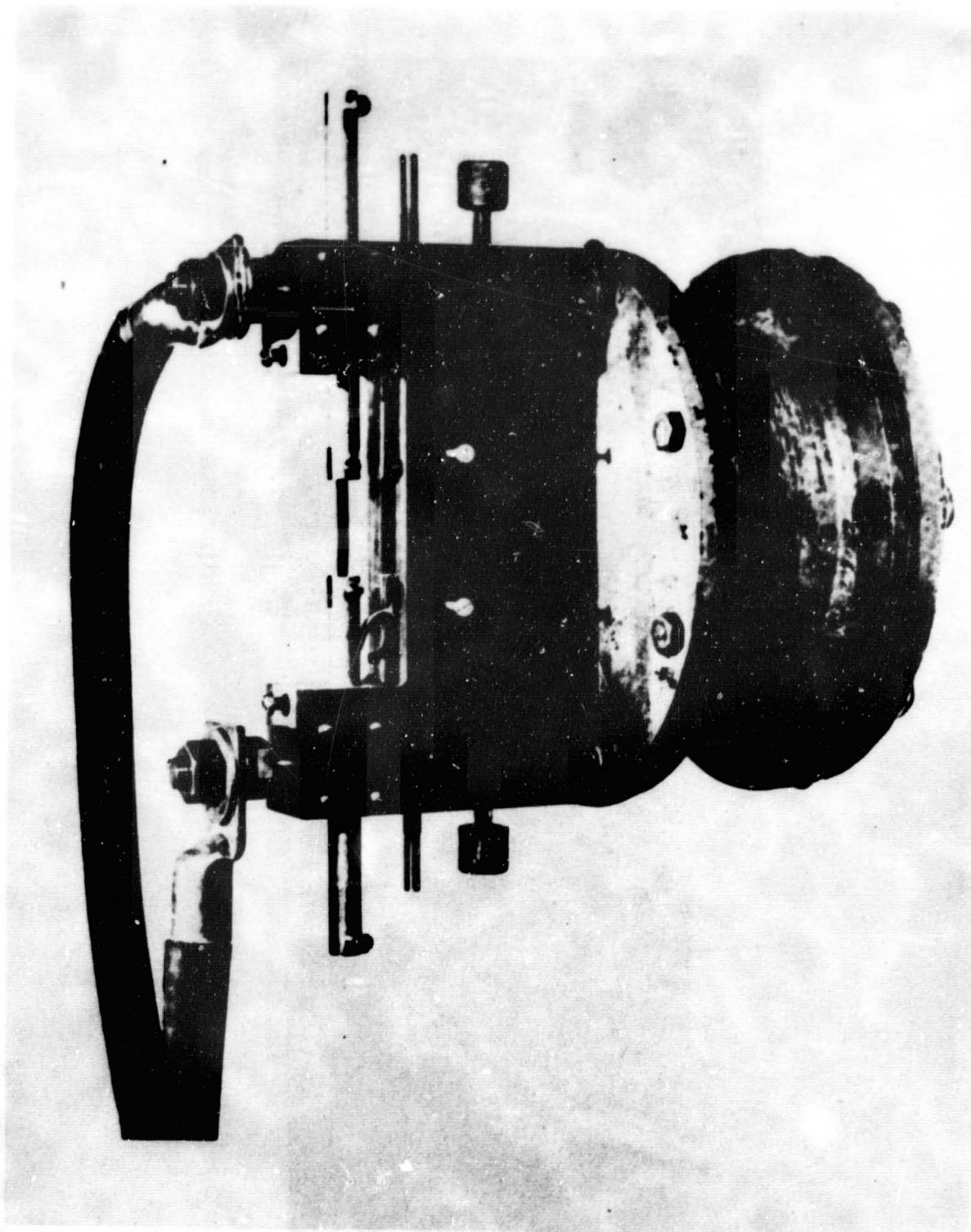


Figure 7.- Wind-tunnel apparatus.

L-58-102a

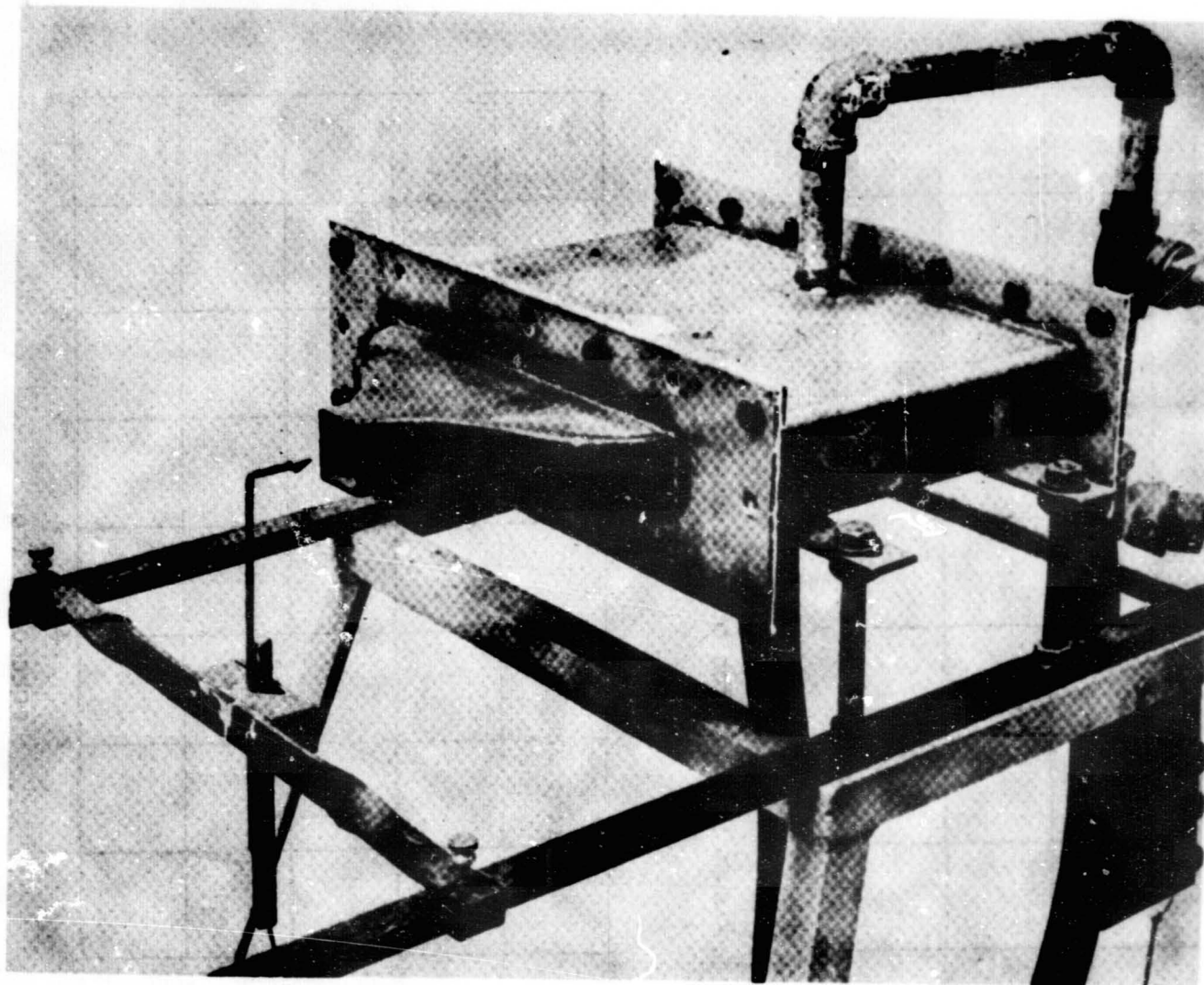


Figure 8.- Hot-air apparatus.

L-58-103a

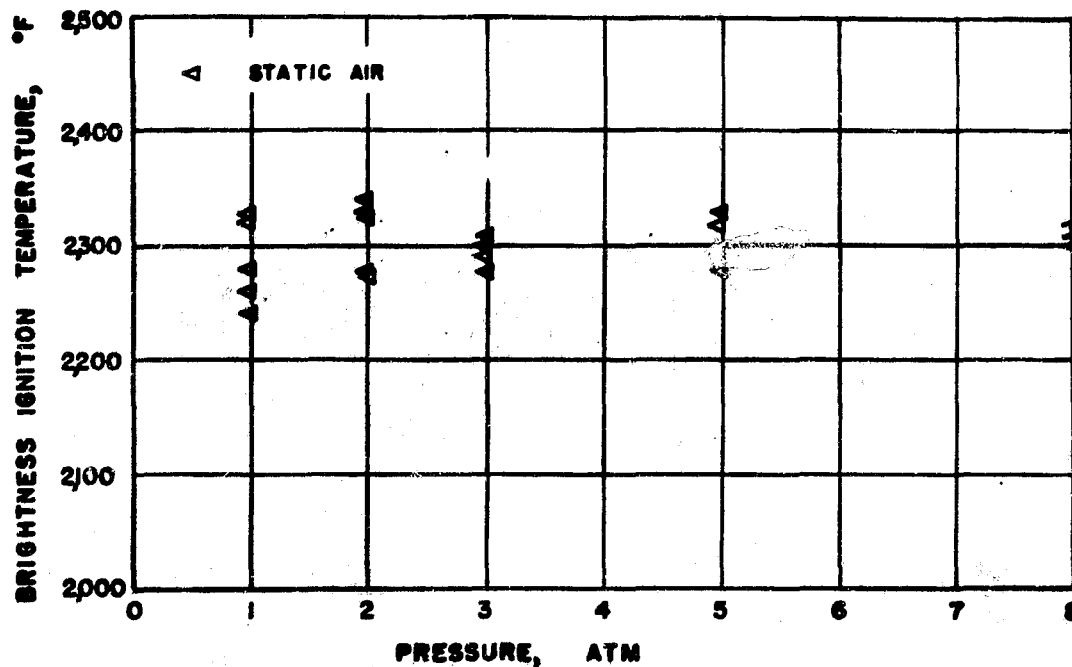


Figure 9.- Ignition temperatures of mild steel.

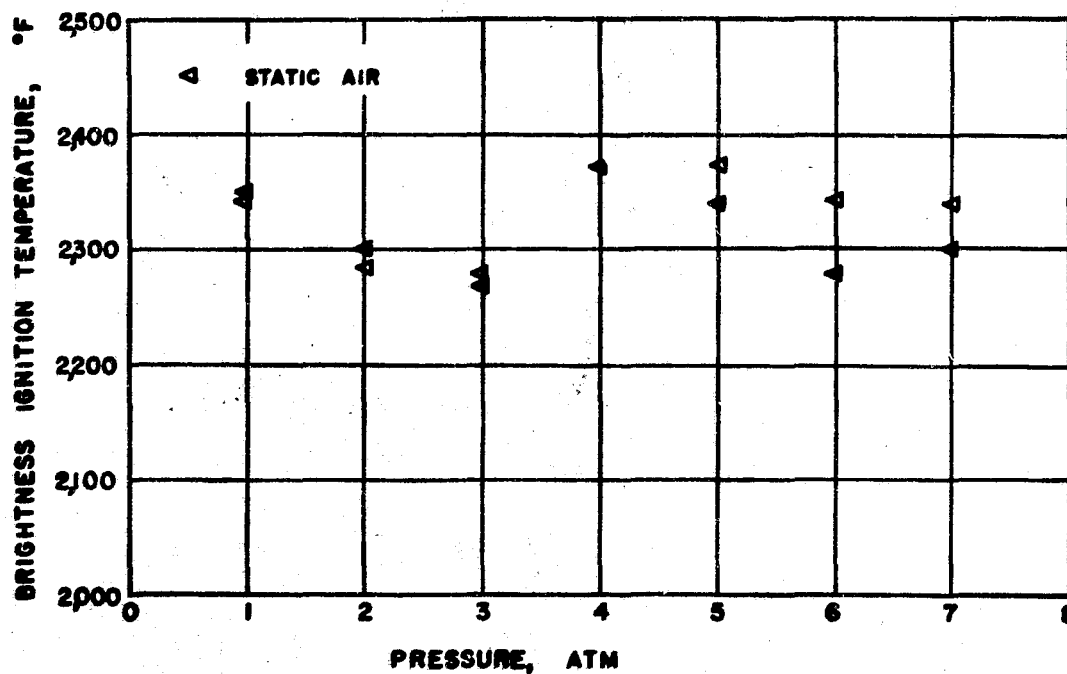


Figure 10.- Ignition temperatures of tungsten.

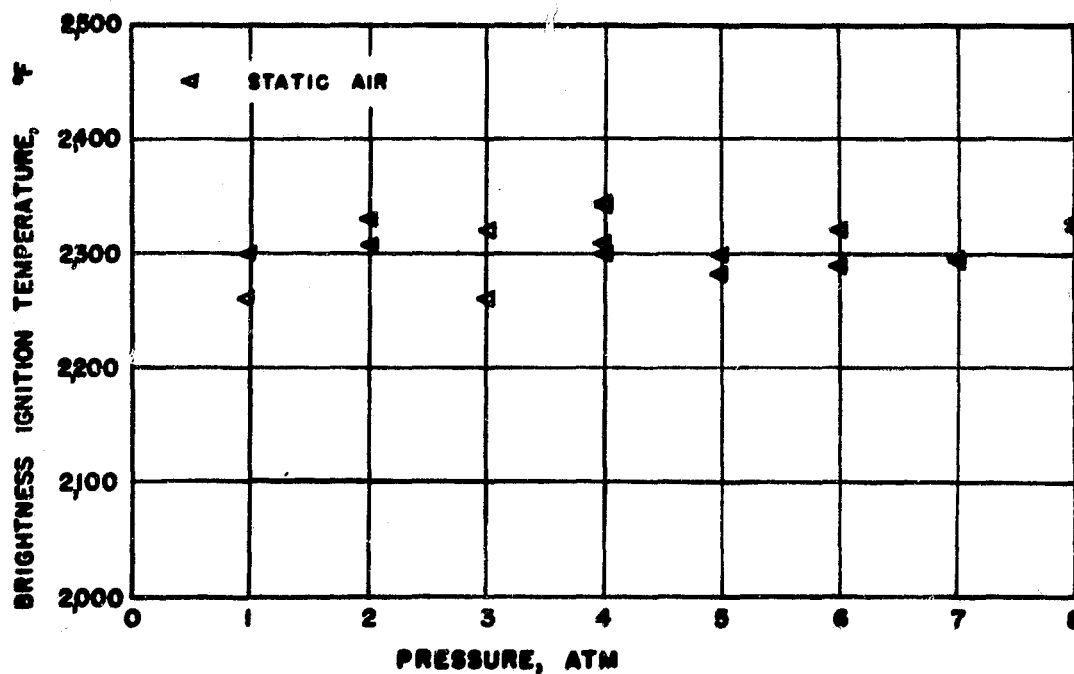


Figure 11.- Ignition temperatures of tantalum.

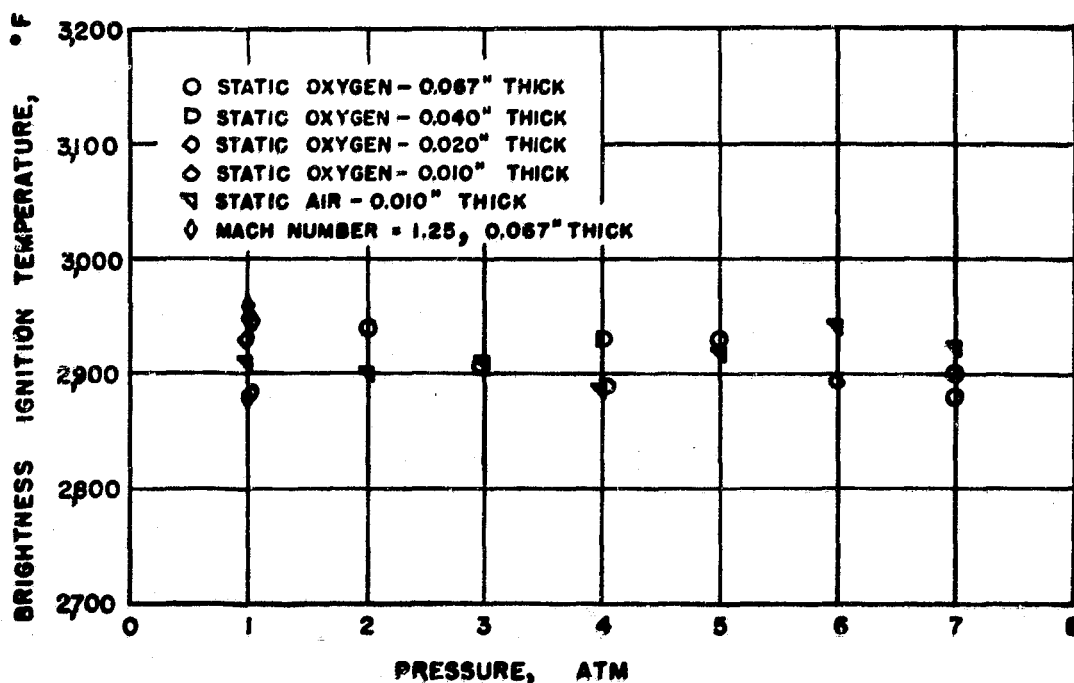


Figure 12.- Ignition temperatures of titanium RC-70.

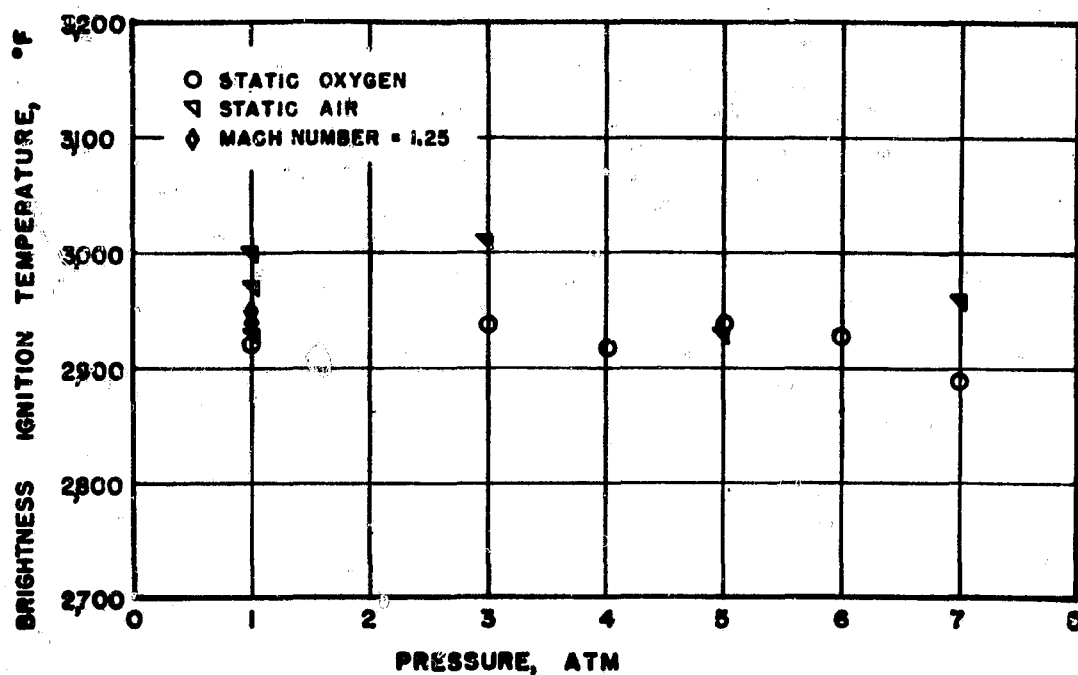


Figure 13.- Ignition temperatures of titanium RS-70.

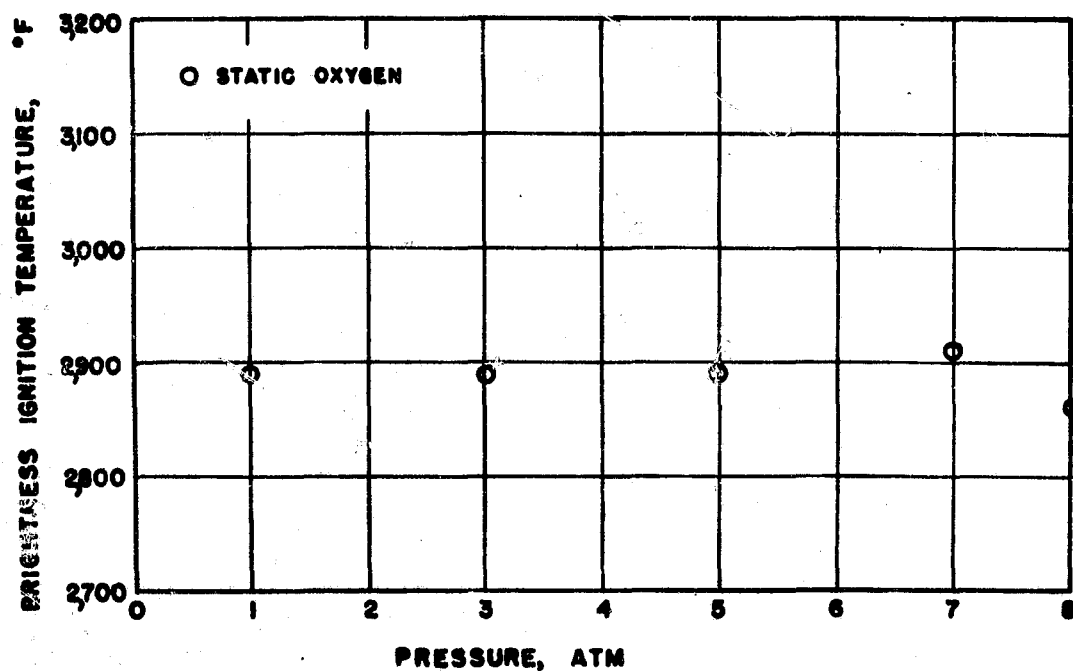


Figure 14.- Ignition temperatures of titanium RS-110-A.

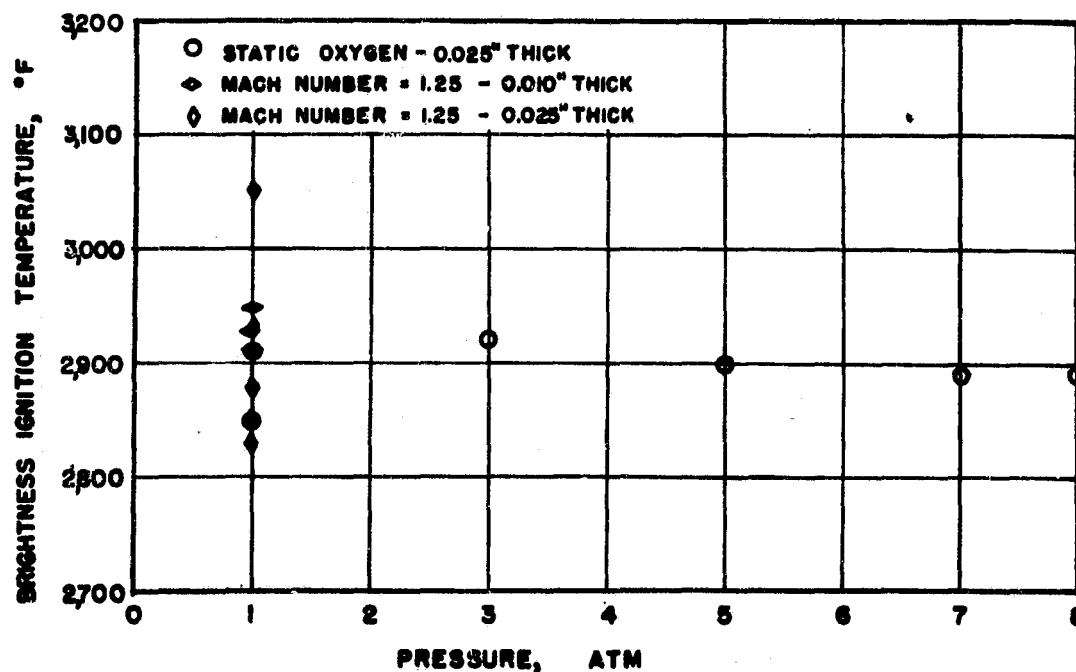


Figure 15.- Ignition temperatures for titanium RS-110-BX.

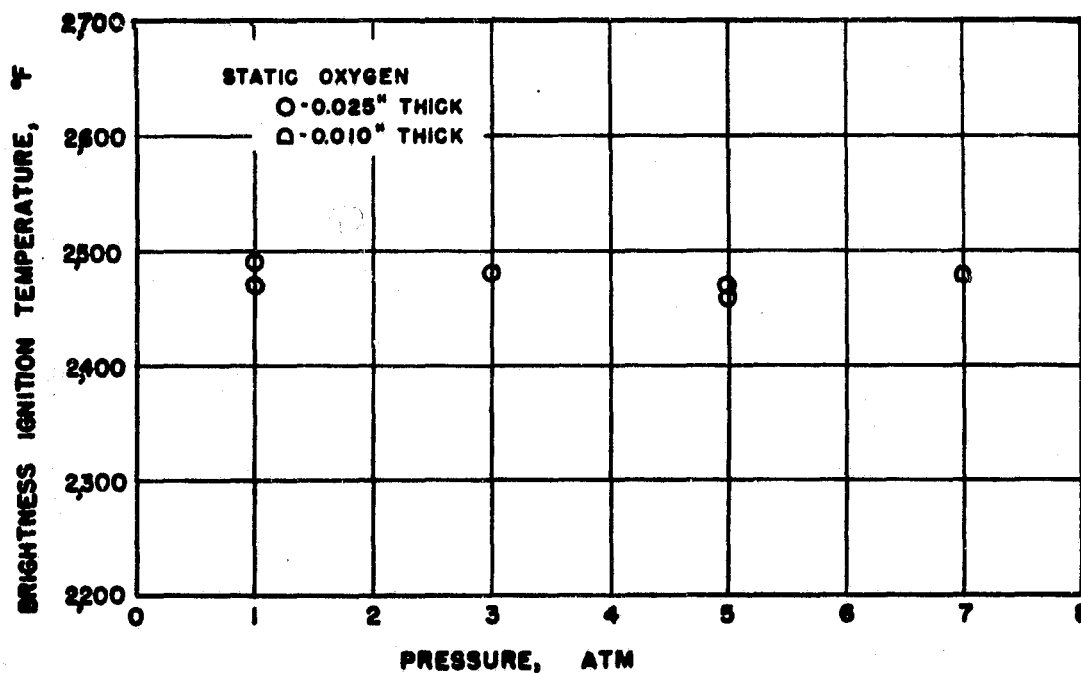


Figure 16.- Ignition temperatures of stainless steel 430.

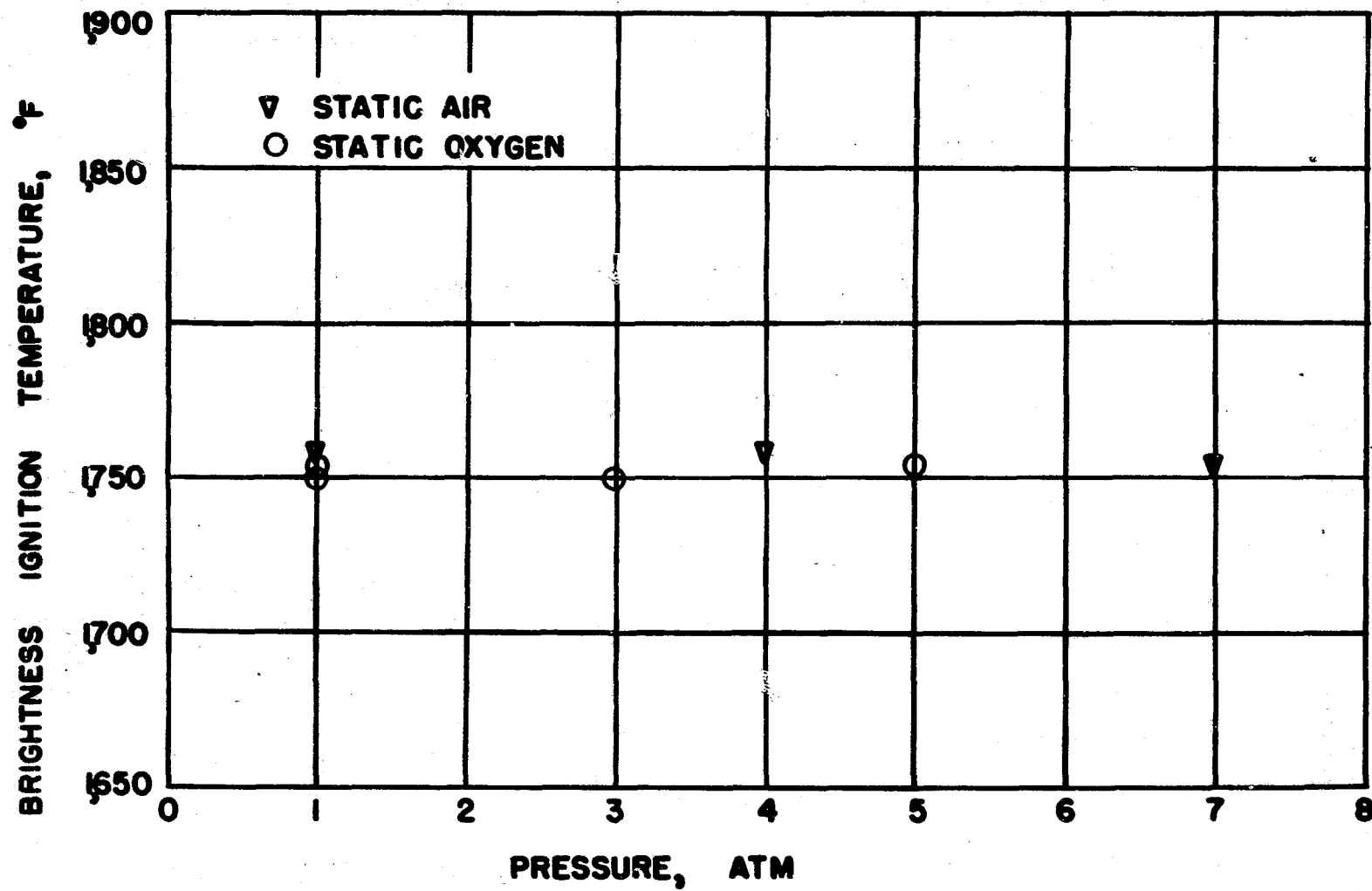


Figure 17.- Ignition temperatures of Berylco 10.

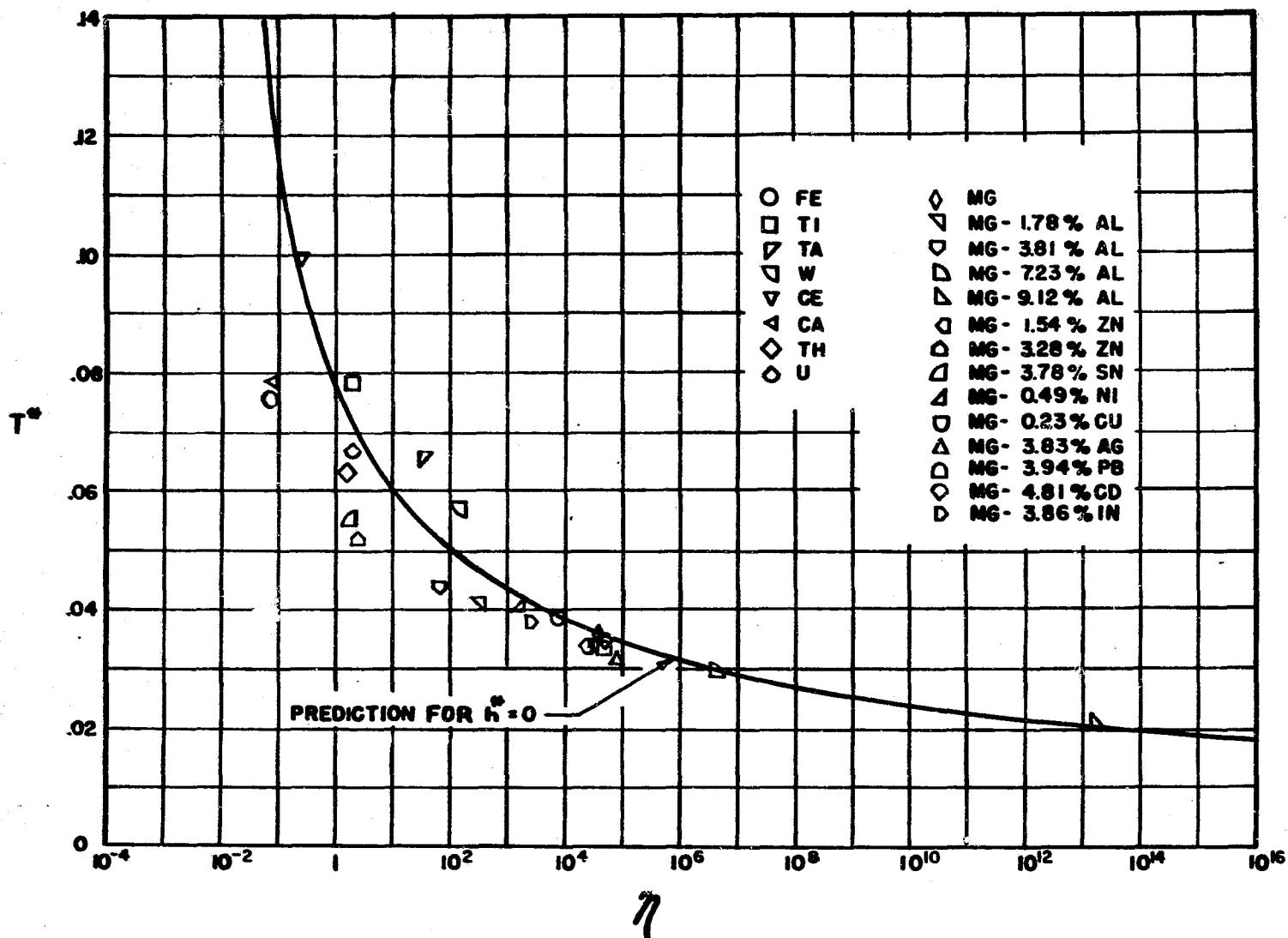


Figure 18.- Comparison of predicted and experimental ignition temperatures.

END OF REFERENCE
28

REFERENCE

29

**GLASSMAN, I.; MELLOR, A. M.; SULLIVAN, H. F.; AND
LAURENDEAU, N. M.: A REVIEW OF METAL IGNITION AND FLAME
MODELS. REACTIONS BETWEEN GASES AND SOLIDS. CONF.
PROC. NO. 52, AGARD, FEB. 1970.**

N 10-24351

AGARD CP No. 52

2.0-0:0

N70-24351

AGARD CONFERENCE PROCEEDINGS No. 52

AGARD

ADVISORY GROUP FOR AEROSPACE RESEARCH & DEVELOPMENT

LEWIS RESEARCH CENTER
Aerospace Safety Research
and Data Institute
MARCH 1 1971

CLEVELAND, OHIO

Reactions between Gases and Solids

LIBRARY COPY

JUL 6 1970

LEWIS LIBRARY, NASA
CLEVELAND, OHIO

NORTH ATLANTIC TREATY ORGANIZATION



INITIAL DISTRIBUTION IS LIMITED
FOR ADDITIONAL COPIES SEE BACK COVER

NORTH ATLANTIC TREATY ORGANIZATION
ADVISORY GROUP FOR AEROSPACE RESEARCH AND DEVELOPMENT
(ORGANISATION DU TRAITE DE L'ATLANTIQUE NORD)

REACTIONS BETWEEN GASES AND SOLIDS

A REVIEW OF METAL IGNITION AND FLAME MODELS

by

I. Glassman, A. M. Meller, H. F. Sullivan and M. M. Laurendeau

Princeton University, Princeton, USA

SUMMARY

Based upon the classic work of Frank Kamenetskii, a physical model of the heterogeneous ignition process of metals was developed. This model is compared with other theories of metal ignition concerned with bulk samples, quiescent piles, single particles and dust dispersions. The new model is based upon the concept of a transition temperature - the temperature at which the oxide layer on the metal becomes non-protective in the sense that a reaction rate independent of time describes the behaviour of the system at constant temperature. The model postulates that the ignition temperature must be greater than both the transition and the critical temperatures. It further relates pyrophoricity to the concept of a transition temperature.

The transition temperature thought to be a unique value characteristic to the metal, such as the oxide melting point, has been shown by Kuehl to be pressure dependent in the case of aluminum. Kuehl's work and the recent supporting evidence of Laurendeau on zinc are reviewed.

With respect to the burning mechanisms of metals, reviewed are the finite reaction zone model of Coffin, liquid oxide bubble model of Fassell, collapsed reaction zone model of Brzustowski and Glassman, extension of the Brzustowski-Glassman model by Khipe, the heterogeneous reaction model of Markstein and the very recent, broad homogeneous reaction zone model of Sullivan.

IN THIS REVIEW OF IGNITION AND FLAME MODELS OF METALS, the authors will use their own work as the central basis of discussion. The work of others will be well-referenced and discussed and various ignition theories will be reviewed extensively in an appendix. The early work in metal combustion at Princeton (1), (2), (3), (4) will be mentioned only briefly. Various compendia and general reviews (5), (6), (7), (8) of metal combustion are readily available.

IGNITION MODELS*

The impetus at Princeton for a study of ignition phenomena came about through certain results obtained in earlier work on combustion which made use of the technique of ohmic heating of wire samples (4), (9), (10), (11), (12).

While investigating the flames produced by aluminum wires, Brzustowski (4), (9), found that the ignition temperature of aluminum in oxygen-argon atmospheres was very close to the melting point of aluminum oxide at pressures greater than 300 torr. In addition, Friedman and Macek (13) had shown that the Al_2O_3 coating must melt in order that aluminum undergo vapor-phase combustion. Later Kuehl (14) showed that in general the ignition temperature of aluminum is very close to $2042^\circ C.$, the melting point of the metal oxide.

Mellor (10), (11) carried out similar experiments with anodized aluminum wires in carbon dioxide-oxygen atmospheres. He observed two things that were very different from the results of Brzustowski. First, in the carbon dioxide-argon mixtures at pressures below 300 torr, a cylindrical vapor-phase diffusion flame appeared before the wire broke. On the other hand, in the oxygen-argon mixtures, the wire broke thereby exposing molten aluminum to the oxidizing atmosphere before a vapor-phase flame appeared (4), (9). Secondly, on the basis of total power required at ignition, it was easier to ignite anodized aluminum wires at similar pressures in CO_2 -Ar atmospheres than it was to ignite them in O_2 -Ar atmospheres (10), (11).

To explain these results it was necessary to consider the pre-ignition oxidation of the metal. In CO_2 -Ar mixtures, little oxidation occurs during the pre-ignition period while in O_2 -Ar mixtures, a very thick oxide coating builds up on the surface of the metal. In general, the anodized film is porous but in oxygen containing atmospheres, these pores are filled by the natural oxidation process during this preignition period (15). Thus, in this case, melting of the oxide occurs before ignition can take place.

For an anodized film of Al_2O_3 considered here, a thin barrier layer of oxide exists between the outer porous layer and the metal substrate. Even in the case of a CO_2 -Ar atmosphere, however, it is suggested that the ignition temperature is still equal to the melting point of Al_2O_3 since only the barrier layer need be melted to expose the molten aluminum to this oxidizing atmosphere (15). Thus, in summary, since little oxidation occurs before ignition in a CO_2 -Ar atmosphere and since the anodized coating is porous, ignition occurs in a cylindrical vapor-phase flame upon melting of the barrier layer before the wire breaks at that point when the anodized coating completely melts**. Obviously, because of the little oxide built up before ignition, the total power at ignition for the anodized wire is less in the CO_2 -Ar mixtures than in the O_2 -Ar mixtures.

This work with aluminum and other work with magnesium ribbons (4), (9), (10), (11) showed primarily that the ignition of metals is strongly dependent on the pre-ignition surface oxidation reaction in the environment of interest. Surface oxidation reactions determine whether or not a particular metal coating is protective in a certain environment in a particular temperature range. If the metal coating is protective, then the metal sample cannot ignite. However, usually the oxide coating becomes nonprotective at higher temperatures and the sample may then ignite.

This surface coating is the unique property of the metal ignition problem that makes it very difficult to analyze mathematically. The ignition problem has been well treated for the homogeneous case, but is not at all well understood in the case of a simple heterogeneous reaction. Here the situation becomes even more difficult since one must consider the complicating factor brought about by the low temperature oxidation process common to all metals of interest.

* This section has been extracted from the M.S.E. thesis of Laurendeau (17). The content is based extensively on the earlier Ph.D. thesis of Mellor (12).

** A more appropriate explanation for the appearance of this cylindrical vapor-phase flame will be offered in a later section.

These findings coupled with the well-known concepts of the homogeneous problem led to Mellor's work on the development of both a model for the heterogeneous ignition of metals and subsequent experimental verification of certain trends predicted by that model (15), (12). Later work by Laurendeau (17) further substantiated and clarified some aspects of the model primarily through an experimental determination of the ignition temperatures of many common non-toxic metals in an oxygen atmosphere.

THE STEADY STATE MODEL OF METAL IGNITION - As mentioned previously, any model which attempts to describe the metal ignition process must take into consideration the formation of solid phase products on the surface during the pre-ignition reaction. Thus, metal ignition is usually much more complicated than the heterogeneous ignition of other simple fuel-oxidizer systems. Because of this difficulty, Mellor developed a qualitative model of metal ignition based to a large extent on the classical thermal theories of homogeneous ignition as demonstrated most lucidly by Fränk-Kamenetskii in his comprehensive work describing the effects of heat and mass transfer in chemical kinetics (16).

As is well known, both a stationary and a non-stationary approach exists for the description of the homogeneous ignition phenomena. Because of the complications involved in any heterogeneous process, it is best to emphasize the stationary approach in this case. It may be shown that the non-stationary approach can equally well describe the metal ignition process, but the argument is somewhat laborious (See Ref. 12). Therefore, since it is of interest here to only describe those aspects of the model directly essential to this particular work, the steady-state approach will be followed in order to make the principal ideas as clear as possible to the reader. Those interested in a detailed description of both the stationary and non-stationary aspects of the model along with an excellent discussion of the relationship between the classical thermal theories of homogeneous ignition and the present model may wish to consult Chapter II of Ref. 12.

It seems important at this time to indicate the intent of the early work at Princeton by Mellor. He attempted to construct a qualitative model which would take into consideration metals of all types and sizes in all possible atmospheres. An investigation of other models of metal ignition (12) (see Appendix I) indicate that they are much more quantitative than the present description in that they attempt to calculate ignition temperatures; however, each of these models is restricted to only a very limited range of practical experimental situations.

HETEROGENEOUS IGNITION WITH GAS-PHASE REACTION PRODUCTS - Before metal ignition, i.e., heterogeneous ignition with solid-phase reaction products is considered, it is of paramount importance that a slightly simpler case be investigated, that is, the ignition of a solid fuel via reaction with a gaseous oxidizer involving only gaseous reaction products. An example of this might perhaps be a carbon particle reacting in air or oxygen (12).

As pointed out by Mellor (12), in the case of a heterogeneous system, where the exothermic reaction occurs on the surface as opposed to throughout a reaction volume as in a homogeneous system, the interaction is characterized by a uniform surface temperature T_s instead of a gas temperature, and all heating terms are expressed per unit area instead of per unit volume. Thus, in order to investigate the case of a spherical metal particle in a static gaseous atmosphere for which all the products are assumed to be in the gaseous state, a heat balance is conveniently made in a thin control volume at uniform surface temperature T_s enclosing only the reacting surface of the metal*.

This heat balance is constructed by examining the rate of heat input and the rate of heat loss from the aforementioned thin control volume, both quantities being functions of the surface temperature T_s . Consider** first then the chemical energy release rate in cal/cm²-sec. It may be written as:

$$\dot{q}_{chem} = \dot{m} Q$$

Eq (1)

where \dot{m} is the molar reaction rate in moles of fuel per cm² per second and Q is the chemical energy release in calories per mole of fuel.

* Since a steady-state is being considered here, it is necessary that the control surface be stationary. Therefore, in this development, reactant depletion is neglected.

** In the present discussion, only chemical heat input will be considered.

The chemical energy release is given by the expression:

$$Q = \sum_{\text{react. } i} n_i \Delta H_{i,T_s} - \sum_{\text{prod. } j} n_j \Delta H_{j,T_s} \quad \text{Eq (2)}$$

where the subscript i indicates reactants and the subscript j products, where

$$\Delta H_{k,T_s} = \Delta H_{f,k}^{298} + (H_{T_s} - H_{298})_k \quad \text{Eq (3)}$$

and where

T_s = surface temperature, °K;
 n_k = no. of moles of species k per mole of fuel;
 $\Delta H_{f,k}^{298}$ = standard heat of formation of species k at 298°K, cal/mole of k ;
 $H_{T,k}$ = enthalpy of species k at T °K, cal/mole of k .

The molar reaction rate is given by two expressions, depending on whether the surface temperature T_s is such that the reaction rate is controlled by kinetics or by diffusion of the oxidizer. At lower temperature, \dot{m} may be given by:

$$\dot{m} = A e^{-E/RT_s} C_s^n \quad \text{Eq (4)}$$

where

A = pre-exponential factor, $\text{cm}^{3n-2}/\text{moles}^{n-1} \cdot \text{sec}$;
 E = activation energy, cal/mole;
 R = universal gas constant, cal/mole, °K;
 C_s = oxidizer concentration at the surface, mole of fuel/ cm^3 ;
 n = order of the reaction, dimensionless, and, therefore, here the dependence of \dot{q}_{chem} on T_s is exponential due to the controlling kinetic Arrhenius factor.

At higher temperatures, \dot{m} may be given by:

$$\dot{m} = \frac{N_u D}{r} (C - C_s) \quad \text{Eq (5)}$$

where

Nu = diffusion Nusselt number, dimensionless;
 D = diffusivity of the oxidizer, cm^2/sec ;
 r = a characteristic dimension of the system, cm;
 C = oxidizer concentration in the gas, moles of fuel/ cm^3 ;
 and, therefore, here the dependence of \dot{q}_{chem} on T_s is given predominantly by the diffusivity D which varies as the 1.67 power of temperature (18).

Thus, as T_s is increased, the value of \dot{q}_{chem} also increases due to the variation of Q with T_s , but the form of \dot{q}_{chem} vs T_s is given by an S-shaped curve (See Fig. 1a) which emphasizes the control of the chemical heat release by the molar reaction rate, \dot{m} . At lower temperatures \dot{m} is controlled by kinetics, but as T_s is increased, diffusion of the oxidizer through the inert gas to the particle surface becomes important and, therefore, \dot{m} then is controlled by the diffusion process. In addition to diffusion, the drop in the slope of the \dot{q}_{chem} vs T_s curve at higher temperatures is partially due to a small amount of dissociation of the reaction products.

Consider next the heat loss rate in $\text{cal}/\text{cm}^2 \cdot \text{sec}$ from the same control volume described previously. Recalling that this control volume includes only the reaction surface, then the rate of heat loss \dot{q}_{loss} may be written as follows:

$$\dot{q}_{\text{loss}} = \dot{q}_{\text{cond},f} + \dot{q}_{\text{cond},g} + \dot{q}_r \quad \text{Eq (6)}$$

where

$\dot{q}_{\text{cond},f}$ = conductive heat loss into the fuel particle, $\text{cal}/\text{cm}^2 \cdot \text{sec}$;
 $\dot{q}_{\text{cond},g}$ = conductive heat loss into the ambient static gas, $\text{cal}/\text{cm}^2 \cdot \text{sec}$;
 \dot{q}_r = radiative heat loss to the environment, $\text{cal}/\text{cm}^2 \cdot \text{sec}$;

and where each of these terms is of course a function of the surface temperature T_s .

Notice that in this equation, there is no term indicating heat loss by means of mass transfer of gaseous products to the environment. In this analysis, the gas phase products are considered to be instantaneously removed as they are produced at temperature T_s and they are not allowed to participate in any heat trans-

fer to the environment. This approach is taken not solely for simplicity, but in looking forward to the adaptation of this model to the case of heterogeneous metal ignition as characterized by the deposition of a solid-phase product on the surface, it is recognized that such a product cannot participate in the transport of heat from the reacting surface to the environment.

By expressing each of the above terms explicitly, Eq (6) can then be written in the following manner:

$$\dot{q}_{loss} = k_f \left. \frac{\partial T}{\partial r} \right|_{r=r_0} + k_g \left. \frac{\partial T}{\partial r} \right|_{r=r_0} + \epsilon \sigma (T_s^4 - T_\infty^4) \quad \text{Eq (7)}$$

where

- k = thermal conductivity of the fuel or oxidizer gas mixture (denoted respectively by subscript f or g), cal/cm.sec.^{°K};
 = temperature gradient evaluated at the surface of the particle ($r=r_0$) either into the fuel ($r=r_-$) or into the oxidizer ($r=r_+$), ^{°K}/cm;
 = total surface emissivity, dimensionless;
 = Stephen-Boltzmann constant, cal/cm².sec. (°K)⁴;
 T_∞ = effective radiation temperature of the environment, °K.

The general form of the \dot{q}_{loss} vs T curve as obtained from the addition of these three heat loss terms is depicted in Fig. 1b. Notice that at the origin, where T_s is equal to the ambient gas temperature T_{amb} , \dot{q}_{loss} is equal to zero. In order that this be true, it is necessary that the overall temperature (both internal and surface) of the sample be equal to T_{amb} before heating begins. If T_{amb} is taken to be room temperature (298 K), then this becomes a perfectly reasonable approximation of an actual physical heating process. In other words, for convenience, the heating of the sample is considered to take place in a room temperature environment in which the original temperature of the sample is also 298 K. Thus, if $T_s = T_{amb} = 298$ K, then \dot{q}_{loss} is equal to zero since only then is $\dot{q}_{cond,f}$ equal to zero.

Other values of T_{amb} can also be considered, but it is felt that this example is the easiest to visualize; indeed the curves can quite simply be extended to other values of T_{amb} as will be made clearer in a discussion of Fig. 2 at the end of this section.

If the most general case is considered, the \dot{q}_{chem} and \dot{q}_{loss} curves may be combined in the fashion depicted in Fig. 1c in which the points of intersection defining equilibrium conditions at the sample surface are obtained. The end points of intersection at the low and high temperature regions of Fig. 1c are both stable equilibrium temperatures with respect to small perturbations of the surface temperature T_s since:

$$\left(\frac{\partial \dot{q}_{chem}}{\partial T_s} \right) \bigg|_{T_s = T_{oxid}} < \left(\frac{\partial \dot{q}_{loss}}{\partial T_s} \right) \bigg|_{T_s = T_{oxid}} \quad \text{Eq (8)}$$

and

$$\left(\frac{\partial \dot{q}_{chem}}{\partial T_s} \right) \bigg|_{T_s = T_f} < \left(\frac{\partial \dot{q}_{loss}}{\partial T_s} \right) \bigg|_{T_s = T_f} \quad \text{Eq (9)}$$

Physically this means that at temperatures somewhat greater than T_{oxid} or T_f , \dot{q}_{loss} is greater than \dot{q}_{chem} and thus T_s tends to decrease; at temperatures somewhat less than T_{oxid} or T_f , \dot{q}_{loss} is less than \dot{q}_{chem} and T_s tends to increase. Therefore, T_{oxid} and T_f are stable temperatures to which the system tends to converge.

The high temperature intersection T_f physically represents the flame temperature and is then the steady-state self-sustained combustion mode of the system. For metals, the flame temperature is limited by enthalpy considerations to the boiling point of the metal oxide.

The low temperature intersection T_{oxid} is referred to as the oxidation temperature. It physically represents the ordinary slow, kinetically controlled, surface oxidation reaction common at this low temperature. However, as can be seen by the fact that the \dot{q}_{chem} and \dot{q}_{loss} curves are nearly tangent at T_{oxid} , the true oxidation process realistically occurs over a short temperature range (12).

The center point of intersection, denoted by T_{crit} is called the critical temperature and is an unstable equilibrium surface temperature since:

$$(\dot{q}_{chem})|_{T_s = T_{crit}} = (\dot{q}_{loss})|_{T_s = T_{crit}}$$

$$\left(\frac{\partial \dot{q}_{chem}}{\partial T_s}\right)|_{T_s = T_{crit}} > \left(\frac{\partial \dot{q}_{loss}}{\partial T_s}\right)|_{T_s = T_{crit}} \quad \text{Eq (10)}$$

Thus, surface temperatures less than T_{crit} tend to decrease to T_{oxid} since here \dot{q}_{loss} is greater than \dot{q}_{chem} and surface temperatures greater than T_{crit} tend to increase to T_s since here \dot{q}_{chem} is less than \dot{q}_{loss} . It is the latter of the above situations that is so important in this development, i.e., once the critical temperature is reached, the system tends to higher temperatures. Because this phenomenon is so vital to a complete understanding of the ignition problem, the critical temperature T_{crit} is defined as follows: T_{crit} is the lowest initial surface temperature from which the surface may self-heat to reach the steady-state combustion configuration.

The critical temperature is commonly called the spontaneous ignition temperature in the literature. It is here labeled the critical temperature in order to avoid confusion with the experimental ignition temperature shortly to be discussed. The existence of this critical temperature is the basic cause of the metal dust explosions that on occasion occur in various industrial plants.

It is now important to define an ignition temperature T_{ign} which can be easily related to the experimental ignition temperature. For most systems, the experimental ignition temperature is usually taken to be that temperature at which the flame appears. When the flame appears, whether it be vapor-phase or surface combustion, there occurs simultaneously the most rapid rate of change with time of both light intensity and sample temperature*. Since temperature runaway is the most obvious phenomenon of the ignition process and since it is the easiest to measure, especially for metals which burn on the surface, it is convenient to define a theoretical ignition temperature in terms of this particular property of the ignition process.

Now, since the aforementioned control volume is assumed to be at a uniform temperature T_s , the time rate of change of the surface temperature can be expressed as a linear function of the quantity $(\dot{q}_{chem} - \dot{q}_{loss})$ as follows:

$$\rho \delta c_p \frac{\partial T_s}{\partial t} = \dot{q}_{chem} - \dot{q}_{loss} \quad \text{Eq (11)}$$

where

- ρ = density of the fuel, g/cm³;
- δ = thickness of the control volume ($\delta \neq 0$), cm;
- c_p = fuel specific heat, cal/g.°K.

According to Eq. (11) then, the ignition temperature can be defined by that point at which the maximum difference between \dot{q}_{chem} and \dot{q}_{loss} exists. Now since the ignition temperature must be above the critical temperature, and below the flame temperature, then the ignition temperature T_{ign} can be represented graphically as in Fig. 2**.

Mathematically, the ignition temperature is defined by looking for the maximum value of $(\dot{q}_{chem} - \dot{q}_{loss})$ above T_{crit} but below T_f . Therefore:

$$\frac{\partial}{\partial T_s} (\dot{q}_{chem} - \dot{q}_{loss})|_{T_s = T_{ign}} = 0 \quad \text{Eq (12)}$$

where

$$T_{crit} \leq T_{ign} \leq T_f \quad \text{Eq (13)}$$

* In the course of many experiments with various metals, the maximum change of light intensity and temperature appear to always coincide.

** In this graph, the internal coordinate system is identical to Fig. 1c.

Thus, the full definition of the experimental ignition temperature becomes the following:

$$\left\{ \left(\frac{d\dot{q}_{chem}}{dT_s} \right) \Big|_{T_s=T_{ign}} = \left(\frac{d\dot{q}_{loss}}{dT_s} \right) \Big|_{T_s=T_{ign}} \right\} \quad T_{crit} \leq T_{ign} \leq T_f \quad \text{Eq (14)}$$

The above then points out the theoretical difference between T_{crit} and T_{ign} as interpreted on a \dot{q} vs T diagram. At T_{crit} , the magnitudes of \dot{q}_{chem} and \dot{q}_{loss} are equal; at T_{ign} , the slopes of the \dot{q}_{chem} and \dot{q}_{loss} curves are equal. Physically, this distinction that has been introduced between the ignition temperature and the critical or spontaneous ignition temperature is a very important one, since it allows for the distinct possibility of the existence of an ignition delay time. This possibly long self-heating time, possibly due to an oxide accumulation on the surface, is what must be prevented when metal particles are used to increase the performance of rocket combustion chambers, for example. Thus, in these applications, the ignition temperature, not the critical temperature, is of prime importance in dealing with ignition inefficiencies.

As intimated above, the ignition delay time in metal ignition may be of the order of minutes rather than a few seconds or milliseconds as in a homogeneous gaseous ignition process. This large difference in ignition delay time between heterogeneous and homogeneous systems is essentially due to the need for oxidizer diffusion to, and absorption on, the fuel surface in the case of a heterogeneous chemical reaction. If the rate of chemical heat input, \dot{q}_{chem} , for a heterogeneous system is represented in Arrhenius form, as for a homogeneous system, then the computed values of \dot{q}_{chem} will indicate the influence upon heterogeneous reaction of the physical processes of diffusion and absorption. The much lower value of \dot{q}_{chem} for a heterogeneous system, as compared to that in a homogeneous system, accounts for the large ignition delay time for such reactions, since $d\dot{q}/dT$ is a linear function of $(\dot{q}_{chem} - \dot{q}_{loss})$ for homogeneous as well as heterogeneous systems.

Now, for both homogeneous and heterogeneous systems in the kinetic range, \dot{q}_{chem} and thus the ignition delay time is a strong function of the kinetic frequency of pre-exponential factor, if the appropriate reaction rate is expressed in Arrhenius form (19). On the basis of collision theory, it has been found that in general the more complicated the chemical reaction process, the smaller in magnitude is the kinetic frequency factor and thus the slower is the reaction rate (20). For homogeneous bimolecular reactions, the frequency factor is on the order of 10^{10} to 10^{14} cm³/mole-sec and for unimolecular reactions, around 10^{13} to 10^{17} sec⁻¹ (19,20). For heterogeneous reactions, the pre-exponential factor has a value for metal systems of 10^{-3} to 10^{-8} gm²/cm⁴-sec for protective oxide systems and 10^{-1} to 10^{-6} gm/cm⁴-sec for non-protective oxide systems (21,22). Thus, for a complicated heterogeneous metal reaction, \dot{q}_{chem} is much smaller in magnitude; in addition, there is a further reduction of \dot{q}_{chem} and thus a longer ignition delay time for a heterogeneous reaction due to the onset of the diffusional control of the reaction rate at higher surface temperatures.

Fig. 2 displays all of the above defined surface temperatures on a diagram covering the entire temperature range starting at 0°K. The internal coordinate system has its origin at $\dot{q}=0$, $T_s=T_{amb}$ and is the coordinate system used in Fig. 1. However, the extension to 0°K is made here in order to discuss some of the properties of the heterogeneous ignition system in more detail.

At 0°K, \dot{q}_{chem} goes to zero; this is appropriate since at lower temperature the molar reaction rate k which is a factor in determining \dot{q}_{chem} is in the kinetic regime and as T goes to zero, indeed the exponential term in Eq. (4) approaches zero thereby forcing k and thus \dot{q}_{chem} to also approach zero. As discussed previously \dot{q}_{loss} approaches zero as T approaches T_{amb} if the temperature of the sample before heating (at $t=0$) is also T_{amb} . The ambient temperature is usually taken to be 298°K since the process is much easier to visualize at room temperature. However, any other value of T_{amb} may be used, but the initial temperature of the sample must also be raised to T_{amb} in order that \dot{q}_{loss} be equal to zero at T_{amb} . This may seem very artificial, but again, it is done in this manner simply for the sake of clarity in the development of the model.

More importantly, however, the ambient temperature is taken to be 298°K because this will give the most general results in terms of the three points of intersection shown in Fig. 1c. In other words, by varying T_{amb} for a fixed value of T , \dot{q}_{chem} stays essentially constant while \dot{q}_{loss} varies a great deal and thus it is possible that only one point of intersection, either at the low temperature or high temperature end of the scale, will appear. In this case, the sample will either never ignite or always ignite. This situation is not of general interest here and thus

T_{amb} is taken to be near room temperature. However, even in this case, if the initial temperature of the sample is kept at the appropriate T_{amb} for the system, then q_{loss} is equal to zero at that particular $T_s = T_{amb}$.

In the unsteady problem, q_{loss} need not always be equal to zero at $T_s = T_{amb}$. At any constant value of T_s , once the heating process has begun, q_{loss} decreases equally over the entire temperature range, due to the conduction losses to the interior of the metal sample (12). In fact, q_{loss} takes on negative values at $T_s = T_{amb}$ since now the internal energy of the sample tends to heat the surface because the interior temperature is greater than the surface temperature, and therefore q_{loss} actually becomes a heat source. Now, a diagram similar to Fig. 2 can be graphed for any time t^* in the heating process. But for any time greater than $t=0$, q_{loss} will not be equal to zero at $T_s = T_{amb}$ since the entire sample has now gained energy from the heating process at a higher surface temperature.

This last paragraph deserves a little more clarification since it implies other details of the model as interpreted here that are not so obvious. Recall that Fig. 2 represents a strictly time-independent system and, therefore, one must use extreme caution in analyzing for example the variation of surface temperature with time in an actual physical heating process. This graph then strictly represents the instantaneous attainment of a surface temperature T_s artificially put on the surface of a fuel sample of original overall temperature T_{amb} in a gaseous atmosphere of temperature T_{amb} . This is somewhat analogous to the dumping of a sample in a heat bath in which the sample surface instantaneously attains the bath temperature, except that here there is another variable in that the atmosphere has an independent temperature T_{amb} equal to the overall temperature of the sample at time $t = 0$.

Now, imagine the sample in equilibrium with the oxidizing atmosphere at T_{amb} . Instantaneously a higher temperature T_s is made to appear on the fuel surface; it remains there until at a later time when instantaneously the original ambient temperature T_s is put on the surface. At this juncture, q_{loss} cannot be equal to zero at $T_s = T_{amb}$ since the interior of the sample is not at temperature T_{amb} , but at a higher temperature, which tends to heat the surface thus making q_{loss} a negative quantity since indeed this process represents a heat gain. Therefore, all the diagrams in this report represent steady-state situations at time $t=0^+$ when q_{loss} is equal to zero at $T_s = T_{amb}$.

Not only is this done for better visualization of the actual theoretical ignition process, but also for a much more practical reason. The essential use for these diagrams is to be able to predict if a fuel sample will or will not ignite. If it does not ignite, it must stabilize at T_{oxid} ; if it does ignite, it must reach T_f . Although the actual values of T_{oxid} and T_f will vary with time somewhat (12), whatever values they represent will eventually be reached in the final steady-state configuration of the fuel sample. In application, the main query is to whether or not the sample will ignite with a given set of initial conditions on the problem. Therefore, the determination of whether or not ignition will take place must be answered practically at time $t = 0^+$, which is really the main reason for graphing these curves at this particular value of time.

Looking again at the q_{loss} curve in Fig. 3, it can be seen that at $T_s = T_{amb}$, q_{loss} becomes an actual heat gain even at time $t=0^+$. This is again true because at $T_s = T_{amb}$, the interior temperature of the sample is greater than the surface temperature.

Also, because q_{loss} is equal to zero at $T_s = T_{amb}$, then for this case in which there is no solid phase product deposited on the sample surface, the stable low-temperature oxidation temperature T_{oxid} is somewhat higher than T_{amb} . Although this may seem peculiar in light of practical experiences with metals, there is a fairly simple explanation that will be discussed in detail in the following section.

HETEROGENEOUS IGNITION WITH SOLID-PHASE REACTION PRODUCTS - All of the preceding has been for the case where the products of combustion appear in the gas phase. For metals, the greatest difficulty comes about through the fact that a solid state metal oxide coating appears on the surface of the sample. This represents one more level of difficulty in the treatment of the heterogeneous ignition problem.

Again, a spherical fuel sample in a static oxidizing atmosphere is considered. The control volume includes those products formed on the reaction surface. In addition, the product temperature is uniform and equal to the surface temperature so that the solid-phase products do not contribute to the heat transfer characteristics of the configuration. Indeed, all the assumptions of the previous section are maintained such that the equations and concepts developed there remain valid for the case of solid-phase product formation.

It has been well-established in isothermal oxidation experiments that, in general, at low temperatures, the presence of the metal oxide film leads to the so-

called protective oxidation rate laws while at higher temperatures, the product film offers no protection to further oxidation and the linear rate law is observed (21,23,24)*. These rate laws in general are of the form:

$$\frac{dx}{dt} = k_n / x^{n-1} \quad \text{Eq (15)}$$

where

x = mass of oxygen consumed per unit surface area at time t , gm/cm^2 ;
 k_n = rate constant, $(\text{gm/cm}^2)^n/\text{sec}$;
 n = oxidation law index, dimensionless.

The variable x may alternatively represent the mass of metal transformed to the oxide or the thickness of the oxide layer in the case of a uniform, plane parallel oxide film. However, the amount of oxygen consumed in the oxidation process per unit surface area is most widely applicable to metals of interest and most measurements of the rate constant have been made in this form (21,22).

Integration of equation (Eq. 15) with $n=2$ or $n=3$ gives respectively the parabolic or cubic protective rate law:

$$x^2 = 2k_2 t + C_2 \quad \text{Eq (16)}$$

$$x^3 = 3k_3 t + C_3 \quad \text{Eq (17)}$$

The logarithmic law is another common example of a protective rate law:

$$x = k \ln t + C \quad \text{Eq (18)}$$

Integration of equation (15) with $n=1$ gives the linear rate law:

$$x = k_1 t + C_1 \quad \text{Eq (19)}$$

In contrast to the protective rate laws (parabolic, cubic, logarithmic), for which the rate of reaction dx/dt decreases with time, the rate of reaction for linear oxidation is independent of time and is thus independent of the amount of gas or metal previously consumed in the reaction. In other words, here the rate of reaction is independent of the amount or thickness of the oxide film on the sample. One explanation of this phenomenon that is most usually experimentally observed (21,23) is that the oxide film has either become porous or has cracked so that the metal surface is not protected from the oxidizing atmosphere.

In most circumstances the parabolic protective oxidation rate law appears at average temperatures; as the temperature increases, the non-protective linear rate law usually appears before ignition occurs. Thus, at lower temperatures, the heterogeneous reaction rate is inhibited by this product film, while at higher temperatures the reaction rate is essentially independent of the product film. Now the temperature at which this changeover occurs is called the transition temperature, T_{trans} . It is the lowest temperature above which the metal-oxidizer system is controlled by a linear oxidation rate law that persists until metal ignition occurs.

Now, since below this transition temperature the metal is protected, the transition temperature must be less than or equal to the ignition temperature. In fact, the transition temperature is the lowest possible ignition temperature for any metal-oxidizer system. This fact will become clearer in the next section.

Mellor (12) attributed the appearance of the transition temperature to a phase change or other changes leading to stress or thermal cracking of the oxide film or perhaps melting of the oxide as in the case of aluminum. Now the linear rate law may not only be due to the non-protectiveness of the oxide layer as intimated by the above mechanisms, but may also arise from other physical mechanisms such as a non-porous barrier layer between the metal substrate and a porous outer oxide layer (12, 23). Therefore, the transition temperature only defines the appearance of a non-protective linear rate law which persists at all higher temperatures between T_{trans} and T_{ign} .

* See these same references for a discussion of the microscopic mechanisms behind these laws.

In view of the significance of the transition temperature in defining the effect of the solid oxide layer in metals, this problem may be graphically analyzed via an uncomplicated extension of the simpler problem of heterogeneous ignition with gas-phase reaction products as displayed in Fig. 1c. At lower temperatures the molar reaction rate \dot{m} will be reduced due to the presence of the protective product film. Since \dot{m} here is in the kinetic regime, \dot{q}_{chem} will decrease following Eqs. (1) and (4) due to a decrease in the pre-exponential factor and an increase in the activation energy. At temperatures above T_{trans} , \dot{q}_{chem} is assumed to approach the value for a clean surface although this is not strictly true in the real case since some oxide always adheres to the exterior of the metal. The \dot{q}_{loss} curve remains the same since the solid oxide coating has been included in the control volume.

Consider now the region near the critical temperature which represents the area of changeover from high temperature oxidation to ignition and subsequent steady-state combustion. Fig. 3a depicts this region for the case of no solid-phase product formation. Figs. 3b and 3c depict the case of solid-phase product formation for the two possible subcases: $T_{trans} < T_{crit}$ and $T_{trans} > T_{crit}$, where T_{crit} is the original critical temperature for the clean surface*. From these graphs, a criterion for metal ignition may be proposed:

$$\text{If } T_{trans} < T_{crit}, \text{ then } T_{ign} \geq T_{crit} \quad \text{Eq (20)}$$

$$\text{If } T_{trans} > T_{crit}, \text{ then } T_{ign} \geq T_{trans} \quad \text{Eq (21)}$$

If $T_{trans} < T_{crit}$, then the ignition temperature is called critical temperature controlled, whereas if $T_{trans} > T_{crit}$, the ignition temperature is called transition temperature controlled. Most metals are critical temperature controlled, while a few metals such as aluminum and beryllium are thought to be transition temperature controlled.

It is important to note here that a transition temperature controlled metal sample of reasonable size cannot in general self-heat to ignition. This statement is supported by the fact that an impervious oxide layer covering the bare metal should protect the surface from producing a large heat of reaction until $T_s \geq T_{trans}$. Thus, the sample would be expected to stabilize at T_{oxid} for all original $T_s \leq T_{trans}$. In order that this occur, it is necessary that the actual critical temperature, as determined by the protective surface (the solid rather than the dashed curve in Fig. 3c) be greater than T_{crit} , but not less than T_{trans} , so that self-heating may not occur below T_{trans} . In other words, \dot{q}_{loss} must be greater than \dot{q}_{chem} for all $T_s \leq T_{trans}$ and necessarily $T_{trans} = T_{crit}$ for the oxide-protected surface of the bulk metal as depicted in Fig. 3c.

In order to summarize the effects of T_{trans} on all previously defined temperatures of interest, it is necessary to study in detail Fig. 4. Fig. 4 is an extension of Fig. 2 to the case of a heterogeneous reaction with a solid-phase oxide product. The typical decrease in \dot{q}_{chem} below T_{trans} for both a critical and a transition temperature controlled metal is shown here but with emphasis on the critical temperature controlled subcase (the T_{trans} controlled subcase is represented by the dashed \dot{q}_{chem} curve). For this subcase, there is theoretically no change in T_{crit} , as well as no change in T_{ign} and T_f , from the case of a heterogeneous reaction with gas-phase reaction products.

For both subcases, the protective quality of the low temperature oxide film results in a significant lowering of the oxidation temperature from T_{oxid} to T_{oxid}^* . The original value of the oxidation temperature T_{oxid} is, as mentioned in the previous section, somewhat higher than the ambient temperature T_{amb} . However, due to the protective qualities of the oxide layer, the new value of the oxidation temperature T_{oxid}^* is postulated to be very near T_{amb} , as would physically be expected for most metals. For example, calcium is known to get fairly warm if exposed to a room temperature environment, and would be expected to stabilize to some temperature higher than T_{amb} if the oxide coating were continually removed during the oxidation reaction. However, it is also a matter of experience that calcium quickly develops a protective oxide coating and that after some time, the temperature stabilizes close to T_{amb} . Also, since some metal oxides, such as Al_2O_3 , are more protective than others, then metals like aluminum stabilize extremely close to room temperature and thus do have $T_{oxid} \approx T_{amb}$ as shown in Fig. 4.

* The \dot{q}_{chem} curve for the clean surface is represented in these figures by the dashed line.

In summary then, a transition temperature has been defined which separates regions of time-dependent and time-independent reaction rates for heterogeneous metal-oxidizer systems. Ignition is postulated to occur only after this temperature is exceeded and, furthermore, the ignition process occurs exactly as in other heterogeneous systems.

APPLICATION OF THE STEADY-STATE MODEL TO METAL PYROPHORICITY - One of the more interesting properties of metals is the ability of a well-dispersed group of small metal particles to spontaneously ignite when exposed to an oxidizer at room temperature. Although this is a difficult problem to analyze because of the cooperative effort between the particles to minimize the rate of heat loss, it is still possible to study instead the effect of metal sample size on the ignition temperature of a single particle. Such studies have indeed been made on this pyrophoric behavior of metal particles, and it has been concluded that a decrease in sample size generally results in a decrease in ignition temperature. It is of interest here to attempt to explain this phenomenon in terms of the present model of metal ignition. First, however, an overall discussion of this problem seems appropriate.

In order for a metal particle to be able to first, self-heat, and second, self-heat to a fairly low ignition temperature, it is necessary that the total heat release increase with respect to the total heat loss as metal particle size is reduced. Now, as particle size decreases, sample surface area increases with respect to sample volume; that is, the ratio of surface area to volume of the sample (S/V , a suitable size index) increases. This increase in S/V is indicative of a relative increase in the total chemical heat release with respect to the total heat capacity of the fuel particle. Therefore, pyrophoric action can be attributed to an increase in the amount of free surface of the metal, since this is responsible for the inability of the metal particle to dissipate its heat of oxidation rapidly enough, because with more surface area and less volume, more heat is liberated that cannot be dissipated by the metal particle itself.

Of course, the heat of oxidation of the metal will be greatly reduced by a protective oxide coating and thus, a metal with a low transition temperature which in all probability is then a critical temperature controlled metal will tend to be more pyrophoric. Of these critical temperature controlled metals, those which have the highest heat of reaction with the oxidizer in the atmosphere of interest will retain the ability to burn spontaneously for a larger-sized particle. In other words, it is generally true that for an oxygen atmosphere, the higher the heat of formation of the metal oxide, the more pyrophoric is the parent metal (27).

TABLE I
HEATS OF FORMATION OF PREDOMINATING METAL OXIDES*

Oxide	$-\Delta H_f^{298}$	Oxide	$-\Delta H_f^{298}$
Ta ₂ O ₅	488.80	SnO ₂	142.01
Al ₂ O ₃	400.40	SrO	141.10
V ₂ O ₅	381.96	WO ₂	140.94
B ₂ O ₃	303.64	Bi ₂ O ₃	139.00
ThO ₂	293.20	BaO	133.50
Cr ₂ O ₃	272.65	ZnO	83.25
HfO ₂	266.05	FeO	63.50
ZrO ₂	261.50	CdO	62.20
UO ₂	259.20	NiO	57.30
TiO ₂	225.50	CoO	57.10
SiO ₂	217.50	PbO	50.39
MoO ₃	182.65	Cu ₂ O	41.80
MgO	143.70	Ag ₂ O	7.20
BeO	143.10	Au ₂ O ₃	0.80

*Data in kcal/gmole taken from Refs. (21,25).

Table I lists the heats of formation of the predominant metal oxide of some metals of interest in order of decreasing magnitude of their heat of formation. In general, those metals which are known to be pyrophoric such as uranium, zirconium, thorium, and vanadium occur at the head of the list while metals which barely oxidize such as silver and gold indeed are at the end of this table.

Now, in dealing with the phenomenon of metal pyrophoricity in terms of the model developed here, it is necessary to ascertain the degree of influence of metal sample size (S/V) on the critical and transition temperatures. Mellor (12) analyzed by means of the available literature the influence of several variables on the latter and found that although the transition temperature may be dependent to some extent on sample purity and non-isothermal conditions, it is generally independent of such things as surface pretreatment, experimental environment, sample size and is so postulated. On the other hand, the critical temperature may be a strong function of some of these environmental factors since the relative values of q_{chem} and q_{loss} could change with these parameters. In particular, as the sample size decreases, S/V increases and therefore the effect of heat loss will decrease since the main heat loss term, the conduction heat loss into the sample, will decrease*. Since q_{chem} is not a function of S/V in the kinetic regime (See Eqs. 1,2,4), then as S/V increases, the critical temperature will decrease, thus theoretically making it possible for a metal sample to self-heat to ignition from a lower value of the initial surface temperature.

Recall that it has been previously postulated that a metal has its ignition temperature controlled by either its critical or transition temperature depending on whether T_{crit} is greater than or less than T_{trans} . Since the transition temperature is here assumed to be independent of sample size, a transition temperature controlled metal is postulated to have its ignition temperature independent of sample size even though its critical temperature is not, while a critical temperature controlled metal has both its critical and ignition temperatures decrease with a decrease in metal sample size**. In short then, metals whose ignition is controlled by T_{crit} will experience a size effect while metals whose ignition is controlled by T_{trans} will experience no size effect.

It is interesting to note that as a sample size is reduced, and thus q_{loss} is decreased, the metal-oxidizer system will shift from a critical temperature controlled system (Figure 3b) to the appropriate transition temperature controlled system (Fig. 3c). As the particle size is further decreased, it is possible as mentioned in the previous section to have q_{loss} become so small that T_{crit} becomes less than T_{trans} and, therefore, the sample may self-heat from temperatures below T_{trans} to eventual ignition. Indeed, it might perhaps be possible that such a process occurs for a transition temperature controlled metal of bulk size, but here the sudden increase in q_{chem} at T_{trans} is usually much larger and the ignition temperature is thus maintained at its bulk value.

When the size of a metal particle has decreased to the point where the system, which was critical temperature controlled in the bulk regime, is now transition temperature controlled, any further decrease in sample size will have little effect on the ignition temperature, as in any transition temperature controlled situation. In other words, as the particle size decreases, the critical temperature will continue to decrease; however, the ignition temperature will never become less than the appropriate transition temperature for that system.

Turning for a moment to the bulk regime, it is postulated that once the sample reaches a certain bulk size, in reference to the surface, the sample volume is infinite. Thus, the q_{loss} curve will tend to stabilize and consequently the critical and ignition temperatures will tend to remain relatively constant with further increases in size.

In summary then, for metals whose bulk ignition is controlled by the critical temperature, the ignition temperature will decrease with decreasing sample size due to a decrease in the critical temperature. For large samples, the ignition temperature is equal to the bulk ignition temperature; in this regime, the critical and ignition temperatures are relatively independent of size. For intermediate-sized samples, the critical and ignition temperatures will decrease with decreasing sample size until the latter nears the transition temperature. Upon further reduction in sample size, the critical temperature continues to decrease, but the ignition temperature remains relatively constant and approaches the transition temperature. This then is the problem of pyrophoricity, where a small particle may self-heat to the transition temperature and thus ignition, but where a larger sample is not allowed to undergo this physical process.

* Inspection of Eq. (7) for q_{loss} shows that only $q_{cond,g}$ and $q_{cond,f}$ are dependent on sample size with the latter much larger since k_g is much larger than k_f in most all cases.

** See Mellor (12) for a mathematically orientated argument that outlines the influence of T_{crit} and T_{trans} on the ignition temperature.

One of the more notable achievements of this theory is the prediction of the size effect as demonstrated by Mellor with the aid of an induction furnace facility and two critical temperature controlled metals, magnesium and calcium (12). The induction furnace accentuates the size effect since it heats on the surface of the sample as is done in the model, and, thus, makes the conduction losses into the sample very important. In other experimental environments where the metal sample is heated uniformly, it is expected that the size effect will be diminished if the source of the size effect has been correctly assumed to be the conduction heat loss into the metal.

Figs. 5 and 6 demonstrate clearly the size effect in various oxidizing atmospheres at 300 torr for the two metals, magnesium and calcium. Unfortunately, it was not possible in both cases to obtain metal samples with a larger S/V ratio because of the difficulties with industrial production of thin sheets of such metals (12). However, the general trend can be seen on these graphs and furthermore, it appears that the ignition temperature may indeed be minimized at the appropriate transition temperature for the metal under consideration.

THE VARIATION OF THE TRANSITION TEMPERATURE

PREVIOUS RESULTS WITH ALUMINUM - In the early work with aluminum at Princeton, Brzustowski (4,9) found, as had other investigators, that the ignition temperature of this metal in oxygen-argon atmospheres was very close to the melting point of its oxide. Brzustowski also noted, however, that the brightness temperature at ignition for anodized aluminum wires, though constant from 20 atm. to 1 atm., slowly decreased from total pressures of 300 torr to 50 torr. Although Brzustowski (4) attributed this behavior to a change in emissivity, it is very possible that the ignition temperature of aluminum decreases with decreasing oxidizer pressure at these lower ambient pressures. Indeed, Kuehl (14) later found that, whereas the ignition temperature of aluminum is constant at the oxide melting point at higher pressures, for pressures lower than approximately 250 torr, the ignition temperature slowly decreases with decreasing ambient pressure.

Since aluminum is transition temperature controlled, the above behavior of its ignition temperature may logically be explained via some mechanism that would allow the transition temperature to decrease with decreasing pressure below 300 torr. Such a mechanism has been proposed by Kuehl (14) and is depicted on the pressure vs. temperature plot in Fig. 7.

The normal transition temperature for aluminum is known to be its metal oxide melting point, 2042°C. This is represented by the straight vertical line in Fig. 7. Consider now the vapor pressure curve for aluminum metal; from Fig. 7, it can be seen that the oxide melting point is equal to the metal boiling point at a pressure of about 700 torr. Thus, at pressures above 700 torr, the pressure of the aluminum vapor enclosed by the oxide coating can never exceed the total ambient pressure without having the temperature of the sample become greater than the melting point of Al_2O_3 . Therefore, at pressures greater than 700 torr, the transition (and ignition) temperature of aluminum is postulated to be the melting point of the metal oxide.

For ambient pressures below 700 torr, the vapor pressure of aluminum inside the solid oxide shell will become larger than the outside ambient pressure for temperatures greater than the appropriate boiling point of aluminum at the pressure of interest. Thus, it is not possible in this pressure range to reach the oxide melting point without causing a pressure differential across the oxide shell. Depending on the strength of the oxide layer then, it is possible that a certain pressure differential may break the oxide coating at temperatures below the melting point of Al_2O_3 . If the oxide coating is thin and weak, but impervious to the ambient oxidizer, then the transition (and ignition) temperature below 700 torr will closely follow the vapor pressure curve. On the other hand, if the oxide coating is thick, strong, and protective, as is usually the case with aluminum, a higher than ambient metal vapor pressure will be needed to break the oxide coating. Therefore, the transition temperature for pressures below 700 torr will follow a path similar to that found by Kuehl (14) as depicted by the lower curve in Fig. 7*. (Note that a pressure drop from 700 to 250 torr is needed in the case of aluminum to have a large enough pressure differential to break the oxide coat.)

In summary then, the ignition temperature for aluminum is postulated to be controlled by the oxide melting point at higher pressures and the metal boiling point at lower pressures. However, aluminum still remains completely transition temperature controlled since the metal boiling point, like the oxide melting point, is a physical

* Notice that the lower curve approaches the vapor pressure curve at very low pressures. This is to be expected since at very low pressures, the oxide shell naturally becomes thin and weak. The heavy lines in Fig. 11 denote the transition temperature variation for both a strong and weak oxide shell.

property of the metal-oxidizer system and not a chemical property, dependent on the heating characteristics of the system. Thus, it is concluded that the transition temperature may vary considerably with the pressure when the metal boiling point interferes with the natural melting process of the oxide.

Adding even more credence to this argument is the fact that it can be used to explain the cylindrical vapor-phase flame that appears upon ignition of aluminum wires in carbon dioxide-argon atmospheres at pressures below 300 torr (14). Earlier this type of flame was explained by arguing that a barrier layer of Al_2O_3 exists which melts before the porous outer layer of oxide, thus, enabling metal vapor to escape before the wire breaks. Although this process may have a part in establishing the vapor-phase flame, the following argument seems to explain the observed phenomenon much more appropriately.

In heating the wire, the pores in the outer layer are only slightly filled by the pre-ignition oxidation process when the atmosphere contains CO_2 -Ar mixtures. At ambient pressures above 300 torr, the oxide coat must melt before ignition can occur and, hence, a cylindrical vapor-phase flame does not appear. However, at pressures less than 300 torr (in agreement with Fig. 7), there exists a large enough pressure differential across the oxide shell to break the coating at its weakest points, specifically, near large pores, and thus allow metal vapor to escape without completely destroying the integrity of the oxide coat and, hence, the anodized aluminum wire. Consequently, it is indeed possible to observe the cylindrical vapor-phase diffusion flame at these lower pressures.

THE INVESTIGATION OF ZINC (17) - Although the boiling point effect as described above seems to bring together and explain various results with aluminum, only Kuehl (14), using pyrometric means, has offered any evidence at all that indeed the ignition temperature of aluminum at low pressures is controlled by a variable transition temperature which is in turn controlled by the metal boiling point. The fact that the ignition temperature of aluminum may be significantly reduced by using low pressures could be very useful in rocket applications (low pressure solid rockets for space applications). Therefore, it appears to be very important to determine if this phenomenon really does occur for metals such as aluminum.

TABLE 2
FUNDAMENTAL TEMPERATURES OF INTEREST FOR METALS*

Metal	Metal Oxide	Metal Melting Point	Metal Oxide Melting Point	Metal Boiling Point	Metal Oxide Boiling Point	Transition Temperature
Ba	BaO	710	1923	1527	2000	17
Bi	Bi ₂ O ₃	271	860	1470	1890	-
Ca	CaO	848	2580	1240	2850	400
Fe	FeO	1536	1420	2872	-	1200
Pb	PbO	328	897	1753	1516	550
Mg	MgO	650	2800	1105	3600	450
Mo	MoO ₃	2620	795	4507	1155	700
Sr	SrO	774	2430	1366	3000	-
Sn	SnO ₂	232	1127	2260	1850	475
Zn	ZnO	419	1975	907	-	700
Co	CoO	1495	1935	3550	-	1350
Cu	Cu ₂ O	1083	1235	2595	-	1000
Ti	TiO ₂	1677	1855	3277	2750	850
W	WO ₂	3410	1580	5900	-	1000
Zr	ZrO ₂	1855	2677	4474	4300	1300

* Taken and extrapolated from Refs. (12,21,23,24,25,26,27); given in °C. Boiling points are for atmospheric pressure (760 torr).

Unfortunately, direct temperature measurements of bulk aluminum in the induction furnace at Princeton was not possible. Consequently, it was thought that perhaps some other metal might be found which would also demonstrate this behavior at lower pressures. By using existing data on ignition temperatures and boiling points, and the data in Table 2, zinc was chosen as perhaps having a transition temperature controlled by a protective oxide layer, and that at lower pressures, its ignition temperature would be controlled by its boiling point. Laurendeau (17) obtained data

using the Princeton induction furnace facility and the data appeared to bear out these original suppositions. Table 3 lists the measured ignition temperatures of zinc to the nearest five degrees.

TABLE 3
IGNITION TEMPERATURES FOR ZINC METAL

<u>Pressure</u>	<u>Ignition Temperature (°C)</u>	<u>Average Ignition Temperature (°C)</u>
200 torr	785	790±5
	795	
300 torr	815	840±30
	835	(830±15)
	840	
	880	
1 atm	895	905±15
	905	
	920	
3 atm	1035	1040±5
	1040	
	1045	
5 atm	1090	1135±35
	1095	(1095±5)
	1140	
	1150	
	1160	
	1165	
7.5 atm	1160	1165±5
	1170	
10 atm	1140	1160±20
	1175	
12.5 atm	1185	-
15 atm	1290	-

In order to ascertain the validity of the boiling point effect, it is necessary to compare the average ignition temperature at each pressure to the boiling point of zinc at these pressures. The vapor pressure curve for zinc metal, as taken and extrapolated from Refs. (28, 35 and 36) is shown in Fig. 8. The data are not plotted as a $\ln p$ vs. $1/T$ to accentuate the constancy of the ignition temperature above 5 atm. Note the near perfect correlation of the average ignition temperature at each pressure up to 7.5 atm with the boiling point of zinc. This indicates that zinc oxide is in all probability a protective oxide, but that it is thin and weak, and therefore only a slight pressure differential is needed to break the oxide shell. In order to see this point better, it is of interest to look closer at the data listed in Table 3.

At the lower pressures, especially at 200 torr, 1 atm, and 3 atm, there is almost perfect correlation with the zinc boiling point (At 760 torr, Table 2 gives 907°C as the boiling point of zinc, for example.). However, at 300 torr, there is a first indication that the oxide coat may at times require a sizeable pressure differential before it will crack. Nevertheless, in most cases at this pressure, the ignition temperature closely follows the vapor pressure curve as can be seen by comparing the average of the three lower experimental points (the average ignition temperature in parentheses) to the boiling point of zinc at 300 torr. A similar behavior is noted at 5 atm, but here the majority of the data points indicates that a higher pressure gives rise to a stronger oxide coat that, in general, remains protective until 1150°C. When, for some reason, a certain oxide shell is unprotective at this pressure, an ignition temperature comparable to the zinc boiling point at 5 atm ($\sim 1100^\circ\text{C}$) is obtained.

For those runs at 300 torr and 5 atm where the oxide shell is protective to a higher temperature than the corresponding metal boiling point, zinc metal scraps are usually found attached to the sides of the pressure vessel after the run has been completed. This indicates that the ignition process here was "explosive" in the sense that the large pressure differential across the oxide shell caused a spewing out of zinc metal upon breaking of the oxide coating just before ignition occurred. In addition, the temperature traces for these particular runs show that immediately upon ignition, the molten zinc metal almost instantaneously drops in temperature to the appropriate metal boiling point. These particular experimental findings again seem to indicate that the zinc oxide shell is indeed protective to fairly high temperatures.

At higher pressures, the reaction is of course very rapid and, at times, the metal is almost completely consumed before the metal fire can be extinguished. At both 7.5 and 10 atm, the ignition temperature is near 1160°C. This corresponds to the zinc boiling point at 7.5 atm, but to a temperature lower than the metal boiling

at 10 atm. It appears then that the protective qualities of the oxide coat are experimentally beginning to level off near 1150°C. Thermal oxidation data indicates that the zinc transition temperature is greater than 700°C; the present results increase the maximum value of the transition temperature to 1150°C or perhaps higher. This, however, is still significantly less than the melting point of ZnO at 1975°C (See Table 4).

The experimental data at 12.5 and 13 atm are not plotted in Fig. 8 because there is some doubt as to the significance of these results. At both of these pressures, the reaction is almost instantaneous and very explosive in the sense described above. At 15 atm, there was a sudden flash of light and no more; however, reaction had occurred since there was a thick layer of zinc oxide particles covering the entire inner surface of the pressure vessel. At 12.5 atm, there was no flash, but the furnace automatically shut down when the metal explosion occurred due to a short circuit across the work coil caused by the flying zinc metal. (This also happened at 15 atm.). After a few seconds, light appeared from the remaining portion of the sample and reaction then proceeded.

Because of the extremely vigorous reaction and the imminent danger that it posed to the work coil, only one run was made at each of these pressures. However, even these very scanty data perhaps indicate that at higher pressures, the oxide coat becomes much thicker, leading to either the possibility of early cracking of the oxide layer or the presence of an extremely strong oxide shell which causes the transition temperature to increase with increasing pressure. The above statement, however, is to be considered very hypothetical in light of the lack of data supporting it*.

The experimental investigation of the ignition temperatures of bulk zinc shows that, in general, the ignition temperature of zinc increases with increasing pressure in almost perfect correlation with its boiling point at the respective pressures involved. Because the ignition temperature may be greater than the metal boiling point, and the range of ignition temperatures is very large, it would appear that the oxide is protective to some high temperature, although not to the oxide melting point as for aluminum**. Indeed the maximum transition temperature, over the observable pressure range investigated here, appears to be near 1150°C, much less than the maximum possible transition temperature for zinc at the melting point of ZnO (1975°C). This maximum transition temperature (1150°C) denotes the end of the control of T_{trans} by the boiling point and the beginning of the control of T_{trans} by the physical characteristics of the zinc oxide coat as determined by the low temperature oxidation process prevalent in all metals.

Assuming that 1150°C is indeed the maximum transition temperature for zinc***, then below the vapor pressure at 1150°C (7.5 atm), the boiling point of zinc will control the transition and thus the ignition temperatures. However, the oxide coat for zinc, although impervious, is thin and weak; therefore, the ignition temperature will follow the vapor pressure curve instead of a curve similar to the lower curve for aluminum below 700 torr as depicted in Fig. 7. At very low pressures, both aluminum and zinc will follow their vapor pressure curves since very little oxidation takes place at these pressures and thus the aluminum oxide coat also becomes thin and weak. At pressures above 7.5 atm, the ignition and transition temperatures are here assumed to be constant at near 1150°C.

The overall results of the zinc investigation show then that a transition temperature controlled metal can have its ignition temperature controlled by its boiling point for a certain range of low pressures. Thus, for metals like zinc and aluminum, the transition temperature is not necessarily a constant but may be a strong function of pressure if the boiling point becomes the controlling influence in the ignition process. Consequently, although not common to most metals, the boiling point effect is indeed a proven influencing factor that very clearly explains the previously observed lowering of the ignition temperature and the cylindrical vapor-phase diffusion flame below 300 torr in early experimental work with aluminum metal.

* In fact, due to the explosive nature of these reactions, it may be possible that the Al_2O_3 crucible perhaps acted as a catalytic agent or even entered into the reaction. There is, however, no evidence for or against this hypothesis.

** If this were true, the ignition temperature would continue to rise until the ambient pressure increased over 260 atm at which pressure, the boiling point is equal to the melting point of the oxide (1975°C). This is highly unlikely based on the high pressure results obtained in the present investigation.

*** Any other assumption for the maximum transition temperature will not change the reasoning in the argument outlined here. Thus, 1150°C corresponds to the melting point of Al_2O_3 at 2042°C shown in Fig. 7. However, 1150°C is not the melting point of ZnO, but instead represents the simple physical failure of the oxide layer to protect the metal substrate. This phenomenon, as for all other metals, is characterized and defined by the transition temperature.

FLAME MODELS*

In this section the various models that have been presented in the literature to represent the flame structure of metal-oxygen diffusion flames will be reviewed. Attention is focused strictly on those metals which burn in the vapor phase.

The evidence to support the proposed models varies significantly. In some cases visual observation alone is the sole criterion suggesting a flame model. Burning rate calculations performed under the guidelines of this postulated model are then compared with experimentally determined burning rates to judge the validity of the model. Other models result from more complete experimental determinations including such diagnostic measurements as optical spectroscopy, electron microscopy and x-ray diffraction studies of the combustion products, quench studies of metal particles in all stages of combustion, and determination of kinetic rate constants. No effort is made to describe the methods of making burning rate calculations. Such methods are described adequately in Ref. (4). The important aspect of the problem is to establish the proper flame model.

It should be pointed out that unknown or uncertain high temperature values for many of the parameters required in order to be able to perform an analytical calculation of a burning rate, preclude the possibility of definitely establishing one flame model as correct on the basis of comparing calculated and measured burning rates. In the same manner it has not been possible to assess critically the various assumptions that have been made in all of these admittedly idealized and simplified models.

FINITE REACTION ZONE MODEL DUE TO COFFIN - The earliest of these models is due to Coffin (9). In his experiments Coffin studied the burning of magnesium ribbons in various mixtures of oxygen with argon, nitrogen, helium and argon-water vapor. His evidence indicated a vapor phase reaction for magnesium combustion bearing some analogy to the combustion of liquid fuel drops. However, the model generally used for liquid droplets, was not used by Coffin. Instead of this "collapsed flame front" model, a finite thickness for the reaction zone was adopted. Coffin's model is illustrated in Figure 9.

In this cylindrical model, there are three concentric zones. The inner zone AB contains only the metal vapor and the inert diluent. Metal, which is vaporized at the fuel surface by the heat conducted back from the reaction zone, diffuses from the ribbon surface at A, where it is at a temperature close to the boiling point of the metal, to the reaction zone which starts at B. The reaction zone was considered to be at the boiling point of the magnesium oxide, as had been suggested by experimental flame temperature measurements (28,29). It was also believed that the oxide dissociated almost completely upon vaporization (30).

The reaction zone BB' thus consisted of a mixture of magnesium vapor, oxygen and condensed oxide at the boiling point of the metal oxide in a stagnant film of inert gas. It was assumed that chemical equilibrium existed among the species in this zone.

The third zone B'C is the zone through which oxidizer diffuses from the surroundings to the constant temperature reaction zone. The oxygen is heated from the ambient temperature of the surroundings to the flame temperature as it diffuses inward. The condensed oxide from the reaction zone cools as it moves outward from the reaction zone through the zone B'C.

Idealized assumptions which were made for this model were as follows: free convection was ignored; the pressure was considered to be 1 atmosphere throughout the system; the inert gas was considered as a stagnant film throughout the system.

LIQUID OXIDE BUBBLE MODEL DUE TO FASSELL AND CO-WORKERS - A second model for the combustion of metal particles has been proposed by Fassell and co-workers (31,32). Although these authors indicated that the gas phase spherical diffusion flame theory adequately accounted for the combustion of magnesium, they suggested that higher boiling metals did not burn in conformity with this model. A particular case of this latter category of metals was aluminum. In the experiments of Fassell et al, aluminum and various aluminum-magnesium alloy particles were burned in two different types of torches in either methane-oxygen mixtures, or a combination of methane, oxygen and air.

Visual observations, high speed photographic measurements and detailed observations including x-ray diffraction of the combustion products suggested to these workers that the diffusion flame model which had apparently been successfully applied to the combustion of magnesium, did not in fact represent the case of aluminum combustion. Based largely on the appearance of the combustion products, Fassell et al proposed the model which is depicted schematically in Figure 10.

* This section is extracted almost in its entirety from Ph.D. thesis of Sullivan.

A continuous layer of molten oxide covers the metal droplet. The evaporating metal from the droplet, which is considered to be at its boiling point, causes the molten oxide layer to form a bubble. The limiting step to further reaction is considered to be diffusion, through this molten oxide layer, of either metal vapor diffusing outward, or oxygen diffusing inward. Reaction is considered to take place at the liquid oxide interface. The authors considered the possibility of the molten oxide bubble exceeding a critical size and bursting, thus scattering fragments of both oxide and freshly exposed metal.

It was thought that this model provided the explanation of the numerous hollow oxide spheres present in the combustion products. It also satisfied one of the difficulties which arose from the x-ray diffraction studies, namely the appearance of species such as $MgAl_2O_4$ which would not be thought likely to occur in a vapor phase diffusion flame.

COLLAPSED REACTION ZONE MODEL DUE TO BRZUSTOWSKI AND GLASSMAN -The first model due to Coffin subsequently came under criticism by Brzustowski and Glassman (9). In addition to certain facets which they felt had to be included in the analytical model (thermal radiation from the flame front to the surroundings and to the droplet surface; diffusion of oxygen toward the flame front being affected by the condensed product), they stated that the thick reaction zone used by Coffin predicted a flame structure "notably different" from observed flames. Coffin's contribution was felt to be the comparison of the diffusion flames of metals and of hydrocarbons. This comparison of the diffusion flames of metals and of hydrocarbons. This comparison was the basis on which Brzustowski and Glassman proceeded to develop a flame model which is outlined below.

The analysis was based on the theory developed to describe the combustion of hydrocarbon droplets, namely the collapsed flame front model depicted in Figure 11, but was modified to account for specific characteristics pertaining to metal combustion. These particular features are presented below:

- (1) The flame temperature will be fixed at the boiling point of the oxide. Some oxide will always form in the condensed state. (Coffin's model was a particular case of this general statement. His model was specifically for magnesium.)
- (2) The presence of the condensed oxide products will affect the diffusion of oxygen to the reaction zone. Movement of these solid or liquid products must occur due to bulk motion of gaseous species since they cannot diffuse.
- (3) Thermal radiation will probably be an important consideration because of the existence of these condensed species in the high temperature regions of the flame. It can possibly result in higher evaporation rates for the fuel due to an increased heat feedback, but it can also lead to significant losses to the surroundings.
- (4) In the case of metal combustion, evaporation rates of the fuel may not be fast compared to diffusional processes.

With the above considerations in mind, the collapsed flame zone model of Figure 11 becomes the metal combustion model proposed by Brzustowski and Glassman. Heat feedback (due to both conduction and radiation) from the thin flame front B, evaporates metal from the fuel surface at A. This metal vapor, at a temperature which may be several hundred degrees lower than the metal boiling point, diffuses through the stagnant film AB toward the high temperature flame front at B.

Oxidizer from the surroundings diffuses toward the flame front through the film BC. This diffusion of the oxidizer is opposed by the outward movement of combustion products which were formed in the thin flame front at B. Heat is conducted and radiated to the surroundings through this film BC.

As in the case of the earlier model of Coffin, idealizations considered in this model include uniform pressures throughout the system, and a system steady in time. It was assumed that combustion products did not diffuse back to the fuel surface through the film AB, but that all products diffused through the film BC to the surroundings. This last assumption was justified in part by the observation of Brzustowski that although oxide was observed on the wire surface (probably from back diffusion of the products) it did not appear to have an appreciable effect on the observed burning mechanism. As will be pointed out later in this chapter, more recent experimental work of other investigators does not support this assumption of no back diffusion of the combustion products.

An important feature of the Brzustowski-Glassman model is the attention paid to the condensed oxide products. Condensed oxide particles can be transported out of the flame zone only if a bulk outward gas velocity exists in the zone BC. The diffusion equation for this zone gives the conditions under which such a bulk velocity can be achieved.

REFERENCE 29 CONTINUED ON CARD 5

A parameter α is defined as the fraction of the condensed oxide product that is vaporized. This parameter is a function of the flame radius when there is dissociation in the flame zone and subsequent recombination in the zone BC. The result, derived analytically by Brzustowski, illustrates that an outward bulk velocity in the zone BC occurs when more than one mole of gaseous products is formed for every mole of oxidizer participating in the reaction.

In the reaction zone itself, the degree of dissociation of the oxide varies according to the balance between heat liberated in the reaction and heat radiated or conducted to the surroundings. If heat losses are large enough, it would be expected that condensed oxide deposits would appear in the flame front itself.

It has sometimes been incorrectly stated in the literature that a collapsed reaction zone assumption would define zero concentrations for the reacting species at the flame front. Brzustowski (4) points out the correct definition of a collapsed flame front as follows: "..... to a desired degree of accuracy, the dimensions of the reaction zone and the changes in reactant concentrations through it are small with respect to the dimensions and concentration differences involved in the diffusion processes."

Brzustowski found Coffin's thick flame zone model unacceptable because, firstly, it assumed that no gaseous oxide was present because of complete dissociation, whereas spectroscopic observations showed significant oxide vapor radiation and, secondly, Brzustowski's interpretation of his flame photographs showed an entirely different structure. Over a large pressure range from 50 torr to 12 atmospheres the bright flame zone thickness was small in comparison with the dimension between the metal surface and the flame front.

EXTENSIONS OF THE BRZUSTOWSKI-GLASSMAN MODEL DUE TO KNIPE - In a survey paper on aluminum particle combustion by Christensen, Knipe and Gordon (6), a critical discussion of aluminum particle combustion models was presented. The two models discussed were the models due to Fassell et al and the Brzustowski-Glassman model discussed in the previous two sections of this chapter.

One of the criticisms of the model of Fassell and co-workers is that the postulated rate-controlling step of diffusion through the oxide shell must be accepted with some caution because of considerable uncertainty about the magnitude of this diffusion rate. This model does take into account the normal metal oxide coating which exists on the metal particle prior to ignition, but the bubble of oxide which is proposed may be unstable.

A criticism of the Brzustowski-Glassman model is that it does not explain the fate of the normal oxide coating which exists on the metal surface. A suggestion is that the oxide may accumulate in one area giving rise to a metal sphere with an agglomerated oxide cap. The basis for this suggestion comes from observations of such metal-oxide configurations in quench studies. However, this is then a considerable departure from the idealized one-dimensional, spherically symmetric model of Brzustowski and Glassman.

Another criticism of this model is the treatment of dissociation fragments in the reaction zone. Allowing for the fact that their precise nature is not known, aluminum and oxygen atoms are the major fragments of dissociation of the oxide. Since the reaction zone is at a high temperature, it is expected that a heterogeneous reaction will be more likely than vapor-phase reaction to gaseous oxides, and as a consequence the conditions favorable to the nucleation of the condensed oxide may play some role in determining the location of the reaction zone.

Christensen et al conclude from this survey of combustion models that the Brzustowski-Glassman model does describe the gross features of aluminum particle combustion but that there are significant features not contained in the idealized model. As a consequence, Knipe (6) sought to extend the Brzustowski-Glassman model as is indicated below.

The Brzustowski-Glassman model does indicate the conditions under which condensed oxide may build up in the reaction zone. Knipe suggests that this fact should raise strong questions about the applicability of a steady state approximation especially in view of the many statements in the literature suggesting that, because of the condensed nature of the products, radiation will be an important heat transfer mechanism in metal flames. As pointed out previously, Knipe also proposes that the principle reaction path will be via heterogeneous processes on the condensed oxide within the reaction zone. It is also stated that the zone of condensed oxide particles has been observed experimentally to possess considerable thickness. This is a plausible observation for such a proposed heterogeneous reaction zone since dissipation of heat, which occurs most efficiently at the edges of this thick zone, significantly affects the progress of the reaction.

In the Brzustowski-Glassman model, back-diffusion of the gaseous combustion products to the metal surface was assumed not to take place. However, experimental observations of Prentice (33) showed that significant amounts of oxide did build up on the metal surface during combustion, indicating that oxygen-containing species were present in the region between the metal particle and the flame front.

Figure 12 is an attempt to represent schematically the model which Knipe proposes.

This model is characterized by a heterogeneous reaction zone of appreciable thickness which probably extends in both directions with time as mentioned previously. A narrow nucleation zone is expected to exist between the reaction zone and a position where the inward-diffusing oxygen-containing species (both evaporation products and partially reacted species) make up a saturated vapor relative to condensation. A second nucleation zone is proposed on the oxidizer side of the reaction zone.

Note that the importance of recognizing the back diffusion of gaseous combustion products is of more significance than merely explaining some of the features attributed to a non-symmetrical burning configuration (e.g., particle spinning). Condensation of oxide on the metal surface would be an appreciable heat transfer mechanism operating between the reaction zone and the particle surface since much of the heat of reaction is in the heat of condensation.

HETEROGENEOUS REACTION MODEL DUE TO MARKSTEIN - Markstein (34), although he has not set out a specific flame model, has discussed vapor-phase burning of metals and has contributed significantly to the problem of whether or not heterogeneous reaction or homogeneous reaction dominates metal combustion, in particular in the case of magnesium.

Figure 13 is reproduced from Markstein's paper (34) and represents a schematic representation of most of the processes that might possibly play a role in vapor-phase combustion.

Markstein states that heterogeneous reaction on the metal surface is not likely a significant process once the vapor phase flame is fully developed. This statement is reflected in the schematic by the dashed lines used to depict this process.

Back diffusion of oxide vapor is also expected to be significant as evidenced by a consideration of the experimental evidence of Macek (35).

Markstein agrees that the question of heterogeneous versus homogeneous reaction is far from settled and, thus far has been an area of speculation and controversy. In an earlier work (36) Markstein seems to have demonstrated the strong role played by heterogeneous reactions in low pressure dilute magnesium-oxygen flames. In these experiments magnesium vapor was carried in an inert carrier gas (Argon). The mixture of magnesium and argon carrier gas entered the stagnant oxygen-argon atmosphere of the combustion chamber through an orifice. Total pressures ranged from about 2 to 10 torr. The spectra of the resulting flame showed no line and band radiation at all, but instead consisted of continuum radiation with several maxima. In addition, it was observed that oxide growths were present near the orifice. The luminescence of these oxide growths was also characterized by a broad maximum in the blue closely resembling that of the dilute flame spectrum. Markstein suggested that the reaction path was following a heterogeneous route. Recent work of Markstein (34,37,38) has been an attempt to determine rate constants for this proposed heterogeneous reaction and to obtain further experimental evidence to elucidate details of the mechanism.

Markstein is cautious about the interpretation of emission spectra by other authors as being an indication of homogeneous reaction, suggesting that the high electronic energies of the states observed in spectra may be difficult to explain on the basis of kinetic steps that are probably not highly exothermic.

If one were to postulate the structure of a combustion model which would fit the particular conditions of Markstein's experiments, namely low pressure highly-diluted flames, it would appear schematically as indicated in Figure 14.

Note that nucleation zones are not specifically defined. Markstein stated (36) that some homogeneous reaction may be required initially to furnish sites for the ensuing heterogeneous reaction but that in the fully developed reaction it would be expected that homogeneous reaction would not be significant. Since oxide vapor is not present due to the lack of homogeneous reaction, it would also be likely that not much oxide would appear on the metal surfaces. This statement is based on two facts. Firstly, most evaporation products dissociate, and thus, very little oxide vapor for back diffusion could be expected from this process. Secondly, it was pointed out earlier that Markstein felt that heterogeneous reaction on the metal

surface was unimportant when fully developed reaction had been established. Thus, the schematic in Figure 14 indicates no back diffusion of oxide vapor to the metal surface.

THE NEW PRINCETON INNER REACTION ZONE MODEL - Sullivan (39) undertook an experimental investigation to determine the flame structure of metal vapor-phase diffusion flames, in particular the low-pressure flames of the alkaline-earth metals Mg, Ca and Sr. In these studies the flames were generated in two types of experiments. In the first type, metal samples in the form of wires or strands were mounted between electrodes and heated to ignition by passing an electric current through the sample. The resulting "wire flame" was studied by color photography and space-resolved spectroscopy which defined the location of emitters in the cylindrically-symmetric flames. In the second type of experiment, a two-dimensional diffusion flame burner was adapted to low-pressure metal combustion studies. The burner provided a flame with a geometry particularly suited for space-resolved spectroscopic observations. The longer exposure times available for obtaining spectra in the burner experiments permitted the observation of oxide band systems which had not been observed in the wire experiments. The observation of these additional band systems aided in the interpretation of the spectral results obtained from the wire experiments.

This investigation has shown that a reaction exists in the inner zone of the luminous envelope surrounding the metal sample. The production of oxide vapor by homogeneous reaction causes a supersaturation of oxide vapor leading to rapid nucleation. Thus, the inner reaction zone is expected to be a high temperature region of the flame due to the liberation of the heat of condensation. Sullivan demonstrated that the major contribution to the observed radiation is due to a thermal excitation mechanism, although some contribution from chemiluminescent radiation may occur in the inner reaction zone. Based on the thermal nature of the radiation, the self-reversal over a portion of their length of the resonance lines of the metals Ca and Sr respectively, indicates that the inner zone of colored radiation in the flame is hotter than the outer zone.

If the trend shown by Markstein's results (38) illustrating the decrease of collision efficiency (for surface reaction) with increasing temperature continues at higher temperatures, it is anticipated that the inner reaction zone of the flames of Ca and Sr is thus a zone of predominantly homogeneous reaction. Heterogeneous reaction would tend to become more important at larger flame radii where it is expected that the temperature is decreasing.

The model described above is pictured schematically in Figure 15. A comparison of this figure with the figures presented at the beginning of this section demonstrates the differences in the flame model as a result of Sullivan's investigation.

The flame zone does not appear to be a "collapsed reaction zone" as in the model of Brzustowski and Glassman. The peak flame temperature is not expected to be located at the outer edge of the luminous envelope. The reaction zone appears to extend to regions very close to the wire surface, and makes it difficult to determine the size of an inner zone such as in the Brzustowski-Glassman model, zone AB, which is assumed to contain only metal vapor and the inert diluent.

The model due to Coffin (40) assumes an extended reaction zone such as the present investigation indicates, but in Coffin's model this zone is assumed to contain no MgO vapor. It would be impossible to explain the spectroscopic observations of Brzustowski (4,9), Courtney (41), and the present investigation, on the basis of Coffin's model. In addition, the two zones observed in the Ca and Sr flames, namely a reaction zone extending almost to the wire surface, and a second zone containing oxide particles surrounding the zone of colored radiation, are not distinguished by Coffin.

In the proposed extensions of the Brzustowski-Glassman model by Knipe (6), it is assumed that reaction probably proceeds predominantly by heterogeneous reaction in the case of aluminum combustion, and that this reaction proceeds at the cloud boundaries. The role played by heterogeneous reaction in the case of aluminum combustion could be significantly different than for the combustion of the alkaline-earth oxides. Unlike the aluminum oxides, the alkaline-earth oxides are observed to have the same composition in the condensed and gaseous phases. However, Knipe's suggestion that reaction proceeds at the cloud boundaries is appropriate to the flames of the alkaline-earth metals as well, in view of the trend illustrated by Markstein's results showing a strong dependence of the heterogeneous reaction mechanism on temperature. It should be stressed, however, that Markstein's results are for a limited temperature range (410°K to 840°K) and that he states that the results should not be taken as "unqualified evidence" that heterogeneous reaction may be unimportant at higher temperatures.

In summary, Sullivan defines a flame structure model in which a predominantly

homogeneous reaction zone is located well inside the luminous envelope. Heat release, which occurs throughout this reaction zone due to oxide vapor condensation, accounts for the excitation of the species observed to radiate. Oxide particles, formed throughout the reaction zone, are swept out of the inner zone of the flame by the bulk velocity of the gaseous product species and thermophoresis effects. Since both effect decrease with increasing distance from the reaction zone, there is a region in which the particles pile up to form the outer luminous edge of the flame which is characteristic of most metal flame photographs.

REFERENCES

1. GLASSMAN, I., "Metal Combustion Processes", Amer. Rocket Soc. Preprint 938-59, 1959.
2. GLASSMAN, I., "Combustion of Metals. Physical Considerations", in Solid Propellant Rocket Research, Ed. by M. Summerfield, Academic Press, New York, 1960, pp 253-258.
3. BRZUSTOWSKI, T. A. and GLASSMAN, I., "Spectroscopic Investigation of Metal Combustion", in Heterogeneous Combustion, Ed. by Wolfhard, H. G., Glassman, I., and Green, L., Jr., Academic Press, New York, 1964, pp 41-74.
4. BRZUSTOWSKI, T. A., "Vapor-Phase Diffusion Flames in the Combustion of Magnesium and Aluminum", Ph.D. Thesis, Princeton University, Dept. of Aeronautical Engineering, 1963.
5. MARKSTEIN, G. H., "Combustion of Metals", AIAA Journal, 1, (1963), pp 550-562.
6. CHRISTENSEN, H. C., KNIPE, R. H., and GORDON, A. S., "Survey of Aluminum Particle Combustion", Pyrodynamics, 3 (1965), pp 91-119.
7. WOLFARD, H. G., GLASSMAN, I., and GREEN, L., JR., Eds. Heterogeneous Combustion Academic Press, New York, 1964.
8. BAHN, G. S., Ed., Pyrodynamics, 3 (1965), pp 29-168.
9. BRZUSTOWSKI, T. A. and GLASSMAN, I., "Vapor-Phase Diffusion Flames in the Combustion of Magnesium and Aluminum: II. Experimental Observations in Oxygen Atmospheres", in Heterogeneous Combustion, Ed. by Wolfhard, H. G., Glassman, I., and Green, L., Jr., Academic Press, New York, 1964, pp 117-158.
10. MELLOR, A. M., "The Combustion of Aluminum and Magnesium in Carbon Dioxide - Oxygen and Carbon Dioxide-Argon Mixtures", B.S.E. Thesis, Princeton University, Dept. of Aeronautical Engineering, 1963.
11. MELLOR, A. M. and GLASSMAN, I., "Vapor-Phase Diffusion Flames in the Combustion of Magnesium and Aluminum: III. Experimental Observations in Carbon Dioxide Atmospheres", in Heterogeneous Combustion, Ed. by Wolfhard, H. G., Glassman, I., and Green, L., Jr., Academic Press, New York, 1964, pp. 159-176.
12. MELLOR, A. M., "Heterogeneous Ignition of Metals: Model and Experiment", Ph.D. Thesis, Princeton University, Department of Aerospace and Mechanical Sciences, 1967.
13. FRIEDMAN, R. and MACEK, A., "Ignition and Combustion of Aluminum Particles in in Hot Ambient Gases", Combustion and Flame, 6 (1965), pp 9-19.
14. KUEHL, D. K., "Ignition and Combustion of Aluminum and Beryllium", AIAA Journal 3, (1965), pp 2239-2247.
15. MELLOR, A. M. and GLASSMAN, I., "A Physical Criterion for Metal Ignition", Pyrodynamics, 3 (1965), pp. 43-64.
16. FRANK-KAMENETSKII, D. A., Diffusion and Heat Exchange in Chemical Kinetics, Thon, N., Translator, Princeton University Press, Princeton, N. J., 1955.
17. LAURENDEAU, N. M., "The Ignition Characteristics of Metals in Oxygen Atmospheres", M.S.E. Thesis, Princeton University, Department of Aerospace and Mechanical Sciences (1968); also AMS Report No. 851 (1968).
18. FRISTOM, R. M. and WESTENBERG, A. A., Flame Structure, McGraw-Hill, New York, 1965.
19. GRAY, P. and HARPER, M. J., "The Thermal Theory of Induction Periods and Ignition Delays", in Seventh Symposium (International) on Combustion, Butterworths, London, 1959, pp. 425-430.
20. LAIDLER, K. J., Chemical Kinetics, Second Edition, McGraw-Hill, New York, 1965.
21. KUBASCHEWSKI, O. and HOPKINS, B. E., Oxidation of Metals and Alloys, Second Revised Edition, Butterworths, London, 1967.
22. REYNOLDS, W. C., "Investigation of Ignition Temperatures of Solid Metals", NASA TN D-182, 1959.
23. KOFSTAD, P., High-Temperature Oxidation of Metals, Wiley, New York, 1966.
24. HAUFFE, K., Oxidation of Metals, English Edition, Plenum Press, New York, 1965.
25. HODGMAN, C. D., Editor, Handbook of Chemistry and Physics, 46th Edition, Chemical Rubber Publishing Co., Cleveland, 1964.
26. JANAF Thermochemical Tables, The Dow Chemical Co., Midland, Mich., March 31, 1965.
27. KAYE, G. W. C. and LABY, T. H., Table of Physical and Chemical Constants, Wiley, New York, 1966.
28. WOLFARD, H. G. and PARKER, W. G., "Temperature Measurements of Flames Containing Incandescent Particles", Proc. Phy. Soc., (London) 62B, 523-9 (1949).
29. SCARTAZZINI, H., "Combustion du magnésium en poudre dans l'oxygène", Compt. Rend. 230, 97-8 (1950).
30. BREWER, L., "The Thermodynamic Properties of the Oxides and Their Vaporization Processes", Chem. Rev. 52, 1-75 (1953).

31. FASSELL, W. M., PAPP, C. A., HILDENBRAND, D. L. and SERNKA, R. P., "The Experimental Nature of the Combustion of Metallic Powders" in Solid Propellant Rocket Research, ed. by M. Summerfield, Progress in Astronautics and Rocketry, Vol. 1, Academic Press, 1960, p. 259-60.
32. BARTLETT, R. W., ONG, J. N., FASSELL, W. M. and PAPP, C. A., "Estimating Aluminum Particle Combustion Kinetics", Combustion and Flame, 7, 227-34 (1963).
33. THE METAL COMBUSTION STUDY GROUP "Aluminum Particle Combustion Progress Report, 1 April 1964-30 June 1965", Technical Progress Report 415, NOTS TD 3916, U. S. Naval Ordnance Test Station (1966).
34. MARKSTEIN, G. H., "Heterogeneous Reaction Processes in Metal Combustion 11th Symposium (International) on Combustion, The Combustion Institute, Pittsburgh, Pa., (1967).
35. MACEK, A., "Fundamentals of Combustion of Single Aluminum and Beryllium Particles", 11th Symposium (International) on Combustion, The Combustion Institute, Pittsburgh, Pa. (1967).
36. MARKSTEIN, G. H., "Magnesium-Oxygen Dilute Diffusion Flame", 9th Symposium (International) on Combustion, Academic Press, New York, (1963).
37. MARKSTEIN, G. H., "Rate of Growth of Magnesium Oxide Deposits Formed by Surface Reaction of Magnesium Vapor and Oxygen", presented at the Spring Meeting of the Western States Section of the Combustion Institute, Denver, Colorado, 25-26 April 1966.
38. MARKSTEIN, G. H., "Study of the Reaction of Magnesium Vapor and Oxygen at the Surface of MgO Deposits by Atomic-Absorption Spectrophotometry" presented at the 12th International Symposium on Combustion, Poitiers, France, July 1968.
39. SULLIVAN, H. F., "The Structure of the Alkaline-Earth Metal Diffusion Flame", Princeton University Ph.D. Thesis (1969), Department of Aerospace and Mechanical Sciences; also AMS Report No. 865 (1969).
40. COFFIN, K. P., "Some Physical Aspects of the Combustion of Magnesium Ribbons", Fifth Symposium (International) on Combustion, Rheinhold, New York, (1955) pp 267-76.
41. COURTNEY, W. G., "Homogeneous Nucleation from Simple and Complex Systems", pp 677-699 Heterogeneous Combustion, Wolfhard, H. G., Glassman, I., and Green, L., Jr., Editors Academic Press, New York (1964).
42. EYRING, H. and ZWOLINSKI, B. J., "The Foundations of Reaction Rate Theory and Some Recent Applications", Record Chem. Prog. 8, (1947), pp 87-102.
43. FASSELL, W. M., JR., GULBRANSEN, L. B., LEWIS, J. R., and HAMILTON, J. H., "Ignition Temperatures of Magnesium and Magnesium Alloys", J. Metals 3, (1951), pp 522-528.
44. HILL, P. R., ADAMSON, D., FOLAND, D. H., and BRESSETTE, W. E., "High-Temperature Oxidation and Ignition of Metals", NACA RM L55L23b, (1956).
45. TALLEY, C. P., "The Combustion of Elemental Boron", Solid Propellant Rocket Research, Summerfield, M., Editor, Academic Press, New York, (pp 279-285) (1960).
46. MACEK, A., FRIEDMAN, R., and SEMPLE, J. M., "Techniques for the Study of Combustion of Beryllium and Aluminum Particles", Heterogeneous Combustion, Wolfhard, H. G., Glassman, I., and Green, L., Jr., Editors, Academic Press, New York, (1964) pp 3-16.
47. NAGY, J. and SURINCIK, D. J., "Thermal Phenomena During Ignition of a Heated Dust Dispersion", Bureau of Mines RI 6811, (1966).
48. ANDERSON, H. C. and BELZ, L. H., "Factors Controlling the Combustion of Zirconium Powders", J. Electrochem. Soc. 100, (1953), pp. 240-249.
49. TETENBAUM, M., MISHLER, L., and SCHNIZLEIN, G., "Uranium Powder Ignition Studies", Nucl. Sci. Eng. 14, (1962), pp. 230-238.

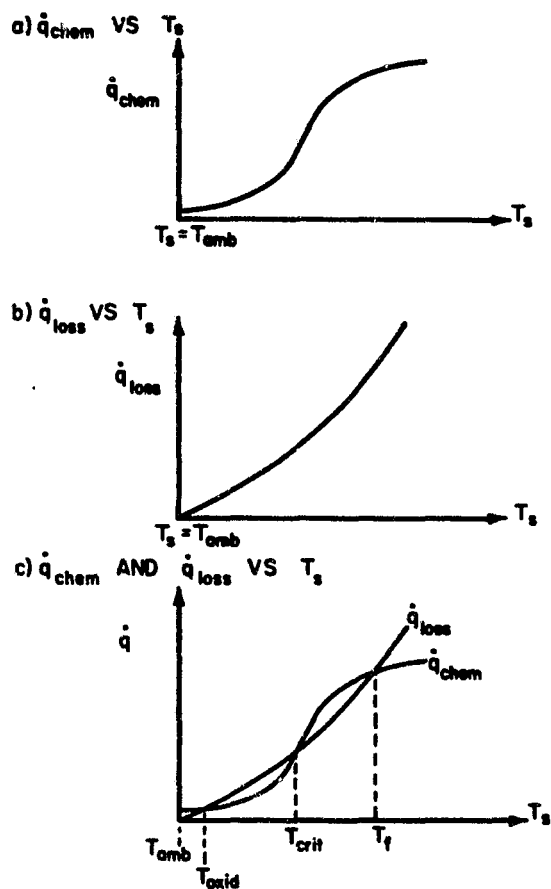


Fig.1 Heterogeneous ignition: rate of chemical energy release and rate of heat loss vs. surface temperature

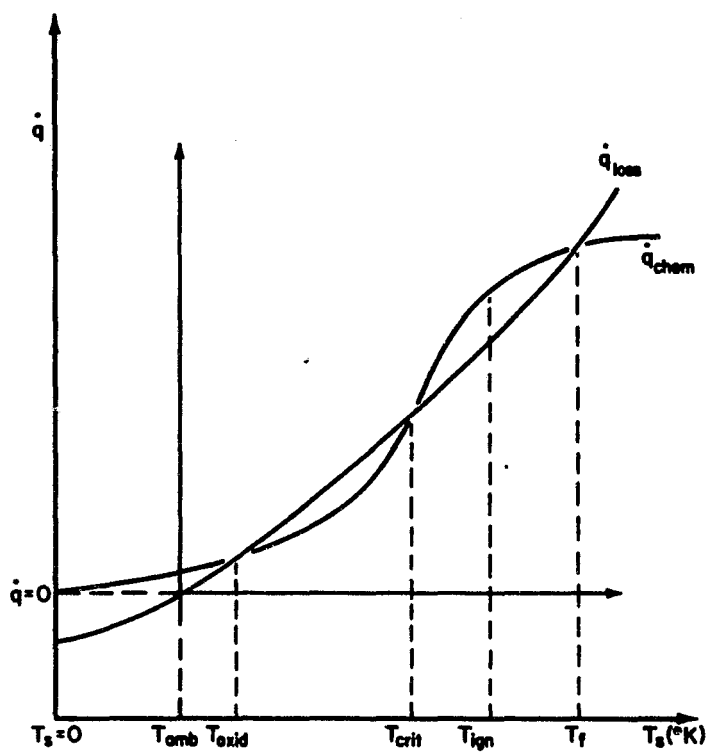


Fig.2 Heterogeneous ignition: complete variation with temperature

a) NO SOLID-PHASE PRODUCT

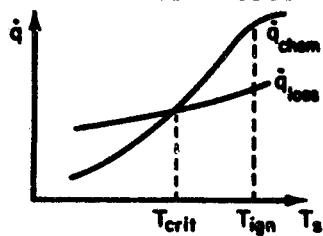
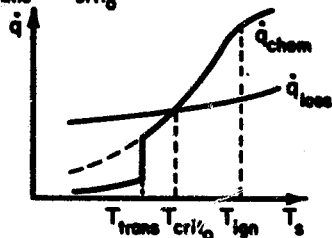
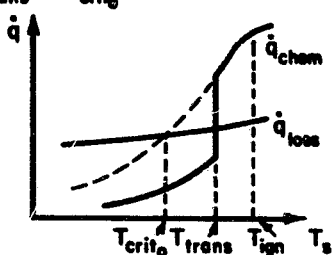
b) $T_{trans} < T_{crit_0}$ c) $T_{trans} > T_{crit_0}$ 

Fig.3 The ignition criterion

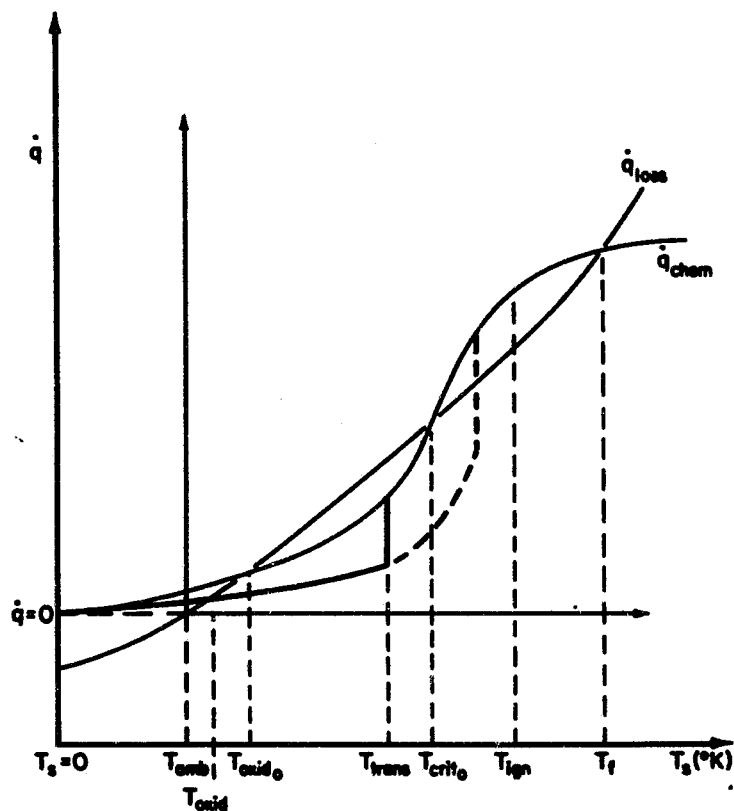


Fig.4 The low temperature effects of the transition temperature

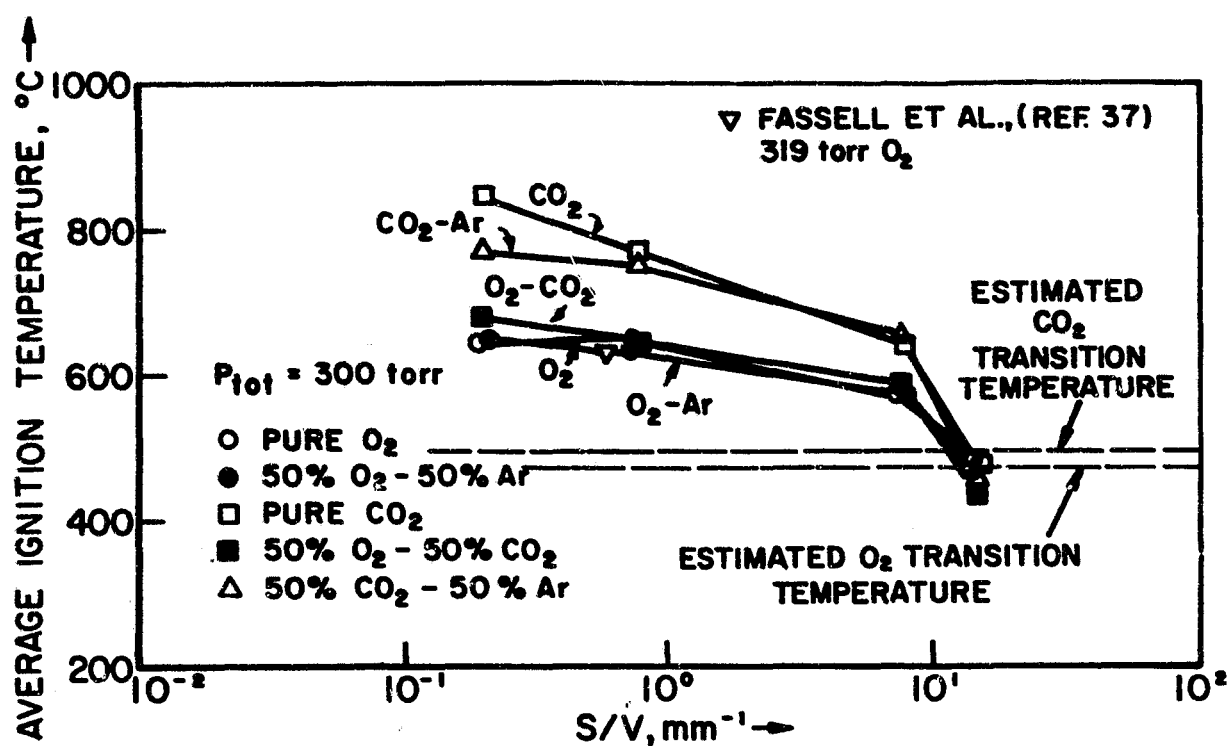


Fig.5 Magnesium average ignition temperature in various oxidizing gases vs. surface to volume ratio (total pressure = 300 torr)

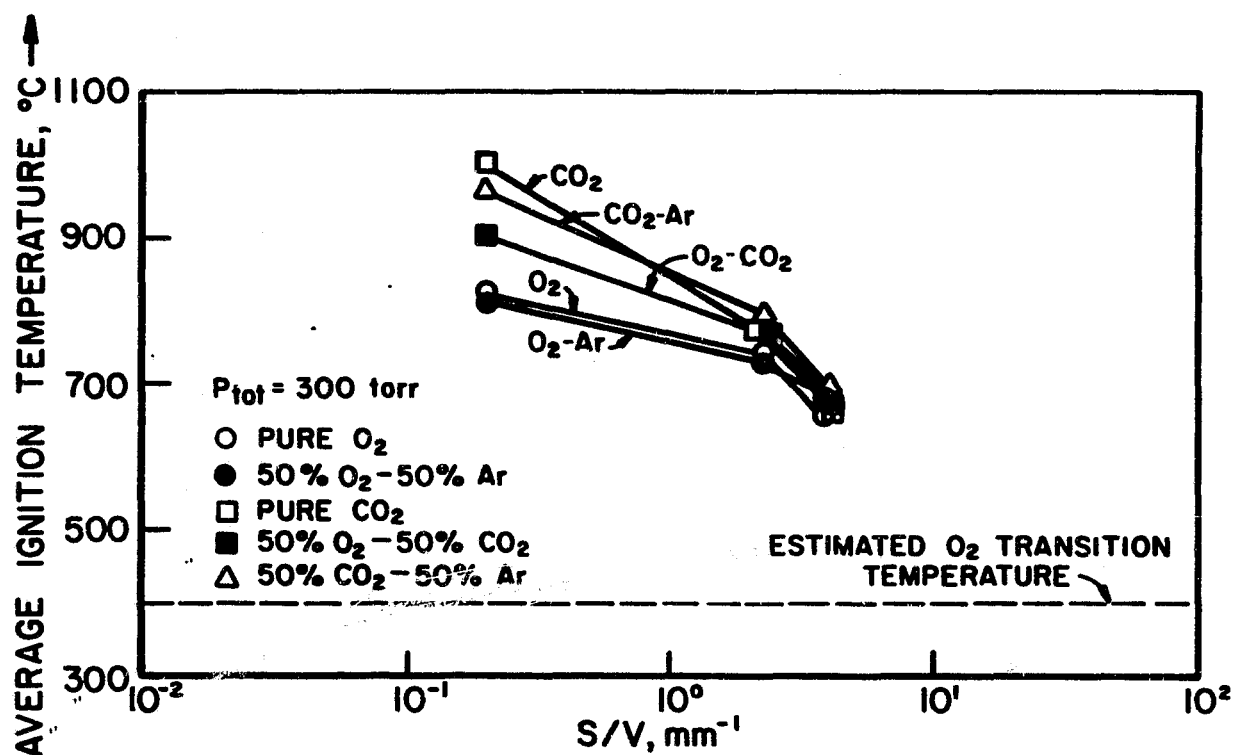


Fig.6 Calcium average ignition temperature in various oxidizing gases vs. surface to volume ratio (total pressure = 300 torr)

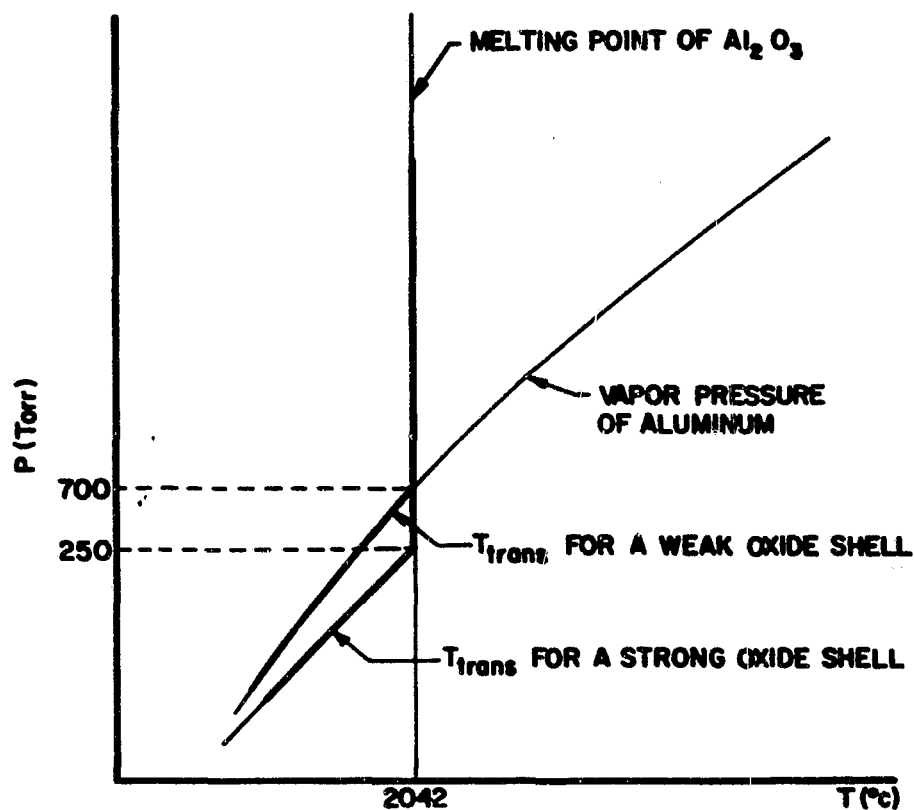


Fig.7 Transition temperature vs. pressure for aluminum

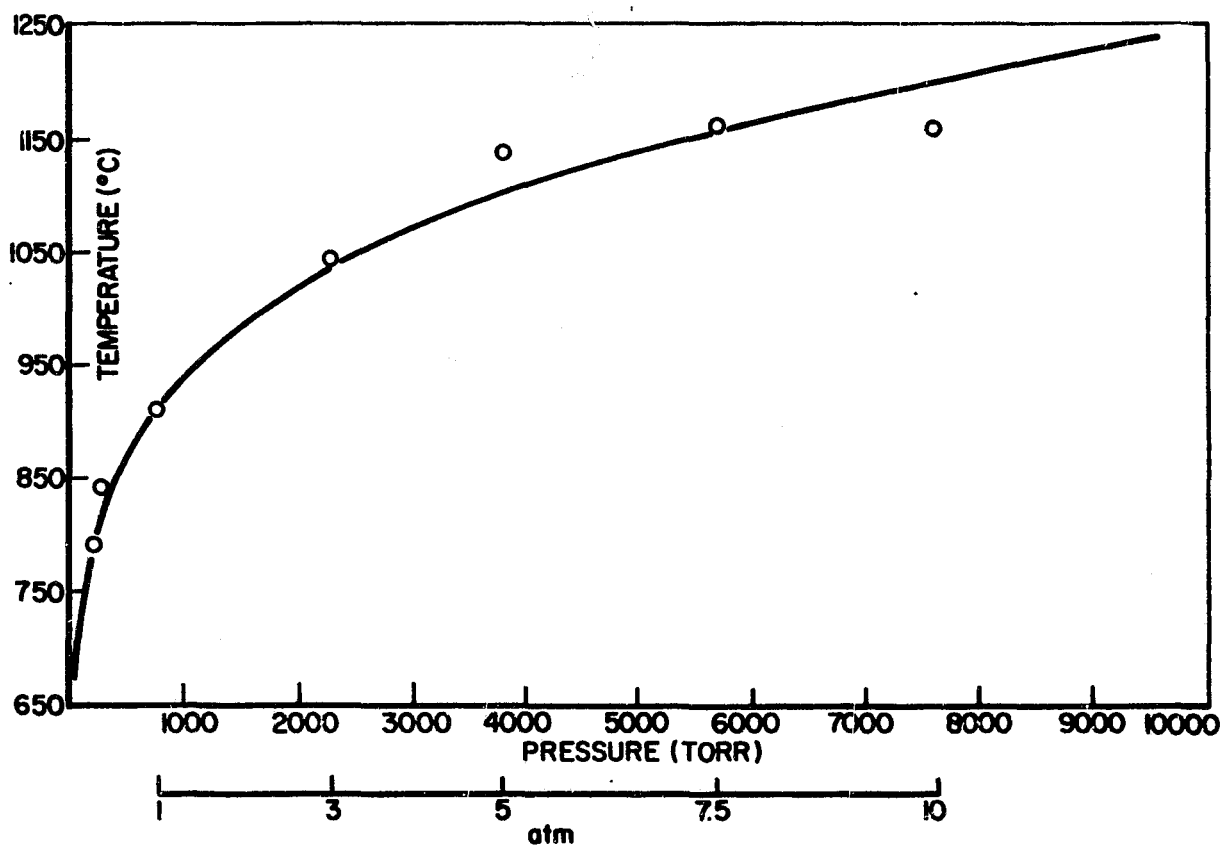


Fig.8 Ignition temperatures vs. boiling points for zinc

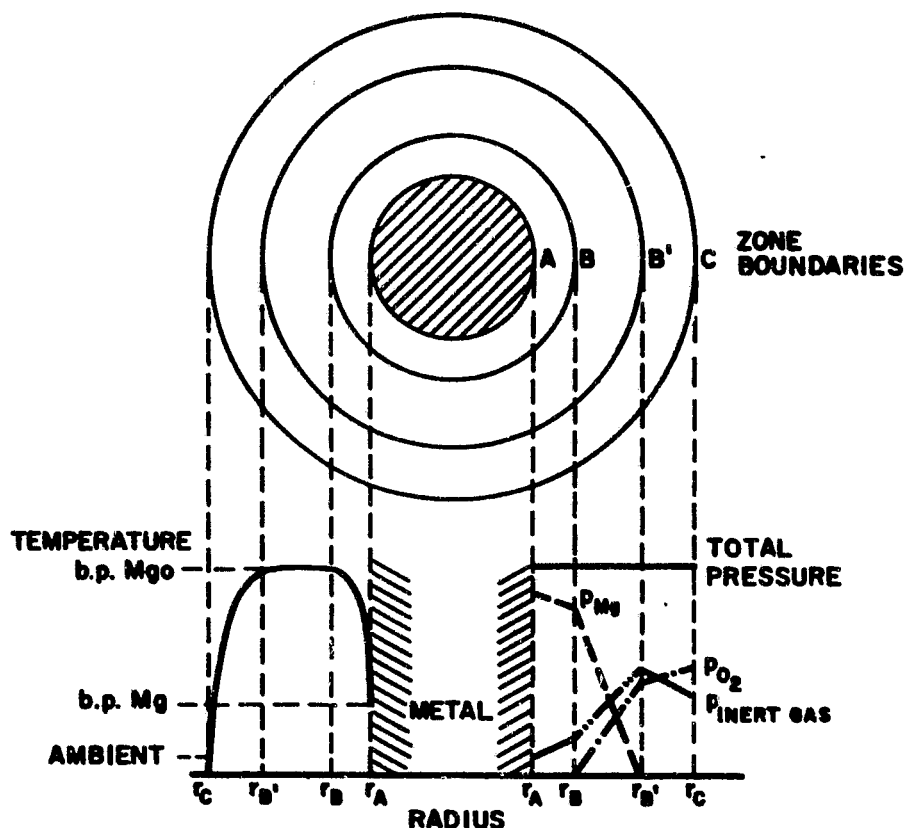


Fig. 9 Cross section of cylindrical stagnant-film model with finite reaction zone; p , partial pressure. Reproduced from Ref. 10

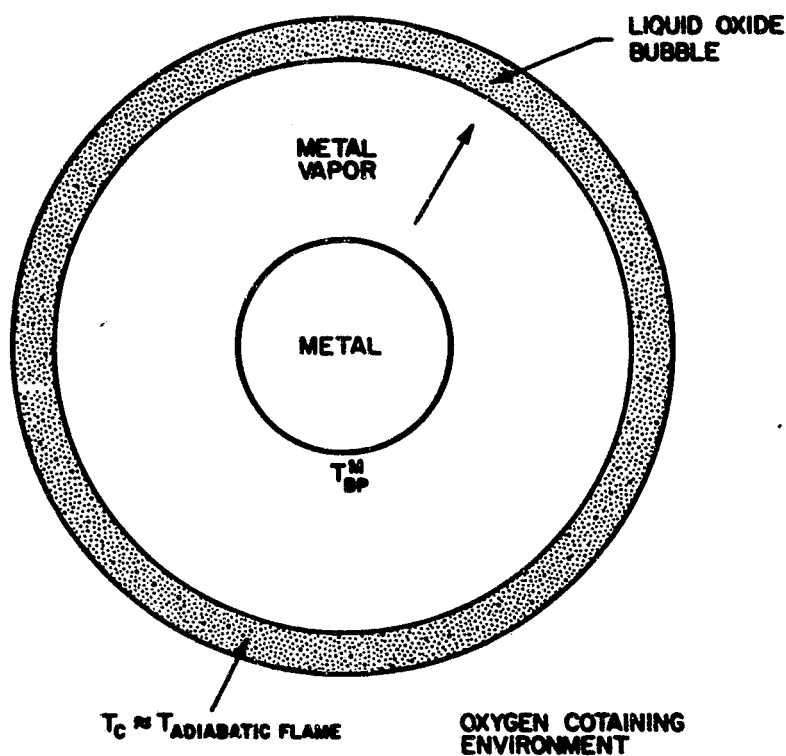


Fig. 10 Model for combustion with metal evaporation and expansion of the liquid oxide shell.

Ref: Fassell et al. Combustion and Flame 7:227-34 (1963)

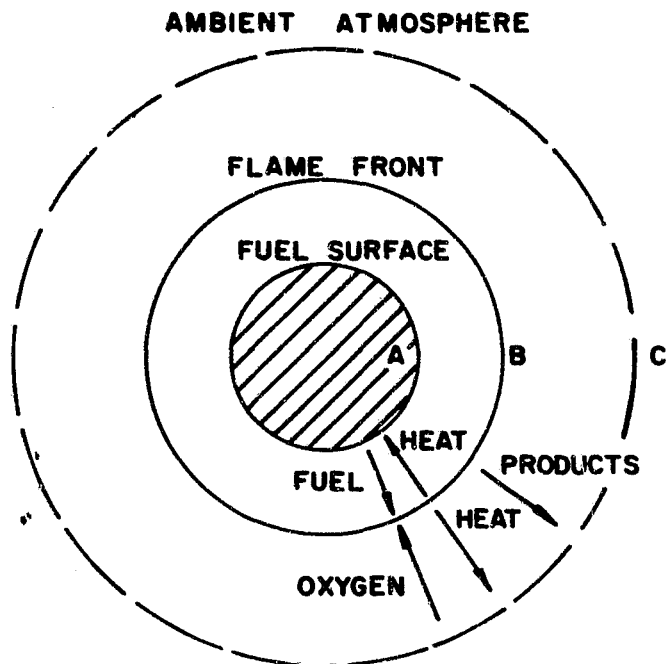


Fig. 11 Droplet burning theory model

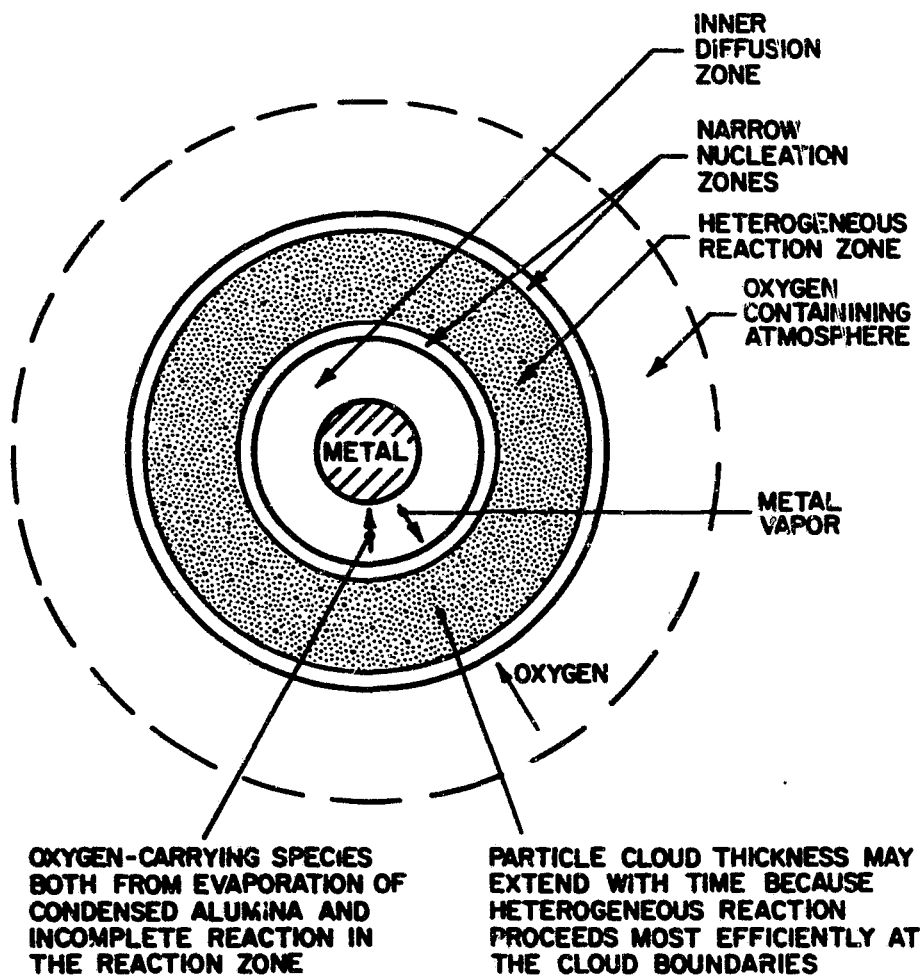


Fig. 12 A model of aluminium particle combustion. Ref: R.H.Knipe. NOTS TP 3916 April 1966. Technical progress report 415

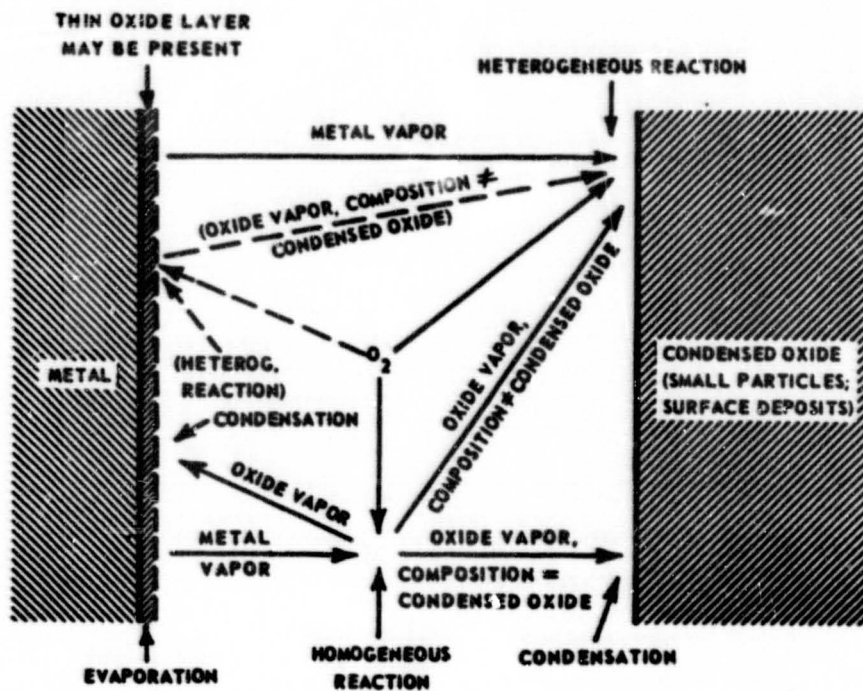


Fig. 13 Schematic representation of vapor-phase burning. Ref: Markstein, G.H. 11th Symposium (International) on combustion pg 219-234, The Combustion Institute, Pittsburgh, Penna.

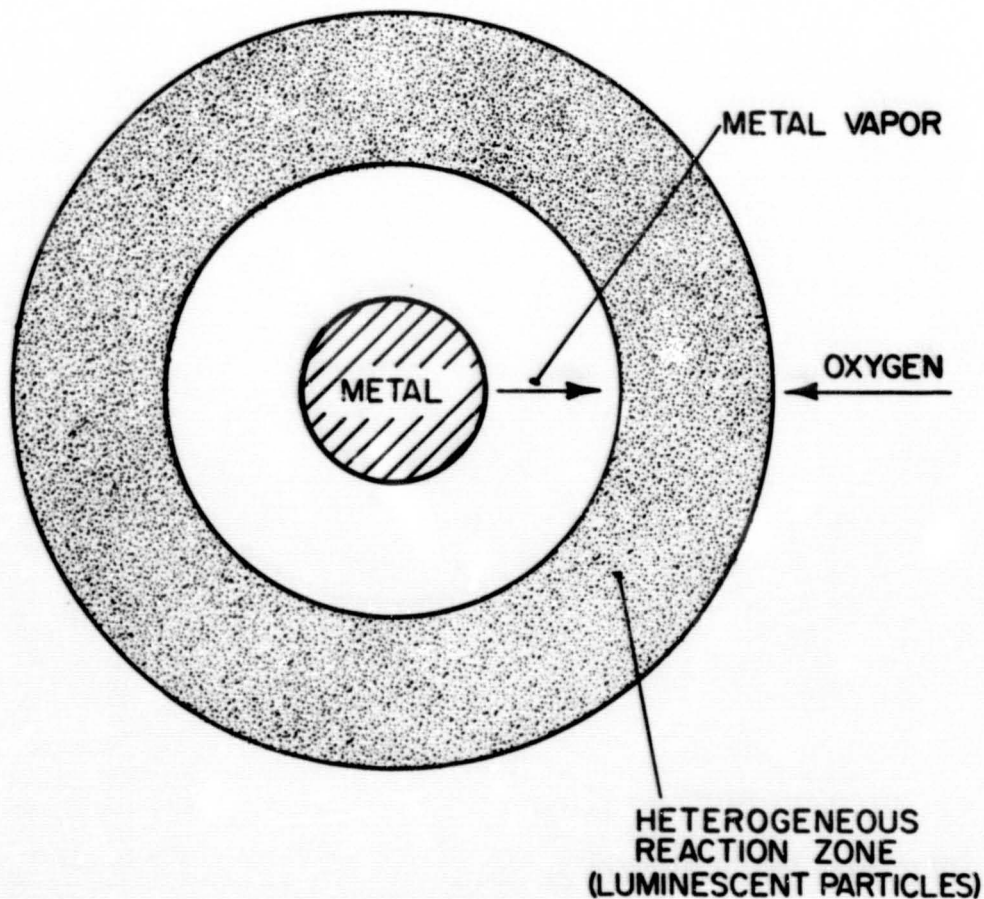


Fig. 14 Heterogeneous reaction model

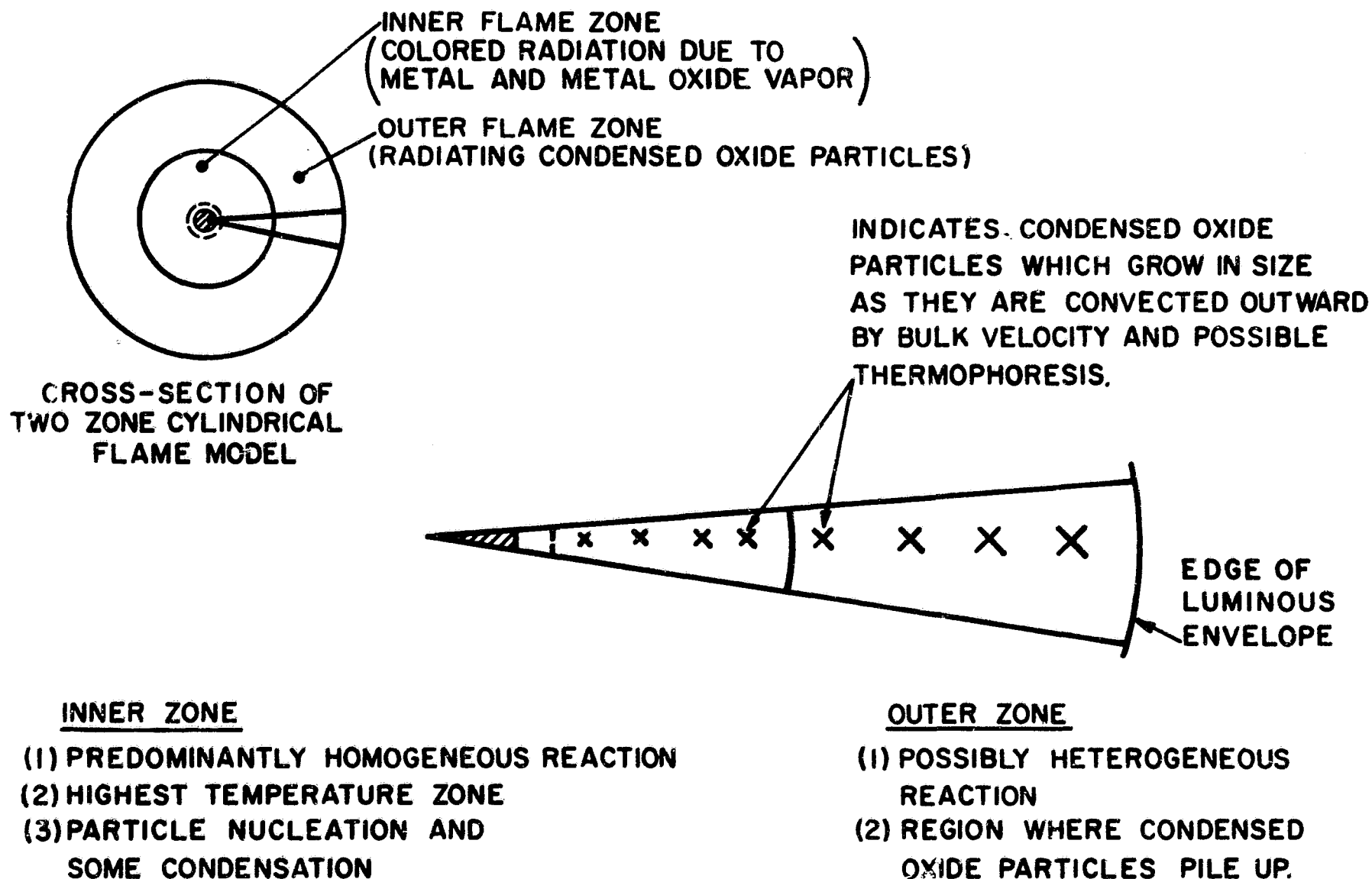


Fig.15 Schematic representation of flame structure

APPENDIX A - THEORIES OF METAL IGNITION*

Several theories of metal ignition have been given by various investigators in the literature; these will now be reviewed. In order to facilitate comparison, the defining equations for the critical and ignition temperatures in Mellor's model are repeated:

$$(\dot{q}_{chem})|_{T_s = T_{crit}} = (\dot{q}_{loss})|_{T_s = T_{crit}} \quad \text{Eq (10)}$$

$$\left(\frac{\partial \dot{q}_{chem}}{\partial T_s}\right)|_{T_s = T_{ign}} = \left(\frac{\partial \dot{q}_{loss}}{\partial T_s}\right)|_{T_s = T_{ign}} \quad \text{Eq (14)}$$

Some of the theories to be discussed are appropriate to systems of any size, that is, are size independent, and others are for particular types of experiments such as those involving dust dispersions.

A - BULK IGNITION ACCORDING TO THE THEORY OF EYRING AND ZWOLINSKI - The earliest theory of metal ignition is due to Eyring and Zvolinski (42). This theory, in terms of the present model, is a calculation for the critical temperatures of a bulk system based on the Theory of Absolute Reaction Rates.

The temperature under consideration was defined by the following heat balance equation:

$$\dot{q}_{chem} = \dot{q}_{loss} \quad \text{Eq (A-19)}$$

The \dot{q}_{chem} term was expressed as:

$$\dot{q}_{chem} = \dot{m} \Delta H_f / N \quad \text{Eq (A-20)}$$

where \dot{m} is the reaction rate (number of metal atoms/cm²sec). ΔH_f is the heat of formation of the product (kcal/mole), and N is Avogadro's number.

It was stated that "the ignition of metal samples will occur when the conduction of heat through the oxide film is inadequate for the removal of the heat produced at the metal-film interface as a result of corrosion". Radiation, conduction into the metal, and conduction into the ambient oxidizing gas are neglected, and thus, \dot{q}_{loss} was written:

$$\dot{q}_{loss} = k_{ox} (T_s - T_o) / d_{ox} \quad \text{Eq (A-21)}$$

where k_{ox} is the thermal conductivity of the oxide (cal/°C cm sec), T_o is the temperature at the metal-oxide interface, T_s is the temperature at the oxide-gas interface (both in °K), and d_{ox} is the oxide film thickness (cm). Eq. (A-19) then becomes:

$$\dot{m} \Delta H_f / N = k_{ox} (T_s - T_o) / d_{ox} \quad \text{Eq (A-22)}$$

The expression for the reaction rate was developed from the Theory of Absolute Reaction Rates and was written:

$$\dot{m} = (C_s k T_s F / h) e^{-E/kT_s} \quad \text{Eq (A-23)}$$

where C_s is the number of absorption sites or metal atoms per unit surface area, k is the Boltzmann constant (ergs/°K), h is Planck's constant (erg sec), E is the activation energy (erg), and F is the ratio of the reaction surface area to the outer area of the oxide film. This rate expression is valid only for regimes of linear oxidation.

Eq. (A-22) and A-23) may be rewritten:

$$T_o = T_s \left[1 - (C_s k F d_{ox} \Delta H_f / k_{ox} h N) e^{-E/kT_s} \right] \quad \text{Eq (A-24)}$$

Since ignition will occur when the heat balance represented by Eq. (A-22) is destroyed, T_s as calculated from Eq. (A-24) is the ignition temperature, which is seen to depend strongly on the oxide film thickness d_{ox} . Note, however, that in terms of the present model, T_s as calculated from Eq. (A-24) is actually the critical temperature by virtue of Eq. (10).

Upon comparison of temperatures calculated from Eq. (A-24) with ignition temperatures measured experimentally for Mg in O₂, Fassell et al. (43) noted the following difficulties with the theory: firstly, the experimental ignition temperature is independent of oxide thickness; secondly, self-heating below the temperature predicted by Eq. (A-24) is impossible (that is, these authors recognized that self-heating below the ignition temperature is possible); and thirdly, the

* Extracted in its entirety from the Ph.D. thesis of Mellor (12).

observed pressure dependence of the ignition temperature is not explained or predicted by the theory.

Recalling that the temperatures calculated by Eyring and Zvolinski are actually critical temperatures, two of the failures of the theory noted by Fassell and co-workers can be explained. It is possible that the critical temperature is a function of oxide film thickness and self-heating is not only possible, but also expected above the critical temperature. A pressure dependence of ignition or critical temperature is predicted by a more complete theory.

Other difficulties with the theory of Eyring and Zvolinski are the independence of critical temperature with respect to sample size and the failure of the theory for zero oxide thicknesses. Also, the theory as developed applies only to temperature regimes of linear oxidation.

In view of the difficulties noted with the theory of Eyring and Zvolinski, Higgins and Schultz proposed the following modifications in which T_s and T_o were defined in terms of microscopic granules of metal: T_s is the mean temperature in the interior of a metallic granule at the metal-oxide interface; T_o is a mean temperature at the external surface of the oxide film associated with the granule; and, allowing for non-uniformities in the oxide film on the granule, d_{ox} is taken as a mean oxide thickness. It was then argued that for an aggregate of small granules, because of the near equality of T_s and T_o from granule to granule, the temperature gradient $(T_s - T_o)/d_{ox}$ becomes vanishingly small and ignition occurs. However, no calculations were attempted.

B-BULK IGNITION ACCORDING TO THE THEORY OF HILL, ADAMSON, FOLAND AND BRESSETTE-A second theory, also based on Eq. (10), was proposed by Hill and co-workers (44). These authors, however, noted that the calculation provided an estimate of the spontaneous ignition temperature, rather than ignition temperature, and is thus consistent with the definitions of the present model.

These authors balanced a rate of chemical energy release with a convection and radiation heat loss:

$$\dot{q}_{chem} = \dot{q}_{conv} + \dot{q}_{rad} \quad \text{Eq (A-25)}$$

A conduction term into the metal was neglected because in their experiments the samples were heated uniformly. Using engineering approximations to the three terms in Eq. (A-25), good agreement between calculated and measured spontaneous ignition temperatures was obtained for 1020 steel in air. The appropriate oxidation rate involved in \dot{q}_{chem} was measured in their own experiments. The calculated values were dependent on the oxide thickness (as in the theory of Eyring and Zvolinski).

A major difficulty with the theory of Hill et al. is that the wrong size dependence of critical temperature is predicted. In their approximation of \dot{q}_{conv} the sample size dependence enters as follows:

$$\dot{q}_{conv} \sim Re^{1/2}/d \quad \text{Eq (A-26)}$$

where d is now the characteristic size of the sample, and Re is the Reynolds number based on this size. Therefore, by virtue of the definition of Reynolds number:

$$\dot{q}_{conv} \sim d^{-1/2} \quad \text{Eq (A-27)}$$

That is, as the sample size is decreased, \dot{q}_{conv} increases, and so does the critical temperature.

As in the theory of Eyring and Zvolinski, the theory of Hill et al fails for clean metal surfaces, that is, for zero oxide thicknesses, because in this case the reaction rate is inversely proportional to oxide film thickness.

C-BULK IGNITION ACCORDING TO THE THEORY OF REYNOLDS - A theory of metal ignition was advanced by Reynolds (22), in which the temperature history of the metallic sample was described by the following energy equation, where conduction into the fuel is neglected:

$$\frac{C}{S} \frac{dT_s}{dt} = \dot{q}_{chem} - h(T_s - T_g) - \epsilon \sigma (T_s^4 - T_a^4) + \dot{q}_{input} \quad \text{Eq (A-28)}$$

where C = total heat capacity of the sample, cal/ $^{\circ}$ K;
 S = surface area of the sample, cm²;
 T_s = surface temperature of the sample, $^{\circ}$ K;
 t = time, sec;
 \dot{q}_{chem} = chemical energy release rate per unit area, cal/cm²sec;
 h = heat transfer coefficient, cal/cm²sec $^{\circ}$ K;
 T_g = sample recovery temperature, K;
 σ = Stefan-Boltzmann constant, cal/cm²sec($^{\circ}$ K)⁴;

ϵ = surface emissivity, dimensionless;
 T_r = effective radiation temperature of the environment, °K;
 \dot{q}_{input} = any heat input independent of the body temperature, cal/cm²sec.

According to Reynolds, "the ignition temperature is seen to be equivalent to the temperature at which the body temperature begins to increase at an increasing rate. This may be expressed mathematically as the temperature at which dT_s/dt is a minimum. Thus, at ignition:

$$\frac{d}{dT_s} \left(\frac{C}{S} \frac{dT_s}{dt} \right) = 0 \quad \text{Eq (A-29)}$$

or, from Eq. (A-28)=

$$\frac{d\dot{q}_{chem}}{dT_s} - h - 4\epsilon\sigma T_s^3 = 0 \quad \text{Eq (A-30)}$$

Reynolds defined ignition to occur at an inflection point in the surface temperature-time curve; as no equilibrium positions (with respect to time) are indicated in his model and as the surface temperature is rising in time, by definition, the critical temperature has been exceeded. He then incorrectly indicated that dT_s/dt goes through a minimum at ignition, above the critical temperature.

In the present model ignition occurs at a maximum value of dT_s/dt above the critical temperature, which is indeed an experimental criterion for ignition. Mathematically, of course, there is no difference in the defining equation for ignition temperature, but the intuitive difference in approach to this equation is stressed.

Reynolds wrote \dot{q}_{chem} as follows:

$$\dot{q}_{chem} = \dot{m} Q_{chem} \quad \text{Eq (A-31)}$$

where \dot{m} is the reaction rate (g O₂/cm²sec) and Q_{chem} is the heat of reaction (cal/g O₂). He considered both linear

$$W = K_L t = A_L t e^{-E_L/RT_s} \quad \text{Eq (A-32)}$$

and parabolic regimes of oxidation

$$W^2 = K_P t = A_P t e^{-E_P/RT_s} \quad \text{Eq (A-33)}$$

where the K_i are the appropriate rate constants, A_i are the appropriate pre-exponential factors, E_i are the appropriate activation energies, and R is the universal gas constant. w is the weight of O₂ per unit area that has reacted with the metal at time t .

Since

$$\dot{m} = \partial W / \partial t \quad \text{Eq (A-34)}$$

then

$$\dot{m}_L = K_L = A_L e^{-E_L/RT_s} \quad \text{Eq (A-35)}$$

and

$$\dot{m}_P = K_P / 2W = K_P \delta / 2\rho_{ox} d_{ox} \quad \text{Eq (A-36)}$$

Therefore*:

$$\dot{m} = (A_P \delta / 2\rho_{ox} d_{ox}) e^{-E_P/RT_s} \quad \text{Eq (A-37)}$$

where ρ_{ox} is the oxide density, d_{ox} is the oxide thickness, and δ is the ratio of the mass of oxide to the mass of O₂ forming it. Multiplying by the heat release per gram O₂, Q_{chem} , the heat release rates are obtained:

$$\dot{q}_{chem,L} = A_L Q_{chem} e^{-E_L/RT_s} \quad \text{Eq (A-38)}$$

$$\dot{q}_{chem,P} = (A_P \delta Q_{chem} / 2\rho_{ox} d_{ox}) e^{-E_P/RT_s} \quad \text{Eq (A-39)}$$

Substitution of Eq. (A-38) or (A-39) into Eq. (A-30) yields:

$$e^{-1/T_{s,i}^*} = (T_{s,i}^*)^5 / \eta_i + h_i^* (T_{s,i}^*)^2 \quad \text{Eq (A-40)}$$

* Markstein (5) has shown that the placement of η_i in the denominators of Eq. (A-36) and A-37), as in the original paper of Reynolds, is in error.

where subscript i equals l or p , and where

$$T_{s,i}^* = T_s R / E_i \quad \text{Eq (A-41)}$$

$$\eta_s = A_s Q_{chem} R^4 / 4 \epsilon \sigma E_s^4 \quad \text{Eq (A-42)}$$

$$\eta_p = A_p \delta Q_{chem} R^4 / 8 \epsilon \sigma_{ox} d_{ox} E_p^4 \quad \text{Eq (A-43)}$$

$$h_s^* = h E_s / A_s Q_{chem} R \quad \text{Eq (A-44)}$$

$$h_{ip}^* = 2 h E_p \sigma_{ox} d_{ox} / A_p \delta Q_{chem} R \quad \text{Eq (A-45)}$$

The T_s^* are dimensionless ignition temperatures, h_s^* are dimensionless heat transfer coefficients, and the η_i are called pyrophoricities by Reynolds.

Reynolds noted that either an increase or decrease in the rate of convective heat transfer (and, furthermore, when this term represents either heating or cooling) will increase the calculated ignition temperature.

Since the ignition temperature is expressed by the universal curve Eq (A-40), all metal-oxidizer systems were expected to agree with this prediction. Reynolds calculated a family of curves of T^* versus η for various values of h^* . He then measured ignition temperatures for various massive systems. For the specific systems, the oxidation rate data were taken from the oxidation literature. Extremely good agreement between the curve of T^* versus η with h^* equal to zero was obtained in all the cases investigated. Reynolds argued that this agreement with the case of zero convective heat transfer was a result of his measuring the ignition temperatures in quiescent atmospheres. Experimentally, ignition was defined by "a sharp break in the temperature curve."

As noted previously, Reynolds' resulting theoretical definition of the ignition temperature, Eq. (A-30), is equivalent to that of the present investigation, Eq. (14). The experimental definition is also equivalent. Thus agreement between theory and experiment, within the experimental error and the theoretical error in estimating the various parameters which appear in Eq. (A-41) - (A-43), is not unexpected. However, in the theory of Reynolds, the ignition temperature is predicted to be independent of sample size, and, furthermore, no pressure dependence is predicted, because of the experimental indication that convective heat losses to the ambient gases are negligible.

D-BULK IGNITION ACCORDING TO THE THEORY OF TALLEY - Talley (45) made a calculation of "the minimum temperature above which the combustion of boron is self-sustaining. . . by equating the rate of heat generation by chemical reaction with the rate of heat loss by radiation as functions of temperature." He referred to this temperature as an ignition temperature, but, of course, in the present model this temperature is defined as the critical temperature. Estimates of the reaction rate were acquired from data about 700°C below the ignition temperature in a temperature regime in which the evaporation of B_2O_3 from the metal surface is rate-determining.

As Talley recognized, because only a radiation heat loss mechanism is assumed, the theory is valid only for large samples. Under these assumptions, an ignition temperature of about 1925°C was predicted for large B samples in O_2 . Because of the experiment employed to investigate the ignition process, critical and ignition temperatures could not be distinguished.

By introducing a 1 mm diameter B rod into an O_2 -rich natural gas flame and using a corrected optical pyrometer to measure surface temperature. Talley made the following observations: "at temperatures about 1800°K the boron was observed to burn relatively slowly. Between 1800 and 2100°K the rate increased evenly. A temperature of 2230°K (1957°C) was the highest temperature before there was a sudden increase in burning rate." The correspondence of the temperature of this sudden rate change and the calculated ignition temperature is excellent.

As is the case with most of the other theories discussed to this point, Talley's theory predicts that the calculated critical temperature is independent of sample size and oxidizer pressure.

E-SINGLE PARTICLE IGNITION ACCORDING TO THE THEORY OF FRIEDMAN AND MACEK - Friedman and Macek (13) developed an ignition theory in order to explain their experimental results on the ignition of Al particles. They later applied similar ideas to the ignition of Be (46).

The attempt to explain their results on the basis of a simple heat balance led to several discrepancies with their experimental results. The theory predicted a strong dependence of the ignition temperature on particle size and on ambient oxidizer concentration, whereas experimentally these parameters had little influence on ignition temperatures. Also, predicted ignition temperatures were considerably higher than the measured temperatures.

In order to circumvent these difficulties, on the basis of the experimental association of the Al ignition temperature with the melting point of Al_2O_3 , they assume that a discontinuous increase in reaction rate occurs at the melting point of the oxide, T_{MP}^{MO} (T_s is the particle temperature):

$$\dot{q}_{chem} = Q_{chem} C_g K \quad T_s < T_{MP}^{MO} \quad \text{Eq (A-46)}$$

$$\dot{q}_{chem} = Q_{chem} C_g K' \quad T_s \geq T_{MP}^{MO} \quad \text{Eq (A-47)}$$

where Q_{chem} is the heat of reaction (cal/mole), c_g is the concentration of oxidizer at the particle surface (mole/cm³), and k and k' are rate constants (cm/sec), with $k' \gg k$.

Two heat fluxes in the ambient gas were considered:

$$\dot{q}_{cond,g} = 2 K_g (T_s - T_g) / d \quad \text{Eq (A-48)}$$

$$\dot{q}_{diff} = 2 Q_{chem} D (C_{g,\infty} - C_g) / d \quad \text{Eq (A-49)}$$

where $\dot{q}_{cond,g}$ is the heat lost by conduction, k_g is the thermal conductivity of the gas (cal/cm² sec K), T_g is the gas temperature (K), d is the particle diameter (cm), \dot{q}_{diff} is the heat flux due to oxidizer diffusion to the reaction zone, D is the oxidizer diffusivity (cm²/sec), and $c_{g,\infty}$ is the oxidizer concentration at infinity (mole/cm³).

Because the particle is assumed to be at uniform temperature, conduction into the particle is neglected. Radiation losses are also neglected in the ignition process.

A temperature defined by an equilibrium:

$$\dot{q}_{cond,g} = \dot{q}_{diff} \quad \text{Eq (A-50)}$$

$$\dot{q}_{chem} = \dot{q}_{cond,g} \quad \text{Eq (A-51)}$$

exists below the oxide melting point; above this temperature the particle may self-heat (that is, this temperature is, in terms of the physical model, the critical temperature). The authors referred to this temperature as the minimum ambient temperature required for ignition.

Friedman and Macek proceeded in this manner in order to evaluate the oxidizer concentration at the particle surface from Eq. (A-50), (A-48), and (A-49):

$$C_g = C_{g,\infty} - K_g (T_s - T_g) / D Q_{chem} \quad \text{Eq (A-52)}$$

Eq. (A-51) may be rewritten:

$$Q_{chem} C_g K = 2 K_g (T_s - T_g) / d \quad \text{Eq (A-53)}$$

Eq. (A-52) is then substituted into Eq. (A-53) and the expression for the minimum ambient temperature required for ignition is obtained:

$$T_g = T_s - C_{g,\infty} Q_{chem} / [K_g (\frac{1}{d} + \frac{2}{dK})] \quad \text{Eq (A-54)}$$

Since at ignition, $T_s = T_{MP}^{MO}$, Eq. (A-54) becomes:

$$T_g = T_{MP}^{MO} - C_{g,\infty} Q_{chem} / [K_g (\frac{1}{d} + \frac{2}{dK})] \quad \text{Eq (A-55)}$$

Friedman and Macek noted that the correction term, the second term on the right hand side of Eq. (A-55), is extremely small compared to T_{MP}^{MO} , which explains the observed small dependence of ignition temperature on d and D .

The theory is applicable only to small particles because conduction into the interior of the particle and radiation to the surroundings are neglected.

A major difficulty with the theory is that as the particle diameter is increased, the minimum ambient temperature required for ignition (or critical temperature) decreases. Also, k , the reaction rate, which appears in Eq. (A-55) is a function of temperature, and pressure.

F-DUST DISPERSION IGNITION ACCORDING TO THE THEORY OF NAGY AND SURINCİK - Nagy and Surincik (47) have recently developed a theory for ignition of dust dispersions. Their theory was tested against experimental results on the ignition of dust dispersions. Their theory was tested against experimental results on the ignition of cornstarch; nevertheless, inasmuch as dust dispersion experiments give ignition temperatures which have little correlation with transition temperatures (12), the ignition temperatures of dust dispersions of cornstarch or metal powders are expected to be predicted equally well by a theory which does not include a transition temperature concept.

Again a simple heat balance is used to define ignition, so that in actuality, a critical rather than ignition temperature is estimated:

$$\dot{q}_{chem} = \dot{q}_{loss} \quad \text{Eq (A-56)}$$

Because of the nature of the sample configuration, somewhat more complicated expressions for the heat fluxes result. Also, heat fluxes per unit volume rather than per unit area are considered.

The following assumptions were made:

1. The entire system (gas plus particles) is described by the equation of state $pV = RT$, where p is pressure, V is volume, R is the universal gas constant, and T is the temperature.
2. The dispersion is uniform with respect to volume, and the volume of the particles is negligible with respect to that of the gas.
3. Mass transfer is negligible during ignition.
4. Heat capacities are temperature independent.
5. Heat transfer occurs primarily by conduction and convection and is linearly proportional to the temperature difference.
6. Any action of the addition of an inert dust to the dispersion is strictly thermal.
7. A bimolecular oxidation process is assumed, and the rate variation of this process with respect to temperature is expressed by an Arrhenius-type function.

The heat release due to reaction per unit volume may then be expressed:

$$\dot{q}_{chem} = A Q_{chem} (F)^{\alpha} (OX)^{\beta} (p/RT)^2 e^{-E/RT} \quad \text{Eq (A-57)}$$

where all symbols have their previous meanings, and where α is the order of the reaction with respect to fuel (F) and β with respect to oxidizer (OX). (F) and (OX) are the relative molar concentrations per unit volume. Several simplifications of Eq. (A-59) are made as indicated below.

Since O_2 is the only reacting component of the gas phase, "the system may be considered unimolecular with respect to the gaseous phase. Thus the term p/RT is taken at the first power rather than at the second power, and the units of A become l/sec . The system contains the inert gases nitrogen and admixed carbon dioxide, and the rate of reaction is lowered by the fraction Z , which represents the proportion of oxygen in the atmosphere." Since at ignition, by definition the concentration of products is negligible:

$$(F) + (OX) = 1 \quad \text{Eq (A-58)}$$

Because the number of moles of O_2 per unit volume is p/RT , the weight of O_2 per unit volume, Z , is:

$$Z = p \theta M_{O_2} / RT \quad \text{Eq (A-59)}$$

where M_{O_2} is the molecular weight of O_2 .

The effective surface area of the dust is included in the chemical heat release rate by modification of the activation energy, that is, $\exp(-E/RT)$ is replaced by $\exp(-\sigma E/RT)$, where σ is the effective surface area of the dust, and E is a property only of the fuel. Finally,

$$(F) = (X/M_d) / (X/M_d + Z/M_{O_2}) \quad \text{Eq (A-60)}$$

where X is the initial dust concentration in g/cm³ and M_d is the molecular weight of the dust. Then:

$$(F)^\alpha [1 - (F)]^\beta = [X/(X + bz)]^\alpha [1 - X/(X + bz)]^\beta \quad \text{Eq (A-61)}$$

$$\equiv f(x) \quad \text{Eq (A-62)}$$

where

$$b \equiv M_d/M_{O_2} \quad \text{Eq (A-63)}$$

Thus combining Eq. (A-57) through (A-62):

$$\dot{q}_{chem} = \{A Q_{chem} Z f(x)/M_{O_2}\} e^{-\sigma E/RT} \quad \text{Eq (A-64)}$$

The rate of heat loss per unit volume is expressed in the following manner:

$$\dot{q}_{loss} = [\sum_i k_i N_i c_{p,i} + V'] (T - T_f) \quad \text{Eq (A-65)}$$

where subscript i includes all constituents of the dust and gas system, k_i is the coefficient of heat transfer of species i (including conduction, convection, and radiation), (1/sec), N_i is the concentration of species i at the furnace temperature T_f (g/cm³), $c_{p,i}$ is the specific heat of species i at T_f (cal/g K), and V' is the rate of heat loss per degree per unit volume to the vessel walls (cal/sec Kcm³).

The experimental results indicated that the heat transfer coefficients, k_i , are all of the same order of magnitude. Thus,

$$k_i = K \quad \text{Eq (A-66)}$$

and

$$V' = V'/K \quad \text{Eq (A-67)}$$

Following Semenov, the approximation is made:

$$T - T_f \approx RT_f^2 / \sigma E \quad \text{Eq (A-68)}$$

(A-65) becomes in its final form:

$$\dot{q}_{loss} = (KR T_f^2 / \sigma E) [\sum_i N_i c_{p,i} + V'] \quad \text{Eq (A-69)}$$

The condition for ignition, Eq. (A-56), is then:

$$\{A Q_{chem} Z f(x)/M_{O_2}\} e^{-\sigma E/RT} = \{KR T_f^2 / \sigma E\} [\sum_i N_i c_{p,i} + V'] \quad \text{Eq (A-70)}$$

Nagy and Surincik obtained the values of σ , k' , V , α , β , and b , where

$$K' \equiv KR M_{O_2} / \sigma A Q_{chem} E \quad \text{Eq (A-71)}$$

from their experimental results on the ignition of cornstarch. They then varied the furnace temperature and concentrations of fuel dust, inert dust, and oxygen over wide ranges, and found an excellent correlation between theory and experiment. Predictions of ignition limits were also verified experimentally.

G-QUIESCENT PILE IGNITION ACCORDING TO THE THEORY OF ANDERSON AND BELZ -
Anderson and Belz (48) proposed a qualitative theory of the ignition of quiescent piles of metal powders. In particular, they considered the ignition of Zr in O₂. It was assumed that a spherical mass of powder of radius r is in perfect contact with a heat reservoir at temperature T₀. This spherical mass of powder consists of spherical particles of diameter d. "If the rate of heat development at the center of the mass is greater than the rate at which the heat can be transported to the container, ignition eventually occurs. Then, the following condition is necessary to ignition: rate of exothermic heat development > rate of heat loss." Therefore, this theory is a discussion of the critical temperature for a quiescent pile experiment.

The appropriate reaction rate law for Zr in O₂ was taken as

$$w = K_p t + \text{const.} \quad \text{Eq (A-72)}$$

where w is the increase in weight of the metal sample per unit area. The reaction rate per unit area is then:

$$\frac{dw}{dt} = \frac{1}{2} \sqrt{\frac{Q_0}{t}} = \frac{\sqrt{A} e^{-E/2RT}}{2 \sqrt{E}} \quad \text{Eq (A-73)}$$

where all symbols have their previous meanings.

The total surface area per gram of a system of uniformly sized particles is $6/\rho d$, where ρ is the metal density*. Anderson and Belz then wrote the rate of heat generation by the center element as

$$g_{chem} = (A' Q_{chem} / \sqrt{E} d) e^{-E/2RT} \quad \text{Eq (A-74)}$$

where A' includes all previous constants.

The heat loss term is assumed to be of the form:

$$g_{loss} = K(T - T_a) / r \quad \text{Eq (A-75)}$$

where k is the appropriate thermal conductivity of the particle plus void configuration. The criterion for ignition then becomes:

$$(A' Q_{chem} / \sqrt{E} d) e^{-E/2RT} > K(T - T_0) / r \quad \text{Eq (A-76)}$$

Anderson and Belz noted that this expression could not be solved for the ignition temperature T in terms of the ambient temperature T_0 . However, simplifications are possible if the assumption that $(T - T_0)$ is equal to a small constant value is made. Then Eq. (A-76) may be written:

$$e^{-E/2RT_0} > A'' \sqrt{E} d / r \quad \text{Eq (A-77)}$$

or

$$T_0 > E / \{ 2 R \ln(1 / A'' \sqrt{E} d) \} \quad \text{Eq (A-78)}$$

Anderson and Belz stated that "various interpretations of the time factor in this expression are possible. If it is interpreted as an inverse function of the external heating rate, then the expression predicts a decrease in ignition temperature with heating rate. This is the experimental case for small samples. In the case of larger samples, the increase of ignition temperature with heating rate is attributed to increased lag of internal temperature with respect to external temperature. . . . The expression is in qualitative agreement with the data, as regards particle size." The trend predicted is that the ignition temperature will decrease with decreasing particle diameter, d .

H-QUIESCENT PILE IGNITION ACCORDING TO THE THEORY OF TETENBAUM, MISHLER, AND SCHWIZLEIN - Tetenbaum et al (49) correlated their experimental results on the ignition of quiescent piles of U powder in O_2 on the basis of the ignition theory of Frank-Kamenetskii. They also applied an ignition theory of Murray, Buddery, and Taylor, which was originally developed in light of the data of Anderson and Belz (48).

Using the stationary homogeneous ignition theory of Frank-Kamenetskii, Tetenbaum and co-workers found excellent agreement between their experimental results and ignition temperatures calculated on the basis of the critical size result of Frank-Kamenetskii (16) with β , the shape constant, equal to 0.88, that is, for a one-dimensional container.

The agreement between a theory developed for homogeneous gas-phase systems with results obtained in a quiescent pile powder experiment no doubt results from the homogeneous nature of this latter experimental configuration, that is, the small metal particles separated by spaces filled with O_2 . Again, Eq (10) is the defining equation in this theory, a critical temperature has been calculated.

Tetenbaum et al then applied a theory due to Murray, Buddery, and Taylor; the physical basis of this theory is questionable. Here no heat losses are included, and all the heat generated by the chemical reaction is used to increase the temperature of the pile of powder. Effectively, then, the critical temperature for this theoretical model is zero, for as long as any exothermic reaction occurs, the temperature of the sample will increase until ignition occurs.

According to Murray et al as quoted by Tetenbaum and co-workers, the rate of heating due to chemical reaction of a metal powder in the linear oxidation rate regime is:

* Anderson and Belz erroneously gave this expression as $6/\rho d^5$, but apparently used $6/\rho d$ in their subsequent calculations.

$$\frac{dH}{dt} = \frac{6 M Q_{chem} A e^{-E/RT}}{\rho D} \quad \text{Eq (A-79)}$$

where H is enthalpy, M is the mass of the powder, d is the diameter of a particle within the powder, and ρ is the density. If the container is heated at the rate $dT/dt = \phi$, then the total enthalpy generated upon heating from 298 K to T° K is:

$$H = \int_{298}^T \frac{6 M Q_{chem} A e^{-E/RT}}{\phi \rho d} dT \quad \text{Eq (A-80)}$$

Also,

$$H = M c_p \Delta T \quad \text{Eq (A-81)}$$

where c_p is the specific heat of the powder and ΔT is the temperature rise resulting from reaction upon raising the container temperature from 298 K to T° K at a rate of ϕ K/min*. Thus,

$$\Delta T = \int_{298}^T \frac{6 Q_{chem} A e^{-E/RT}}{\phi \rho c_p d} dT \quad \text{Eq (A-82)}$$

After integration, Eq. (A-82) may be written:

$$\log \left\{ R \rho d \phi c_p \Delta T / 6 Q_{chem} A E \right\} = -E/4.56 T_0 + \log \left\{ \left(\frac{RT_0}{E} \right)^2 - 2 \left(\frac{RT_0}{E} \right)^3 \right\} \quad \text{Eq (A-83)}$$

where T_0 is the container temperature at which ignition occurs. ΔT is "the difference in temperature between the sample and container at ignition."

On the basis of the data of Anderson and Belz obtained with Zr powder (48), Murray and co-workers took $T=50^\circ$ K. Tetenbaum et al. used this value of T and calculated ignition temperatures, T_0 , for their experiments from Eq. (A-83). Again, excellent agreement between theory and experiment was obtained.

At first sight, there is an apparent contradiction between these two theories. Critical temperatures are calculated from the theory of Frank-Kamenetskii because of the starting equation, Eq. (10). Because no heat losses are involved in the theory of Murray et al., the critical temperature is zero and the calculated temperature may be an ignition temperature. Yet temperatures calculated from both theories agree extremely well with each other and with experiment. This could mean that the critical and ignition temperatures are equivalent in this particular experiment.

First, however, it is not clear that the temperature calculated from the Murray theory is an ignition temperature, and particularly the ignition temperature as defined in the physical model of metal ignition. Secondly, in this theory, ignition is regarded to occur when the amount of sample self-heating over the container temperature, ΔT , is equal to 50° K. This value, however, was estimated on the basis of results of Anderson and Belz.

It was shown in the previous sections of this chapter that these latter investigators most likely measured critical temperatures rather than ignition temperatures. Thus, the agreement of the Murray and Frank-Kamenetskii theories is not fortuitous, because the choice of $\Delta T=50^\circ$ K was based on critical temperature data.

* There is a typographical error in the definition of H in Ref. (49), in which $H = M c_p \Delta T$. Eq. (A-81) above is correct.

END OF REFERENCE
29

REFERENCE

30

**CARSLAW, H. S.; AND JAEGER, J. C.: CONDUCTION OF HEAT
IN SOLIDS. CLARENDON PRESS, 1950.**

**THIS REFERENCE IS COPYRIGHTED MATERIAL AND THEREFORE
THE CONTENTS HAVE NOT BEEN REPRODUCED FROM THE TEXT.**

END OF REFERENCE 30

REFERENCE

31

ARPACI, VEDAT S.: CONDUCTION HEAT TRANSFER. ADDISON-WESLEY PUB. CO., 1966.

**THIS REFERENCE IS COPYRIGHTED MATERIAL AND THEREFORE
THE CONTENTS HAVE NOT BEEN REPRODUCED FROM THE TEXT.**

END OF REFERENCE 3I